Survival and proliferation of human pathogenic *Candida* species within phagocytes

Dissertation

To Fulfill the

Requirements for the Degree of

„doctor rerum naturalium" (Dr. rer. nat.)

FRIEDRICH-SCHILLER-UNIVERSITÄT JENA

Submitted to the Council of the Faculty

of Biological Sciences

of the Friedrich Schiller University Jena

by M.Sc. Biochemistry Marcel Sprenger

born on 1st April 1990 in Erfurt

Reviewers:

1) Prof. Dr. Bernhard Hube
   Dept of Microbial Pathogenicity Mechanisms, Leibniz-Institute for Natural Product
   Research and Infection Biology (Hans-Knoell Institute) Jena, Germany

2) Prof. Dr. Kai Papenfort
   Institute of Microbiology, Friedrich-Schiller University Jena, Germany

3) Prof. Ph.D. Michael C. Lorenz
   Department of Microbiology and Molecular Genetics, University of Texas McGovern
   Medical School, USA

Date of defense: 15.09.2020

Table of contents

Summary

The two most prevalent, but phylogenetically distant pathogenic *Candida* species, *C. albicans* and *C. glabrata*, normally exist as harmless commensals on mucosal surfaces of most healthy humans. However, under certain circumstances, these species can become opportunistic pathogens causing superficial or systemic candidiasis, of which the latter is associated with high mortality rates.

During systemic infections, *C. albicans* and *C. glabrata* grow in different morphological forms and follow distinct infection strategies, but also show a common pattern of pathogenicity. Both species are able to colonize multiple organs, though face different humoral and cellular defense activities of the host's immune system. These include internalization by innate immune cells, like macrophages. Inside phagosomes of macrophages, fungal cells face a hostile environment with a low pH, containing high levels of reactive oxygen species and antimicrobial substances, but also low nutrient levels.

C. albicans and *C. glabrata* cells are efficiently phagocytosed by macrophages, but have evolved different strategies to survive phagocytosis, proliferate within, and escape from these cells. Besides a comprehensive detoxification system against the antimicrobial activities, *C. albicans* and *C. glabrata* cells adapt to nutrient limitations inside the phagosome by adjusting their central metabolic pathways. The prerequisite for essential micronutrients, however, cannot be bypassed as these are often co-factors of important metabolic enzymes. Micronutrients comprise trace metals but also vitamins, like biotin (vitamin H) – a vitamin for which both *Candida* species are auxotrophic. The main aim of this thesis was to gain new insights into the relevance of biotin acquisition of *C. albicans* and *C. glabrata* on fungal proliferation, survival in specific host niches, such as the phagosome of macrophages, and virulence.

The transcription factor gene *VHR1* and its biotin-related target genes were characterized in *C. albicans* and *C. glabrata*. One major finding of this thesis was the identification of the putative biotin transporter gene *VHT1* in both species. Similar to its ortholog in *S. cerevisiae*, *VHT1 of C. albicans* and *C. glabrata* contributed to biotin-dependent growth. The expression of *VHT1* in both species was shown to be regulated by biotin availability and was modulated by Vhr1 in a species-specific manner. Expression analyses further suggested that *VHT1* is regulated by yet unknown additional factors besides Vhr1 and growth assays hinted at the involvement of *VHR1* in other metabolic processes independent of biotin. *In silico* and growth analyses showed that some, but not all, medically important *Candida* species possess an incomplete biotin biosynthesis gene cluster which allows growth on biotin biosynthesis intermediates. This gene cluster was not required for *C. albicans* during interaction with

macrophages. Instead, biotin pre-starvation of *C. albicans* and *C. glabrata* or the deletion of *VHR1* diminished survival within macrophages. The importance of Vht1-mediated biotin acquisition for intraphagosomal proliferation together with the increased expression of *VHR1*, *VHT1*, and other biotin-related genes in phagocytosed *C. albicans* and *C. glabrata* cells was a fundamental observation in this study. These data suggest that biotin access is limited in phagosomes containing these *Candida* cells. Finally, the Vht1-mediated biotin acquisition was also crucial for efficient colonization of *C. glabrata* and *C. albicans* in distinct organs and for virulence of *C. albicans* during systemic candidiasis. Overall, these results propose that *C. albicans* and *C. glabrata* experience biotin limitation in certain host niches and that Vht1-dependent biotin import represents a mechanism by which fungi can overcome this limitation.

The evolutionary adaptation of pathogenic *Candida* species may have originated from ancient interactions of these fungi with environmental amoebae. In another project of this thesis it was shown that amoeba predation targets fungal copper and redox homeostasis to incapacitate ingested *C. parapsilosis* cells. A peroxiredoxin-mediated redox homeostasis system depending on the gene *PRX1* was shown to be essential for survival of *C. parapsilosis* in this alternative phagocyte model and to withstand killing by macrophages. Since *PRX1* is conserved among different pathogenic *Candida* species it can be concluded that peroxiredoxins are part of a basic survival package to resist phagocytic attacks.

Taken together, these data showed the importance of micronutrient and redox homeostasis as counterstrategies of different pathogenic *Candida* species to survive phagocytosis and pivotal virulence determinants. Future studies to elucidate fungal pathogenicity mechanisms will benefit from sophisticated gene manipulation approaches in *Candida* species, in particular non-*albicans* species. New gene reintegration, overexpression and complementation, and RNA-mediated gene knock-down protocols established in this thesis will contribute to future analyses of gene functions in *C. glabrata*.

Zusammenfassung

Die häufigsten, aber phylogenetisch voneinander separaten, *Candida* Spezies *C. albicans* und *C. glabrata* existieren als harmlose Kommensale auf Schleimhäuten von vielen gesunden Menschen. Unter bestimmten Umständen können beide Spezies allerdings opportunistische Infektionen verursachen, die sich entweder oberflächlich oder systemisch manifestieren, wobei letztere durch hohe Mortalitätsraten gekennzeichnet sind. *C. albicans* und *C. glabrata* unterschieden sich während einer systemischen Blutstrominfektion in ihren morphologischen Wachstumsformen und Infektionsstrategien, folgen aber einem ähnlichen Pathogenitätsmuster. Beide *Candida* Spezies können verschiedene Organe kolonisieren, werden aber mit verschiedenen Verteidigungslinien des humoralen und zellulären Immunsystems konfrontiert. Diese beinhalteten die Aufnahme durch Immunzellen der angeborenen Immunität, wie beispielsweise durch Makrophagen. Pilzzellen finden im Phagosom von Makrophagen eine feindliche Umgebung vor, die durch einen niedrigen pH, hohe Konzentrationen an reaktiven Sauerstoffspezies und antimikrobiellen Substanzen, aber auch durch eine niedrige Nährstoffverfügbarkeit charakterisiert ist.

C. albicans und *C. glabrata* Zellen werden erfolgreich durch Makrophagen phagozytiert, haben jedoch Mechanismen entwickelt die Phagozytose zu überleben, intrazellulär zu proliferieren und aus Makrophagen auszubrechen. Neben den ausgeprägten Systemen zur Detoxifizierung der antimikrobiellen Aktivitäten im Phagosom können sich *C. albicans* und *C. glabrata* durch die Umstrukturierung von zentralen metabolischen Strömen an die Nährstofflimitierung in diesem Kompartiment anpassen. Die Anforderung an essentielle Mikronährstoffe kann allerdings nicht umgangen werden, da diese oftmals Kofaktoren von wichtigen metabolischen Enzymen sind. Zur Gruppe der Mikronährstoffe gehören neben Spurenelementen auch Vitamine, wie beispielswiese Biotin (Vitamin H), für das beide *Candida* Spezies auxotroph sind. Der Fokus dieser Arbeit lag darin, neue Erkenntnisse über die Biotinaufnahme von *C. albicans* und *C. glabrata* zu erlangen und dessen Relevanz für das Wachstum, das Überleben in bestimmten Wirtsnischen, wie beispielsweise einem Phagosom von Makrophagen, und die Virulenz zu bestimmen.

Das Gen des Transkriptionsfaktors *VHR1* sowie dessen Biotin-assoziierten Zielgene wurden in *C. albicans* und *C. glabrata* charakterisiert. Ein wichtiger Fund dieser Arbeit war die Identifizierung des putativen Biotintransportergens *VHT1* in beiden *Candida* Spezies. *VHT1* von *C. albicans* und *C. glabrata* förderte das Biotin-abhängigen Wachstum, vergleichbar mit der Funktion des Orthologs in *S. cerevisiae*. Es konnte verdeutlicht werden, dass die Expression von *VHT1* durch die Verfügbarkeit von Biotin reguliert und durch Vhr1 Spezies-spezifisch moduliert wird. Expressions- und

Zusammenfassung

Wachstumsanalysen legten zusätzlich nahe, dass *VHT1* außer durch Vhr1 von anderen bis jetzt unbekannten Faktoren reguliert wird. Darüber hinaus scheint Vhr1 an anderen Biotin-unabhängigen Stoffwechselprozessen beteiligt zu sein. Das Vorhandensein von unvollständigen Biotinsynthese Genclustern konnte über *in silico* und Wachstumsanalysen in einigen medizinisch-relevanten *Candida* Spezies gezeigt werden. Ein solches Gencluster ermöglicht das Wachstum mit Biotinvorstufen, war jedoch nicht relevant für die Interaktion von *C. albicans* mit Makrophagen. Stattdessen verminderte das Aushungern von *C. albicans* und *C. glabrata* für Biotin oder die Inaktivierung von *VHR1* das Überleben in Makrophagen. Eine wesentliche Beobachtung in dieser Arbeit war die Bedeutsamkeit der Vht1-vermittelten Biotinaufnahme auf die intraphagosomale Proliferation sowie die erhöhte Expression von *VHR1*, *VHT1* und anderen Biotin-assoziierten Genen in *C. glabrata* und *C. albicans* Zellen nach dessen Phagozytose. Diese Daten suggerieren eine verminderte Biotinverfügbarkeit in Phagosomen, welche *Candida* Zellen enthalten. Schließlich war der Vht1-vermittelte Biotintransport auch essentiell für die erfolgreiche Kolonisierung von bestimmten Organen in Mäusen durch *C. glabrata* und *C. albicans* sowie die Virulenz von *C. albicans* bei systemischen Mausinfektionen. Insgesamt deuten die Ergebnisse darauf hin, dass *C. albicans* und *C. glabrata* in bestimmten Wirtsnischen Biotinmangel ausgesetzt sind, welcher durch die Vht1-abhängige Biotinaufnahme überwunden werden kann.

Die evolutionäre Anpassung von pathogenen *Candida* Spezies könnte ihren Ursprung in einer Interaktion zwischen Pilzen und in der Umwelt vorkommenden Amöben haben. In einem weiteren Projekt dieser Arbeit konnte gezeigt werden, dass die Kupfer- und Redoxhomöostase von Pilzzellen durch die Prädation von Amöben angegriffen wird, um aufgenommene *C. parapsilosis* Zellen abzutöten. Das Peroxidoxin-vermittelte System der Redoxhomöostase ist abhängig von dem *PRX1* Gen und notwendig für das Überleben von *C. parapsilosis* in diesem alternativen Phagozytenmodell, sowie in Makrophagen. Da *PRX1* in verschiedenen *Candida* Spezies konserviert ist, kann geschlussfolgert werden, dass Peroxiredoxine ein Teil eines grundlegenden Überlebensprogramms gegenüber Angriffen durch Phagozyten sind.

Zusammenfassend konnten die Daten dieser Arbeit die Bedeutung der Mikronährstoff- und Redoxhomöostase als Gegenstrategie von pathogenen *Candida* Spezies zum Überleben in Phagozyten, sowie als wichtige Virulenzdeterminanten zeigen. Zukünftige Studien zur Aufklärung von pilzlichen Pathogenitätsmechanismen werden von weiter entwickelten Genmanipulationsansätzen in *Candida* Spezies und insbesondere in nicht-*albicans* Spezies profitieren. Die in dieser Arbeit neu entwickelten Methoden zur Genintegration, -Überexpression und -Komplementierung, sowie zu einem RNA-

vermittelten Gen-Knockdown Protokoll, werden zu zukünftigen funktionalen Genanalysen in *C. glabrata* beitragen.

1 Introduction

1.1 *Candida* spp. infections

Candida species are the second most common agents causing invasive fungal infections worldwide and belong to the fourth leading cause of nosocomial infections [1]. In contrast to most other fungal pathogens, *Candida* species exist as human commensals and belong to the normal microbiota of 30-70% of the human population [2], while they are rarely found in soil, insects, and on fruits or plants [3]. Under certain circumstances, some *Candida* species can become opportunistic pathogens causing candidiasis. This encompasses superficial infections, either of the skin (cutaneous candidiasis) or mucosal surfaces (oropharyngeal, esophageal, vulvovaginal candidiasis) and systemic bloodstream infections leading to invasive candidiasis (IC) of internal organs. The latter are associated with high mortality rates ranging from 15 to 75% dependent on different patient groups and *Candida* species [1, 4-6], and each episode of IC costs approximately $ 40,000 per patient [7, 8]. The highest mortality rates among the most common four *Candida* species are documented for infection with *C. albicans*, *C. tropicalis*, and *C. glabrata* and the lowest mortality rates are caused by *C. parapsilosis* [9-11].

Predisposing risk factors leading to mucosal or systemic candidiasis vary significantly. The development of disseminated candidiasis occurs under common iatrogenic and/or nosocomial conditions, prolonged hospitalization, parenteral nutrition, breakdown of anatomical barriers by surgery, vascular catheter insertion, anticancer chemotherapy, and broad-spectrum antibacterial therapies and require the colonization with *Candida* cells [12-14]. Other risk factors that predominantly predispose to mucosal candidiasis are an immunosuppressive status, for example caused by chemotherapy (neutropenia, corticosteroids), infection with HIV, metabolic dysfunction (diabetes), impaired salivary gland function, dentures or pregnancy [15, 16]. An early diagnosis of invasive *Candida* infections is essential for a timely initiation of antifungal therapy [17]. Unfortunately, the lack of highly sensitive and specific diagnosis tools and the limited number of available antifungal agents (which cause few side effects) contribute to the high mortality rates of systemic candidiasis [18]. The understanding of pathogenicity mechanisms is therefore critical as a basis for the development of new diagnosis tools or antifungal therapies [19].

1.2 *Candida* genetics, phylogeny and pathogenicity mechanisms

The genus *Candida* is member of the subphylum Saccharomycotina (phylum ascomycota) [20] and currently consists of about 150 species [21, 22]. However, only fifteen species were so far isolated from patients and the majority of *Candida* infections (> 90%) are caused by *C. albicans*, *C. glabrata*, *C. tropicalis*, *C. parapsilosis* and a few other species [4, 23] (**Table 1**). Medically important *Candida* species are different in their frequency of isolation, the morphology and the ploidy (**Table 1**).

Table 1: Characteristics of clinically important *Candida* species (adapted from [24]).

species	frequency range	morphologies	ploidy
C. albicans	49 – 68%	yeast, pseudohyphae, hyphae	diploid
C. glabrata	7 – 21%	yeast, pseudohyphae[1]	haploid
C. tropicalis	5 – 13%	yeast, pseudohyphae, hyphae	diploid
C. parapsilosis	4 – 14%	yeast, pseudohyphae	diploid
C. krusei	1 – 4%	yeast, pseudohyphae	diploid
C. guilliermondii	0.1 – 2%	yeast, pseudohyphae	haploid
C. lusitaniae	0.5 – 0.6%	yeast, pseudohyphae	haploid
C. dubliniensis	0.1 – 0.2%	yeast, pseudohyphae, hyphae	diploid
C. auris	few outbreaks reported [25]	yeast, pseudohyphae[2]	haploid

[1] pseudohyphae rarely described [26]

[2] pseudohyphae found in some isolates and under certain conditions [27]
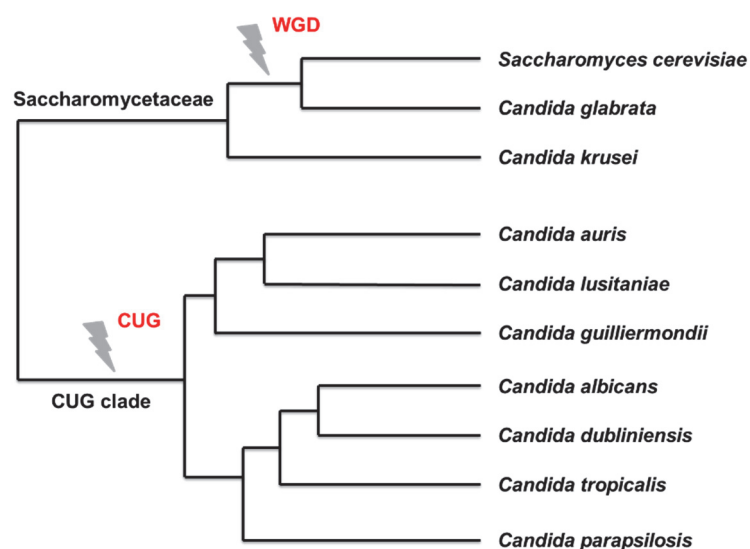
Figure 1: Phylogeny of *Candida* species. Important pathogenic *Candida* species belong to either the Saccharomycetaceae or the CUG clade. A common ancestor of *C. glabrata* and the baker´s yeast *S. cerevisiae* underwent the whole genome duplication (WGD). The figure is adapted from [24].

Candida species belong to different clades. The CUG clade contains organisms that translate the triplet codon CUG as serine instead of leucine, including *C. albicans* and *C. parapsilosis* [28]. A second major clade (Saccharomycetaceae) contains species whose genomes have undergone whole genome duplication (WGD) and in which the CUG codon encodes leucine **(Figure 1)** [29], including *C. glabrata*. Furthermore, *Candida* species differ in their ploidy (**Table 1**), independent from the CUG and WGD clades, and the ploidy can be different in different clinical isolates [30].

1.2.1 *Candida albicans*

C. albicans has a diploid genome with 6198 ORFs (haploid total) [31] and is the most prevalent (**Table 1**) and best-investigated *Candida* species. The transition between yeast and hypha (**Figure 2**) in response to changing environmental conditions represent an important virulence factor of *C. albicans* [32], and mutant strains of *C. albicans*, either locked in the yeast or hypha morphology, are attenuated in virulence [33]. Moreover, other morphologies, including pseudohyphae [34] and chlamydospores [35] contribute to a high morphological flexibility of *C. albicans*. Furthermore, *C. albicans* can undergo phenotypic switching (white-to-opaque switching with is associated with different characteristic [36]) and mating [37].
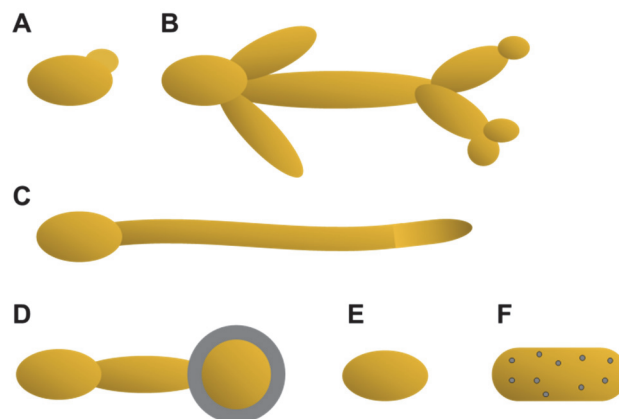
Figure 2: Common morphotypes of *Candida albicans*. During certain environmental circumstances *C. albicans* can grow as (A) yeast, (B) pseudohypha (elongated non-separated yeast cells) or (C) true hypha (divided by septa), and can develop (D) chlamydospores, characterized by a thick cell wall (gray) [38]. *C. albicans* can undergo the transition into an (D) white or (E) opaque phenotype.

The hyphal form of *C. albicans* has increased adhesion, invasion, and host tissue damage potential during interaction with epithelial cells due to the expression of hypha-associated factors like adhesins (Hwp1 [39] and Als3 [40]), invasins (Als3 [40, 41] and Ssa1 [42]), the peptide toxin candidalysin [43], and secretory aspartic proteases (Saps) [44]. The yeast form is believed to be important for spreading and disseminating during

systemic infection [45] and promoting colonization and persistence on mucosal surfaces [46, 47]. Interestingly, commensal and infecting *C. albicans* are genetically similar or identical [48, 49] and it is believed that the gut represents a main reservoir of systemic *C. albicans* infections [50, 51].

1.2.2 Non-*albicans Candida* species

The prevalence of infections with non-*albicans Candida* species (NAC) species increased in the last decades, and NAC account now for 35-65% of all systemic candidiasis cases with geographic and patient group variations [9, 22, 52, 53]. *C. glabrata* represents the most common NAC species in many studies (**Table 1**) and is frequently isolated in North America, whereas *C. tropicalis* is more frequently found in Asia-Pacific and *C. parapsilosis* is three times more often found in America than in Europe [52]. Recently, *C. auris* emerged in different countries all over the world, a species that can cause severe illness of hospitalized patients [54, 55] and is often multidrug-resistant [56].

1.2.2.1 *Candida glabrata*

C. glabrata has a haploid genome with 5293 ORFs and was described as strict asexual yeast [31]. It is mainly found in the yeast form, does not form true hyphae and only infrequently forms pseudohyphae [26]. This yeast is phylogenetically more related to the baker´s yeast *Saccharomyces cerevisiae* than to other *Candida* species (**Figure 1**) [57]. Surprisingly, not only the genetic machinery for phenotypic switching [58], but also the potential for sexual recombination has been identified [59]. Therefore, it seems that *C. glabrata* can potentially mate [60], and it has been suggested that mating probably occurs at sites of infection [61]. *C. glabrata* is found as a commensal among the microbiota of warm-blooded animals and frequently colonizes the oral cavity, with increased colonization rates in elderly individuals and diabetic patients [62, 63]. Possibly because of that, systemic *C. glabrata* infections are commonly found in these individuals [64, 65].

C. glabrata is, compared to *C. albicans*, less virulent in mouse models of systemic candidiasis without causing mortality in immunocompetent mice [66-68]. However, *C. glabrata* can adhere to human epithelial cells dependent on fungal GPI-anchored cell wall adhesins (Epa, epithelial adhesin), mainly Epa1, Epa6, and Epa7 [69, 70]. *C. glabrata* lacks any secreted proteolytic activity [71], but the genome contains eleven genes encoding for extracellular GPI-anchored aspartic proteases (*CgYPS1-11*) [72], regulating cell wall remodeling, biofilm formation, and cellular homeostasis, which in turn can influence the interaction with host cells [72-75]. *C. glabrata* possesses a

relative high level of intrinsic fluconazole resistance and rapidly develops further resistance potential after fluconazole prophylaxis by different mechanisms, which likely contributes significantly to the high frequency of *C. glabrata* infections [76-78]. *C. glabrata* is, in contrast to other pathogenic *Candida* species, auxotrophic for niacin, pyridoxine, thiamine and cannot catabolize galactose and allantoin [79, 80].

1.2.2.2 *Candida parapsilosis*

C. parapsilosis has a diploid genome with 5837 ORFs (haploid total) [31] and grows as yeast or pseudohyphae, but in contrast to *C. albicans,* it cannot form true hyphae [81, 82]. *C. parapsilosis* is part of the healthy microbiota of skin and nails [83], however, the yeast is also found in diverse environmental sources and insects [82, 84-86]. The presence of *C. parapsilosis* on the skin of health care personnel and the frequent isolation from medical devices (catheters and surfaces) are potential iatrogenic factors leading to nosocomial infection with this fungus. Therefore, it is not surprising that *C. parapsilosis* is an emerging pathogen of invasive infections in neonates, which are caused by direct transmission through health care workers, catheterization or inunction [87-89]. Contrary to *C. albicans*-caused disseminated infections, the majority of *C. parapsilosis* infections are due to exogenous sources [90, 91]. *C. parapsilosis* displays, compared to *C. albicans*, a lower virulence, probably due to the lack of true hypha formation [21], and is less virulent in mouse models [92]. The adhesion to medial plastic devices and catheters, and the subsequent formation of a tenacious and carbohydrate-rich biofilm is an important virulence factor of *C. parapsilosis* [93, 94]. In addition to that, secreted aspartic proteases and lipases contribute to its virulence [95-98].

1.3 Genetic tools to investigate pathogenicity mechanisms of *Candida* spp.

The genomes of all medically important *Candida* species are now sequenced and publically available *via* the *Candida* Genome Database (CGD) [31]. Over the last three decades, researchers developed several genetic manipulation techniques to elucidate the function of *C. albicans* genes, especially of those required for pathogenicity of *C. albicans* (summarized in [99]). The most frequently used strategy is the classical gene disruption method, using different nutritional or drug-resistant selection marker genes [100-102] and based on homologous recombination. Other techniques were developed to study the role of essential genes by using conditional knock-outs [103] or to epitope-tag proteins [104]. These new techniques permit a more dynamic view about the importance and function of certain genes (during infection). Pleiotropic effects of

ectopically expressed selection marker genes can have an impact on the pathogenicity and virulence potential of *C. albicans* [105-107]. Therefore, researchers are encouraged to reintroduce the gene into the mutated organism (which lack this gene), fulfilling molecular Koch's postulates [108]. The *SAT1* flipper and CIp10-based protocols were established to recycle drug-resistant marker genes in clinical isolates, and to standardize the localization of genomic reintegration, respectively [109, 110]. Some of these techniques were also transferable to other *Candida* species, like the replacement of genes by nutritional and drug-resistant marker genes. However, noncanonical translation of CUG codons of classically used markers [111], the decreased homologous recombination efficiency [112-114], and the haploid genome architecture in *C. glabrata* reduced the transferability.

1.4   Immunology of *Candida* spp. infections

Mammals are equipped with a complex innate and adaptive immune system consisting of humoral and cellular components to fight against invading microbes [115]. The innate immune system is an ancient part of the host defense mechanism and responds very fast and efficient [116]. If natural barriers are surmounted by *Candida* cells and these cells reach the bloodstream, they can colonize multiple organs. The complement cascade represents the first line of innate immune response to coordinate further cellular responses of the innate and adaptive immune system [117]. *C. albicans* induces the complement system followed by a pro-inflammatory response [118-120], which decreases the susceptibility for systemic candidiasis [121, 122]. As a part of an invading *C. albicans* population survives within a complement-competent host, it is not surprising that this fungus evolved specific mechanisms to evade the complement system by direct binding of inhibitory proteins, proteolytic degradation or invasion into host cells [123, 124]. A second wave of host activities towards invading *Candida* cells is facilitated by the innate immune cell population involved in phagocytosis, fungal killing and induction of pro-inflammatory responses, mainly encompassing macrophages, neutrophils, and monocytes (only in the blood) [125, 126]. An activated innate immune response is important for coping with invading *Candida* cells, but is also required for subsequent stimulation of the cellular adaptive immune response, needed to sufficiently eradicate the fungus [127]. Especially, a protective T-cell response (Th1 and Th17), mediated by dendritic cells (DCs)[128], decreases the susceptibility to systemic candidiasis [129].

The outer structure of the fungal cell, the cell wall, exposes different pathogen-associated molecular patterns (PAMPs) - absent in mammalian cells - which can be recognized by the host innate immune system [130, 131]. The cell wall consists of an

outer *O*- and *N*-linked mannose polymer (mannan layer), followed by an inner three-dimensional network of microfibrils consisting of covalently bound β-glucan and chitin [132]. Host immune cells detect fungal PAMPs by pattern recognition receptors (PRRs), consisting of Toll-like receptors (TLRs), C-type lectins (CLRs), Nucleotide-binding oligomerization domain (NOD)-like receptors (NLRs), and retinoic-acid-inducible gene I (RIGI)-like receptors (RLRs) [133, 134]. These receptor families are differently expressed in innate immune cells and recognize different fungal PAMPs, either extracellularly on the plasma membrane or intracellularly in endosomes or the cytoplasm [126, 134]. Each fungal pathogen possesses species-specific differences in their recognition and cytokine response, probably due to slightly different cell wall structures [131].

The process of phagocytosis by specialized cells, called phagocytes, was discovered by Ilya Mechnikov and awarded with the Nobel prize in 1908 [135]. He observed that leucocytes can migrate towards infectious agents, can take them up and digest them intracellularly [136]. Today, we know that phagocytes can migrate towards the pathogen and use the dynamic and proceeded receptor-mediated process, named phagocytosis to engulf the pathogen in membrane-enclosed compartments, termed phagosomes [137, 138]. Subsequently, the phagosome matures by different fusion events with other intracellular compartments (endosomes and lysosomes), creating a hostile environment for microbes. Their highly microbicidal activity is attributed to the acidification of the phagosomal lumen, the production of reactive oxygen (ROS) and nitrogen species (RNS) and the release of antimicrobial peptides (mostly cationic antimicrobial peptides) and lysosomal acidic hydrolases (summarized in [139, 140]).

1.4.1 Surveillance by neutrophilic granulocytes

Neutrophilic granulocytes (short: neutrophils or polymorphonuclear leukocytes (PMNs)) are important innate immune cells and play a pivotal role in elimination of invading pathogens [141]. They are produced in the bone marrow and are released into the bloodstream for constant patrolling [142].

Neutropenia is a major risk factor for systemic candidiasis, associated with a poor prognosis [143-145]. Neutrophils are essential to control *C. albicans* cells infecting the liver, spleen and kidney during invasive candidiasis [143, 146, 147], as well as mucosal tissues [148, 149], and are the most potent leukocytes that can inhibit the yeast to hypha transition [150]. The fast neutrophil recruitment into *C. albicans*-infected organs such as the liver and the spleen lead to fungal clearance, whereas the late neutrophil infiltration in kidneys is linked to immunopathology [147]. Neutrophils use phagocytosis, degranulation and NETosis (Neutrophil extracellular traps) as main killing strategies

[151, 152]. Further on, the NADPH-oxidase and myeloperoxidase (MPO)-dependent killing is essential for fungal control [153-156] and the inhibition of NADPH-oxidase decreases the fungicidal activity against *C. albicans* [157, 158]. *Candida* cells, phagocytosed by neutrophils, react towards these oxidative stresses with a transcriptional activation of stress-responsive genes [159-161].

1.4.2 Surveillance by mononuclear phagocytes

Mononuclear phagocytes are a heterogeneous subset of leukocytes that mature in the bone marrow and comprise monocytes, monocyte-derived macrophages (MDMs), tissue-resident macrophages, and DCs with cell type-specific characteristics [162-164]. Circulating monocytes represent 2% to 8% of the whole blood count (WBC) count in humans and app. 1% to 2% in mice [165]. They can differentiate into MDMs and DCs, determined by the inflammatory milieu and location, to contribute directly to immune defense against microbial pathogens, inflammation, and adaptive immune response [163, 164, 166, 167]. Tissue-resident macrophages are essential for maintaining homeostasis in all organs by clearance of apoptotic cells. They differ from monocyte-derived phagocytes as they are still able in self-renewing [163, 168], except macrophages of the intestine, dermis, pancreas and heart [167].

The role of mononuclear phagocytes during disseminated candidiasis is, compared to neutrophils, less investigated and originated mostly from *in vivo* studies. First studies revealed a controversial role of mononuclear phagocytes during systemic candidiasis. While splenic macrophage elimination *in vivo* decreased clearance of *C. albicans* from the bloodstream and increased mortality [169], monocytopenia alone did not increase the susceptibility to systemic candidiasis [170]. Recent studies, however, showed an expansion of inflammatory monocytes in the blood and all organs, and the disrupted trafficking of these cells into the kidneys worsened fungal clearance and survival outcome [147, 171]. Recently, it was shown that the protective effect of inflammatory monocytes is dependent on phagocytosis of *C. albicans* and further activation of other immune cells [172, 173]. Also, macrophages accumulate during systemic candidiasis in spleen and liver [147] and tissue-resident macrophages in the liver, called Kupffer cells, are involved in limiting fungal dissemination [174].

In addition to studies based on animal models, isolated immune cells and environmental phagocytic organisms (like amoebae) are used to investigate the interaction with *Candida* cells. These *in vitro* models help to identify host factors which mediate fungal killing, and fungal factors which promote resistance against antimicrobial activities. Therefore, different host cell models, like immortalized cell lines

[33, 175, 176] or primary monocytes and macrophages [177, 178] as well as predatory amoebae [179, 180] have been used.

1.5 Survival and immune evasion strategies of *Candida* cells towards mononuclear phagocytes

The resistance against the host immune system is a striking feature of pathogens, that can help establishing and maintaining infections in a susceptible host. Cells of all *Candida* species are efficiently phagocytosed by macrophages, exemplary shown for *Candida* species of the CUG clade [181], but have evolved different strategies to prevent detection or prohibit intracellular killing by these phagocytes.

1.5.1 Evading immune recognition

The recognition of invading pathogens is essential for generating a protective antimicrobial response. Fungal pathogens have evolved sophisticated strategies to avoid the recognition of highly immunogenic cell wall components like β-glucan by the host immune system [182]. For example, shielding of β-1,3-glucan on the cell wall surface of *Candida* spp. by highly mannosylated glycoproteins promotes escape from immune cell recognition [131, 183, 184]. Several environmental and host-derived signals or drug treatment can dynamically influence the exposure of β-1,3-glucan and, indeed, a differential exposure modulates immune recognition and pro-inflammatory response [185-190]. Besides shielding PAMPs, hiding in non-immune cells can serve as an immune evasion strategy. *C. parapsilosis* can be internalized by and replicate within endothelial cells thereby preventing killing by immune cells [191].

1.5.2 Modulating immune cell function

The recognition of fungal cell wall components is associated with immune cell activation coupled to downstream processes like phagocytosis and cytokine response [192]. Not surprisingly, alterations in fungal recognition or masking of immunogenic components and *Candida* species-specific surface properties influence these immune cell functions. Furthermore, *Candida* cells can interfere with immune cells causing dampening of their antifungal activities or the modulating of one immune cell type, which then diminished the antifungal response of a second immune cell [182]. One interesting example is *C. glabrata*, which hardly elicits any pro-inflammatory responses in macrophages [178, 193]. *Ex vivo* whole blood models and isolated immune cells studies showed that *C. glabrata* attracts monocytes or associates more with these cells compared to other medially relevant *Candida* spp. and that *C. glabrata* increases phagocytosis by monocytes to prevent engulfment by neutrophils [Kaemmer *et al.*,

unpublished data]. Additionally, *C. glabrata* activates neutrophils differently compared to *C. albicans*, and *C. glabrata*-infected neutrophils secrete less chemokines and cytokines, which are known to recruit further PMNs [194]. These *ex vivo* studies confirmed the situation observed during systemic infection and *vise versa*. *In vivo*, *C. glabrata* cells are mostly associated with mononuclear cells in murine organs and cause almost no infiltration of neutrophils [68]. In stark contrast, a predominant association with neutrophils in a whole blood model and a massive neutrophil infiltration during systemic infections are characteristic for *C. albicans* [147, 195, 196], which is mostly caused by candidalysin [197].

Pathogenic *Candida* species are also able to modulate immune cell function directly. Increased chitin exposure of *C. albicans* induces the expression of the host arginase and modulates macrophage polarization with impact on fungal killing [198]. Prostaglandin production of *C. parapsilosis* increases the fungal survival and diminishes pro-inflammatory cytokine secretion influencing fungal persistence *in vivo* [199, 200]. Interestingly, *C. albicans* is also known as producer of immunomodulatory prostaglandins in presence of arachidonic acid [201].

1.5.3 Escaping from or persisting in the phagosome

Successful pathogens either escape early from hostile phagosomes or stay in and adapt to the phagosomal niche and may escape later. Microbial escape strategies are myriad and widely described for bacterial intracellular pathogens [202-204]. Sooner or later, all facultative intracellular microbes have to exit from the phagosome to disseminate or transmit in the host. Fungal pathogens have evolved different strategies to escape from the phagosome. An non-lytic expulsion from macrophages, as described for *Cryptococcus (Cr.) neoformans* [205, 206], is rarely observed in *C. albicans* [207] and *C. parapsilosis* [208]. *C. glabrata* can replicate or persist in macrophages, probably due the protective shielding from detection, missing filamentation, immune cell activation, and elimination [68, 75, 178, 209]. An increase in fungal biomass by intracellular proliferation of *C. glabrata* yeast cells and of *C. parapsilosis* pseudohyphal cells can finally lead to bursting of the infected macrophage and the release of fungal cells [178, 208].

C. albicans proliferates inside phagosomes as well, but does so in the hyphal growth form, which is induced early after phagocytosis [33, 210]. Within hours, *C. albicans* escapes from macrophages by intraphagosomal hypha formation *in vitro* [211, 212], and mutants with defects in filamentation are typically more sensitive to phagocytosis-mediated killing [176]. Another early escape mechanism, the triggering of host cell pyroptosis and/or damage, is used by *C. albicans* [213, 214] and requires cell wall

remodeling [215, 216], hypha formation [211, 213, 214, 217], and the fungal peptide toxin candidalysin [218]. Expanding filaments generate discontinuities in the phagosomal membrane integrity and luminal alkalinization, which probably allows the fungus to have access to the nutrient-rich cytosol [219].

1.5.4 Coping with the intraphagosomal environment

Phagocytes destruct invading microorganisms by engulfment into phagosomes to bundle their antimicrobial activities and prevent damage of surrounding host cells. Some *Candida* species, however, found ways to create their own less-hostile intracellular environment.

Modulating intracellular trafficking

Many intracellular pathogens modulate the maturation of phagosomes by interfering with intracellular signaling cascades to prevent the formation of an antimicrobial and hostile compartment [139]. Viable *C. glabrata* cells block phagosome acidification and remain in a late endosomal compartment [178, 220]. *C. albicans* delays phagolysosome maturation dependent on cell wall composition and morphogenesis [221, 222] until the phagosomal membrane is ruptured by hyphal expansion [219].

Withstanding phagocyte-induced stress and nutrient limitation

Phagocytosis by macrophages induces DNA damage repair mechanisms, detoxification systems and significant reorganization of metabolic processes in *C. albicans* [175] and *C. glabrata* [72, 178]. Phagocytosed fungal cells also have to cope with ROS and RNS inside the phagosome. The rapid induction of genes encoding proteins with antioxidant properties, like fungal catalases, glutathione peroxidases, thioredoxines, and superoxide dismutases are important to detoxify and withstand the oxidative burst of phagocytes [160, 223-227]. While both, *C. albicans* and *C. glabrata*, have nearly the same enzymatic systems for oxidative stress responses, these two species react differently to this stress [228]. *C. albicans* suppresses the production of nitric oxide and ROS in macrophages in a dose-dependent manner [229], while *C. glabrata* possesses a high intrinsic oxidative stress resistance partially due to a highly active and phagocytosis-induced catalase Cta1 [230, 231].

Phagocytes use the intoxication with trace metals inside phagosomes, mainly by copper and zinc to kill engulfed microbes due to redox cycling, mismetallation and further excessive oxidative and nitrosative stress due to the generation of free radicals [232-234]. In line with this, an efficient copper detoxification system is essential for survival of *C. albicans* during copper stress within phagosomes [235-237] and zinc

intoxication by macrophages is used as fungicidal response to phagocytosed *C. glabrata* cells [238].

Phagocytosed *Candida* cells are not only bombarded with toxic compounds. The limitation of preferred macronutrients and essential micronutrients in the phagosome, as indicated by transcriptional data [72, 175], represents a major stress factor fungal cells have to deal with. *C. albicans* and *C. glabrata* have evolved strategies to counteract the severe deprivation of favorable nutrients [72, 175, 224, 239], by constantly sensing carbon- and nitrogen sources and changing its metabolism. Different nutritional sensors [240, 241] and signaling pathways [242-245] are closely intertwined for adaptation to nutritional conditions on transcriptional, translational and posttranslational levels.

Intracellular *C. albicans* and *C. glabrata* cells induce the expression of genes involved in alternative carbon source utilization (glyoxylate cycle, β-oxidation of fatty acids, gluconeogenesis, methyl citrate cycle) [72, 175]. Moreover, these cells activate their proteolytic machinery, possibly to degrade phagosomal proteins or to recycle own proteins, and simultaneously induce genes associated with the uptake and assimilation of amino acids and ammonium [72, 175]. Interestingly, arginine biosynthesis pathway is upregulated in both *Candida* species [72, 175]. At the same time phagocytosed cells represses the energy consuming protein synthesis to safe energy [72, 175]. The starvation mode of phagocytosed *C. glabrata* cells is underlined by the fact that phagocytosed fungal cells activate autophagy (protein degradation process) and pexophagy, a process to degrade damaged peroxisomes [231, 246]. Not surprisingly, defects in alternative carbon utilization pathways worsen survival within phagocytes, immune evasion, and fungal virulence [247-258].

1.6   Nutrition during infection

The efficient utilization of nutrients and especially the adaptation to changes in nutritional composition or nutritionally restrictive environments represents an important pathogenicity mechanism as it is essential for pathogens to drive nutritional homeostasis and establish an acute infection [239, 259, 260].

When nutrients are getting limited inside phagocytes, *Candida* cells have to use alternative strategies to overcome the lack of nutrients essential for cellular homeostasis of metabolic pathways, development, production of energy, and biomass – all processes that are needed to colonize and survive in different host niches [261]. During colonization of different mucosal surfaces in the commensal state, *Candida* cells have access to several favorable nutrients despite their competition with the bacterial microbiota, which often restrict nutrient availability and fungal overgrowth

[262]. This is especially true for the orogastrointestinal tract, a nutrient-rich environment due to regular food uptake of the host [263]. However, the host and the host's immune system has developed mechanisms to actively restrict the accessibility of nutrients, thereby limiting microbial growth, a phenomenon called 'nutritional immunity' [264-266]. This process is best investigated for trace metals like iron, zinc and manganese. Phagocytes sequestrate these trace metals from the phagosome using the cation transporter NRAMP1 [267] or iron exporter Fpn1 [268, 269]. *Candida* species have evolved the reductive pathway, the receptor-mediated uptake, and siderophore-mediated iron acquisition as high affinity systems to cope with iron limitation [270]. A siderophore (Sit1)-mediated iron uptake system and iron homeostasis in general are essential for *C. glabrata* to survive macrophage killing [271, 272].

The preferred carbon source glucose of many microbes [273] including *C. albicans* and *C. glabrata* is present in the blood but often scarce in other host niches [274]. Instead, other carbon sources like lactate and acetate are potentially available in the gut, in the kidney tissue or within phagocytes [72, 175, 259, 275-277]. The sensing and metabolism of glucose trigger the resistance against oxidative stress and antifungal agents as well as cell wall remodeling [278-282] reflecting that carbon source availability within different host niches have a strong impact on fungal virulence [259]. On the other hand, amino acid sensing and metabolism trigger important virulence features of *C. albicans* like morphogenesis [283-285] and biofilm formation [286].

1.7   Vitamin acquisition during host-pathogen interaction

As described above, intracellular *Candida* cells face a phagosomal environment that lacks certain nutrients. So far, it is unknown whether vitamins are present in the phagosome, but it is likely that vitamins are not present in excess. The uptake or synthesis of essential vitamins by *Candida* cells could therefore be crucial for survival and fitness during an intracellular lifestyle. Vitamins, belonging to micronutrients, are required in very small quantities for any organism [287]. Vitamins are chemically diverse, involved in different cellular functions and the uptake from the environment is essential in case an organism is not able to synthesize the corresponding vitamin *de novo* [287-289]. Depending on their abilities to synthesize or take up certain vitamins, different successful pathogens have their own vitamin requirements when growing in the host [290]. Vitamin auxotrophies increase the dependency of pathogens on external supply by the host or the microbial community in certain micro-niches [291]. The biosynthesis and uptake of vitamins is particularly well characterized in bacteria. For example, *Mycobacterium tuberculosis* depends on its own synthesis of riboflavin, biotin, pyridoxine and pantothenic acid synthesis [292-295]. Contrary, some other

bacterial pathogens lack the biosynthetic pathway and need riboflavin transporter systems, probably for their survival in host niches [296, 297]. For example, the uptake of riboflavin modulates important virulence traits of *Listeria monocytogenes* [298]. Vitamin biosynthesis pathways of pathogens, that lack vitamin uptake machineries and which dependent on endogenous vitamin biosynthesis, have been considered as potential drug targets [293, 299-302].

Table 2: Currently described vitamins impairing pathobiology of fungal pathogens.

vitamin	essential for	reference
riboflavin (B$_2$)	*Aspergillus* spp.	[303]
		[304]
	H. capsulatum	[305]
	C. albicans	[306]
pantothenic acid (B$_5$)	*A. fumigatus*	[303]
	H. capsulatum	[305]
pyridoxine (B$_6$)	*Aspergillus* spp.	[303]
		[304]
folate (B$_9$)	*Aspergillus* spp.	[307, 308]

The role of vitamin biosynthesis for fungal pathogens during the interaction with their host is less investigated and only a few examples are described by now (**Table 2**). As described for bacterial pathogens, not only the biosynthesis, but also the uptake from the host may be essential during infection in case the pathogen is auxotrophic for that vitamin. *C. glabrata* possesses more vitamin auxotrophies than *C. albicans*. It possesses an intrinsic auxotrophy for niacin, pyridoxine and thiamine, whereas *S. cerevisiae* and *C. albicans* are prototrophic for these vitamins [79, 80, 309]. All medically relevant *Candida* species are biotin auxotrophic, and some isolates are also thiamine auxotrophic [310, 311], suggesting that an transport system for these vitamins might be essential for viability, the survival in specific host niches, and probably virulence.

1.8   Aim of this study

Candida species are common colonizers of mucosal surfaces, but can also cause superficial and life-threatening systemic infections under predisposing conditions [2]. Infections are characterized by recruitment of innate immune cells which limit fungal proliferation and spreading [147-149]. However, pathogenic *Candida* species have evolved mechanisms to survive phagocytosis, proliferate within and escape from innate immune cells [312].

This study aimed to convey a better understanding on how *Candida* species cope with nutrient limitation within the phagosome of macrophages, representing an important phagocytic immune cell during candidiasis [147, 313]. **Manuscript I** of this thesis was written in order to compare nutrient acquisition and adaptation strategies of different bacterial and fungal pathogens with a facultative intracellular lifestyle within macrophages (**manuscript I**).

Since *Candida* species are naturally dependent on biotin, and the putative regulator of biotin-related processes Vhr1 was shown to promote survival within macrophages and virulence of *C. glabrata* [314, 315], the focus was set on this essential vitamin. Hence, this study aimed to characterize *VHR1* and its downstream target genes to unveil new insights into the regulation and maintenance of biotin homeostasis in *C. glabrata*, but also in the phylogenetically distant pathogenic *Candida* species, *C. albicans*, using transcriptional analysis, mutagenesis of biotin-metabolic genes, biotin-dependent growth analyses, as well as macrophage infection experiments and a systemic murine infection model (**manuscript II**).

As further improvement of genetic and molecular tools for assaying *C. glabrata*-host interaction, a RNA-mediated gene knock-down, a gene complementation strategy in *C. glabrata* and a flow cytometry-based method for determination of intraphagosomal replication rates were established and described in further manuscripts (**manuscript II, III & V**).

Finally, predatory amoebae are often used to understand how fungal pathogens evolved resistance strategies against mammalian phagocytes [316] and why species-specific differences occur in fungal immune evasion mechanisms [180]. Therefore, transcriptional analyses and mutagenesis approaches were used to gain new insights into the interaction of *C. parapsilosis* with amoeba and to compare these to the established macrophage model (**manuscript IV**).

2   Manuscripts

2.1   Manuscript I: Sprenger *et al., Int J Med Microbiol.*, 2018

Metabolic adaptation of intracellular bacteria
and fungi to macrophages

Marcel Sprenger, Lydia Kasper, Michael Hensel, Bernhard Hube

Summary

Successful intracellular pathogens evolved strategies to withstand antimicrobial activities within macrophages and resist destruction by these immune cells. Nutrient limitation within the phagosomal compartment represents one important mechanism to restrict microbial growth and further spreading in the host. This review focusses on adaptation mechanisms of selected bacterial and fungal pathogens to metabolic conditions of the phagosomal compartment as well as the cytosolic environment, with a focus on species-specific requirements.

Own contribution

Marcel Sprenger conceived the topic, conducted the literature research, wrote the review article and conceptualized the tables and figures.

Estimated authors' contributions:

Marcel Sprenger	**62%**
Lydia Kasper	18%
Michael Hensel	8%
Bernhard Hube	12%

Prof. Bernhard Hube

Review

Metabolic adaptation of intracellular bacteria and fungi to macrophages

Marcel Sprenger[a], Lydia Kasper[a], Michael Hensel[b], Bernhard Hube[a,c,d,*]

[a] Department of Microbial Pathogenicity Mechanisms, Leibniz Institute for Natural Product Research and Infection Biology, Hans-Knoell-Institute, Jena, Germany
[b] Division of Microbiology, University Osnabrück, Osnabrück, Germany
[c] Friedrich Schiller University, Jena, Germany
[d] Center for Sepsis Control and Care, University Hospital, Jena, Germany

ARTICLE INFO

ABSTRACT

The mature phagosome of macrophages is a hostile environment for the vast majority of phagocytosed microbes. In addition to active destruction of the engulfed microbes by antimicrobial compounds, restriction of essential nutrients in the phagosomal compartment contributes to microbial growth inhibition and killing. However, some pathogenic microorganisms have not only developed various strategies to efficiently withstand or counteract antimicrobial activities, but also to acquire nutrients within macrophages for intracellular replication. Successful intracellular pathogens are able to utilize host-derived amino acids, carbohydrates and lipids as well as trace metals and vitamins during intracellular growth. This requires sophisticated strategies such as phagosome modification or escape, efficient nutrient transporters and metabolic adaptation. In this review, we discuss the metabolic adaptation of facultative intracellular bacteria and fungi to the intracellular lifestyle inside macrophages.

1. Antimicrobial mechanisms of macrophages

Macrophages are phagocytic cells of the innate immune system patrolling in nearly all human tissues and on mucosal surfaces and thus contributing to the first line of defence against invading microbes (Pollard, 2009). Defined microbe-associated molecular patterns (MAMPs) of invading microorganisms are recognized by vesicular or cytosolic pattern recognition receptors (PRRs) of macrophages (reviewed by (Erwig and Gow, 2016; Ren et al., 2017; Weiss and Schaible, 2015)) leading to host signalling cascades, which regulate downstream processes such as immune cell activation, changes in host cell metabolism, inflammation and phagocytosis (Ren et al., 2017; Weiss and Schaible, 2015). Phagocytosis represents a cellular uptake machinery required for efficient destruction of invading microbes (reviewed in (Mao and Finnemann, 2015)). Following phagocytosis, ingested microbes are localized within defined membrane-enclosed phagosomal compartments, which mature to phagolysosomes *via* a tightly regulated series of fusion events with the endocytic machinery (Jeschke and Haas, 2016; Mao and Finnemann, 2015; Pauwels et al., 2017; Stein et al., 2012). In the maturated phago(lyso)some, microbes are exposed to an acidic hostile environment with antimicrobial activities due to lysosomal proteases, reactive oxygen species and antimicrobial peptides (Flannagan et al., 2015). Nevertheless, an astonishing number of microbes have developed strategies to survive within this intracellular compartment.

Intracellular survival strategies are manifold and extensively reviewed elsewhere (Awuh and Flo, 2017; Gilbert et al., 2014; Ramond et al., 2012; Sarantis and Grinstein, 2012). Some microbes adapt to antimicrobial activities within the phagosome, while others either actively modify the phagosome, inhibit phagosome maturation (thereby generating a less hostile replicative environment), or escape from the phagosomal compartment into the cytoplasm.

In addition to the above-mentioned direct antimicrobial mechanisms, phagocytosed pathogens also face an environment with a reduced supply of nutrients as compared to the extracellular milieu. For example, essential trace metals like iron or manganese and other nutrients are scarce due to host induced sequestration activities (Appelberg, 2006; Flannagan et al., 2015). Thus, microbial growth inhibition or killing within phagocytes may not only be based on the toxic environment in the phagosome, but may also result from the scarcity of

nutrients. Consequently, successful facultative intracellular pathogens must not only be equipped with strategies that ensure avoidance of or resistance to toxic mechanisms of macrophages, but also be able to adapt to the special nutritional conditions inside macrophages.

In this review, we focus on the impact of nutrients within macrophages for intracellular pathogens, as well as on the adaptation of pathogens to these nutritional conditions. We discuss strategies of selected examples of bacterial and fungal pathogens with diverse infection cycles including stages of intracellular proliferation within macrophages. In addition to macrophages, we discuss intracellular survival within amoebae (e.g. *Acanthamoeba castellanii*). Amoebae show macrophage-like behaviour and microbicidal activity (Guimaraes et al., 2016), and successful environmental mammalian pathogens, such as *Legionella pneumophila* or *Cryptococcus neoformans,* are known to have the potential to resist antimicrobial activities and to replicate intracellularly in environmental amoebae (Guimaraes et al., 2016). Selected exemplary bacterial and fungal pathogenic species discussed in this review are briefly introduced in the following paragraphs.

Mycobacterium tuberculosis, a Gram-positive bacterium with an exceptional hydrophobic cell wall, is the causative agent of tuberculosis and has evolved strategies to use macrophages as a replicative niche, thus evading host immune responses and allowing it to persist and/or spread in the host (Awuh and Flo, 2017). *M. tuberculosis* prevents phagosome-lysosome fusions and efficiently manipulates host macrophages to obtain sufficient host-derived nutrients to ensure survival, replication and intracellular persistence (Neyrolles et al., 2015).

The Gram-negative bacterium *Legionella pneumophila*, etiological agent of severe pneumonia (Legionnaire's disease), replicates in environmental amoebae, accidentally infects humans and resists human alveolar macrophages after phagocytosis (Khodr et al., 2016). Inside macrophages, *L. pneumophila* induces the formation of a replicative non-endosomal vacuole, where the pathogen is able to acquire nutrients, replicate and further differentiate into a flagellated form, which mediates escape from the phagosome into the cytoplasm and finally from the macrophage into the extracellular space (Eisenreich and Heuner, 2016; Robertson et al., 2014).

Francisella tularensis is a Gram-negative, highly virulent, zoonotic bacterium, which can infect a broad range of mammalian species and cause tularemia (Meibom and Charbit, 2010). During infection, this facultative intracellular bacterium primarily infects macrophages and enters the phagosomal compartment, but to survive and replicate within infected macrophages, *F. tularensis* needs to escape from the phagosome into the cytosol (Ramond et al., 2012).

Listeria monocytogenes is a facultative intracellular Gram-positive bacterium that causes the fatal foodborne disease listeriosis (Vazquez-Boland et al., 2001). After phagocytosis by macrophages, *L. monocytogenes* prevents the maturation of the phagosome, escapes to and replicates within the cytosol (Ireton et al., 2014).

Salmonella enterica is a facultative intracellular Gram-negative pathogen that causes a range of diseases in humans. *S. enterica* serovars such as Typhimurium or Enteritidis are frequently transmitted from reservoirs in livestock and cause gastroenteritis, a self-limiting infection of the small intestine with local inflammation. High human-adapted serovars Typhi and Paratyphi A are transmitted from infected humans and cause a systemic, often fatal disease termed typhoid fever. The ability of certain *Salmonella* spp. to survive and replicate within phagocytic cells is generally considered as requirement to cause systemic diseases (Fields et al., 1986). However, this notion is mainly based on experimental studies in a systemic infection model with *S.* Typhimurium in susceptible mouse strains.

Candida albicans and *C. glabrata* are commensal yeasts of warm-blooded animals and humans as well as opportunistic fungal pathogens that provoke superficial mucosal infections, but also life-threatening systemic candidiasis (Odds, 1988). Both *Candida* species can resist elimination by macrophages and have evolved strategies to proliferate within phagocytes (Erwig and Gow, 2016; Gilbert et al., 2014; Kasper

et al., 2015). Phagocytosis of *C. albicans* by macrophages induces intracellular filamentation, which mediates damage of the host cell and escape, whereas *C. glabrata* is not able to form hypha and grows in the phagosome as yeast cells until the host macrophages burst (Miramon et al., 2013; Seider et al., 2010).

The encapsulated and opportunistic fungus *Cryptococcus neoformans* is able to cause life-threatening respiratory and systemic infections (cryptococcosis) in immunocompromised individuals (Johnston and May, 2013). Inhaled airborne yeast cells, or sexually produced basidiospores, of environmental *Cr. neoformans* switch to capsulated yeast morphology (Kwon-Chung et al., 2014). Although capsules inhibit phagocytosis by alveolar macrophages, *Cr. neoformans* is known to persist and proliferate within a mature phagolysosome once phagocytosed (Gilbert et al., 2014; Johnston and May, 2013; Leopold Wager et al., 2016).

The environmental fungal pathogen *Histoplasma capsulatum*, causing most endemic respiratory mycoses in the USA, is able to infect macrophages, resist the antimicrobial activities and proliferates intracellularly (Garfoot and Rappleye, 2016; Horwath et al., 2015). Engulfed by macrophages, *H. capsulatum* enters the phagosomal compartment, blocks acidification and avoids killing e.g. due to detoxification of reactive oxygen radicals (Gilbert et al., 2014).

2. Nutrient limitation as an antimicrobial strategy

Phagocytosis by macrophages is thought to generate an environment with restricted nutrient availability as compared to the extracellular milieu, and there is evidence that macrophages actively deprive pathogens of accessible nutrients (Appelberg, 2006). However, intracellular pathogens have developed specific virulence mechanisms that target host biosynthetic and degradation pathways or nutrient-rich sources to enhance supplies of limiting nutrients, a paradigm termed as 'nutritional virulence' (Abu Kwaik and Bumann, 2013). However, the defined characterization of the biochemical composition of pathogen-containing compartments in macrophages has been challenging, and knowledge about nutrient composition has mostly been derived indirectly from microbial responses to conditions in their intracellular niche (Appelberg, 2006; Weiss and Schaible, 2015). For example, it has been assumed from transcriptional profiling approaches and metabolic flux analysis that intraphagosomal pathogens encounter glucose and trace metal limitation and rely on alternative C_2 and C_3 carbon sources like amino acids or lipid degradation products. Examples for such proposed nutritional conditions come from studies dealing with intracellular bacterial (*M. tuberculosis*) and fungal pathogens (*C. albicans*) (Lorenz et al., 2004; Lorenz and Fink, 2002; McKinney et al., 2000). However, it is unlikely that these observations can be generalized for an intracellular life style *per se*, as the replicative niche used inside macrophages differs among pathogens. For example, the cytosol, used by several intracellular bacteria, is thought to be less nutrient-deprived as compared to membrane-enclosed compartments (Appelberg, 2006). Further, the fact that *L. pneumophila* uses amino acids, glucose and glycerol as major nutrients during intra-vacuolar growth (in contrast to *M. tuberculosis* and *C. albicans*) (Eisenreich and Heuner, 2016), points to a defined nutrient composition depending on the pathogen-associated membrane-enclosed compartment. In line with this, the active manipulation of the host endocytic pathways by intracellular pathogens results in not only a less hostile niche, but in a distinct replication-permissive pathogen vacuole with rather favourable conditions including sufficient access to nutrients (e.g. *Salmonella*, *Legionella*) (Hilbi and Haas, 2012).

Due to incomplete amino acid biosynthesis clusters, pathogens like *F. tularensis* require host-derived amino acids within the intracellular milieu of macrophages (Meibom and Charbit, 2010). Interestingly, some of these amino acids, for example cysteine, are strongly limited within host cells (Meibom and Charbit, 2010). Therefore, intracellular growth of some intracellular pathogens maybe suppressed by limiting

certain amino acids, which has been termed a 'nutritional rheostat' (Abu Kwaik and Bumann, 2013). A similar defence strategy of macrophages to limit intracellular microbial growth is amino acid deprivation by activation of degradation pathways (Weiss and Schaible, 2015).

Engulfment of pathogens induces not only host signalling cascades that activate antimicrobial responses, but also a change in metabolism, which is associated with macrophage polarization. In fact, clear metabolic differences exist between M1 and M2 macrophages (Galvan-Pena and O'Neill, 2014). Classically activated M1 macrophages exhibit high glucose and glutamine turnover, supporting the synthesis of NADPH, which is essential for the generation of ROS within the phagosome (reviewed in (Ganeshan and Chawla, 2014)). In contrast, alternatively activated M2 macrophages change their metabolism to oxidative phosphorylation and β-oxidation (Ganeshan and Chawla, 2014). Many pathogens have evolved strategies to interfere with macrophage polarization, taking advantage of the various (immune) functions of the different macrophage phenotypes (Ren et al., 2017). It is tempting to speculate that interference with macrophage polarization may also be a strategy to generate an optimal metabolic niche for the pathogen.

Host strategies used to limit the access of essential trace metals for invading microorganisms are well-investigated and extensively reviewed elsewhere (Caza and Kronstad, 2013; Cerasi et al., 2013; Juttukonda and Skaar, 2015; Nairz et al., 2015b)). The host transporter NRAMP1 (SLC11A1), for example, removes divalent cations (manganese, iron and cobalt) from the phagosomal compartment to starve intracellular pathogens and limit intracellular fitness (Forbes and Gros, 2003; Jabado et al., 2000; Juttukonda and Skaar, 2015; Nairz et al., 2009). Also, iron-binding proteins like transferrin, ferritin and the manganese, calcium and zinc binding protein calprotectin are important to sequester metal ions to prevent microbial growth (Hood and Skaar, 2012; Zackular et al., 2015). In contrast, intoxication with high levels of zinc and copper are used as antimicrobial mechanisms. These host strategies of trace metal withholding, but also intoxication are summarized as 'nutritional immunity' (Hood and Skaar, 2012).

3. The intracellular lifestyle—nutrients as a limiting factor within macrophages

Microbial replication requires large amounts of energy, as well as macro- and micronutrients to maintain metabolic and cellular processes. This is driven by the degradation of macromolecules, such as carbohydrates, lipids and proteins (macronutrients), and consumption of their degradation products (e.g. amino acids). Further, trace metals or vitamins (micronutrients) are needed, e.g. as cofactors of essential metabolic enzymes. Thus, intracellular pathogens have to acquire macro- and micronutrients from the host.

Pathogens prefer to metabolize certain nutrients and strictly control their nutrient assimilation pathways on transcriptional and post-transcriptional levels (Lorenz, 2013). For example, glucose is an essential and preferred nutrient for many microbes to generate energy and to synthesize cellular components (Towle, 2005). However, glucose is often restricted in biological systems. Therefore, pathogens compete with their hosts and have evolved strategies to efficiently sense, acquire and metabolise this nutrient (Sabina and Brown, 2009). Furthermore, since glucose is not readily available within macrophages, alternative carbon and energy resources for an intracellular lifestyle are crucial to permit survival and replication in this niche. Therefore, intracellular pathogens have developed several different strategies to efficiently acquire nutrients during intracellular growth as summarized in Table 1.

Many pathogens are well adapted to the nutrient-restrictive situation of their intracellular environments and rely on efficient acquisition systems or utilize various alternative nutrient sources during intracellular stages (Table 1). For example, many pathogens express distinct transporters for the respective nutrients. *M. tuberculosis* is able to utilize extracellular amino acids, glycolytic C_3-sources, C_2-sources (acetyl-CoA), host lipids and even CO_2 (Beste et al., 2013; Pandey and

Sassetti, 2008). Similarly, *F. tularensis* possesses high affinity transporters for different amino acids that facilitate efficient escape from the phagosome and multiplication within the cytosol (Ziveri et al., 2017). Other pathogens have evolved mechanisms to successfully manipulate the host cell to import or degrade host-derived nutrients, which are then used to replicate within macrophages. For example, *L. pneumophila* and *F. tularensis* manipulate the host amino acid pool by inducing the expression of the host amino acid transporter gene SLC1A5 to create a more favourable microenvironment (Barel et al., 2012; Wieland et al., 2005).

The unique environment with its nutritional restrictions inside macrophages is not only a trigger for pathogens to quickly adapt their up-take systems and own metabolism to the particular demands of their specialized niche, but also triggers 'adaptive prediction' (Brunke and Hube, 2014), including morphological differentiation or expression of virulence factors, which promote subsequent stages of pathogenesis.

In the following paragraphs, we discuss (i) how intracellular pathogens adapt their metabolism to utilize amino acids, carbohydrates, polyols, lipids and micronutrients (summarized in Table 1) and (ii) what impact these nutrients have on intracellular survival and proliferation (summarized in Table 2).

4. Utilization of macronutrients

4.1. Amino acids

Amino acids can be used as a source of energy, carbon, nitrogen and sulphur to maintain microbial metabolism and thus are an important nutrient source for intracellular pathogens. There are major differences in the metabolism of amino acids. For example, the majority of prokaryotes, plants and fungi is able to synthesize amino acids *de novo*, whereas higher eukaryotes synthesize only twelve out of 20 amino acids (non-essential amino acids) and require essential amino acids from external sources.

Host-derived amino acids are considered as a 'nutritional rheostat' for intracellular multiplication, because the basal microbial pool of amino acids is thought to be insufficient for intracellular replication even for normally prototrophic pathogens (Abu Kwaik and Bumann, 2013). Therefore, additional amounts of amino acids are required during an intracellular lifestyle. Furthermore, some pathogens, like *F. tularensis* (Ziveri et al., 2017) or *L. pneumophila* (Eisenreich and Heuner, 2016), have multiple intrinsic auxotrophies for amino acids and thus have to find special solutions to thrive intracellularly. In fact, the cysteine auxotrophy of *L. pneumophila* can be bypassed through the exploitation of the host proteasomal degradation system to boost the intracellular level of free available cysteine (Price et al., 2011).

Uptake and metabolism of different amino acids and nucleotides by *L. pneumophila* within macrophages is mediated via the phagosomal transporter family (*Pht*) and studies by Schunder et al. demonstrated that uptake and metabolism of amino acids is crucial within the *Legionella*-containing vacuole (LCV) of infected *Acanthamoeba castellanii* (Schunder et al., 2014). The acquisition of threonine and valine is executed by *phtA* and *phtJ*, respectively, and is required for differentiation into the replicative form (Fonseca and Swanson, 2014; Sauer et al., 2005). The transporter *phtC-D* facilitates thymidine uptake, crucial for intracellular proliferation (Fonseca et al., 2014). A similar important role is played by the uptake of serine, which is metabolised via the TCA cycle and represents a crucial intracellular energy supply (Eylert et al., 2010; Gillmaier et al., 2016). As discussed above, sensing the nutrient availability in intracellular compartments may also induce a 'predictive adaptation' response. For example, the arginine repressor ArgR senses arginine levels within the LCV and derepresses the transcription of a set of genes involved in detoxification, stress adaptation, amino acid metabolism and Icm/Dot-translocated substrates during intracellular growth (Hovel-Miner et al., 2010).

In *L. monocytogenes*, the transcriptional activity of PrfA, which

Table 1
Overview of strategies used for nutrient acquisition and nutritional adaptation inside macrophages.

Strategies for intracellular nutrient acquisition	Nutrient class	Species	Reference
Transcriptional up-regulation of transporter genes	Amino acids	*L. monocytogenes*	(Lobel et al., 2012)
		Candida spp.	(Lorenz et al., 2004)
	Carbohydrates/ polyols	*Candida* spp.	(Kaur et al., 2007; Lorenz et al., 2004)
		Cr. neoformans	(Fan et al., 2005)
		L. monocytogenes	(Joseph et al., 2006)
High affinity uptake systems	Amino acids	*L. pneumophila*	(Fonseca and Swanson, 2014; Sauer et al., 2005)
		L. monocytogenes	(Haber et al., 2017)
		M. tuberculosis	(Gouzy et al., 2013)
		F. tularensis	(Gesbert et al., 2014; Gesbert et al., 2015; Ramond et al., 2015; Ramond et al., 2014)
	Carbohydrates/ polyols	*F. tularensis*	(Ziveri et al., 2017)
		L. monocytogenes	(Joseph et al., 2006)
	Lipids	*M. tuberculosis*	(Pandey and Sassetti, 2008)
	Trace metals	*L. pneumophila*	(Portier et al., 2015)
		M. tuberculosis	(De Voss et al., 2000; Rodriguez and Smith, 2006)
		F. tularensis	(Perez and Ramakrishnan, 2014; Ramakrishnan et al., 2012)
		H. capsulatum	(Hilty et al., 2011; Hwang et al., 2008; Newman and Smulian, 2013)
		C. glabrata	(Nevitt and Thiele, 2011; Seider et al., 2014; Srivastava et al., 2014)
Degradation of macromolecules	Lipids	*M. tuberculosis*	(Crowe et al., 2017; Speer et al., 2015)
		Cr. neoformans	(Evans et al., 2015)
Modulation of host transporters	Amino acids	*F. tularensis*	(Barel et al., 2012)
		L. pneumophila	(Wieland et al., 2005)
		S. enterica	(Das et al., 2010)
Activation of pathogen autophagy pathway	Amino acids	*C. glabrata*	(Roetzer et al., 2010)
		Cr. neoformans	(Gontijo et al., 2017)
Activation of host cell autophagy pathway	Amino acids	*F. tularensis*	(Chong et al., 2012; Steele et al., 2013)
		L. pneumophila	(Choy et al., 2012)
		C. albicans	(Smeekens et al., 2014)
Activation of alternative carbon source utilization pathways	Carbon sources	*S. enterica*	(Becker et al., 2006)
		M. tuberculosis	(McKinney et al., 2000; Munoz-Elias and McKinney, 2005)
		Candida spp.	(Childers et al., 2016; Derengowski Lda et al., 2013; Kaur et al., 2007; Lorenz et al., 2004)
		Cr. neoformans	(Derengowski Lda et al., 2013)
		H. capsulatum	(Isaac et al., 2013)
Redirection of host cell endosomal transport, vesicle fusion	Vesicular content	*S. enterica*	(Liss et al., 2017)
		L. pneumophila	(Michard et al., 2015)

controls essential virulence attributes, is modulated by host-derived amino acids (Scortti et al., 2007). PrfA transcription is positively regulated by the transcription regulator CodY, which responds to the low availability of branched chain amino acids (BCAA) within host cells (Lobel and Herskovits, 2016; Lobel et al., 2015; Lobel et al., 2012). PrfA induces the expression of the *Listeria* virulence factors listeriolysin O and phospholipase B, which facilitate escape from the phagosomal compartment into the cytosol (de las Heras et al., 2011). Once cells have entered the reducing environment of the cytosol, host-derived glutathione can modulate PrfA to positively regulate the expression of the actin polymerization factor gene *actA*, which is essential for spreading into adjacent cells (de las Heras et al., 2011; Freitag et al., 2009; Reniere et al., 2015). In addition, glutamine can function as an environmental sensor, controlling the expression of virulence-related *Listeria* genes (Haber et al., 2017): the expression of virulence factors is induced when the listerial glutamine pool increases over a certain threshold, depending on the high affinity uptake system GlnPQ and probably due to modulation of PrfA. Interestingly, intracellular *Listeria* cells directly use host-derived amino acids for protein biosynthesis or modulation of gene expression and not for catabolism and energy supply (Grubmuller et al., 2014).

In *M. tuberculosis*, the uptake of aspartate and asparagine within macrophage phagosomes by AnsP1 and AnsP2 transporters is important for assimilation of nitrogen (Gouzy et al., 2014; Gouzy et al., 2013). The utilization of asparagine offers two important advantages for *M. tuberculosis* during intracellular stages, as this amino acid can not only serve as a nitrogen source, but can also contribute to reducing acidic stress within the phagosome. The latter is achieved by cleavage of asparagine to aspartate and ammonia, which neutralizes the phagosomal pH (Gouzy et al., 2014). A similar neutralization strategy of the phagosomal compartment has been observed in *C. albicans* (Vylkova and Lorenz, 2014).

Since *F. tularensis* is auxotrophic for some amino acids, uptake of host-derived amino acids is essential (Meibom and Charbit, 2010). *F. tularensis* uses an amino acid uptake system similar to *M. tuberculosis*, which is also based on asparagine import by an AnsP transporter. In contrast to *M. tuberculosis*, however, asparagine is imported during the cytosolic replication stage within infected macrophages (Gesbert et al., 2014). Besides asparagine, *F. tularensis* can take up glutamate *via* the glutamate permease GadC within the phagosomal compartment. GadC-mediated glutamate uptake supports resistance against oxidative stress by modulating the redox status of the bacterium and positively affects escape from the phagosome into the cytosol (Ramond et al., 2014). As inactivation of *gadC* reduced the bacterial pool of TCA cycle metabolites, glutamate uptake seems to be necessary for bacterial energy supply (Ramond et al., 2014). In addition to GadC, two other amino acid permeases, one for isoleucine (IleP) and one for arginine (ArgP), facilitate the uptake of the respective amino acids during different stages of the intracellular lifestyle and contribute to phagosomal escape as well as cytosolic bacterial replication (Gesbert et al., 2015; Ramond et al., 2015; Ziveri et al., 2017).

Most serovars of *S. enterica* are prototrophic and able to synthesize all amino acids *de novo* using intermediates of primary carbon metabolism. Mutant strains deficient in amino acid biosynthesis pathways are attenuated in macrophage infections and in a murine model of systemic infection. Human-adapted serovars such as *S. enterica* serovar Typhi and Paratyphi A require supplementation by tryptophan and cysteine for growth in minimal media, indicating defective biosynthetic pathways. Since *S.* Typhi and *S.* Paratyphi are able to proliferate in host tissue, a continuous supply of these amino acids during growth in the

Table 2
Overview of the impact of different nutrient sources on the intracellular lifestyle. BCAA; branched-chain amino acids.

Nutrient class	Impact	Nutrient source	Species	Influence on intracellular lifestyle	Reference
Amino acids	Expression of virulence genes Morphological differentiation	BCAA glutamine	*L. monocytogenes*	Phagosomal escape	(Lobel et al., 2015) (Haber et al., 2017)
		Arginine	*L. pneumophila*	Intracellular proliferation	(Hovel-Miner et al., 2010)
		Arginine	*C. albicans*	Phagosomal escape	(Ghosh et al., 2009)
	Protein synthesis	Arginine	*L. monocytogenes*	Intracellular proliferation	(Grubmuller et al., 2014)
	Nitrogen assimilation	Asparagine	*M. tuberculosis*	Modification of phagosomal pH	(Gouzy et al., 2014)
		unknown	*C. albicans*	Modification of phagosomal pH	(Vylkova and Lorenz, 2014)
	Resistance against oxidative stress	Glutamate	*F. tularensis*	Phagosomal escape	(Ramond et al., 2014)
	Energy source	Asparagine	*F. tularensis*	Intracellular proliferation	(Gesbert et al., 2014) (Ramond et al., 2014)
		Glutamate			
		Isoleucine			(Gesbert et al., 2015)
		Serine	*L. pneumophila*	Intracellular proliferation	(Gillmaier et al., 2016; Hauslein et al., 2016)
		Leucine	*H. capsulatum*	Modification of phagosomal pH	(Isaac et al., 2013)
	Phagosomal escape	Arginine	*F. tularensis*	Phagosomal escape	(Ramond et al., 2015)
		Isoleucine			(Gesbert et al., 2015)
	Sulphur source	Cysteine/ glutathione	*F. tularensis*	Intracellular proliferation	(Meibom and Charbit, 2010)
Carbohydrates and polyols	Expression of virulence genes	Glycerol Glucose-6-phosphate	*L. monocytogenes*	Phagosomal escape	(Joseph et al., 2008) (Mertins et al., 2007) (Stoll et al., 2008)
	Energy source	Glycerol	*L. monocytogenes*	Intracellular proliferation	(Grubmuller et al., 2014)
	Carbon source	Glycerol	*F. tularensis*	Intracellular proliferation	(Ziveri et al., 2017)
		Glycerol	*S. enterica*	Intercellular proliferation	(Eriksson et al., 2003)
		Glucose-6-phosphate	*L. monocytogenes*	Intracellular proliferation	(Grubmuller et al., 2014)
		Glucose	*S. enterica*	Intracellular proliferation	(Eriksson et al., 2003)
Lipids	Energy source	Cholesterol	*M. tuberculosis*	Intraphagosomal replication	(Pandey and Sassetti, 2008)
	Carbon, nitrogen and phosphorus source	Sphingomyelin	*M. tuberculosis*	Intraphagosomal replication	(Speer et al., 2015)
Vitamins	Cofactor activity (own biosynthesis)	Biotin	*F. tularensis*	Phagosomal escape	(Napier et al., 2012)
			M. marinum	Intracellular proliferation	(Yu et al., 2011)
		Riboflavin	*H. capsulatum*	Intracellular proliferation	(Garfoot et al., 2014)
	Cofactor activity (host derived)	Lipoic acid	*L. monocytogenes*	Intracellular proliferation	(O'Riordan et al., 2003)

host is anticipated. A study by Popp et al. investigated the requirement for amino acids, which are non-essential for mammalian host cells (Popp et al., 2015). The work showed that mutant strains auxotrophic for proline were highly attenuated in proliferation in macrophages. Supplementation of the growth medium of infection macrophages with proline complemented intracellular proliferation, but only if the *Salmonella* pathogenicity island-2 type III secretion system (SPI2-T3SS) was functional in manipulating host cell endosomal transport. Work by Das et al. revealed that cationic amino acid transporters (CAT) of the host cell were up-regulated in *Salmonella* infected phagocytes and that host cell CAT were sequestered to the *Salmonella*-containing vacuole (SCV) (Das et al., 2010). In addition, *Salmonella* uses its arginine transporter ArgT for uptake of arginine from the SCV. This suggests that *Salmonella* in the SCV deploy host cell CAT to access the cytosolic pool of arginine. In line with this model, a *Salmonella* mutant deficient in arginine biosynthesis was attenuated in intracellular proliferation and systemic virulence (Das et al., 2010).

Amino acid utilization is also described for facultative intracellular fungal pathogens. The last enzyme in the catabolism of leucine, the HMG-CoA lyase Hcl1, plays a critical role for intracellular replication of *H. capsulatum* (Isaac et al., 2013). The degradation of this amino acid may be an important intracellular energy supply for *H. capsulatum* and this observation suggests therefore that the *H. capsulatum*-containing phagosome provides sufficient amounts of leucine to support growth (Isaac et al., 2013). The catabolism of leucine generates acetyl-CoA, which can be used through the glyoxylate cycle. This metabolic pathway is an important hub for the utilization of several alternative carbon sources used in the host, such as acetyl-CoA generated through degradation of amino acids, cholesterol or fatty acids. Interestingly, mutants of both, *M. tuberculosis* (McKinney et al., 2000; Munoz-Elias

and McKinney, 2005) and *C. albicans* (Childers et al., 2016; Lorenz and Fink, 2001), lacking genes of the glyoxylate cycle show reduced intracellular fitness and virulence. In fact, genes encoding enzymes of the glyoxylate cycle are up-regulated in *C. albicans* (Lorenz et al., 2004), *C. glabrata* (Kaur et al., 2007) and *Cr. neoformans* (Derengowski Lda et al., 2013; Fan et al., 2005) after phagocytosis by macrophages.

The opportunistic pathogenic fungus *C. albicans* undergoes a dramatic transcriptional reprogramming process upon phagocytosis by macrophages (Lorenz et al., 2004). This response involves the up-regulation of genes coding for amino acid and ammonia transporters, enzymes involved in alternative carbon source utilization as well as a repression of energy-consuming processes. Expression of amino acid permease and oligopeptide transporter genes is induced by the transcription factor Stp2, which is proteolytically activated through the plasma membrane located SPS amino acid sensor system, consisting of Ssy1 (sensor), Ptr3 (mediator) and Ssy5 (endoprotease) in the presence of amino acids as a sole carbon source (Miramon and Lorenz, 2016). This allows nitrogen assimilation and also promotes neutralization of the phagosomal compartment by release of ammonia − a process that induces hyphal morphogenesis, killing of and escape from macrophages (Miramon and Lorenz, 2016; Vylkova and Lorenz, 2014). The carbon backbone of amino acids is used by *C. albicans* as a sole carbon source and fulfils another important aspect, the maintenance of metabolic pathways to generate essential metabolites and energy (Vylkova et al., 2011). Similar to *C. albicans*, other fungal pathogens like *C. glabrata* and *Cr. neoformans* shift their metabolism to a starvation mode and activate the expression of genes coding for enzymes of the glyoxylate cycle, gluconeogenesis, fatty acid degradation and amino acid biosynthesis and uptake (Fan et al., 2005; Kaur et al., 2007; Lorenz et al., 2004; Rai et al., 2012). As in most cases, this up-regulation coincides with the

repression of protein biosynthesis (Fan et al., 2005; Kaur et al., 2007; Lorenz et al., 2004), suggesting that ingested fungal pathogens encounter both carbon and nitrogen deprivation inside phagocytes.

A main difference between *C. albicans* and *C. glabrata* is the ability of *C. albicans* to form true hyphae, while *C. glabrata* only grows in the yeast form (Brunke and Hube, 2013). The hyphal outgrowth from the phagosome may be a useful strategy of *C. albicans* to escape the harmful and nutrient-poor environment within hours (Hummert et al., 2010), while *C. glabrata* cells can remain intracellular for several days without damaging the host macrophage (Kasper et al., 2015; Seider et al., 2011). Therefore, it is not surprising that *C. albicans* does not require its own autophagy machinery for survival within macrophages (Palmer et al., 2007), whereas the viability of *C. glabrata* within the phagosomal compartment of macrophages is enhanced by autophagy, probably to efficiently recycle resources to maintain its own metabolism (Roetzer et al., 2010). Recently, it was shown that autophagy is also an essential cellular process for survival of *Cr. neoformans* within macrophages (Gontijo et al., 2017).

Besides the role of pathogeńs autophagy machinery in intracellular adaptation, the hostś autophagy machinery also plays an important role during the interaction of pathogens with macrophages. Host cells use autophagy to digest damaged proteins, degrade whole organelles and also intracellular microbes. Therefore, host cell autophagy can be disadvantageous for intracellular microbes and some have evolved strategies to block induction of autophagy (Deretic and Levine, 2009; Steele et al., 2015). *L. pneumophila*, for example, secretes the bacterial effector RacZ, which irreversibly disrupts macrophage Atg8 proteins to prevent degradation by autophagy (Choy et al., 2012). Autophagy limits early replication of *L. monocytogenes* within macrophages, and intraphagosomal bacteria co-localize with autophagy markers in initial stages of infection (Birmingham et al., 2007; Py et al., 2007). However, *L. monocytogenes* hijacks host cell proteins to counteract autophagy upon entering the cytosol (Dortet et al., 2011). *M. tuberculosis* remains in a self-modified phagosome, which prevents association with the hostś autophagy machinery, and permeabilization of the phagosomal membrane increases association with autophagy markers (Watson et al., 2012). In contrast, the induction of host autophagy is used by some pathogens to gain nutrients (Deretic and Levine, 2009). *F. tularensis* induces autophagy, evades autophagic degradation and harvests nutrients from this process (Chong et al., 2012; Steele et al., 2013). Furthermore, *C. albicans* induces a shift of the cytosolic protein LC3-I to autophagosome-associated LC3-II, which indicates autophagy induction by this fungus (Smeekens et al., 2014). However, macrophage autophagy plays a role in nutrient restriction to *C. albicans*, as inactivation of autophagy in macrophages reduces the phagocytosis of *C. albicans* as well as fungistatic activity (Nicola et al., 2012).

In summary, intracellular pathogens seem to rely on the utilization of a set of host-derived amino acids to maintain their own metabolism, and each pathogen (e.g. *F. tularensis* and *Legionella* spp.) has its own requirements for nutrients due to different intrinsic auxotrophies. The examples discussed in this chapter show that amino acid uptake is achieved by specialized transporters and sophisticated regulatory mechanisms. Additionally, intracellular pathogens are also able to modulate the host to promote the release of free available amino acids by exploiting host transporters or protein turnover by autophagy.

4.2. Carbohydrates and polyols

Glucose and glycolytic intermediates and metabolites are normally channelled into the glycolysis or other alternative pathways, such as the Entner-Doudoroff (ED), Embden-Meyerhof-Parnas (EMP) or pentose phosphate (PP) pathway (Harada et al., 2010; Hauslein et al., 2016). Glucose is generally a preferred nutrient source for the host and most pathogens. Within membrane-engulfed compartments, glucose is assumed to be less available to intraphagosomal pathogens (*Candida*, *Cryptococcus* and *Mycobacterium* spp.) since transcriptional profiling indicates increased expression of alternative carbon source utilization genes (Derengowski Lda et al., 2013; Lorenz et al., 2004; McKinney et al., 2000). However, this may not be a general phenomenon for all pathogen-containing compartments. For example, parts of the alternative glucose degradation (ED) pathway, are necessary for intracellular growth of *L. pneumophila* (Harada et al., 2010). It was also shown that the polyol glycerol promotes the growth of *L. pneumophila* within macrophages. This intracellular growth depends on the glycerol-3-phosphate dehydrogenase and glucose, as well as glycerol, which are used for anabolic purposes (gluconeogenesis and PP pathway) (Hauslein et al., 2016). Recently, it was shown that catabolic degradation of *myo*-inositol promotes the intracellular growth of *L. pneumophila* within macrophages or amoeba (Manske et al., 2016).

Transcriptional profiling of *L. monocytogenes* grown in macrophages demonstrated that intracellular growth induces genes involved in the uptake of glycerol and glucose-6-phosphate as well as metabolic pathways associated with these molecules, namely the gluconeogenesis and PP pathway (Joseph et al., 2006). In line with this, ^{13}C-Isotopologue-profiling analysis demonstrated the dependence of intracellular *Listeria* spp. on host-derived C_3-substrates as carbon sources, which were subsequently incorporated into amino acids (Eylert et al., 2008). Glycerol as a main C_3-substrate is channelled into glycolysis to generate ATP, and the remaining pyruvate is converted to oxaloacetate *via* the pyruvate carboxylase PycA (Grubmuller et al., 2014; Schar et al., 2010). Glucose-6-phosphate enters glycolysis at an earlier step and is metabolised *via* the PP pathway to predominantly fulfil anabolic purposes (Grubmuller et al., 2014). Interestingly, glycerol and glucose-6-phosphate modulate the activity of the transcription factor PrfA, resulting in optimal expression of virulence genes, which represents a general mechanism of metabolic modulation of virulence (Joseph et al., 2008; Mertins et al., 2007; Stoll et al., 2008).

M. tuberculosis is also able to utilize a glycolytic C_3-source at the midpoint of the glycolysis/gluconeogenesis pathway channelled into the PP pathway, demonstrating that this pathogen has access to glycolytic intermediates within the phagosomal compartment for anabolic purposes (Beste et al., 2013). Moreover, this anabolic gluconeogenic flux of intermediates of the TCA cycle is necessary for *M. tuberculosis* to maintain infection (Marrero et al., 2010).

F. tularensis similarly possesses glycerol as well as glycerol-3-phosphate transporters, which probably support intracellular carbon source utilization besides amino acids (Ziveri et al., 2017). Compared to *Listeria* spp., permeases for glucose-6-phosphate are missing in *F. tularensis*, demonstrating a completely different requirement of carbohydrates by two intracellular pathogens, which both can escape into the host cell cytosol.

S. enterica is a metabolic 'all-rounder' and is considered to be able to adapt to a wide variety of C-sources for growth inside macrophages. Equipped with fully functional EMD, PP, ED pathways, reductive and oxidative modes of TCA cycle, respiratory chains with oxygen and alternative electron acceptors, *S. enterica* can easily adapt to the changing availability of C- and energy sources. Furthermore, this pathogen can synthesize all cellular macromolecules from single C-sources as basic as C_3 or C_2. Indeed, only a few mutations in carbon catabolic pathways led to decreased intracellular survival and replication, and the attenuation most likely results from toxicity of accumulated metabolites such as phosphorylated hexoses.

Proteomic analyses of *S.* Typhimurium in the murine model of systemic infection demonstrated that multiple nutrient sources as utilized in parallel (Steeb et al., 2013). Glycerol catabolism was most highly induced, and high levels of proteins involved in transport and catabolism of glucose, gluconate, lactate, and *N*-acetyl-glucosamine (GlcNAc) were determined. In addition, transport/catabolism of various amino acids, fatty acids and nucleotides was induced. As the analyses were performed with *Salmonella* recovered from spleens of infected mice, the parallel activity of metabolic pathways may result from various subpopulations in distinct microhabitats or type of host cells.

Transcriptomic profiling of *S.* Typhimurium in macrophages revealed strong up-regulation of EMD and PP pathways, while the expression of ED genes was not altered (Eriksson et al., 2003). The analysis also revealed up-regulation of genes for gluconate, gluconurate, galactonate and related carbonic acids, suggesting preferential use of these compounds in the SCV in macrophages.

Upon phagocytosis by macrophages, *C. albicans* not only up-regulates the expression of amino acid permease and oligopeptide transporter genes (see above); but also genes encoding lactate and GlcNAc transporters (Alvarez and Konopka, 2007; Lorenz et al., 2004; Miramon and Lorenz, 2016; Vieira et al., 2010). It is not known whether lactate and GlcNAc are used as nutrients within the phagosome or whether these metabolites serve as a host-derived signal that modulates virulence-associated functions. Clearly, growth with lactate as an alternative carbon source (as compared to glucose − the preferred carbon source) leads to a modulated cell wall architecture and increased stress resistance of *C. albicans* (Ene et al., 2012). It remains to be elucidated whether these phenotypes occur inside macrophages and whether they affect the intraphagosomal lifestyle of *C. albicans*. The uptake of GlcNAc through the Ngt1 transporter and GlcNAc signalling through Ngs1 induce the transcription of genes mediating hypha development and could thus support escape of *C. albicans* from macrophages (Alvarez and Konopka, 2007; Su et al., 2016).

Similar to *C. albicans*, membrane transporter-encoding genes of *Cr. neoformans* are induced upon internalization by macrophages. This mainly includes carbohydrate and polyol transporters as well as ammonia and amino acid permeases, indicating a restriction in nutrient availability encountered by intracellular *Cr. neoformans* cells (Derengowski Lda et al., 2013; Fan et al., 2005).

In summary, the utilization of carbohydrates is less investigated compared to amino acids, but it seems clear that all pathogens require carbohydrates for different anabolic (gluconeogenesis or PP pathway) or catabolic processes (glycolysis or ED pathway).

4.3. Lipids

M. tuberculosis can feed well on host lipids within macrophages and metabolises fatty acids via β-oxidation and the glyoxylate cycle (Barisch and Soldati, 2017). β-oxidation can facilitate adaptation of *M. tuberculosis* to changing metabolite conditions during infection (Toledo and Benach, 2015). The glyoxylate cycle is essential to synthesize C₄-intermediates for the TCA cycle and gluconeogenesis, when acetyl-CoA is produced by fatty acid degradation in the absence of glucose. Cholesterol, a distinctive host membrane lipid, is not only essential for uptake of *M. tuberculosis* by macrophages, but also essential for survival within lysosomes (Gatfield and Pieters, 2000). *M. tuberculosis* requires the import system Mce4 and the catabolism of steroid rings to use cholesterol as a carbon source during its intracellular lifestyle in activated macrophages (Crowe et al., 2017; Pandey and Sassetti, 2008). Cholesterol breakdown generates acetyl-CoA and propionyl-CoA. Propionyl-CoA needs to be detoxified via the methylcitrate cycle or the methylmalonyl pathway. Both pathways supply TCA cycle intermediates that are used for energy generation (Munoz-Elias et al., 2006; Savvi et al., 2008). In addition, propionyl-CoA is used for the biosynthesis of methyl-branched long chain fatty acids, which are incorporated into virulence-associated bacterial cell wall lipids (Lee et al., 2013; Russell et al., 2010). Host phagosomal sphingomyelin is cleaved by *M. tuberculosis* through the activity of an outer membrane sphingomyelinase. As this enzyme is necessary for intraphagosomal replication of *M. tuberculosis*, the pathogen likely uses sphingomyelin as a carbon, nitrogen and phosphorus source (Speer et al., 2015). On the other hand, phospholipids can also serve as a carbon and energy source for intracellular growing *M. tuberculosis*, by degradation through cell wall anchored phospholipase C (PLC), which has its expression up-regulated during infection of macrophages (Raynaud et al., 2002). However, it seems as PLCs are only marginally required for virulence, and the up-

regulation of PLCs during intracellular phases of *M. tuberculosis* might rather be linked to a phosphate-limited phagosomal compartment (Le Chevalier et al., 2015).

Fatty acids catabolism of *S. enterica* is up-regulated in the murine infection model (Steeb et al., 2013), while transcriptional profiling of *Salmonella* in macrophages did not indicate a specific response to fatty acids as a nutrient source (Eriksson et al., 2003). As discussed for carbohydrates, the metabolic flexibility may allow intracellular *Salmonella* to readily switch been carbohydrates, fatty acids and further nutritional sources depending on local availability and preference.

Presumably, other intracellular pathogens can also use host lipids as an additional nutrient source *via* lipases or other lipid degrading enzymes. For example, transcriptional analysis of *C. albicans* engulfed by macrophages revealed an up-regulation of secretory lipase and phospholipase genes (Lorenz et al., 2004). An intracellular growth defect of a *Cr. neoformans* mutant lacking a phospholipase B (*plb1Δ*) suggested that the degradation of host phospholipids may promote intracellular proliferation (Evans et al., 2015). One earlier study suggests that *Cr. neoformans* can in fact use lipids derived from macrophages by phospholipase B (Wright et al., 2007).

5. Utilization of micronutrients during the intracellular lifestyle

5.1. Trace metals

Trace metals are often cofactors of transcription factors (zinc finger proteins) or enzymes, and trace metal limitation leads to dys- or nonfunctional proteins. Iron-sulphur clusters are essential for the enzymatic activity of essential metabolic enzymes such as aconitase, catalyzing the conversion of citrate into isocitrate (Miller and Auerbuch, 2015). Zinc has an important role as a structural and catalytic cofactor of many proteins, mainly transcription factors or enzymes, which function in diverse biological processes (Capdevila et al., 2016). Copper and manganese predominantly fulfil catalytic functions in superoxide detoxifying enzymes (SODs), cytochrome c oxidases (COXs) and DNA synthesis (Besold et al., 2016; Broxton and Culotta, 2016; Culotta et al., 2006; Juttukonda and Skaar, 2015). In contrast, high levels of iron, zinc or copper can lead to cell-toxic effects by generation of toxic radicals damaging DNA. For example, excess zinc can antagonize the uptake of other trace metals and can inhibit key enzymes by displacing other metals (Besold et al., 2016; Djoko et al., 2015). Consequently, trace metals are essential for both host and pathogen, and there is a constant tug of war for trace metals in the human body during infection. Thus, metal homeostasis is crucial and the metabolism of trace metals has to be tightly regulated. Within the host, micronutrients are often limited, and the host restricts access to essential trace metals to prevent microbial growth, a process termed 'nutritional immunity' (Hood and Skaar, 2012).

In the last decades, the role of trace metals for survival and replication of intracellular pathogens within macrophages has been extensively studied. The host immune system has evolved multiple sequestration strategies to limit the availability of trace metals (iron, zinc and manganese) from invading microorganisms (reviewed by (Becker and Skaar, 2014; Johnson and Wessling-Resnick, 2012; Zackular et al., 2015)). On the other hand, metal intoxication, mainly with copper and zinc, is used as an antimicrobial strategy by the host (Besold et al., 2016; Djoko et al., 2015). Therefore, intracellular pathogens not only need efficient import of trace metals, they also require potent export systems to prevent toxicity.

Iron is the most prominent example of an inorganic micronutrient essential for growth of all organisms and virulence of most intracellular pathogens (summarized in (Crawford and Wilson, 2015; Leon-Sicairos et al., 2015; Neyrolles et al., 2015)), and depletion of iron from host macrophages diminishes intracellular growth of pathogens (Paradkar et al., 2008). Therefore, it is not surprising that many intracellular pathogens can express high affinity uptake systems that compete with

host iron binding proteins. These high affinity uptake systems are highly regulated and encompass the (1) reductive pathway to exploit ferric iron from iron-chelating proteins or the environment, (2) receptor-mediated uptake of iron-containing hemoproteins from the host (hemoglobin, transferrin, lactoferrin) and (3) the siderophore-mediated iron acquisition (Leon-Sicairos et al., 2015).

Genetic or chemical inactivation of either high affinity transporter systems or transcription factors regulating the transport system often reduces intracellular fitness, as shown for *L. pneumophila* (Portier et al., 2015), *C. glabrata* (Seider et al., 2014; Srivastava et al., 2014), *H. capsulatum* (Hilty et al., 2011; Hwang et al., 2008; Newman and Smulian, 2013), *F. tularensis* (Perez and Ramakrishnan, 2014; Ramakrishnan et al., 2012) and *M. tuberculosis* (De Voss et al., 2000; Rodriguez and Smith, 2006). Iron availability is also critical for intracellular *S. enterica. Salmonella* processes several iron uptake systems such as EntC or Feo and can synthesize several siderophores. Transcriptomic analyses showed that in the J774-A.1 macrophage line derived from NRAMP1$^{-/-}$ mice, iron uptake systems are down-regulated suggesting non-limited iron supply. This situation is different in macrophages from NRAMP1$^{+/+}$ donors and especially in activated macrophages (Nairz et al., 2009) suggesting a key role for NRAMP1 in iron restriction. For example, NRAMP1 function is linked to expression of lipocalin-2 and antimicrobial peptides restricting the availability of iron-loaded siderophores (Nairz et al., 2015a). In addition, intracellular pathogens manipulate the host metabolism to acquire iron. For example, phagocytosed *M. tuberculosis* recruits holotransferrin to the phagosome and this molecule is internalized across the mycobacterial cell wall to acquire iron (Boradia et al., 2014). Upon filamentous growth, *C. albicans* expresses the multifunctional protein Als3 on the cell surface, which enables the fungus to utilize iron from host ferritin (Almeida et al., 2008; Liu and Filler, 2011). However, it is unclear whether this utilization pathway plays a role during interaction with macrophages. Recently it was shown that the disruption of the siderophore transporter LbtP and the resulting iron limitation response lead to a premature escape of *L. pneumophila* from infected cells (O'Connor et al., 2016). This example shows that *L. pneumophila* iron acquisition inside macrophages promotes intracellular survival and replication (Portier et al., 2015), while conditions that further lower iron availability or uptake options may drive the escape of the pathogen from its intracellular niche. Siderophore-mediated iron acquisition by Sit1 also improves intracellular survival of *C. glabrata* within macrophages (Nevitt and Thiele, 2011).

Besides iron restriction, zinc and manganese are sequestered by vertebrates intra- and extracellularly to protect against infection thus contributing to nutritional immunity (Kehl-Fie and Skaar, 2010).

Bacterial pathogens have evolved strategies to deal with low zinc concentrations by a zinc-responsive ZnuABC transport system (Cerasi et al., 2013), but so far there are rare observations that this system is essential, e.g. in *Salmonella* (Ammendola et al., 2007).

Accumulation of zinc and copper within *M. tuberculosis*-containing phagosomes is used by the host to intoxicate the microbe (Botella et al., 2012; Soldati and Neyrolles, 2012). Similarly to *M. tuberculosis*, the supplementation of macrophages with zinc reduces the ability of *L. monocytogenes* to replicate and a combination with vitamin A enhances the antimicrobial activity (Castillo et al., 2015). Interestingly, the proinflammatory stimulation of macrophages with IFN-γ induces the recruitment of host cell transporters, like ATP7A and ZnT1, to the phagosome thereby increasing the concentration of toxic metals (Soldati and Neyrolles, 2012; White et al., 2009). Nevertheless, *M. tuberculosis* resists metal intoxication by expressing several efflux pumps of the P-type ATPase class and an inactivation of these efflux pumps affects intracellular survival and growth (Botella et al., 2011; Neyrolles et al., 2013; Rowland and Niederweis, 2012; Ward et al., 2010).

Fungal pathogens like *C. albicans* and *Cr. neoformans* activate the expression of zinc importers, and the zincophore Pra1 in the case of *C. albicans*, after engulfment by macrophages, indicating a zinc-restricted intracellular environment (Citiulo et al., 2012; Do et al., 2016; Lorenz et al., 2004; Marcil et al., 2008). In line with this, the induction of zinc restriction in macrophages by GM-CSF induces export of zinc from the *Histoplasma*-containing phagosome and inhibits intracellular growth of *H. capsulatum*, while treatment with anti-inflammatory cytokines like Interleukin 4 (IL-4) increases zinc stores and promotes survival and persistence (Subramanian Vignesh et al., 2013; Subramanian Vignesh et al., 2016; Winters et al., 2010).

Excess of copper within the phagosome is used by host macrophages to kill ingested *M. tuberculosis* and an efficient detoxification system is required for *M. tuberculosis* cells to survive within the intraphagosomal compartment (Wolschendorf et al., 2011). The increased copper sensitivity combined with slow growth within macrophages of a strain lacking *SUR7* in *C. albicans* suggests that copper detoxification is important for survival within the *Candida*-containing phagosome (Douglas et al., 2012). Intriguingly, *C. albicans* possesses a P-type ATPase encoded by *CRP1*, mediating copper resistance. However, it is unclear, whether this efflux pump plays a role within the phagosomal compartment (Weissman et al., 2000). The survival of *Cr. neoformans* in macrophages is dependent on a balanced copper homeostasis, mediated by a Cuf1-induced expression of the copper transporter gene *CTR4* and the copper-detoxifying metallothionein genes *CMT1/2* (Ding et al., 2013; Waterman et al., 2007; Waterman et al., 2012). Pathogenic microorganisms possess a redundant manganese transport system (MntH in bacteria and Smf1/2 in fungi (Juttukonda and Skaar, 2015; Reddi et al., 2009). The active expulsion of manganese through host NRAMP1 from the phagosome suggests that intraphagosomal pathogens require uptake of this trace element, and the host is limiting its availability (Juttukonda and Skaar, 2015). So far, however, the necessity of manganese import within macrophages has only been shown for *Shigella flexneri* (Runyen-Janecky et al., 2006). In contrast, the requirement of manganese acquisition systems is well studied for several extracellular-localized pathogens, which reside in an environment restricted for manganese due to sequestration by host calprotectin (Juttukonda and Skaar, 2015; Lisher and Giedroc, 2013).

The murine model for systemic *S. enterica* infections, i.e. mimicking typhoid fever, uses *Salmonella*-sensitive mouse strains such as C57BL/6 or BALB/c. These strains are NRAMP1-deficient and cannot control the proliferation of *Salmonella* in systemic sites. In contrast, NRAMP1-proficient strains are able to control the infection and much higher dose of *Salmonella* inoculums are required to induce systemic disease. Based on these observations, availability of zinc, iron, and further divalent cations is likely to be a limiting factor for intracellular growth of *Salmonella* (Nairz et al., 2009).

5.2. Vitamins

Some vitamins are essential for intracellular pathogens due to intrinsic auxotrophies. For example, *L. monocytogenes* requires lipoate (O'Riordan et al., 2003) and *C. glabrata* is auxotrophic for niacin (Ma et al., 2007). Vitamins are synthesized by many bacteria, fungi and plants, but rarely by mammals, which thus need to assimilate essential vitamins from the daily food and host cells express vitamin-specific transporters (Suzuki and Kunisawa, 2015). Within pro- and eukaryotic cells, vitamins execute diverse cellular functions (Suzuki and Kunisawa, 2015; Zempleni et al., 2009). Therefore, host cells and invading pathogens, including intracellular pathogens, have to acquire or synthesize essential vitamins.

To date the number of studies dealing with the importance of microbial vitamin acquisition or synthesis for intracellular fitness is low. Recent studies, however, show that bacterial and fungal mutants that lack certain vitamin-biosynthetic pathways are attenuated in intracellular fitness. While *H. capsulatum* requires the biosynthesis of riboflavin for intracellular proliferation in macrophages (Garfoot et al., 2014), *Mycobacterium marinum*, a fish and amphibian pathogen (Tobin and Ramakrishnan, 2008), needs its own biotin biosynthesis for
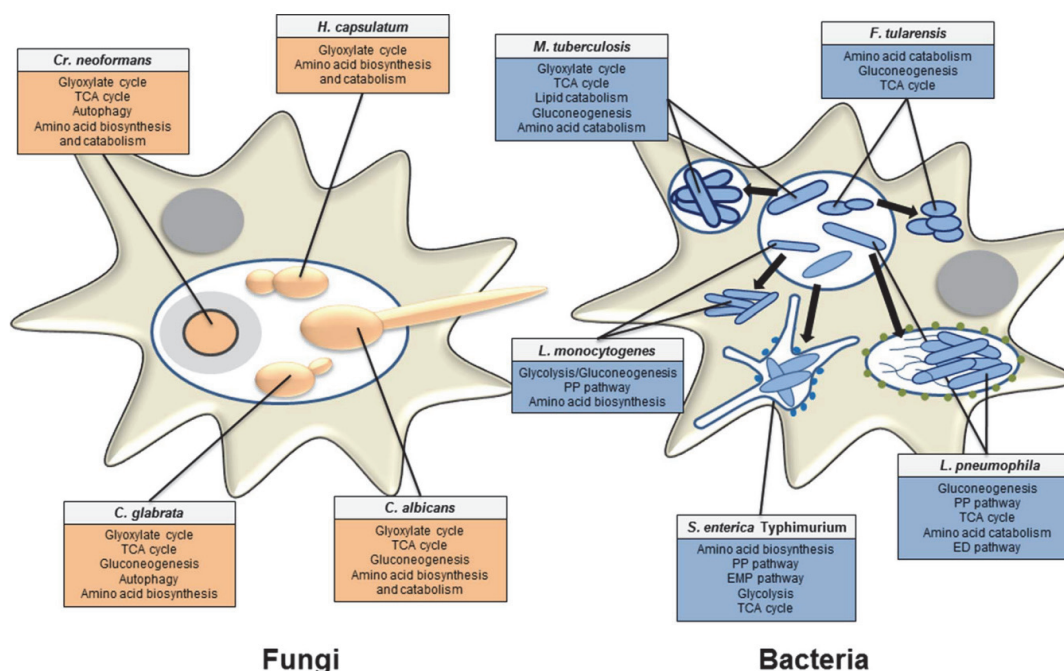
Fig. 1. Examples of metabolic pathways adopted by different facultative intracellular fungal (left) and bacterial (right) pathogens during intracellular stages within macrophages and discussed in this review. Different fungal and bacterial pathogens enter the phagosomal compartment of macrophages after engulfment. Left: *C. albicans*, *C. glabrata*, *H. capsulatum*, and *Cr. neoformans* can grow and replicate within a membrane-surrounded intracellular compartment. While capsulated *Cr. neoformans* cells can escape from their intracellular compartments via expulsion into the extracellular space (not shown), *C. albicans* can escape via hypha, thereby piercing the phagosomal and cell membrane. All fungal pathogens activate a starvation mode and induce pathways to utilize alternative carbon sources.

Right: After phagocytosis, *S. enterica* and *L. pneumophila* redirect the host cell endosomal transport machinery to create their own nutrient-optimized intracellular compartment (SCV or LCV; indicated by the blue and green dots, respectively). Initially, *L. monocytogenes* and *F. tularensis* enter the phagosome, but rapidly escape into the nutrient rich host cell cytosol, thereby also avoiding phagosomal antimicrobial activities. *M. tuberculosis* resides within the phagosome, arrests the maturation into a phagolysosome and is able to acquire different host nutrient sources to replicate within the phagosome. ED, Entner-Doudoroff; EMP, Embden-Meyerhof-Parnas; LCV, *Legionella*-containing vacuole; PP, pentose phosphate; SCV, *Salmonella*-containing vacuole; TCA, tricarboxylic acid.

proliferation within macrophages (Yu et al., 2011). Biotin biosynthesis also contributes to virulence and escape of *F. tularensis* from the phagosome into the cytosol. Phagosomal escape in turn is essential for this pathogen to assimilate nutrients for proper growth (Feng et al., 2015; Feng et al., 2014; Napier et al., 2012). This implies that the availability of at least certain vitamins is limited to different classes of pathogens in macrophages. The uptake of lipoic acid, a cofactor required for enzymatic activity of pyruvate dehydrogenase, is essential for intracellular multiplication of *L. monocytogenes*, indicating a necessity of this enzymatic reaction for intracellular stages (O'Riordan et al., 2003). As a prototrophic organism, *S. enterica* does not depend on the supply of vitamins or their organic precursors from macrophages. Indeed, the attenuation of mutant strains defective in respective biosynthesis pathways indicate that this pathogen may not have evolved strategies to sequester vitamins from the macrophage host cell (Bäumler et al., 1994).

A specific strategy for nutrition of intracellular pathogens is the biogenesis of specific compartments what alleviate nutritional restrictions encountered in the canonical endocytic pathway. Two prominent examples are *L. pneumophila* and *S. enterica,* both forming pathogen containing vacuoles with unique properties. *Legionella* inhabits a vacuole with markers characteristic for endosomes, macropinosomes and endoplasmic reticulum (ER) (Finsel and Hilbi, 2015). This unique compartment is formed by the action of effector proteins transported *via* the Icm/Dot type IV secretion system, resulting in deviation of the

normal phagosomal maturation process and atypical fusion events, such as fusions with the ER. The unique environment of the LCV provides a range of nutrients for the intracellular replication of the pathogen (Manske and Hilbi, 2014). Several host cell transporters for amino acids, carbohydrates or fatty acids remain present in the LCV membrane and mediate transport into the LCV lumen. In addition, *Legionella* secretes various hydrolytic enzymes into the lumen of LCV, resulting in degradation host molecules for subsequent uptake by the pathogen.

S. enterica deploys the SPI2-T3SS and a cocktail of about 30 effector proteins to manipulate various mechanisms of the host cell (LaRock et al., 2015). A subset of these effector proteins, most prominently SifA, interferes with the function of microtubule motor proteins. This manipulation leads to recruitment of various endosomal compartments to the SCV and their fusion. These events allow the continuous extension of the SCV to accommodate the growing intracellular *Salmonella* population. Furthermore, various types of tubular vesicular extensions are formed, for example *Salmonella*-induced filaments or (SIF) (Liss and Hensel, 2015). Recent work by Liss et al. demonstrated that SCV and SIF form an interconnected network with rapid interchanges of membranes and luminal content. The formation of this network allows *Salmonella* to access nutrients present in the lumen of the redirected and fused vesicles (Liss et al., 2017).

In summary, successful intracellular pathogens have evolved efficient acquisition mechanisms to compete with the host for essential trace metals and vitamins. In contrast to other nutrients, high amounts

of iron, copper and zinc appear to be toxic for intracellular pathogens and are actively pumped into the pathogen-containing compartment. Thus, intracellular pathogens also require detoxification systems. Further, intracellular pathogens have different requirements for vitamins due to intrinsic auxotrophies and incomplete biosynthesis gene clusters, respectively. Therefore, some pathogens require efficient uptake systems hijacking vitamins from the host or rely on their own biosynthesis.

6. Conclusions

In this review we summarized the current knowledge on how different intracellular pathogens are specifically adapted to the metabolic conditions of the phagosomal compartment as well as the cytosolic environment with a focus on species-specific needs regarding specific nutrients utilized for intracellular adaptation and replication (summarized in Fig. 1). Despite these species differences, fungal pathogens seem to share a common transcriptional response leading to repression of energy consuming processes like protein biosynthesis and activation of alternative carbon- and nitrogen assimilation pathways (Fig. 1).

Studying strategies of nutrient deprivation as an antimicrobial mechanism of macrophages to restrict microbial transmission is more challenging than the search for toxic and microbicidal activities of macrophages. Due to different intracellular trafficking stages and fusion-events with other organelles or even the escape from a membrane-surrounded compartment, the availability of nutrients and the requirement could differ dramatically. Several studies observed that intraphagosomal pathogens employ nutrient acquisition strategies suggesting that the phagosome represents a niche with limited nutrient supply. However, the phagosome is not completely nutrient restricted. Amino acids seem to be a main nutrient source for all intracellularly adapted pathogens and can function as a regulatory signal for the pathogen. Additionally, carbohydrates, lipids and micronutrients are used to directly generate energy or maintain metabolic fluxes for anabolic purposes.

The struggle for nutrients at the host-pathogen interface has put evolutionary pressure on intracellular pathogens to evolve powerful microbial acquisition systems. Effective nutrient acquisition from the host is essential to successfully maintain the metabolism of the pathogen as a prerequisite to survive and replicate within this niche. Therefore, therapeutic strategies to selectively inactivate these acquisition pathways are promising options for the development of antimicrobial drugs.

References

Abu Kwaik, Y., Bumann, D., 2013. Microbial quest for food *in vivo*: 'nutritional virulence' as an emerging paradigm. Cell. Microbiol. 15, 882–890.

Almeida, R.S., Brunke, S., Albrecht, A., Thewes, S., Laue, M., Edwards, J.E., Filler, S.G., Hube, B., 2008. The hyphal-associated adhesin and invasin Als3 of *Candida albicans* mediates iron acquisition from host ferritin. PLoS Pathog. 4, e1000217.

Alvarez, F.J., Konopka, J.B., 2007. Identification of an N-acetylglucosamine transporter that mediates hyphal induction in *Candida albicans*. Mol. Biol. Cell 18, 965–975.

Ammendola, S., Pasquali, P., Pistoia, C., Petrucci, P., Petrarca, P., Rotilio, G., Battistoni, A., 2007. High-affinity Zn2+ uptake system ZnuABC is required for bacterial zinc homeostasis in intracellular environments and contributes to the virulence of *Salmonella enterica*. Infect. Immun. 75, 5867–5876.

Appelberg, R., 2006. Macrophage nutriprive antimicrobial mechanisms. J. Leukoc. Biol. 79, 1117–1128.

Awuh, J.A., Flo, T.H., 2017. Molecular basis of mycobacterial survival in macrophages. Cell. Mol. Life Sci. 74, 1625–1648.

Bäumler, A.J., Kusters, J.G., Stojiljkovic, I., Heffron, F., 1994. *Salmonella typhimurium* loci involved in survival within macrophages. Infect. Immun. 62, 1623–1630.

Barel, M., Meibom, K., Dubail, I., Botella, J., Charbit, A., 2012. *Francisella tularensis* regulates the expression of the amino acid transporter SLC1A5 in infected THP-1 human monocytes. Cell. Microbiol. 14, 1769–1783.

Barisch, C., Soldati, T., 2017. Breaking fat! How *Mycobacteria* and other intracellular pathogens manipulate host lipid droplets. Biochimie. 141 (October), 54–61.

Becker, K.W., Skaar, E.P., 2014. Metal limitation and toxicity at the interface between host and pathogen. FEMS Microbiol. Rev. 38, 1235–1249.

Becker, D., Selbach, M., Rollenhagen, C., Ballmaier, M., Meyer, T.F., Mann, M., Bumann, D., 2006. Robust *Salmonella* metabolism limits possibilities for new antimicrobials. Nature 440, 303–307.

Besold, A.N., Culbertson, E.M., Culotta, V.C., 2016. The Yin and Yang of copper during infection. J. Biol. Inorg. Chem. 21, 137–144.

Beste, D.J., Noh, K., Niedenfuhr, S., Mendum, T.A., Hawkins, N.D., Ward, J.L., Beale, M.H., Wiechert, W., McFadden, J., 2013. 13C-Flux spectral analysis of host-pathogen metabolism reveals a mixed diet for intracellular *Mycobacterium tuberculosis*. Chem. Biol. 20, 1012–1021.

Birmingham, C.L., Canadien, V., Gouin, E., Troy, E.B., Yoshimori, T., Cossart, P., Higgins, D.E., Brumell, J.H., 2007. *Listeria monocytogenes* evades killing by autophagy during colonization of host cells. Autophagy 3, 442–451.

Boradia, V.M., Malhotra, H., Thakkar, J.S., Tillu, V.A., Vuppala, B., Patil, P., Sheokand, N., Sharma, P., Chauhan, A.S., Raje, M., Raje, C.I., 2014. *Mycobacterium tuberculosis* acquires iron by cell-surface sequestration and internalization of human holo-transferrin. Nat. Commun. 5, 4730.

Botella, H., Peyron, P., Levillain, F., Poincloux, R., Poquet, Y., Brandli, I., Wang, C., Tailleux, L., Tilleul, S., Charriere, G.M., Waddell, S.J., Foti, M., Lugo-Villarino, G., Gao, Q., Maridonneau-Parini, I., Butcher, P.D., Castagnoli, P.R., Gicquel, B., de Chastellier, C., Neyrolles, O., 2011. Mycobacterial p(1)-type ATPases mediate resistance to zinc poisoning in human macrophages. Cell Host Microbe 10, 248–259.

Botella, H., Stadthagen, G., Lugo-Villarino, G., de Chastellier, C., Neyrolles, O., 2012. Metallobiology of host-pathogen interactions: an intoxicating new insight. Trends Microbiol. 20, 106–112.

Broxton, C.N., Culotta, V.C., 2016. SOD enzymes and microbial pathogens: surviving the oxidative storm of infection. PLoS Pathog. 12, e1005295.

Brunke, S., Hube, B., 2013. Two unlike cousins: *Candida albicans* and *C. glabrata* infection strategies. Cell. Microbiol. 15, 701–708.

Brunke, S., Hube, B., 2014. Adaptive prediction as a strategy in microbial infections. PLoS Pathog. 10, e1004356.

Capdevila, D.A., Wang, J., Giedroc, D.P., 2016. Bacterial strategies to maintain zinc metallostasis at the host-pathogen interface. J. Biol. Chem. 291, 20858–20868.

Castillo, Y., Tachibana, M., Nakatsu, Y., Watanabe, K., Shimizu, T., Watarai, M., 2015. Combination of zinc and all-trans retinoic acid promotes protection against *Listeria monocytogenes* infection. PLoS One 10, e0137463.

Caza, M., Kronstad, J.W., 2013. Shared and distinct mechanisms of iron acquisition by bacterial and fungal pathogens of humans. Front. Cell. Infect. Microbiol. 3, 80.

Cerasi, M., Ammendola, S., Battistoni, A., 2013. Competition for zinc binding in the host-pathogen interaction. Front. Cell. Infect. Microbiol. 3, 108.

Childers, D.S., Raziunaite, I., Mol Avelar, G., Mackie, J., Budge, S., Stead, D., Gow, N.A., Lenardon, M.D., Ballou, E.R., MacCallum, D.M., Brown, A.J., 2016. The rewiring of ubiquitination targets in a pathogenic yeast promotes metabolic flexibility, host colonization and virulence. PLoS Pathog. 12, e1005566.

Chong, A., Wehrly, T.D., Child, R., Hansen, B., Hwang, S., Virgin, H.W., Celli, J., 2012. Cytosolic clearance of replication-deficient mutants reveals *Francisella tularensis* interactions with the autophagic pathway. Autophagy 8, 1342–1356.

Choy, A., Dancourt, J., Mugo, B., O'Connor, T.J., Isberg, R.R., Melia, T.J., Roy, C.R., 2012. The *Legionella* effector RavZ inhibits host autophagy through irreversible Atg8 deconjugation. Science 338, 1072–1076.

Citiulo, F., Jacobsen, I.D., Miramon, P., Schild, L., Brunke, S., Zipfel, P., Brock, M., Hube, B., Wilson, D., 2012. *Candida albicans* scavenges host zinc via Pra1 during endothelial invasion. PLoS Pathog. 8, e1002777.

Crawford, A., Wilson, D., 2015. Essential metals at the host-pathogen interface: nutritional immunity and micronutrient assimilation by human fungal pathogens. FEMS Yeast Res. 15.

Crowe, A.M., Casabon, I., Brown, K.L., Liu, J., Lian, J., Rogalski, J.C., Hurst, T.E., Snieckus, V., Foster, L.J., Eltis, L.D., 2017. Catabolism of the last two steroid rings in *Mycobacterium tuberculosis* and other bacteria. mBio 8 (2) pii: e00321-17.

Culotta, V.C., Yang, M., O'Halloran, T.V., 2006. Activation of superoxide dismutases: putting the metal to the pedal. Biochim. Biophys. Acta 1763, 747–758.

Das, P., Lahiri, A., Lahiri, A., Sen, M., Iyer, N., Kapoor, N., Balaji, K.N., Chakravortty, D., 2010. Cationic amino acid transporters and *Salmonella* Typhimurium ArgT collectively regulate arginine availability towards intracellular *Salmonella* growth. PLoS One 5, e15466.

de las Heras, A., Cain, R.J., Bielecka, M.K., Vazquez-Boland, J.A., 2011. Regulation of *Listeria* virulence: prfA master and commander. Curr. Opin. Microbiol. 14, 118–127.

De Voss, J.J., Rutter, K., Schroeder, B.G., Su, H., Zhu, Y., Barry 3rd, C.E., 2000. The salicylate-derived mycobactin siderophores of *Mycobacterium tuberculosis* are essential for growth in macrophages. Proc. Natl. Acad. Sci. U. S. A. 97, 1252–1257.

Derengowski Lda, S., Paes, H.C., Albuquerque, P., Tavares, A.H., Fernandes, L., Silva-Pereira, I., Casadevall, A., 2013. The transcriptional response of *Cryptococcus* neoformans to ingestion by *Acanthamoeba castellanii* and macrophages provides insights into the evolutionary adaptation to the mammalian host. Eukaryot. Cell 12, 761–774.

Deretic, V., Levine, B., 2009. Autophagy, immunity, and microbial adaptations. Cell Host Microbe 5, 527–549.

Ding, C., Festa, R.A., Chen, Y.L., Espart, A., Palacios, O., Espin, J., Capdevila, M., Atrian, S., Heitman, J., Thiele, D.J., 2013. *Cryptococcus neoformans* copper detoxification

machinery is critical for fungal virulence. Cell Host Microbe 13, 265–276.

Djoko, K.Y., Ong, C.L., Walker, M.J., McEwan, A.G., 2015. The role of copper and zinc toxicity in innate immune defense against bacterial pathogens. J. Biol. Chem. 290, 18954–18961.

Do, E., Hu, G., Caza, M., Kronstad, J.W., Jung, W.H., 2016. The ZIP family zinc transporters support the virulence of *Cryptococcus neoformans*. Med. Mycol. 54, 605–615.

Dortet, L., Mostowy, S., Samba-Louaka, A., Gouin, E., Nahori, M.A., Wiemer, E.A., Dussurget, O., Cossart, P., 2011. Recruitment of the major vault protein by InlK: a *Listeria monocytogenes* strategy to avoid autophagy. PLoS Pathog. 7, e1002168.

Douglas, L.M., Wang, H.X., Keppler-Ross, S., Dean, N., Konopka, J.B., 2012. Sur7 promotes plasma membrane organization and is needed for resistance to stressful conditions and to the invasive growth and virulence of *Candida albicans*. mBio 3 (1) pii: e00254-11.

Eisenreich, W., Heuner, K., 2016. The life stage-specific pathometabolism of *Legionella pneumophila*. FEBS Lett. 590, 3868–3886.

Ene, I.V., Heilmann, C.J., Sorgo, A.G., Walker, L.A., de Koster, C.G., Munro, C.A., Klis, F.M., Brown, A.J., 2012. Carbon source-induced reprogramming of the cell wall proteome and secretome modulates the adherence and drug resistance of the fungal pathogen *Candida albicans*. Proteomics 12, 3164–3179.

Eriksson, S., Lucchini, S., Thompson, A., Rhen, M., Hinton, J.C., 2003. Unravelling the biology of macrophage infection by gene expression profiling of intracellular *Salmonella enterica*. Mol. Microbiol. 47, 103–118.

Erwig, L.P., Gow, N.A., 2016. Interactions of fungal pathogens with phagocytes. Nat. Rev. Microbiol. 14, 163–176.

Evans, R.J., Li, Z., Hughes, W.S., Djordjevic, J.T., Nielsen, K., May, R.C., 2015. *Cryptococcal* phospholipase B1 is required for intracellular proliferation and control of titan cell morphology during macrophage infection. Infect. Immun. 83, 1296–1304.

Eylert, E., Schar, J., Mertins, S., Stoll, R., Bacher, A., Goebel, W., Eisenreich, W., 2008. Carbon metabolism of *Listeria monocytogenes* growing inside macrophages. Mol. Microbiol. 69, 1008–1017.

Eylert, E., Herrmann, V., Jules, M., Gillmaier, N., Lautner, M., Buchrieser, C., Eisenreich, W., Heuner, K., 2010. Isotopologue profiling of *Legionella pneumophila*: role of serine and glucose as carbon substrates. J. Biol. Chem. 285, 22232–22243.

Fan, W., Kraus, P.R., Boily, M.J., Heitman, J., 2005. *Cryptococcus neoformans* gene expression during murine macrophage infection. Eukaryot. Cell 4, 1420–1433.

Feng, Y., Napier, B.A., Manandhar, M., Henke, S.K., Weiss, D.S., Cronan, J.E., 2014. A *Francisella* virulence factor catalyses an essential reaction of biotin synthesis. Mol. Microbiol. 91, 300–314.

Feng, Y., Chin, C.Y., Chakravartty, V., Gao, R., Crispell, E.K., Weiss, D.S., Cronan, J.E., 2015. The atypical occurrence of two biotin protein ligases in *Francisella novicida* is due to distinct roles in virulence and biotin metabolism. mBio 6, e00591.

Fields, P.I., Swanson, R.V., Haidaris, C.G., Heffron, F., 1986. Mutants of *Salmonella typhimurium* that cannot survive within the macrophage are avirulent. Proc. Natl. Acad. Sci. U. S. A. 83, 5189–5193.

Finsel, I., Hilbi, H., 2015. Formation of a pathogen vacuole according to *Legionella pneumophila*: how to kill one bird with many stones. Cell. Microbiol. 17, 935–950.

Flannagan, R.S., Heit, B., Heinrichs, D.E., 2015. Antimicrobial mechanisms of macrophages and the immune evasion strategies of *Staphylococcus aureus*. Pathogens 4, 826–868.

Fonseca, M.V., Swanson, M.S., 2014. Nutrient salvaging and metabolism by the intracellular pathogen *Legionella pneumophila*. Front. Cell. Infect. Microbiol. 4, 12.

Fonseca, M.V., Sauer, J.D., Crepin, S., Byrne, B., Swanson, M.S., 2014. The phtC-phtD locus equips *Legionella pneumophila* for thymidine salvage and replication in macrophages. Infect. Immun. 82, 720–730.

Forbes, J.R., Gros, P., 2003. Iron, manganese, and cobalt transport by Nramp1 (Slc11a1) and Nramp2 (Slc11a2) expressed at the plasma membrane. Blood 102, 1884–1892.

Freitag, N.E., Port, G.C., Miner, M.D., 2009. *Listeria monocytogenes* – from saprophyte to intracellular pathogen. Nat. Rev. Microbiol. 7, 623–628.

Galvan-Pena, S., O'Neill, L.A., 2014. Metabolic reprograming in macrophage polarization. Front. Immunol. 5, 420.

Ganeshan, K., Chawla, A., 2014. Metabolic regulation of immune responses. Annu. Rev. Immunol. 32, 609–634.

Garfoot, A.L., Rappleye, C.A., 2016. *Histoplasma capsulatum* surmounts obstacles to intracellular pathogenesis. FEBS J. 283, 619–633.

Garfoot, A.L., Zemska, O., Rappleye, C.A., 2014. *Histoplasma capsulatum* depends on *de novo* vitamin biosynthesis for intraphagosomal proliferation. Infect. Immun. 82, 393–404.

Gatfield, J., Pieters, J., 2000. Essential role for cholesterol in entry of *mycobacteria* into macrophages. Science 288, 1647–1650.

Gesbert, G., Ramond, E., Rigard, M., Frapy, E., Dupuis, M., Dubail, I., Barel, M., Henry, T., Meibom, K., Charbit, A., 2014. Asparagine assimilation is critical for intracellular replication and dissemination of *Francisella*. Cell. Microbiol. 16, 434–449.

Gesbert, G., Ramond, E., Tros, F., Dairou, J., Frapy, E., Barel, M., Charbit, A., 2015. Importance of branched-chain amino acid utilization in *Francisella* intracellular adaptation. Infect. Immun. 83, 173–183.

Ghosh, S., Navarathna, D.H., Roberts, D.D., Cooper, J.T., Atkin, A.L., Petro, T.M., Nickerson, K.W., 2009. Arginine-induced germ tube formation in *Candida albicans* is essential for escape from murine macrophage line RAW 264.7. Infect. Immun. 77, 1596–1605.

Gilbert, A.S., Wheeler, R.T., May, R.C., 2014. Fungal pathogens: survival and replication within macrophages. Cold Spring Harbor Perspect. Med. 5, a019661.

Gillmaier, N., Schunder, E., Kutzner, E., Tlapak, H., Rydzewski, K., Herrmann, V., Stammler, M., Lasch, P., Eisenreich, W., Heuner, K., 2016. Growth-related metabolism of the carbon storage poly-3-hydroxybutyrate in *Legionella pneumophila*. J. Biol. Chem. 291, 6471–6482.

Gontijo, F.A., de Melo, A.T., Pascon, R.C., Fernandes, L., Paes, H.C., Alspaugh, J.A., Vallim, M.A., 2017. The role of Aspartyl aminopeptidase (Ape4) in *Cryptococcus neoformans* virulence and authophagy. PLoS One 12, e0177461.

Gouzy, A., Larrouy-Maumus, G., Wu, T.D., Peixoto, A., Levillain, F., Lugo-Villarino, G., Guerquin-Kern, J.L., de Carvalho, L.P., Poquet, Y., Neyrolles, O., 2013. *Mycobacterium tuberculosis* nitrogen assimilation and host colonization require aspartate. Nat. Chem. Biol. 9, 674–676.

Gouzy, A., Larrouy-Maumus, G., Bottai, D., Levillain, F., Dumas, A., Wallach, J.B., Caire-Brandli, I., de Chastellier, C., Wu, T.D., Poincloux, R., Brosch, R., Guerquin-Kern, J.L., Schnappinger, D., Sorio de Carvalho, L.P., Poquet, Y., Neyrolles, O., 2014. *Mycobacterium tuberculosis* exploits asparagine to assimilate nitrogen and resist acid stress during infection. PLoS Pathog. 10, e1003928.

Grubmuller, S., Schauer, K., Goebel, W., Fuchs, T.M., Eisenreich, W., 2014. Analysis of carbon substrates used by *Listeria monocytogenes* during growth in J774A.1 macrophages suggests a bipartite intracellular metabolism. Front. Cell. Infect. Microbiol. 4, 156.

Guimaraes, A.J., Gomes, K.X., Cortines, J.R., Peralta, J.M., Peralta, R.H., 2016. *Acanthamoeba* spp. as a universal host for pathogenic microorganisms: one bridge from environment to host virulence. Microbiol. Res. 193, 30–38.

Haber, A., Friedman, S., Lobel, L., Burg-Golani, T., Sigal, N., Rose, J., Livnat-Levanon, N., Lewinson, O., Herskovits, A.A., 2017. L-glutamine induces expression of *Listeria monocytogenes* virulence genes. PLoS Pathog. 13, e1006161.

Harada, E., Iida, K., Shiota, S., Nakayama, H., Yoshida, S., 2010. Glucose metabolism in *Legionella pneumophila*: dependence on the Entner-Doudoroff pathway and connection with intracellular bacterial growth. J. Bacteriol. 192, 2892–2899.

Hauslein, I., Manske, C., Goebel, W., Eisenreich, W., Hilbi, H., 2016. Pathway analysis using (13) C-glycerol and other carbon tracers reveals a bipartite metabolism of *Legionella pneumophila*. Mol. Microbiol. 100, 229–246.

Hilbi, H., Haas, A., 2012. Secretive bacterial pathogens and the secretory pathway. Traffic 13, 1187–1197.

Hilty, J., George Smulian, A., Newman, S.L., 2011. *Histoplasma capsulatum* utilizes siderophores for intracellular iron acquisition in macrophages. Med. Mycol. 49, 633–642.

Hood, M.I., Skaar, E.P., 2012. Nutritional immunity: transition metals at the pathogen-host interface. Nat. Rev. Microbiol. 10, 525–537.

Horwath, M.C., Fecher, R.A., Deepe Jr., G.S., 2015. *Histoplasma capsulatum*, lung infection and immunity. Future Microbiol. 10, 967–975.

Hovel-Miner, G., Faucher, S.P., Charpentier, X., Shuman, H.A., 2010. ArgR-regulated genes are derepressed in the *Legionella*-containing vacuole. J. Bacteriol. 192, 4504–4516.

Hummert, S., Hummert, C., Schroter, A., Hube, B., Schuster, S., 2010. Game theoretical modelling of survival strategies of *Candida albicans* inside macrophages. J. Theor. Biol. 264, 312–318.

Hwang, L.H., Mayfield, J.A., Rine, J., Sil, A., 2008. Histoplasma requires SID1, a member of an iron-regulated siderophore gene cluster, for host colonization. PLoS Pathog. 4, e1000044.

Ireton, K., Rigano, L.A., Dowd, G.C., 2014. Role of host GTPases in infection by *Listeria monocytogenes*. Cell. Microbiol. 16, 1311–1320.

Isaac, D.T., Coady, A., Van Prooyen, N., Sil, A., 2013. The 3-hydroxy-methylglutaryl coenzyme A lyase HCL1 is required for macrophage colonization by human fungal pathogen *Histoplasma capsulatum*. Infect. Immun. 81, 411–420.

Jabado, N., Jankowski, A., Dougaparsad, S., Picard, V., Grinstein, S., Gros, P., 2000. Natural resistance to intracellular infections: natural resistance-associated macrophage protein 1 (Nramp1) functions as a pH-dependent manganese transporter at the phagosomal membrane. J. Exp. Med. 192, 1237–1248.

Jeschke, A., Haas, A., 2016. Deciphering the roles of phosphoinositide lipids in phago-lysosome biogenesis. Commun. Integr. Biol. 9, e1174798.

Johnson, E.E., Wessling-Resnick, M., 2012. Iron metabolism and the innate immune response to infection. Microbes Infect. 14, 207–216.

Johnston, S.A., May, R.C., 2013. *Cryptococcus* interactions with macrophages: evasion and manipulation of the phagosome by a fungal pathogen. Cell. Microbiol. 15, 403–411.

Joseph, B., Przybilla, K., Stuhler, C., Schauer, K., Slaghuis, J., Fuchs, T.M., Goebel, W., 2006. Identification of *Listeria monocytogenes* genes contributing to intracellular replication by expression profiling and mutant screening. J. Bacteriol. 188, 556–568.

Joseph, B., Mertins, S., Stoll, R., Schar, J., Umesha, K.R., Luo, Q., Muller-Altrock, S., Goebel, W., 2008. Glycerol metabolism and PrfA activity in *Listeria monocytogenes*. J. Bacteriol. 190, 5412–5430.

Juttukonda, L.J., Skaar, E.P., 2015. Manganese homeostasis and utilization in pathogenic bacteria. Mol. Microbiol. 97, 216–228.

Kasper, L., Seider, K., Hube, B., 2015. Intracellular survival of *Candida glabrata* in macrophages: immune evasion and persistence. FEMS Yeast Res. 15, fov042.

Kaur, R., Ma, B., Cormack, B.P., 2007. A family of glycosylphosphatidylinositol-linked aspartyl proteases is required for virulence of *Candida glabrata*. Proc. Natl. Acad. Sci. U. S. A. 104, 7628–7633.

Kehl-Fie, T.E., Skaar, E.P., 2010. Nutritional immunity beyond iron: a role for manganese and zinc. Curr. Opin. Chem. Biol. 14, 218–224.

Khodr, A., Kay, E., Gomez-Valero, L., Ginevra, C., Doublet, P., Buchrieser, C., Jarraud, S., 2016. Molecular epidemiology, phylogeny and evolution of *Legionella*. Infect. Genet. Evol. 43, 108–122.

Kwon-Chung, K.J., Fraser, J.A., Doering, T.L., Wang, Z., Janbon, G., Idnurm, A., Bahn, Y.S., 2014. *Cryptococcus neoformans* and *Cryptococcus gattii*, the etiologic agents of cryptococcosis. Cold Spring Harbor Perspect. Med. 4, a019760.

LaRock, D.L., Chaudhary, A., Miller, S.I., 2015. *Salmonellae* interactions with host processes. Nat. Rev. Microbiol. 13, 191–205.

Le Chevalier, F., Cascioferro, A., Frigui, W., Pawlik, A., Boritsch, E.C., Bottai, D., Majlessi, L., Herrmann, J.L., Brosch, R., 2015. Revisiting the role of phospholipases C in virulence and the lifecycle of *Mycobacterium tuberculosis*. Sci. Rep. 5, 16918.

Lee, W., VanderVen, B.C., Fahey, R.J., Russell, D.G., 2013. Intracellular *Mycobacterium tuberculosis* exploits host-derived fatty acids to limit metabolic stress. J. Biol. Chem. 288, 6788–6800.

Leon-Sicairos, N., Reyes-Cortes, R., Guadron-Llanos, A.M., Maduena-Molina, J., Leon-Sicairos, C., Canizalez-Roman, A., 2015. Strategies of intracellular pathogens for obtaining iron from the environment. BioMed Res. Int. 2015, 476534.

Leopold Wager, C.M., Hole, C.R., Wozniak, K.L., Wormley Jr., F.L., 2016. *Cryptococcus* and phagocytes: complex interactions that influence disease outcome. Front. Microbiol. 7, 105.

Lisher, J.P., Giedroc, D.P., 2013. Manganese acquisition and homeostasis at the host-pathogen interface. Front. Cell. Infect. Microbiol. 3, 91.

Liss, V., Hensel, M., 2015. Take the tube: remodelling of the endosomal system by intracellular *Salmonella enterica*. Cell. Microbiol. 17, 639–647.

Liss, V., Swart, A.L., Kehl, A., Hermanns, N., Zhang, Y., Chikkaballi, D., Bohles, N., Deiwick, J., Hensel, M., 2017. *Salmonella enterica* remodels the host cell endosomal system for efficient intravacuolar nutrition. Cell Host Microbe 21, 390–402.

Liu, Y., Filler, S.G., 2011. *Candida albicans* Als3, a multifunctional adhesin and invasin. Eukaryot. Cell 10, 168–173.

Lobel, L., Herskovits, A.A., 2016. Systems level analyses reveal multiple regulatory activities of CodY controlling metabolism, motility and virulence in *Listeria monocytogenes*. PLoS Genet. 12, e1005870.

Lobel, L., Sigal, N., Borovok, I., Ruppin, E., Herskovits, A.A., 2012. Integrative genomic analysis identifies isoleucine and CodY as regulators of *Listeria monocytogenes* virulence. PLoS Genet. 8, e1002887.

Lobel, L., Sigal, N., Borovok, I., Belitsky, B.R., Sonenshein, A.L., Herskovits, A.A., 2015. The metabolic regulator CodY links *Listeria monocytogenes* metabolism to virulence by directly activating the virulence regulatory gene prfA. Mol. Microbiol. 95, 624–644.

Lorenz, M.C., Fink, G.R., 2001. The glyoxylate cycle is required for fungal virulence. Nature 412, 83–86.

Lorenz, M.C., Fink, G.R., 2002. Life and death in a macrophage: role of the glyoxylate cycle in virulence. Eukaryot. Cell 1, 657–662.

Lorenz, M.C., Bender, J.A., Fink, G.R., 2004. Transcriptional response of *Candida albicans* upon internalization by macrophages. Eukaryot. Cell 3, 1076–1087.

Lorenz, M.C., 2013. Carbon catabolite control in *Candida albicans*: new wrinkles in metabolism. mBio 4, e00034–00013.

Ma, B., Pan, S.J., Zupancic, M.L., Cormack, B.P., 2007. Assimilation of NAD(+) precursors in *Candida glabrata*. Mol. Microbiol. 66, 14–25.

Manske, C., Hilbi, H., 2014. *Metabolism of the vacuolar pathogen Legionella* and implications for virulence. Front. Cell. Infect. Microbiol. 4, 125.

Manske, C., Schell, U., Hilbi, H., 2016. Metabolism of myo-inositol by *Legionella pneumophila* promotes infection of amoebae and macrophages. Appl. Environ. Microbiol. 82, 5000–5014.

Mao, Y., Finnemann, S.C., 2015. Regulation of phagocytosis by rho GTPases. Small GTPases 6, 89–99.

Marcil, A., Gadoury, C., Ash, J., Zhang, J., Nantel, A., Whiteway, M., 2008. Analysis of PRA1 and its relationship to *Candida albicans*- macrophage interactions. Infect. Immun. 76, 4345–4358.

Marrero, J., Rhee, K.Y., Schnappinger, D., Pethe, K., Ehrt, S., 2010. Gluconeogenic carbon flow of tricarboxylic acid cycle intermediates is critical for *Mycobacterium tuberculosis* to establish and maintain infection. Proc. Natl. Acad. Sci. U. S. A. 107, 9819–9824.

McKinney, J.D., Honer zu Bentrup, K., Munoz-Elias, E.J., Miczak, A., Chen, B., Chan, W.T., Swenson, D., Sacchettini, J.C., Jacobs Jr., W.R., Russell, D.G., 2000. Persistence of *Mycobacterium tuberculosis* in macrophages and mice requires the glyoxylate shunt enzyme isocitrate lyase. Nature 406, 735–738.

Meibom, K.L., Charbit, A., 2010. The unraveling panoply of *Francisella tularensis* virulence attributes. Curr. Opin. Microbiol. 13, 11–17.

Mertins, S., Joseph, B., Goetz, M., Ecke, R., Seidel, G., Sprehe, M., Hillen, W., Goebel, W., Muller-Altrock, S., 2007. Interference of components of the phosphoenolpyruvate phosphotransferase system with the central virulence gene regulator PrfA of *Listeria monocytogenes*. J. Bacteriol. 189, 473–490.

Michard, C., Sperandio, D., Bailo, N., Pizarro-Cerda, J., LeClaire, L., Chadeau-Argaud, E., Pombo-Gregoire, I., Hervet, E., Vianney, A., Gilbert, C., Faure, M., Cossart, P., Doublet, P., 2015. The *Legionella* kinase LegK2 targets the ARP2/3 complex to inhibit actin nucleation on phagosomes and allow bacterial evasion of the late endocytic pathway. mBio 6, e00354–00315.

Miller, H.K., Auerbuch, V., 2015. Bacterial iron-sulfur cluster sensors in mammalian pathogens. Metallomics 7, 943–956.

Miramon, P., Lorenz, M.C., 2016. The SPS amino acid sensor mediates nutrient acquisition and immune evasion in *Candida albicans*. Cell. Microbiol. 18, 1611–1624.

Miramon, P., Kasper, L., Hube, B., 2013. Thriving within the host: *Candida* spp. interactions with phagocytic cells. Med. Microbiol. Immunol. 202, 183–195.

Munoz-Elias, E.J., McKinney, J.D., 2005. *Mycobacterium tuberculosis* isocitrate lyases 1 and 2 are jointly required for in vivo growth and virulence. Nat. Med. 11, 638–644.

Munoz-Elias, E.J., Upton, A.M., Cherian, J., McKinney, J.D., 2006. Role of the methylcitrate cycle in *Mycobacterium tuberculosis* metabolism, intracellular growth, and virulence. Mol. Microbiol. 60, 1109–1122.

Nairz, M., Fritsche, G., Crouch, M.L., Barton, H.C., Fang, F.C., Weiss, G., 2009. Slc11a1 limits intracellular growth of *Salmonella enterica* sv. Typhimurium by promoting macrophage immune effector functions and impairing bacterial iron acquisition. Cell. Microbiol. 11, 1365–1381.

Nairz, M., Ferring-Appel, D., Casarrubea, D., Sonnweber, T., Viatte, L., Schroll, A., Haschka, D., Fang, F.C., Hentze, M.W., Weiss, G., Galy, B., 2015a. Iron regulatory proteins mediate host resistance to *Salmonella* infection. Cell Host Microbe 18, 254–261.

Nairz, M., Schroll, A., Demetz, E., Tancevski, I., Theurl, I., Weiss, G., 2015b. 'Ride on the ferrous wheel'–the cycle of iron in macrophages in health and disease.

Immunobiology 220, 280–294.

Napier, B.A., Meyer, L., Bina, J.E., Miller, M.A., Sjostedt, A., Weiss, D.S., 2012. Link between intraphagosomal biotin and rapid phagosomal escape in *Francisella*. Proc. Natl. Acad. Sci. U. S. A. 109, 18084–18089.

Nevitt, T., Thiele, D.J., 2011. Host iron withholding demands siderophore utilization for *Candida glabrata* to survive macrophage killing. PLoS Pathog. 7, e1001322.

Newman, S.L., Smulian, A.G., 2013. Iron uptake and virulence in *Histoplasma capsulatum*. Curr. Opin. Microbiol. 16, 700–707.

Neyrolles, O., Mintz, E., Catty, P., 2013. Zinc and copper toxicity in host defense against pathogens: *Mycobacterium tuberculosis* as a model example of an emerging paradigm. Front. Cell. Infect. Microbiol. 3, 89.

Neyrolles, O., Wolschendorf, F., Mitra, A., Niederweis, M., 2015. *Mycobacteria*, metals, and the macrophage. Immunol. Rev. 264, 249–263.

Nicola, A.M., Albuquerque, P., Martinez, L.R., Dal-Rosso, R.A., Saylor, C., De Jesus, M., Nosanchuk, J.D., Casadevall, A., 2012. Macrophage autophagy in immunity to *Cryptococcus neoformans* and *Candida albicans*. Infect. Immun. 80, 3065–3076.

O'Connor, T.J., Zheng, H., VanRheenen, S.M., Ghosh, S., Cianciotto, N.P., Isberg, R.R., 2016. Iron limitation triggers early egress by the intracellular bacterial pathogen *Legionella pneumophila*. Infect. Immun. 84, 2185–2197.

O'Riordan, M., Moors, M.A., Portnoy, D.A., 2003. *Listeria* intracellular growth and virulence require host-derived lipoic acid. Science 302, 462–464.

Odds, F.C., 1988. *Candida* and Candidosis: a Review and Bibliography, 2nd edition. Bailliere Tindall, London, UK.

Palmer, G.E., Kelly, M.N., Sturtevant, J.E., 2007. Autophagy in the pathogen *Candida albicans*. Microbiology 153, 51–58.

Pandey, A.K., Sassetti, C.M., 2008. Mycobacterial persistence requires the utilization of host cholesterol. Proc. Natl. Acad. Sci. U. S. A. 105, 4376–4380.

Paradkar, P.N., De Domenico, I., Durchfort, N., Zohn, I., Kaplan, J., Ward, D.M., 2008. Iron depletion limits intracellular bacterial growth in macrophages. Blood 112, 866–874.

Pauwels, A.M., Trost, M., Beyaert, R., Hoffmann, E., 2017. Patterns, receptors, and signals: regulation of phagosome maturation. Trends Immunol. 38, 407–422.

Perez, N.M., Ramakrishnan, G., 2014. The reduced genome of the *Francisella tularensis* live vaccine strain (LVS) encodes two iron acquisition systems essential for optimal growth and virulence. PLoS One 9, e93558.

Pollard, J.W., 2009. Trophic macrophages in development and disease. Nat. Rev. Immunol. 9, 259–270.

Popp, J., Noster, J., Busch, K., Kehl, A., Zur Hellen, G., Hensel, M., 2015. Role of host cell-derived amino acids in nutrition of intracellular *Salmonella enterica*. Infect. Immun. 83, 4466–4475.

Portier, E., Zheng, H., Sahr, T., Burnside, D.M., Mallama, C., Buchrieser, C., Cianciotto, N.P., Hechard, Y., 2015. IroT/mavN, a new iron-regulated gene involved in *Legionella pneumophila* virulence against amoebae and macrophages. Environ. Microbiol. 17, 1338–1350.

Price, C.T., Al-Quadan, T., Santic, M., Rosenshine, I., Abu Kwaik, Y., 2011. Host proteasomal degradation generates amino acids essential for intracellular bacterial growth. Science 334, 1553–1557.

Py, B.F., Lipinski, M.M., Yuan, J., 2007. Autophagy limits *Listeria monocytogenes* intracellular growth in the early phase of primary infection. Autophagy 3, 117–125.

Rai, M.N., Balusu, S., Gorityala, N., Dandu, L., Kaur, R., 2012. Functional genomic analysis of *Candida glabrata*-macrophage interaction: role of chromatin remodeling in virulence. PLoS Pathog. 8, e1002863.

Ramakrishnan, G., Sen, B., Johnson, R., 2012. Paralogous outer membrane proteins mediate uptake of different forms of iron and synergistically govern virulence in *Francisella tularensis tularensis*. J. Biol. Chem. 287, 25191–25202.

Ramond, E., Gesbert, G., Barel, M., Charbit, A., 2012. Proteins involved in *Francisella tularensis* survival and replication inside macrophages. Future Microbiol. 7, 1255–1268.

Ramond, E., Gesbert, G., Rigard, M., Dairou, J., Dupuis, M., Dubail, I., Meibom, K., Henry, T., Barel, M., Charbit, A., 2014. Glutamate utilization couples oxidative stress defense and the tricarboxylic acid cycle in *Francisella* phagosomal escape. PLoS Pathog. 10, e1003893.

Ramond, E., Gesbert, G., Guerrera, I.C., Chhuon, C., Dupuis, M., Rigard, M., Henry, T., Barel, M., Charbit, A., 2015. Importance of host cell arginine uptake in *Francisella* phagosomal escape and ribosomal protein amounts. Mol. Cell. Proteomics 14, 870–881.

Raynaud, C., Guilhot, C., Rauzier, J., Bordat, Y., Pelicic, V., Manganelli, R., Smith, I., Gicquel, B., Jackson, M., 2002. Phospholipases C are involved in the virulence of *Mycobacterium tuberculosis*. Mol. Microbiol. 45, 203–217.

Reddi, A.R., Jensen, L.T., Naranuntarat, A., Rosenfeld, L., Leung, E., Shah, R., Culotta, V.C., 2009. The overlapping roles of manganese and Cu/Zn SOD in oxidative stress protection. Free Radic. Biol. Med. 46, 154–162.

Ren, Y., Khan, F.A., Pandupuspitasari, N.S., Zhang, S., 2017. Immune evasion strategies of pathogens in macrophages: the potential for limiting pathogen transmission. Curr. Issues Mol. Biol. 21, 21–40.

Reniere, M.L., Whiteley, A.T., Hamilton, K.L., John, S.M., Lauer, P., Brennan, R.G., Portnoy, D.A., 2015. Glutathione activates virulence gene expression of an intracellular pathogen. Nature 517, 170–173.

Robertson, P., Abdelhady, H., Garduno, R.A., 2014. The many forms of a pleomorphic bacterial pathogen-the developmental network of *Legionella pneumophila*. Front. Microbiol. 5, 670.

Rodriguez, G.M., Smith, I., 2006. Identification of an ABC transporter required for iron acquisition and virulence in *Mycobacterium tuberculosis*. J. Bacteriol. 188, 424–430.

Roetzer, A., Gratz, N., Kovarik, P., Schuller, C., 2010. Autophagy supports *Candida glabrata* survival during phagocytosis. Cell. Microbiol. 12, 199–216.

Rowland, J.L., Niederweis, M., 2012. Resistance mechanisms of *Mycobacterium*

tuberculosis against phagosomal copper overload. Tuberculosis (Edinb) 92, 202–210.

Runyen-Janecky, L., Dazenski, E., Hawkins, S., Warner, L., 2006. Role and regulation of the *Shigella flexneri* sit and MntH systems. Infect. Immun. 74, 4666–4672.

Russell, D.G., VanderVen, B.C., Lee, W., Abramovitch, R.B., Kim, M.J., Homolka, S., Niemann, S., Rohde, K.H., 2010. *Mycobacterium tuberculosis* wears what it eats. Cell Host Microbe 8, 68–76.

Sabina, J., Brown, V., 2009. Glucose sensing network in *Candida albicans*: a sweet spot for fungal morphogenesis. Eukaryot. Cell 8, 1314–1320.

Sarantis, H., Grinstein, S., 2012. Subversion of phagocytosis for pathogen survival. Cell Host Microbe 12, 419–431.

Sauer, J.D., Bachman, M.A., Swanson, M.S., 2005. The phagosomal transporter A couples threonine acquisition to differentiation and replication of *Legionella pneumophila* in macrophages. Proc. Natl. Acad. Sci. U. S. A. 102, 9924–9929.

Savvi, S., Warner, D.F., Kana, B.D., McKinney, J.D., Mizrahi, V., Dawes, S.S., 2008. Functional characterization of a vitamin B12-dependent methylmalonyl pathway in *Mycobacterium tuberculosis*: implications for propionate metabolism during growth on fatty acids. J. Bacteriol. 190, 3886–3895.

Schar, J., Stoll, R., Schauer, K., Loeffler, D.I., Eylert, E., Joseph, B., Eisenreich, W., Fuchs, T.M., Goebel, W., 2010. Pyruvate carboxylase plays a crucial role in carbon metabolism of extra- and intracellularly replicating *Listeria monocytogenes*. J. Bacteriol. 192, 1774–1784.

Schunder, E., Gillmaier, N., Kutzner, E., Eisenreich, W., Herrmann, V., Lautner, M., Heuner, K., 2014. Amino acid uptake and metabolism of *Legionella pneumophila* hosted by *Acanthamoeba castellanii*. J. Biol. Chem. 289, 21040–21054.

Scortti, M., Monzo, H.J., Lacharme-Lora, L., Lewis, D.A., Vazquez-Boland, J.A., 2007. The PrfA virulence regulon. Microbes Infect. 9, 1196–1207.

Seider, K., Heyken, A., Luttich, A., Miramon, P., Hube, B., 2010. Interaction of pathogenic yeasts with phagocytes: survival, persistence and escape. Curr. Opin. Microbiol. 13, 392–400.

Seider, K., Brunke, S., Schild, L., Jablonowski, N., Wilson, D., Majer, O., Barz, D., Haas, A., Kuchler, K., Schaller, M., Hube, B., 2011. The facultative intracellular pathogen *Candida glabrata* subverts macrophage cytokine production and phagolysosome maturation. J. Immunol. 187, 3072–3086.

Seider, K., Gerwien, F., Kasper, L., Allert, S., Brunke, S., Jablonowski, N., Schwarzmuller, T., Barz, D., Rupp, S., Kuchler, K., Hube, B., 2014. Immune evasion, stress resistance, and efficient nutrient acquisition are crucial for intracellular survival of *Candida glabrata* within macrophages. Eukaryot. Cell 13, 170–183.

Smeekens, S.P., Malireddi, R.K., Plantinga, T.S., Buffen, K., Oosting, M., Joosten, L.A., Kullberg, B.J., Perfect, J.R., Scott, W.K., van de Veerdonk, F.L., Xavier, R.J., van de Vosse, E., Kanneganti, T.D., Johnson, M.D., Netea, M.G., 2014. Autophagy is redundant for the host defense against systemic *Candida albicans* infections. Eur. J. Clin. Microbiol. Infect. Dis. 33, 711–722.

Soldati, T., Neyrolles, O., 2012. *Mycobacteria* and the intraphagosomal environment: take it with a pinch of salt(s)!. Traffic 13, 1042–1052.

Speer, A., Sun, J., Danilchanka, O., Meikle, V., Rowland, J.L., Walter, K., Buck, B.R., Pavlenok, M., Holscher, C., Ehrt, S., Niederweis, M., 2015. Surface hydrolysis of sphingomyelin by the outer membrane protein Rv0888 supports replication of *Mycobacterium tuberculosis* in macrophages. Mol. Microbiol. 97, 881–897.

Srivastava, V.K., Suneetha, K.J., Kaur, R., 2014. A systematic analysis reveals an essential role for high-affinity iron uptake system, haemolysin and CFEM domain-containing protein in iron homoeostasis and virulence in *Candida glabrata*. Biochem. J. 463, 103–114.

Steeb, B., Claudi, B., Burton, N.A., Tienz, P., Schmidt, A., Farhan, H., Maze, A., Bumann, D., 2013. Parallel exploitation of diverse host nutrients enhances *Salmonella* virulence. PLoS Pathog. 9, e1003301.

Steele, S., Brunton, J., Ziehr, B., Taft-Benz, S., Moorman, N., Kawula, T., 2013. *Francisella tularensis* harvests nutrients derived via ATG5-independent autophagy to support intracellular growth. PLoS Pathog. 9, e1003562.

Steele, S., Brunton, J., Kawula, T., 2015. The role of autophagy in intracellular pathogen nutrient acquisition. Front. Cell. Infect. Microbiol. 5, 51.

Stein, M.P., Muller, M.P., Wandinger-Ness, A., 2012. Bacterial pathogens commandeer Rab GTPases to establish intracellular niches. Traffic 13, 1565–1588.

Stoll, R., Mertins, S., Joseph, B., Muller-Altrock, S., Goebel, W., 2008. Modulation of PrfA activity in *Listeria monocytogenes* upon growth in different culture media. Microbiology 154, 3856–3876.

Su, C., Lu, Y., Liu, H., 2016. N-acetylglucosamine sensing by a GCN5-related N-acetyltransferase induces transcription via chromatin histone acetylation in fungi. Nat. Commun. 7, 12916.

Subramanian Vignesh, K., Landero Figueroa, J.A., Porollo, A., Caruso, J.A., Deepe Jr., G.S., 2013. Granulocyte macrophage-colony stimulating factor induced Zn

sequestration enhances macrophage superoxide and limits intracellular pathogen survival. Immunity 39, 697–710.

Subramanian Vignesh, K., Landero Figueroa, J.A., Porollo, A., Divanovic, S., Caruso, J.A., Deepe Jr., G.S., 2016. IL-4 induces metallothionein 3- and SLC30A4-dependent increase in intracellular Zn(2+) that promotes pathogen persistence in macrophages. Cell Rep. 16, 3232–3246.

Suzuki, H., Kunisawa, J., 2015. Vitamin-mediated immune regulation in the development of inflammatory diseases. Endocr. Metab. Immune Disord. Drug Targets 15, 212–215.

Tobin, D.M., Ramakrishnan, L., 2008. Comparative pathogenesis of *Mycobacterium marinum* and *Mycobacterium tuberculosis*. Cell. Microbiol. 10, 1027–1039.

Toledo, A., Benach, J.L., 2015. Hijacking and use of host lipids by intracellular pathogens. Microbiol. Spectrum 3.

Towle, H.C., 2005. Glucose as a regulator of eukaryotic gene transcription. Trends Endocrinol. Metab. 16, 489–494.

Vazquez-Boland, J.A., Kuhn, M., Berche, P., Chakraborty, T., Dominguez-Bernal, G., Goebel, W., Gonzalez-Zorn, B., Wehland, J., Kreft, J., 2001. *Listeria* pathogenesis and molecular virulence determinants. Clin. Microbiol. Rev. 14, 584–640.

Vieira, N., Casal, M., Johansson, B., MacCallum, D.M., Brown, A.J., Paiva, S., 2010. Functional specialization and differential regulation of short-chain carboxylic acid transporters in the pathogen *Candida albicans*. Mol. Microbiol. 75, 1337–1354.

Vylkova, S., Lorenz, M.C., 2014. Modulation of phagosomal pH by *Candida albicans* promotes hyphal morphogenesis and requires Stp2p, a regulator of amino acid transport. PLoS Pathog. 10, e1003995.

Vylkova, S., Carman, A.J., Danhof, H.A., Collette, J.R., Zhou, H., Lorenz, M.C., 2011. The fungal pathogen *Candida albicans* autoinduces hyphal morphogenesis by raising extracellular pH. mBio 2, e00055–00011.

Ward, S.K., Abomoelak, B., Hoye, E.A., Steinberg, H., Talaat, A.M., 2010. CtpV: a putative copper exporter required for full virulence of *Mycobacterium tuberculosis*. Mol. Microbiol. 77, 1096–1110.

Waterman, S.R., Hacham, M., Hu, G., Zhu, X., Park, Y.D., Shin, S., Panepinto, J., Valyi-Nagy, T., Beam, C., Husain, S., Singh, N., Williamson, P.R., 2007. Role of a CUF1/CTR4 copper regulatory axis in the virulence of *Cryptococcus neoformans*. J. Clin. Invest. 117, 794–802.

Waterman, S.R., Park, Y.D., Raja, M., Qiu, J., Hammoud, D.A., O'Halloran, T.V., Williamson, P.R., 2012. Role of CTR4 in the virulence of *Cryptococcus neoformans*. mBio 3 (5) pii: e00285-12.

Watson, R.O., Manzanillo, P.S., Cox, J.S., 2012. Extracellular *M. tuberculosis* DNA targets bacteria for autophagy by activating the host DNA-sensing pathway. Cell 150, 803–815.

Weiss, G., Schaible, U.E., 2015. Macrophage defense mechanisms against intracellular bacteria. Immunol. Rev. 264, 182–203.

Weissman, Z., Berdicevsky, I., Cavari, B.Z., Kornitzer, D., 2000. The high copper tolerance of *Candida albicans* is mediated by a P-type ATPase. Proc. Natl. Acad. Sci. U. S. A. 97, 3520–3525.

White, C., Lee, J., Kambe, T., Fritsche, K., Petris, M.J., 2009. A role for the ATP7A copper-transporting ATPase in macrophage bactericidal activity. J. Biol. Chem. 284, 33949–33956.

Wieland, H., Ullrich, S., Lang, F., Neumeister, B., 2005. Intracellular multiplication of *Legionella pneumophila* depends on host cell amino acid transporter SLC1A5. Mol. Microbiol. 55, 1528–1537.

Winters, M.S., Chan, Q., Caruso, J.A., Deepe Jr., G.S., 2010. Metallomic analysis of macrophages infected with *Histoplasma capsulatum* reveals a fundamental role for zinc in host defenses. J. Infect. Dis. 202, 1136–1145.

Wolschendorf, F., Ackart, D., Shrestha, T.B., Hascall-Dove, L., Nolan, S., Lamichhane, G., Wang, Y., Bossmann, S.H., Basaraba, R.J., Niederweis, M., 2011. Copper resistance is essential for virulence of *Mycobacterium tuberculosis*. Proc. Natl. Acad. Sci. U. S. A. 108, 1621–1626.

Wright, L.C., Santangelo, R.M., Ganendren, R., Payne, J., Djordjevic, J.T., Sorrell, T.C., 2007. *Cryptococcal* lipid metabolism: phospholipase B1 is implicated in transcellular metabolism of macrophage-derived lipids. Eukaryot. Cell 6, 37–47.

Yu, J., Niu, C., Wang, D., Li, M., Teo, W., Sun, G., Wang, J., Liu, J., Gao, Q., 2011. MMAR_2770, a new enzyme involved in biotin biosynthesis, is essential for the growth of *Mycobacterium marinum* in macrophages and zebrafish. Microbes Infect. 13, 33–41.

Zackular, J.P., Chazin, W.J., Skaar, E.P., 2015. Nutritional immunity: S100 proteins at the host-pathogen interface. J. Biol. Chem. 290, 18991–18998.

Zempleni, J., Wijeratne, S.S., Hassan, Y.I., 2009. Biotin. Biofactors 35, 36–46.

Ziveri, J., Barel, M., Charbit, A., 2017. Importance of metabolic adaptations in *Francisella* pathogenesis. Front. Cell. Infect. Microbiol. 7, 96.

2.2 Manuscript II: Sprenger *et al., Cell. Microbiol.*, 2020

Fungal biotin homeostasis is essential for immune evasion after macrophage phagocytosis and virulence

Marcel Sprenger, Teresa Sofie Hartung, Stefanie Allert, Stephanie Wisgott, Maria Joanna Niemiec, Katja Graf, Ilse D. Jacobsen, Lydia Kasper and Bernhard Hube

Summary

The vitamin biotin is essential for all organisms, including human pathogenic microbes like fungi of the genus *Candida* as well as their mammalian hosts. *Candida* spp. are auxotrophic for this vitamin and must thus possess an efficient uptake system to allow biotin acquisition during infection. This study characterized a conserved metabolic pathway facilitating biotin homeostasis in two medically important *Candida* species, *C. albicans* and *C. glabrata*.

Biotin-related genes are upregulated upon phagocytosis by macrophages and the transcription factor Vhr1 is mainly involved in this regulation. The intracellular proliferation of both *Candida* species was reduced by biotin pre-starvation and deletion of *VHR1* or the biotin importer gene *VHT1*. Moreover, *VHT1* was essential for full virulence of *C. albicans* and the colonization of certain mouse organs. This study showed the first time biotin acquisition of *C. albicans* and *C. glabrata* mediated by Vht1 is linked to immune evasion and virulence.

Own contribution

Marcel Sprenger planned, performed and evaluated all experiments, interpreted the data of following experiments: construction of deletion and complementation strains (Cgvhr1Δ, *Cgvhr1Δ - CgVHR1*, *Cgvht1Δ*, *Cgvht1Δ - CgVHT1*, *Cavht1Δ/Δ*, and *Cavht1Δ/Δ - CaVHT1*), their verification by PCR and Southern blot, growth and filamentation assays in different formats, RNA isolation and qRT-PCR, macrophage confrontation assays and animal experiments. The co-authors assisted in the generation and verification of mutant strains, the design and conceptualization of the study, the application and performance of the animal experiments, and editing of the initial manuscript. Marcel Sprenger wrote the manuscript and generated all figures.

Estimated authors' contributions:

Marcel Sprenger	**54%**
Teresa Sofie Hartung	6%
Stefanie Allert	5%
Stephanie Wisgott	2%
Maria Joanna Niemiec	1%
Katja Graf	1%
Ilse D. Jacobsen	4%
Lydia Kasper	20%
Bernhard Hube	7%

_____

Prof. Bernhard Hube

RESEARCH ARTICLE

WILEY

Fungal biotin homeostasis is essential for immune evasion after macrophage phagocytosis and virulence

Marcel Sprenger[1] | Teresa S. Hartung[1] | Stefanie Allert[1] |
Stephanie Wisgott[1] | Maria J. Niemiec[2,3] | Katja Graf[1] | Ilse D. Jacobsen[2,3,4] |
Lydia Kasper[1] | Bernhard Hube[1,4]

[1]Department of Microbial Pathogenicity Mechanisms, Leibniz Institute for Natural Product Research and Infection Biology, Hans Knoell Institute, Jena, Germany

[2]Research Group Microbial Immunology, Leibniz Institute for Natural Product Research and Infection Biology, Hans Knoell Institute, Jena, Germany

[3]Center for Sepsis Control and Care (CSCC), Jena University Hospital, Jena, Germany

[4]Institute of Microbiology, Friedrich Schiller University, Jena, Germany

Correspondence
Lydia Kasper and Bernhard Hube, Department of Microbial Pathogenicity Mechanisms, Leibniz Institute for Natural Product Research and Infection Biology, Hans Knoell Institute, Jena, Germany.
Email: lydia.kasper@leibniz-hki.de (L. K.) and bernhard.hube@leibniz-hki.de (B. H.)

Present address
Teresa S. Hartung, Department of Medical Immunology, Charité, Berlin, Germany

Funding information
Deutsche Forschungsgemeinschaft SPP 1580, Grant/Award Number: Hu 528/17-1

Abstract

Biotin is an important cofactor for multiple enzymes in central metabolic processes. While many bacteria and most fungi are able to synthesise biotin *de novo*, *Candida* spp. are auxotrophic for this vitamin and thus require efficient uptake systems to facilitate biotin acquisition during infection. Here we show that *Candida glabrata* and *Candida albicans* use a largely conserved system for biotin uptake and regulation, consisting of the high-affinity biotin transporter Vht1 and the transcription factor Vhr1. Both species induce expression of biotin-metabolic genes upon *in vitro* biotin depletion and following phagocytosis by macrophages, indicating low biotin levels in the *Candida*-containing phagosome. In line with this, we observed reduced intracellular proliferation of both *Candida* cells pre-starved of biotin and deletion mutants lacking *VHR1* or *VHT1* genes. *VHT1* was essential for the full virulence of *C. albicans* during systemic mouse infections, and the lack of *VHT1* led to reduced fungal burden in *C. glabrata*-infected brains and *C. albicans*-infected brains and kidneys. Together, our data suggest a critical role of Vht1-mediated biotin acquisition for *C. glabrata* and *C. albicans* during intracellular growth in macrophages and systemic infections.

KEYWORDS

biotin, *Candida albicans*, *Candida glabrata*, macrophage, metabolism, virulence

1 | INTRODUCTION

The ability to acquire macronutrients, such as carbon and nitrogen sources, and micronutrients, such as trace metals and vitamins, is of vital importance for all organisms. Vitamins, although required in very small quantities, are involved in numerous cellular processes (Combs & McClung, 2017; Dakshinamurti, 2005). During microbial infections, vitamin availability becomes important at the host–pathogen interface. On one hand, the host vitamin status is important for immune functions, on the other hand, pathogens need to synthesise or acquire vitamins in order to proliferate in the host (Combs & McClung, 2017; Mikkelsen, Stojanovska, Prakash, & Apostolopoulos, 2017; Stephensen, 2001). In this study, we investigate the requirement of biotin (vitamin H or vitamin B7) for human pathogenic *Candida* species. This vitamin is known to be crucial for key metabolic pathways, like gluconeogenesis and amino acid and fatty acid metabolism, which require the activity of

Lydia Kasper and Bernhard Hube contributed equally to this work.

biotin-dependent carboxylases (Knowles, 1989; Tong, 2013; Zempleni, Wijeratne, & Hassan, 2009).

While mammals need to take up biotin as part of their diet (Zempleni et al., 2009), many bacterial and fungal pathogens are able to synthesise biotin *de novo* (Garfoot, Zemska, & Rappleye, 2014; Magliano, Flipphi, Sanglard, & Poirier, 2011; Magnusdottir, Ravcheev, de Crecy-Lagard, & Thiele, 2015; Napier et al., 2012; Salaemae, Booker, & Polyak, 2016). In contrast, yeasts belonging to the *Candida* genus, including opportunistic pathogens (Pfaller & Diekema, 2007), are biotin auxotrophs (Littman & Miwatani, 1963; McVeigh & Bell, 1951). Medically important *Candida* spp. colonise the oral cavity, urogenital, or gastrointestinal tract as harmless commensals (Huffnagle & Noverr, 2013), but can also cause disease ranging from superficial mucosal to systemic infections with dissemination throughout the body and infection of internal organs (Odds, 1988). *Candida albicans* is the most prevalent cause of systemic candidiasis, followed by *Candida glabrata* and other non-*albicans Candida* species (Horn et al., 2009; Lindberg, Hammarstrom, Ataollahy, & Kondori, 2019).

The fact that *Candida* species are successful pathogens despite biotin-auxotrophy and blocking biotin biosynthesis in fungi like *Histoplasma capsulatum* or *Aspergillus nidulans* does not reduce virulence (Garfoot et al., 2014; Purnell, 1973), suggests that there is sufficient biotin in the host to allow normal growth and virulence of fungal pathogens (Meir & Osherov, 2018). These findings, however, also implicate that fungal pathogens, especially *Candida* species, must possess efficient uptake systems to acquire biotin during infection. This may be especially challenging in nutrient-poor host compartments, like the macrophage phagosome. Macrophages are important effectors of the innate immune system, which can recognise, ingest, and kill microbes including *Candida* species (Erwig & Gow, 2016; Miramón, Kasper, & Hube, 2013). The compartmentalisation in phagosomes is assumed to be a major mechanism to control microbial growth by increasing the efficiency of antimicrobial activities, but also by restricting nutrients (Haas, 2007; Sprenger, Kasper, Hensel, & Hube, 2017). Indeed, transcriptional profiling of fungal responses to macrophage phagocytosis suggests that *C. albicans* and *C. glabrata* experience nutrient limitation inside the phagosome (Chew et al., 2019; Childers et al., 2016; Kaur, Ma, & Cormack, 2007; Lorenz, Bender, & Fink, 2004; Roetzer, Gratz, Kovarik, & Schüller, 2010). Both *C. albicans* and *C. glabrata*, however, can adapt to macrophage antimicrobial activities and phagosomal nutrient conditions, proliferate intracellularly, and escape from these phagocytes (Miramón et al., 2013). Survival strategies, although sharing basic concepts, differ between the two species. Phagocytosed *C. albicans* yeast cells rapidly start to form hyphae, damage macrophage membranes, and escape after host cell death and via hyphal outgrowth (Kasper et al., 2018; McKenzie et al., 2010; Vylkova & Lorenz, 2014; Westman, Moran, Mogavero, Hube, & Grinstein, 2018). In contrast, *C. glabrata* replicates as yeast cells, is able to persist intracellularly for several days without causing damage, and finally escapes from macrophage by unknown mechanisms (Kaur et al., 2007; Seider et al., 2011).

In this study, we investigated the relevance of biotin acquisition of *C. albicans* and *C. glabrata* for growth, during interaction with macrophages, and systemic infection.

2 | RESULTS

2.1 | Pathogenic *Candida* species require biotin or biotin precursors for growth

While many bacterial and fungal species are able to synthesise the essential vitamin biotin *de novo*, most multicellular eukaryotes (excluding plants) and many yeasts are biotin auxotrophic (Roje, 2007). To find out how different medically important *Candida* species cope with biotin limitation, we analysed growth of *C. albicans*, *C. glabrata*, *C. dubliniensis*, *C. parapsilosis*, *C. tropicalis* and *C. auris* in minimal medium lacking biotin or containing different biotin sources. As expected, all tested species grew well in the presence of biotin, but showed drastically reduced growth rates in the absence of biotin (Figures 1a,b and Figure S1). Growth defects in biotin-depleted media were more pronounced when *C. albicans* and *C. glabrata* were pre-starved in biotin-free medium prior to the experiment, suggesting that both yeasts can use biotin from intracellular stores (Figure 1b). In host niches like the gut, which are colonised by multiple microbes of the microbiota, *Candida* cells may have access to biotin biosynthesis intermediates such as 7-keto-8-aminopelargonic acid (KAPA) or desthiobiotin (DTB) produced by these other microbes (Hill, 1997). While *C. albicans* and *C. tropicalis* grew in the presence of either KAPA or DTB, *C. dubliniensis* and *C. auris* only grew in the presence of DTB, and *C. glabrata* and *C. parapsilosis* were unable to effectively utilise these biotin intermediates (Figures 1a,b and S1a).

Candida albicans, in contrast to *C. glabrata*, is a polymorphic fungus that can grow as yeast or hyphae depending on the environmental conditions (Sudbery, 2011). The induction of germ tubes was unaffected by biotin pre-starvation or the availability of biotin, DTB or KAPA (Figure 1c). However, filament elongation was significantly reduced in medium lacking biotin or its precursors, as seen by reduced hyphal length after 4 hr with pre-starved *C. albicans* cells (Figure 1d) and reduced size of hyphal microcolonies after 24 hr (Figure 1e).

Mammalian cells can recycle biotin by proteolytic digestion of biotinylated proteins, releasing biocytin, which is further degraded to lysine and biotin (Zempleni, Hassan, & Wijeratne, 2008). To determine whether *Candida* spp. cells are able to utilise these potential host biotin sources, we analysed the growth of *C. albicans* and *C. glabrata* in the presence of biotinylated BSA or biocytin. Indeed, both species grew in the presence of biotinylated BSA or biocytin (Figure S1b).

Of note, biotin is not essential under all growth conditions. We found that the growth defect of *C. glabrata* and *C. albicans* in the absence of biotin was partly rescued when aspartate was added as a nitrogen source instead of ammonium sulfate (Figure S1c) or when casamino acids were present as the sole carbon and nitrogen source (Figure S3b,d). In fact, aspartate can be converted to the central metabolite oxaloacetate in a biotin-independent reaction (Yagi,
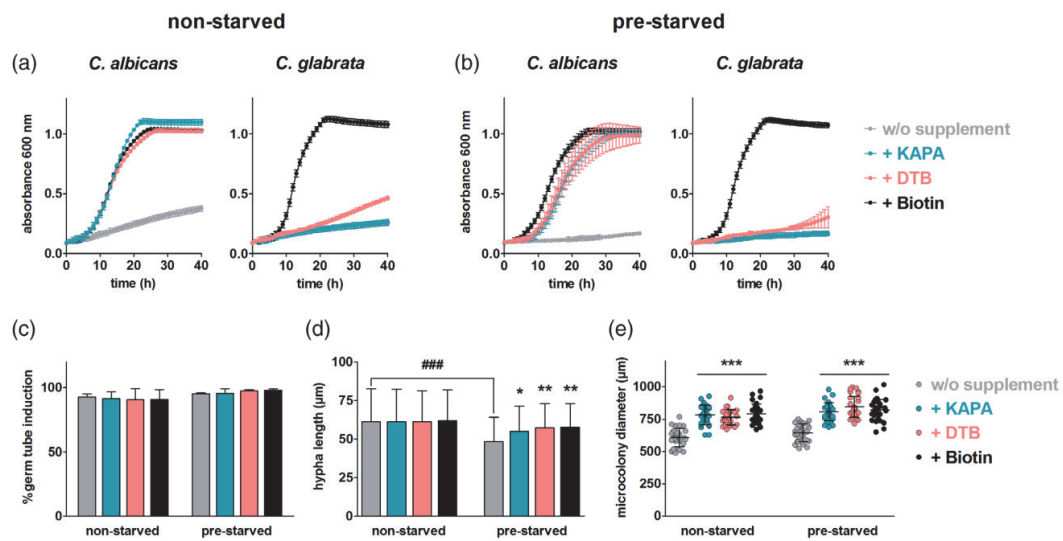
FIGURE 1 *Candida* spp. are auxotrophic for biotin. Yeast growth of (a) biotin non-starved (pre-cultured in YPD) or (b) biotin pre-starved (pre-cultured in biotin-free minimal medium) *Candida* cells in minimal medium containing biotin or biotin precursors (2 μg/L) or no biotin (w/o supplement) at 30°C. (c–e) Hyphal growth of non-starved or pre-starved *Candida albicans* cells in RPMI1640 containing biotin or biotin precursors (2 μg/L) or no biotin (w/o supplement) at 37°C and 5% CO2. (c) Percentage of germ tube-forming cells at 2 hr. (d) Hyphal length at 4 hr (mean + SD of individual hyphae from three replicates). (e) Microcolony size at 24 hr, as a measure for long-term hypha formation (each single dot represents one individual microcolony). Values are represented as mean ± SD (a,b) or mean + SD (c–e) of at least three replicates. For statistical analysis, a repeated measures ANOVA with Bonferroni's multiple comparison test was used (*p ≤ .05, **p ≤ .01, ***p ≤ .001; comparing biotin or precursor supplementation to control w/o supplement and ###p ≤ .001; comparing non-starved to pre-starved cells)

Kagamiyama, & Nozaki, 1982). This likely bypasses the need of the biotin-dependent pyruvate carboxylase for production of oxaloacetate by carboxylation of pyruvate (Ruiz-Amil, De Torrontegui, Palacian, Catalina, & Losada, 1965).

These data show that, under standard culture conditions, the presence of biotin, its precursors, or potential host biotin sources are essential for the growth of different pathogenic *Candida* species.

2.2 | *C. glabrata* and *C. albicans* genomes contain potential biotin-metabolic and regulatory genes

Biotin acquisition, biosynthesis, and regulation of these processes have been described in the model yeast *Saccharomyces cerevisiae* (Phalip, Kuhn, Lemoine, & Jeltsch, 1999; Stolz, 2009; Stolz, Hoja, Meier, Sauer, & Schweizer, 1999; Weider, Machnik, Klebl, & Sauer, 2006). To identify genes necessary for biotin acquisition and the maintenance of biotin homeostasis in the most frequently isolated *Candida* species, *C. glabrata* and *C. albicans*, we searched the genomes of these species for potential orthologs of *S. cerevisiae* biotin-related genes.

The biotin biosynthesis pathway was completely lost in the last common ancestor of *Candida* and *Saccharomyces* species, but has been partially rebuilt through horizontal gene transfer from bacterial

species, resulting in the *S. cerevisiae BIO2-5* incomplete biotin biosynthesis cluster which allows biotin synthesis from the precursor KAPA or DTB (Fitzpatrick, O'Gaora, Byrne, & Butler, 2010; Hall & Dietrich, 2007; Figure 2a). The *C. albicans* genome contains potential orthologs of the *S. cerevisiae* genes encoding the enzymes Bio2, Bio3 and Bio4 (CR_01930C, *CaBIO2*; CR_01920W, *CaBIO3*; CR_01910C, *CaBIO4*) (Fitzpatrick et al., 2010; Figures 2b and Figure S4). Although *C. glabrata* is more closely related to *S. cerevisiae* than to *C. albicans*, we did not identify potential Bio2-4 orthologs in this yeast, indicating a loss of biotin biosynthetic genes (Figure 2b). Orthologs of the potential KAPA and 7,8-Diaminopelargonic Acid (DAPA) transporter Bio5 (Phalip et al., 1999), however, were identified in both genomes (CR_01900C and CAGL0H03399g). The uptake of biotin or its precursor, DTB, is facilitated by the *S. cerevisiae* high-affinity H$^+$-biotin symporter, Vht1 (vitamin H transporter 1) (Stolz et al., 1999). We found two putative *C. glabrata* orthologs (CAGL0K04609g, CAGL0K04565g), while the two best hits in *C. albicans* were CR_06790C and CR_06660W (Figure 2b). In addition, *C. albicans* CR_03270W has recently been described as a putative biotin transporter gene (Gaur et al., 2008). All potential orthologs contain 10–12 putative transmembrane helices, a feature common in plasma membrane transporters (Sonnhammer, von Heijne, & Krogh, 1998). To narrow down potential functional orthologs of biotin or biotin precursor transporter genes, we analysed gene expression in *C. albicans* and *C. glabrata* at different biotin levels
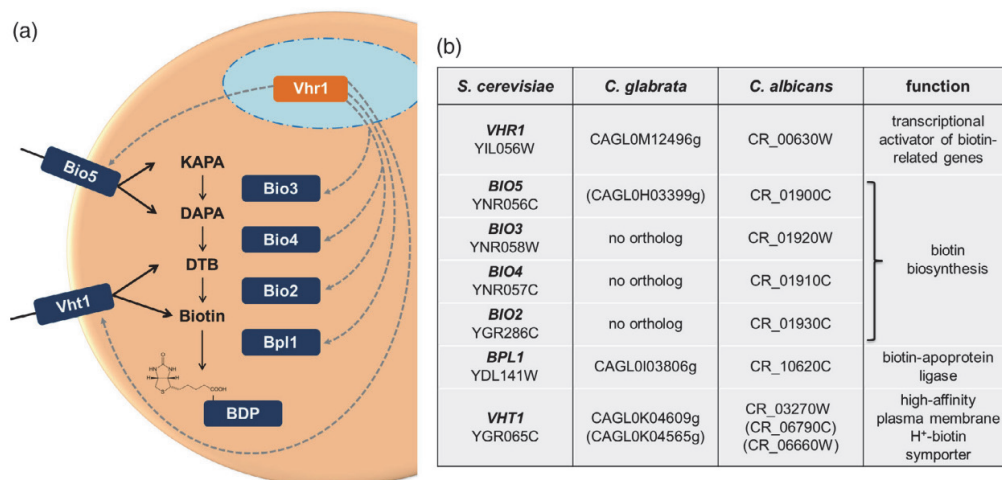
FIGURE 2 *In silico* identification of biotin transport, biosynthesis and regulatory genes. (a) Overview of *S. cerevisiae* biotin biosynthesis, transport and gene regulation. The incomplete biotin biosynthesis pathway consists of Bio5 (transporter for KAPA and DAPA), the metabolic enzymes Bio3 (7,8-diamino-pelargonic acid aminotransferase), Bio4 (desthiobiotin synthetase) and Bio2 (biotin synthase). The uptake of biotin (or DTB) from the environment is facilitated by the high-affinity transporter Vht1 (vitamin H transporter 1). The transcription factor Vhr1 regulates the expression of *BIO*-genes and *VHT1* in response to biotin availability. Biotin is covalently linked to biotin-dependent proteins (BDP) by the activity of Bpl1 (biotin:apoprotein ligase 1). The scheme is adapted from Stolz (2009). (b) Putative orthologs of *S. cerevisiae* biotin-related genes in *Candida glabrata* and *Candida albicans*. Gene names in brackets showed no biotin-dependent regulation (see Figure S2) and were excluded from further analysis

(Figure S2). Of the potential *ScVHT1* orthologs, only the *C. glabrata* gene CAGL0K04609g (*CgVHT1*) and the *C. albicans* gene CR_03270W (*CaVHT1*) showed clear biotin-dependent expression (Figure S2). In addition, the potential *C. albicans* ortholog (CR_01900C, *CaBIO5*), but not the *C. glabrata* ortholog of *ScBIO5*, was induced upon biotin limitation (Figure S2). In *S. cerevisiae*, the expression of genes associated with biotin metabolism is induced by the transcriptional activator Vhr1 in response to low biotin (Weider et al., 2006). We found one potential *ScVHR1* ortholog in *C. glabrata* and *C. albicans*— CAGL0M12496g (*CgVHR1*) and CR_00630W (*CaVHR1*), respectively (Figure 2b). Both orthologs share a highly conserved N-terminal putative DNA-binding domain and a C-terminal putative activation domain with their *S. cerevisiae* ortholog (Weider et al., 2006). CAGL0M12496g is currently annotated as a pseudogene with a premature translational stop codon (http://www.candidagenome.org/). Sequencing of CAGL0M12496g in *C. glabrata* genomic DNA revealed a frameshift in comparison to the annotated sequence (four cytosines at ORF position 473–476 in the annotated sequence [Skrzypek et al., 2017], but only three cytosines in our strain, see Appendix S2). The predicted protein deduced from our sequence data lacks the early translational stop codon and has a similar length as the *S. cerevisiae* ortholog (689 and 640 amino acids, respectively; Appendix S2). Finally, the biotin protein ligase Bpl1 is needed for the transfer of biotin to biotin-accepting proteins in baker's yeast. The genes CAGL0I03806g (*CgBPL1*) and orf19.7645 (*CaBPL1*) represent potential orthologs in *C. glabrata* and *C. albicans*.

2.3 | *VHT1* is essential for biotin-dependent growth of *C. glabrata* and *C. albicans*

To test whether *CgVHT1* and *CaVHT1* have a role in biotin acquisition, we generated deletion strains of the respective genes by targeted mutagenesis. Indeed, these strains were unable to grow in the presence of intermediate biotin levels (2 μg/L biotin) and required high amounts (2 mg/L) of this vitamin for growth comparable to that of the wildtype. A delayed growth was observed with elevated biotin concentrations (0.2 mg/L). The growth defect was restored after re-introduction of either *CgVHT1* or *CaVHT1* (Figure 3a,b). Similarly, *C. albicans* hyphal induction and extension after 2, 4 and 24 hr was significantly reduced in the *Cavht1Δ/Δ* mutant as compared to the wildtype in medium containing 2 μg/L or 0.2 mg/L of biotin (Figure 3c–e). Again, high amounts of biotin or reintegration of *CaVHT1* were able to restore wildtype-like filamentation. These data strongly indicate that *CgVHT1* and *CaVHT1* indeed encode biotin importers.

2.4 | Vhr1 is a transcriptional regulator of biotin-metabolic genes in *C. glabrata* and *C. albicans*

To elucidate whether *CgVhr1* and *CaVhr1* regulate biotin-related genes in *C. glabrata* and *C. albicans*, we analysed gene expression of potential target genes under biotin limitation (no biotin or 0.2 μg/L biotin) as compared to intermediate biotin levels (2 μg/L biotin) in wildtype strains and mutants lacking *CgVHR1* and *CaVHR1*. Both,
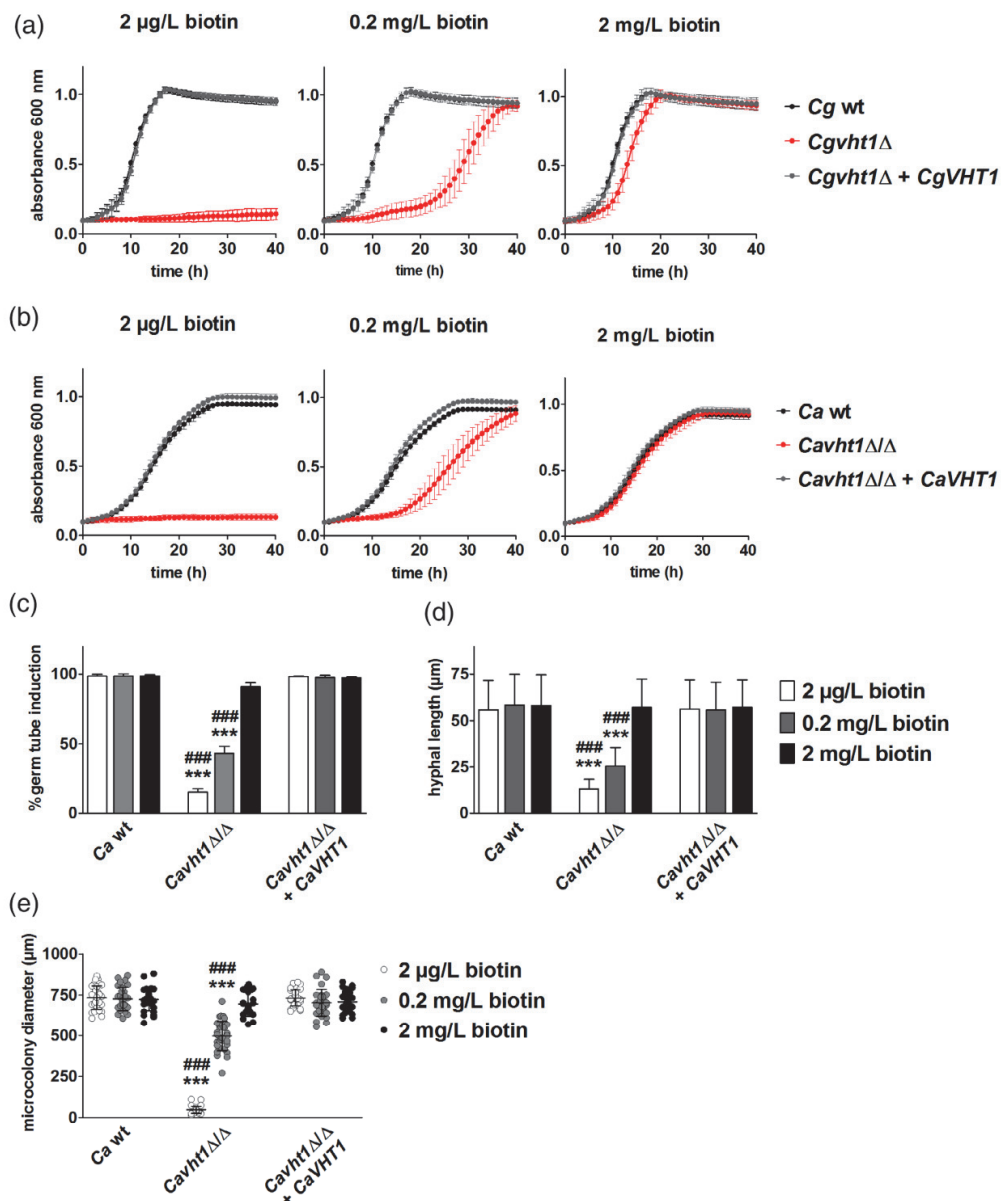
FIGURE 3 *VHT1* is essential for biotin-dependent growth. Yeast growth of biotin pre-starved wt, mutant (*vht1Δ*), or complemented strain (*vht1Δ + VHT1*) of (a) *Candida glabrata* (37°C) or (b) *Candida albicans* (30°C) in minimal medium containing 2 μg/L, 0.2 or 2 mg/L biotin. (c–e) Hyphal growth of non-starved or pre-starved *C. albicans* cells in RPMI1640 containing 2 μg/L, 0.2 or 2 mg/L biotin at 37°C and 5% CO_2. (c) Percentage of germ tube-forming cells at 2 hr. (d) Hyphal length at 4 hr (mean + SD of individual hyphae from three replicates). (e) Microcolony size at 24 hr, as a measure for long-term hypha formation (each single dot represents one individual microcolony). Values are represented as mean ± SD (a,b) or mean + SD (c–e) of at least three replicates. For statistical analysis, a one-way ANOVA with Bonferroni's multiple comparison test was used (***$p ≤ .001$ comparing wt and *VHT1* deletion mutant; ###$p ≤ .001$ comparing *VHT1* deletion mutant to *VHT1* complemented strain)

*Cg*VHT1 and *Cg*BPL1 were induced upon biotin limitation in wildtype or the *Cg*VHR1-complemented strain while *Cg*VHR1 itself was steadily expressed independent of the biotin levels. The up-regulation of *Cg*VHT1 and *Cg*BPL1 was almost abolished in the *Cgvhr1Δ* mutant (Figure 4a).

Similarly, *C. albicans*' incomplete biotin biosynthesis cluster genes *CaBIO2-5*, as well was *CaVHT1*, *CaBPL1* and *CaVHR1* showed the highest expression under biotin-limiting conditions in wildtype cells and the *CaVHR1*-complemented strain (Figure 4b). Expression of *CaBIO3*, *CaBIO4* and *CaBIO5* was strongly reduced in the absence of *CaVHR1*, while *CaVHT1* and *CaBIO2* expression was unaffected by *CaVHR1* deletion under biotin-limiting conditions and even increased in the presence of 2 μg/L biotin. *CaBPL1* showed a mixed expression pattern with slightly reduced expression in the *Cavhr1Δ/Δ* mutant

under biotin limitation, but higher expression in the presence of 2 μg/L biotin.

These data show that both *Cg*Vhr1 and *Ca*Vhr1 are important for the fungal response to environmental biotin availability. While *Cg*Vhr1, similar to its *S. cerevisiae* ortholog, activates genes associated with biotin import and intracellular transfer to proteins upon biotin limitation, *Ca*Vhr1-dependent activation seems to be limited to the biotin biosynthesis genes *CaBIO3-5*. Meanwhile, biotin uptake in *C. albicans* is reduced and depends on *Ca*Vhr1 when sufficient environmental biotin is available.

C. albicans and *C. glabrata* mutants lacking *CgVHR1* and *CaVHR1* were further tested for growth under biotin limitation (0.2 μg/L biotin). In contrast to the deletion of *VHT1*, the deletion of *VHR1* did not lead to growth or hyphal defects under biotin limitation (Figure S3). In host
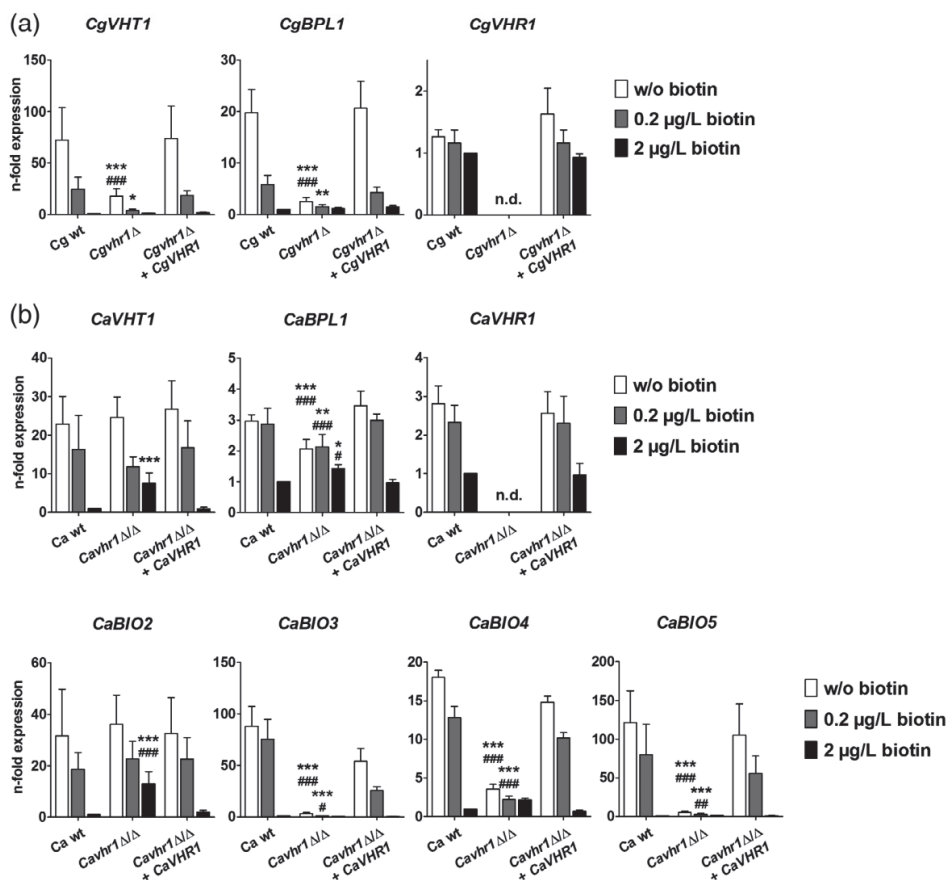
FIGURE 4 *VHR1* regulates biotin-metabolic genes. Non-starved (a) *Candida glabrata* or (b) *Candida albicans* cells were cultivated in minimal medium with indicated biotin concentrations for 90 min (*C. glabrata*) or 180 min (*C. albicans*) at 37°C. Target gene expression was analysed by qRT-PCR and normalised to *CgACT1*, *CgEFB1*, *CgEFT2* and *CaTDH3*, *CaEFT2*. Values are represented as mean + SD of three independent experiments, whereby *n*-fold expression for each gene is shown relative to the wt in 2 μg/L biotin. For statistical analysis, a two-way ANOVA with Bonferroni post-tests was used (*$p \leq .05$, **$p \leq .01$, ***$p \leq .001$; comparing wt and *VHR1* deletion mutant; #$p \leq .05$, ##$p \leq .01$, ###$p \leq .001$; comparing *VHR1* deletion mutant to *VHR1* complemented strain; n.d., not detectable)

niches like the macrophage phagosome, *Candida* cells likely do not encounter their preferred carbon and nitrogen sources in high amounts, but rather alternative sources like amino acids (Kaur et al., 2007; Lorenz, 2013; Lorenz et al., 2004). Therefore, we combined biotin limitation with the presence of casamino acids as the sole carbon and nitrogen source, instead of the optimal nutrients glucose and ammonium sulfate. Under these conditions, the *Cgvhr1Δ* mutant grew less than the wildtype (Figure S3b), whereas the *Cavhr1Δ/Δ* mutant grew similarly to the wildtype (Figure S3g). This suggests that *C. glabrata* requires *CgVHR1* for growth under conditions that combine low biotin with limitations of optimal C- and N-sources.

2.5 | The fungal biotin pool influences intracellular fitness inside macrophages

Metabolic plasticity is essential for the adaptation of *Candida* species to the changing environment of different, often nutrient-limited, host niches including the macrophage phagosome (Lorenz, 2013; Miramón & Lorenz, 2017). Both *C. albicans* and *C. glabrata* are able to survive macrophage phagocytosis and even replicate inside macrophages (*C. glabrata*, Seider et al., 2011) or form hypha and escape (*C. albicans*, McKenzie et al., 2010). Both species must have developed strategies to counteract macrophage killing activities, but also adapt to phagosomal nutrient conditions (Miramón et al., 2013). To elucidate how biotin impacts the fungal fitness inside macrophages, we first confronted biotin-starved (pre-incubation in medium without biotin) or biotin-fed (pre-incubation in medium with high biotin 2 mg/L) *C. glabrata* or *C. albicans* cells with primary human monocyte-derived macrophages (hMDMs). As a control, we used fungal cells pre-incubated in medium with intermediate biotin levels (2 μg/L) that are sufficient to promote growth. In macrophage confrontation assays, biotin pre-starvation increased the susceptibility of *C. glabrata* and *C. albicans* to phagocytosis-mediated killing (Figure 5a,c).

Moreover, biotin-starved *C. glabrata* cells were significantly reduced in intracellular replication in macrophages (Figure 5b) and biotin-starved *C. albicans* cells developed shorter filaments and showed reduced levels of hyphal outgrowth compared to fungal cells pre-cultivated with intermediate or high amounts of biotin (Figure 5d,e). To exclude that the observed effects were due to a
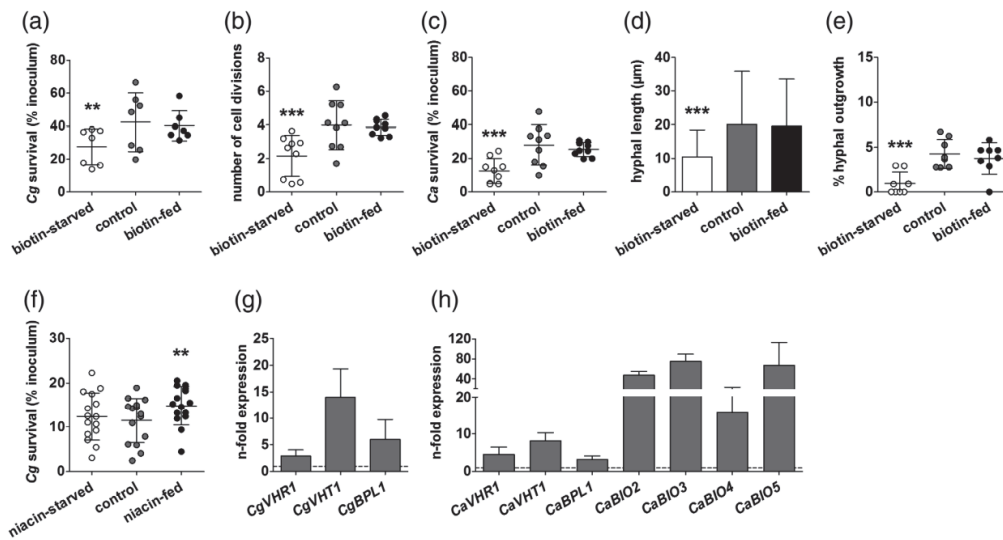
FIGURE 5 Biotin pre-starvation reduces fungal fitness inside macrophages, while phagocytosis induces up-regulation of biotin-related *Candida* genes. (a,b) *Candida glabrata* or (c–e) *Candida albicans* cells were pre-cultivated in minimal medium without (biotin-starved), with 2 μg/L (control), or with 2 mg/L (biotin-fed) biotin before confrontation with human blood monocyte-derived macrophages (hMDMs). (a) Survival of *C. glabrata* after 3 hr (% of inoculum). (b) Intracellular replication of *C. glabrata* after 20 hr, shown as number of cell divisions − $\log_2[1/1 − (\%$ daughter cells/100)]. (c) Survival of *C. albicans* after 3 hr (% of inoculum). (d) Length of hyphae formed 10 hr after phagocytosis. (e) Outgrowth of *C. albicans* hyphae from macrophages after 10 hr (% of ingested hyphae piercing the macrophage membrane). (f) Survival in hMDMs (after 3 hr; % of inoculum) of *C. glabrata* cells pre-cultivated in minimal medium without (niacin-starved), with 0.4 mg/L (control) or with 400 mg/L (niacin-fed) niacin. (g,h) hMDMs were infected with non-starved (g) *C. glabrata* or (h) *C. albicans* cells and fungal RNA was isolated after 3 hr. Target gene expression was analysed by qRT-PCR and normalised to *CgACT1*, *CgEFT2* and *CaEFT2*, *CaACT1*. Expression is shown relative to wt (grown without hMDMs with 0.2 mg/L biotin). Values are represented as scatterplot with mean ± SD (a–c, e and f), with each single dot corresponding to one blood donor (total at least seven different donors in at least two independent experiments). Values in d, g and h are represented as mean + SD of individual hyphae from three replicates (d) or three replicates (g,h). For statistical analysis, a repeated measures ANOVA was performed followed by Dunnett's multiple comparison test (**p ≤ .01, ***p ≤ .001; compared to control condition)

general detrimental effect of vitamin limitation on fungus-macrophage interactions, we infected macrophages with *C. glabrata* cells pre-starved for niacin (nicotinic acid), a vitamin needed for *C. glabrata* to

overcome NAD$^+$ auxotrophy (Domergue et al., 2005). Nicotinic acid starvation did not reduce *C. glabrata* survival inside macrophages (Figure 5f), indicating that the observed effect of biotin starvation is
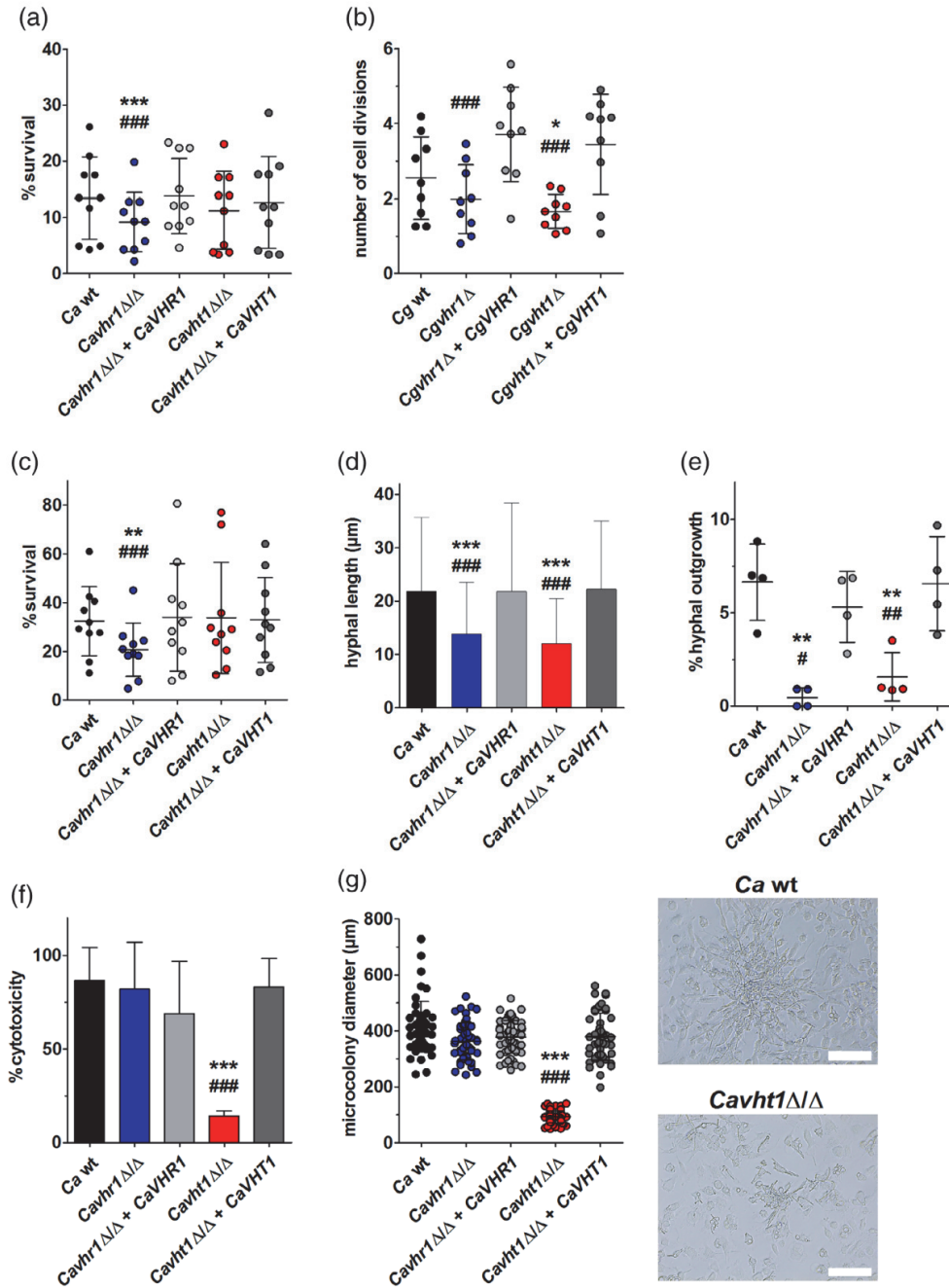
FIGURE 6 Legend on next page.

specific. Up-regulation of biotin homeostasis and biosynthesis genes after phagocytosis by macrophages suggests that *C. glabrata* and *C. albicans* indeed experience biotin limitation inside macrophages (Figure 5g,h). Combined, these data indicate that biotin is crucial for survival and proliferation of *C. glabrata* and *C. albicans* in macrophages and that biotin availability for *C. glabrata* and *C. albicans* upon macrophage phagocytosis is limited.

2.6 | *VHR1* and *VHT1* are essential for fungal fitness within macrophages

Next, we wanted to know whether disturbance of biotin uptake or biotin-dependent regulation would affect fungal fitness after macrophage phagocytosis. Therefore, we confronted hMDMs with biotin-fed *C. glabrata* or *C. albicans VHT1* and *VHR1* knockout strains and evaluated survival and intracellular proliferation of phagocytosed fungal cells (Figure 6).

The *Cgvhr1Δ*, but not the *Cgvht1Δ* mutant, was significantly attenuated in intracellular survival as compared to the complemented strain or the wildtype (Figure 6a). Similarly, the *Cavhr1Δ/Δ*, but not the *Cavht1Δ/Δ* mutant, showed reduced survival rates. To rule out that stored biotin from the pre-culture compensates the need for *VHT1* early after infection, we did parallel survival assays with pre-starved fungal strains (Figure S5). Indeed, pre-starved *Cavht1Δ/Δ* cells showed significantly lower survival rates than the wildtype. However, survival of the *Cgvht1Δ* mutant was not reduced. In addition, a lower survival rate of *vhr1Δ* mutants was only observed when fungal cells were pre-grown in biotin-containing medium (Figure 6a,c), but not when biotin-starved fungal cells were used (Figure S5).

Even after biotin feeding, *C. glabrata* intracellular replication was reduced for both the *Cgvhr1Δ* and *Cgvht1Δ* mutants (Figure 6b). Also, *C. albicans* hyphae formed early after phagocytosis were shorter in both *Cavhr1Δ* and *Cavht1Δ* as compared to the wildtype or the complemented strain and both mutants showed reduced rates of hyphal outgrowth (Figure 6c–e).

While *C. glabrata* can replicate inside macrophages without causing substantial damage (Seider et al., 2011), *C. albicans* hyphal growth and other factors cause macrophage lysis within hours (Kasper et al.,

2018; McKenzie et al., 2010; Vylkova & Lorenz, 2014). Therefore, we looked at macrophages confronted for 24 hr with *C. albicans* and measured macrophage lactate dehydrogenase (LDH) release to determine host cell lysis. In addition, we quantified the sizes of *C. albicans* microcolonies as a measure for sustained hyphal growth during contact with macrophages. While the *Cavht1Δ/Δ* mutant formed smaller microcolonies and was severely attenuated in macrophage damage, the *Cavhr1Δ/Δ* showed wildtype-like microcolonies and cytotoxicity (Figure 6f,g).

Besides biotin, precursors like KAPA or DTB may support *C. albicans* growth depending on its *BIO2-5* partial biosynthesis cluster (see above). Such precursors may potentially be provided by co-inhabiting bacteria, for example, during gut colonisation, but are likely not available during direct *C. albicans*–host interactions, as these intermediates are not produced by host cells. We constructed a *C. albicans* mutant lacking *CaBIO2-5* and found that the *BIO2-5* cluster is indeed necessary for growth with KAPA and DTB, but not biotin (Figure S4a). Intracellular survival, hyphal growth and damage of macrophages were unaffected in the *Cabio2-5Δ/Δ* mutant (Figure S4b–e), indicating that KAPA or DTB utilisation is dispensable for the *C. albicans*–macrophage interaction.

Collectively, these data indicate that in both *Candida* species, Vhr1-regulated processes are important for short-term responses to macrophage antifungal activities and intracellular proliferation. Vht1-dependent biotin acquisition is needed for survival of *C. albicans* cells that have experienced biotin limitation prior to phagocytosis. Vht1 also becomes relevant for *C. glabrata* replication and early and sustained intracellular growth of *C. albicans* hyphae and hypha-induced damage of macrophages.

2.7 | The biotin transporter Vht1 is required for colonisation of the brain during systemic infection

Our *in vitro* growth experiments show that both *C. albicans* and *C. glabrata* similarly require *VHT1* for biotin acquisition, and mutants lacking *VHT1* need at least ×1,000 more biotin than wildtype cells for proliferation (Figure 3). To learn more about the availability of and requirement for biotin during *Candida* infections, we analysed both

FIGURE 6 Genes related to biotin homeostasis are necessary for fungal fitness within macrophages. Wildtype (wt), mutant (*vht1Δ*), or complemented strains (*vht1Δ* + *VHT1*) of (a,b) *Candida glabrata* or (c–g) *Candida albicans* cells were pre-cultivated in YPD + 2 mg/L biotin before confrontation with human blood monocyte-derived macrophages (hMDMs). (a) Survival of *C. glabrata* strains after 3 hr, (% survival of inoculum). (b) Intracellular proliferation of *C. glabrata* after 20 hr, shown as number of cell divisions − $\log_2[1/1 − (\%$ daughter cells/100)] ($n = 3$). (c) Survival of *C. albicans* strains after 3 hr (% survival of inoculum). (d) Length of hyphae formed 10 hr after phagocytosis. (e) Outgrowth of hyphae from macrophages after 10 hr (% of ingested hyphae piercing the macrophage membrane). (f) Macrophage damage by *C. albicans* after 24 hr (% cytotoxicity; 100% refers to full lysis). (g) Microcolony size at 24 hr, as a measure for long-term hypha formation. Exemplary microscopy pictures of microcolonies of *C. albicans* wt and *Cavht1Δ/Δ* + *CaVHT1* on infected macrophages are shown; scale bar: 100 μm. Values are represented as scatterplots with mean ± SD (a–c, e and g) or mean + SD of individual hyphae from four donors in two independent experiments (d,f). Each single dot in a-c and e corresponds to one blood donor (total of at least four different donors in at least two independent experiments). Scatterplot in (g) shows a single dot for one individual microcolony (five donors of two independent experiments). For statistical analysis, a repeated measures ANOVA with Bonferroni's multiple comparison test was performed (*$p ≤ .05$, **$p ≤ .01$, ***$p ≤ .001$ comparing wt and deletion mutant; ##$p ≤ .01$, ###$p ≤ .001$ comparing deletion mutant to the respective complemented strain)

Candida species in established systemic infection mouse models (Jacobsen et al., 2010; Jacobsen, Lüttich, Kurzai, Hube, & Brock, 2014). First, we infected mice via the tail vein with biotin pre-starved or biotin-fed *C. glabrata* wildtype, *Cgvhr1*Δ or *Cgvht1*Δ mutant, or the respective complemented strains. As expected from previous studies, systemic infection with *C. glabrata* caused no clinical symptoms and the only alteration upon necropsy was moderate splenomegaly, indicating an immune response to infection (Jacobsen et al., 2010) (not shown). Fungal burdens of infected organs were highest at Day

2 post-infection and decreased over time for all tested strains (Figures 7a and Figure S6). The biotin transporter mutant *Cgvht1*Δ was strongly attenuated in colonisation of the brain and caused less MCP-1 (monocyte chemoattractant protein 1; CCL-2) production, while the complemented strain showed wildtype-like behaviour (Figures 7a and Figure S7). In contrast, mice infected with the *Cgvhr1*Δ or *Cgvht1*Δ mutant showed wildtype-like fungal burdens and comparable cytokine levels in the kidney, liver and spleen (Figures S6a–c and S7). Since, according to our *in vitro* experiments,
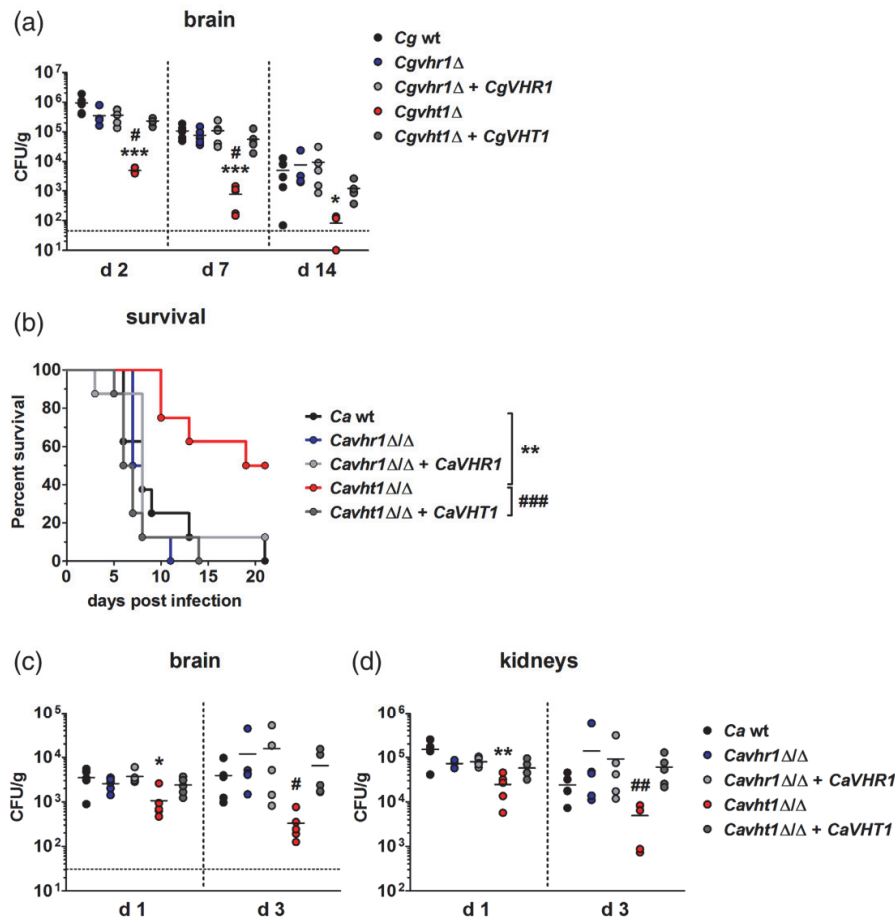
FIGURE 7 *VHT1* is required for *in vivo* persistence of *Candida glabrata* and virulence of *Candida albicans*. (a) Five CD-1 mice per group were intravenously infected with biotin-starved *C. glabrata* wildtype (wt), mutant, or complemented strains (2.5×10^7 yeast cells/20 g body weight in 100 μL PBS) on Day 0. The fungal burden of the brain was determined by quantifying cfu in tissue homogenates at indicated time points. (b–d) Balb/C mice were intravenously infected with biotin-starved *C. albicans* wildtype, mutant, or complemented strains (2×10^5 yeast cells/20 g body weight in 100 μL PBS) on Day 0 and (b) survival of eight mice was followed up for 21 days. The fungal burden of (c) brain and (d) kidneys was evaluated by quantifying cfu in tissue homogenates of five mice at indicated time points. Statistical analysis was performed with a one-way ANOVA on datasets from the same day to compare the strains, followed by Dunn's multiple comparison test. Survival curves were compared using the log rank (Mantel-Cox) test. (*$p \leq .05$, **$p \leq .01$, ***$p \leq .001$ comparing wt and *VHT1* deletion mutant; #$p \leq .05$, ##$p \leq .01$, ###$p \leq .001$ comparing *VHT1* deletion mutant to *VHT1* complemented strain). Dashed lines represent the detection limit and dots below this line mean no cfu were detected

CgVht1 in particular is essential for full fitness and proliferation in biotin-poor microniches, we concluded that infecting *Cgvht1Δ* cells may either find sufficient, accessible biotin for proliferation in these organs or that these cells persist in a non-proliferating stage. To provide proof that *C. glabrata* can remain viable in the absence of nutrients, we incubated the different *C. glabrata* strains in PBS without carbon, nitrogen or vitamin sources. The numbers of colony forming units (cfu) dropped over time, but stayed above 10% of the initial cell count, confirming that a fraction of *C. glabrata* cells can survive for 2 weeks, even in the absence of nutrients, and independent of *CgVHR1* or *CgVHT1* (Figure S6d).

Fungal burdens after infection with biotin pre-starved *C. glabrata* were slightly (but not significantly) increased as compared to non-starved *C. glabrata* in the liver, kidneys and brain on Day 2, but not on Day 7 and 14 (Figures 7a and S6a,c). Thus, biotin pre-starved *C. glabrata* may be slightly better adapted to early conditions during *in vivo* infection; however, the biotin status before infection has no substantial impact on fungal persistence. Secondly, we infected mice via the tail vein with biotin pre-starved *C. albicans* wildtype, *Cavhr1Δ/Δ* or *Cavht1Δ/Δ* mutant cells, or the respective complemented strains. Mouse morbidity was analysed by monitoring the development of clinical symptoms over a maximum of 21 days and mice were euthanized after reaching humane endpoints. The *Cavht1Δ/Δ* mutant was significantly attenuated in virulence, whereas the *Cavhr1Δ/Δ* mutant showed wildtype-like virulence (Figure 7b). Additionally, to gain insights into the organ-specific *C. albicans* fungal loads, a time course experiment analogous to the *C. glabrata* infection model was performed. We found that the *Cavht1Δ/Δ* mutant showed significantly lower fungal burdens in the brain and kidneys (Figure 7c,d), while those of the liver and spleen were comparable to the wildtype (Figure S6f,g). Correspondingly, the inflammatory response in the *Cavht1Δ/Δ*-infected brain and kidney but also liver was reduced, while the complemented strain induced a wildtype-like cytokine response (Figure S7).

Based on these data we conclude that Vhr1-dependent regulatory processes are dispensable for *in vivo* persistence of *C. glabrata* and virulence of *C. albicans*. However, Vht1-mediated biotin acquisition is required for persistence of *C. glabrata* in the mouse brain and virulence of *C. albicans*.

3 | DISCUSSION

Candida albicans and *C. glabrata* are two successful opportunistic pathogenic fungi. These two yeast species are able to rapidly adapt to changing environments with varying nutrient availability (Miramón & Lorenz, 2017). Both *C. glabrata* and *C. albicans* are auxotrophic for the essential micronutrient biotin and, thus, must have found ways to acquire this vitamin during commensal growth and systemic infection (Ahmad Hussin et al., 2016; Firestone & Koser, 1960). On mucosal surfaces, *C. albicans* and *C. glabrata* live in close proximity to other microbes, which are often able to synthesise biotin and likely provide this vitamin or biosynthesis intermediates to colonising *Candida* cells

(Hill, 1997). While *C. albicans* contains the incomplete biotin biosynthesis cluster *BIO2-5*, which enables this fungus to synthesise biotin when growing in the presence of KAPA or DTB (Figures 1, 2 and S4; Ahmad Hussin et al., 2016; Fitzpatrick et al., 2010), *C. glabrata* has apparently lost the biotin biosynthesis pathway (Figure 2) and cannot utilise these biotin precursors (Figure 1). This underlines the remarkable metabolic flexibility of *C. glabrata*, which can thrive in the host despite loss of several metabolic genes and resulting auxotrophies, such as NAD^+, pyridoxine and thiamine (Brunke & Hube, 2013; Dujon et al., 2004; Kaur, Domergue, Zupancic, & Cormack, 2005). Presence or absence of *BIO2-5* genes in other medically important yeasts (Fitzpatrick et al., 2010) similarly correlated with their ability to utilise biotin precursors (Figure S2): *C. tropicalis* (possessing *BIO2-5*), grew on KAPA and DTB while *C. dubliniensis* and *C. auris* (possessing *BIO2* only) grew on DTB and *C. parapsilosis* (lacking *BIO2-5*) was unable to utilise either biotin precursor. The *BIO2-5* cluster may therefore be an advantage for *C. albicans* (and *C. tropicalis*) over *C. glabrata* (and *C. dubliniensis*, *C. auris* and *C. parapsilosis*), allowing for better host colonisation in the presence of bacteria. Therefore, these genes may be seen as commensal factors. However, these genes are likely dispensable during systemic infection, as mammals are biotin auxotrophs and provide no biosynthesis intermediates. In agreement, *BIO2-5* was dispensable for *C. albicans*–macrophage interaction (Figure S4).

The ability of *C. albicans* to undergo a morphological transition between yeast and hyphae is considered to be a main virulence attribute of this fungus (Jacobsen et al., 2012). Our data show that biotin is necessary for *in vitro* proliferation of *C. glabrata* and *C. albicans* yeast cells, but also for *C. albicans* hyphal growth (Figure 1). These data are supported by a previous study (Ahmad Hussin et al., 2016), which showed that biotin enhances *C. albicans* germ tube formation.

We have identified two major players of biotin homeostasis in *C. albicans* and *C. glabrata*—the ortholog of the *S. cerevisiae* biotin transporter Vht1 and the ortholog of the *S. cerevisiae* regulator of biotin-metabolic genes Vhr1. As mutants lacking *VHT1* were unable to grow *in vitro* unless high amounts of biotin were present and as *VHT1* expression was highly up-regulated in medium with low biotin in both *Candida* spp., we conclude that Vht1 is the main factor facilitating biotin acquisition in both, *C. albicans* and *C. glabrata* (Figures 3, 4 and S2). Genomes of other biotin-auxotrophic *Candida* spp. such as *C. tropicalis*, *C. dubliniensis*, *C. auris* and *C. parapsilosis*, also contain potential *VHT1* orthologs (Skrzypek et al., 2017), indicating that the biotin uptake machinery is conserved among other medically important *Candida* species.

Our data show that Vhr1 regulates the expression of biotin-metabolic genes, including *VHT1* in *C. albicans* and *C. glabrata*. While *C. glabrata* Vhr1 induces *CgVHT1* expression upon biotin limitation, *C. albicans* Vhr1 was required for keeping *CaVHT1* expression low under biotin-replete conditions (Figure 4). This suggests that a yet unknown regulator activates *CaVHT1* expression in *C. albicans*. A *Cgvhr1Δ* mutant was still able to express *VHT1* to some extent, suggesting the presence of additional regulators in *C. glabrata* as well. This may also explain why mutants lacking *VHR1* were still able to grow under biotin-limiting conditions (Figure S3) or showed

wildtype-like fitness *in vivo* (Figures 7 and S6). In contrast, a *Cgvhr1Δ* mutant was outcompeted by the wildtype in a previous infection study, suggesting an involvement of *CgVHR1* in *in vivo* fitness (Brunke et al., 2015). However, that mutant was generated in a strain background with amino acid auxotrophies. Such auxotrophies alone have no impact on *C. glabrata* fitness in the mouse (Jacobsen et al., 2010), but may be detrimental when combined with the absence of Vhr1-dependent regulation. Our data, however, show that *VHR1* is required for survival and proliferation in macrophages (*C. albicans* and *C. glabrata*) as well as growth when biotin limitation is combined with the replacement of glucose by casamino acids (Figure S3). These data suggest that Vhr1-dependent regulation becomes important in specific niches, when biotin limitation is combined with the limitation of other nutrients and/or antimicrobial activities of immune cells (see below).

Our data obtained from macrophage confrontation assays implies that the *Candida*-containing phagosome is limited in biotin, as biotin-pre-starvation reduced *Candida* survival, as the biotin transporter gene *VHT1* was up-regulated in both *Candida* species upon biotin pre-starvation and after phagocytosis, and as deletion of *VHT1* led to slower replication of *C. glabrata* and slower hyphal extension of *C. albicans* inside macrophages (Figures 3, 5, 6 and S5). This concept of biotin limitation inside the phagosome is supported by studies in bacterial pathogens like *Francisella* spp. and *Mycobacterium* spp., which require a functional *de novo* biotin biosynthesis pathway for intracellular fitness within macrophages (Feng et al., 2015; Napier et al., 2012; Rengarajan, Bloom, & Rubin, 2005; Yu et al., 2011). Correlating with the reduction in hyphal formation of a *Cavht1Δ/Δ* mutant during the course of macrophage interaction, we observed a reduction in macrophage damage—a phenotype confirmed by a previous study (O'Meara et al., 2018).

Vhr1 was similarly important for replication (*C. glabrata*) or early hypha formation in macrophages (*C. albicans*), but not for sustained *C. albicans* filamentation and late macrophage damage. Of note, a *Cavhr1Δ/Δ* mutant exhibited wildtype-like *VHT1* expression in macrophages (not shown). In addition, *VHR1* was only necessary for *Candida* survival under conditions were *VHT1* was dispensable (when biotin was high before phagocytosis, Figure S5). These data suggest that *Ca*Vhr1 functions during early stages of macrophage interaction are independent of Vht1 regulation and become dispensable at later stages. Instead, *Ca*Vht1-dependent biotin uptake is needed for sustained proliferation inside macrophages. In *C. glabrata* we observe reduced *CgVHT1* expression in the absence of *CgVHR1* (not shown), which likely limits biotin import and consequently replication after phagocytosis.

Together, our macrophage confrontation data suggest that Vht1-dependent biotin uptake is required for sustained proliferation of *C. glabrata* and *C. albicans* inside macrophages, while initial fitness depends on *VHT1*-independent Vhr1 functions in fungal survival.

Our main conclusions on the importance of biotin during *Candida* infection are based on *in vivo* data with *C. glabrata* and *C. albicans vht1Δ* mutants, which are unable to synthesise and acquire biotin unless high amounts are present (Figure 3). Our data

clearly show that Vht1 is essential for the full virulence of *C. albicans* (Figures 7 and S6). Fungal organ burdens, however, were reduced in the kidney and brain, but not in the spleen or liver. Similarly, *C. glabrata* persistence in mice was not generally reduced upon *VHT1* deletion (Figures 7 and S6). In fact, *VHT1* deletion mutants of *C. glabrata* showed wildtype-like fungal burden in the kidney, liver, and spleen and reduced cfu numbers were only observed in mouse brains. These data indicate that biotin availability is high enough to support *Candida* growth in organs like the liver and spleen, while access to biotin is limited in the brain. In line with this, avidin-based histology staining suggested that hepatocytes and proximal tubular epithelial cells in the kidney contain high amounts of biotin (Combs & McClung, 2017; Cooper, Kennedy, McConnell, Kennedy, & Frigg, 1997), while biotin levels in the extracellular space of the brain tissue are lower (8 nM in rabbit [2 µg/L]) (Spector & Johanson, 2007). Such levels would be sufficient to promote growth of *Candida* wildtype cells, but not *VHT1* deletion strains (Figure 3). An alternative explanation is that certain nutrients, like aspartate or other amino acids, may bypass the need for biotin in certain host niches as suggested by our *in vitro* data (Figures S1 and S3).

Of note, biotin levels available in humans may be substantially lower than in mice, as a recent study showed a 40-fold higher biotin concentration in mouse plasma compared to human plasma (Carfrae et al., 2020). In line with this, the same study showed that growth of bacterial pathogens, which lack biotin transporters and are deficient in biotin biosynthesis, is diminished in human plasma, but not mouse (Carfrae et al., 2020).

Biotin may become dispensable for colonising *Candida* cells in cases of weak or no fungal metabolic activity or proliferation. Fungal burdens of *C. glabrata* in brains, but not kidney, liver, or spleen of mice increase between 12 hr and 3 days post-infection, which may indeed point to *C. glabrata* replication in the brain, but not in the other tested organs soon after infection (Beyer et al., 2018). This exciting possibility of non-proliferating *C. glabrata* cells in the host may also contribute to the high tolerance of *C. glabrata* towards fungistatic antifungal drugs. Similarly, increases of *C. albicans* fungal burdens in mouse kidney and brain, but not in liver or spleen (Lionakis, Lim, Lee, & Murphy, 2011) point to replication in those organs in which we observed reduced cfu of the *Cavht1Δ/Δ* mutant.

Collectively, our data show for the first time that Vht1-dependent fungal biotin acquisition is linked with intracellular proliferation of the opportunistic fungal pathogens *C. albicans* and *C. glabrata* in macrophages and *in vivo* persistence of *C. glabrata* and virulence of *C. albicans* in mice. Our results underline the importance of micronutrients, such as biotin, for fungal pathogens.

4 | EXPERIMENTAL PROCEDURES

4.1 | Ethics statement

Human blood was taken from healthy volunteers with written, informed consent. The blood donation protocol and use of blood for

this study were approved by the institutional ethics committee of the university hospital Jena (Ethik-Kommission des Universitätsklinikums Jena, Permission No. 2207–01/08). Animal experiments were performed in compliance with the European and German animal protection laws and were approved by the ethics committee "Beratende Kommission nach §15 Abs. 1 Tierschutzgesetz" and the responsible Federal State authority Thüringer Landesamt für Verbraucherschutz, Bad Langensalza, Germany (Permit No. 03-026/16, HKI-19-005). All mice were cared for in accordance with the principles outlined in the European Convention for the Protection of Vertebrate Animals Used for Experimental and Other Scientific Purposes.

4.2 | Strains and general growth conditions

All strains used in this study are listed in Table S1. *Escherichia coli* was cultivated in liquid lysogeny broth with 50 µg/ml ampicillin for plasmid generation. For growth on solid medium, 2% agar was added. *Candida* strains were pre-cultured overnight in liquid Yeast Peptone Dextrose (YPD) broth (2% glucose, 2% peptone and 1% yeast extract) at 30 or 37°C, with shaking at 180 rpm for 14–16 hr. The biotin concentration in standard YPD is 10–20 µg/L (Ogoshi et al., 2014 and own observations). As gene deletion of *VHT1* led to strong growth defects in standard media, we routinely pre-cultured strains for experiments including the biotin transporter mutant *vht1Δ* in YPD + 2 mg/L biotin. Stationary phase yeast cells from pre-cultures were washed three times in PBS and the cell number was adjusted in PBS or culture medium.

For biotin and niacin pre-starvation, the YPD-grown, PBS-washed cell suspension was adjusted to an OD of 0.2 in minimal medium either without biotin (0.69% yeast nitrogen base [YNB] without biotin, amino acids, with ammonium sulfate [Formedium]; 2% glucose) or without niacin (0.69% YNB without niacin, amino acids, with ammonium sulfate [Formedium]; 2% glucose) and incubated for further 24 hr at 30 or 37°C and 180 rpm. Media with defined biotin concentrations were prepared on the basis of biotin-free medium (see above), with addition of 0.2 µg/L biotin (low biotin), 2 µg/L biotin (intermediate, standard), 0.2 mg/L biotin (elevated biotin) or 2 mg/L biotin (high biotin).

4.3 | Growth assays

Twenty microliters of a yeast cell suspension (5×10^6 cells/ml) were added to 180 µL media in a 96-well plate (Tissue Culture Test Plate, TPP Techno Plastic Products AG). The growth was monitored by measuring the absorbance at 600 nm every 30 min for 100 cycles at 30 or 37°C using a Tecan Reader (Plate Reader infinite M200 PRO, Tecan Group GmbH) with orbital shaking (30 s, amplitude: 6 mm, wait: 10 s) before each measurement and multiple reads per well. All experiments were done in technical duplicates and, at least, biological triplicates.

Filamentation of *C. albicans* was induced in biotin-free RPMI1640 medium (PAN-Biotech) with ʟ-glutamine (Thermo Fisher Scientific)

either without biotin or with 2 µg/L of biotin/KAPA/DTB at 37°C and 5% CO_2 in a 24-well plate. Briefly, 5×10^4 cells/well were incubated for 2 and 4 hr to allow formation of short hyphae. In parallel, to measure long hyphae in vitro, 100 cells/well were incubated for 24 hr to generate microcolonies originating from single yeast cells that formed radially branching filamentous hyphae (McCall, Kumar, & Edgerton, 2018). Following this, cells were fixed by adding one-tenth of the volume of 37% paraformaldehyde. Microscopy images were recorded using the Zeiss Axio Vert.A1 (Carl Zeiss Microscopy). Germ tube formation (2 hr) and hyphal length (4 hr) were measured for at least 200 cells/sample and the diameter of at least 10 microcolonies was determined (both in at least three replicates).

4.4 | *C. glabrata* mutant generation

For construction of *C. glabrata* *vhr1Δ* and *vht1Δ* mutants, the upstream and downstream homologous regions of CAGL0M12496g (*VHR1*) and CAGL0K04609g (*VHT1*) were first subcloned with flanking restriction enzyme recognition sites (5' SphI- and 3' SacII for upstream region of *VHR1*, 5' SphI and 3' NcoI for upstream region of *VHT1*, 5' SpeI- and 3' SacI for downstream regions of *VHR1* and *VHT1*) using the TOPO Cloning Kit (Invitrogen). The homologous regions were then excised and cloned into the plasmid pTS50 (Schwarzmüller et al., 2014) to generate cassettes containing the *NAT1* selection marker (Schwarzmüller et al., 2014; Table S3) surrounded by gene-specific regions. Integration was confirmed by restriction digestion. Deletion constructs were amplified from generated plasmids using P1 and P4 primers (Table S2) and purified with QIAquick PCR purification kit (Qiagen). Next, 4 µg of the PCR product was transformed into the parental strain wildtype strain ATCC2001 or a tryptophan-auxotrophic derivative (*trp1Δ*) using a modified heat-shock method (Sanglard, Ischer, Monod, & Bille, 1996 with heat shock: 15 min at 45°C). Mutants were selected for on YPD agar plates with 250 µg/ml nourseothricin. Growth of *vht1Δ* clones was facilitated by adding 2 mg/L biotin to selective agar plates.

Complemented strains were generated by reintegrating *VHR1* and *VHT1* into the *TRP1* locus. This locus was chosen as tryptophan auxotrophy (*trp1Δ*) had no negative impact on *C. glabrata* in vivo fitness and in vitro mutant growth phenotypes (Jacobsen et al., 2010; Yanez-Carrillo et al., 2015). In detail, the *TRP1* gene and its 5' upstream region (−984 bp to +750 bp) was PCR-amplified with primers introducing flanking SphI restriction sites and ligated into the SphI-linearized pUC19 vector (In-Fusion HD Cloning Kit) to generate pUC19-*TRP1*. Subsequently, the *TRP1* 3' downstream region (+751 bp to +1,570 bp) was PCR-amplified with primers introducing XmaI and SacI restriction sites and was ligated into the XmaI/SacI opened plasmid pUC19-*TRP1* to create the final p*TRP1*. Plasmids p*TRP1-VHR1* and p*TRP1-VHT1* were generated by PCR amplifying the coding sequences of *VHR1* and *VHT1* together with the up- and downstream intergenic regions with primers introducing 15 bp flanks of the empty p*TRP1* (*VHR1*) or SalI and XbaI restriction sites (*VHT1*). Constructs were cloned into XbaI-digested p*TRP1*

(to generate pTRP1-VHR1) or SphI and XbaI-digested pTRP1 (to generate pTRP1-VHT1). Resulting plasmids were confirmed by sequencing. The TRP1 or TRP1-VHR1/TRP1-VHT1 cassettes were amplified by PCR, purified and transformed into a trp1Δ background strain to generate tryptophan prototrophic mutants or complemented strains, respectively. Resulting clones were selected for on solid minimal medium. All deletions and re-integrations were confirmed by PCR and Southern blot.

4.5 | *C. albicans* mutant generation

Candida albicans vhr1Δ/Δ (CR_00630WΔ/Δ) and vht1Δ/Δ (CR_03270WΔ/Δ) mutants were generated with a gene disruption method (Wilson, Davis, & Mitchell, 1999) and lithium acetate transformation protocol (Walther & Wendland, 2003). Briefly, the Arg-, His- and Ura-auxotrophic parental strain BWP17 was sequentially transformed with 10 μg of PCR-amplified and purified HIS1 and ARG4 deletion cassettes, which were flanked by 100 bp of the target homology region, resulting in disruption of the open reading frames of both alleles of CR_00630W (VHR1) or CR_03270W (VHT1). Primers used for PCR amplification and verification are listed in Table S2. Growth of vht1Δ/Δ clones was facilitated by adding 2 mg/L biotin to selective agar plates. Homozygous uridine-auxotrophic deletion mutants were then transformed with the StuI-linearized empty CIp10 plasmid (Murad, Lee, Broadbent, Barelle, & Brown, 2000) to generate prototrophic mutants or with StuI-linearized CIp10-VHR1 or CIp10-VHT1 plasmids to generate complemented strains. For the generation of CIp10-VHR1 or CIp10-VHT1, the coding sequences of VHR1 as well as VHT1 together with their native up- and downstream intergenic regions were cloned into CIp10 using KpnI and SalI (CIp10-VHR1) or XhoI (CIp10-VHT1). Constructed plasmids were verified by sequencing and the correct integration of deletion and complementation cassettes was confirmed by PCR and Southern blot.

4.6 | Isolation and differentiation of hMDMs

Human peripheral blood mononuclear cells (PBMCs) from buffy coats donated by healthy volunteers were separated through Lymphocytes Separation Media (Capricorn Scientific) in Leucosep tubes (Greiner Bio-One) by density centrifugation. Magnetically labelled CD14-positive monocytes were selected for by automated cell sorting (autoMACs; MiltenyiBiotec). To differentiate monocytes into adherent hMDMs, 1.7×10^7 cells were seeded into 175 cm^2 cell culture flasks in RPMI1640 media with L-glutamine (Thermo Fisher Scientific) containing 10% heat-inactivated foetal bovine serum (FBS; Bio&SELL) and 50 ng/ml recombinant human macrophage colony stimulating factor (M-CSF) (Immunotools) and incubated for 5 days at 37°C and 5% CO$_2$ until the medium was exchanged. After another 2 days, adherent hMDMs were detached with 50 mM EDTA in PBS and seeded in 6-well plates (1×10^6 hMDMs/well), 12-well plates (4×10^5 hMDMs/well), 24-well plates (2×10^5 hMDMs/well) or 96-well plates (4×10^4

hMDMs/well) in RPMI with 50 ng/mL M-CSF and incubated overnight. Prior to macrophage infection, medium was exchanged with serum- and biotin-free RPMI medium with L-glutamine (Thermo Fisher Scientific) to exclude biotin uptake by *Candida* prior to phagocytosis.

4.7 | Macrophage killing assay

Fungal survival was quantified as described previously (Seider et al., 2014). Briefly, macrophages in 24-well plates were stimulated for at least 24 hr with 20 ng/mL of recombinant human IFN-γ (Immunotools) in RPMI containing 50 ng/mL M-CSF and 10% FBS (see above) to favour a pro-inflammatory macrophage phenotype. Intracellular fungal survival was evaluated after 3 hr of coincubation with *C. glabrata* or *C. albicans* at a multiplicity of infection (MOI) of 1. Extracellular *Candida* cells were removed by washing three times with PBS and intracellular yeast cells were released by lysing the macrophages with 0.1% Triton-X-100 for 10 min. Appropriate dilutions were plated in duplicate on YPD plates containing 2 mg/L biotin and incubated for 1–2 days at 37°C. Colonies were counted with an automated colony counter ProtoCOL3 (Synbiosis, Cambridge, UK). To correct for inoculation differences between strains, colony numbers determined from intracellular lysates were normalised to colony numbers from plated culture inocula before calculating survival.

In experiments investigating the influence of niacin, hMDMs were seeded in 96-well plates and stimulated for at least 24 hr with 5 ng/mL of recombinant human IFN-γ (Immunotools) in RPMI1640 medium containing 50 ng/mL M-CSF and 10% FBS. Before confrontation with yeast cells, macrophages were washed with RPMI1640 medium without FBS and niacin. Niacin-free RPMI1640 medium was self-made and contains L-glutamine, phenol red, and sodium bicarbonate, but lacks niacinamide. The medium was adjusted to pH 7.2 and filter sterilised. Intracellular fungal survival was evaluated after 3 hr of coincubation with *C. glabrata* at an MOI of 1 in technical triplicates. The following steps were performed as described above.

4.8 | Differential staining after macrophage infection

Macrophages (1.5×10^5 hMDMs/well) were allowed to adhere onto coverslips in a 24-well plate overnight in RPMI containing 50 ng/mL M-CSF and 10% FBS and infected with *C. albicans* at an MOI of 2 for 10 hr. Phagocytosis was synchronised on ice for 30 min followed by two washing steps with pre-warmed medium to remove unbound *Candida* cells. The staining protocol was adapted from Kasper et al. (2018). Briefly, infected macrophages were fixed with Roti-Histofix 4% and stained with 50 μg/mL Concanavalin A conjugated with Alexa Fluor 647 (ConA-AF647; Thermo Fisher Scientific) at 37°C for 30 min to visualise external *Candida* cells. After permeabilisation with 0.5% Triton-X-100, extra- and intracellular fungal cells were stained with 35 μg/mL Calcofluor White. Coverslips were mounted with Mowiol mounting medium and fluorescence images were recorded using the

Zeiss AXIO Observer.Z1 (Carl Zeiss Microscopy). Outgrowth rates of intracellular hyphae and hyphal length of internalised *C. albicans* were calculated by manually counting a minimum of 100 yeast cells/sample.

4.9 | Macrophage damage assay

Macrophages were allowed to adhere in 96-well plates overnight in RPMI containing 50 ng/mL M-CSF and 10% FBS and infected in technical triplicates with *C. albicans* at an MOI of 2 for 24 hr at 37°C and 5% CO_2. Macrophage lysis was determined by measuring the release of LDH into the cell culture supernatant using the Cytotoxicity Detection kit (Roche). A low (non-infected cells) and a high control (cells lysed with 0.2% Triton-X-100) were performed to calculate the percentage of cytotoxicity. In the same samples, the diameter of microcolonies was measured to determine *C. albicans* hyphal length after 24 hr (≥10 colonies per sample).

4.10 | Determination of intracellular replication in macrophages

The protocol was adapted from Dagher et al. (2018) with minor changes. Prior to infection, *C. glabrata* cells were stained with 0.2 mg/mL fluorescein isothiocyanate (FITC) in carbonate buffer (0.15 M NaCl, 0.1 M Na_2CO_3, pH 9.0) for 30 min. Afterwards, yeast cells were washed three times in PBS and macrophages were infected at an MOI of 2 for 20 hr. To evaluate intracellular replication, macrophages were washed three times with PBS and lysed with 0.5% Triton-X-100 for 10 min. Released yeast cells were washed once with PBS, then with 2% BSA in PBS, and counterstained with 50 μg/mL ConA-AF647 in PBS at 37°C for 30 min. The ConA-AF647-stained yeast cells were washed two times with PBS and fixed with Roti-Histofix 4% (Roth) for at least 20 min at room temperature. The ratio of FITC-positive and -negative yeast cells was evaluated with BD FACS Verse (BD Biosciences, Franklin Lakes) counting 10,000 events. Data analysis was performed using the FlowJO 10.2 software (FlowJO LLC, Ashland). The gating strategy was based on the detection of single, ConA positive cells and exclusion of cellular debris. The assessment of intracellular replication with FACS allows the relative distinction between mother and daughter cells.

4.11 | Fungal RNA isolation

For preparation of RNA from in vitro cultured *Candida* cells, stationary phase yeast cells were washed three times in PBS and 2×10^7 *Candida* cells/mL were inoculated into minimal medium with different biotin concentrations. At indicated time points, cells were harvested and centrifuged (4,000*g*, 10 min and 4°C). The cell pellet was washed with ice-cold water, centrifuged again, and immediately frozen in liquid nitrogen. For preparation of RNA from phagocytosed *Candida* cells, stationary phase yeast cells were washed three times in PBS.

Macrophages (1×10^6 hMDMs/well) were infected at an MOI of 10 in serum and biotin-free RPMI (PAN Biotech) with L-glutamine (Thermo Fisher Scientific). Phagocytosis was synchronised for 30 min on ice and unbound *Candida* cells were removed by two washing steps with warm RPMI medium. After 3 hr of incubation at 37°C and 5% CO_2, infected macrophages were washed three times with ice-cold PBS and lysed with 750 μL RLT buffer (Qiagen) containing β-mercaptoethanol. Phagocytosed fungal cells were collected by using a cell scraper to loosen the host cells and centrifuged (20,000*g*, 12 min and 4°C). The fungal cells were washed once with RLT buffer to remove most of the host RNA and immediately frozen in liquid nitrogen.

The isolation of the fungal RNA was performed as previously described (Lüttich, Brunke, & Hube, 2012). The fungal RNA from infected host cells was treated with 3 U Baseline-ZERO DNase (Biozym) in a total volume of 50 μL at 37°C for 45 min. The RNA was then precipitated by adding 1 volume of isopropyl alcohol and one-tenth volume of sodium acetate (pH 5.5). The quantity of the RNA was determined using the NanoDrop Spectrophotometer ND-1000 (NRW International GmbH).

4.12 | Expression analysis by reverse transcription-quantitative PCR

DNase-treated RNA (600 ng) was transcribed into cDNA using 0.5 μg of oligo-dT_{12-18}, 100 U Superscript III Reverse Transcriptase and 20 U RNaseOUT Recombinant RNase Inhibitor (all: Thermo Fischer Scientific) in a total volume of 35 μL for 2 hr at 42°C followed by heat inactivation for 15 min at 70°C. The cDNA was diluted from 1:5 to 1:20 in Diethyl pyrocarbonate (DEPC)-treated water and used for quantitative PCR with EvaGreen QPCR Mix II (Bio&SELL) performed in a CFX96 thermocycler (Bio-Rad). Primers (Table S2) were used at a final concentration of 500 nM. Target gene expression was calculated using the $\Delta\Delta Ct$ method (Pfaffl, 2001), with normalisation to the housekeeping genes *CgACT1*, *CgEFB1*, *CgEFT2* for *C. glabrata* or *CaACT1*, *CaTDH3*, *CaEFT2* for *C. albicans*.

4.13 | Mouse model of systemic *C. glabrata* infection

Female, specific-pathogen-free CD-1 mice (Charles River, Germany; 8–10 weeks, 20–22 g) were randomly assigned into groups of five upon arrival and housed in individually ventilated cages. All *Candida* strains were either pre-starved for or fed with biotin for 24 hr before infection. On Day 0, mice were intravenously challenged with 2.5×10^7 cfu/20 g body weight in 100 μL PBS via the lateral tail vein. The health status was monitored at least twice a day. On days 2, 7 and 14, five mice per strain were euthanised with an overdose of ketamine (10 mg/20 g body weight) and xylazine (0.5 mg/20 g body weight) applied intraperitoneally.

4.14 | Mouse model of systemic *C. albicans* infection

Female, specific-pathogen-free BALB/cAnNRj mice (Janvier, France; 8 weeks, 18–22 g) were randomly assigned into groups of four (survival) and five (kinetics) upon arrival and housed in individually ventilated cages for the course of the experiment. On Day 0, mice were intravenously challenged with biotin pre-starved 2×10^5 cfu/20 g body weight in 100 μL PBS via the lateral tail vein. The health status was monitored at least twice a day. Mice which reached the humane endpoints (corresponding to moderate suffering and determined by a scoring system based on body weight, general appearance, changes in posture and behaviour, and body surface temperature) were euthanised with an overdose of ketamine (10 mg/20 g body weight) and xylazine (0.5 mg/20 g body weight) applied intraperitoneally. To determine the kinetics of fungal burden and inflammatory response in different organs, groups of five mice per strain were sacrificed 24 and 72 hr post-infection as described above.

4.15 | Quantification of fungal burden and cytokine levels in infected tissues

The mouse spleen, liver, kidneys and brain were removed aseptically, weighed and homogenised in tissue lysis buffer (200 mM NaCl, 5 mM EDTA, 10 mM Tris, 10% glycerol, 1 mM phenylmethylsulfonyl fluoride, 1 μg/ml leupeptin and 28 μg/ml aprotinin; pH 7.4) using an Ika T10 basic Ultra-Turrax homogeniser (Ika, Staufen, Germany). To determine fungal burden, serial dilutions of homogenates were cultivated on YPD plates containing 2 mg/L biotin and 80 μg/mL chloramphenicol. Colonies were counted after 24–48 hr of incubation at 30–37°C with an automated colony counter ProtoCOL3 (Synbiosis, Cambridge, UK). The fungal burden was calculated as cfu per gram of tissue.

For cytokine profiling, tissue homogenates were immediately centrifuged (1,500*g*, 15 min, 4°C) and supernatants were stored at −80°C. For cytokine measurement, frozen tissue homogenates were thawed on ice and centrifuged once (1,500*g*, 15 min, 4°C). The supernatants were diluted in supplied assay diluent supplied by manufacturer and enzyme and cytokine levels were determined by commercially available mouse enzyme-linked immunosorbent assay (ELISA) kits (Interleukin 1β [IL-1β], monocyte-chemoattractant protein-1 [CCL-2 or MCP-1], Interleukin 6 [IL-6] and Interferon-γ [IFN-γ] ELISA Ready SET Go! eBioscience, Thermo Fisher Scientific and myeloperoxidase [MPO] DuoSet, R&D systems) according to the manufacturer's instructions.

4.16 | *In silico* analysis and statistical analysis

Information about gene orthologs was obtained from the *Candida* Genome Database (Skrzypek et al., 2017) and the *Saccharomyces* Genome Database (Cherry et al., 2012). Potential orthologs were identified by BLAST search, based on *S. cerevisiae* protein sequences. Direct comparison of two sequences was done using BLAST (https://blast.ncbi.nlm.nih.gov/Blast.cgi). Transmembrane prediction analysis was done using TMHMM Server v. 2.0 (prediction of transmembrane helices in proteins, http://www.cbs.dtu.dk/services/TMHMM/) and TMpred (membrane-spanning region prediction, https://embnet.vital-it.ch/software/TMPRED_form.html; Hofmann & Stoffel, 1993). Data are reported as scatterplot with mean ± SD, line charts with mean ± SD, or bar charts showing mean + SD. Data were analysed using GraphPad Prism 5 (GraphPad Software, San Diego) and a one-way analysis of variance (ANOVA) with Bonferroni's or Dunn's multiple comparison test. For statistical analysis of matched observations in macrophage experiments and experiments on wildtype filamentation, a repeated measures ANOVA with Dunnett's or Bonferroni's multiple comparison test was performed. To represent the scattering of hyphal length, we illustrate the mean and standard deviation of all measured hypha in three replicates, but have used the mean of each replicate for statistical analysis. Reverse transcription-quantitative PCR data were statistically analysed using a two-way ANOVA with Bonferroni's post-tests to evaluate differences between the strains and biotin concentrations. Statistically significant results are marked with a single asterisk or hash meaning $p \leq .05$, double asterisks or hashes meaning $p \leq .01$ or triple asterisks or hashes meaning $p \leq .001$, n.d., not detectable. If symbol/colour explanations apply to several graphs in a row, one legend is given for neighbouring sub-panels on the right.

CONFLICT OF INTEREST

The authors have no conflict of interest.

AUTHOR CONTRIBUTIONS

ORCID

Marcel Sprenger https://orcid.org/0000-0002-8757-1230
Stefanie Allert https://orcid.org/0000-0003-0823-4824
Maria J. Niemiec https://orcid.org/0000-0001-5667-6032
Ilse D. Jacobsen https://orcid.org/0000-0002-6033-9984
Lydia Kasper https://orcid.org/0000-0002-4552-7063
Bernhard Hube https://orcid.org/0000-0002-6028-0425

REFERENCES

Ahmad Hussin, N., Pathirana, R. U., Hasim, S., Tati, S., Scheib-Owens, J. A., & Nickerson, K. W. (2016). Biotin auxotrophy and biotin enhanced germ tube formation in *Candida albicans*. *Microorganisms*, *4*(3), 37. https://doi.org/10.3390/microorganisms4030037

Beyer, R., Jandric, Z., Zutz, C., Gregori, C., Willinger, B., Jacobsen, I. D., ... Schüller, C. (2018). Competition of *Candida glabrata* against *Lactobacillus* is Hog1 dependent. *Cellular Microbiology*, *20*(12), e12943. https://doi.org/10.1111/cmi.12943

Brunke, S., & Hube, B. (2013). Two unlike cousins: *Candida albicans* and *C. glabrata* infection strategies. *Cellular Microbiology*, *15*(5), 701–708. https://doi.org/10.1111/cmi.12091

Brunke, S., Quintin, J., Kasper, L., Jacobsen, I. D., Richter, M. E., Hiller, E., ... Ferrandon, D. (2015). Of mice, flies—and men? Comparing fungal infection models for large-scale screening efforts. *Disease Models & Mechanisms*, *8*(5), 473–486. https://doi.org/10.1242/dmm.019901

Carfrae, L. A., MacNair, C. R., Brown, C. M., Tsai, C. N., Weber, B. S., Zlitni, S., ... Brown, E. D. (2020). Mimicking the human environment in mice reveals that inhibiting biotin biosynthesis is effective against antibiotic-resistant pathogens. *Nature Microbiology*, *5*(1), 93–101. https://doi.org/10.1038/s41564-019-0595-2

Cherry, J. M., Hong, E. L., Amundsen, C., Balakrishnan, R., Binkley, G., Chan, E. T., ... Wong, E. D. (2012). *Saccharomyces* genome database: The genomics resource of budding yeast. *Nucleic Acids Research*, *40*, D700–D705. https://doi.org/10.1093/nar/gkr1029

Chew, S. Y., Ho, K. L., Cheah, Y. K., Ng, T. S., Sandai, D., Brown, A. J. P., & Than, L. T. L. (2019). Glyoxylate cycle gene *ICL1* is essential for the metabolic flexibility and virulence of *Candida glabrata*. *Scientific Reports*, *9*(1), 2843. https://doi.org/10.1038/s41598-019-39117-1

Childers, D. S., Raziunaite, I., Mol Avelar, G., Mackie, J., Budge, S., Stead, D., ... Brown, A. J. (2016). The rewiring of ubiquitination targets in a pathogenic yeast promotes metabolic flexibility, host colonization and virulence. *PLoS Pathogens*, *12*(4), e1005566. https://doi.org/10.1371/journal.ppat.1005566

Combs, G. F., & McClung, J. P. (2017). *The vitamins: Fundamental aspects in nutrition and health* (5th ed.). Cambridge, Massachusetts: Academic Press.

Cooper, K. M., Kennedy, S., McConnell, S., Kennedy, D. G., & Frigg, M. (1997). An immunohistochemical study of the distribution of biotin in tissues of pigs and chickens. *Research in Veterinary Science*, *63*(3), 219–225.

Dagher, Z., Xu, S., Negoro, P. E., Khan, N. S., Feldman, M. B., Reedy, J. L., ... Mansour, M. K. (2018). Fluorescent tracking of yeast division clarifies the essential role of spleen tyrosine kinase in the intracellular control of *Candida glabrata* in macrophages. *Frontiers in Immunology*, *9*, 1058. https://doi.org/10.3389/fimmu.2018.01058

Dakshinamurti, K. (2005). Biotin—A regulator of gene expression. *The Journal of Nutritional Biochemistry*, *16*(7), 419–423. https://doi.org/10.1016/j.jnutbio.2005.03.015

Domergue, R., Castaño, I., De Las Peñas, A., Zupancic, M., Lockatell, V., Hebel, J. R., ... Cormack, B. P. (2005). Nicotinic acid limitation regulates silencing of *Candida* adhesins during UTI. *Science*, *308*(5723), 866–870. https://doi.org/10.1126/science.1108640

Dujon, B., Sherman, D., Fischer, G., Durrens, P., Casaregola, S., Lafontaine, I., ... Souciet, J. L. (2004). Genome evolution in yeasts. *Nature*, *430*(6995), 35–44. https://doi.org/10.1038/nature02579

Erwig, L. P., & Gow, N. A. (2016). Interactions of fungal pathogens with phagocytes. *Nature Reviews. Microbiology*, *14*(3), 163–176. https://doi.org/10.1038/nrmicro.2015.21

Feng, Y., Chin, C. Y., Chakravartty, V., Gao, R., Crispell, E. K., Weiss, D. S., & Cronan, J. E. (2015). The atypical occurrence of two biotin protein ligases in *Francisella novicida* is due to distinct roles in virulence and biotin metabolism. *MBio*, *6*(3), e00591. https://doi.org/10.1128/mBio.00591-15

Firestone, B. Y., & Koser, S. A. (1960). Growth promoting effect of some biotin analogues for *Candida albicans*. *Journal of Bacteriology*, *79*, 674–676.

Fitzpatrick, D. A., O'Gaora, P., Byrne, K. P., & Butler, G. (2010). Analysis of gene evolution and metabolic pathways using the *Candida* gene order browser. *BMC Genomics*, *11*, 290. https://doi.org/10.1186/1471-2164-11-290

Garfoot, A. L., Zemska, O., & Rappleye, C. A. (2014). *Histoplasma capsulatum* depends on de novo vitamin biosynthesis for intraphagosomal proliferation. *Infection and Immunity*, *82*(1), 393–404. https://doi.org/10.1128/IAI.00824-13

Gaur, M., Puri, N., Manoharlal, R., Rai, V., Mukhopadhayay, G., Choudhury, D., & Prasad, R. (2008). MFS transportome of the human pathogenic yeast *Candida albicans*. *BMC Genomics*, *9*, 579. https://doi.org/10.1186/1471-2164-9-579

Haas, A. (2007). The phagosome: Compartment with a license to kill. *Traffic*, *8*(4), 311–330. https://doi.org/10.1111/j.1600-0854.2006.00531.x

Hall, C., & Dietrich, F. S. (2007). The reacquisition of biotin prototrophy in *Saccharomyces cerevisiae* involved horizontal gene transfer, gene duplication and gene clustering. *Genetics*, *177*(4), 2293–2307. https://doi.org/10.1534/genetics.107.074963

Hill, M. J. (1997). Intestinal flora and endogenous vitamin synthesis. *European Journal of Cancer Prevention*, *6*(Suppl. 1), S43–S45.

Hofmann, K., & Stoffel, W. (1993). TMbase—A database of membrane spanning proteins segments. *Biological Chemistry Hoppe-Seyler*, *347*, 166.

Horn, D. L., Neofytos, D., Anaissie, E. J., Fishman, J. A., Steinbach, W. J., Olyaei, A. J., ... Webster, K. M. (2009). Epidemiology and outcomes of candidemia in 2019 patients: Data from the prospective antifungal therapy alliance registry. *Clinical Infectious Diseases*, *48*(12), 1695–1703. https://doi.org/10.1086/599039

Huffnagle, G. B., & Noverr, M. C. (2013). The emerging world of the fungal microbiome. *Trends in Microbiology*, *21*(7), 334–341. https://doi.org/10.1016/j.tim.2013.04.002

Jacobsen, I. D., Brunke, S., Seider, K., Schwarzmüller, T., Firon, A., d'Enfert, C., ... Hube, B. (2010). *Candida glabrata* persistence in mice does not depend on host immunosuppression and is unaffected by fungal amino acid auxotrophy. *Infection and Immunity*, *78*(3), 1066–1077. https://doi.org/10.1128/IAI.01244-09

Jacobsen, I. D., Lüttich, A., Kurzai, O., Hube, B., & Brock, M. (2014). In vivo imaging of disseminated murine *Candida albicans* infection reveals unexpected host sites of fungal persistence during antifungal therapy. *The Journal of Antimicrobial Chemotherapy*, *69*(10), 2785–2796. https://doi.org/10.1093/jac/dku198

Jacobsen, I. D., Wilson, D., Wächtler, B., Brunke, S., Naglik, J. R., & Hube, B. (2012). *Candida albicans* dimorphism as a therapeutic target.

Expert Review of Anti-Infective Therapy, 10(1), 85–93. https://doi.org/10.1586/eri.11.152

Kasper, L., König, A., Koenig, P. A., Gresnigt, M. S., Westman, J., Drummond, R. A., ... Hube, B. (2018). The fungal peptide toxin Candidalysin activates the NLRP3 inflammasome and causes cytolysis in mononuclear phagocytes. *Nature Communications, 9*(1), 4260. https://doi.org/10.1038/s41467-018-06607-1

Kaur, R., Domergue, R., Zupancic, M. L., & Cormack, B. P. (2005). A yeast by any other name: *Candida glabrata* and its interaction with the host. *Current Opinion in Microbiology, 8*(4), 378–384. https://doi.org/10.1016/j.mib.2005.06.012

Kaur, R., Ma, B., & Cormack, B. P. (2007). A family of glycosylphosphatidylinositol-linked aspartyl proteases is required for virulence of *Candida glabrata*. *Proceedings of the National Academy of Sciences of the United States of America, 104*(18), 7628–7633. https://doi.org/10.1073/pnas.0611195104

Knowles, J. R. (1989). The mechanism of biotin-dependent enzymes. *Annual Review of Biochemistry, 58*, 195–221. https://doi.org/10.1146/annurev.bi.58.070189.001211

Lindberg, E., Hammarstrom, H., Ataollahy, N., & Kondori, N. (2019). Species distribution and antifungal drug susceptibilities of yeasts isolated from the blood samples of patients with candidemia. *Scientific Reports, 9*(1), 3838. https://doi.org/10.1038/s41598-019-40280-8

Lionakis, M. S., Lim, J. K., Lee, C. C., & Murphy, P. M. (2011). Organ-specific innate immune responses in a mouse model of invasive candidiasis. *Journal of Innate Immunity, 3*(2), 180–199. https://doi.org/10.1159/000321157

Littman, M. L., & Miwatani, T. (1963). Effect of water soluble vitamins and their analogues on the growth of *Candida albicans*. I. Biotin, pyridoxamine, pyridoxine and fluorinated pyrimidines. *Mycopathologia et Mycologia Applicata, 21*, 81–108.

Lorenz, M. C. (2013). Carbon catabolite control in *Candida albicans*: New wrinkles in metabolism. *MBio, 4*(1), e00034–e00013. https://doi.org/10.1128/mBio.00034-13

Lorenz, M. C., Bender, J. A., & Fink, G. R. (2004). Transcriptional response of *Candida albicans* upon internalization by macrophages. *Eukaryotic Cell, 3*(5), 1076–1087. https://doi.org/10.1128/EC.3.5.1076-1087.2004

Lüttich, A., Brunke, S., & Hube, B. (2012). Isolation and amplification of fungal RNA for microarray analysis from host samples. *Methods in Molecular Biology, 845*, 411–421. https://doi.org/10.1007/978-1-61779-539-8_28

Magliano, P., Flipphi, M., Sanglard, D., & Poirier, Y. (2011). Characterization of the *Aspergillus nidulans* biotin biosynthetic gene cluster and use of the bioDA gene as a new transformation marker. *Fungal Genetics and Biology, 48*(2), 208–215. https://doi.org/10.1016/j.fgb.2010.08.004

Magnusdottir, S., Ravcheev, D., de Crecy-Lagard, V., & Thiele, I. (2015). Systematic genome assessment of B-vitamin biosynthesis suggests cooperation among gut microbes. *Frontiers in Genetics, 6*, 148. https://doi.org/10.3389/fgene.2015.00148

McCall, A. D., Kumar, R., & Edgerton, M. (2018). *Candida albicans* Sfl1/Sfl2 regulatory network drives the formation of pathogenic microcolonies. *PLoS Pathogens, 14*(9), e1007316. https://doi.org/10.1371/journal.ppat.1007316

McKenzie, C. G., Koser, U., Lewis, L. E., Bain, J. M., Mora-Montes, H. M., Barker, R. N., ... Erwig, L. P. (2010). Contribution of *Candida albicans* cell wall components to recognition by and escape from murine macrophages. *Infection and Immunity, 78*(4), 1650–1658. https://doi.org/10.1128/IAI.00001-10

McVeigh, I., & Bell, E. (1951). The amino acid and vitamin requirements of *Candida albicans* Y-475 and *Mycoderma vini* Y-939. *Bulletin of the Torrey Botanical Club, 78*(2), 134–144. https://doi.org/10.2307/2482046

Meir, Z., & Osherov, N. (2018). Vitamin biosynthesis as an antifungal target. *Journal of Fungi, 4*(2), 72. https://doi.org/10.3390/jof4020072

Mikkelsen, K., Stojanovska, L., Prakash, M., & Apostolopoulos, V. (2017). The effects of vitamin B on the immune/cytokine network and their involvement in depression. *Maturitas, 96*, 58–71. https://doi.org/10.1016/j.maturitas.2016.11.012

Miramón, P., Kasper, L., & Hube, B. (2013). Thriving within the host: *Candida* spp. interactions with phagocytic cells. *Medical Microbiology and Immunology, 202*(3), 183–195. https://doi.org/10.1007/s00430-013-0288-z

Miramón, P., & Lorenz, M. C. (2017). A feast for *Candida*: Metabolic plasticity confers an edge for virulence. *PLoS Pathogens, 13*(2), e1006144. https://doi.org/10.1371/journal.ppat.1006144

Murad, A. M., Lee, P. R., Broadbent, I. D., Barelle, C. J., & Brown, A. J. (2000). Clp10, an efficient and convenient integrating vector for *Candida albicans*. *Yeast, 16*(4), 325–327. https://doi.org/10.1002/1097-0061(20000315)16:4<325::AID-YEA538>3.0.CO;2-#

Napier, B. A., Meyer, L., Bina, J. E., Miller, M. A., Sjostedt, A., & Weiss, D. S. (2012). Link between intraphagosomal biotin and rapid phagosomal escape in *Francisella*. *Proceedings of the National Academy of Sciences of the United States of America, 109*(44), 18084–18089. https://doi.org/10.1073/pnas.1206411109

Odds, F. C. (1988). *Candida and candidosis: A review and bibliography* (2nd ed.). London - Philadelphia - Toronto - Sydney - Tokyo: Baillière Tindall.

Ogoshi, R. C., Zangeronimo, M. G., Dos Reis, J. S., Franca, J., Santos, J. P., Pires, C. P., ... Saad, F. M. (2014). Acidifying and yeast extract in diets for adults cats. *Animal Science Journal, 85*(5), 555–561. https://doi.org/10.1111/asj.12166

O'Meara, T. R., Duah, K., Guo, C. X., Maxson, M. E., Gaudet, R. G., Koselny, K., ... Cowen, L. E. (2018). High-throughput screening identifies genes required for *Candida albicans* induction of macrophage pyroptosis. *MBio, 9*(4), pii: e01581–18. https://doi.org/10.1128/mBio.01581-18

Pfaffl, M. W. (2001). A new mathematical model for relative quantification in real-time RT-PCR. *Nucleic Acids Research, 29*(9), e45.

Pfaller, M. A., & Diekema, D. J. (2007). Epidemiology of invasive candidiasis: A persistent public health problem. *Clinical Microbiology Reviews, 20*(1), 133–163. https://doi.org/10.1128/CMR.00029-06

Phalip, V., Kuhn, I., Lemoine, Y., & Jeltsch, J. M. (1999). Characterization of the biotin biosynthesis pathway in *Saccharomyces cerevisiae* and evidence for a cluster containing *BIO5*, a novel gene involved in vitamer uptake. *Gene, 232*(1), 43–51.

Purnell, D. M. (1973). The effects of specific auxotrophic mutations on the virulence of *Aspergillus nidulans* for mice. *Mycopathologia et Mycologia Applicata, 50*(3), 195–203.

Rengarajan, J., Bloom, B. R., & Rubin, E. J. (2005). Genome-wide requirements for *Mycobacterium tuberculosis* adaptation and survival in macrophages. *Proceedings of the National Academy of Sciences of the United States of America, 102*(23), 8327–8332. https://doi.org/10.1073/pnas.0503272102

Roetzer, A., Gratz, N., Kovarik, P., & Schüller, C. (2010). Autophagy supports *Candida glabrata* survival during phagocytosis. *Cellular Microbiology, 12*(2), 199–216. https://doi.org/10.1111/j.1462-5822.2009.01391.x

Roje, S. (2007). Vitamin B biosynthesis in plants. *Phytochemistry, 68*(14), 1904–1921. https://doi.org/10.1016/j.phytochem.2007.03.038

Ruiz-Amil, M., De Torrontegui, G., Palacian, E., Catalina, L., & Losada, M. (1965). Properties and function of yeast pyruvate carboxylase. *The Journal of Biological Chemistry, 240*(9), 3485–3492.

Salaemae, W., Booker, G. W., & Polyak, S. W. (2016). The role of biotin in bacterial physiology and virulence: A novel antibiotic target for *Mycobacterium tuberculosis*. *Microbiology Spectrum, 4*(2): VMBF-0008-2015. https://doi.org/10.1128/microbiolspec.VMBF-0008-2015

Sanglard, D., Ischer, F., Monod, M., & Bille, J. (1996). Susceptibilities of *Candida albicans* multidrug transporter mutants to various antifungal

agents and other metabolic inhibitors. *Antimicrobial Agents and Chemotherapy*, *40*(10), 2300–2305.

Schwarzmüller, T., Ma, B., Hiller, E., Istel, F., Tscherner, M., Brunke, S., ... Kuchler, K. (2014). Systematic phenotyping of a large-scale *Candida glabrata* deletion collection reveals novel antifungal tolerance genes. *PLoS Pathogens*, *10*(6), e1004211. https://doi.org/10.1371/journal.ppat.1004211

Seider, K., Brunke, S., Schild, L., Jablonowski, N., Wilson, D., Majer, O., ... Hube, B. (2011). The facultative intracellular pathogen *Candida glabrata* subverts macrophage cytokine production and phagolysosome maturation. *Journal of Immunology*, *187*(6), 3072–3086. https://doi.org/10.4049/jimmunol.1003730

Seider, K., Gerwien, F., Kasper, L., Allert, S., Brunke, S., Jablonowski, N., ... Hube, B. (2014). Immune evasion, stress resistance, and efficient nutrient acquisition are crucial for intracellular survival of *Candida glabrata* within macrophages. *Eukaryotic Cell*, *13*(1), 170–183. https://doi.org/10.1128/EC.00262-13

Skrzypek, M. S., Binkley, J., Binkley, G., Miyasato, S. R., Simison, M., & Sherlock, G. (2017). The *Candida* Genome Database (CGD): Incorporation of Assembly 22, systematic identifiers and visualization of high throughput sequencing data. *Nucleic Acids Research*, *45*(D1), D592–D596. https://doi.org/10.1093/nar/gkw924

Sonnhammer, E. L., von Heijne, G., & Krogh, A. (1998). A hidden Markov model for predicting transmembrane helices in protein sequences. *Proceedings. International Conference on Intelligent Systems for Molecular Biology*, *6*, 175–182.

Spector, R., & Johanson, C. E. (2007). Vitamin transport and homeostasis in mammalian brain: Focus on vitamins B and E. *Journal of Neurochemistry*, *103*(2), 425–438. https://doi.org/10.1111/j.1471-4159.2007.04773.x

Sprenger, M., Kasper, L., Hensel, M., & Hube, B. (2017). Metabolic adaptation of intracellular bacteria and fungi to macrophages. *International Journal of Medical Microbiology*, *308*, 215–227. https://doi.org/10.1016/j.ijmm.2017.11.001

Stephensen, C. B. (2001). Vitamin A, infection, and immune function. *Annual Review of Nutrition*, *21*, 167–192. https://doi.org/10.1146/annurev.nutr.21.1.167

Stolz, J. (2009). Das Vitamin für Haut, Haar und Hefe. *BIOspektrum*, 132–135.

Stolz, J., Hoja, U., Meier, S., Sauer, N., & Schweizer, E. (1999). Identification of the plasma membrane H$^+$-biotin symporter of *Saccharomyces cerevisiae* by rescue of a fatty acid-auxotrophic mutant. *The Journal of Biological Chemistry*, *274*(26), 18741–18746.

Sudbery, P. E. (2011). Growth of *Candida albicans* hyphae. *Nature Reviews. Microbiology*, *9*(10), 737–748. https://doi.org/10.1038/nrmicro2636

Tong, L. (2013). Structure and function of biotin-dependent carboxylases. *Cellular and Molecular Life Sciences*, *70*(5), 863–891. https://doi.org/10.1007/s00018-012-1096-0

Vylkova, S., & Lorenz, M. C. (2014). Modulation of phagosomal pH by *Candida albicans* promotes hyphal morphogenesis and requires Stp2p, a regulator of amino acid transport. *PLoS Pathogens*, *10*(3), e1003995. https://doi.org/10.1371/journal.ppat.1003995

Walther, A., & Wendland, J. (2003). An improved transformation protocol for the human fungal pathogen *Candida albicans*. *Current Genetics*, *42*(6), 339–343. https://doi.org/10.1007/s00294-002-0349-0

Weider, M., Machnik, A., Klebl, F., & Sauer, N. (2006). Vhr1p, a new transcription factor from budding yeast, regulates biotin-dependent expression of *VHT1* and *BIO5*. *The Journal of Biological Chemistry*, *281*(19), 13513–13524. https://doi.org/10.1074/jbc.M512158200

Westman, J., Moran, G., Mogavero, S., Hube, B., & Grinstein, S. (2018). *Candida albicans* hyphal expansion causes phagosomal membrane damage and luminal alkalinization. *MBio*, *9*(5), pii: e01226–18. https://doi.org/10.1128/mBio.01226-18

Wilson, R. B., Davis, D., & Mitchell, A. P. (1999). Rapid hypothesis testing with *Candida albicans* through gene disruption with short homology regions. *Journal of Bacteriology*, *181*(6), 1868–1874.

Yagi, T., Kagamiyama, H., & Nozaki, M. (1982). Aspartate: 2-Oxoglutarate aminotransferase from bakers' yeast: Crystallization and characterization. *Journal of Biochemistry*, *92*(1), 35–43. https://doi.org/10.1093/oxfordjournals.jbchem.a133929

Yanez-Carrillo, P., Orta-Zavalza, E., Gutierrez-Escobedo, G., Patron-Soberano, A., De Las Penas, A., & Castano, I. (2015). Expression vectors for C-terminal fusions with fluorescent proteins and epitope tags in *Candida glabrata*. *Fungal Genetics and Biology*, *80*, 43–52. https://doi.org/10.1016/j.fgb.2015.04.020

Yu, J., Niu, C., Wang, D., Li, M., Teo, W., Sun, G., ... Gao, Q. (2011). MMAR_2770, a new enzyme involved in biotin biosynthesis, is essential for the growth of *Mycobacterium marinum* in macrophages and zebrafish. *Microbes and Infection*, *13*(1), 33–41. https://doi.org/10.1016/j.micinf.2010.08.010

Zempleni, J., Hassan, Y. I., & Wijeratne, S. S. (2008). Biotin and biotinidase deficiency. *Expert Review of Endocrinology and Metabolism*, *3*(6), 715–724. https://doi.org/10.1586/17446651.3.6.715

Zempleni, J., Wijeratne, S. S., & Hassan, Y. I. (2009). Biotin. *BioFactors*, *35*(1), 36–46. https://doi.org/10.1002/biof.8

SUPPORTING INFORMATION

Additional supporting information may be found online in the Supporting Information section at the end of this article.

1 **Data files**

2
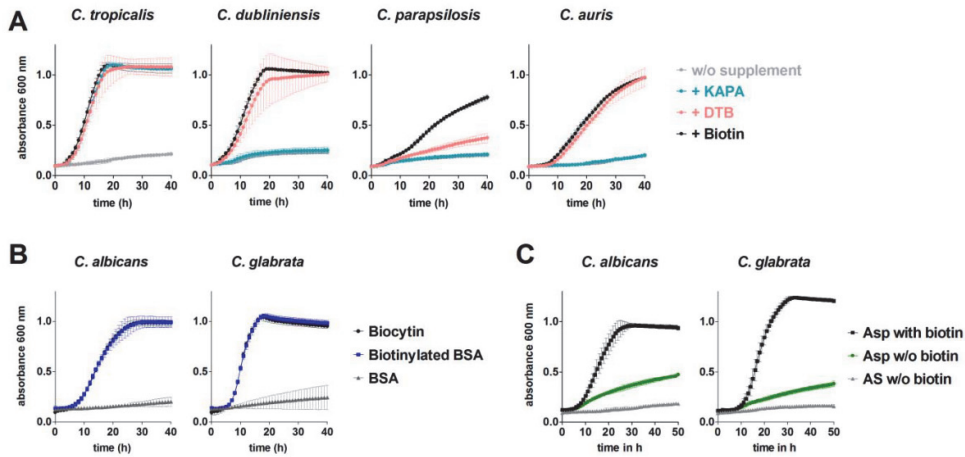
3

4 **FIGURE S1 Growth of pathogenic *Candida* species depending on biotin, biotin**

5 **biosynthesis intermediates, biotin-containing compounds, or aspartate.**

6 Yeast growth of biotin pre-starved (pre-cultured in biotin-free minimal medium) *Candida* spp.

7 cells in minimal medium (A) containing biotin or biotin precursors (each 2 µg/L) or no biotin

8 (w/o supplement), (B) biocytin, biotinylated BSA or BSA (each 2 µg/L) and (C) 0.4 %

9 aspartate (Asp) or 0.5 % ammonium sulfate (AS) as nitrogen source with or without 2 µg/L

10 biotin at 30°C. Values are represented as mean ± SD of at least three replicates.
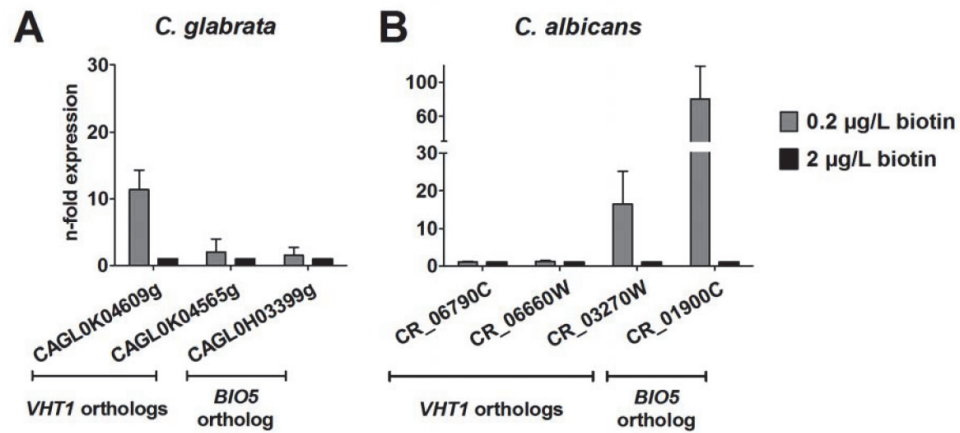
FIGURE S2 Biotin limitation induces up-regulation of putative orthologs of S. cerevisiae VHT1 and BIO5.

Non-starved (A) *C. glabrata* (ATCC2001) and (B) *C. albicans* (SC5314) wild type strains (2×10^7 cells/mL) were cultivated in medium with indicated biotin concentrations for 3 h at 37 °C and 180 rpm. Transcript abundance of the putative *VHT1* orthologs CAGL0K04609g, CAGL0K04565g, CR_06790C, CR_06660W and CR_03270W as well as the putative *BIO5* orthologs CAGL0H03399g and CR_01900C was analyzed by quantitative RT-PCR and normalized to the housekeeping genes *CgACT1*, *CgEFB1* and *CaTDH3*, *CaEFT2*. Values are represented as mean + SD of three independent experiments, whereby n-fold expression for each gene is shown relative to 2 µg/L biotin.
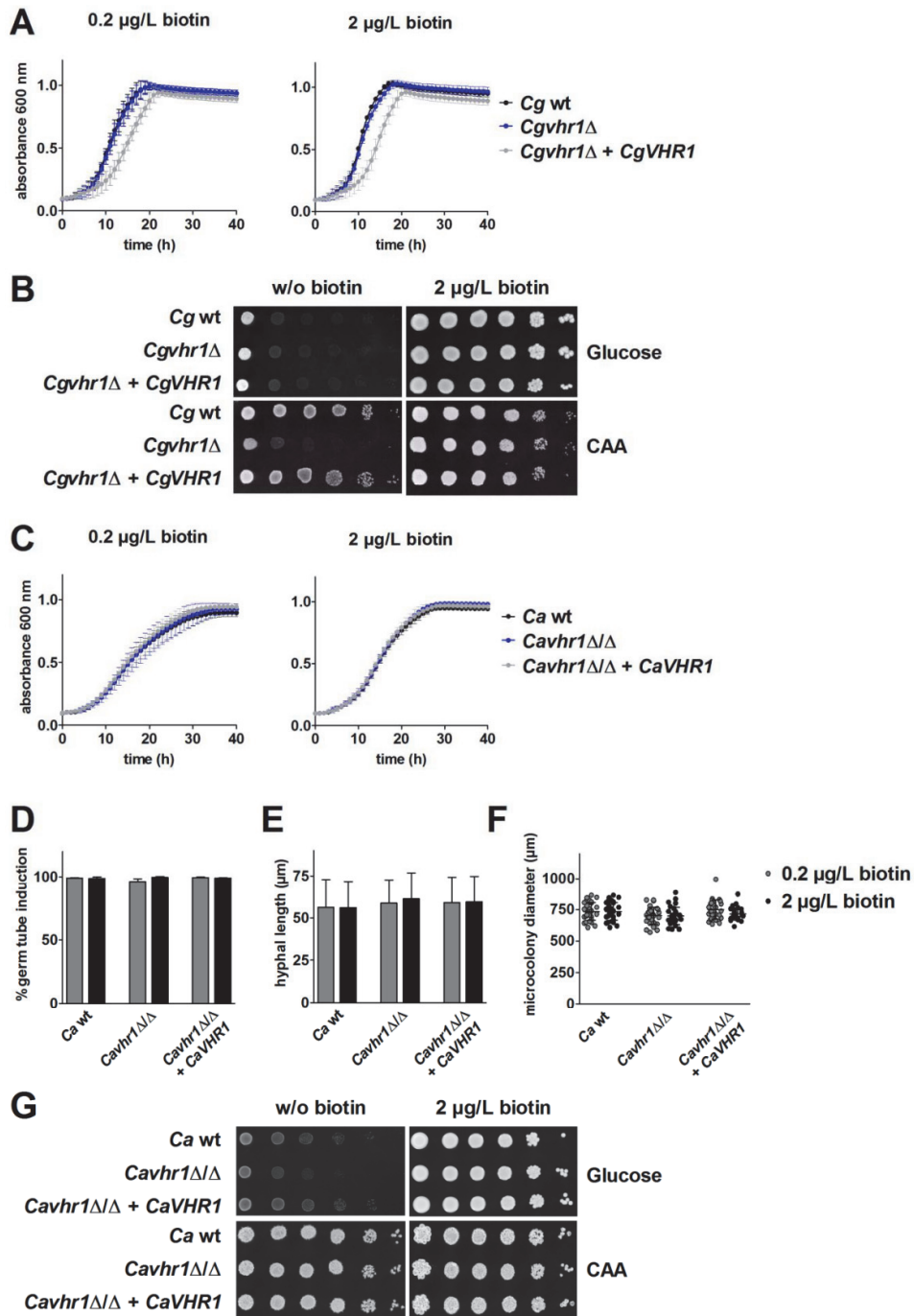
FIGURE S3 ***VHR1* is mostly dispensable for biotin-dependent growth *in vitro*.**

Yeast growth of biotin pre-starved *C. glabrata* wt, mutant (*Cgvhr1*Δ) and complemented strains (*Cgvhr1*Δ + *CgVHR1*) (A) in minimal medium with addition of 0.2 or 2 µg/L biotin or (B) on solid minimal medium with either casamino acids (CAA) as a sole carbon- and nitrogen source or glucose and ammonium sulfate without or with biotin by spotting serial dilutions ranging from 10^6 to 10^1 cells at 37 °C. A representative picture out of three independent experiments is shown. (C) Yeast growth and (D-F) hyphal growth of biotin pre-starved *C. albicans* wt, mutant (*Cavhr1*Δ/Δ) and complemented strains (*Cavhr1*Δ/Δ + *CaVHR1*) in (C) minimal medium at 30 °C and (D-F) in RPMI1640 at 37 °C and 5 % CO_2 with addition of 0.2 or 2 µg/L biotin. (D) Percentage of germ tube-forming cells at 2 h. (D) Hyphal length at 4 h (mean + SD of individual hyphae from three replicates). (E) Microcolony size at 24 h (each single dot represents one individual microcolony). Values are represented as mean ± SD (A,C, and F) or mean + SD (D-E) of at least three replicates. (G) Serial dilutions ranging from 10^6 to 10^1 biotin pre-starved *C. albicans* cells were spotted on solid minimal medium with either CAA as a sole carbon- and nitrogen source or glucose and ammonium sulfate without or with biotin. A representative picture out of three independent experiments is shown.

42
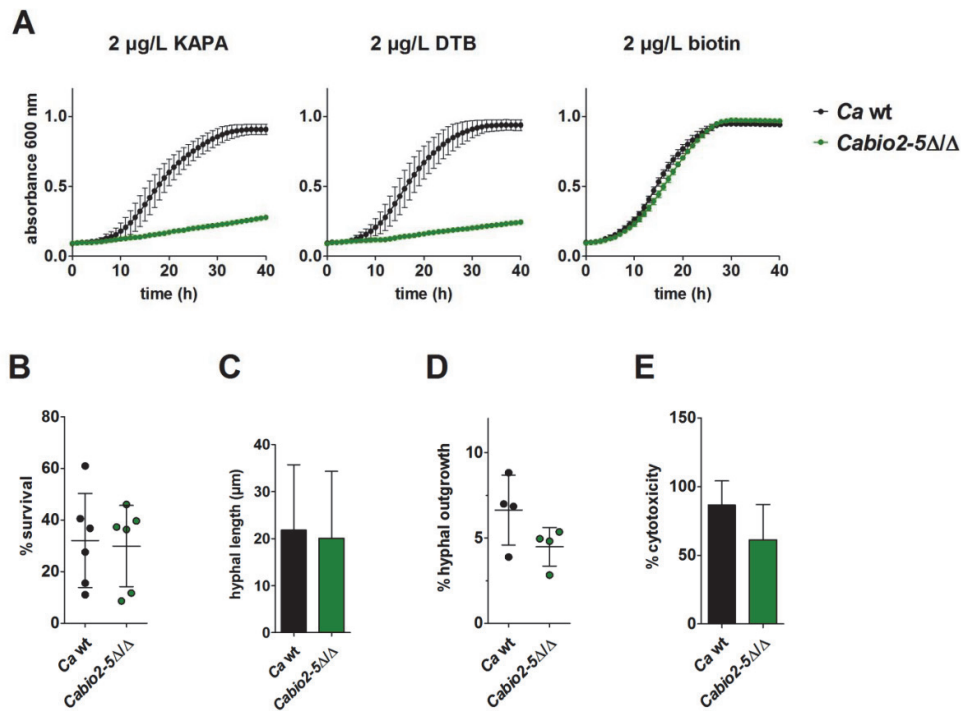
FIGURE S4 *CaBIO2-5* **allows utilization of biotin precursors but is dispensable for macrophage infectivity.**

(A) Yeast growth of biotin pre-starved *C. albicans* wt or *Cabio2-5Δ/Δ* mutant in minimal medium containing biotin or biotin precursors (each 2 μg/L) at 30 °C of five biological replicates. (B) *C. albicans* wild type (wt) and mutant (*bio2-5Δ/Δ*) were pre-cultivated in YPD with 2 mg/L biotin before confrontation with human blood monocyte-derived macrophages (hMDMs). (B) Survival after 3 h (% survival of inoculum). (C) Length of hyphae formed 10 h after phagocytosis. (D) Outgrowth of *C. albicans* hyphae from macrophages after 10 h (% of ingested hyphae piercing the macrophage membrane). (E) Macrophage damage by *C. albicans* after 24 h (% cytotoxicity; 100 % refers to full lysis).

Values in C are represented as mean + SD of individual hyphae from four donors in two independent experiments. Values are represented as mean ± SD (A), mean + SD (E) or as scatterplot with mean ± SD (B,D) with each single dot corresponding to one blood donor (total at least six (B) or four (C-D) different donors in at least two independent experiments).

57

58
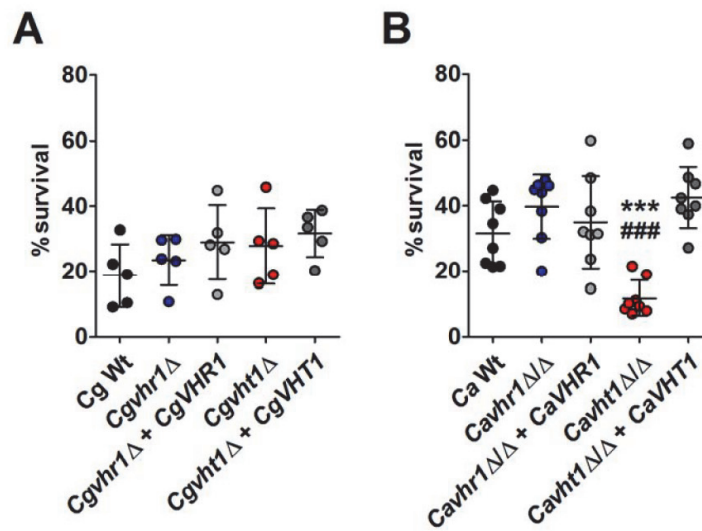
FIGURE S5 Biotin pre-starvation affects survival within macrophages.

Wild type (wt), mutant (*vht1Δ*), or complemented strains (*vht1Δ + VHT1*) of (A) *C. glabrata* or (B) *C. albicans* cells were biotin pre-starved for 24 h in minimal medium without biotin before confrontation with human blood monocyte-derived macrophages (hMDMs). Survival of *C. glabrata* (A) and *C. albicans* (B) strains after 3 h (% survival of inoculum). Values are represented as scatterplot with mean ± SD, with each single dot corresponding to one blood donor (at least five different donors in two independent experiments). For statistical analysis, a Repeated Measures ANOVA with Bonferroni's multiple comparison test was performed (* $p \leq 0.05$, ** $p \leq 0.01$, *** $p \leq 0.001$ comparing wt and deletion mutant; ## $p \leq 0.01$, ### $p \leq 0.001$ comparing deletion mutant to the respective complemented strain).

69
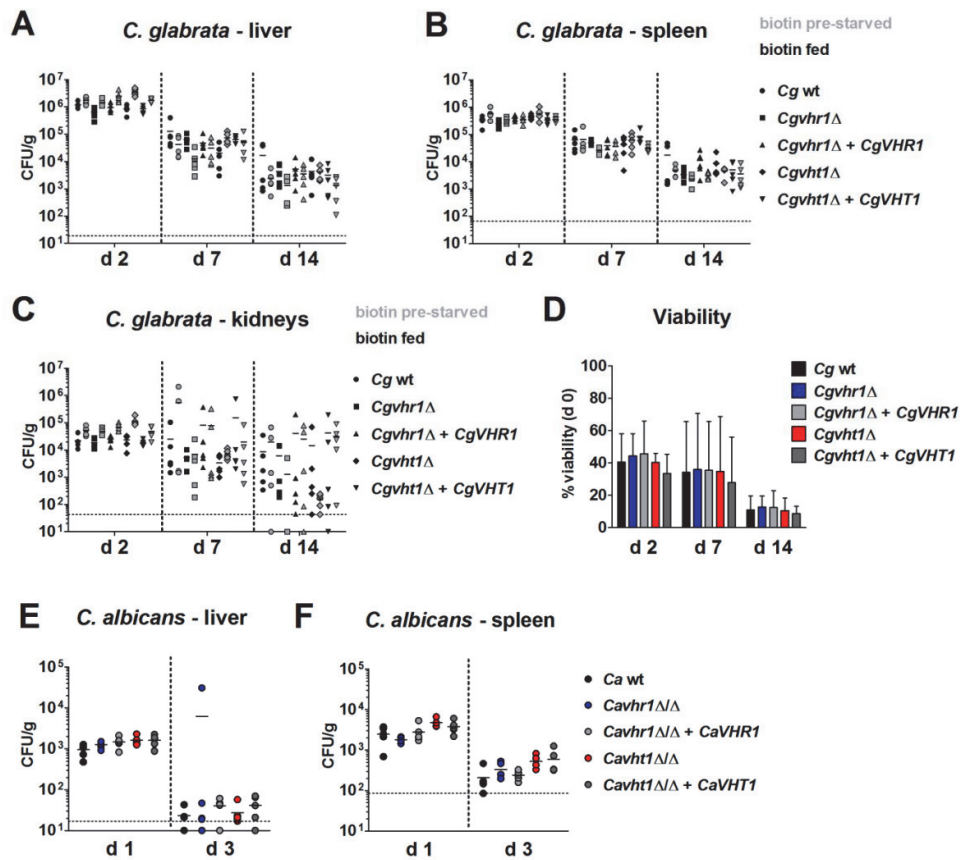
FIGURE S6 Fungal burden in mouse organs after systemic *C. glabrata* and *C. albicans* infection and long term viability of *C. glabrata*.

(A-C) Fungal burden in organs of mice infected either with biotin-starved (gray) or biotin-fed (black) *C. glabrata* wild type, mutant or complemented strains. Five mice per group were intravenously infected with 2.5×10^7 yeast cells/20 g body weight on day 0. The fungal burden was determined by quantifying cfu in tissue homogenates of (A) liver, (B) spleen and (C) kidney. (D) The viability of biotin-fed *C. glabrata* cells in PBS was monitored over 14 days, determined by cfu plating at indicated time points and normalized to inoculum control (d 0; set as 100 %) in four independent experiments. (E-F) Fungal burden in liver (E) and spleen (F) of mice infected intravenously with 2×10^5 *C. albicans* wild type, mutant or complemented strain cells/20 g body weight on day 0. Each dot represents the fungal burden in the respective organ of one mouse. No statistically significant differences were observed for

82   liver, spleen and kidney. Dashed lines represent the detection limit and dots below this line

83   mean no cfu were detected in the respective organ.

A brain

Legend: low / intermediate / high / not detectable

CCL-2 (pg/g)

	wt	vhr1Δ	vhr1Δ-VHR1	vht1Δ	sig.	vht1Δ-VHT1	
d 2	520	375	296	193	**	292	*C. glabrata*
d 7	209	160	222	140	*	166	*C. glabrata*
d 14	149	151	171	141		205	*C. glabrata*
d 1	1231	1247	1049	524	***/#	893	*C. albicans*
d 3	450	540	554	120	*	504	*C. albicans*

MPO (ng/g)

	wt	vhr1Δ	vhr1Δ-VHR1	vht1Δ	sig.	vht1Δ-VHT1	
d 2	14	11	12	13		11	*C. glabrata*
d 7	11	11	11	6		8	*C. glabrata*
d 14	8	10	12	7		12	*C. glabrata*
d 1	169	192	169	78	***/###	171	*C. albicans*
d 3	165	172	175	49	***/###	159	*C. albicans*

IL-1β (pg/g)

	wt	vhr1Δ	vhr1Δ-VHR1	vht1Δ	sig.	vht1Δ-VHT1	
d 2	not detectable						*C. glabrata*
d 7	not detectable						*C. glabrata*
d 14	not detectable						*C. glabrata*
d 1	207	168	231	86		159	*C. albicans*
d 3	132	161	163	69		147	*C. albicans*

IL-6 (pg/g)

	wt	vhr1Δ	vhr1Δ-VHR1	vht1Δ	sig.	vht1Δ-VHT1	
d 2	not detectable						*C. glabrata*
d 7	not detectable						*C. glabrata*
d 14	not detectable						*C. glabrata*
d 1	334	407	286	105	**	197	*C. albicans*
d 3	123	144	117	19		107	*C. albicans*

B kidneys

Legend: low / intermediate / high / not detectable

CCL-2 (pg/g)

	wt	vhr1Δ	vhr1Δ-VHR1	vht1Δ	sig.	vht1Δ-VHT1	
d 2	316	363	317	368		361	*C. glabrata*
d 7	305	207	256	193		210	*C. glabrata*
d 14	221	307	264	216		305	*C. glabrata*
d 1	4789	5127	4506	1401	**	2391	*C. albicans*
d 3	1376	1658	939	183		1352	*C. albicans*

MPO (ng/g)

	wt	vhr1Δ	vhr1Δ-VHR1	vht1Δ	sig.	vht1Δ-VHT1	
d 2	508	480	815	504		1077	*C. glabrata*
d 7	1005	661	713	459		462	*C. glabrata*
d 14	320	472	460	261		463	*C. glabrata*
d 1	2309	2420	2287	1215		2179	*C. albicans*
d 3	2773	3346	3139	684	**/###	3862	*C. albicans*

IL-1β (pg/g)

	wt	vhr1Δ	vhr1Δ-VHR1	vht1Δ	sig.	vht1Δ-VHT1	
d 2	162	156	119	98		100	*C. glabrata*
d 7	226	115	151	101		71	*C. glabrata*
d 14	100	84	83	0		138	*C. glabrata*
d 1	1752	1744	1529	825		1424	*C. albicans*
d 3	2227	3403	2818	455	*	2627	*C. albicans*

IL-6 (pg/g)

	wt	vhr1Δ	vhr1Δ-VHR1	vht1Δ	sig.	vht1Δ-VHT1	
d 2	not detectable						*C. glabrata*
d 7	not detectable						*C. glabrata*
d 14	not detectable						*C. glabrata*
d 1	5362	6299	5242	2678		3874	*C. albicans*
d 3	6089	8752	6154	1683	##	7658	*C. albicans*

IFN-γ (pg/g)

	wt	vhr1Δ	vhr1Δ-VHR1	vht1Δ	sig.	vht1Δ-VHT1	
d 2	427	393	374	464		499	*C. glabrata*
d 7	301	253	512	195		273	*C. glabrata*
d 14	269	302	328	228		380	*C. glabrata*
d 1	1585	2418	1994	1864		1486	*C. albicans*
d 3	200	151	159	143		189	*C. albicans*

C | liver

CCL-2 (pg/g)

	wt	vhr1 Δ	vhr1 Δ - VHR1	vht1 Δ		vht1 Δ - VHT1	
d 2	94	81	63	100		77	*C. glabrata*
d 7	79	66	83	47		64	*C. glabrata*
d 14	59	66	81	56		82	*C. glabrata*
d 1	1060	893	986	603	***	739	*C. albicans*
d 3	532	472	512	372		526	*C. albicans*

MPO (ng/g)

	wt	vhr1 Δ	vhr1 Δ - VHR1	vht1 Δ		vht1 Δ - VHT1	
d 2	296	251	286	325		252	*C. glabrata*
d 7	426	393	349	272		344	*C. glabrata*
d 14	289	222	302	237		294	*C. glabrata*
d 1	267	235	291	184		278	*C. albicans*
d 3	463	443	403	213	***/##	429	*C. albicans*

IL-1β (pg/g)

	wt	vhr1 Δ	vhr1 Δ - VHR1	vht1 Δ		vht1 Δ - VHT1	
d 2	223	203	183	222		195	*C. glabrata*
d 7	366	261	376	153		249	*C. glabrata*
d 14	242	271	249	155		267	*C. glabrata*
d 1	540	441	432	305	***/##	444	*C. albicans*
d 3	357	429	349	275		374	*C. albicans*

IL-6 (pg/g)

	wt	vhr1 Δ	vhr1 Δ - VHR1	vht1 Δ		vht1 Δ - VHT1	
d 2			not detectable				*C. glabrata*
d 7			not detectable				*C. glabrata*
d 14			not detectable				*C. glabrata*
d 1	71	47	52	20	**	46	*C. albicans*
d 3	68	74	60	21	*/#	62	*C. albicans*

IFN-γ (pg/g)

	wt	vhr1 Δ	vhr1 Δ - VHR1	vht1 Δ		vht1 Δ - VHT1	
d 2	146	156	137	143		142	*C. glabrata*
d 7	156	132	148	119		146	*C. glabrata*
d 14	123	148	158	149		191	*C. glabrata*
d 1	226	167	197	169		239	*C. albicans*
d 3	200	151	159	143		189	*C. albicans*

Legend: low / intermediate / high / not detectable

D | spleen

CCL-2 (pg/g)

	wt	vhr1 Δ	vhr1 Δ - VHR1	vht1 Δ	vht1 Δ - VHT1	
d 2			not detectable			*C. glabrata*
d 7			not detectable			*C. glabrata*
d 14			not detectable			*C. glabrata*
d 1			not detectable			*C. albicans*
d 3			not detectable			*C. albicans*

MPO (ng/g)

	wt	vhr1 Δ	vhr1 Δ - VHR1	vht1 Δ	vht1 Δ - VHT1	
d 2	2428.2	2343.5	2276.6	2102.6	2047.2	*C. glabrata*
d 7	2095.1	2078.1	2161.2	2084.4	2319.3	*C. glabrata*
d 14	1997.5	2435.5	2373.3	2647.5	1798.0	*C. glabrata*
d 1	15012	14975	15897	13715	14111	*C. albicans*
d 3	11403	11884	10042	8943	10706	*C. albicans*

IL-1β (pg/g)

	wt	vhr1 Δ	vhr1 Δ - VHR1	vht1 Δ	vht1 Δ - VHT1	
d 2	1777	1692	1474	1635	1349	*C. glabrata*
d 7	1581	1711	1761	1386	1642	*C. glabrata*
d 14	1443	1612	1895	1375	1478	*C. glabrata*
d 1	5040	4578	5002	3712	4477	*C. albicans*
d 3	3754	4506	3605	2585	3180	*C. albicans*

IL-6 (pg/g)

	wt	vhr1 Δ	vhr1 Δ - VHR1	vht1 Δ	vht1 Δ - VHT1	
d 2			not detectable			*C. glabrata*
d 7			not detectable			*C. glabrata*
d 14			not detectable			*C. glabrata*
d 1			not detectable			*C. albicans*
d 3			not detectable			*C. albicans*

IFN-γ (pg/g)

	wt	vhr1 Δ	vhr1 Δ - VHR1	vht1 Δ	vht1 Δ - VHT1	
d 2			not detectable			*C. glabrata*
d 7			not detectable			*C. glabrata*
d 14			not detectable			*C. glabrata*
d 1			not detectable			*C. albicans*
d 3			not detectable			*C. albicans*

Legend: low / intermediate / high / not detectable

84 **FIGURE S7 Inflammatory response during systemic *C. glabrata* and *C. albicans***

85 **infections.**

86 Five mice per group were intravenously infected with $2.5×10^7$ *C. glabrata* or

87 $2×10^5$ *C. albicans* cells/20 g body weight on day 0 and sacrificed at indicated time points.

88 The cytokine and MPO amount in tissue homogenates of (A) brain, (B) kidneys, (C) liver and

89 (D) spleen was quantified by ELISA, normalized to the body weight of the respective mouse,

90 and the mean values are represented. A color code ranging from red (highest) to blue

91 (lowest) is shown for both *Candida* species and each cytokine separately and tables

92 highlighted in grey means not detectable. Statistical analysis was performed with a one-way

93 ANOVA on data sets from the same day to compare the wild type with the mutant or the

94 mutant with his respective complemented strain, followed by Dunn´s multiple comparison test

95 (* $p ≤ 0.05$, ** $p ≤ 0.01$, *** $p ≤ 0.001$ comparing wt and deletion mutant; ## $p ≤ 0.01$, ### $p ≤$

96 0.001 comparing deletion mutant to the respective complemented strain).

97   **Table S1. Strains used in this study.**

name	internal ID	designation/ genotype	reference
C. albicans strains			
SC5314	C55	clinical isolate	(Gillum, Tsay, & Kirsch, 1984)
BWP17	M130	**parental strain** (derivative of SC5314) *ura3::λimm434/ura3::λimm434* *his1::hisG/his1::hisG* *arg4::hisG/arg4::hisG*	(Wilson, Davis, & Mitchell, 1999)
BWP17 CIp30 (*Ca* wt)	M1477	**isogenic wild type** *ura3::λimm434/ura3::λimm434* *his1::hisG/his1::hisG* *arg4::hisG/arg4::hisG* *RPS1/rps1::CIp30-URA3-HIS1-ARG4*	(Citiulo et al., 2012)
Cavhr1Δ/Δ	M2565	*orf19.7468::ARG4/orf19.7468::HIS1* *RPS1/rps1::CIp10-URA3*	This work
Cavhr1Δ/Δ + CaVHR1	M2567	*orf19.7468::ARG4/orf19.7468::HIS1* *RPS1/rps1::CIp10-URA3-orf19.7468*	This work
Cabio2-5Δ/Δ	M2573	*orf19.2587-orf19.2590-orf19.2591-orf19.2593::ARG4/orf19.2587-orf19.2590-orf19.2591-orf19.2593::HIS1* *RPS1/rps1::CIp10-URA3*	This work
Cavht1Δ/Δ	M2667	*orf19.2397::ARG4/orf19.2397::HIS1* *RPS1/rps1::CIp10-URA3*	This work
Cavht1Δ/Δ + CaVHT1	M2668	*orf19.2397::ARG4/orf19.2397::HIS1* *RPS1/rps1::CIp10-URA3-orf19.2397*	This work
C. glabrata strains			
ATCC2001	C94	clinical isolate	(Schwarzmüller et al., 2014)
Cgtrp1Δ	G17	**parental strain** (derivative of ATCC2001) *trp1::FRT*	(Kitada, Yamaguchi, & Arisawa, 1995)

98

Cgtrp1Δ + CgTRP1 (*Cg* wt)	G203	**isogenic wild type** *trp1::TRP1*	This work
Cgvhr1Δ	G241	*trp1::TRP1; CAGL0M12496g::NAT1*	This work
Cgvhr1Δ + CgVHR1	G279	*CAGL0M12496g::NAT1; trp1::(TRP1-CAGL0M12496g)*	This work
Cgvht1Δ	G243	*trp1::TRP1; CAGL0K04609g::NAT1*	This work
Cgvht1Δ + CgVHT1	G269	*CAGL0K04609g::NAT1; trp1::(TRP1-CAGL0K04609g)*	This work
Other			
C. auris	C221	B8441	(Munoz et al., 2018)
C. dubliniensis	C97	Wü284	(Morschhäuser, Ruhnke, Michel, & Hacker, 1999)
C. parapsilosis	C118	GA-1	(Gácser, Salomon, & Schafer, 2005)
C. tropicalis	C30	DSM 4959	(Rüchel, 1984)
S. cerevisiae, S288c	C92	*MATα SUC2 gal2 mal2 mel flo1 flo8-1 hap1 ho bio1 bio6*	EuroGenTec
E. coli - Stellar™ Competent Cells		*F–, endA1, supE44, thi-1, recA1, relA1, gyrA96, phoA, Φ80d lacZΔ M15, Δ (lacZYA-argF) U169, Δ (mrr - hsdRMS - mcrBC), mcrA, λ–*	Part of the In-Fusion® HD Cloning Plus Kit

99

100 **References:**
101 Citiulo, F., Jacobsen, I. D., Miramón, P., Schild, L., Brunke, S., Zipfel, P., . . . Wilson, D.
102   (2012). *Candida albicans* scavenges host zinc via Pra1 during endothelial invasion.
103   *PLoS Pathog, 8*(6), e1002777. doi:10.1371/journal.ppat.1002777
104 Gácser, A., Salomon, S., & Schafer, W. (2005). Direct transformation of a clinical isolate of
105   *Candida parapsilosis* using a dominant selection marker. *FEMS Microbiol Lett,*
106   *245*(1), 117-121. doi:10.1016/j.femsle.2005.02.035
107 Gillum, A. M., Tsay, E. Y., & Kirsch, D. R. (1984). Isolation of the *Candida albicans* gene for
108   orotidine-5'-phosphate decarboxylase by complementation of *S. cerevisiae* ura3 and
109   *E. coli* pyrF mutations. *Mol Gen Genet, 198*(2), 179-182.

110 Kitada, K., Yamaguchi, E., & Arisawa, M. (1995). Cloning of the *Candida glabrata TRP1* and
111   *HIS3* genes, and construction of their disruptant strains by sequential integrative
112   transformation. *Gene, 165*(2), 203-206.
113 Morschhäuser, J., Ruhnke, M., Michel, S., & Hacker, J. (1999). Identification of CARE-2-
114   negative *Candida albicans* isolates as *Candida dubliniensis*. *Mycoses, 42*(1-2), 29-32.
115 Munoz, J. F., Gade, L., Chow, N. A., Loparev, V. N., Juieng, P., Berkow, E. L., . . . Cuomo,
116   C. A. (2018). Genomic insights into multidrug-resistance, mating and virulence in
117   *Candida auris* and related emerging species. *Nat Commun, 9*(1), 5346.
118   doi:10.1038/s41467-018-07779-6
119 Rüchel, R. (1984). A variety of *Candida* proteinases and their possible targets of proteolytic
120   attack in the host. *Zentralbl Bakteriol Mikrobiol Hyg A, 257*(2), 266-274.
121 Schwarzmüller, T., Ma, B., Hiller, E., Istel, F., Tscherner, M., Brunke, S., . . . Kuchler, K.
122   (2014). Systematic phenotyping of a large-scale *Candida glabrata* deletion collection
123   reveals novel antifungal tolerance genes. *PLoS Pathog, 10*(6), e1004211.
124   doi:10.1371/journal.ppat.1004211
125 Wilson, R. B., Davis, D., & Mitchell, A. P. (1999). Rapid hypothesis testing with *Candida*
126   *albicans* through gene disruption with short homology regions. *J Bacteriol, 181*(6),
127   1868-1874.

128   **Table S2. Oligonucleotides used in this study**

oligonucleotide name	sequence (5´→ 3`)	used for	reference
CgTRP1 cloning			
5'-SphI-*TRP1*	CATGCATGCCACAACGCAGAACTGGCTGCAGTG	Amplification of *CgTRP1* coding region + promotor and 98 bp of *CgTRP1* terminator	This study
3'-SphI-*TRP1*	CATGCATGCAATGAGTCAGTATATTCAGTATTC		This study
5'-XmaI-*TRP1*term	GATCCCGGGATATTCTTTAATTGTAGTTTCTC	Amplification of *CgTRP1* downstream homologous region	This study
3'-SacI-*TRP1*term	CATGAGCTCAGATGGTGACTCGTCTCGCTGTAG		This study
TRP1-F	GCTGTGGCTCGTGAAATATC	Verification	This study
M13 forward	TTGTAAAACGACGGCCAG		Universal primer
TRP1-R	CAGCCTCGACGGTTTGAATC		This study
M13 reverse	GGAAACAGCTATGACCATG		Universal primer
*TRP1*term-R	CTTACTGCCGTGAATGAGAG		This study
p*TRP1*-Seq fwd	AGAGACTGACGGCGTCAAAG		This study
TRP1-amp-f	ACTCGTCTCGCTGTAGCACTTG	Amplification of complementation construct	This study
TRP1-amp-r	GCTGCAGTGCAAAGGCATTTCC		This study
TRP1-up-ctrl-f	TTATGACCAGGCGGCTACTAAG	Verification	This study
TRP1-down-ctrl-r	CAAGGATAACTTAAGAGAGCAATTC		This study
Generation of deletion and complementation strains in *C. glabrata*			
VHT1-P1 R-SphI	GATGCATGCTTGATGACCCTCTTTCTTCC	Cloning of *VHT1* deletion construct	This study
VHT1-P2 R-NcoI	GCGCCATGGTTGAATATGGAAAAGGAAATGA		This study
VHT1-P3 R-SpeI	GCGACTAGTAATTGTGTTTTGAGAAAGTTTTG		This study
VHT1-P4 R-SacI	GTAGAGCTCTGAATACATTGACGACCACA		This study
VHT1-P1	TTGATGACCCTCTTTCTTCC	Amplification of *VHT1* deletion construct from plasmid	This study
VHT1-P4	TGAATACATTGACGACCACA		This study
CoP1 *VHT1*	AAAAGTGTGAAAGCCCATCG	Verification	This study
CoP4 *VHT1*	AACCTGAATGTCCCAGCAAT		This study
VHT1-up-F1	GATGCCTCACTTGGGTCATTAG	Amplification of *VHT1* deletion construct	This study
VHT1-down-R1	GCTACACTAAGCGTTTGTGTTC		This study
5'-SalI-*VHT1*-F	CATGTCGACGATGCCTCACTTGGGTCATTAG	Cloning of *VHT1* complementation construct	This study
3'-XbaI-*VHT1*-R	CAGTCTAGAGAATCGAATTCTTACACGGTATTG		This study

VHT1-R1	ACTTCCAGCGAGACTTGTTAGC		This study
VHT1-Seq-f1	CAAGTGCTATCGCCTTAC	Verification	This study
VHT1-Seq-f2	CCAACGCTTATGTGTCTC		This study
VHT1-Seq-f3	GGTGTCGATAGGTCAAAG		This study
VHT1-Seq-f4	CTGGATTCCGACACTTAC		This study
VHR1-P1 R-SphI	GATGCATGCGCCATGGCAAGTTGTG		This study
VHR1-P2 R-SacII	GTACCGCGGAAGGAGGCGTTTCGTC	Cloning of *VHR1* deletion construct	This study
VHR1-P3 R-SpeI	GGCACTAGTCTGCATCCCAGCTTCA		This study
VHR1-P4 R-SacI	GATGAGCTCTTGCAGGCAAGTGAGC		This study
VHR1-P1	GCCATGGCAAGTTGTG	Amplification of *VHR1* deletion construct from plasmid	This study
VHR1-P4	TTGCAGGCAAGTGAGC		This study
CoP1 *VHR1* new	CGTTGAGCTCCTCGAACACT	Verification	This study
CoP4 *VHR1* new	CAGGGCCAAAGTAGTTCGTT		This study
p*TRP1-VHR1* fwd	GCAGGTCGACTCTAGTTATTTTTTTGCCCCCCACCAC	Cloning of *VHR1* complementation construct	This study
p*TRP1-VHR1* rev	CCGGGGATCCTCTAGCGGAAAGTCTTTATATTTTTATG		This study
VHR1-R1	CGAGCTGCTCCCTGATCTTGTG		This study
VHR1-Seq-f1	AGACGAAACGCCTCCTTG		This study
VHR1-Seq-f2	CAATGCCAATGCCAATGC	Verification	This study
VHR1-Seq-f3	GCTATTCACCACCTCATC		This study
VHR1-Seq-f4	CTGCATCCCAGCTTCATC		This study
NAT1 fwd South	CTGTTCCAGGTGATGCTGAAG	Southern Blot probe	(Gerwien et al., 2016)
NAT1 rev South	CGAATTCAGTAGCCAAACCCAT		(Gerwien et al., 2016)
CgTRP1-term Sonde fwd	TCGCTGTAGCACTTGCTTGGTAGC	Southern Blot probe	This study
CgTRP1-term Sonde rev	TAGCCTCTCATTCACGGCAGTAAG		This study
CgVHR1-prom Sonde new fwd	TAGAAGTGGAAGCACAGCAGTAG	Southern Blot probe	This study
CgVHR1-prom Sonde new rev	CGTTCTTGGAGTGCTTGTTC		This study
CgVHR1-term Sonde new fwd	CCTATCACAAGGTCGCTAAG	Southern Blot probe	This study
CgVHR1-term Sonde new rev	TGGTCGCATAATCGCCGTTC		This study
CgVHT1-prom Sonde new fwd	GAAATGAATTGAATGAGGTATAAAG	Southern Blot probe	This study
CgVHT1-prom Sonde new rev	CAGCGTTGTGACTCAAGGTTACTC		This study

129

CgVHT1-term Sonde fwd	ACTTTGATTCTGTTTTTAAATGC	Southern Blot probe	This study
CgVHT1-term Sonde rev	TGGGTTTCGTCTACTAATCAAATC		This study
Generation of deletion and complementation strains in *C. albicans*			
*CaBIO2-5*del fwd	GAGAATTGTTGAGTCGACTGCGCA ACACCTCATACCCACCAATTAAAAA CAAATTATTCGTAATCTTTCTGTTTT TTTTTTCTTTAATCTTCAACGTTTAT ACA **gaagcttcgtacgctgcaggtc**	Deletion construct *BIO2-5*	This study
*CaBIO2-5*del rev	GGACAACGTCAGAAGATTTCTGCTA GAATTGTCGTGTAAAATGCTCACTA CTTTACTCCACAGCAAACTCAAATT CATTCAGCTGGCCCACTAGCAGAA CAGCA**tctgatatcatcgatgaattcgag**		This study
CaBIO2-5 fwd	AGGAGGCATTTCCGTCTTAG	Verification	This study
CaBIO2-5 rev	GGTATGCGAAACAGAGCTGG		This study
*CaVHR1*del fwd	TTCAGAGTCATGGTTGACTTTAAGT CGGTCAATAAATGATTTCTTTAATAC CATTTCCTCATAAACACAATATATTT ATATAAACTACAAACATTAAGCA **gaagcttcgtacgctgcaggtc**	Deletion construct orf19.7468	This study
*CaVHR1*del rev	TATAGTTAGGAAAAACCGTTTTTTTT CATACACACACACATTTATACTTCTA CAACAAAAAACATAACCCACTATCT ATTAATCTTACCATCTCTCTAAA **tctgatatcatcgatgaattcgag**		This study
*CaVHR1*prom 1 fwd	AACACGACCTCGAGAGGATG	Verification	This study
*CaVHR1*term 1 rev	CCTCAGACTGAAAGGGAAAG		This study
Ca19.2397del fwd	ATTTCCTGTTAGACAAGCCCTTTCT TTTTTTTTA TCAATTGTTCTACATCCAAAAAAGA AATAAATCA CCTATCCCGGTTGCTTAGTTAATAG GAAGAT **gaagcttcgtacgctgcaggtc**	Deletion construct orf19.2397	This study
Ca19.2397del rev	ATTATCACTTAACATCTAATTATTAA TCAACACATA TATCTAAGAAGAATGTGACATATAA TTAGTATTGT CTTTGCTTAAATGGTTAACGAAACA CATT **tctgatatcatcgatgaattcgag**		This study
Ca19.2397prom fwd	TCCTTGGGCTACATAACCAG	Verification	This study
Ca19.2397term rev	TAGGACAGCCACACTGAACG		This study

KpnI*VHR1*_REV	GGGGTACCGTTTCTGTTGGTGTTTTGTGTATATGTG	Cloning of *VHR1* complementation construct	This study
SalI*VHR1*_REV	CATGTCGACAAAAAATCGAAGAAATAAAGCAAGTG		This study
CaVHR1-RT 2 rev	TTGGACCCGGAACATCATCTG	Verification	This study
pCIp10-2397 fwd	TACCGTCGACCTCGAAAAAAAGCACCAAGAAATTTTCATT	Cloning of *VHT1* complementation construct	This study
pCIp10-2397 rev	CGGGCCCCCCCTCGAGGTTTTAATTTTGATGTTGATAGAA		This study
Ca19.2397 ctrl rev	CTTAATCCCGGCCAAGTACC	Verification	This study
2397 seq 1 fwd	CCTGTTAGACAAGCCCTTTC		This study
2397 seq 2 fwd	TTGTGGTGGTTACCCGATAG		This study
VHR1-prom Sonde new 2 rev	CTCTAAACTCTCCCTGCCTATATG	Southern Blot probe	This study
ARG4-F1	GGATATGTTGGCTACTGATTTAGC	Verification	(Gola, Martin, Walther, Dunkler, & Wendland, 2003)
ARG4-R1	AATGGATCAGTGGCACCGGTG		(Gola et al., 2003)
HIS1-F1	GGACGAATTGAAGAAAGCTGGTGCAACCG		(Gola et al., 2003)
HIS1-R1	CAACGAAATGGCCTCCCCTACCACAG		(Gola et al., 2003)
URA3-F2	GGAGTTGGATTAGATGATAAAGGTGATGG	Verification of complementation	(Gola et al., 2003)
RPF-F1	GAGCAGTGTACACACACACATCTTG		(Wilson et al., 2014)
RPF-2	CGCCAAAGAGTTTCCCCTATTATC		(Crawford et al., 2018)
SB *bio2-5* FWD	GCGAAGGGTTCTCCGGTTTG	Southern Blot probe	This study
SB *bio2-5* REV	CTAAGACGGAAATGCCTCCT		This study
SB_*VHR1*_profwd	ACCAGGCTAAGATGACTGAG	Southern Blot probe	This study
SB_*VHR1*_prorev	CATCCTCTCGAGGTCGTGTT		This study
Ca19.2397term Sonde fwd	TTCCGTTCAGTGTGGCTGTC	Southern Blot probe	This study
Ca19.2397term Sonde rev	TCGGCTCTTCAGTGGATACC		This study
Quantitative RT-PCR oligonucleotids			
***C. glabrata* genes**			
CgBPL1 RT fwd	CTTACCCGTTCGAATCAAGTG		This study
CgBPL1 RT rev	CTCGACCTGAATAGGAGGTAG		This study
CgVHR1-RT-P1	ACCAATGAAACCCGAGAGTG		This study
CgVHR1-RT-P2	ATTGAAGAACAGGCCCAATG		This study

CAGL0K04609g_vht1_RT_fwd	CATACAGTGGATCCTACACATT	This study
CAGL0K04609g_vht1_RT_rev	AGCAAACCATTTTGTCGAACTA	This study
CAGL0K04565g_vht1_RT_fwd	TTTACACAGGTTCTTATACCCA	This study
CAGL0K04565g_vht1_RT_rev	AAACCATTTGGTGCTCTCT	This study
CgACT1-RT-P1	CCTACGAATTGCCAGATGGT	This study
CgACT1-RT-P2	CACCGGACATGACGATGTTA	This study
CgEFB1-RT-P1	GACACTGTCAAGGAATTGAACAC	(Gerwien et al., 2016)
CgEFB1-RT-P2	GAAGCAGCTGGGAAGGAGT	(Gerwien et al., 2016)
qRT *CgEFT2* HK fwd	TACTCTAAACTCCGACCCATTG	(Gerwien et al., 2016)
qRT *CgEFT2* HK rev	TCCTTCATACCGTGTCTCTTAC	(Gerwien et al., 2016)
C. albicans genes		
orf19.2397 RT fwd	TGGATTGGGTCCTACAGTTC	This study
orf19.2397 RT rev	CCCCCAACATAAGTACCAAC	This study
orf19.700 RT fwd	GAACTCTTAAAGATAGTGCTG	This study
orf19.700 RT rev	TGATACTAAAACCACTTGTCG	This study
orf19.1855 RT fwd	GTGCTATTTTATTTACTCAAG	This study
orf19.1855 RT rev	AGGCAAAAGCACTACAAGCTG	This study
CaBIO5-RT fwd_new	CTGATGTGTCCGAGGTTGTC	This study
CaBIO5-RT rev_new	CTTCTGATCCGGCCAATGTC	This study
CaBIO4-RT fwd	AGTAGCTCGGAGTGGATTGG	This study
CaBIO4-RT rev	TTCAGTTTAGAATGAGGGATG	This study
CaBIO3-RT fwd	TGCGTACGTATCATCCTCAG	This study
CaBIO3-RT rev	CGGTTCGTCCACCACTGATG	This study
CaBIO2-RT fwd	ACCCGTACATACGACGAAAG	This study
CaBIO2-RT rev	GACCGGCGGCCAATCTAATG	This study
CaTDH3-RT-fwd	ATCCCACAAGGACTGGAGA	(Polke et al., 2017)
CaTDH3-RT-rev	GCAGAAGCTTTAGCAACGTG	(Polke et al., 2017)
CaBPL1-RT fwd	GTTTCAGGGCAAGGCGTTGG	This study
CaBPL1-RT rev	CCCTTTCCACGTCTGATCTC	This study
CaEFT2-RT fwd	GCTGCTTTCCAATGGGCTAC	This study
CaEFT2-RT rev	GGAGTACCTGGTCTTTGTTC	This study

132 <u>underlined:</u>   restriction enzyme recognition motif

133 **lowercase:**   pFA plasmid annealing site

134 green: homolog to *Xba*I-linearized vector p*TRP1*

135 blue: homolog to *Xho*I- linearized vector CIp10

136

137

138

139 **References:**

140 Crawford, A. C., Lehtovirta-Morley, L. E., Alamir, O., Niemiec, M. J., Alawfi, B., Alsarraf, M., .
141   . . Wilson, D. (2018). Biphasic zinc compartmentalisation in a human fungal
142   pathogen. *PLoS Pathog, 14*(5), e1007013. doi:10.1371/journal.ppat.1007013
143 Gerwien, F., Safyan, A., Wisgott, S., Hille, F., Kaemmer, P., Linde, J., . . . Hube, B. (2016). A
144   Novel Hybrid Iron Regulation Network Combines Features from Pathogenic and
145   Nonpathogenic Yeasts. *MBio, 7*(5). doi:10.1128/mBio.01782-16
146 Gola, S., Martin, R., Walther, A., Dunkler, A., & Wendland, J. (2003). New modules for PCR-
147   based gene targeting in *Candida albicans*: rapid and efficient gene targeting using
148   100 bp of flanking homology region. *Yeast, 20*(16), 1339-1347. doi:10.1002/yea.1044
149 Polke, M., Sprenger, M., Scherlach, K., Albán-Proaño, M. C., Martin, R., Hertweck, C., . . .
150   Jacobsen, I. D. (2017). A functional link between hyphal maintenance and quorum
151   sensing in *Candida albicans*. *Mol Microbiol, 103*(4), 595-617. doi:10.1111/mmi.13526
152 Wilson, D., Mayer, F. L., Miramón, P., Citiulo, F., Slesiona, S., Jacobsen, I. D., & Hube, B.
153   (2014). Distinct roles of *Candida albicans*-specific genes in host-pathogen
154   interactions. *Eukaryot Cell, 13*(8), 977-989. doi:10.1128/EC.00051-14

155 **Table S3. Plasmids used in this study.**

plasmid	features/Use	reference
pTS50	Amplification of *CgNAT1* cassette	(Schwarzmüller et al., 2014)
pUC19	Backbone for pUC19-*TRP1 and* p*TRP1* with ampicillin resistance cassette (*ampR*)	Part of the In-Fusion® HD Cloning Plus Kit
pFA-*HIS1*	Amplification of *CaHIS1* cassette, complementation of histidine auxotrophy	(Gola, Martin, Walther, Dunkler, & Wendland, 2003)
pFA-*ARG4*	Amplification of *CaARG4* cassette, complementation of arginine auxotrophy	(Gola et al., 2003)
CIp10	Integration of *CaURA3* into *RPS1* locus, complementation of uridine auxotrophy	(Murad, Lee, Broadbent, Barelle, & Brown, 2000)
CIp10-*CaVHR1*	Integration of *CaURA3* and orf19.7468 into *RPS1* locus, complementation of uridine auxotrophy and *CaVHR1* deletion	this study
CIp10-*CaVHR1*	Integration of *CaURA3* and orf19.2397 into *RPS1* locus, complementation of uridine auxotrophy and *CaVHT1* deletion	this study
pUC19-*TRP1*	Intermediate plasmid (contains promotor and coding sequence of *CgTRP1* without downstream terminator)	this study
p*TRP1*	Amplification of *CgTRP1* cassette, complementation of tryptophan auxotrophy	this study
p*TRP1*-*CgVHR1*	Amplification of *CgTRP1* and CAGL0M12496g, complementation of tryptophan auxotrophy and *CgVHR1* deletion	this study
p*TRP1*-*CgVHT1*	Amplification of *CgTRP1* and CAGL0K04609g, complementation of tryptophan auxotrophy and *CgVHT1* deletion	this study

156

157 **References:**
158 Gola, S., Martin, R., Walther, A., Dunkler, A., & Wendland, J. (2003). New modules for PCR-
159   based gene targeting in *Candida albicans*: rapid and efficient gene targeting using
160   100 bp of flanking homology region. *Yeast, 20*(16), 1339-1347. doi:10.1002/yea.1044
161 Murad, A. M., Lee, P. R., Broadbent, I. D., Barelle, C. J., & Brown, A. J. (2000). Clp10, an
162   efficient and convenient integrating vector for *Candida albicans*. *Yeast, 16*(4), 325-
163   327. doi:10.1002/1097-0061(20000315)16:4<325::AID-YEA538>3.0.CO;2-#
164 Schwarzmüller, T., Ma, B., Hiller, E., Istel, F., Tscherner, M., Brunke, S., . . . Kuchler, K.
165   (2014). Systematic phenotyping of a large-scale *Candida glabrata* deletion collection
166   reveals novel antifungal tolerance genes. *PLoS Pathog, 10*(6), e1004211.
167   doi:10.1371/journal.ppat.1004211

168 **Appendix S1. Supplementary methods.**

169

170 **Growth assays**

171 Growth of *Candida* on solid agar was tested by spotting serial dilutions (1×10^6 to 1×10^1) of

172 biotin pre-starved yeast cells on YNB plates (2 % oxoid-agar; 0.19 % YNB without amino

173 acids, biotin and ammonium sulfate [Formedium], containing either 2 % glucose and 0.5 %

174 ammonium sulfate or 1 % casamino acids [CAA]).

175

176 **Viability Assay**

177 Biotin-fed *C. glabrata* cells were washed three times in PBS and 2×10^7 cells/mL were

178 incubated in 20 mL of PBS (pH 7.4) at 37 °C and 180 rpm. After 2, 7 and 14 days, 1 mL cell

179 suspension was collected and appropriate dilutions were plated on YPDB plates in technical

180 duplicates and incubated 1 day at 37 °C. Colonies were counted with an automated colony

181 counter ProtoCOL3 (Synbiosis, Cambridge, UK). The cfu of inoculum were used as control.

Appendix S2. DNA- and protein sequence of CAGL0M12496g *(CgVHR1)*.

The open reading frame was sequenced using Sanger sequencing (capillary electrophoresis, ABI Prism, 3130XL Genetic Analyzer). The coding sequence of CAGL0M12496g is shown in black with the translated protein sequence in green. The currently annotated sequence (GCD, (Skrzypek et al., 2017)) contains an insertion of a cytosine at position 476 (depicted in red) which results in an early translational stop codon (underlined, position 834-836).

```
   1 atg gcc ccg aac aag cac tcc aag aac ggg act acc cac aag atc agg gag cag ctc ggg ttc acg gat gag aag atg tgg aag cgg ttc agc agc aga cgg ctg gag ctc atc gac aag ttc cag ctg tcg cag ttc aaa gcg agc gag
     m   a   p   n   k   h   s   k   n   g   t   t   h   k   i   r   e   q   l   g   f   t   d   e   k   k   w   k   r   f   s   s   r   r   l   e   l   i   d   k   f   q   l   s   q   f   k   a   s   e

 151 caa gac ctg aac atc aag cag ata gcc aat atc ctg cgg acg gag ttc ggg tac ccc gtg acg tgc tcg atg gag ttc gag aag ctg gtg acc gcg gca atc cag tcc gtc agg agg aac agg aag cgc tcg aaa aag aag agc tac atg
     q   d   l   n   i   k   q   i   a   n   i   l   r   t   e   f   g   y   p   v   t   c   s   m   e   f   e   k   l   v   t   a   a   i   q   s   v   r   r   n   r   k   r   s   k   k   k   s   y   m

 301 ctg cac ggc gcc aag aac atg agc tac tcg acc agc gag gag gag ccg gag tcc cgc gcc acg tcc cgc atc acg tcc cct gtg ggc acg ctc tcc cag tcc cac tcc cag cca gca gcg agc gtg tcg ccg ctg tcc aac atg tcc acg
     l   h   g   a   k   n   m   s   y   s   t   s   e   e   e   p   e   s   r   a   t   s   r   i   t   s   p   v   g   t   l   s   q   s   h   s   q   p   a   a   s   v   s   p   l   s   n   m   s   t

 451 ggg tcc gcc atg acg cag ggc tcc cctg ccc gtg cac atg ccg gtg cca gtg ccc gtg caa gtg caa gca ccc atg tcc atg tcc atg cca atg ccc atg cca atg cca atg cac gta cca gtg cct atc tcc cta caa caa cag
     g   s   a   m   t   q   g   s   l   p   v   h   m   p   v   p   v   p   v   q   v   q   a   p   m   s   m   s   m   p   m   p   m   p   m   p   m   h   v   p   v   p   i   s   l   q   q   q

 601 caa cag cca gca cca caa caa caa cca caa caa caa cag aac gac cct atg cgg ttc gtg agg tca acg act cca ttg cca gac cac aag ttc cag cgg ttg ctg agc ccg ctc tcg tcg tcg aga ccg ccc cgc cgg atg tcg aac cca
     q   q   p   a   p   q   q   q   p   q   q   q   q   n   d   p   m   r   f   v   r   s   t   t   p   l   p   d   h   k   f   q   r   l   l   s   p   l   s   s   s   r   p   p   r   p   m   s   n   p

 751 cag cgc gtg ctt cca ccc atg gcc cag agc tcg tcc gcg ccc gct gct cag aag tac gac gac atc atc aag aac ata gtc gct aac ctg gtg cac aac ata gta ccg ctc gct gag cag gcc aac agg gac aac aac ggc cta gcg ctg
     q   r   v   l   p   p   m   a   q   s   s   s   a   p   a   a   q   k   y   d   d   i   i   k   n   i   v   a   d   l   v   h   n   i   v   p   l   a   e   q   a   n   r   d   n   n   g   l   a   l

 901 aag ctc tcc acg ttc gac ccg aac aac ccg gtc aag agc gag cac cct ccg tcc ata gac cag gaa cca gcg cat ggc ggc ctg cct tac ttc ttc ctg gag aag ctg ctc ctg cag atc caa aag tca aag acg tgc ctg gaa atc gca
     k   l   s   t   f   d   p   n   n   p   v   k   s   e   h   p   p   s   i   d   q   e   p   a   h   g   g   l   p   y   f   l   r   e   k   l   l   l   q   i   q   k   s   k   t   c   l   e   i   a

1051 acg agc cag ggg tcc atg gaa ctc tac gct aac ctg gag aca ctc ggt gaa atg gca ata cgg acc tcg ata gca ttc cta gtc gaa aga ttc ttc tcg aac atg ctg tcc atg tcc atg gag tac atc tcc aga aag tct tcc tcc gac
     t   s   q   g   s   m   e   l   y   a   n   l   e   t   l   g   e   m   a   i   r   t   s   i   a   f   l   v   e   r   f   f   s   n   m   l   s   m   a   m   e   y   i   s   r   k   s   s   d

1201 gaa aac ttg gcc aac ctg gct ttg aag ctg atg tca ccc gct gtg aga ata aac ctg gct aac atg cca atg cat gaa gta cag ata aag acc ctt tac tta cta gta ggc ggt ata gtg aag gac ttc ggc ttc gat ccg tgc cta tac
     e   n   l   a   n   l   a   l   k   l   m   s   p   a   v   r   i   n   l   a   n   m   p   m   h   e   v   q   i   k   t   l   y   l   l   v   g   g   i   v   k   d   f   g   f   d   p   c   l   y

1351 ccg ctg agt gag gct att cac cac ctc atc atg aca cag tac cct cta gtt acc aac aac aac aac aac aac aac aac ggc caa gcc atg agc gat aac agc agc gag tcg agc aac ctc gtg aac cct ata ccg acc tcc gca tcc
     p   l   s   e   a   i   h   h   l   i   m   t   q   y   p   l   v   t   n   n   n   n   n   n   n   n   n   n   g   q   a   m   s   d   n   s   s   e   s   s   h   l   v   n   p   i   p   t   s   a   s

1501 cag aga gcc act ctg ctg tcc aca tta cca atg aaa ccc gag agt gca aac cag gac atc aac aag aag gtg tac atc aaa tac cgt gat aac gag cat gtt ttc aca ttc cac caa cta agc aac gga act cca acg atc ata gag ata
     q   r   a   t   l   l   s   t   l   p   m   k   p   e   s   a   n   q   d   i   n   k   k   v   y   i   k   y   r   d   n   e   h   v   f   t   f   h   q   l   s   n   g   t   p   t   i   i   e   i

1651 atg gaa aat tgc aag agc ctc ttc aat att gtc aac tca gat ttc tca ttg ggc ctg ttc ttc aat gga agc att atc aat gat gac att cta tcc agg ttg ttc aac gat ctc tct aat aat gaa atc cac ttg gag ata aga caa aca
     m   e   n   c   k   s   l   f   n   i   v   n   s   d   f   s   l   g   l   f   f   n   g   s   i   i   n   d   d   i   l   s   r   l   f   n   d   l   s   n   n   e   i   h   l   e   i   r   q   t

1801 gat caa gca gtt cca aaa ctg agt gat act gga atc aca acg ggc agc att gta cca tct atc cca att cca aca aga cca aat agt gtg aaa gca cta gat gac atc ata gga aga atg ggt aag aac gga tta cct tct cag aac gag
     d   q   a   v   p   k   l   s   d   t   g   i   t   t   g   s   i   v   p   s   i   p   i   p   t   r   p   n   s   v   k   a   l   d   d   i   i   g   r   m   g   k   n   g   l   p   s   q   n   e

1951 cag atg gta cca cct cct cca cca acc att ata acg cct tca aat tac tct aac aac tct tct cgt gag agg ttc cca aac aac acg ttg cct caa cca gta tac caa cct ttg ctt taa
     q   m   v   p   p   p   p   p   t   i   i   t   p   s   n   y   s   n   n   s   s   r   e   r   f   p   n   n   t   l   p   q   p   v   y   q   p   l   l   -
```

Reference:

Skrzypek, M. S., Binkley, J., Binkley, G., Miyasato, S. R., Simison, M., & Sherlock, G. (2017). The *Candida* Genome Database (CGD): incorporation of Assembly 22, systematic identifiers and visualization of high throughput sequencing data. *Nucleic Acids Res, 45*(D1), D592-D596. doi:10.1093/nar/gkw924

2.3   Manuscript III: Ishchuk *et al.*, *Front. Microbiol.*, 2019

RNAi as a tool to study virulence in the
pathogenic yeast *Candida glabrata*

Olena P. Ishchuk, Khadija Mohamed Ahmad, Katarina Koruza, Klara Bojanovič,
Marcel Sprenger, Lydia Kasper, Sascha Brunke, Bernhard Hube, Torbjörn Säll,
Thomas Hellmark, Birgitta Gullstrand, Christian Brion, Kelle Freel, Joseph Schacherer,
Birgitte Regenberg, Wolfgang Knecht and Jure Piškur

Summary:

For a better understanding and treatment of infections caused by *C. glabrata*, it is essential to investigate the molecular basis of fungal virulence and resistance. The established RNA interference (RNAi) system in *C. glabrata* uses Dicer and Argonaute genes from *Saccharomyces castellii* and results in 30 and 70% knockdown of reporter genes and putative virulence genes. The screening of an RNAi mutant library identified new virulence-related genes involved in the maintenance of cell integrity, antifungal drug and ROS resistance, which could be promising targets for the treatment of *C. glabrata* infections.

Own contribution:

Marcel Sprenger performed and analyzed the macrophage survival experiments, and edited the manuscript.

Estimated authors' contributions:

Olena P. Ishchuk	47%
Khadija Mohamed Ahmad	5%
Katarina Koruza	7%
Klara Bojanovič	3%
Marcel Sprenger	**3%**
Lydia Kasper	3%
Sascha Brunke	3%
Bernhard Hube	3%
Torbjörn Säll	3%

Thomas Hellmark	2%
Birgitta Gullstrand	2%
Christian Brion	3%
Kelle Freel	3%
Joseph Schacherer	3%
Birgitte Regenberg	3%
Wolfgang Knecht	2%
Jure Piškur	5%

_____

Prof. Bernhard Hube

RNAi as a Tool to Study Virulence in the Pathogenic Yeast *Candida glabrata*

Olena P. Ishchuk[1,2]*, Khadija Mohamed Ahmad[1], Katarina Koruza[1], Klara Bojanovič[1], Marcel Sprenger[3], Lydia Kasper[3], Sascha Brunke[3], Bernhard Hube[3,4], Torbjörn Säll[1], Thomas Hellmark[5], Birgitta Gullstrand[5], Christian Brion[6], Kelle Freel[6], Joseph Schacherer[6], Birgitte Regenberg[7], Wolfgang Knecht[1,8] and Jure Piškur[1]

[1] Department of Biology, Lund University, Lund, Sweden, [2] Department of Biology and Biological Engineering, Systems and Synthetic Biology, Chalmers University of Technology, Gothenburg, Sweden, [3] Department of Microbial Pathogenicity Mechanisms, Hans Knöll Institute, Jena, Germany, [4] Institute of Microbiology, Friedrich Schiller University, Jena, Germany, [5] Department of Nephrology, Lund University, Lund, Sweden, [6] Department of Molecular Genetics, Genomics and Microbiology, Strasbourg University, Strasbourg, France, [7] Department of Biology, Faculty of Science, University of Copenhagen, Copenhagen, Denmark, [8] Lund Protein Production Platform, Lund University, Lund, Sweden

The yeast *Candida glabrata* is a major opportunistic pathogen causing mucosal and systemic infections in humans. Systemic infections caused by this yeast have high mortality rates and are difficult to treat due to this yeast's intrinsic and frequently adapting antifungal resistance. To understand and treat *C. glabrata* infections, it is essential to investigate the molecular basis of *C. glabrata* virulence and resistance. We established an RNA interference (RNAi) system in *C. glabrata* by expressing the Dicer and Argonaute genes from *Saccharomyces castellii* (a budding yeast with natural RNAi). Our experiments with reporter genes and putative virulence genes showed that the introduction of RNAi resulted in 30 and 70% gene-knockdown for the construct-types antisense and hairpin, respectively. The resulting *C. glabrata* RNAi strain was used for the screening of a gene library for new virulence-related genes. Phenotypic profiling with a high-resolution quantification of growth identified genes involved in the maintenance of cell integrity, antifungal drugs, and ROS resistance. The genes identified by this approach are promising targets for the treatment of *C. glabrata* infections.

Keywords: Candida glabrata, pathogenic yeast, RNA interference, RNAi, gene library, antifungal drugs, virulence factors, macrophages

INTRODUCTION

The yeast *Candida glabrata* is an opportunistic human pathogen that causes relatively benign mucosal or fatal systemic infections. The incidence of infections caused by this *Candida* species has significantly increased particularly in immune-deficient patients, in addition to those that undergo chemotherapy, treated with broad-spectrum antibiotics for prolonged time, or have undergone a higher number of invasive surgeries (Pfaller and Diekema, 2007). In healthy humans, *Candida* species colonize the oral cavity, vagina, and gut (Mårdh et al., 2002; Moyes and Naglik, 2011). In many studies, *C. glabrata* and *C. albicans* are considered the most common causes of candidiasis (Fidel et al., 1999; Brunke and Hube, 2013). While *C. glabrata* is a distant relative of *C. albicans,* it is a close relative of bakers' yeast *Saccharomyces cerevisiae*

(Dujon et al., 2004). In evolutionary time scales, *C. glabrata* only "recently" became pathogenic (Brunke and Hube, 2013; Ahmad et al., 2014). The mechanisms behind *C. glabrata* pathogenicity are thus far not well understood, but appear to differ greatly from *C. albicans*. Immune evasion strategies, possibly via intracellular survival and replication in macrophages contribute to the virulence of *C. glabrata* (Seider et al., 2011, 2014; Brunke and Hube, 2013; Kasper et al., 2014). *C. glabrata* also readily rearranges its genome (Ahmad et al., 2014) at a frequency one order of magnitude higher than in *C. albicans* (Gabaldón and Fairhead, 2018). Genome rearrangements could be evolutionary advantageous for this yeast, allowing it to adapt rapidly to its host environment and to antifungal treatments.

Research focused on *C. glabrata* pathogenicity can benefit greatly from the development of molecular tools. In *S. cerevisiae*, the strategy of gene deletion has been used for decades as an approach to study gene function. However, Giaever et al. (2002) found that approximately 1000 mutants (representing ∼17% of all *S. cerevisiae* genes) failed to grow as a result of a specific gene deletion in haploids, proving that these genes are essential for this yeast. The genome of *C. glabrata* has 5283 predicted coding sequences, and extensive research has been devoted to the creation of a whole genome deletion library for this haploid yeast (Schwarzmüller et al., 2014). Large-scale gene deletions for *C. glabrata* proved less feasible than for *S. cerevisiae* due to gene essentiality or technical reasons (lower homologous recombination rates). However it must be assumed that *C. glabrata* contains a similar number of essential genes as *S. cerevisiae*.

Other techniques, such as down-regulating gene expression can provide alternative ways to study genes' functions. The RNA interference (RNAi), which relies on manipulating the levels of a gene's transcript, has become a widespread tool to analyze the function of genes in organisms ranging from protozoa to human. Unlike gene deletions, RNAi can be applied to any gene, even those that are essential. It has, however, not found many applications in baker's yeast, which naturally lack important components of the RNAi machinery (Drinnenberg et al., 2009). The RNAi approach relies on the activity of two proteins, Dicer (ribonuclease III) and Argonaute (the carrier of small interfering RNA [siRNAs]). The process is initiated by the cleavage of double stranded RNA (complementary to the target transcript) by Dicer into siRNAs, which are then loaded on Argonaute and, by base-pair interaction, target the gene's transcript. This ultimately interferes with gene expression by down-regulation. RNAi is found widely in nature (plants, animals, and fungi), and provides evolutionary advantages by protecting these organisms from viruses, taking part in gene silencing, heterochromatin organization, and chromosome segregation (Tijsterman et al., 2002; Martienssen et al., 2005; Moazed, 2009).

Remarkably, although RNAi is well preserved among some fungi (Drinnenberg et al., 2009), it has been lost in several budding yeasts such as *S. cerevisiae* and *C. glabrata*. The aim of this study was to develop a RNAi system for *C. glabrata* and to use it as a tool to identify and functionally analyze genes known to be putatively required for virulence.
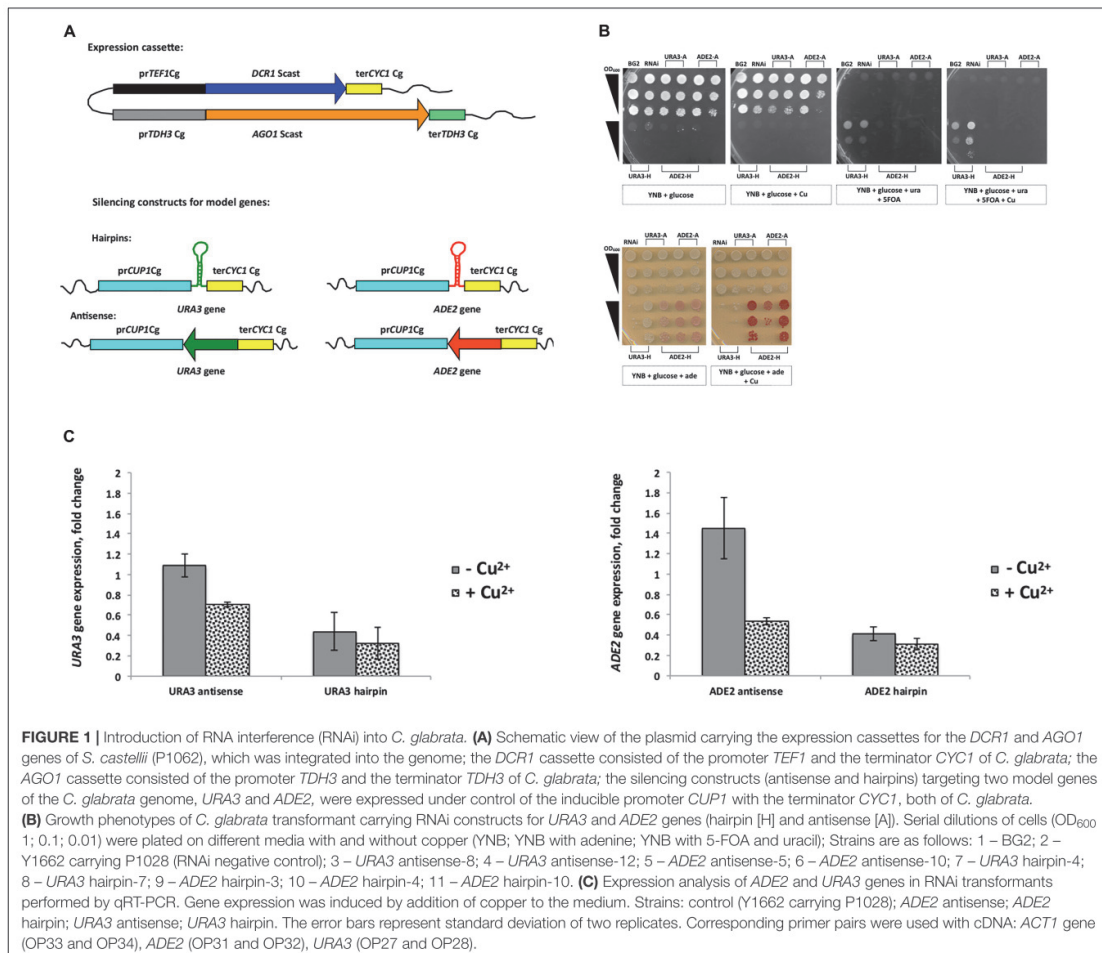
RESULTS

Introduction of RNAi Into *C. glabrata*

For the reconstitution of an RNAi mechanism in *C. glabrata*, two heterologous *Saccharomyces castellii* genes, *DCR1* and *AGO1* (coding for Dicer and Argonaute, correspondingly) were introduced into the *C. glabrata* genome. For this purpose we first evaluated the activity of several constitutive and inducible promoters by their ability to induce expression of a functional enzyme, deoxyribonucleoside kinase of *Drosophila melanogaster* (**Supplementary Figure S1**, Methods). The *dNK* gene encoding this enzyme was successfully expressed in *C. glabrata* and different enzyme activity was observed when expressed from different promoters (**Supplementary Figure S1**). For the expression of *DCR1* and *AGO1* genes in the *C. glabrata*, we used the strong constitutive promoters *TEF1* and *TDH3* of *C. glabrata* (**Figure 1A** and **Supplementary Figure S1**). The plasmid carrying the *DCR1* and *AGO1* constructs (P1062, **Supplementary Table S2**) was linearized by *Sph*I and integrated into the genome of three standard laboratory *C. glabrata* strains, BG2, CBS138 and BG14 (**Table 1**).

To first prove that the RNAi pathway can function in *C. glabrata*, we generated silencing constructs targeting the two genes *URA3* (encoding orotidine 5′-phosphate decarboxylase) and *ADE2* (encoding phosphoribosylaminoimidazole carboxylase) in the *C. glabrata* genome. They are part of the uracil (*URA3* gene) and adenine (*ADE2* gene) biosynthesis pathway and are popular auxotrophic markers in yeast genetics. Lack or loss of function of these genes products result in following phenotypes: requirement of uracil/adenine for growth, accumulation of *p*-ribosylaminoimidazolecarboxylate (red pigment) in the absence of *ADE2* transcript, and resistance to 5-FOA without *URA3*. We used two different silencing constructs for these genes (antisense and hairpin), which we introduced into the *lys2* auxotrophic variant of BG2 carrying RNAi genes (Y1662, **Table 1**) by transforming it with integrative plasmids. The design of silencing constructs was similar to that used by Drinnenberg et al. (2009), were the antisense constructs consisted of 339 bp of antisense DNA strand of the gene and hairpins had 339 bp of both antisense and sense DNA strand separated by 79 bp "loop" (**Supplementary Data**). *Sal*I linearized the plasmids with antisense constructs, and *Sma*I linearized hairpin plasmids before the transformation. For the expression of silencing constructs we selected the strong inducible *C. glabrata* promoter *CUP1* (**Figure 1A** and **Supplementary Figure S1**).

Two to three selected transformants of the RNAi strain carrying different silencing constructs were grown on different selective media (**Figure 1B**). We observed a decreased growth among transformants carrying antisense constructs (*URA3*, *ADE2*) under conditions of *CUP1* promoter induction (medium supplemented with copper) on minimal medium lacking uracil or adenine. For hairpin constructs (*URA3, ADE2*), a growth inhibition by several orders of magnitudes was observed with

Ishchuk et al.   *RNAi Tool for Candida glabrata*

FIGURE 1 | Introduction of RNA interference (RNAi) into *C. glabrata*. **(A)** Schematic view of the plasmid carrying the expression cassettes for the *DCR1* and *AGO1* genes of *S. castellii* (P1062), which was integrated into the genome; the *DCR1* cassette consisted of the promoter *TEF1* and the terminator *CYC1* of *C. glabrata;* the *AGO1* cassette consisted of the promoter *TDH3* and the terminator *TDH3* of *C. glabrata;* the silencing constructs (antisense and hairpins) targeting two model genes of the *C. glabrata* genome, *URA3* and *ADE2,* were expressed under control of the inducible promoter *CUP1* with the terminator *CYC1*, both of *C. glabrata*. **(B)** Growth phenotypes of *C. glabrata* transformant carrying RNAi constructs for *URA3* and *ADE2* genes (hairpin [H] and antisense [A]). Serial dilutions of cells (OD_{600} 1; 0.1; 0.01) were plated on different media with and without copper (YNB; YNB with adenine; YNB with 5-FOA and uracil); Strains are as follows: 1 – BG2; 2 – Y1662 carrying P1028 (RNAi negative control); 3 – *URA3* antisense-8; 4 – *URA3* antisense-12; 5 – *ADE2* antisense-5; 6 – *ADE2* antisense-10; 7 – *URA3* hairpin-4; 8 – *URA3* hairpin-7; 9 – *ADE2* hairpin-3; 10 – *ADE2* hairpin-4; 11 – *ADE2* hairpin-10. **(C)** Expression analysis of *ADE2* and *URA3* genes in RNAi transformants performed by qRT-PCR. Gene expression was induced by addition of copper to the medium. Strains: control (Y1662 carrying P1028); *ADE2* antisense; *ADE2* hairpin; *URA3* antisense; *URA3* hairpin. The error bars represent standard deviation of two replicates. Corresponding primer pairs were used with cDNA: *ACT1* gene (OP33 and OP34), *ADE2* (OP31 and OP32), *URA3* (OP27 and OP28).

and without *CUP1* promoter induction. Apparently, the *CUP1* promoter was leaky (**Supplementary Figure S1**) and the hairpin constructs had a strong effect on gene expression. In agreement with this, silencing of the *URA3* gene with the hairpins allowed growth on 5-FOA (**Figure 1B**), a compound, which is toxic to cells with an active *URA3* gene. Further, *ADE2* silencing with hairpins resulted in accumulation of the red pigment *P*-ribosylamino imidazole on adenine-limited media (10 mg/L), which indicates a block in adenine synthesis (**Figure 1B**). These results show a strong silencing of model target genes by both *URA3* and *ADE2* hairpin constructs.

To confirm our phenotypic observations, the expression of *URA3* and *ADE2* genes was studied by qRT-PCR in transformants carrying either antisense or hairpin silencing constructs (**Figure 1C**). Compared to the control strain, both *ADE2* antisense and *URA3* antisense constructs caused 1.4-times and 2-times down-regulation, respectively, of their target genes

specifically in the medium with copper (**Figure 1C**). In contrast, gene expression in transformants with hairpin constructs was repressed further than that even in the medium without copper, with only slight additional increase in the presence of Cu ions (**Figure 1C**).

The experiment showed that the reconstituted RNAi pathway in *C. glabrata* is functional and can be applied for gene silencing in this yeast.

Knock-Down of a Known Virulence Gene

In addition to model genes, we designed silencing constructs for *PUP1*/CAGL0M12947g gene of *C. glabrata* to be tested in our RNAi system in *C. glabrata* CBS 138 strain. The deletion of this gene, encoding a mitochondria localized protein, decreases the virulence of azole resistant strain DSY565 of *C. glabrata* in an immuno-compromised mouse model (Vermitsky et al., 2006; Ferrari et al., 2011). Both DSY565 and CBS 138 strains are
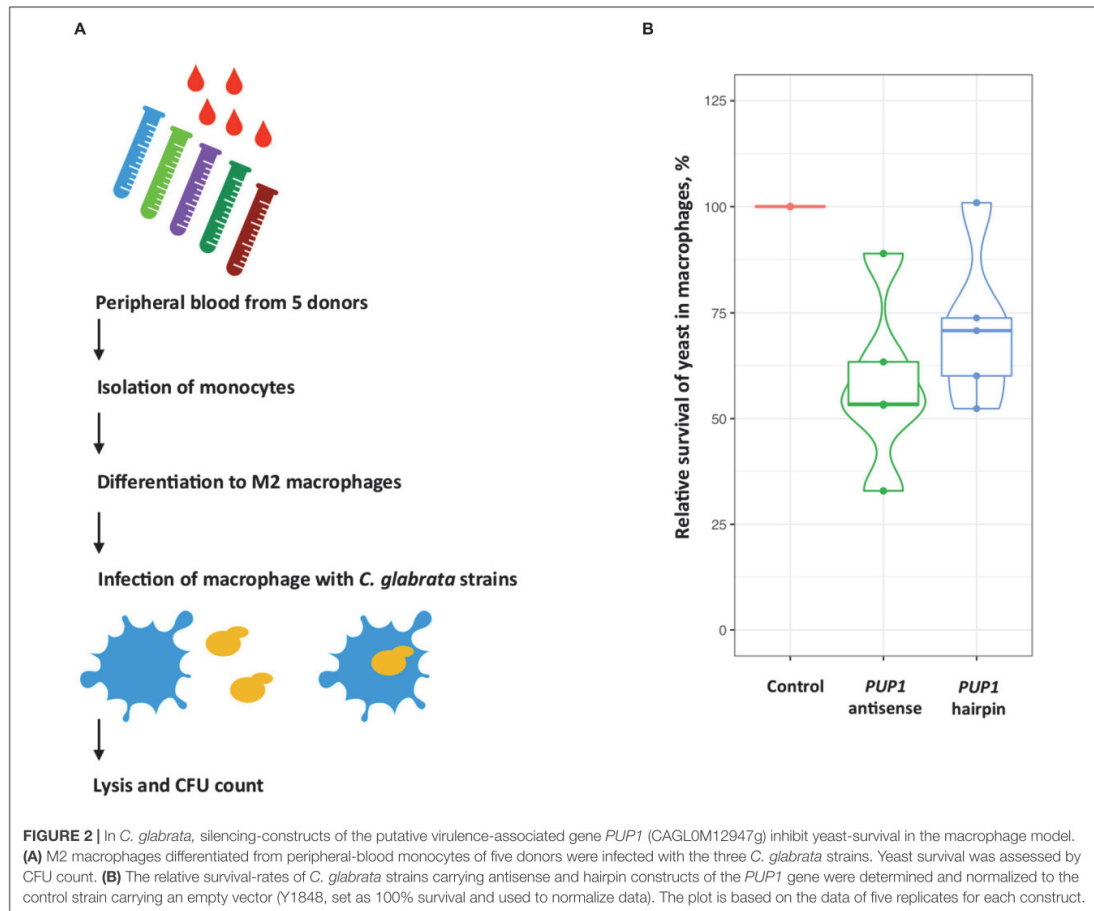
TABLE 1 | Strains used in this study.

Laboratory designation	Original name	Origin	Description	Source
Y1092	CBS 138 (ATCC 2001)		Wild type	Reference strain
Y1630	BG2	Clinical isolate	Wild type	(Fidel et al., 1996) Kindly provided by Cormack B.
Y1638	BG14	BG2	*ura3*	(Cormack and Falkow, 1999) Kindly provided by Cormack B.
Y1636	Y1092 *lys2*	CBS 138 (Y1092)	*lys2*	This study
Y1637	BG2 *lys2*	BG2	*lys2*	This study
Y1662	BG2 *lys2 DCR1 AGO1*	BG2	RNAi master strain, *lys2* carrying P1062 (stable transformant)	This study
Y1699	Y1092 *lys2 DCR1 AGO1*	CBS 138	RNAi master strain, *lys2* carrying P1062 (stable transformant)	This study
Y2121	BG14 ura3 *DCR1 AGO1*	BG14	RNAi master strain, *ura3* carrying P1062 (stable transformant)	This study
Y1663	Y1637 *DCR1 AGO1 URA3* antisense-8	Y1662	Y1662 carrying P1029	This study
Y1664	Y1637 *DCR1 AGO1 URA3* antisense-12	Y1662	Y1662 carrying P1029	This study
Y1665	Y1637 *DCR1 AGO1 URA3* hairpin-4	Y1662	Y1662 carrying P1030	This study
Y1667	Y1637 *DCR1 AGO1 URA3* hairpin-7	Y1662	Y1662 carrying P1030	This study
Y1660	Y1637 *DCR1 AGO1 ADE2* antisense-5	Y1662	Y1662 carrying P1065	This study
Y1661	Y1637 *DCR1 AGO1 ADE2* antisense-10	Y1662	Y1662 carrying P1065	This study
Y1671	Y1637 *DCR1 AGO1 ADE2* hairpin-3	Y1662	Y1662 carrying P1066	This study
Y1672	Y1637 *DCR1 AGO1 ADE2* hairpin-4	Y1662	Y1662 carrying P1066	This study
Y1673	Y1637 *DCR1 AGO1 ADE2* hairpin-10	Y1662	Y1662 carrying P1066	This study
Y1843	Y1699 *DCR1 AGO1 PUP1* antisense	Y1699	Y1699 carrying P1125	This study
Y2172	Y1699 *DCR1 AGO1 PUP1* hairpin	Y1699	Y1699 carrying P1151	This study
Y1847	Y1637 *DCR1 AGO1*	Y1662	Y1662 carrying empty P1061	This study
Y1848	Y1636 *DCR1 AGO1*	Y1699	Y1699 carrying empty P1061	This study

fluconazole resistant. As estimated in our lab, the CBS138 strain has fluconazole MIC of 129 mg/L, which is higher than that of DSY565 (fluconazole MIC of 64 mg/L, Vale-Silva et al., 2017). To achieve a stable integration for silencing constructs in the genome, we targeted the 18S rDNA locus of *C. glabrata* CBS 138 strain with RNAi. For a constitutive expression level, the promoter *PGK1* of *C. glabrata* was selected (**Supplementary Figure S1**).

We constructed two recombinant plasmids carrying antisense or hairpin constructs for the *PUP1* (**Supplementary Table S2**). These vectors (P1125 and P1151) were linearized with *SacII* (this restriction site is present in the 18S rDNA sequence) and transformed into CBS 138-based *C. glabrata* master strain Y1699 carrying both *DCR1* and *AGO1* genes (**Table 1**). The plasmid linearization in 18S rDNA region generated homologous regions for ends-in homologous recombination with 18S rDNA loci. To check the stability of the plasmids' integration into the genome, the recombinant colonies were grown for several generations on non-selective YPD medium. The strains were analyzed by PCR to confirm the presence of antisense or hairpin "bullets" and

integration of both *DCR1* and *AGO1*. Then 90% of all strains carrying the inserts were stable for 60 generations.

Using this approach, we constructed two strains, Y1843 and Y2172, which carry antisense and hairpin constructs for the *C. glabrata PUP1* gene, respectively. As survival in macrophages may be one important virulence determinant of *C. glabrata* (Brunke and Hube, 2013), we used a macrophage-confrontation assay for the analysis of fitness of our mutant. In this macrophage confrontation assay, the strains carrying the *PUP1* antisense and hairpin constructs showed decreased intracellular survival of 42% (for antisense construct) and 29% (for hairpin construct) of their mean values compared to the empty-vector control strain Y1848 (**Figure 2**). While the silencing constructs reduced survival comparing to the control (ANOVA, $p = 0.02$ and $p = 0.1$), the difference between the antisense and hairpin transformants survival was not significantly different (ANOVA, $p = 0.42$). Compared to the control strain, the *PUP1* gene expression was 10-fold lower in the *PUP1* antisense strain, and 1000-fold lower in *PUP1* hairpin strain (**Supplementary Figure S2**). The ratio of gene size to antisense region was ∼2. Our results of the

FIGURE 2 | In *C. glabrata*, silencing-constructs of the putative virulence-associated gene *PUP1* (CAGL0M12947g) inhibit yeast-survival in the macrophage model. **(A)** M2 macrophages differentiated from peripheral-blood monocytes of five donors were infected with the three *C. glabrata* strains. Yeast survival was assessed by CFU count. **(B)** The relative survival-rates of *C. glabrata* strains carrying antisense and hairpin constructs of the *PUP1* gene were determined and normalized to the control strain carrying an empty vector (Y1848, set as 100% survival and used to normalize data). The plot is based on the data of five replicates for each construct.

down regulation of *PUP1* gene by silencing constructs prove that our RNAi system can be used to study gene functions in an infection model and show that *PUP1* is required for *C. glabrata* survival in macrophages.

Construction of RNAi Gene Library to Detect New Virulence-Associated Genes of *C. glabrata*

To use our RNAi system as a basis for the identification of infection-relevant *C. glabrata* genes, we constructed a library of *C. glabrata* genome fragments on a plasmid vector (P1226) carrying an ARS-like sequence, which results in about 10 copies per cell (Hanic-Joyce and Joyce, 1998) (**Figure 3A**). The expression cassette for genomic fragments contained the strong constitutive promoter *TEF1* and the terminator *CYC1* of *C. glabrata*. The resulting gene-library plasmids were isolated from 400,000 bacterial transformants, and 40% of these carried inserts ranging from 1 to 5 kb in size as estimated by *Sau*3AI

enzyme digestion of the plasmid DNA. The constructed gene library therefore represented at least a 10× genome coverage of *C. glabrata* as estimated by the number of clones and their plasmid insert sizes. This library was used to transform the BG2-based *C. glabrata* strain with the reconstituted RNAi pathway, Y1662 (**Figure 3**). In this case, both sense and antisense DNA fragments (depending on the orientation of the ligated genomic fragments) could determine the transformant's phenotype. We expected that the sense fragments lead to gene up-regulation, while the antisense fragments lead to gene down-regulation (silencing).

RNAi Gene Library Phenotypic Screening Identifies Putative Virulence-Associated Genes

A total of 1080 *C. glabrata* strains with the gene library were selected randomly from ∼5000 colonies obtained after transformation, and subjected to phenotypic profiling in search

91

FIGURE 3 | Cloning of putative virulence genes from a gene library. **(A)** Genomic DNA for gene library construction was isolated from the *C. glabrata* BG2 strain. The DNA was partially digested with *Sau*3AI and cloned into the *C. glabrata* multi-copy expression vector P1226 under control of the *TEF1* promoter and with *CYC1* terminator. This library was transformed into the RNAi-capable *C. glabrata* strain Y1662. **(B)** 1080 transformants of Y1662 containing gene library plasmids were plated from liquid YNB onto different media of interest (amphotericin B, fluconazole, menadione, hydrogen peroxide, SDS, bromocresol green) using a robotic system in 384-colony format plates. The growth of colonies was monitored by the digital imaging over 96 h.

of novel virulence-related genes involved in ROS tolerance, and antifungal drug resistance (**Figure 3**), attributes that help *C. glabrata* survive in the host. In addition, we selected medium with SDS for the large-scale cloning of genes responsible for *C. glabrata* cell integrity, and pH indicator for monitoring the colonies surface pH (**Figure 3**). Later can be explored further as targets for the development of new antifungals to destroy the cell or studied for its pH alteration properties in macrophages.

In the first round of screening, 1080 transformants were analyzed for their growth capacity in two replicates at high resolution using a robotic platform. The plating and growth screening were carried out on solid media containing fluconazole, amphotericin B, menadione, hydrogen peroxide, SDS, or the pH indicator bromocresol green. As shown in **Figure 4**, the *C. glabrata* transformant colonies varied in their growth phenotypes with a high correlation between two replicates. In comparison to the control medium (YNB with 2% glucose), the addition of selected compounds in most conditions resulted in more divergent transformant phenotypes (colony sizes) relative to the control transformant with an empty vector (used for the normalization and has value 1). Transformants with colony size

different to the control strain under the conditions studied are of interest for further study, as the genes, which can contribute to this superior or diminished growth, are potential antifungal targets. Several transformants were resistant or sensitive to different stress conditions (**Figure 4**).

The second round of screening was performed for the sensitivity to the potent new antifungal peptides 6, 9, and 11 developed by Larsen et al. (2015). For this, we used selected transformants with stress-related phenotypes (identified in the first round, 139 transformants) and 54 previously untested randomly picked up transformants. Transformants were tested in replicate and 11 transformants proved to be sensitive or resistant to one or all of the antifungal peptides tested (**Table 2**).

In total, we randomly selected 82 gene library transformants for sequencing, all of which showed increased or decreased stress sensitivity, and/or changed resistance to antifungal drugs tested, for sequencing. The inserts of the isolated plasmids were sequenced from the promoter *TEF1* and the terminator *CYC1* and 24 inserts sequences, which were obtained in full, contained one gene (or portion of a gene) in either the sense or anti-sense orientation (**Table 2**). The *C. glabrata*

FIGURE 4 | The gene library transformants had different growth phenotypes. **(A)** Relative colony size of two replicates of 1080 gene library transformants of the RNAi-capable strain under different conditions estimated at 48 h of incubation. Colony size of transformants with the library was normalized to the control (Y1662 with empty vector, which was set to 1.0) on each plate. Conditions: 0 (no treatment), antifungals (fluconazole [50 and 400 μg/ml], amphotericin B [0.05 and 0.25 μg/ml]), ROS-generating compounds (hydrogen peroxide [3 and 12 mM], menadione [0.02 and 0.06 mM]), and surfactant (SDS, 0.0025 and 0.01%). **(B)** Growth for 96 h of transformants (two replicates each) selected for sequencing on the medium with AmB (0.25 μg/ml).

CAGL0G05335g gene, (*TPS2*) encoding a subunit of trehalose-6-phosphate synthase/phosphatase complex and known to be associated with virulence in *C. albicans* (Van Dijck et al., 2002), was found on two plasmids. Most of the genes isolated were so far uncharacterized (**Table 2**). Potential gene functions predicted form orthologs of identified genes in other species cover numerous cellular processes including RNA processing and transcription regulation, adhesins, trehalose biosynthesis, ethanol production, protein folding, chromosome maintenance and recombination, and metabolite transport. We also found two clones with antisense fragments to genes, whose orthologs in *S. cerevisiae* are essential: CAGL0H00891g (*S. cerevisiae IQG1* encodes protein required cytokinesis (Epp and Chant, 1997), and CAGL0A01430g [*S. cerevisiae TRP5* gene encodes tryptophan synthase and whose mutations results in tryptophan auxotrophy (Braus, 1991)].

Seven transformants proved to be sensitive to one or to all antifungal peptides tested (**Table 2**). For example, transformant 81C6 (5N2) was sensitive to peptide 6, 9, and 11 (**Table 2** and **Figure 5**), and was found to carry the plasmid with antisense fragment to the *C. glabrata* CAGL0J02464g gene, which encodes a putative isopeptidase, that is possibly able to directly cleave or modify the tested peptides. Four transformants proved to be resistant to one or to all antifungal peptides tested (**Table 2**). Transformant 81E12 (2A3) was resistant to peptide 9 (**Table 2** and **Figure 5**), and was found to carry the plasmid with sense fragment of the *C. glabrata* CAGL0B01683g/*TMN2* gene's open reading frame, which ortholog in *S. cerevisiae* is a membrane protein, which take part in endosome-vacuolar trafficking. The degradation of other antimicrobial peptides by targeting to yeast vacuole was reported by other studies (Lis et al., 2009; Muñoz et al., 2013).

In addition sensitivity to antifungal drugs, the transformant 3F3 displayed more acidic colony surface on medium with pH indicator bromocresol green, as the colonies of this strain had darker yellow color than the control strain (**Figure 6A**), indicating acid pH ($\leq$3) of 3F3 colonies. The observed properties of 3F3 on bromocresol green could affect its survival after phagocytosis. Sequencing of the insert of the gene library plasmid isolated from 3F3 showed that it carried an antisense insert of the uncharacterized gene of CAGL0K11968g of *C. glabrata*. In *S. cerevisiae*, the gene-ortholog has a 3-hydroxyisobutyryl-CoA hydrolase activity and a role in the stress-activated MAPK cascade with its mutation affecting the fluid-phase endocytosis[1]. Indeed, vacuolar staining revealed that as in deletion mutants of *S. cerevisiae*, the down-regulation of this gene in *C. glabrata* affects the vacuolar morphology (**Figure 6B**). We tested the 3F3 strain in our macrophage model, where it was 50% more susceptible to killing after macrophage phagocytosis (**Figure 6C**). The macrophages phagosome maturation is accompanied with high level of ROS, and one of *C. glabrata* strategies to proliferate inside the macrophages is lowering ROS (Seider et al., 2011). Our study of 3F3 strain showed that it had lowered proliferating properties inside the macrophages (lowered survival). The expression of the 3F3 plasmid (antisense) was also found to confer hydrogen peroxide sensitivity in RNAi strain but not in wild type (**Supplementary Figure S3**).

In summary, using high resolution of mitotic growth screening of gene library in RNAi strain we cloned several putative virulence-related genes.

RNAi Gene Library Antisense Plasmids Inhibit the Expression of Their Target Genes

Further studies are needed to verify each isolated gene by the gene overexpression studies or gene deletions. Moreover, the antisense and truncated gene constructs may have off target effects on other gene expression as observed in mammalian cells (El-Brolosy and

[1]www.yeastgenome.org

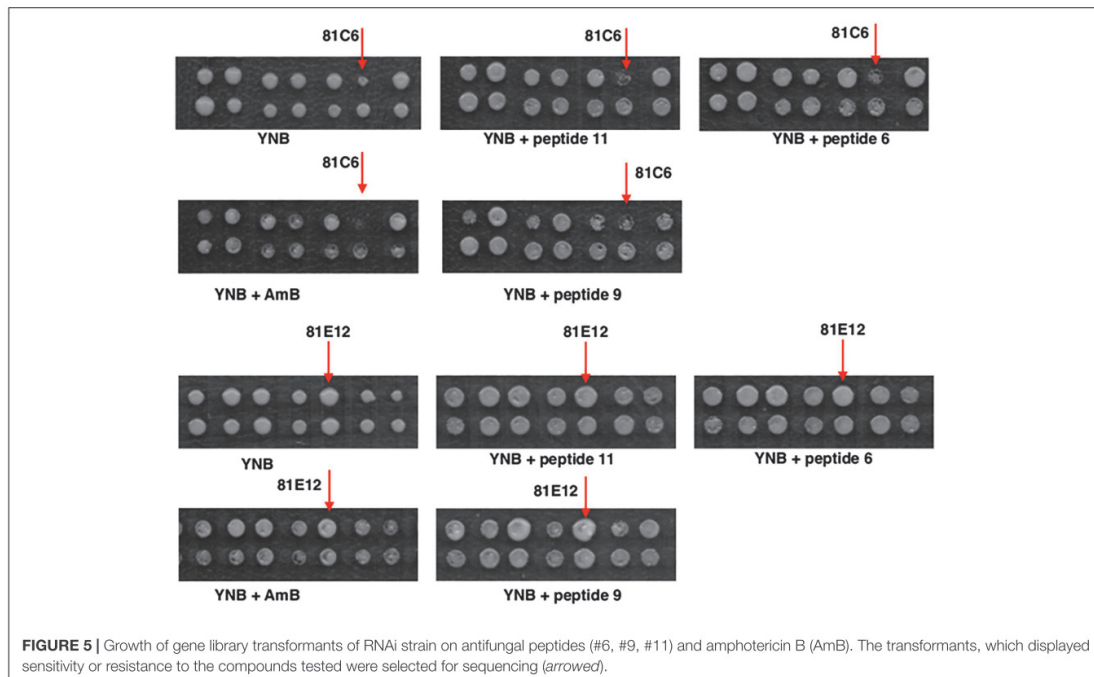**TABLE 2 |** Sequencing analysis of gene library plasmids.

Plasmid name from robot screening	Plasmid name from manual screening	Gene present on the plasmid insert	Gene description (www.candidagenome.org)	Insert orientation	Phenotype
2C23, #220	81E18	CAGL0L00157g	Uncharacterized, homologous to other adhesion-like GPI-anchored proteins of *C. glabrata* (*EPA11, EPA19,* etc.).	Antisense	Fluconazole (−) Amphotericin B (−) Menadione (−) pH (modified) SDS (−)
2E5, #235	81C18	CAGL0E00231g	Uncharacterized, putative adhesin-like protein; contains tandem repeats and a predicted GPI-anchor; belongs to adhesin cluster III.	Antisense	Fluconazole (−) Amphotericin B (−) Menadione (−) SDS (−) H_2O_2 (−)
2G7, #260	81E14	CAGL0I11011g	Uncharacterized, putative adhesin; belongs to adhesin cluster V.	Antisense	Fluconazole (−) Amphotericin B (−) Menadione (−) SDS (−) H_2O_2 (-)
2A3, #186	81E12	CAGL0B01683g	*TMN2,* uncharacterized, ortholog(s) have role in cellular copper ion homeostasis, invasive growth in response to glucose limitation, pseudohyphal growth, vacuolar transport and fungal-type vacuole membrane localization.	Sense	Fluconazole (−) Menadione (−) SDS (−) pH (modified) Peptide 9 (+) H_2O_2 (−) SDS (−)
2I5, #283		CAGL0G05335g	*TPS2*, uncharacterized, ortholog(s) have trehalose-phosphatase activity.	Antisense	Fluconazole (−) Amphotericin B (−) Menadione (−) SDS (−) H_2O_2 (−)
5N2, #893	81C6	CAGL0J02464g	Uncharacterized, Ortholog(s) have SUMO-specific isopeptidase activity, role in chromosome condensation, mitotic spindle assembly checkpoint, plasmid maintenance, protein desumoylation, and nucleus localization.	Antisense	Fluconazole (−) Amphotericin B (−) Menadione (−) SDS (−) Peptide 6 (−) Peptide 9 (−) Peptide 11 (−) H_2O_2 (−)
3F3, #430	81C4	CAGL0K11968g	Uncharacterized, ortholog(s) have 3-hydroxyisobutyryl-CoA hydrolase activity and mitochondrial ribosome localization.	Antisense	Fluconazole (−) Amphotericin B (−) Menadione (−) SDS (−) pH (modified) H_2O_2 (−)
2A5, #187	81E4	CAGL0H05049g	Uncharacterized, ortholog(s) have leucine-tRNA ligase activity, mRNA binding activity, role in Group I intron splicing, leucyl-tRNA aminoacylation, mitochondrial translation and mitochondrion localization.	Sense	Fluconazole (+) Amphotericin B (+) Menadione (+) SDS (+) Peptide 9 (+) H_2O_2 (+)
2N23, #352	81C22	CAGL0D05588g	Uncharacterized, ortholog(s) have role in maturation of SSU-rRNA from tricistronic rRNA transcript (SSU-rRNA, 5.8S rRNA, LSU-rRNA) and nucleolus, small-subunit processome localization.	Sense	Fluconazole (+) Amphotericin B (+) H_2O_2 (+) Menadione (+) SDS (+)
	81N8	CAGL0A01430g	Uncharacterized, putative tryptophan synthase; protein abundance increased in *ace2* mutant cells.	Antisense	Amphotericin B (−)
6D19, #966	81A16	CAGL0E00539g	Uncharacterized, ortholog(s) have role in attachment of spindle microtubules to kinetochore involved in homologous chromosome segregation, chromatin silencing at rDNA, protein localization to nucleolar rDNA repeats, rDNA condensation.	Antisense	Fluconazole (+) Amphotericin B (+) SDS (+) Peptide 6 (+) Peptide 9 (+) Peptide 11 (+)
6K21, #1051	81A14	CAGL0J01661g	Uncharacterized, has domain(s) with predicted transmembrane transporter activity and role in transmembrane transport.	Sense	Fluconazole (−) Amphotericin B (−) Menadione (−) SDS (−) H_2O_2 (−)

(Continued)

TABLE 2 | Continued

Plasmid name from robot screening	Plasmid name from manual screening	Gene present on the plasmid insert	Gene description (www.candidagenome.org)	Insert orientation	Phenotype
3F1, #429		CAGL0M04741g	Uncharacterized, ortholog(s) have protein disulfide isomerase activity, protein disulfide oxidoreductase activity, protein-disulfide reductase (glutathione) activity and role in protein folding.	Sense	Amphotericin B (+) SDS (+)
4E7, #604		CAGL0K01991g	Uncharacterized, has domain(s) with predicted tRNA (cytosine-5-)-methyltransferase activity.	Sense	Fluconazole (−) Amphotericin B (−) Menadione (−) SDS (−) H_2O_2 (-)
5B5, #751	81G5	CAGL0J03652g	Uncharacterized, has domain(s) with predicted ATP binding, aminoacyl-tRNA editing activity, leucine-tRNA ligase activity, role in leucyl-tRNA aminoacylation and cytoplasm localization.	Sense	Fluconazole (−) Amphotericin B (−) Peptide 9 (−)
6J23, #1040		CAGL0A03630g	Uncharacterized, ortholog(s) have RNA polymerase III general transcription initiation factor activity, chromatin insulator sequence binding activity and role in transcription initiation from RNA polymerase III promoter.	Sense	Fluconazole (−) Amphotericin B (−) Menadione (−) H_2O_2 (−)
3I5, #467	81I15	CAGL0I07843g	*ADH1*, Putative alcohol dehydrogenase isoenzyme III; increased protein abundance in azole resistant strain.	Sense	Fluconazole (−) Amphotericin B (−) Menadione (−) SDS (−) Peptide 6 (−) Peptide 9 (−) Peptide 11 (−) H_2O_2 (−)
3C9, #397	81I21	CAGL0A00781g	Uncharacterized, has domain(s) with predicted zinc ion binding activity.	Sense	Fluconazole (−) Amphotericin B (−) Menadione (−) SDS (−) Peptide 9 (−) H_2O_2 (−)
	82H20	CAGL0B05049g	Uncharacterized, ortholog(s) have ubiquitin-protein transferase activity and role in double-strand break repair via non-homologous end joining, double-strand break repair via synthesis-dependent strand annealing.	Sense	Amphotericin B (−) Peptide 6 (−) Peptide 9 (−) Peptide 11 (−)
	82N22	CAGL0H00891g	Uncharacterized, ortholog(s) have actin filament binding, calmodulin binding activity.	Antisense	Amphotericin B (−) Peptide 6 (−) Peptide 9 (−) Peptide 11 (−)
	81E20	CAGL0G05335g	*TPS2*, uncharacterized, ortholog(s) have trehalose-phosphatase activity.	Antisense	Amphotericin B (−)
	82M12	CAGL0L13392g	Protein of unknown function.	Sense	Amphotericin B (−) Peptide 6 (+) Peptide 9 (+) Peptide 11 (+)
	83K4	CAGL0D06446g	*STT4*, uncharacterized, ortholog(s) have 1-phosphatidylinositol 4-kinase activity.	Sense	Fluconazole (+)
	83K11	CAGL0H07623g	Uncharacterized, ortholog(s) have role in meiotic gene conversion, reciprocal meiotic recombination.	Antisense	Amphotericin B (−) Peptide 6 (−)

"#", location on the graph, **Figure 4**. "+", resistant. "−", sensitive.

Stainier, 2017; Ma et al., 2019; Wilkinson, 2019), and studying the global gene expression of these strains could give more information on this in future studies. In this study, to rule-out the possibility of off-target gene inhibitions we have investigated the target gene expression of 10 antisense constructs in both wild type and RNAi strains.

For this purpose we took ten gene library antisense plasmids (2C23, 2E5, 81E20, 6D19, 3F3, 2I5, 82N22, 81N8, 83K11, and 2G7) and transformed them into the wild type and RNAi strains. Two transformants of each plasmid were selected for the analysis. The RNA was extracted from their cultures grown in YNB

with 2% glucose and gene expression was studied by qRT-PCR (**Figure 7** and **Supplementary Figure S4**). Plasmids 2C23, 2E5, 81E20, 2I5, and 82N22 had stronger gene expression inhibition in RNAi strain than in WT. Plasmids 6D19, 3F3, 81N8, 83K11, and 2G7 proved to inhibit the target genes in RNAi strain but not in the WT strain (**Figure 7**). This suggests that the gene inhibition is indeed mediated through RNAi. Phenotypes observed during the robotics screening were re-confirmed for most plasmids after the re-transformation (**Supplementary Figure S3**). While some of the phenotypes were unique to RNAi transformants (H_2O_2 sensitivity in 2I5, 3F3, 82N22, and 81E20), 2I5 conferred

FIGURE 5 | Growth of gene library transformants of RNAi strain on antifungal peptides (#6, #9, #11) and amphotericin B (AmB). The transformants, which displayed sensitivity or resistance to the compounds tested were selected for sequencing (*arrowed*).

the amphotericin resistance to both RNAi and wild type strain (**Supplementary Figure S3**).

DISCUSSION

The yeast *C. glabrata* is an important opportunistic human pathogen, which has become of interest over recent decades, particularly due to its increasing occurrence and resistance to antifungal drugs.

Unlike for *S. cerevisiae* and *C. albicans,* there are no extensive genetics toolboxes available for *C. glabrata* and thus this yeast remains poorly studied. Gene deletions in this yeast for gene function elucidations are not easy to obtain. With a higher rate of non-homologous recombination in *C. glabrata* than that in *S. cerevisiae* (Cormack and Falkow, 1999; Corrigan et al., 2013), longer homology regions are required for more efficient gene knockouts in *C. glabrata*; haploid asexual nature of *C. glabrata* prohibits many techniques based on mating developed for *S. cerevisiae*. In this study, we developed a new tool for *C. glabrata* based on RNA interference (RNAi), which relies on gene silencing through double-stranded RNA intermediates and siRNA. This ancient mechanism of protection from foreign DNA and chromatin organization is lost in Hemiascomycetes (Axelson-Fisk and Sunnerhagen, 2006) with the exception of *Saccharomyces castellii* (Drinnenberg et al., 2009). We therefore cloned the *DCR1* and *AGO1* genes from *S. castellii* and overexpressed them in *C. glabrata* together

with silencing constructs. Judging from our data on silencing of metabolic genes (endogenous *ADE2* and *URA3* genes), the introduced RNAi pathway is functional and can be applied to additional genes of interest in this yeast. We found that gene silencing was stronger with hairpin compared to antisense constructs in this study similarly to Drinnenberg et al. (2009). Although our data indicate that the *CUP1* promoter used for RNAi is leaky, the antisense constructs resulted in decreased gene expression and detectable phenotypes only upon its induction by copper. In contrast, the hairpin constructs displayed high inhibition of gene expression regardless of the *CUP1* promoter induction, which suggests that the designed hairpins are very effective in our system.

Our RNAi tool proved to be active when we tested it with an established virulence-associated gene CAGL0M12947g (*PUP1*) of *C. glabrata*, which was shown by deletion to be important for a survival in a mouse model (Ferrari et al., 2011). Here, we showed that down-regulation of this gene affects survival in human macrophages. Its ortholog (*RCI37/YIL077C*) is poorly studied in *S. cerevisiae*. Although it is known to localize in the mitochondria and interact with the respiratory chain (Morgenstern et al., 2017), the mechanistic connections of its *C. glabrata* ortholog to virulence remain unknown.

We were interested to apply the developed RNAi for the discovery of new virulence-associated genes of *C. glabrata*. We did this by using the RNAi strain with a gene library as the basis for screening of virulence-related phenotypes and the identification of responsible genes. To this end we created a

FIGURE 6 | *Candida glabrata* CAGL0K11968g contributes to vacuolar morphology and survival in macrophages. **(A)** On the medium with pH indicator bromocresol green the 3F3 strains had darker yellow color than control strain, indicating more acidic pH. **(B)** Fluorescent microscopy images of *C. glabrata* strains after staining showing abnormal vacuolar morphology of the 3F3 strain. **(C)** The transformant 3F3, which carries an antisense CAGL0K11968g gene, displayed 50% loss of viability in our macrophage model. The experiment was performed in four replicates with cells originating from blood of two donors. The plot is based on data of four replicates. The control strain data (CFU) was set as 100% and used to normalize data. According to Poisson Regression analysis of raw data, the 3F3 strains CFU response was significantly different (***p-value $\leq$ 0.0005).

library of random genome fragments in the expression vector. In contrast to hairpin constructs, this approach is feasible on the genomic level (the library represents 10-fold genome coverage), and we can assume that a significant portion of clones will carry the antisense regions of genes to induce RNAi. Since the inhibitory effect of the antisense constructs was less efficient than

FIGURE 7 | The target genes expression studies of the transformants of RNAi and wild type strain carrying antisense gene library plasmids. *Y*-axis – logarithmic scale. RNAi strain was Y1662, and the wild type was Y1637, which were newly re-transformed with plasmids. Antisense plasmids: 1 – 2C23 (CAGL0L00157g gene), 2 – 2E5 (CAGL0E00231g gene), 3 – 81E20 (CAGL0G05335g gene), 4 – 6D19 (CAGL0E00539g gene), 5 – 3F3 (CAGL0K11968g gene), 6 – 2I5 (CAGL0G05335g gene), 7 – 82N22 (CAGL0H00891g gene), 8 – 81N8 (CAGL0A01430g gene), 9 – 83K11 (CAGL0H07623g gene), and 10 – 2G7 (CAGL0I11011g gene). The untreated controls were used to calculate gene expression fold change: RNAi and wild type carrying empty vector (P1226). Primer pair ACT1-1 and ACT1-2 was used for *ACT1* gene.

hairpins in our model and required a high expression level, the gene library was constructed using the strong constitutive *TEF1* promoter and a multi-copy vector.

Our primary interest was to discover genes, which affect *C. glabrata* resistance to antifungal drugs, and to stress conditions that *C. glabrata* may face during survival in macrophages. Therefore, we selected the following conditions for cell growth *in vitro*, which have overlap in their targets in yeast. In our screening we selected fluconazole and amphotericin B, which are both antifungal drugs currently in use against candidiasis, and which target the plasma membrane. Although the mechanism of action of many azole drugs and resistance to them are quite extensively studied (Vale-Silva and Sanglard, 2015), the molecular mechanism of amphotericin B action and resistance remains poorly understood. We also tested hydrogen peroxide and menadione since ROS are elevated upon amphotericin B exposure (Mesa-Arango et al., 2014), and are produced inside

the macrophages phagosomes (Seider et al., 2014), and resistance against ROS is important for pathogen survival. SDS was tested to mimic damage to the plasma membrane. In addition, we used new antifungal drugs for the *C. glabrata* gene library screening including three peptidomimetics with an arginine-[β-(2,5,7-tri-tert-butylindol-3-yl)alanine]-arginine motif, which were recently developed (Larsen et al., 2015), and are effective against *S. cerevisiae* as well as *Zygosaccharomyces bailii*, known to spoil food. Interestingly, *C. glabrata* was previously shown to be resistant to these peptides (Larsen et al., 2015) and finding the resistance genes in pathogenic yeasts can help to develop potent antifungals further.

The frequent and large size differences of transformants colonies in our screening indicated that a broad range of genes was covered by the RNAi library strains. We selected representative resistant and sensitive transformants for sequencing of their plasmid inserts to determine the original

genome loci. Using this approach, we found that several positive clones of our RNAi library corresponded to putative virulence-associated genes. This shows that our approach allows us to recover genes with relevance for *C. glabrata* pathobiology, which can be exploited further for the development of treatments for *C. glabrata* infections.

The gene down-regulation and expression of truncated genes might affect the expression of other genes in the genome, their genes network as described for mammalian cells (El-Brolosy and Stainier, 2017; Ma et al., 2019; Wilkinson, 2019). This effect, genetic compensation, is also common for gene knockouts in yeasts (He and Zhang, 2006; Teng et al., 2013). The expression of antisense constructs spanning the coding regions in *S. cerevisiae* from the plasmid vectors were reported to inhibit the *ATH1* and *CAR1* gene expression (Park et al., 2001; Jung and Park, 2005) suggesting the natural antisense interference without RNAi (Donaldson and Saville, 2012). The whole genome sequencing and global gene expression profiling can give more information on any off-target effects of isolated gene library clones in the future studies. When we analyzed ten antisense constructs, all 10 down-regulated the target genes, and 5 of 10 worked through the RNAi because they did not down-regulate the gene expression in the wild type strain without RNAi pathway.

Three of the genes identified in our screen were predicted glycosylphosphatidylinositol (GPI)-anchored proteins and adhesins (CAGL0L00157g, CAGL0E00231g, and CAGL0I11011g), and the expression of their antisense regions leads to sensitivity to fluconazole, amphotericin B, menadione, hydrogen peroxide, and SDS. GPI-anchored proteins are abundant membrane and cell wall proteins with multiple roles, and their biosynthesis is reportedly linked ergosterol biosynthesis and azole drug response, Ras signaling (Yadav et al., 2014). The GPI-anchored proteins are therefore important antifungal targets, and are in the focus of drug discovery studies (Mann et al., 2015). It is important to note that the antisense region of the 2C23 isolate of our study included a part of the GPI-anchored protein transmembrane domain (CAGL0L00157g), which is a fragment of 17 other GPI-genes sequences in the *C. glabrata* genome. This suggests that the construct affected several GPI proteins, likely resulting in altered plasma membrane structure.

The 6K21 strain, which was sensitive to antifungals and ROS, carried the overexpression plasmid for a sense fragment of transporter gene CAGL0J01661g, whose ortholog in *S. cerevisiae* (YPR011C) encodes a mitochondrial transporter for adenosine 5′-phosphosulfate (APS) and 3′-phospho-adenosine 5′-phosphosulfate (PAPS), the deletion of whish causes the decreased glutathione and methionine levels and temperature sensitive phenotype (Todisco et al., 2014), and glutathione is known ROS scavenger (Jamieson, 1998).

Our results point at the *TPS2* gene, encoding trehalose-6 phosphate phosphatase of *C. glabrata,* as a potential drug target with virulence-associated roles in this yeast. The *TPS2* antisense construct expression resulted in sensitivity to fluconazole, amphotericin B, and other stressors. The deletion of *TPS2* in both *S. cerevisiae* and *C. albicans* causes the accumulation of increased amounts of trehalose-6 phosphate upon stress, which is toxic to the cell, and results in thermo-sensitive phenotype

(De Virgilio et al., 1993; Van Dijck et al., 2002). In *C. albicans*, it was also found to reduce the virulence as the survival of infected mice in systemic infection model was increased (Van Dijck et al., 2002). Indeed, the deletion of this gene leads to impaired growth in *C. albicans,* and other species, and the gene product itself is considered as a potential target for antifungal therapy (Van Dijck et al., 2002; Pianalto and Alspaugh, 2016).

The transformant 3I5 carried a gene library plasmid with a complete *ADH1* open reading frame in the sense direction. It proved to be sensitive to fluconazole, amphotericin B, peptides, SDS, and reactive oxygen species. The *ADH1* gene is encoding alcohol dehydrogenase, responsible for the conversion of acetaldehyde to ethanol. In *C. albicans,* the expression of the *ADH1* and azole resistance is inversely correlated in clinical isolates (Siikala et al., 2011). On the contrary, increased abundance of the Adh1 protein was previously observed in an azole resistant strain of *C. glabrata* (Rogers et al., 2006). Since we do not have the data on the *ADH1* expression in 3I5 strain, further study is needed.

Due to their low toxicity, the peptidomimetics are potent antifungal drugs (Larsen et al., 2015). A mode of action of these peptides is likely the interaction with sphingolipids, as determined by the analysis of deletion mutants' library in *S. cerevisiae* (Larsen et al., 2015). Larsen et al. (2015) pointed out that higher resistance in pathogenic yeasts (*C. albicans* and *C. glabrata*) to these compounds might be due to the secretion of extracellular proteases, which sequester or degrade the antifungals. One of the isolated *C. glabrata* antisense plasmids carried part of the CAGL0J02464g gene, whose orthologs have SUMO (Small Ubiquitin-like Modifier)-specific isopeptidase and protein deSUMOylation activities. The encoded isopeptidase could be important for the resistance to peptidomimetics in this yeast and could be involved in their direct cleavage, in support of the hypothesis proposed by Larsen et al. (2015). In addition, fragments of two putative aminoacyl-tRNA genes were found with our system affecting the peptidomimetics resistance. We hypothesize that they could directly interact with peptidomimetics or their targets by acylating them. Aminoacyl-tRNA dependent acylation is involved in several cellular processes and resistance to antifungal peptides reported in other species (Raina and Ibba, 2014). Acylation of membrane lipids is known to change the membrane surface and subsequently the affinity of the membrane to antifungal peptides in other species (Ernst and Peschel, 2011; Raina and Ibba, 2014). The direct acylation of macromolecules using aminoacyl-tRNA can change their activity, recognition or directs them to degradation (Katz et al., 2016).

Taking a step further, we validated the importance of one of the identified target in the macrophage model. We confirmed the vital importance of the *C. glabrata* CAGL0K11968g gene affecting colony pH and vacuolar function with this screening method. With the antisense construct for this gene the *C. glabrata* strain was less viable upon exposure to human macrophages.

We have thus established a working RNAi system for the investigation of *C. glabrata* pathobiology. Our initial testing showed that the system can be used to interfere with the expression of a broad range of genes, including those assumed

Manuscript III

Ishchuk et al.   RNAi Tool for *Candida glabrata*

to be essential for *C. glabrata*. The RNAi strains can be used in *in vitro* stress tests and in interaction with immune cells, which will be invaluable in attributing functions to the many genes of *C. glabrata*, which are unannotated so far. Our screening of a RNAi library with genome fragments is a first step into that direction. Especially, as this method enables us to tackle new genes, which are central for fungal growth and survival, we believe that it will allow us to find important new potential targets for *C. glabrata* antifungals, a yeast that is notorious for its inherent and acquired resistances.

MATERIALS AND METHODS

Growth Conditions

All strains used in this study were grown in rich medium (YPD [yeast extract 1%, peptone 2%, glucose 2%, Bactoagar 2%] or synthetic minimal medium (YNB [yeast nitrogen base without amino acid and ammonium sulfate] 1.9 g/L, glucose 2%, ammonium sulfate 0.5%) at 25°C, unless stated otherwise. For the uracil-deficient mutant BG14, 50 mg/L uracil was added to the YNB medium. For the lysine-deficient mutants, 40 mg/L lysine was added to the minimal medium. *C. glabrata* transformants carrying plasmids with the *LYS2* gene as a selectable marker were selected and propagated on YNB medium. For *C. glabrata* transformants carrying the *Streptoalloteichus hindustanus ble* gene as a selective marker, 200 μg/ml of zeocin was added to the YPD medium. For the induction of the *CUP1* promoter, 0.05 mM CuSO$_4$ was added to the YNB medium.

For gene library yeast transformants different compounds were added to YNB medium as follows: amphotericin B (0.05 and 0.25 μg/ml), fluconazole (50 and 400 mg/L), SDS (0.01 and 0.0025%), hydrogen peroxide (3 and 12 mM), menadione (0.02 and 0.06 mM), and antifungal peptidomimetics (peptide 6 [H-Arg-Tbt-Arg-Phe-NH2], 9 [H-Arg-Tbt-Arg-hPhe-NH2], and 11 [H-Arg-Tbt-Arg-[NPhe]-NH2] (Larsen et al., 2015) at 25 μg/ml. Gene library transformants were propagated at 37°C.

RNA Extraction and qRT-PCR

Total RNA was extracted from the *C. glabrata* cultures grown in selective media (supporting plasmids propagation) using the PureLink RNA Mini Kit (Thermo Fisher Scientific). The concentration and purity of RNA were determined by NanoDrop spectrophotometer. The isolated RNA was treated with DNase I (RNase-Free DNase Set, Qiagen) according to the manufacturer's recommendations. The RNA integrity was checked by electrophoresis using precast RNA MOPS agarose gels (Sigma-Aldrich). Five microgram of pure RNA was used for the synthesis of cDNA. The SuperScript III Reverse Transcriptase kit with RNaseOUT Ribonuclease Inhibitor and random primers (Thermo Fisher Scientific) was used. The cDNA produced was used as a template with gene-specific primers in qRT-PCR reactions with the SYBR GreenER qPCR SuperMix (Thermo Fisher Scientific). qRT-PCRs were run in duplicate in the RotorGene 2000

cycler (Corbett Research) under the conditions specified by Thermo Fisher Scientific. The take off and amplification values were obtained using the RotorGene 2000 software. The β-actin gene was treated as the endogenous reference gene (housekeeping gene), while Y1848 was used as untreated strain. Primer pairs for the 3′-region of the gene ORFs of interest of *C. glabrata* were used in qRT-PCR experiments as follows for the: *ACT1* (OP33 and OP34; ACT1-1 and ACT1-2), *ADE2* (OP31 and OP32), *URA3* (OP27 and OP28), *PUP1* (947-1 and 947-2), CAGL0L00157g (157-1 and 157-2), CAGL0E00231g (231-3 and 231-4), CAGL0G05335g (5335-3 and 5335-4), CAGL0E00539g (539-1 and 539-2), CAGL0K11968g (968-1 and 968-2), CAGL0H00891g (891-1 and 891-2), CAGL0A01430g (1430-3 and 1430-4), CAGL0H07623g (7623-1 and 7623-2), and CAGL0I11011g (11-1 and 11-2) (**Supplementary Table S1**). The gene expression fold change was calculated by the ΔΔCt method (Livak and Schmittgen, 2001).

Macrophage Culture and Infection With Yeast

Human monocyte-derived macrophages (hMDMs) were prepared according to the protocol used before (Seider et al., 2011, 2014). Monocytes were isolated from human peripheral blood (donated by healthy volunteers with written consent) with CD14 magnetic beads by automated cell sorting (autoMACs, MiltenyiBiotec). CD14-positive monocytes differentiated to M2 macrophages for 7 days in RPMI1640 media with L-glutamine (Thermo Fisher Scientific) with 10% heat-inactivated FCS (Bio&Sell GmbH), and with 50 ng/ml recombinant human macrophage colony stimulating factor (rh M-CSF; Immunotools). Adherent MDMs were detached with 10 mM EDTA in PBS and seeded in 96-well plates (4 × 10^4 hMDMs/well) in RPMI with 50 ng/ml rh M-CSF and 10% FCS and incubated overnight. Prior macrophage infection yeast cells from a stationary YNB culture were washed three times with PBS. M2 macrophages were infected by adding the yeast cells at multiplicity of infection of one (MOI 1) in RPMI w/o FCS. The cells were further diluted and incubated for 3 h at 5% CO$_2$ and 37°C. Unattached yeast cells were removed by washing the macrophages two times with 60 μl PBS. Next, 20 μl of 0.5% Triton X-100 was added to lysate the macrophages, and incubated 10 min under gentle shaking. After the incubation, cells were diluted, plated on YPD, and incubated at 37°C for 1 day. After incubation, the yeast CFU were counted. The reference strain Y1848 carrying empty vector was used to normalize obtained data and was set to 100% survival.

Robotics Screening

Individual transformants of the *C. glabrata* RNAi strain (Y1662) containing the gene library plasmids were grown overnight in flat bottom polystyrene 96-well plates in 200 μl of liquid YNB at 37°C (12 plates in total). The next day, yeast transformants were plated onto the solid media YNB supplemented with antifungal drugs

[amphotericin B (0.05 and 0.25 μg/ml) or fluconazole (50 and 400 μg/ml)], ROS generating compounds [menadione (0.02 and 1 0.06 mM) and hydrogen peroxide (3 and 12 mM)], surfactant (SDS 0.01 and 0.0025%) and a pH indicator (bromocresol green 0.01 g/ml, YNB medium pH was adjusted to 4.5) using a robotic system (Siger RoToR HDA robot). Each 96-well plate liquid culture was plated on solid medium in duplicate, and four were combined onto one 384 format solid medium plate. The colonies growth was scored by the colony size in pixels from the digital images of the plates during 96 h of incubation.

Vacuolar Staining and Fluorescent Microscopy

Cells were re-suspended in 10 mM HEPES buffer pH 7.4 supplemented with 5% glucose. The fluorescent dye CMAC-Ala-Pro (7-amino-4-chloromethylcoumarin, l-alanyl-l-proline amide, Yeast Vacuolar Marker Sampler Kit [Thermo Fisher Scientific]) was added to the cell suspension at 100 μM and then incubated in the dark for 30 min. The staining was visualized by fluorescent microscopy (automated inverted wide-field microscope Observer Z1 [Carl Zeiss] equipped with a sCMOS camera).

Statistical Analysis

The software packages R (Version 1.1.463– ©2009–2018 RStudio, Inc.), JMP®, Pro 13.0.0 (SAS Institute Inc., Cary, NC, United States, 1989–2019) and Minitab®18.1, were used to analyze the obtained data.

DEDICATION

In loving memory of JP who sadly deceased on May 18, 2014.

DATA AVAILABILITY

All datasets generated for this study are included in the manuscript and/or the **Supplementary Files**.

ETHICS STATEMENT

AUTHOR CONTRIBUTIONS

OI and JP designed the study. OI, KA, KK, KB, and TS developed the RNAi tool. LK, SB, MS, BH, TH, BG, and OI performed the macrophage experiments. CB, KF, JS, BR, and OI analyzed the gene library. OI, KA, WK, and JP wrote the manuscript. All authors commented on and reviewed the manuscript.

FUNDING

ACKNOWLEDGMENTS

SUPPLEMENTARY MATERIAL

The Supplementary Material for this article can be found online at: https://www.frontiersin.org/articles/10.3389/fmicb.2019.01679/full#supplementary-material

REFERENCES

Ahmad, K. M., Kokošar, J., Guo, X., Gu, Z., Ishchuk, O. P., and Piškur, J. (2014). Genome structure and dynamics of the yeast pathogen *Candida glabrata*. *FEMS Yeast Res.* 14, 529–535. doi: 10.1111/1567-1364.12145

Axelson-Fisk, M., and Sunnerhagen, P. (2006). "Comparative genomics and gene finding in fungi," in *Comparative Genomics Using Fungi as Models. Topics in Current Genetics*, Vol. 15, eds P. Sunnerhagen and J. Piškur (Berlin: Springer), doi: 10.1007/4735_111

Braus, G. H. (1991). Aromatic amino acid biosynthesis in the yeast *Saccharomyces cerevisiae*: a model system for the regulation of a eukaryotic biosynthetic pathway. *Microbiol Rev.* 55, 349–370.

Brunke, S., and Hube, B. (2013). Two unlike cousins: *Candida albicans* and *C. glabrata* infection strategies. *Cell. Microbiol.* 15, 701–708. doi: 10.1111/cmi.12091

Cormack, B. P., and Falkow, S. (1999). Efficient homologous and illegitimate recombination in the opportunistic yeast pathogen *Candida glabrata*. *Genetics* 151, 979–987.

Corrigan, M. W., Kerwin-Iosue, C. L., Kuczmarski, A. S., Amin, K. B., and Wykoff, D. D. (2013). The fate of linear DNA in *Saccharomyces cerevisiae* and *Candida glabrata*: the role of homologous and non-homologous end joining. *PLoS One* 8:e69628. doi: 10.1371/journal.pone.0069628

De Virgilio, C., Bürckert, N., Bell, W., Jenö, P., Boller, T., and Wiemken, A. (1993). Disruption of *TPS2*, the gene encoding the 100-kDa subunit of the trehalose-6-phosphate synthase/phosphatase complex in *Saccharomyces cerevisiae,* causes accumulation of trehalose-6-phosphate and loss of trehalose-6-phosphate phosphatase activity. *Eur. J. Biochem.* 212, 315–323. doi: 10.1074/jbc.M113.528802

Donaldson, M. E., and Saville, B. J. (2012). Natural antisense transcripts in fungi. *Mol. Microbiol.* 85, 405–417. doi: 10.1111/j.1365-2958.2012.08125.x

101

Drinnenberg, I. A., Weinberg, D. E., Xie, K. T., Mower, J. P., Wolfe, K. H., Fink, G. R., et al. (2009). RNAi in budding yeast. *Science* 326, 544–550. doi: 10.1126/science.1176945

Dujon, B., Sherman, D., Fischer, G., Durrens, P., Casaregola, S., Lafontaine, I., et al. (2004). Genome evolution in yeasts. *Nature* 430, 35–44. doi: 10.1038/nature02579

El-Brolosy, M. A., and Stainier, D. Y. R. (2017). Genetic compensation: a phenomenon in search of mechanisms. *PLoS Genet.* 13:e1006780. doi: 10.1371/journal.pgen.1006780

Epp, J. A., and Chant, J. (1997). An IQGAP-related protein controls actin-ring formation and cytokinesis in yeast. *Curr. Biol.* 7, 921–929. doi: 10.1016/s0960-9822(06)00411-8

Ernst, C. M., and Peschel, A. (2011). Broad-spectrum antimicrobial peptide resistance by MprF-mediated aminoacylation and flipping of phospholipids. *Mol. Microbiol.* 80, 290–299. doi: 10.1111/j.1365-2958.2011.07576.x

Ferrari, S., Sanguinetti, M., Torelli, R., Posteraro, B., and Sanglard, D. (2011). Contribution of CgPDR1-regulated genes in enhanced virulence of azole-resistant *Candida glabrata*. *PLoS One* 6:e17589. doi: 10.1371/journal.pone.0017589

Fidel, P. L. Jr., Cutright, J. L., Tait, L., and Sobel, J. D. (1996). A murine model of *Candida glabrata* vaginitis. *J. Infect. Dis.* 173, 425–431. doi: 10.1093/infdis/173.2.425

Fidel, P. L. Jr., Vazquez, J. A., and Sobel, J. D. (1999). Candida glabrata: review of epidemiology, pathogenesis, and clinical disease with comparison to *C. albicans*. *Clin. Microbiol. Rev.* 12, 80–96. doi: 10.1128/CMR.12.1.80

Gabaldón, T., and Fairhead, C. (2018). Genomes shed light on the secret life of *Candida glabrata*: not so asexual, not so commensal. *Curr. Genet.* 65, 93–98. doi: 10.1007/s00294-018-0867-z

Giaever, G., Chu, A. M., Ni, L., Riles, L., Véronneau, S., Dow, S., et al. (2002). Functional profiling of the *Saccharomyces cerevisiae* genome. *Nature* 418, 387–391. doi: 10.1038/nature00935

Hanic-Joyce, P. J., and Joyce, P. B. (1998). A high-copy-number *ADE2*-bearing plasmid for transformation of *Candida glabrata*. *Gene* 211, 395–400. doi: 10.1016/s0378-1119(98)00157-7

He, X., and Zhang, J. (2006). Toward a molecular understanding of pleiotropy. *Genetics* 173, 1885–1891. doi: 10.1016/S0378-1119(98)00157-7

Jamieson, D. J. (1998). Oxidative stress responses of the yeast *Saccharomyces cerevisiae*. *Yeast* 14, 1511–1527. doi: 10.1002/(SICI)1097-0061(199812)14:16<1511::AID-YEA356>3.0.CO;2-S

Jung, Y. J., and Park, H. D. (2005). Antisense-mediated inhibition of acid trehalase (*ATH1*) gene expression promotes ethanol fermentation and tolerance in *Saccharomyces cerevisiae*. *Biotechnol. Lett.* 27, 1855–1859. doi: 10.1007/s10529-005-3910-3

Kasper, L., Seider, K., Gerwien, F., Allert, S., Brunke, S., Schwarzmüller, T., et al. (2014). Identification of *Candida glabrata* genes involved in pH modulation and modification of the phagosomal environment in macrophages. *PLoS One* 9:e96015. doi: 10.1371/journal.pone.0096015

Katz, A., Elgamal, S., Rajkovic, A., and Ibba, M. (2016). Non-canonical roles of tRNAs and tRNA mimics in bacterial cell biology. *Mol. Microbiol.* 101, 545–558. doi: 10.1111/mmi.13419

Larsen, C. E., Larsen, C. J., Franzyk, H., and Regenberg, B. (2015). Antifungal properties of peptidomimetics with an arginine-[β-(2,5,7-tri-tert-butylindol-3-yl)alanine]-arginine motif against *Saccharomyces cerevisiae* and *Zygosaccharomyces bailii*. *FEMS Yeast Res.* 15:fov011. doi: 10.1093/femsyr/fov011

Lis, M., Fuss, J. R., and Bobek, L. A. (2009). Exploring the mode of action of antimicrobial peptide MUC7 12-mer by fitness profiling of *Saccharomyces cerevisiae* genomewide mutant collection. *Antimicrob. Agents Chemother.* 53, 3762–3769. doi: 10.1128/AAC.00668-09

Livak, K. J., and Schmittgen, T. D. (2001). Analysis of relative gene expression data using real-time quantitative PCR and the $2^{-\Delta\Delta C_T}$ Method. *Methods* 25, 402–408. doi: 10.1006/meth.2001.1262

Ma, Z., Zhu, P., Shi, H., Guo, L., Zhang, Q., Chen, Y., et al. (2019). PTC – bearing mRNA elicits a genetic compensation response via Upf3a and COMPASS components. *Nature* 568, 259–263. doi: 10.1038/s41586-019-1057-y

Mann, P. A., McLellan, C. A., Koseoglu, S., Si, Q., Kuzmin, E., Flattery, A., et al. (2015). Chemical genomics-based antifungal drug discovery: targeting glycosylphosphatidylinositol (GPI) precursor biosynthesis. *ACS Infect. Dis.* 1, 59–72. doi: 10.1021/id5000212

Mârdh, P. A., Rodrigues, A. G., Genç, M., Novikova, N., Martinez-de-Oliveira, J., and Guaschino, S. (2002). Facts and myths on recurrent vulvovaginal candidosis–a review on epidemiology, clinical manifestations, diagnosis, pathogenesis and therapy. *Int. J. STD. AIDS.* 13, 522–539. doi: 10.1258/095646202760159639

Martienssen, R. A., Zaratiegui, M., and Goto, D. B. (2005). RNA interference and heterochromatin in the fission yeast *Schizosaccharomyces pombe*. *Trends Genet.* 21, 450–456. doi: 10.1016/j.tig.2005.06.005

Mesa-Arango, A. C., Trevijano-Contador, N., Román, E., Sánchez-Fresneda, R., Casas, C., Herrero, E., et al. (2014). The production of reactive oxygen species is a universal action mechanism of Amphotericin B against pathogenic yeast and contributes to the fungicidal effect of this drug. *Antimicrob. Agents Chemother.* 58, 6627–6638. doi: 10.1128/AAC.03570-14

Moazed, D. (2009). Molecular biology. *Rejoice–RNAi for yeast*. *Science* 326, 533–534. doi: 10.1126/science.1182102

Morgenstern, M., Stiller, S. B., Lübbert, P., Peikert, C. D., Dannenmaier, S., Drepper, F., et al. (2017). Definition of a high-confidence mitochondrial proteome at quantitative scale. *Cell Rep.* 19, 2836–2852. doi: 10.1016/j.celrep.2017.06.014

Moyes, D. L., and Naglik, J. R. (2011). Mucosal immunity and *Candida albicans* infection. *Clin. Dev. Immunol.* 2011:346307. doi: 10.1155/2011/346307

Muñoz, A., Harries, E., Contreras-Valenzuela, A., Carmona, L., Read, N. D., and Marcos, J. F. (2013). Two functional motifs define the interaction internalization and toxicity of the cell-penetratingantifungal peptide PAF26 on fungal cells. *PLoS One* 8:e54813. doi: 10.1371/journal.pone.0054813

Park, H., Shin, M., and Woo, I. (2001). Antisense-mediated inhibition of arginase (*CAR1*) gene expression in *Saccharomyces cerevisiae*. *J. Biosci. Bioeng.* 92, 481–484. doi: 10.1263/jbb.92.481

Pfaller, M. A., and Diekema, D. J. (2007). Epidemiology of invasive candidiasis: a persistent public health problem. *Clin. Microbiol. Rev.* 20, 133–163. doi: 10.1128/CMR.00029-06

Pianalto, K. M., and Alspaugh, J. A. (2016). New horizons in antifungal therapy. *J. Fungi.* 2:26. doi: 10.3390/jof2040026

Raina, M., and Ibba, M. (2014). tRNAs as regulators of biological processes. *Front. Genet.* 5:171. doi: 10.3389/fgene.2014.00171

Rogers, P. D., Vermitsky, J. P., Edlind, T. D., and Hilliard, G. M. (2006). Proteomic analysis of experimentally induced azole resistance in *Candida glabrata*. *J. Antimicrob. Chemother.* 58, 434–438. doi: 10.1093/jac/dkl221

Schwarzmüller, T., Ma, B., Hiller, E., Istel, F., Tscherner, M., Brunke, S., et al. (2014). Systematic phenotyping of a large-scale *Candida glabrata* deletion collection reveals novel antifungal tolerance genes. *PLoS Pathog.* 10:e1004211. doi: 10.1371/journal.ppat.1004211

Seider, K., Brunke, S., Schild, L., Jablonowski, N., Wilson, D., Majer, O., et al. (2011). The facultative intracellular pathogen *Candida glabrata* subverts macrophage cytokine production and phagolysosome maturation. *J. Immunol.* 187, 3072–3086. doi: 10.4049/jimmunol.1003730

Seider, K., Gerwien, F., Kasper, L., Allert, S., Brunke, S., Jablonowski, N., et al. (2014). Immune evasion, stress resistance, and efficient nutrient acquisition are crucial for intracellular survival of *Candida glabrata* within macrophages. *Eukaryot. Cell.* 13, 170–183. doi: 10.1128/EC.00262-13

Siikala, E., Bowyer, P., Richardson, M., Saxen, H., Sangland, D., and Rautemaa, R. (2011). *ADH1* expression inversely correlates with *CDR1* and *CDR2* in *Candida albicans* from chronic oral candidosis in APECED (APS-I) patients. *FEMS Yeast Res.* 11, 494–498. doi: 10.1111/j.1567-1364.2011.00739.x

Teng, X., Dayhoff-Brannigan, M., Cheng, W. C., Gilbert, C. E., Sing, C. N., Diny, N. L., et al. (2013). Genome-wide consequences of deleting any single gene. *Mol. Cell.* 52, 485–494. doi: 10.1016/j.molcel.2013.09.026

Tijsterman, M., Ketting, R. F., and Plasterk, R. H. (2002). The genetics of RNA silencing. *Annu. Rev. Genet* 36, 489–519. doi: 10.1146/annurev.genet.36.043002.091619

Todisco, S., Di Noia, M. A., Castegna, A., Lasorsa, F. M., Paradies, E., and Palmieri, F. (2014). The *Saccharomyces cerevisiae* gene *YPR011c* encodes a mitochondrial transporter of adenosine 5′-phosphosulfate and 3′-phospho-adenosine 5′-phosphosulfate. *Biochim. Biophys. Acta.* 1837, 326–334. doi: 10.1016/j.bbabio.2013.11.013

Ishchuk et al.   RNAi Tool for *Candida glabrata*

Vale-Silva, L., Beaudoing, E., Tran, V. D. T., and Sanglard, D. (2017). Comparative genomics of two sequential *Candida glabrata* clinical isolates. *G3.* 7, 2413–2426. doi: 10.1534/g3.117.042887

Vale-Silva, L. A., and Sanglard, D. (2015). Tipping the balance both ways: drug resistance and virulence in *Candida glabrata*. *FEMS Yeast Res.* 15:fov025. doi: 10.1093/femsyr/fov025

Van Dijck, P., De Rop, L., Szlufcik, K., Van Ael, E., and Thevelein, J. M. (2002). Disruption of the *Candida albicans TPS2* gene encoding trehalose-6 phosphate phosphatase decreases infectivity without affecting hypha formation. *Infect. Immunol* 70, 1772–1782. doi: 10.1128/IAI.70.4.1772-1782.2002

Vermitsky, J. P., Earhart, K. D., Smith, W. L., Homayouni, R., Edlind, T. D., and Rogers, P. D. (2006). Pdr1 regulates multidrug resistance in *Candida glabrata*: gene disruption and genome-wide expression studies. *Mol. Microbiol.* 61, 704–722. doi: 10.1111/j.1365-2958.2006.05235.x

Wilkinson, M. F. (2019). Genetic paradox explained by nonsense. *Nature* 568, 179–180. doi: 10.1038/d41586-019-00823-5

Yadav, B., Bhatnagar, S., Ahmad, M. F., Jain, P., Pratyusha, V. A., Kumar, P., et al. (2014). First step of glycosylphosphatidylinositol (GPI) biosynthesis cross-talks with ergosterol biosynthesis and Ras signaling in Candida albicans. *J. Biol. Chem.* 289, 3365–3382. doi: 10.1074/jbc.M113.528802

103

Complete supplemental material for this article can be found at:

https://www.frontiersin.org/articles/10.3389/fmicb.2019.01679/full#supplementary-material

2.4   Manuscript IV: Radosa *et al*., in revision *Cell. Microbiol.*

Phagocytic predation by the fungivorous amoeba *Protostelium aurantium* targets metal ion and redox homeostasis

Silvia Radosa, Jakob L. Sprague, Renáta Tóth, Thomas Wolf, **Marcel Sprenger**, Sascha Brunke, Jörg Linde, Gianni Panagiotou, Attila Gácser, and Falk Hillmann

Summary:

Predatory interactions among microbes are considered as a major evolutionary driving force for defense against phagocytic killing. The transcriptional response induced in *C. parapsilosis* upon confrontation with the fungivorous amoeba *Protostelium aurantium* highlights fungal copper- and redox homeostasis as primary targets during intracellular killing. Site-directed mutagenesis confirmed the role of the copper exporter Crp1 and the thioredoxin peroxidase Prx1 in copper and redox homeostasis, respectively and identified methionine biosynthesis as a metabolic target during predation. Both genes contributed to survival of *C. parapsilosis* encountering *P. aurantium*, but *PRX1* additionally impacts on the survival within human macrophages. The fact that both genes are conserved within the entire *Candida* clade suggested that they could be part of a basic toolkit to survive phagocytic attacks.

Own contribution:

Marcel Sprenger assisted the macrophage experiments for fungal RNA isolation, performed and analyzed the macrophage survival experiments for the revised manuscript. Marcel Sprenger edited the manuscript.

Estimated authors' contributions:

Silvia Radosa	45%
Jakob L. Sprague	5%
Renáta Tóth	5%
Thomas Wolf	5%
Marcel Sprenger	**5%**

Sascha Brunke	5%
Jörg Linde	5%
Gianni Panagiotou	5%
Attila Gácser	5%
Falk Hillmann	15%

Prof. Bernhard Hube

Phagocytic predation by the fungivorous amoeba *Protostelium aurantium* targets metal ion and redox homeostasis

Silvia Radosa[1,2], Jakob L. Sprague[1,2], Renáta Tóth[3], Thomas Wolf[4,5], Marcel Sprenger[2,6], Sascha Brunke[6], Jörg Linde[4¶], Gianni Panagiotou[5], Attila Gácser[3], and Falk Hillmann[1*]

[1]Junior Research Group *Evolution of Microbial Interaction*, Leibniz Institute for Natural Product Research and Infection Biology - Hans Knöll Institute (HKI), Jena, Germany

[2] Institute of Microbiology, Friedrich Schiller University Jena, Jena, Germany

[3] Department of Microbiology, University of Szeged, Szeged, Hungary

[4]Research Group PIDOMICS, Leibniz Institute for Natural Product Research and Infection Biology - Hans Knöll Institute (HKI), Jena, Germany

[¶]current address: Institute of Bacterial Infections and Zoonoses, Federal Research Institute for Animal Health – Friedrich-Löffler-Institute, Jena, Germany.

[5]Research Group Systems Biology and Bioinformatics, Leibniz Institute for Natural Product Research and Infection Biology - Hans Knöll Institute (HKI), Jena, Germany

[6]Department of Microbial Pathogenicity Mechanisms, Leibniz Institute for Natural Product Research and Infection Biology - Hans Knöll Institute (HKI), Jena, Germany

*for correspondence

Email: Falk.hillmann@leibniz-hki.de

Phone: +49-3641-532-1445

Fax: +49-3641-532-2445

Summary

Predatory interactions among microbes are considered as a major evolutionary driving force for biodiversity and the defence against phagocytic killing. Here we show that confrontation with the fungivorous amoeba *Protostelium aurantium* triggers selective predatory responses in three different yeasts of the genus *Candida.* While *C. albicans* escaped initial recognition, *C. glabrata* was rapidly taken up, but remained undigested with prolonged survival. Phagocytic killing and feeding by *P. aurantium* were highly effective for the third major pathogen, *C. parapsilosis.* These three different outcomes of the confrontation with the predator were reflected by distinct transcriptional responses, indicating fungal copper- and redox homeostasis as primary targets during intracellular killing. Gene deletions for the highly expressed copper exporter *Crp1* and the peroxiredoxin *Prx1* confirmed their role in copper and redox homeostasis, respectively and identified methionine biosynthesis as a metabolic target during predation. Both, intact Cu export and redox homeostasis contributed to the survival of *C. parapsilosis* not only when encountering *P. aurantium,* but also in the presence of human macrophages. As both genes were found to be widely conserved within the entire *Candida* clade, our results suggest that they could be part of a basic tool-kit to survive phagocytic attacks by environmental predators.

Introduction

Members of the genus *Candida* are among the leading causative agents of fungal infections worldwide with *Candida albicans* being responsible for the majority of candidiasis cases, followed by *C. glabrata* and *C. parapsilosis* (Dadar *et al.*, 2018). All three *Candida* species are known to be commensals being frequent residents of the oral cavities, the gastrointestinal tract or the skin. Environmental reservoirs for any of these species have rarely been documented, but recent isolations of *C. parapsilosis* or *C. albicans* from pine and oak trees, respectively, suggest that these might exist (Bensasson *et al.*, 2018, Robinson *et al.*, 2016, Maganti *et al.*, 2012). *C. glabrata,* in turn, has been enriched from fermented foods and grape juice (Greppi *et al.*, 2015, Morrison-Whittle *et al.*, 2018). Within the human host, all three are able to counteract the phagocytic attacks of macrophages and neutrophilic granulocytes to some extent, using different strategies and molecular tool-kits (Erwig & Gow, 2016).

An outer layer of mannoproteins masks pathogen-associated molecular patterns (PAMPs) on the surface of *C. albicans*, hence hindering their initial recognition via cell wall ß-glucans (Seider *et al.*, 2010). Even after its ingestion, *C. albicans* can escape from innate immune phagocytes following a morphological switch from yeast to hyphae which triggers the cytolytic death of the host cell (Uwamahoro *et al.*, 2014, Wellington *et al.*, 2014, Kasper *et al.*, 2018). *C. parapsilosis* is also able to survive the restricted phagosomal environment and forms pseudohyphae after internalization by macrophages (Toth *et al.*, 2014). However, its rates of ingestion and killing by neutrophils and macrophages were reported to be higher than for *C. albicans* (Linden *et al.*, 2010, Sasada & Johnston, 1980, Toth et al., 2014). Intracellular filamentation, in turn, is not the typical escape strategy for *C. glabrata*, which can survive and even replicate inside modified phagosomal compartments of macrophages (Kasper *et al.*, 2015).

Estimates indicate that *C. glabrata* may be separated from the other two *Candida* species by more than 300 million years (Pesole *et al.*, 1995), and hence, well before their time as commensals. Comparative genome analysis of *C. glabrata* and its closest relatives have suggested that adaptations preceding its commensal stage may have facilitated traits that later enabled pathogenicity (Gabaldon *et al.*, 2013, Turner & Butler, 2014, Gabaldon & Fairhead, 2019). The increasing clinical records of fungal infections originating from species even without any clear history of commensalism have further raised questions on the role of environmental factors as early promoters of virulence-associated traits.

Predator-prey interactions are considered as drivers of an evolutionary arms race and frequently occur also among microbes. Humans and higher animals are indirectly affected as some microbial defences against phagocytic predators are thought to be effective against innate immune cells such as macrophages and neutrophilic granulocytes. These trained defences may have favoured certain microbes to establish commensalism or appear as new pathogens (Casadevall *et al.*, 2019). Experimental studies have corroborated this idea using well-known model organisms such as *Dictyostelium discoideum* or *Acanthamoeba castellanii* (Steenbergen *et al.*, 2003, Steenbergen *et al.*, 2001, Van Waeyenberghe *et al.*, 2013, Hillmann *et al.*, 2015, Koller *et al.*, 2016). *Protostelium aurantium* is a representative of a widely spread group of amoebae with a fungivorous life-style (Aguilar *et al.*, 2007, Ndiritu *et al.*, 2009, Shadwick *et al.*, 2009a, Zahn *et al.*, 2014, Hillmann *et al.*, 2018). The amoeba was recently found to feed on a wide range of basidiomycete and ascomycete yeast species with *C. parapsilosis* being the most efficient food source, while *C. albicans* and *C. glabrata* were discriminated at the stage of recognition or intracellular processing, respectively (Radosa *et al.*, 2019). In this study, we investigated the responses of *C. albicans, C. glabrata*, and *C. parapsilosis* when confronted with the fungivorous predator. Our findings demonstrate that copper and redox homeostasis are central targets during phagocytic predation by *P. aurantium* and suggest that such basic anti-phagocytic defence strategies may have been trained during an arms race with an environmental predator.

Results

The predation responses of the three *Candida* species reflect their different prey patterns

While *C. albicans* and *C. glabrata* can escape *P. aurantium* at the stage of recognition or intracellular processing, respectively, *C. parapsilosis* serves as a comparably efficient food source (Radosa et al., 2019). To elucidate common, as well as species-specific reactions to the presence of the predator, we conducted high-throughput RNA sequencing of each of the three *Candida* species in co-cultures with *P. aurantium.* Yeast cells were confronted with trophozoites of *P. aurantium* for 30 and 60 minutes *prior* to sampling for RNA isolation. For *C. parapsilosis*, a total of 667 genes were upregulated ($\log_2$FC > 1.5), and 588 genes were downregulated ($\log_2$FC < -1.5), while in *C. albicans*, a total of 903 genes were significantly upregulated, and 937 genes were downregulated at both time points (Fig. 1A). In *C. glabrata,* 1218 genes were upregulated, while only 273 genes were found to be downregulated (Fig. 1A). A complete list of DEGs for each species and time point is listed in Dataset S1.

To address the biological significance of up- and downregulated genes, we analysed their annotations for the enrichment of defined categories in molecular function, cell component and biological process (Fig. 1B, Fig. S1, Dataset S2). Overall, the enriched categories for all three *Candida* species partially overlapped, most likely resulting from general metabolic adaptations, e. g. when grouped by molecular function, transferase and ligase activity were categories common to all three fungi among the upregulated genes. However, for *C. glabrata*, there was no significantly enriched biological process among the downregulated genes (Fig. S1) Also, transporter and kinase activity were the only two molecular functions which were enriched among the downregulated genes of *C. glabrata*. In sharp contrast, transporters were found to be generally upregulated in *C. albicans* and *C. parapsilosis*. Higher expression of RNA binding, helicases, and nucleotidyl transferases was unique to *C. parapsilosis*, the preferred prey, implicating that transcription and translation could be most severely affected in this fungus. The finding that the nucleolus and that the biological process categories for RNA metabolism and ribosome biogenesis were all enriched only in *C. parapsilosis* provides additional support for this idea. Further, the extracellular region and the cell wall were more severely affected in *C. parapsilosis* than in *C. albicans* or *C. glabrata* (Fig. 1B).
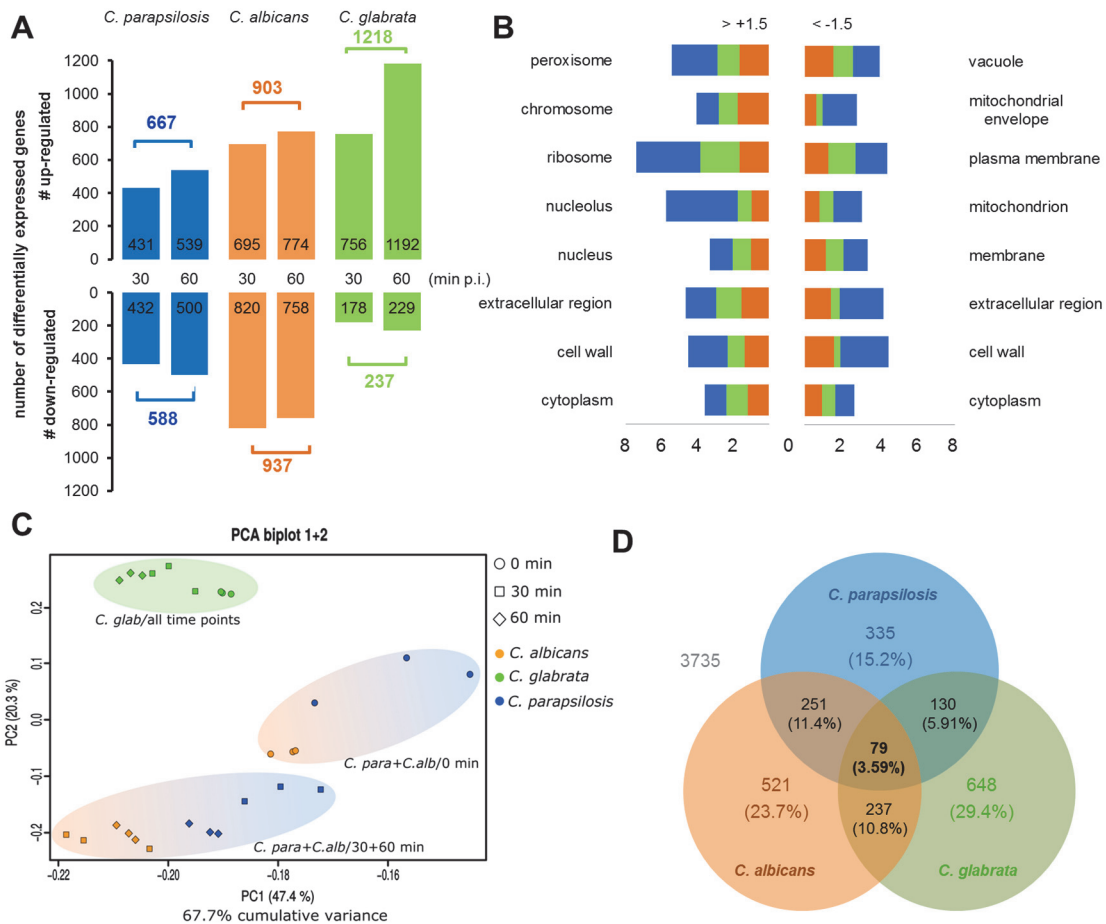
Fig. 1: Differentially gene expression in *C. parapsilosis, C. albicans* and *C. glabrata* in response to *P. aurantium*. A, Total numbers of differentially expressed genes (DEGs) of *Candida* spp. in the presence *of P. aurantium* after 30 and 60 min. Genes were considered as differentially expressed when the log$_2$ fold-change in the transcript level was ≥1.5 or ≤-1.5 and p≤0.01 according to EdgeR at either of the two tested time points. **B,** Gene ontology (GO) clusters for cellular components enriched in up- and downregulated genes of *C. parapsilosis* (blue) and their expression in *C. glabrata* (green) and *C. albicans* (orange) **C,** Principle component analysis (PCA) for read count values from orthologous genes of the three *Candida* species. PC1 and PC2 explain about 68% of the overall variance within the data set and clearly separate all *C. glabrata* samples (green, top left) from those of *C. albicans* (orange) and *C. parapsilosis* (blue). For the two latter species, there is an additional separation between control time point at 0 min (round) and time points 30/60 min (square/diamond). **D**, Venn diagram displaying an overlap in the differential expression of orthologues at 30 and 60 min. Of 3,735 orthologues in total, 2,201 were differentially expressed orthologues (DEOs) and 79 were common (3.6%) to all three species.

The core response of *C. albicans, C. parapsilosis*, and *C. glabrata* to the presence of *P. aurantium*

A principal component analysis was used to determine the dynamic variations in the orthologous DEGs. The response of *C. glabrata* to amoeba predation showed less variation between the time points (see the cluster dendrogram in Fig. S2) and was clearly distinguishable from *C. parapsilosis* and *C. albicans* (Fig 1C). For the latter two, it was evident, that their transcription profiles at time point 30 and 60 min clustered

closer together and displayed a higher variance when compared to the initial time point. To identify a commonly responsive gene set of all three fungi, we compared the differential expression among all their orthologues (DEOs). Overall, 3735 orthologous genes showed differential expression at either one of the two time points (Fig. 1D). Within all three *Candida* species, 79 genes were differentially regulated, representing a core response to the presence of *P. aurantium* (Fig. 1D). Among those, 48 genes were commonly induced, and eight genes were commonly repressed in all three species at either of the time points, while 23 genes showed opposite regulation between the species (Fig.2).
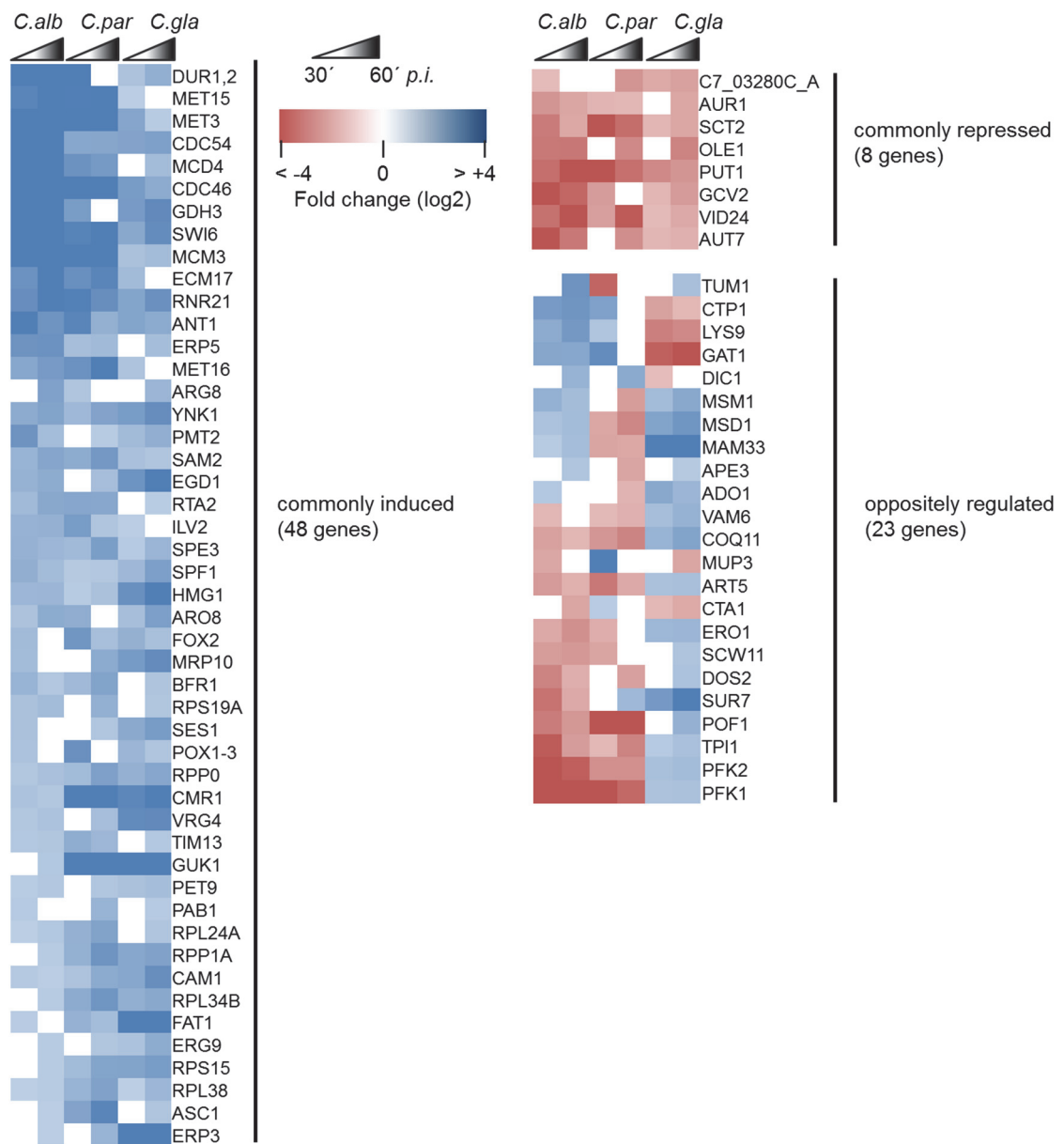
Fig. 2: Heat map of expression for all 79 differentially expressed orthologues (DEOs) during the confrontation with _P. aurantium_. All DEOs were grouped according to their transcript profile at 30 min and 60 min _p.i._ and considered as commonly induced or commonly repressed if they shared the expression pattern within all three species. DEOs were considered as oppositely regulated if their expression differed between two species. Red and blue colors represent down- and upregulated genes, respectively. Gene names are based on the orthologues of _C. albicans_.

The corresponding sets of genes were further analysed for significantly shared GO terms in biological processes (Dataset S3). Enriched categories included the sulfur amino acid metabolic process (GO:0000096) comprising genes such as _SAM2, MET3, ECM17_ (_MET5_)_, MET15, MET16,_ all playing a role in the metabolism of methionine. A plethora of genes, predicted to be involved in organo-nitrogen compound biosynthetic process (GO:1901566) such as the amino acid biosynthesis enzymes _ILV2_ and _ARG8_, a P-type calcium-transporting ATPase encoded by _SPF1_ or genes with role in fatty acid beta-oxidation (GO:0006635) like _ANT1, FOX2_ or _POX1-3_, were commonly induced as well. The most highly enriched GO term was found to be "negative regulation of helicase activity" comprising three _MCM_ genes: _CDC54_ (_MCM4_), _CDC46_ (_MCM5_) and _MCM3_; all known to be a part of MCM complex, necessary for unwinding the DNA double helix and triggering fork progression during DNA replication (Bochman & Schwacha, 2009).

Noteworthy is further the induction of the _DUR1,2_ gene, encoding the urea amidolyase and shown to be important for the survival of _C. albicans_ in macrophages (Navarathna _et al._, 2012). No GO category was found to be enriched within the eight commonly downregulated genes. Nevertheless, three out of eight genes, namely _OLE1, SCT2_ and _AUR1_, function in lipid biosynthetic processes and most probably play an important role in the integrity of cell membrane. Interestingly, GO enrichment analysis revealed the glycolytic process through fructose-6-phosphate (GO:0061615) as a highly overrepresented category within the oppositely regulated set of genes: all genes annotated to this category, namely _TPI1, PFK1_ and _PFK2,_ were downregulated in _C. albicans_ and _C. parapsilosis_, while in _C. glabrata_ they showed an increase in transcript level.

P. aurantium predation targets copper and redox homeostasis in _C. parapsilosis_

Of all three species, _C. parapsilosis_ represented the preferential food source for _P. aurantium,_ and thus, we conducted a deeper characterization of the 1255 DEGs (667 genes with log2FC > 1.5, and 588 genes with log2FC > -1.5) from _C. parapsilosis_ using

the GO Slim tool which maps DEGs to more general terms and broad categories (Skrzypek *et al.*, 2017). Most genes could not be categorized, were involved in unknown biological processes, or mapped to regulation as a general category. These were not analysed further. Transport and stress response were the two most frequent biological processes and were further selected to search for more specific categories (Fig. 3). The extra-nuclear transport of ribonucleoproteins was highly enriched as could be expected from the results obtained from the general enrichment analysis for *C. parapsilosis*. We further found the transport of transition metal ions to be overrepresented with several genes encoding orthologous proteins for the transport of Fe and Zn being deregulated in response to *P. aurantium* (Tables S1 and S2).
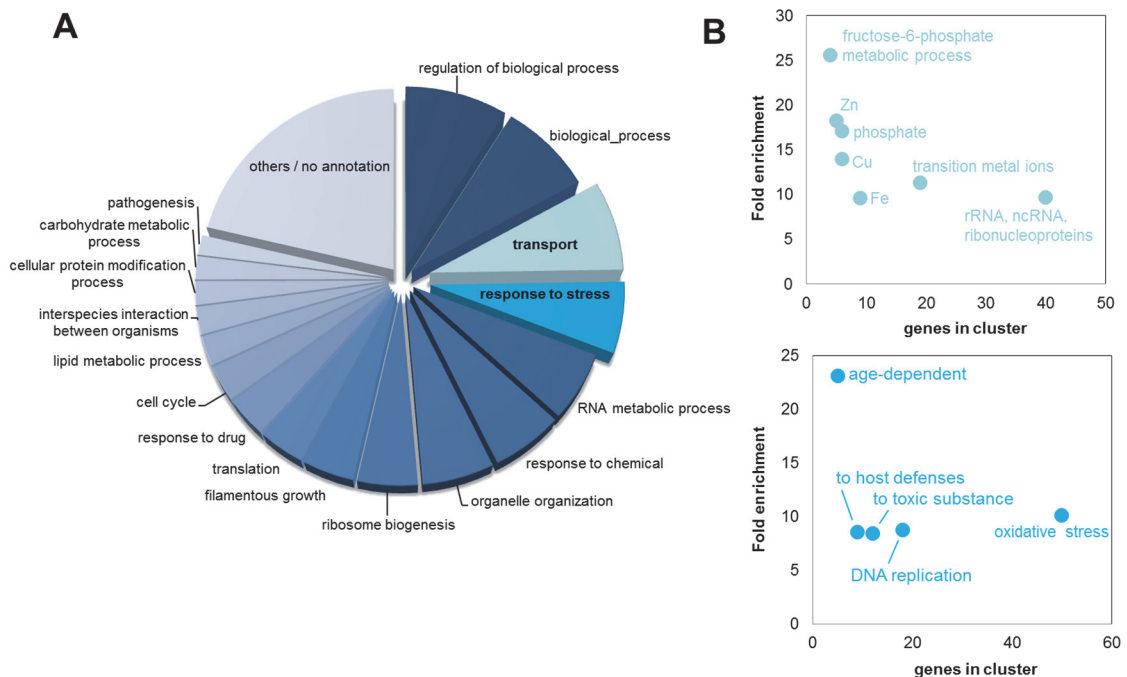
Fig. 3: GO Slim categorization of the DEGs from *C. parapsilosis* during the confrontation with *P. aurantium*. A, All 1255 DEGs from 30 min and 60 min after the confrontation with *P. aurantium* were categorized according to GO SLIM processes. **B,** Genes mapped to the GO SLIM categories *transport* and *response to stress* were further analyzed for more specific GO Terms. Categories with the highest enrichment (top 7 for *transport* and top 5 for *response to stress*) are displayed as a 2D dot plot for the number of genes in the respective cluster and fold enrichment (p-value <0.005).

Two Cu transporters were among the most highly deregulated genes in *C. parapsilosis* (Table 1.) The most upregulated gene upon amoeba predation (log$_2$FC of approx. 9 at 30 min and 8 at 60 min) was found to be CPAR2_203720. This gene is an orthologue to *C. albicans CRP1* (orf19.4784), encoding a copper-transporting P1-type ATPase, which

mediates copper resistance and is induced by high copper concentrations (Weissman *et al.*, 2000).

Interestingly, the second most downregulated gene at 30 min ($\log_2$FC = -9.8), we identified CPAR2_602990, an orthologue of *C. albicans CTR1* (orf19.3646) with copper importing activity. Four other genes annotated as copper transporters were also repressed at both time points.

Table 1: Expression of *C. parapsilosis* genes involved in the transport of Cu ions (GOID 6825)

name	log2FC 30 min	log2FC 60 min	Description	Ortholog in *C. albicans*
CPAR2_203720	9.36	8.18	copper-exporting ATPase activity, role in cadmium ion transport, cellular copper ion homeostasis, copper ion transport, silver ion transport and plasma membrane localization	C1_09250W_A/CRP1
CPAR2_210510	-2.36	-2.46	copper uptake transmembrane transporter activity, role in cellular copper ion homeostasis, copper ion import, intracellular copper ion transport and fungal-type vacuole membrane localization	C1_08620W_A/CTR2
CPAR2_300620	-7.66	-8.01	ferric-chelate reductase activity, role in copper ion import, iron ion transport and plasma membrane localization	C7_00430W_A
CPAR2_406100	-1.81	-3.67	copper ion transmembrane transporter activity, inorganic phosphate transmembrane transporter activity and role in cellular copper ion homeostasis, copper ion transmembrane transport, phosphate ion transmembrane transport	C2_09590C_A
CPAR2_701290	-3.09	-3.26	copper ion binding activity, role in cellular protein-containing complex assembly, copper ion transport and mitochondrial inner membrane, plasma membrane localization	CR_09300C_A/SCO1
CPAR2_602990	-9.79	- Inf	Ortholog(s) have copper uptake transmembrane transporter activity, role in copper ion import, high-affinity iron ion transport and cytoplasm, nucleus, plasma membrane localization	C6_00790C_A/CTR1

The differential expression of these genes was validated by quantitative real-time PCR and further tested, whether they would also respond to phagocytosis by monocyte-derived human primary macrophages (MDMs). Only for the Cp*CRP1* gene, expression in response to *P. aurantium* and MDMs was fully in accordance, while the expression of Cp*CTR1* was regulated in an opposite manner when the yeast encountered MDMs (Fig. 4A+B). We further investigated the expression of Cp*CRP1* and Cp*CTR1* during copper excess and depletion. As expected, the putative copper exporter gene Cp*CRP1* showed induction when *Candida* was treated with 100 μM of Cu, and repression in the presence of the copper chelator BCS (Fig. 4C). Even though the expression of Cp*CTR1* was not significantly influenced by the presence of BCS in the media, remarkable downregulation of this gene was measured at high copper concentration. It is noteworthy that differences in the expression levels for both genes, Cp*CRP1* and Cp*CTR1*, were more pronounced during encounters with *P. aurantium* than with macrophages or the metal itself.
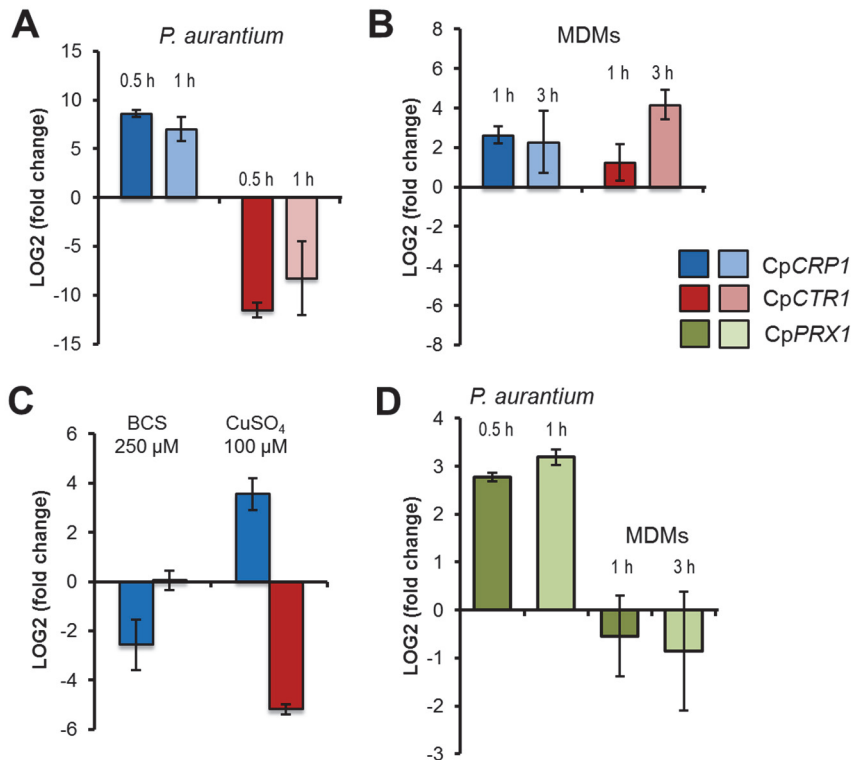
Fig. 4: Expression of copper and redox homeostasis genes. Expression of the *CRP1* (CPAR2_203720), *CTR1* (CPAR2_602990), and *PRX1* (CPAR2_805590) of *C. parapsilosis* was analyzed by qRT-PCR using total RNA isolated after the exposure to *P. aurantium* (A, D), human monocyte-derived macrophages (MDMs, B, D), and in the presence of the copper ion chelator BCS or CuSO$_4$. All data show average expression levels relative to time point 0 based on three biological and three technical replicates. Error bars indicate the standard deviation.

Intriguingly, four genes encoding superoxide dismutases (SODs) of the Cu/Zn type (CPAR2_500330, CPAR2_500390, CPAR2_213540, CPAR2_213080) and one Fe/Mn-SOD (CPAR2_109280) were strongly repressed in the presence of *P. aurantium* (Table 2).

In contrast, genes involved in the thioredoxin antioxidant pathway were found to be highly upregulated, such as CPAR2_304080, CPAR2_500130 or CPAR2_805590. The latter one is an orthologous gene to *C. albicans PRX1,* a thioredoxin-linked peroxidase, shown to be primarily involved in the reduction of cellular organic peroxides (Srinivasa *et al.*, 2012). More than a 5-fold increase in transcript level was observed in *C. parapsilosis* after 30 min of co-incubation with *P. aurantium*. This upregulation further increased up to 9-fold after another 30 min of co-incubation with the predator but remained unaffected in response to primary macrophages (Fig. 4D).

Table 2: Expression of *C. parapsilosis* genes involved in response to oxidative stress (GOID 6979)*

name	log2FC 30 min	log2FC 60 min	Description	Ortholog in *C. albicans*
CPAR2_805590	2.03	2.9	thioredoxin peroxidase activity and role in cell redox homeostasis, cellular response to oxidative stress, response to cadmium ion, sporocarp development involved in sexual reproduction	C7_02810W_A/PRX1
CPAR2_101390	2.16	2.84	NAD binding, nucleoside diphosphate kinase activity	C5_02890W_A/YNK1
CPAR2_802460	3.24	3.75	ribosomal large subunit binding, ribosomal small subunit binding activity and role in cellular response to oxidative stress, cytoplasmic translation	CR_00860C_A/TMA19
CPAR2_213080	-7.18	-Inf	Ortholog(s) have superoxide dismutase activity and role in cellular response to superoxide, evasion or tolerance by symbiont of host-produced reactive oxygen species	C2_00660C_A/SOD4
CPAR2_803850	-6.74	-6.14	Has domain(s) with predicted catalase activity, heme binding activity and role in oxidation-reduction process, response to oxidative stress	orf19.6229/CAT1
CPAR2_806310	-6.47	-5.89	ATPase activity, GTPase activity	C2_09220W_A/DDR48
CPAR2_500330	-5	-6.92	superoxide dismutase activity	orf19.2770.1/SOD1
CPAR2_808660	-4.59	-4.53	alditol:NADP+ 1-oxidoreductase activity and role in D-xylose catabolic process, arabinose catabolic process, cellular response to oxidative stress	C3_06860C_A
CPAR2_406810	-4.42	-4.59	role in cellular response to oxidative stress, pathogenesis and plasma membrane localization	C2_06870C_A/PST1
CPAR2_101680	-3.97	-5.25	nitric oxide dioxygenase activity, nitric oxide reductase activity	CR_07790C_A/YHB1
CPAR2_101350	-3.67	-2.87	D-xylose:NADP reductase activity, NADPH binding, mRNA binding activity	C5_02930C_A/GRE3
CPAR2_204330	-3.52	-3.07	ADP binding, ATP binding, ATPase activity, coupled, chaperone binding, misfolded protein binding, unfolded protein binding activity	CR_08250C_A/HSP104
CPAR2_806210	-3.41	-4.03	role in NADH oxidation, positive regulation of apoptotic process, regulation of reactive oxygen species metabolic process, response to singlet oxygen and mitochondrion, nucleus localization	C2_08100W_A
CPAR2_804600	-3.36	-3.12	Ortholog(s) have glutamate decarboxylase activity and role in cellular response to oxidative stress, glutamate catabolic process	C1_11660W_A/GAD1
CPAR2_406510	-3.35	-4.7	DNA-binding transcription factor activity, RNA polymerase II-specific, RNA polymerase II proximal promoter sequence-specific DNA binding activity	C2_07170C_A/AFT2
CPAR2_208070	-3.26	-2.69	superoxide dismutase copper chaperone activity and role in cellular copper ion homeostasis, cellular response to metal ion, protein maturation by copper ion transfer, removal of superoxide radicals	C1_07180W_A/CCS1
CPAR2_103080	-2.63	-2.89	glyoxalase III activity and role in cellular response to nutrient levels, cellular response to oxidative stress, methylglyoxal catabolic process to D-lactate via S-lactoyl-glutathione	C3_02610C_A/GLX3
CPAR2_209930	-2.54	-3.54	DNA-binding transcription factor activity, RNA polymerase II-specific activity	C2_05860C_A
CPAR2_109280	-2.51	-3.01	manganese ion binding, superoxide dismutase activity	C1_01520C_A/SOD2
CPAR2_808750	-2.47	-2.08	alditol:NADP+ 1-oxidoreductase activity, glycerol dehydrogenase [NAD(P)+] activity, mRNA binding activity	C3_07340W_A/GCY1
CPAR2_601800	-2.4	-1.84	cytochrome-b5 reductase activity, acting on NAD(P)H activity and role in cellular response to oxidative stress, ergosterol biosynthetic process	C6_02040W_A/MCR1
CPAR2_704130	-2.39	-2.77	role in cellular response to drug, cellular response to oxidative stress and filamentous growth of a population of unicellular organisms in response to biotic stimulus, more	C7_03220C_A/ZCF29
CPAR2_804070	-2.34	-3.4	DNA-binding transcription factor activity, RNA polymerase II-specific, RNA polymerase II regulatory region sequence-specific DNA binding activity	CR_00630W_A
CPAR2_105790	-2.28	-2.5	disulfide oxidoreductase activity, glutathione peroxidase activity, glutathione transferase activity and role in cellular response to oxidative stress, glutathione metabolic process, pathogenesis	C1_00490C_A/TTR1
CPAR2_200560	-2.04	-2.15	S-(hydroxymethyl)glutathione dehydrogenase activity, alcohol dehydrogenase (NAD) activity, hydroxymethylfurfural reductase (NADH) activity	CR_10250C_A/FDH3
CPAR2_301730	-1.88	-2.27	DNA-binding transcription factor activity, RNA polymerase II-specific, proximal promoter sequence-specific DNA binding activity	C1_08940C_A/MSN4
CPAR2_500390	-1.75	-1.73	superoxide dismutase activity	C4_02320C_A/SOD1
CPAR2_204160	-1.72	-2.44	role in cellular response to oxidative stress, chromatin silencing at silent mating-type cassette, pathogenesis	CR_05390W_A/PST3
CPAR2_600070	-1.59	-1.73	actin filament binding, protein binding, bridging activity	C6_02730W_A/SAC6
CPAR2_102830	-1.37	-1.72	Ortholog(s) have cytochrome-c peroxidase activity, role in cellular response to reactive oxygen species and mitochondrial intermembrane space, mitochondrial membrane localization	C3_02480C_A/CCP1

*only genes with p <0.01 according to EdgeR are displayed

C. parapsilosis* is exposed to ROS during phagocytosis by *P. aurantium

The induction of genes involved in redox homeostasis prompted us to analyse whether this occurred as a direct response to ROS production by the amoeba. When co-incubating *C. parapsilosis* with *P. aurantium* in the presence of the superoxide ($O_2^{\bullet-}$) indicator dihydroethidium (DHE), an increase in red fluorescence of cultures was specific to the presence of amoebae and reached a maximum after 10 min of co-incubation (Fig. 5A). Fluorescence microscopy of single cells of *P. aurantium* using either DHE or the alternative ROS sensor CellROX®Deep Red further revealed that ROS production was locally specific to *P. aurantium* actively feeding on *C. parapsilosis* (Fig. 5B) suggesting that yeast cells are exposed to increased levels of ROS upon phagocytic processing in *P. aurantium*.
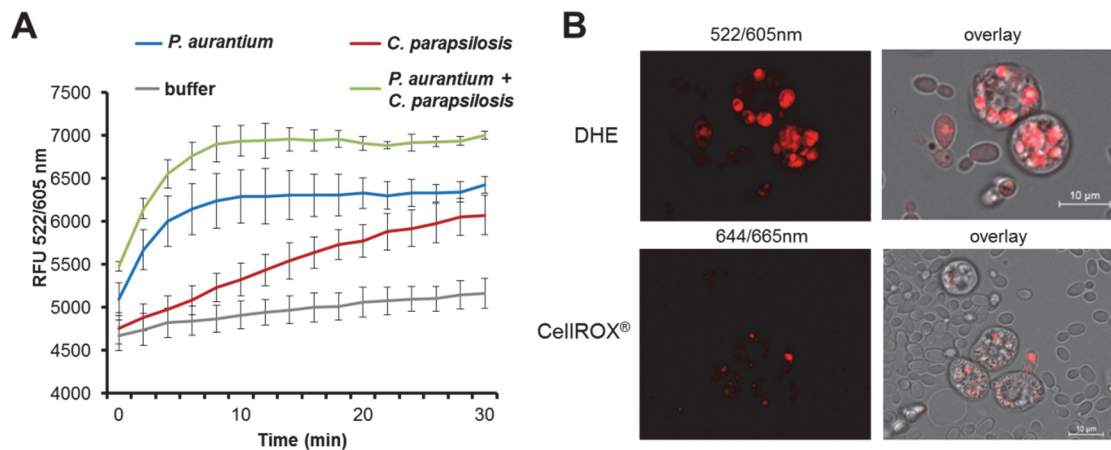
Fig. 5: ROS production by *P. aurantium* during phagocytosis of *C. parapsilosis*. A, ROS were determined indirectly as the increase in DHE oxidation over 30 min in co-incubations of *C. parapsilosis* with *P. aurantium*. Data represent mean RFU (λ_{ex} 522/ λ_{em} 605 nm) of three independent samples over 30 min. **B,** ROS production was primarily localized to feeding cells of *P. aurantium*. Cells were co-incubated with *C. parapsilosis* in the presence of ROS sensitive probes DHE or CellROX® Deep Red and images were taken after 30 min.

Copper and redox homeostasis contribute to the resistance against *P. aurantium* and macrophages

The expression profile and its similarity to its orthologue of *C. albicans* suggested a role for Crp1p of *C. parapsilosis* in detoxification of high Cu levels. Deleting Cp*CRP1* ($\Delta/\Delta crp1$) displayed no apparent growth defect in SD medium at 30°C and the mutant strain tolerated even high concentrations of Cu above 1 mM. Its sensitivity towards this transition metal changed dramatically when cells were exposed to a more acidic pH on solid or in liquid media (Fig. 6). At a pH of 3*,* Cp*CRP1* proved to be essential for

growth at Cu concentrations between 500 and 1000 µM, indicating that the function of Crp1p could be crucial under the acidic conditions of the phagolysosome.
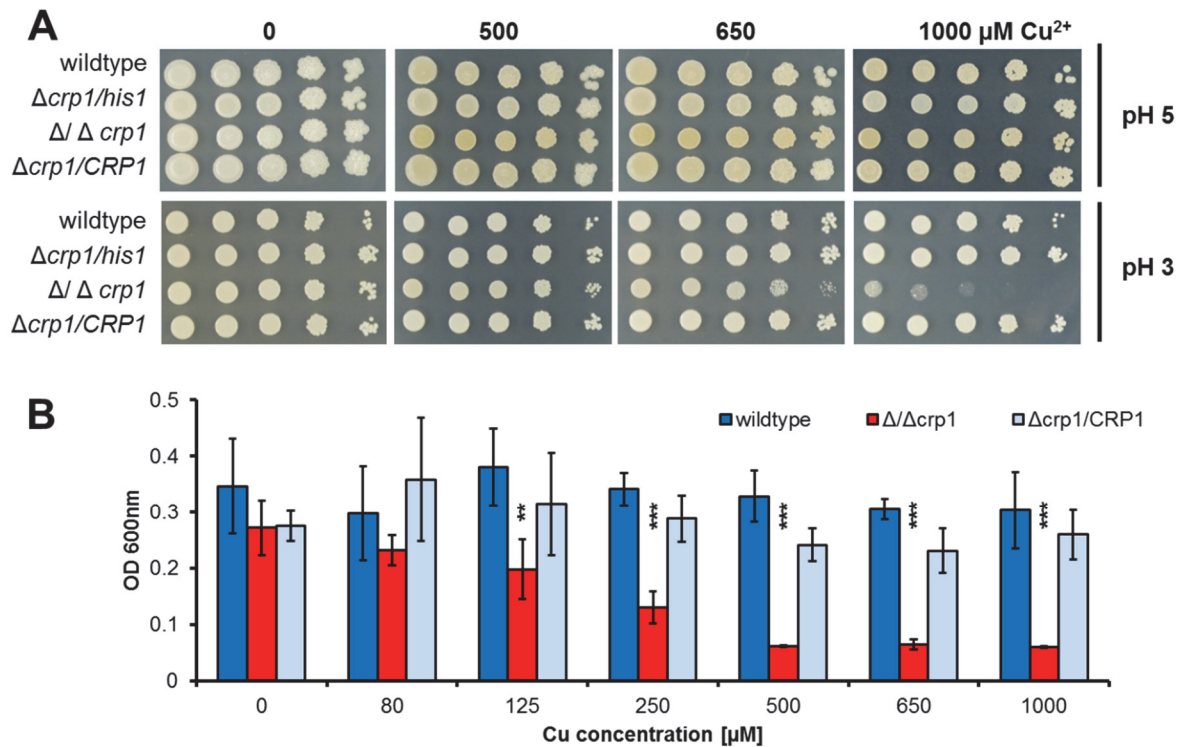
Fig. 6: Crp1 protects *C. parapsilosis* from high Cu levels at acidic pH. A, The Δ/Δ *crp1* mutant strain showed a pH-dependent copper sensitivity in comparison to the wildtype during growth at pH 3. **B,** Increased sensitivity of Δ/Δ *crp1* mutant strain to high Cu concentrations in liquid medium with malt extract broth (pH=3) in comparison to the wildtype and complementation strains. Data represent the mean and standard deviation of three biological replicates with asterisks indicating statistical significance in an unpaired Student's t-test between the values obtained for the Δ/Δ*crp1* strain and the wild type (∗∗∗, p < 0.001).

We also addressed the antioxidant function of *PRX1* in *C. parapsilosis*, by subjecting a homozygous mutant (*Δ/Δprx1*) to oxidative stress delivered by hydrogen peroxide (H_2O_2) and *tert*-butyl hydroperoxide (*t*-bOOH). The sensitivity of the mutant towards H_2O_2 was nearly indistinguishable from the wild type, and even the organic peroxide had only a mild effect on the growth of Δ*prx1* on a solid medium supplemented with adenine, uracil, and 9 amino acids (Fig. 7A). However, the impact of oxidative stress was more severe when these supplements were omitted from the medium. Under these conditions, growth in liquid medium was significantly reduced for *Δ/Δprx1* even in the absence of an external stressor (Fig. 7B). When using 11 selective dropouts with each one lacking a different component, we found that a lack of methionine was responsible for the growth defect of *Δ/Δprx1*. The Omission of methionine from the normal

medium, in combination with the organic peroxide, affected the wild type and the mutant strains to similar extents (Fig. 7C).
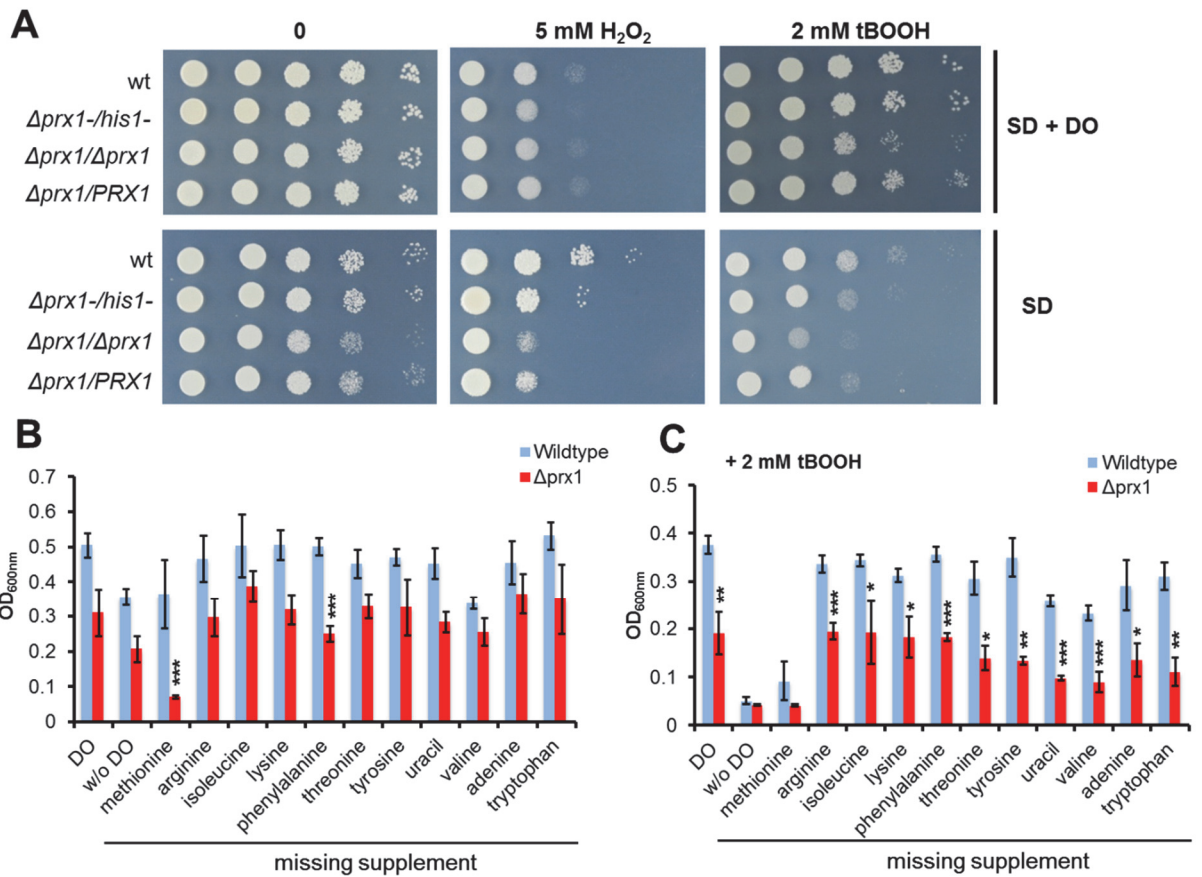
Fig. 7: The antioxidant role of *PRX1* in *C. parapsilosis*. A, Growth of *C. parapsilosis* on solid SD media with or without amino acid drop-out supplement (DO) in the presence of tBOOH or H_2O_2 as oxidative stressors. **B and C,** Growth of the wildtype and the $\Delta prx1$ null mutant in liquid SD media, supplemented with drop-out solutions, selectively missing one essential amino acid (B) and in the presence of tbOOH (C). Growth was measured as optical density at 600 nm. Data represent the mean and standard deviation of three biological replicates with asterisks indicating statistical significance in an unpaired Student's t-test between the values obtained for the $\Delta prx1$ null mutant in comparison to the parental strain, wt ($*p < 0.05$, $** p < 0.01$, $***p < 0.001$).

Both, *CRP1* and *PRX1*, are widely conserved across the *Candida* clade, including several species without any record as commensals or pathogens (Fig. S3). To test whether these two genes are part of the defence against amoeba predation, deletion mutants for *CRP1* and *PRX1* were confronted with *P. aurantium.* Both mutants showed decreased survival in comparison to the wild type after 3 hours of co-incubation (Fig. 8A). As we hypothesized that both mechanisms for stress defence could also contribute to survival when encountering innate immunity, we performed another co-incubation assay with primary macrophages (MDMs) from healthy donors. Both, *Δ/Δcrp1* and

Δ/Δprx1 displayed reduced survival when confronted with MDMs (Fig. 8B), indicating that these genes mediating resistance to copper and oxidative stress during predation could also play a role during evasion in the human host.
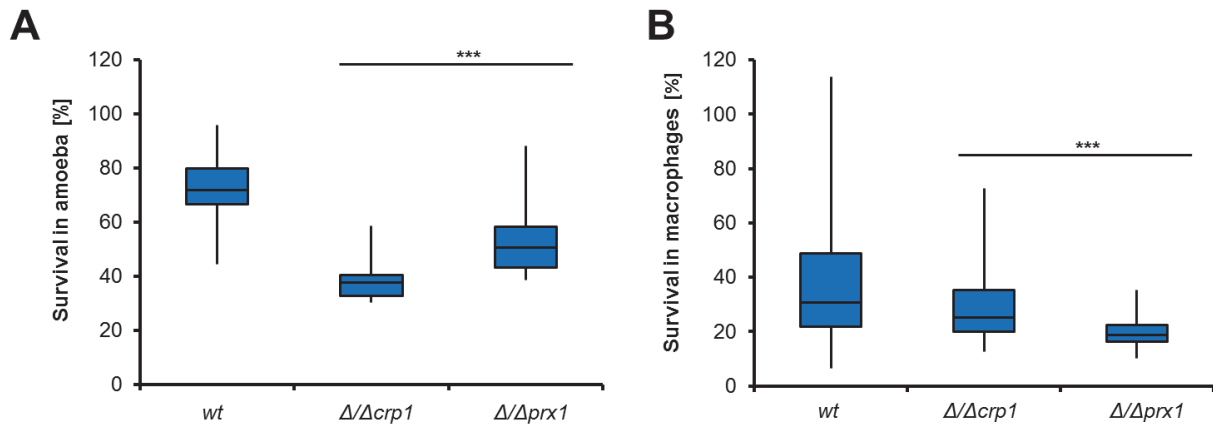
Fig. 8: Survival of *C. parapsilosis* mutant strains during amoeba predation (A) and phagocytosis by primary macrophages (B). Strains of *C. parapsilosis* were incubated with *P. aurantium* for 3 h at a yeast-to-amoeba ratio of 10:1 (A) or with primary macrophages isolated from at least 6 different anonymous donors at a yeast-to-macrophage ratio of 1:1 (B). The number of survivors was determined by plating the cells on YPD media and counting the CFUs. The boxes signify the 25th and 75th percentile. The median is represented by a short black line within the box for each strain. The whiskers indicate the highest and lowest values from three independent biological and six technical replicates. Asterisks show statistical significance in an unpaired Student's t-test between the values obtained for the null mutants in comparison to the parental strain, wt (∗∗∗, p<0.001).

Discussion

The arms race between phagocytic predators and their microbial prey is thought to have shaped virulence determinants of bacteria and fungi (Casadevall et al., 2019, Brussow, 2007). Amoebae are predominant environmental micro-predators, but only a few of them have been described to actively feed on fungi (Old & Darbyshire, 1978, Old, 1977, Chakraborty *et al.*, 1983). Such a fungivorous lifestyle was also described for *Protostelium mycophagum*, the type species for the polyphyletic group of protosteloid amoebae that form microscopic, stalked fruiting bodies from single cells and are found on nearly all continents (Spiegel *et al.*, 2017, Kang *et al.*, 2017, Shadwick *et al.*, 2009b, Shadwick *et al.*, 2018). We have recently isolated and characterized a strain of *P. aurantium* (formerly known as *Planoprotostelium aurantium*), which was found to selectively recognize, kill and feed on a wide range of ascomycete and basidiomycete yeasts, including major human pathogens of the *Candida* clade (Radosa et al., 2019). While *C. parapsilosis* acted as a preferred food source, *C. albicans* was found to be protected from initial recognition by an extensive coat of mannoproteins, and *C. glabrata* showed delayed processing after ingestion. A similar survival strategy seems to rescue *C. glabrata* when encountering macrophages. Here, its ability to persist and even replicate inside the phagocyte has been well documented and characterized to the level of single genes (Seider *et al.*, 2011, Kasper et al., 2015, Kaur *et al.*, 2007). A functional genomic approach identified 23 genes in *C. glabrata* which were critically involved in the survival of macrophage phagocytosis (Seider *et al.*, 2014). When comparing this set of 23 genes to all genes expressed during predation by *P. aurantium*, we found 7 genes to be highly upregulated ($\log_2$FC >1.5) at both time points. The three most upregulated genes with a $\log_2$FC of more than 2 were *GNT1* (CAGL0I09922g) *OST6* (CAGL0G07040g), and *PMT2* (CAGL0J08734g), all involved either in cell wall modification or protein glycosylation.

All these genes share orthologues with the other two *Candida* species, but when confronted with *P. aurantium*, only *PMT2* was upregulated in *C. parapsilosis* and even more so in *C. albicans*. In the latter, the gene encodes an essential protein O-mannosyltransferase, which renders the cell more resistant to antifungals and cell wall perturbing agents (Lengeler *et al.*, 2007, Peltroche-Llacsahuanga *et al.*, 2006). The upregulation of mannan synthesis in *C. albicans* in the presence of the predator seems not to be limited to O-linked mannans, but was also observed for the N-linked type. *MNN2* and *MNN22* are two members of another well-characterized family of N-

mannosyltranferses which absence severely affects the mannoprotein coat of *C. albicans* (Hall *et al.*, 2013, Hall & Gow, 2013). Both genes showed induction levels comparable to *PMT2*. The pivotal role of the mannan coat of *C. albicans* during an interaction with phagocytes of the innate immunity is well documented, as defective O- and N-linked mannosylation led to an increased uptake and phagosomal maturation, most likely through unmasking of β-glucans and enhanced recognition of *C. albicans* *via* the Dectin-1 receptor (Bain *et al.*, 2014, McKenzie *et al.*, 2010). The fact that mannan biosynthesis was upregulated in *C. albicans* supports the previous finding that mannosidase treated cells were internalized more frequently by *P. aurantium* (Radosa et al., 2019).

The different interaction patterns of the three yeasts were partially reflected throughout the transcriptome of their orthologous genes. The general response to the predator comprised only 79 orthologues. Of these 48 were commonly induced, among them the orthologues of CDC54, CDC46, and MCM3, indicating that all three yeast species were metabolically active in the M/G1 phase of the cell cycle (Cote *et al.*, 2009). Genes involved in fatty acid catabolism were generally induced while their biosynthesis was rather repressed. In contrast, amino acid biosynthesis was commonly upregulated, presumably in response to the nutrient-deprived growth medium used during the confrontation.

Of over 1500 orthologous genes that were differentially regulated in either *C. albicans* or *C. parapsilosis*, only 251 were common DEOs for both species. Within this gene set, the impact on copper homeostatic genes was preeminent especially for *C. parapsilosis* and the null mutant for *CRP1*, the gene with the highest induction, pointed towards a vital role of copper during predation by *P. aurantium*. Intoxication by copper is especially effective in highly acidic environments as occurring during early maturation of the phagolysosome. This strategy was also found to be effective in the bacteriovorous amoeba *Dictyostelium discoideum* and has most likely contributed to the spread of copper resistance islands among bacterial pathogens (Hao *et al.*, 2016). From this perspective, it cannot be surprising that highly tuned copper homeostatic systems were elucidated in the major environmentally acquired fungal pathogens *A. fumigatus* and *Cryptococcus neoformans* (Ding *et al.*, 2013, Wiemann *et al.*, 2017). Both fungi also exploit similar escape strategies when confronted with amoebae or innate immune phagocytes (Hillmann et al., 2015, Novohradska *et al.*, 2017, Steenbergen et al., 2001).

A recent screening approach identified SUR7 as a Cu-protective protein which reduces membrane permeability to Cu in *C. albicans* (Douglas & Konopka, 2019). Although downregulation of *SUR7* was observed at both time points after confrontation with the amoeba, its putative orthologue (CPAR2_602600) showed higher expression in *C. parapsilosis* after one hour of co-incubation with *P. aurantium*. Also, for *C. glabrata* which seems to lack a *CRP1* orthologue, *SUR7* (CAGL0L01551g) was highly induced at both time-points.

At least some of the toxic effects of Cu are inflicted via Fenton-type chemistry with ROS, which were actively produced in feeding *P. aurantium.* Their impact on the yeast will likely be further aggravated by the downregulation of nearly all SODs, as seen for *C. parapsilosis* during confrontation with the predator. In contrast, expression of the one-cysteine peroxiredoxin *PRX1* was increased in *C. parapsilosis*. Higher expression of the orthologous gene from *C. albicans* was also found during co-incubation with macrophages (Lorenz *et al.*, 2004). We found that an essential cellular function of *PRX1* is tightly linked to a lack of methionine. Intriguingly, among the only 48 commonly upregulated genes in all three *Candida* species, 5 are involved in the metabolism of sulfur-containing amino acids (ECM17, MET15, MET16, MET3, SAM2). For all five genes, the induction was lowest for *C. glabrata*. Amino acid deprivation, and more specifically, a limitation in methionine, also occurs in the phagolysosome of neutrophilic granulocytes (Rubin-Bejerano *et al.*, 2003, Miramón *et al.*, 2012). Its sensitivity to ROS is phenotypically well established for baker's yeast, as mutants lacking either SOD1 or its chaperone CCS1 were unable to grow in normoxic environments due to a methionine auxotrophic phenotype (Chang & Kosman, 1990, Culotta *et al.*, 1997).

In conclusion, our results show that the fungivorous feeding of the predator *P. aurantium* affects essential biosynthetic pathways by targeting the fungal Cu and redox homeostasis. With regard to the millions of years of coevolution of amoebae and fungi, it is well conceivable that basic molecular tool-kits for resistance against environmental phagocytes were later expanded for survival in other hosts.

Material and Methods

Strains and growth conditions

Protostelium aurantium var. fungivorum has been isolated in Jena, Germany, as described in (Hillmann et al., 2018). Isolated amoebae were further grown in standard size Petri dishes (94x16 mm, Greiner Bio-One, Austria) in PBS (80 g l^{-1} NaCl, 2 g l^{-1} KCl, 26.8 g l^{-1} Na_2HPO_4 x 7 H_2O, 2.4 g l^{-1} KH_2PO_4, pH 6.6) with *Rhodotorula mucilaginosa* as a food source at 22°C, if not stated differently. All yeast strains are listed in Table S3. If not indicated otherwise, all fungi were grown in YPD medium at 30°C, supplemented with 1.5 % [w/v] agar for growth on solid media. Mutant strains of *C. parapsilosis* were grown on the SD-agar (0.4 % [w/v] yeast nitrogen base with ammonium sulfate, 2 % [w/v] glucose, 1.5 % [w/v] agar), supplemented with 10 % [v/v] of a selective drop-out solution excluding leucine or histidine. Complemented strains were grown on YPD agar supplemented with 100 µg/ml nourseothricin (clonNAT, Werner BioAgents, Jena, Germany).

RNA isolations from yeast cells and co-cultures with *P. aurantium*

Frozen cell pellets from yeast cultures or co-incubations with *P. aurantium* were resuspended in TES buffer (10 mM Tris-HCl, pH 7.5, 10 mM EDTA, 0.5% [w/v] SDS) and transferred into a chilled tube containing zirconia beads (ZYMO Research, Irvine, CA, USA). Primary extractions of RNA were performed with acidic phenol:chloroform (5:1) shaking at 1500 rpm at 65°C for 30 min in a thermoblock. Afterwards, samples were frozen at -80°C for 30 min, centrifuged at 10.000 g for 15 min for phase separation. Samples underwent two more extractions using phenol:chloroform (5:1) and chloroform:isoamyl alcohol (24:1). The RNA was equilibrated with 10% [w/v] of 3 M sodium acetate (pH 5.2) and precipitated in ice-cold ethanol. After centrifugation, pellets were washed in 70 % [v/v] ethanol, air dried and resuspended in nuclease-free water. RNA samples were stored at -80°C.

RNA isolations from yeast cells after confrontation with monocyte-derived macrophages (MDMs)

Adherent macrophages with attached and ingested yeast cells were washed and subsequently lysed by adding RLT lysis buffer containing β-mercaptoethanol (Qiagen, Hilden, Germany) and shock-freezing the plate in liquid nitrogen. Cells were detached

by scraping and transferred into screw cap tube, sedimented by centrifugation and washed once with RLT buffer to remove most of the host RNA. Yeast pellets were shock-frozen again in liquid nitrogen and stored at -80°C. For RNA isolation, pellets were resuspended in 400 µl of AE buffer (50 mM Na-acetate pH 5.3 and 10 mM EDTA) and 40 µl of 10% [w/v] SDS. After mixing for 30 sec, cells were extracted with phenol: chloroform: isoamyl alcohol [25:24:1] for 5 min at 65°C and then frozen at -80°C. Phase separations, precipitation and resuspension of the purified RNA were performed as above.

RNA sequencing and analysis of expression data

The preparation of cDNA libraries from total RNA and the sequencing was performed at LGC Genomics GmbH (Berlin, Germany). Briefly, the quality of RNA samples was first controlled using 2100 Bioanalyzer (Agilent, CA, USA). Next, samples were enriched for mRNA using oligo-dT binding and magnetic separation using the NEBNext Poly(A) Magnetic Isolation Module (New England Biolabs). Samples were reverse transcribed using the NEBNext RNA First and Second Strand Synthesis Modules (New England Biolabs) and purified. The Encore Rapid DR Multiplex system (Nugen) was used for preparation cDNA-libraries which were amplified in a volume of 100 µl for 15 cycles using MyTaq (Bioline) and standard Illumina primers. From these libraries, 2 x 75 bp (*C. parapsilosis*) or 2x 150 bp (*C. albicans* and *C. glabrata*) paired-end reads were sequenced on an Illumina MiSeq platform. FastQC (Andrew, 2010) and Trimmomatic v0.32 (Bolger *et al.*, 2014) were used for quality control and trimming of library adaptors. Mapping of reads was achieved with TopHat2 v2.1.0 (Kim *et al.*, 2013) against the reference genomes of *C. parapsilosis*, *C. glabrata* and *C. albicans,* in combination with the genome of *P. aurantium*. Differential gene expression between time points was analysed with DEseq2 (Love *et al.*, 2014) and EdgeR (Robinson *et al.*, 2010). A list of all differentially expressed genes is provided as Dataset S1. All sequencing data is available from the GEO repository under the accession number GSE116535. The Venn diagram was computed using the package "VennDiagram" from the statistical programming language R. The genes in all areas of the Venn diagram are listed in supplementary dataset III. The PCA was conducted using the method "prcomp" from the "stats" package of R.

Gene ontology analysis

Gene ontology (GO) clustering analysis was performed on all differentially up- and downregulated genes of three *Candida* species using GO Slim (Mi *et al.*, 2017) -Mapper tool available at the Candida Genome Database (http://www.candidagenome.org/cgi-bin/GO/goTermMapper) for biological process, molecular function and cellular component. All data from the Gene Ontology analysis is provided as Dataset S2.

Quantitative real-time reverse transcription-PCR (qRT-PCR)

For all qRT-PCR reactions, RNA concentration was determined via NanoDrop ND1000 Spectrophotometer (NanoDrop Technologies Inc., USA). 1 µg of RNA was treated with DNase using RQ1 RNase-free DNase (Promega, USA) and transcribed into cDNA (RevertAid First Strand cDNA Synthesis Kit, Thermo Scientific). The cDNA was diluted 1:10 and used for qRT-PCR that included SYBR Select Master Mix (Applied Biosystems). The experiments were performed in a thermal cycler (Step One Plus, Applied Biosystems), in three biological and three technical replicates. The expression rates reported here are relative to the expression values of the housekeeping gene *ACT1* of *C. parapsilosis*. All primers are listed in Table S4.

Detection of reactive oxygen species

The production of reactive oxygen species during amoeba predation was measured using dihydroethidium (DHE; Thermofisher, Dreieich, Germany) at a final concentration of 10 µM. Amoebae and yeasts were seeded at the MOI of 10. Increased fluorescence, indicating ROS production, was measured using an Infinite M200 Pro fluorescence plate reader (Tecan, Männedorf, Switzerland) in intervals of 2 min over 30 min period at λ_{ex} 522 nm/λ_{em} 605 nm. ROS production was further visualized by using DHE staining as mentioned above or CellROX®Deep Red staining (Thermofisher) at a final concentration of 5 µM. Fluorescence images were captured using the Zeiss Axio Observer 7 Spinning Disk Confocal Microscope (Zeiss, Germany) at the λ_{ex} 370 nm/λ_{em} 420 nm (for non-oxidized DHE), λ_{ex} 535 nm/λ_{em} 610 nm (for oxidized DHE), and at λ_{ex} 640 nm/λ_{em} 665 nm for Cell Rox Deep Red staining.

Construction of gene deletions and complementations in *C. parapsilosis*

Target genes were deleted from the *leu2⁻/his1⁻* CLIB2014 parental strain using a fusion PCR method described previously (Noble & Johnson, 2005) and adapted to *C. parapsilosis* (Holland et al., 2014). All primer sequences and target genes are listed in Table S4. Briefly, approximately 500 bp of the upstream and downstream DNA loci of

the coding sequence were amplified by PCR with the primer pairs P1/P3 and P4/P6, respectively. The selectable markers, *C. dubliniensis HIS1* and *C. maltosa LEU2* genes were amplified with the P2/P5 primer pair from the plasmids pSN52 and pSN40, respectively. All PCR products were further purified using Gel/PCR DNA Fragments Extraction Kit (Geneaid Biotech, New Taipei City, Taiwan) and connected via PCR through overlapping sequences of the P2/P3 and P4/P5 primer pairs. The entire deletion cassette was amplified using primers P1 and P6 and transformed into the recipient strain in two rounds of transformation. The first allele was replaced by the *Cm*LEU2 marker and the second allele with the *Cd*HIS1 marker. Site-specific integration of the selection marker was checked by PCR at both ends of the deletion constructs. Loss of expression was also confirmed by qRT-PCR targeting the respective ORF (Supplementary Fig. S4A-D).

To generate reintegrant strains, the neutral locus NEUT5L was targeted as described in (Gerami-Nejad *et al.*, 2013). The promoter-OR-terminator regions were amplified from the CLIB214 parental strain using specific rec_F/R primers listed in Table S4. The dominant nourseothricin resistance marker *NAT1*, and a modified sequence of *C. parapsilosis* NEUT5L locus, were amplified from plasmid pDEST_TDH3_NAT_CpNEUT5L_NheI using Clon_F/Clon_R primers. The 5' tails of *gene name*_rec_F/*gene name*_rec_R primers contained flanking regions complementary to the sequence of Clon_F/Clon_R primers to allow fusion via circular polymerase extension cloning (CPEC cloning). The completely assembled plasmids (Supplementary Fig. S4E) were directly used for transformation of *E. coli* DH5α without further purification. After purification from *E. coli* up to 3 µg of plasmid were enzymatically digested with StuI or HpaI and EcoRI to confirm their correct size. The modified sequence of *C. parapsilosis* NEUT5L locus contains a specific restriction site for StuI which linearised the plasmid and enables the integration of the vector into the NEUT5L locus of *C. parapsilosis* via duplication. Integration of the vector into the genome of the parental strain was confirmed by PCR.

Chemical transformation of *C. parapsilosis*

Overnight culture of *C. parapsilosis leu2-/his1-* were diluted to an OD_{600} of 0.2 in YPD media and grown at 30°C/180 rpm to an OD_{600} of 1. The culture was harvested by centrifugation at 4000 g for 5 min and the pellet was suspended in 3 ml of ice-cold water. After collecting the cells, the pellet was resuspended in 1 ml of TE with LiAc

(0.1 M Lithium acetate, 10 mM Tris-HCl, 1 mM EDTA, pH 7.5), followed by centrifugation for 30 s at 14,000 g. Cells were then suspended in 200 µl of the ice-cold TE-LiAc buffer. For transformation 10 µl of boiled herring sperm DNA (2 mg/ml), 20 µl of transforming DNA were added to 100 µl of competent cells. The mixture was incubated at 30°C without shaking for 30 min followed by the addition of 700 µl of PLATE solution (0,1 M Lithium acetate, 10 mM Tris-HCl, 1 mM EDTA, pH = 7,5 and 40 % PEG 3350). Afterwards, the samples were incubated overnight at 30°C. The next day, samples were heat-shocked at 44°C for 15 min, centrifuged and washed twice with YPD medium. Following incubation in 100 µl of YPD for 2 hours (180 rpm, 30°C), samples were plated on SD agar plates, supplemented with essential amino acids, and histidine or leucine to obtain heterozygous mutant strains. To select for homozygous mutant histidine and leucine were omitted from the medium. Selective plates were incubated for two days at 30°C. To select for reintegrants, cells were plated on YPD agar with 100 µg ml^{-1} of nourseothricin.

Sensitivity assays

Yeasts were grown overnight in YPD at 30°C/180 rpm, harvested by centrifugation at 10,000 g for 1 min and washed twice with PBS. For droplet assays, cells were diluted to the concentration of 5×10^7 ml^{-1} and 5 µl of serial 10-fold dilutions were dropped on agar plates. To determine the MIC$_{50}$ of Cu, 2.5×10^4 cells were seeded in a 96 well plate with malt extract broth buffered to pH 3 and CuSO$_4$. For oxidative stress sensitivity assays, 11 selective drop-out solutions, each missing one component, were added to SD base (0.4 % yeast nitrogen base with ammonium sulfate, 2 % glucose) with or without 2 mM of t-BOOH (Luperox® TBH70X, Sigma-Aldrich, USA) and approx. 3×10^2 cells were seeded in 48 well plates. All plates were incubated at 30°C for two days. Growth in well plates was evaluated by measuring the optical density (OD$_{600}$) in a plate reader (Infinite M200 Pro, Tecan, Männedorf, Switzerland). Data represent the average of 3 biological replicates.

Isolation of monocyte-derive macrophages (MDMs)

Human peripheral blood mononuclear cells (PBMCs) were isolated by density centrifugation. PBMCs from buffy coats donated by healthy volunteers were separated through Lymphocytes Separation Media (Capricorn Scientific, Ebersdorfergrund, Germany) in Leucosep™ centrifuge tubes (Greiner Bio-One). Magnetically labelled

CD14 positive monocytes were selected by automated cell sorting (autoMACs; Miltenyi Biotec, Bergisch-Gladbach, Germany). To differentiate monocytes into MDMs, 1.7×10^7 cells were seeded into 175 cm² cell culture flasks in RPMI 1640 media with L-glutamine (Thermo Fisher Scientific) containing 10 % heat-inactivated fetal bovine serum (FBS; Bio&SELL, Feucht, Germany) and 50 ng ml^{-1} recombinant human M-CSF (ImmunoTools, Friesoythe, Germany) and incubated for five days at 37 °C and 5 % CO_2 until the medium was exchanged. Stimulation with human M-CSF favours the differentiation to M2-type macrophages. After two additional days, adherent MDMs were detached with 50 mM EDTA in PBS and seeded in 6-well plates (for expression analysis) or in 96-well plates (for killing assay) to a final concentration of 1×10^6 or 4×10^4 MDMs/well, respectively in RPMI complete and incubated overnight. Macrophage infection experiments were performed in serum-free RPMI medium.

Ethics statement

Blood donations for subsequent isolation of PBMCs were obtained from healthy donors after written informed consent. This is in accordance with the Declaration of Helsinki, all protocols were approved by the Ethics Committee of the University Hospital Jena (permission number *2207-01/08*).

Co-incubation of *C. parapsilosis* with monocyte-derived macrophages (MDMs)

Overnight cultures of yeast cells were harvested by centrifugation at 5 000 rpm/4°C for 5 min and cells were washed three times in ice-cold H_2O. Cells were counted in a Neubauer-improved cell counting chamber and added to macrophages in 96-well plates at an MOI of 1 (killing assays) or in 6-well plates at an MOI of 10 (isolation of total RNA) with RPMI medium. Media control wells for each time point were included, where the yeast cells were incubated in RPMI alone without the macrophages. Plates were incubated at 37°C in atmosphere 5% CO_2.

***P. aurantium* and macrophage killing assays**

Yeast strains were grown overnight in YPD medium at 30°C/180 rpm, harvested by centrifugation and counted in CASY® TT Cell Counter (OLS Bio, Bremen, Germany). Amoebae were grown to confluency in PB, harvested by scraping and counted. Yeast cells were co-incubated with amoebae or macrophages in 96-well plates at MOIs of 10 and 1, respectively, and incubated at 22°C or 37°C/5% CO_2, respectively, for 3 hours. Yeast cells surviving the amoeba predation were collected by vigorous pipetting and

plated on YPD agar. Cells surviving the macrophage killing were first collected from the supernatant, then, intracellular survivors were obtained after lysis of macrophages with 0.5% Triton-X-100 for 15 min. The number of survived yeast cells was calculated as a percentage of CFUs compared to the inoculum. Data are based on three biological and six technical replicates (*P. aurantium*) and six different anonymous donors with 6 technical replicates (macrophages), respectively.

Author contributions

SR performed most experimental work with input from JLS, RT, and MS. FH, AG, SB and GP supervised the experimental work. Bioinformatic processing and analysis of RNA-Seq data was performed by JL and TW. SR and FH wrote the paper. All authors analysed the data and commented on the manuscript.

Declaration of Interests

The authors declare no competing interests.

References

Aguilar, M., C. Lado & F. W. Spiegel, (2007) Protostelids from deciduous forests: first data from southwestern Europe. *Mycological research* **111**: 863-872.

Andrew, S., (2010) FastQC: a quality control tool for high throughput sequence data. Available online at: http://www.bioinformatics.babraham.ac.uk/projects/fastqc. In., pp.

Bain, J. M., J. Louw, L. E. Lewis, B. Okai, C. A. Walls, E. R. Ballou, L. A. Walker, D. Reid, C. A. Munro, A. J. Brown, G. D. Brown, N. A. Gow & L. P. Erwig, (2014) Candida albicans hypha formation and mannan masking of beta-glucan inhibit macrophage phagosome maturation. *MBio* **5**: 01874-01814.

Bensasson, D., J. Dicks, J. M. Ludwig, C. J. Bond, A. Elliston, I. N. Roberts & S. A. James, (2018) Diverse lineages of Candida albicans live on old oaks. *bioRxiv*.

Bochman, M. L. & A. Schwacha, (2009) The Mcm Complex: Unwinding the Mechanism of a Replicative Helicase. *Microbiology and Molecular Biology Reviews : MMBR* **73**: 652-683.

Bolger, A. M., M. Lohse & B. Usadel, (2014) Trimmomatic: a flexible trimmer for Illumina sequence data. *Bioinformatics* **30**: 2114-2120.

Brussow, H., (2007) Bacteria between protists and phages: from antipredation strategies to the evolution of pathogenicity. *Molecular microbiology* **65**: 583-589.

Casadevall, A., M. S. Fu, A. J. Guimaraes & P. Albuquerque, (2019) The 'Amoeboid Predator-Fungal Animal Virulence' Hypothesis. *J Fungi* **5**.

Chakraborty, S., K. M. Old & J. H. Warcup, (1983) Amoebae from a take-all suppressive soil which feed on Gaeumannomyces graminis tritici and other soil fungi. *Soil Biology and Biochemistry* **15**: 17-24.

Chang, E. C. & D. J. Kosman, (1990) O2-dependent methionine auxotrophy in Cu,Zn superoxide dismutase-deficient mutants of Saccharomyces cerevisiae. *J Bacteriol* **172**: 1840-1845.

Cote, P., H. Hogues & M. Whiteway, (2009) Transcriptional analysis of the Candida albicans cell cycle. *Mol Biol Cell* **20**: 3363-3373.

Culotta, V. C., L. W. Klomp, J. Strain, R. L. Casareno, B. Krems & J. D. Gitlin, (1997) The copper chaperone for superoxide dismutase. *J Biol Chem* **272**: 23469-23472.

Dadar, M., R. Tiwari, K. Karthik, S. Chakraborty, Y. Shahali & K. Dhama, (2018) Candida albicans - Biology, molecular characterization, pathogenicity, and advances in diagnosis and control - An update. *Microbial pathogenesis* **117**: 128-138.

Ding, C., R. A. Festa, Y.-L. Chen, A. Espart, Ò. Palacios, J. Espín, M. Capdevila, S. Atrian, J. Heitman & D. J. Thiele, (2013) Cryptococcus neoformans copper detoxification machinery is critical for fungal virulence. *Cell host & microbe* **13**: 265-276.

Douglas, L. M. & J. B. Konopka, (2019) Plasma membrane architecture protects Candida albicans from killing by copper. *PLoS Genet* **15**: e1007911-e1007911.

Erwig, L. P. & N. A. Gow, (2016) Interactions of fungal pathogens with phagocytes. *Nat Rev Microbiol* **14**: 163-176.

Gabaldon, T. & C. Fairhead, (2019) Genomes shed light on the secret life of Candida glabrata: not so asexual, not so commensal. *Curr Genet* **65**: 93-98.

Gabaldon, T., T. Martin, M. Marcet-Houben, P. Durrens, M. Bolotin-Fukuhara, O. Lespinet, S. Arnaise, S. Boisnard, G. Aguileta, R. Atanasova, C. Bouchier, A. Couloux, S. Creno, J. Almeida Cruz, H. Devillers, A. Enache-Angoulvant, J. Guitard, L. Jaouen, L. Ma, C. Marck, C. Neuveglise, E. Pelletier, A. Pinard, J. Poulain, J. Recoquillay, E. Westhof, P. Wincker, B. Dujon, C. Hennequin & C. Fairhead, (2013) Comparative genomics of emerging pathogens in the Candida glabrata clade. *BMC Genomics* **14**: 1471-2164.

Gerami-Nejad, M., L. F. Zacchi, M. McClellan, K. Matter & J. Berman, (2013) Shuttle vectors for facile gap repair cloning and integration into a neutral locus in Candida albicans. *Microbiology (Reading, England)* **159**: 565-579.

Greppi, A., Ł. Krych, A. Costantini, K. Rantsiou, D. J. Hounhouigan, N. Arneborg, L. Cocolin & L. Jespersen, (2015) Phytase-producing capacity of yeasts isolated from traditional African fermented food products and PHYPk gene expression of Pichia kudriavzevii strains. *International Journal of Food Microbiology* **205**: 81-89.

Hall, R. A., S. Bates, M. D. Lenardon, D. M. Maccallum, J. Wagener, D. W. Lowman, M. D. Kruppa, D. L. Williams, F. C. Odds, A. J. Brown & N. A. Gow, (2013) The Mnn2 mannosyltransferase family modulates mannoprotein fibril length, immune recognition and virulence of Candida albicans. *PLoS Pathog* **9**: 25.

Hall, R. A. & N. A. R. Gow, (2013) Mannosylation in Candida albicans: role in cell wall function and immune recognition. *Molecular microbiology* **90**: 1147-1161.

Hao, X., F. Luthje, R. Ronn, N. A. German, X. Li, F. Huang, J. Kisaka, D. Huffman, H. A. Alwathnani, Y. G. Zhu & C. Rensing, (2016) A role for copper in protozoan grazing - two billion years selecting for bacterial copper resistance. *Molecular microbiology* **102**: 628-641.

Hillmann, F., G. Forbes, S. Novohradska, I. Ferling, K. Riege, M. Groth, M. Westermann, M. Marz, T. Spaller, T. Winckler, P. Schaap & G. Glockner, (2018) Multiple Roots of Fruiting Body Formation in Amoebozoa. *Genome biology and evolution* **10**: 591-606.

Hillmann, F., S. Novohradska, D. J. Mattern, T. Forberger, T. Heinekamp, M. Westermann, T. Winckler & A. A. Brakhage, (2015) Virulence determinants of the human pathogenic fungus Aspergillus fumigatus protect against soil amoeba predation. *Environ Microbiol* **17**: 2858-2869.

Holland, L. M., M. S. Schroder, S. A. Turner, H. Taff, D. Andes, Z. Grozer, A. Gacser, L. Ames, K. Haynes, D. G. Higgins & G. Butler, (2014) Comparative phenotypic analysis of the major fungal pathogens Candida parapsilosis and Candida albicans. *PLoS Pathog* **10**: e1004365.

Kang, S., A. K. Tice, F. W. Spiegel, J. D. Silberman, T. Panek, I. Cepicka, M. Kostka, A. Kosakyan, D. M. C. Alcantara, A. J. Roger, L. L. Shadwick, A. Smirnov, A. Kudryavtsev, D. J. G. Lahr & M. W. Brown, (2017) Between a Pod and a Hard Test: The Deep Evolution of Amoebae. *Mol Biol Evol* **34**: 2258-2270.

Kasper, L., A. Konig, P. A. Koenig, M. S. Gresnigt, J. Westman, R. A. Drummond, M. S. Lionakis, O. Gross, J. Ruland, J. R. Naglik & B. Hube, (2018) The fungal peptide toxin Candidalysin activates the NLRP3 inflammasome and causes cytolysis in mononuclear phagocytes. *Nat Commun* **9**: 018-06607.

Kasper, L., K. Seider & B. Hube, (2015) Intracellular survival of Candida glabrata in macrophages: immune evasion and persistence. *FEMS yeast research* **15**: fov042.

Kaur, R., B. Ma & B. P. Cormack, (2007) A family of glycosylphosphatidylinositol-linked aspartyl proteases is required for virulence of Candida glabrata. *Proceedings of the National Academy of Sciences of the United States of America* **104**: 7628-7633.

Kim, D., G. Pertea, C. Trapnell, H. Pimentel, R. Kelley & S. L. Salzberg, (2013) TopHat2: accurate alignment of transcriptomes in the presence of insertions, deletions and gene fusions. *Genome Biology* **14**: R36.

Koller, B., C. Schramm, S. Siebert, J. Triebel, E. Deland, A. M. Pfefferkorn, V. Rickerts & S. Thewes, (2016) Dictyostelium discoideum as a Novel Host System to Study the Interaction between Phagocytes and Yeasts. *Frontiers in microbiology* **7**.

Lengeler, K. B., D. Tielker & J. F. Ernst, (2007) Protein-O-mannosyltransferases in virulence and development. *Cellular and Molecular Life Sciences* **65**: 528.

Linden, J. R., M. A. Maccani, S. S. Laforce-Nesbitt & J. M. Bliss, (2010) High Efficiency Opsonin-Independent Phagocytosis of Candida parapsilosis by Human Neutrophils. *Medical mycology : official publication of the International Society for Human and Animal Mycology* **48**: 10.1080/13693780903164566.

Lorenz, M. C., J. A. Bender & G. R. Fink, (2004) Transcriptional Response of Candida albicans upon Internalization by Macrophages. *Eukaryotic Cell* **3**: 1076-1087.

Love, M. I., W. Huber & S. Anders, (2014) Moderated estimation of fold change and dispersion for RNA-seq data with DESeq2. *Genome Biology* **15**: 550.

Maganti, H., D. Bartfai & J. Xu, (2012) Ecological structuring of yeasts associated with trees around Hamilton, Ontario, Canada. *FEMS yeast research* **12**: 9-19.

McKenzie, C. G., U. Koser, L. E. Lewis, J. M. Bain, H. M. Mora-Montes, R. N. Barker, N. A. Gow & L. P. Erwig, (2010) Contribution of Candida albicans cell wall components to recognition by and escape from murine macrophages. *Infect Immun* **78**: 1650-1658.

Mi, H., X. Huang, A. Muruganujan, H. Tang, C. Mills, D. Kang & P. D. Thomas, (2017) PANTHER version 11: expanded annotation data from Gene Ontology and Reactome pathways, and data analysis tool enhancements. *Nucleic Acids Res* **45**: D183-D189.

Miramón, P., C. Dunker, H. Windecker, I. M. Bohovych, A. J. P. Brown, O. Kurzai & B. Hube, (2012) Cellular Responses of Candida albicans to Phagocytosis and the Extracellular Activities of Neutrophils Are Critical to Counteract Carbohydrate Starvation, Oxidative and Nitrosative Stress. *PloS one* **7**: e52850.

Morrison-Whittle, P., S. A. Lee, B. Fedrizzi & M. R. Goddard, (2018) Co-evolution as Tool for Diversifying Flavor and Aroma Profiles of Wines. *Frontiers in microbiology* **9**.

Navarathna, D. H., M. S. Lionakis, M. J. Lizak, J. Munasinghe, K. W. Nickerson & D. D. Roberts, (2012) Urea amidolyase (DUR1,2) contributes to virulence and kidney pathogenesis of Candida albicans. *PloS one* **7**: e48475.

Ndiritu, G. G., S. L. Stephenson & F. W. Spiegel, (2009) First records and microhabitat assessment of protostelids in the Aberdare Region, Central Kenya. *The Journal of eukaryotic microbiology* **56**: 148-158.

Noble, S. M. & A. D. Johnson, (2005) Strains and strategies for large-scale gene deletion studies of the diploid human fungal pathogen Candida albicans. *Eukaryot Cell* **4**: 298-309.

Novohradska, S., I. Ferling & F. Hillmann, (2017) Exploring Virulence Determinants of Filamentous Fungal Pathogens through Interactions with Soil Amoebae. *Frontiers in cellular and infection microbiology* **7**: 497.

Old, K. M., (1977) Giant soil amoebae cause perforation of conidia of Cochliobolus sativus. *Transactions of the British Mycological Society* **68**: 277-281.

Old, K. M. & J. F. Darbyshire, (1978) Soil fungi as food for giant amoebae. *Soil Biology and Biochemistry* **10**: 93-100.

Peltroche-Llacsahuanga, H., S. Goyard, C. d'Enfert, S. K. Prill & J. F. Ernst, (2006) Protein O-mannosyltransferase isoforms regulate biofilm formation in Candida albicans. *Antimicrob Agents Chemother* **50**: 3488-3491.

Pesole, G., M. Lotti, L. Alberghina & C. Saccone, (1995) Evolutionary origin of nonuniversal CUGSer codon in some Candida species as inferred from a molecular phylogeny. *Genetics* **141**: 903-907.

Radosa, S., I. Ferling, J. L. Sprague, M. Westermann & F. Hillmann, (2019) The different morphologies of yeast and filamentous fungi trigger distinct killing and feeding mechanisms in a fungivorous amoeba. *Environ Microbiol* **13**: 1462-2920.

Robinson, H. A., A. Pinharanda & D. Bensasson, (2016) Summer temperature can predict the distribution of wild yeast populations. *Ecol Evol* **6**: 1236-1250.

Robinson, M. D., D. J. McCarthy & G. K. Smyth, (2010) edgeR: a Bioconductor package for differential expression analysis of digital gene expression data. *Bioinformatics* **26**: 139-140.

Rubin-Bejerano, I., I. Fraser, P. Grisafi & G. R. Fink, (2003) Phagocytosis by neutrophils induces an amino acid deprivation response in Saccharomyces cerevisiae and Candida albicans. *Proceedings of the National Academy of Sciences of the United States of America* **100**: 11007-11012.

Sasada, M. & R. B. Johnston, Jr., (1980) Macrophage microbicidal activity. Correlation between phagocytosis-associated oxidative metabolism and the killing of Candida by macrophages. *J Exp Med* **152**: 85-98.

Seider, K., S. Brunke, L. Schild, N. Jablonowski, D. Wilson, O. Majer, D. Barz, A. Haas, K. Kuchler, M. Schaller & B. Hube, (2011) The facultative intracellular pathogen Candida glabrata subverts macrophage cytokine production and phagolysosome maturation. *J Immunol* **187**: 3072-3086.

Seider, K., F. Gerwien, L. Kasper, S. Allert, S. Brunke, N. Jablonowski, T. Schwarzmuller, D. Barz, S. Rupp, K. Kuchler & B. Hube, (2014) Immune evasion, stress resistance, and efficient nutrient acquisition are crucial for intracellular survival of Candida glabrata within macrophages. *Eukaryot Cell* **13**: 170-183.

Seider, K., A. Heyken, A. Luttich, P. Miramon & B. Hube, (2010) Interaction of pathogenic yeasts with phagocytes: survival, persistence and escape. *Current opinion in microbiology* **13**: 392-400.

Shadwick, J. D., S. L. Stephenson & F. W. Spiegel, (2009a) Distribution and ecology of protostelids in Great Smoky Mountains National Park. *Mycologia* **101**: 320-328.

Shadwick, J. D. L., J. D. Silberman & F. W. Spiegel, (2018) Variation in the SSUrDNA of the Genus Protostelium Leads to a New Phylogenetic Understanding of the Genus and of the Species Concept for Protostelium mycophaga (Protosteliida, Amoebozoa). *The Journal of eukaryotic microbiology* **65**: 331-344.

Shadwick, L. L., F. W. Spiegel, J. D. L. Shadwick, M. W. Brown & J. D. Silberman, (2009b) Eumycetozoa = Amoebozoa?: SSUrDNA Phylogeny of Protosteloid Slime Molds and Its Significance for the Amoebozoan Supergroup. *PloS one* **4**: e6754.

Skrzypek, M. S., J. Binkley, G. Binkley, S. R. Miyasato, M. Simison & G. Sherlock, (2017) The Candida Genome Database (CGD): incorporation of Assembly 22, systematic identifiers and visualization of high throughput sequencing data. *Nucleic acids research* **45**: D592-D596.

Spiegel, F. W., L. L. Shadwick, G. G. Ndiritu, M. W. Brown, M. Aguilar & J. D. Shadwick, (2017) Protosteloid Amoebae (Protosteliida, Protosporangiida, Cavosteliida, Schizoplasmodiida, Fractoviteliida, and Sporocarpic Members of Vannellida, Centramoebida, and Pellitida). In: Handbook of the Protists. J. M. Archibald, A. G. B. Simpson, C. H. Slamovits, L. Margulis, M. Melkonian, D. J. Chapman & J. O. Corliss (eds). Cham: Springer International Publishing, pp. 1-38.

Srinivasa, K., N. R. Kim, J. Kim, M. Kim, J. Y. Bae, W. Jeong, W. Kim & W. Choi, (2012) Characterization of a putative thioredoxin peroxidase prx1 of Candida albicans. *Molecules and cells* **33**: 301-307.

Steenbergen, J. N., J. D. Nosanchuk, S. D. Malliaris & A. Casadevall, (2003) Cryptococcus neoformans virulence is enhanced after growth in the genetically malleable host Dictyostelium discoideum. *Infect Immun* **71**: 4862-4872.

Steenbergen, J. N., H. A. Shuman & A. Casadevall, (2001) Cryptococcus neoformans interactions with amoebae suggest an explanation for its virulence and intracellular pathogenic strategy in macrophages. *Proceedings of the National Academy of Sciences of the United States of America* **98**: 15245-15250.

Toth, R., A. Toth, C. Papp, F. Jankovics, C. Vagvolgyi, M. F. Alonso, J. M. Bain, L. P. Erwig & A. Gacser, (2014) Kinetic studies of Candida parapsilosis phagocytosis by macrophages and detection of intracellular survival mechanisms. *Frontiers in microbiology* **5**: 633.

Turner, S. A. & G. Butler, (2014) The Candida pathogenic species complex. *Cold Spring Harb Perspect Med* **4**.

Uwamahoro, N., J. Verma-Gaur, H.-H. Shen, Y. Qu, R. Lewis, J. Lu, K. Bambery, S. L. Masters, J. E. Vince, T. Naderer & A. Traven, (2014) The Pathogen Candida albicans Hijacks Pyroptosis for Escape from Macrophages. *mBio* **5**.

Van Waeyenberghe, L., J. Bare, F. Pasmans, M. Claeys, W. Bert, F. Haesebrouck, K. Houf & A. Martel, (2013) Interaction of Aspergillus fumigatus conidia with Acanthamoeba castellanii parallels macrophage-fungus interactions. *Environ Microbiol Rep* **5**: 819-824.

Weissman, Z., I. Berdicevsky, B. Z. Cavari & D. Kornitzer, (2000) The high copper tolerance of Candida albicans is mediated by a P-type ATPase. *Proceedings of the National Academy of Sciences of the United States of America* **97**: 3520-3525.

Wellington, M., K. Koselny, F. S. Sutterwala & D. J. Krysan, (2014) Candida albicans triggers NLRP3-mediated pyroptosis in macrophages. *Eukaryot Cell* **13**: 329-340.

Wiemann, P., A. Perevitsky, F. Y. Lim, Y. Shadkchan, B. P. Knox, J. A. Landero Figueora, T. Choera, M. Niu, A. J. Steinberger, M. Wuthrich, R. A. Idol, B. S. Klein, M. C. Dinauer, A. Huttenlocher, N. Osherov & N. P. Keller, (2017) Aspergillus fumigatus Copper Export Machinery and Reactive Oxygen Intermediate Defense Counter Host Copper-Mediated Oxidative Antimicrobial Offense. *Cell Rep* **19**: 1008-1021.

Zahn, G., S. L. Stephenson & F. W. Spiegel, (2014) Ecological distribution of protosteloid amoebae in New Zealand. *PeerJ* **2**: e296.

Complete supplemental material for this article can be found at:

https://www.biorxiv.org/content/10.1101/690503v2.supplementary-material

2.5 Manuscript V: Sprenger *et al.*, prepared for submission to FEMS Yeast Research

A *TRP1*-marker-based system for gene complementation, overexpression, reporter gene expression and gene modification in *Candida glabrata*

Marcel Sprenger, Sascha Brunke, Bernhard Hube, and Lydia Kasper

Summary:

The molecular Koch´s postulates define criteria that must be satisfied to show that a certain gene has a role during pathogenesis. This includes reintroduction of the gene of interest into the mutated organism. However, gene complementation strategies are only rarely used in the haploid yeast *C. glabrata* so far. Here we developed a new gene complementation strategy, expressing the selection marker *TRP1* at its native locus. In addition, we used our strategy to overexpress fluorescence markers, the antigen ovalbumin, or to overexpress and modify genes associated with the vitamin biotin in *C. glabrata*. The *TRP1* locus in *C. glabrata* is a suitable locus to reintegrate gene of interest, either with their native DNA sequence, with specific sequence variations or with alternative promotors, to investigate the role and function of these genes for fungal pathobiology.

Own contribution:

Marcel Sprenger planned, performed and evaluated all experiments, and interpreted the data. The co-authors assisted in the conceptualization of the study and editing of the initial manuscript. Marcel Sprenger wrote the manuscript and generated all figures.

Estimated authors' contributions:

Marcel Sprenger	**66%**
Sascha Brunke	12%
Bernhard Hube	4%
Lydia Kasper	18%

Prof. Bernhard Hube

A *TRP1*-marker-based system for gene complementation, overexpression, reporter gene expression and gene modification in *Candida glabrata*

Marcel Sprenger[1], Sascha Brunke[1], Bernhard Hube[1,2], and Lydia Kasper[1]

[1] Department Microbial Pathogenicity Mechanisms, Leibniz Institute for Natural Product Research and Infection Biology, Hans Knoell Institute, Jena, Germany.

[2] Institute of Microbiology, Friedrich Schiller University, Jena, Germany.

* Corresponding author

Email: lydia.kasper@leibniz-hki.de

Abstract

Although less prevalent than its relative *Candida albicans*, *Candida glabrata* is a successful human-pathogenic yeast, causing life threatening candidiasis. It is thus vital to understand the pathogenicity mechanisms and the contributing genes of *C. glabrata*. However, gene complementation as a tool to restore the function of a previously deleted gene is not standardized in *C. glabrata* and less frequently used as compared to *C. albicans*.

In this study, we established a gene complementation strategy using genomic integration at the *TRP1* locus. We prove that our approach can not only be used for integration of complementation cassettes but also for overexpression of fluorescence markers, the antigen ovalbumin or the putative biotin transporter gene *VHT1*. On the example of urea amidolyase Dur1,2 we show that the complementation cassettes can also be used to study the effects of sequence-modifications in genes. With this approach, we found that changes in the lysine-residue within the biotinylation motif of Dur1,2 impaired the usage of urea by *C. glabrata*. Taken together, the *TRP1*-based gene complementation approach is a valuable tool for investigating novel gene functions and for elucidating their role in pathobiology of *C. glabrata*.

Key words

Candida glabrata, *TRP1*, **gene complementation, overexpression, green fluorescent protein**

Introduction

The opportunistic pathogen *Candida glabrata* is a constitutively haploid fungus. It belongs to the Nakaseomyces clade (Kurtzman & Robnett, 2003) and is evolutionarily related to the baker's yeast *Saccharomyces cerevisiae* (Gabaldón & Carrete, 2016). *C. glabrata* is normally associated with the mammalian host and is the second most prevalent *Candida* species to cause life-threatening candidasis, after *Candida albicans* (Diekema *et al.*, 2012). It is therefore necessary to understand and characterize mechanisms and genes contributing to the pathogenicity of this fungus.

The molecular Koch´s postulates define criteria that must be satisfied to show that a certain gene has a role during pathogenesis (Falkow, 1988). One of these criteria states that gene reintegration into a mutated organism (complementation) should restore the pathogenic potential of the organism. Thus, complementation is an important step in elucidating gene functions and to exclude potential pleiotropic effects that originated from genetic manipulation. However, to date gene complementation strategies in *C. glabrata* are less well developed than *e.g.* in *C. albicans*, less frequently used, and each have certain disadvantages. The first strategy used for *C. glabrata* is based on extrachromosomal episomal replicative vectors (Kitada *et al.*, 1996, Frieman *et al.*, 2002, Zordan *et al.*, 2013), which contain the autonomously replicating sequence (ARS) and a centromere (CEN) together with the gene of interest (GOI). An example is the centromere-based plasmid pCgACT which contains the nutritional marker *TRP1* to restore prototrophy of a *trp1Δ* deletion mutant (Miyazaki *et al.*, 2011, Hosogaya *et al.*, 2013, Noble *et al.*, 2013). A strong disadvantage of episomal vectors is, however, the unforeseeable multimerizations or recombinations with the genome, causing unwanted genetic alterations (Pla *et al.*, 1996). Additionally, plasmid loss (for example in environments where tryptophan is readily available) or copy number variations could increase population heterogeneity.

A second strategy for the generation of *C. glabrata* complementation strains relies on genomic integration, either by reintroducing the original GOI together with specific

selection markers at its native locus (Yánez-Carrillo *et al.*, 2015) or by replacing the *URA3* gene by the GOI and the dominant *NAT1* marker (Nevitt & Thiele, 2011). Both these strategies have the potential to restore the gene of interest to a wild type-like state. The *NAT1* selection marker is, however, widely used for gene deletions in *C. glabrata* (Schwarzmüller *et al.*, 2014) and therefore often not available anymore for later gene complementation, and changes in *URA3* expression levels might influence virulence phenotypes (Brand *et al.*, 2004).

Gene complementation in the diploid *C. albicans* often uses the CIp10 strategy (Murad *et al.*, 2000)*,* whereby the selection marker *URA3* is ectopically expressed at one of alleles of the neutral *RPS1* locus. In contrast to *C. albicans*, the haploid genome of *C. glabrata* makes it more difficult to find suitable loci, since single-allele knock-outs and dosage effects of ectopic expression of nutritional selection markers cannot be compensated by an alternative allele, with unknown influences on the phenotype.

In this study we describe a novel gene complementation strategy for *C. glabrata* based on transformation with and stable genomic integration of a complementation cassette into the *TRP1* locus. We show that reintegration of *TRP1* at this native chromosomal location can restore tryptophan auxotrophy to wild type-like levels. This strategy can not only be used for gene complementation but also for reporter gene expression, gene overexpression, heterologous expression, or expression of genetically modified gene variants in the haploid yeast *C. glabrata*.

We validate the functionality of our complementation system by heterologous expression of fluorescence reporter genes or ovalbumin (OVA), by inducing point mutations in the urea amidolyase gene Dur1,2, and by overexpressing the biotin acquisition gene *VHT1* in *C. glabrata*. Artificial OVA expression by pathogens is frequently used as a tool to investigate the cross-reactivity between effector and memory T cells in response to the microbe (Ishizuka *et al.*, 2009, Krummey *et al.*, 2014, Harms *et al.*, 2018). Vitamins are involved in a broad range of cellular processes (Dakshinamurti, 2005, Combs, 2017). Biotin (vitamin H or B$_7$) is covalently linked to

several proteins, including enzymes involved in carboxylation reactions (Zempleni *et al.*, 2008). All target proteins possess a conserved lysine residue (Lane *et al.*, 1964), which is biotinylated by the biotin ligase Bpl1 *via* an amide bond (Sternicki *et al.*, 2017). Yeasts belonging to the *Candida* and *Saccharomyces* genus are biotin auxotrophs (McVeigh, 1951, Littman & Miwatani, 1963) due to intrinsic loss of biosynthetic genes (Fitzpatrick *et al.*, 2010, Madsen *et al.*, 2015) and have to take up biotin from the environment. *C. glabrata* and *C. albicans* strictly rely on the putative biotin importer Vht1 for biotin acquisition (Sprenger *et al.*, 2020).

Materials and methods

Ethics statement

Human blood was taken from healthy volunteers with written, informed consent. The blood donation protocol and use of blood for this study were approved by the institutional ethics committee of the university hospital Jena (Ethik-Kommission des Universitätsklinikums Jena, Permission No. 2207–01/08).

Strains and growth conditions

All strains used in this study are listed in **Table S1**. *Escherichia coli* was cultured in liquid lysogeny broth (LB) at 37°C with shaking at 180 rpm and with 50 µg/mL ampicillin for plasmid propagation. *Candida* strains were cultured in liquid Yeast Peptone Dextrose (YPD) broth (2% glucose, 2% peptone, 1% yeast extract) at 30°C (*C. albicans*) or 37°C (*C. glabrata*), with shaking at 180 rpm for 14-16 h. For growth on solid medium, 2% agar was added. Routinely, stationary phase yeast cells from pre-cultures were washed three times in PBS, and the cell number was adjusted in PBS or culture medium.

For growth analyses in liquid media, twenty microliters of a yeast cell suspension (5×10^6 cells/mL) were added to 180 µL media in a 96-well plate (Tissue Culture Test

Plate, TPP Techno Plastic Products AG). In some experiments minimal medium (0.19% yeast nitrogen base (YNB) without biotin, amino acids, ammonium sulfate [Formedium]; 2% glucose) with varying biotin concentrations and different nitrogen sources (0.5% ammonium sulfate, 0.5% urea) was used. The growth was monitored by measuring the absorbance at 600 nm every 30 min for 100 cycles at 30°C or 37°C using a microplate reader (Plate Reader infinite M200 PRO, Tecan Group GmbH) with orbital shaking (30 sec, amplitude: 6 mm, wait: 10 sec) before each measurement and multiple reads per well. All experiments were done in technical duplicates and, at least, biological triplicates. Growth of *Candida* on solid agar was tested by spotting serial dilutions (1×10^6 to 1×10^1) of yeast cells on YNB plates (0.19 % YNB without amino acids and biotin; 2% glucose and either 0.5% ammonium sulfate or 0.5% urea; 2% oxoid agar).

Construction of *VHT1* overexpression, OVA overexpression and fluorescently labelled strains

The prototrophic *trp1Δ* + *TRP1* strain was generated by reintroducing *TRP1* into the native *TRP1* locus, amplified from pTRP1 and replacing the FRT sequence in the *trp1Δ* strain. The *C. glabrata vhr1Δ* mutant was generated, as previously described (Sprenger *et al.*, 2020), in a *trp1Δ* strain background, with reintroduction of *TRP1* into the native *TRP1* locus. The overexpression constructs of the biotin transporter gene *VHT1*, the fluorescence markers yeGFP and mCherry, or ovalbumin (OVA) were integrated into the *TRP1* locus by selecting for tryptophan prototrophy. Briefly, plasmids pTRP1-*TEF1*prom-*yEGFP*, pTRP1-*PDC1*prom-*yEGFP*, pTRP1-*LYS21* prom-*yEGFP*, pTRP1-*TEF1*prom-*mCherry*, and pTRP1-*TEF1*prom-*OVA* listed in **Table S2**, were generated by PCR, via amplification of the coding sequences of yEGFP (from pCN-PDC1-GFP (Zordan *et al.*, 2013)), mCherry (from pYC56 (Yánez-Carrillo *et al.*, 2015)) and OVA (codon-optimized) together with the specific promotor and terminator sequences (*HIS3* terminator for yEGFP and *CTA1* terminator for mCherry) with primers, listed in **Table**

S3, with 15 bp overlap to the pTRP1 sequence. The generation of pTRP1 has been previously described in detail (Sprenger *et al.*, 2020). The plasmids pTRP1-*TEF1*prom-*VHT1*, pTRP1-*PDC1*prom-*VHT1*, and pTRP1-*LYS21*prom-*VHT1* were generated by PCR, amplifying the coding sequences of *VHT1* together with the native terminator sequence with primers overlapping 15 bp to the pTRP1 sequence.

All constructs were cloned by In-Fusion HD cloning system into *Xba*I-digested pTRP1, and the resulting plasmids were confirmed by PCR and sequencing. The cassettes were amplified by PCR, purified and used to transform a *trp1*Δ strain background to generate tryptophan prototrophic strains using the modified heat-shock method ((Sanglard *et al.*, 1996) with heat shock: 15 min at 45 °C). Resulting clones were selected on solid minimal medium. The correct integration into the *TRP1* locus was verified by PCR, and positive clones were analyzed for yEGFP and mCherry fluorescence by microscopy and FACS (only yEGFP).

Construction of *DUR1,2* deletion mutants

The *C. glabrata dur1,2*Δ mutant (CAGL0M05533gΔ) was generated in the *trp1*Δ parental strain using the deletion cassette amplified from an existing deletion mutant (Schwarzmüller *et al.*, 2014). Deletion constructs were amplified using P1 and P4 primers (**Table S2**) and purified with QIAquick® PCR purification kit (Qiagen). The transformation was done as described above.

For interspecies comparison, a *C. albicans dur1,2*Δ/Δ (C1_04660WΔ/Δ) mutant was generated by a standard gene disruption method (Wilson *et al.*, 1999) using lithium acetate transformation (Walther & Wendland, 2003). Briefly, the Arg-, His-, and Ura-auxotrophic parental strain BWP17 was sequentially transformed with 10 μg of PCR-amplified and purified *HIS1* and *ARG4* deletion cassettes, which were flanked by 100 bp of the target homology region, resulting in disruption of the open reading frames of both alleles of C1_04660W. The correct deletion of *DUR1,2* in *C. glabrata* and *C. albicans* was confirmed by PCR and Southern blot.

Construction of *DUR1,2* complementation strains

Plasmids pTRP1-*DUR1,2* and pTRP1-*DUR1,2*[K1798R] were generated by In-Fusion HD cloning of PCR-amplified *DUR1,2* wild-type allele (one fragment) together with the up- and downstream intergenic regions with primers with 15 bp overlap to the pTRP1 sequence. The mutated version was created by In-Fusion HD cloning using primers with the codon for arginine instead of lysine (two fragments). Constructs were cloned into *Xba*I-digested pTRP1 and resulting plasmids were confirmed by sequencing. Cassettes containing only *TRP1* or *TRP1-DUR1,2*[Wt] and *TRP1-DUR1,2*[K→R] were amplified by PCR, purified, and used to transform a *trp1Δdur1,2Δ* mutant background strain to generate tryptophan prototrophic mutants and complemented strains, respectively. Resulting clones were selected for on solid minimal medium.

For the generation of CIp10-*DUR1,2*[WT] or CIp10-*DUR1,2*[K1779R], the coding sequences of *DUR1,2* with either the wild-type allele together with the native up- and downstream intergenic regions were amplified. The mutated version was created by In-Fusion HD cloning using primers with the codon for arginine instead of lysine (two fragments). The wild-type allele (one fragment) and the mutated allele (two fragments) were cloned into CIp10 using *Xho*I. Constructed plasmids were verified by sequencing. Homozygous uridine-auxotrophic deletion mutants were transformed with the *Stu*I-linearized empty CIp10 plasmid (Murad *et al.*, 2000) to generate prototrophic mutants or with *Stu*I-linearized CIp10-*DUR1,2*[WT] or CIp10-*DUR1,2*[K1779R] plasmids to generate complemented strains with the native or mutated biotinylation motif. The correct integration of *C. glabrata* and *C. albicans* complementation cassettes was confirmed by PCR and Southern blot.

Genomic DNA isolation and Southern blot

Yeast cells were harvested, resuspended in 1 mL lysis buffer (1 M sorbitol; 100 mM sodium citrate, pH 5.8; 50 mM EDTA, pH 8.0; 0.6 mg/mL lyticase and 2.5% β-

mercaptoethanol) and incubated at 37°C for 45 min. Afterwards the cells pellet was resuspended in 800 µL proteinase buffer (10 mM Tris-HCl, pH 7.5; 50 mM EDTA, pH 7.5; 0.5% SDS; 1 mg/mL proteinase K) and incubated at 60°C for 30 min. The cell debris was precipitated by adding 800 µL phenol/chloroform/isoamylalcohol (25:24:1), mixed with vortex device for 4 min and centrifuged (20,000g, 5 min, RT). The hydrophilic phase was transferred into a new microcentrifuge tube containing 750 µL isopropanol. The precipitated DNA was centrifuged (20,000g, 5 min, RT), washed with 600 µL 70% ethanol and air-dried. The transparent DNA pellet was reconstituted in 200 µL ddH$_2$O containing 10 mg/mL RNase A. The DNA quantity was evaluated using a NanoDrop Spectrophotometer (ND-100, Peqlab). The DNA was stored at 4 °C (short term) or -20 °C (long term). Dilutions of DNA were made freshly.

Thirty µg DNA were digested with *Hind*III (NEB) according to the manufacturer's recommendations. The digested DNA and the DNA Molecular Weight Marker III, DIG-labeled (50 pg per lane, Roche) was separated in a 1% agarose gel. The DNA was pretreated in acid to ensure efficient transfer. The agarose gel was rinsed 10 min in depurination solution (0.25 M HCl) and shortly in water. The gel was denatured two times for 15 min in denaturing solution (0.5 M NaOH, 1.5 M NaCl) and washed briefly in water. Finally, the gel was rinsed in neutralization buffer (1 M Tris-HCl pH 7.5; 1.5 M NaCl) two times for 15 min and equilibrated for at least 10 min in 20× SSC (3 M NaCl, 0.3 M sodium citrate; pH 7.0).

The nylon membrane (positively charged, Roche) was rinsed 2 min in water and 15 min in 20× SSC to activate the membrane, before the DNA was vacuum blotted 1.5 h at 50-100 mbar (Biometra). Before DNA crosslinking, the membrane was rinsed 30 sec in 0.4 M NaOH, 30 sec in 0.2 M Tris-HCl pH 7.5 and dried 10-15 min on a piece of Whatman™ filter paper. The DNA was crosslinked to the membrane by UV light (120 mJ/cm^2) for at least 60 sec and the membrane was rinsed with 2× SSC. Further steps were performed according the DIG nonradioactive nucleic acid labeling and detection

system (Roche), using the PCR DIG Probe Synthesis Kit, DIG Easy Hyb™, Anti-Digoxigenin-AP, Fab fragments, and CDP-Star.

Fungal RNA isolation and reverse transcription-quantitative PCR (qRT-PCR)

For preparation of RNA from *in vitro* cultures of *Candida*, stationary phase yeast cells were washed three times in PBS, and 2×10^7 *Candida* cells per mL were inoculated into minimal medium with different biotin concentrations. At indicated time points, cells were harvested and centrifuged (4,000*g*, 10 min and 4°C). The cell pellet was washed with ice cold water, centrifuged again, and immediately frozen in liquid nitrogen. The isolation of the fungal RNA was performed as previously described (Lüttich *et al.*, 2012). The quantity of the RNA was determined using the NanoDrop Spectrophotometer ND-1000 (NRW International GmbH). DNase-treated RNA (600 ng) was transcribed into cDNA using 0.5 µg oligo-dT$_{12\text{-}18}$, 100 U Superscript™ III Reverse Transcriptase and 20 U RNaseOUT™ Recombinant RNase Inhibitor (all: Thermo Fischer Scientific) in a total volume of 35 µL for 2 h at 42 °C, followed by heat-inactivation for 15 min at 70°C. The cDNA was diluted 1:20 in DEPC-treated water and used for quantitative PCR with EvaGreen® QPCR Mix II (Bio&SELL) performed in a CFX96 thermocycler (Bio-Rad). Primers (**Table S3**) were used at a final concentration of 500 nM. Target gene expression was calculated using the $\Delta\Delta Ct$ method (Pfaffl, 2001), with normalization to the housekeeping genes *ACT1* and *EFB1*.

Protein isolation and Western blot

For preparation of whole protein extracts, stationary phase cells were washed three times in PBS, diluted to OD$_{600}$ 0.2 into minimal medium and incubated at 37°C at 180 rpm overnight. The cells were harvested and mechanically lysed in PBS-KMT (PBS + 3 mM KCl, 2.5 mM MgCl$_2$, 0.1% Triton-X-100) + protease inhibitor cocktail (Roche) with acid-washed glass beads by bead beating in a Precellys 24 homogenizer (Peqlab; 6.500 rpm, 2 cycles, each 30 sec, 15 sec pause). The lysate was centrifuged

(14,000 rpm, 4°C for 5 min) and the protein concentration of the supernatant was determined by Pierce™ BCA Protein Assay Kit (Thermo Fisher Scientific). Two aliquots of twenty μg protein of each sample were denatured in one-fourth volume of 4× Lämmli buffer (125 mM Tris-HCl pH 6.8, 50% glycerol, 4% SDS, 0.02% bromophenol blue, 1:10 β-mercaptoethanol) at 95°C for 5 min and separated by denaturizing SDS-PAGE with Rotiphorese® Gel 30 (final 12% acrylamide mix (Roth)). Proteins were electro-transferred to nitrocellulose membranes (Whatman) in blotting buffer (25 mM Tris, 192 mM glycine, 10% methanol and 0.1% SDS) and free binding sites were blocked with 5% milk powder in TBS (0.5 M Tris, 1.5 M NaCl, pH 7.6) + 0.05% Tween®-20 (TBS-T) for 3 hr at room temperature. One membrane was incubated with monoclonal mouse anti-chicken egg albumin antibody (Sigma), diluted 1:2000 in TBS-T containing 2% milk powder. The other membrane was incubated with rat anti-α-tubulin antibody (AbD Serotec), diluted 1:1000 in TBS-T containing 2% BSA. Both were incubated at 4°C overnight and gentle shaking. The membranes were rinsed three times in TBS-T, incubated with goat anti-mouse IgG-HRP (1:1000 in 2% milk powder) or goat anti-rat IgG-HRP (1:2000 in 2% BSA) (both Santa Cruz Biotech) to detect ovalbumin and α-tubulin, respectively. Finally, the membranes were rinsed three times in TBS-T and two times in TBS, followed by chemiluminescence detection using Pierce™ ECL Plus Western Blotting Substrate (Thermo Fisher Scientific) according to the manufactures' instructions.

Experiments with human monocyte-derived macrophages (hMDMs)

Primary macrophages were differentiated from CD14-positive monocytes as previously described (Sprenger *et al.*, 2020), seeded in 24-well plates (2×10^5 hMDMs/well) in RPMI with 50 ng/mL M-CSF, and incubated overnight. Prior to macrophage infection, the medium was exchanged to serum- and biotin-free RPMI with L-glutamine (Thermo Fisher Scientific) to exclude biotin uptake by *Candida* prior to phagocytosis. The fungal survival within macrophages was evaluated after 3 h of coincubation with *C. glabrata* at

a multiplicity of infection (MOI) of 1, by plating of appropriate dilutions on YPD agar as previously described (Sprenger *et al.*, 2020). Macrophages (1.5×10⁵ hMDMs/well) were allowed to adhere onto coverslips in a 24-well plate overnight in RPMI containing 50 ng/mL M-CSF and 10 % FBS, and then infected with *C. glabrata* at an MOI of 2 for the indicated time points. Phagocytosis was synchronized on ice for 30 min followed by two washing steps with pre-warmed medium to remove unbound *Candida* cells.

Fluorescence analysis by flow cytometry and microscopy

Stationary phase cells were diluted 1:20 into fresh YPD medium and incubated at 37 °C for 2 h and 180 rpm. Then, cells were harvested and washed once with PBS, fixed with 500 µL Roti®-Histofix 4% for 20 min and washed again with PBS. The median fluorescence intensity (MFI) of *C. glabrata* yeast cells was evaluated with BD FACS Verse® (BD Biosciences, Franklin Lakes (USA)) counting 50,000 events. Data analysis was performed using the FlowJO™ 10.2 software (FlowJO LLC, Ashland (USA)). The gating strategy was based on blotting forward (FSC) and side scatter (SSC) to exclude cellular debris.

The staining of phagocytosed yeast cells was adapted from (Kasper *et al.*, 2018). Infected macrophages were fixed with Roti®-Histofix 4% and stained with 50 µg/mL Concanavalin A conjugated with Alexa Fluor™ 647 (ConA-AF647; Thermo Fisher Scientific) at 37°C for 30 min to visualize external *Candida* cells. Coverslips were mounted with ProLong™ Gold Antifade Mountant with DAPI and fluorescence images were recorded using the Zeiss AXIO Observer.Z1 (Carl Zeiss Microscopy).

***In silico* analysis and statistics**

Information about gene orthologs was obtained from the *Candida* Genome Database (CGD) (Skrzypek *et al.*, 2017) and the *Saccharomyces* Genome Database (SGD) (Cherry *et al.*, 2012). Data are reported as scatterplot with mean ± SD, line charts with mean ± SD, or bar charts showing mean + SD. Data were analyzed using

GraphPad Prism 5 (GraphPad Software, San Diego, USA). For statistical analysis of matched observations in macrophage experiments, a repeated measures ANOVA with Bonferroni's multiple comparison test was performed. Statistically significant results are marked with a single asterisk meaning $p \leq 0.05$, double asterisks meaning $p \leq 0.01$.

Results and discussion

Complementation of tryptophan auxotrophy in *C. glabrata* by genomic reintegration

Gene complementation in the best-studied diploid *Candida* species, *C. albicans*, is often achieved by genomic integration targeting specific promotor regions (*HIS1* (Davis *et al.*, 2002) and *ENO1* (Staab *et al.*, 2003)) or neutral ORFs (*ADH1* (Hünniger *et al.*, 2014), *RPS1*, (Murad *et al.*, 2000), and *ACT1* (Morschhäuser *et al.*, 1998, Xu *et al.*, 2014). However, similar approaches in the haploid genome of *C. glabrata* would lead to an additional knock-out of the targeted gene. To define a suitable locus for gene integration, we therefore first carefully reviewed the literature to exclude unwanted side-effects upon genetic modification, especially during infection experiments. We chose the tryptophan biosynthesis gene *TRP1* as a target locus for integration, as previous data has shown that genetic manipulation in this locus has no influence on fungal fitness in a systemic *C. glabrata* infection model (Jacobsen *et al.*, 2010) and on the interaction with macrophages (Schwarzmüller *et al.*, 2014, Seider *et al.*, 2014). In addition, the *TRP1* gene is, besides *HIS3*, *LEU2*, and *URA3* widely used as selection marker in different plasmid vectors in *S. cerevisiae* and *C. glabrata*.

As a basis for complementation constructs, we created a pTRP1 plasmid vector based on the plasmid pUC19, which harbors the *TRP1* gene as the selection marker together with its up- and downstream regions for homologous recombination at the native *TRP1* locus. The remaining part of the multiple cloning site of the pUC19 backbone downstream of the *TRP1* terminator allows easy insertion of any GOI (**Figure 1A**). A *trp1Δ* mutant, which can be used as the parental strain for integration of pTRP1, has been previously created with the *SAT1* flipper protocol (Jacobsen *et al.*, 2010), where only one recombination site (FRT) of the flip-recombinase (FLP) remains at the *TRP1* locus (**Figure 1B**). To generate a *TRP1* complementation strain in a strain background that harbors no additional gene deletions, the *TRP1* construct was PCR-amplified from

pTRP1 and transformed into *trp1Δ*. We used this PCR-amplified complementation cassette instead of the whole plasmid to rule out the unspecific genomic integration of additional vector DNA. Correct integration into the *TRP1* locus was then verified by Southern blotting (**Figure 1C**). Phenotypically, the growth of the complemented strain (*trp1Δ + TRP1*) was restored in minimal medium lacking tryptophan (**Figure 1D**). We can therefore conclude that the *TRP1* locus is suitable for expression of target genes, which is similar to the CIp10 strategy in *C. albicans* (Murad *et al.*, 2000), but uses the native chromosomal location of the *TRP1* locus.

To apply our approach for the analysis of gene functions of a *C. glabrata* GOI, a mutant strain lacking the GOI has to be generated in *trp1Δ* strain background. This mutant will then be transformed with the above-described *TRP1* cassette for restoring *TRP1* prototrophy, or with the *TRP1* cassette containing the GOI together with promotor and terminator region, to restore *TRP1* prototrophy and function of the GOI. This method then allows the direct comparison of three prototrophic strains – the *trp1Δ + TRP1* wild type strain (**Figure 1**), the *trp1ΔGOIΔ + TRP1* mutant strain and the *trp1ΔGOIΔ + TRP1+GOI* complemented strain. This strategy has successfully been applied for complementation of *C. glabrata* with the biotin-metabolic genes *VHR1* and *VHT1*, for which recovery of wild type phenotypes after complementation was proven (Sprenger *et al.*, 2020).

Of note, our strategy of restoring the tryptophan prototrophy of a *trp1*-auxotrophic parental strain can be used to complement genes in a published triple auxotrophic *his3Δ leu2Δ trp1Δ C. glabrata* mutant library remaining leucine and histidine auxotrophy (Schwarzmüller *et al.*, 2014). A good alternative strategy might be the integration of complementation cassettes into intergenic regions, which is already established in *C. albicans* (Gerami-Nejad *et al.*, 2013) and in *C. glabrata* (Ueno *et al.*, 2011). However, genomic integration in these regions can raise the problem of inefficient transcriptional activity due to a silenced chromatin structure (Rando & Winston, 2012, Gartenberg & Smith, 2016).

Heterologous expression of yEGFP, mCherry, and ovalbumin in *C. glabrata*

In order to determine whether the *TRP1* locus is suitable for heterologous expression of fluorescent markers and ovalbumin, an antigen used for immunological studies, we used the In-Fusion HD cloning system to fuse different promotors with these GOIs and into the *Xba*I-digested pTRP1 vector (**Figure 2A**). This technique allows the combination of promotor, protein-encoding, and terminator sequences by one cloning step. Several well-investigated promotors (Zordan *et al.*, 2013) were fused with yEGFP (yeast-enhanced green fluorescent protein (Cormack *et al.*, 1997)) to achieve constitutive expression under *in vitro* conditions (*TEF1*prom and *PDC1*prom), but also induced expression upon phagocytosis by macrophages (*LYS21*prom). The correct integration into the *TRP1* locus into the *trp1*Δ strain was verified by PCR and positive clones were analyzed for yEGFP fluorescence by microscopy and FACS.

The expression of yEGFP under control of the *TEF1* promotor led to the highest median fluorescence intensity among all tested promotors in culture medium (**Figure 2B-C**). This construct was expressed by *C. glabrata* cells internalized by macrophages, but also non-internalized cells (**Figure 2D**). The *PDC1*-controlled yEGFP expression showed fluorescence levels similar to *TEF1* in culture medium, which were also similar between phagocytosed and non-phagocytosed yeast cells (Figure 2D). Comparing logarithmically growing to stationary cells, yEGFP fluorescence with *TEF1* and *PDC1* promotors was higher in logarithmic cells (**Figure 2B**). When the expression was controlled by the *LYS21* promotor, the fluorescence signal was higher in phagocytosed *vs* extracellular *C. glabrata* cells (**Figure 2D**, as expected from a previous study (Zordan *et al.*, 2013)). In contrast to the other promotors, the expression of yEGFP remained low in the logarithmic growth phase when controlled by the *LYS21* promotor (**Figure 2B**).

In addition to yEGFP, the *TEF1* promotor was fused with mCherry (red fluorescent protein), cloned into the *Xba*I-digested pTRP1 and transformed into the *trp1*Δ strain background. The expression of mCherry controlled by the strong constitutive promotor

TEF1 again led to a strong fluorescence signal of logarithmically growing cells (**Figure 2E**).

The expression of fluorescent markers under control of constitutive or inducible promotors is not only useful for generating fluorescently labeled fungal wild type or mutant strains that can be traced during infection, it also generates reporter strains that can be used to identify promotor-inducing conditions during infection (Miramón *et al.*, 2012). Similarly, the efficiency of transcription and translation based on promotors of interest can be quantified, even by measuring the fluorescence intensity on a single cell level. The method presented here can be expanded by using more than one fluorophores which can be integrated into other genomic regions, like the *HIS3* or *LEU2* locus of *his3Δ* or *leu2Δ* single mutants or the triple auxotrophic *his3Δ leu2Δ trp1Δ* mutant (Jacobsen *et al.*, 2010, Schwarzmüller *et al.*, 2014).

The heterologous expression of ovalbumin (OVA) in pathogens can be used to induce OVA-specific immune responses for investigation of the immune recognition of and T cell activation by the pathogen (Ishizuka *et al.*, 2009, Krummey *et al.*, 2014, Harms *et al.*, 2018). To generate an OVA-expressing *C. glabrata* strain, we fused a codon-optimized OVA gene with the *TEF1* promotor and cloned it into the *Xba*I-digested p*TRP1*. The expression of OVA in *C. glabrata* was verified by Western blot **(Figure 2F)**. The heterologously expressed OVA in *C. glabrata* was smaller in size than native ovalbumin from egg white (42.8 kDa) and was detected as two bands. A previous study in *Pichia pastoris* demonstrated that mono- and diglycosylation of OVA correspond to these two bands. The smaller size is therefore likely due to missing *N*-acetylation and phosphorylation in this yeast expression system (Ito & Matsudomi, 2005).

In summary, we have constructed a set of plasmids for fluorescence reporter-based analysis using *TRP1* integration in *C. glabrata*. We have shown that the fluorescence levels depend on the strength of the promotor and promotor-specific induction conditions. Moreover, we used this system for heterologous expression of the well-characterized model antigen OVA as a basis for measuring the specific immune

response of T cells against *C. glabrata*. Additionally, this system can be used for epitope-tagging of proteins or for competitive infection or interspecies competition models, by combining different fluorescently labeled *C. glabrata* strains in one experiment.

Overexpression of the biotin transporter gene *VHT1* modulates intracellular survival within macrophages

To evaluate the suitability of our *TEF1*, *LYS21* and *PDC1* promotor constructs for overexpression of *C. glabrata*'s own genes, we used the system with the biotin transporter gene *VHT1* of *C. glabrata*. The expression of the biotin transporter gene *VHT1* is normally induced when availability of biotin in the environment is low, and its expression is dependent on the transcriptional regulator Vhr1 (Sprenger *et al.*, 2020). Similar constructs as described for yEGFP were created, and transformed into a *trp1*Δ strain (wild type) and a *trp1*Δ *vhr1*Δ strain (mutant). Resulting strains were analyzed for the transcriptional abundance of *VHT1* after inoculation into nutrient-rich medium. The transcript abundance of *VHT1* was strongly increased compared to the wild type when the gene was controlled by *TEF1*prom or *PDC1*prom, both constitutively active promotors, whereas the *LYS21*-controlled *VHT1* expression was only marginally increased (**Figure 3A**). The overexpression of *VHT1* was independent of its native regulator, Vhr1, as the additional deletion of *VHR1* had no impact on the transcript abundance of *VHT1.*

VHR1 is needed for survival of *C. glabrata* in macrophages. This gene contributes to upregulation of *VHT1* under biotin limitation, it may also have regulatory targets in addition to *VHT1* regulation (Sprenger *et al.*, 2020). To elucidate whether *VHR1*-depentent *VHT1* induction is important during *C. glabrata*-macrophage interaction, we tested whether overexpression of *VHT1* by our system can diminish the survival defect of the *vhr1*Δ mutant. We confronted hMDMs with *VHT1* overexpression strains and evaluated survival of phagocytosed fungal cells. The *vhr1*Δ strain showed an

attenuated intracellular survival within hMDMs as previously described (Sprenger *et al.*, 2020), while both *VHT1*-overexpressing strains showed survival rates comparable to the wild type (**Figure 3B**). These data imply that the overexpression of *VHT1* can indeed compensate the deletion of *VHR1*, whereas the wild type with its functional Vhr1 does not benefit from higher *VHT1* expression (**Figure 3B**).

Mutations in the biotinylation motif of Dur1,2 prevent the utilization of urea

Biotinylation is a covalent posttranslational modification of lysine residues in target proteins (Lane *et al.*, 1964). Most of these lysine residues lie in highly conserved AMKM sequence motifs of biotin-dependent enyzmes (Samols *et al.*, 1988, Chapman-Smith & Cronan, 1999). The enzyme urea amidolyase Dur1,2 is important for utilizing urea as a nitrogen source, and its expression is highly induced by urea (Navarathna *et al.*, 2011). It possesses a conserved biotinylation motif in its carboxylase-acting C-terminal domain in both, *C. glabrata* and *C. albicans* (**Figure 4A,** (Samols *et al.*, 1988, Chapman-Smith & Cronan, 1999)). *DUR1,2* is important for the pathogenicity of *C. albicans* (Ghosh *et al.*, 2009, Navarathna *et al.*, 2012) and *C. glabrata* (Brunke *et al.*, 2015). To study whether biotinylation is important for Dur1,2 functionality, we mutated the lysine codon AAA into the arginine-coding AGA (amino acid position 1798 in *C. glabrata* and 1779 in *C. albicans* (**Figure 4B**)), using our newly developed complementation strategy in *C. glabrata* and the established CIp10 strategy in *C. albicans* (Murad *et al.*, 2000). Growth of the mutant strains in liquid (**Figure 4C, E**) and solid (**Figure 4D, F**) medium showed a growth defect in media with urea as the sole nitrogen source. The K→R mutation strains exhibited similar phenotypes as the *dur1,2* deletion mutants of both species (**Figure 4C-F**). Interestingly, the *Cadur1,2Δ/Δ* mutant and the K→R mutation strain not only showed reduced growth on agar plates containing urea, but also failed to induce colony wrinkling at 37°C (**Figure 4F**). These data suggest that biotinylation of Dur1,2 is indeed essential for urea utilization in *C. glabrata* and *C. albicans*.

In summary, we conclude that the *TRP1* locus is a suitable locus to reintegrate genes of interest, either with their native DNA sequence, with specific sequence variations or with alternative promotors, to investigate the role and function of these genes for fungal (patho)biology.

References

Brand A, MacCallum DM, Brown AJ, Gow NA & Odds FC (2004) Ectopic expression of URA3 can influence the virulence phenotypes and proteome of *Candida albicans* but can be overcome by targeted reintegration of *URA3* at the *RPS10* locus. *Eukaryot Cell* **3**: 900-909.

Brunke S, Quintin J, Kasper L*, et al.* (2015) Of mice, flies--and men? Comparing fungal infection models for large-scale screening efforts. *Dis Model Mech* **8**: 473-486.

Chapman-Smith A & Cronan JE, Jr. (1999) Molecular biology of biotin attachment to proteins. *J Nutr* **129**: 477S-484S.

Cherry JM, Hong EL, Amundsen C*, et al.* (2012) *Saccharomyces* Genome Database: the genomics resource of budding yeast. *Nucleic Acids Res* **40**: D700-705.

Combs JGFM, J.P. (2017) *The Vitamins: Fundamental Aspects in Nutrition and Health*. Academic Press.

Cormack BP, Bertram G, Egerton M, Gow NA, Falkow S & Brown AJ (1997) Yeast-enhanced green fluorescent protein (yEGFP): a reporter of gene expression in *Candida albicans*. *Microbiology* **143 (Pt 2)**: 303-311.

Dakshinamurti K (2005) Biotin--a regulator of gene expression. *J Nutr Biochem* **16**: 419-423.

Davis DA, Bruno VM, Loza L, Filler SG & Mitchell AP (2002) *Candida albicans* Mds3p, a conserved regulator of pH responses and virulence identified through insertional mutagenesis. *Genetics* **162**: 1573-1581.

Diekema D, Arbefeville S, Boyken L, Kroeger J & Pfaller M (2012) The changing epidemiology of healthcare-associated candidemia over three decades. *Diagn Microbiol Infect Dis* **73**: 45-48.

Falkow S (1988) Molecular Koch's postulates applied to microbial pathogenicity. *Rev Infect Dis* **10 Suppl 2**: S274-276.

Fitzpatrick DA, O'Gaora P, Byrne KP & Butler G (2010) Analysis of gene evolution and metabolic pathways using the *Candida* Gene Order Browser. *BMC Genomics* **11**: 290.

Frieman MB, McCaffery JM & Cormack BP (2002) Modular domain structure in the *Candida glabrata* adhesin Epa1p, a beta1,6 glucan-cross-linked cell wall protein. *Mol Microbiol* **46**: 479-492.

Gabaldón T & Carrete L (2016) The birth of a deadly yeast: tracing the evolutionary emergence of virulence traits in *Candida glabrata*. *FEMS Yeast Res* **16**: fov110.

Gartenberg MR & Smith JS (2016) The Nuts and Bolts of Transcriptionally Silent Chromatin in *Saccharomyces cerevisiae*. *Genetics* **203**: 1563-1599.

Gerami-Nejad M, Zacchi LF, McClellan M, Matter K & Berman J (2013) Shuttle vectors for facile gap repair cloning and integration into a neutral locus in *Candida albicans*. *Microbiology* **159**: 565-579.

Ghosh S, Navarathna DH, Roberts DD, Cooper JT, Atkin AL, Petro TM & Nickerson KW (2009) Arginine-induced germ tube formation in *Candida albicans* is essential for escape from murine macrophage line RAW 264.7. *Infect Immun* **77**: 1596-1605.

Harms JS, Khan M, Hall C, Splitter GA, Homan EJ, Bremel RD & Smith JA (2018) Brucella Peptide Cross-Reactive Major Histocompatibility Complex Class I Presentation Activates SIINFEKL-Specific T Cell Receptor-Expressing T Cells. *Infect Immun* **86**.

Hosogaya N, Miyazaki T, Nagi M*, et al.* (2013) The heme-binding protein Dap1 links iron homeostasis to azole resistance via the P450 protein Erg11 in *Candida glabrata*. *FEMS Yeast Res* **13**: 411-421.

Hünniger K, Lehnert T, Bieber K, Martin R, Figge MT & Kurzai O (2014) A virtual infection model quantifies innate effector mechanisms and *Candida albicans* immune escape in human blood. *PLoS Comput Biol* **10**: e1003479.

Ishizuka J, Grebe K, Shenderov E*, et al.* (2009) Quantitating T cell cross-reactivity for unrelated peptide antigens. *J Immunol* **183**: 4337-4345.

Ito K & Matsudomi N (2005) Structural characteristics of hen egg ovalbumin expressed in yeast *Pichia pastoris*. *Biosci Biotechnol Biochem* **69**: 755-761.

Jacobsen ID, Brunke S, Seider K, Schwarzmüller T, Firon A, d'Enfert C, Kuchler K & Hube B (2010) *Candida glabrata* persistence in mice does not depend on host immunosuppression and is unaffected by fungal amino acid auxotrophy. *Infect Immun* **78**: 1066-1077.

Kasper L, Konig A, Koenig PA*, et al.* (2018) The fungal peptide toxin Candidalysin activates the NLRP3 inflammasome and causes cytolysis in mononuclear phagocytes. *Nat Commun* **9**: 4260.

Kitada K, Yamaguchi E & Arisawa M (1996) Isolation of a *Candida glabrata* centromere and its use in construction of plasmid vectors. *Gene* **175**: 105-108.

Krummey SM, Floyd TL, Liu D, Wagener ME, Song M & Ford ML (2014) *Candida*-elicited murine Th17 cells express high Ctla-4 compared with Th1 cells and are resistant to costimulation blockade. *J Immunol* **192**: 2495-2504.

Kurtzman CP & Robnett CJ (2003) Phylogenetic relationships among yeasts of the 'Saccharomyces complex' determined from multigene sequence analyses. *FEMS Yeast Res* **3**: 417-432.

Lane MD, Rominger KL, Young DL & Lynen F (1964) The Enzymatic Synthesis of Holotranscarboxylase from Apotranscarboxylase and (+)-Biotin. Ii. Investigation of the Reaction Mechanism. *J Biol Chem* **239**: 2865-2871.

Littman ML & Miwatani T (1963) Effect of Water Soluble Vitamins and Their Analogues on the Growth of *Candida Albicans*. I. Biotin, Pyridoxamine, Pyridoxine and Fluorinated Pyrimidines. *Mycopathol Mycol Appl* **21**: 81-108.

Lüttich A, Brunke S & Hube B (2012) Isolation and amplification of fungal RNA for microarray analysis from host samples. *Methods Mol Biol* **845**: 411-421.

Madsen CT, Sylvestersen KB, Young C*, et al.* (2015) Biotin starvation causes mitochondrial protein hyperacetylation and partial rescue by the SIRT3-like deacetylase Hst4p. *Nat Commun* **6**: 7726.

McVeigh IB, E. (1951) The amino acid and vitamin requirements of *Candida albicans* Y-475 and *Mycoderma vini* Y-939. *Bull Torrey Botan Club* **Vol. 78**: 134–144.

Miramón P, Dunker C, Windecker H, Bohovych IM, Brown AJ, Kurzai O & Hube B (2012) Cellular responses of *Candida albicans* to phagocytosis and the extracellular activities of neutrophils are critical to counteract carbohydrate starvation, oxidative and nitrosative stress. *PLoS One* **7**: e52850.

Miyazaki T, Izumikawa K, Yamauchi S*, et al.* (2011) The glycosylphosphatidylinositol-linked aspartyl protease Yps1 is transcriptionally regulated by the calcineurin-Crz1 and Slt2 MAPK pathways in *Candida glabrata*. *FEMS Yeast Res* **11**: 449-456.

Morschhäuser J, Michel S & Hacker J (1998) Expression of a chromosomally integrated, single-copy GFP gene in *Candida albicans*, and its use as a reporter of gene regulation. *Mol Gen Genet* **257**: 412-420.

Murad AM, Lee PR, Broadbent ID, Barelle CJ & Brown AJ (2000) CIp10, an efficient and convenient integrating vector for *Candida albicans*. *Yeast* **16**: 325-327.

Navarathna DH, Das A, Morschhauser J, Nickerson KW & Roberts DD (2011) Dur3 is the major urea transporter in *Candida albicans* and is co-regulated with the urea amidolyase Dur1,2. *Microbiology* **157**: 270-279.

Navarathna DH, Lionakis MS, Lizak MJ, Munasinghe J, Nickerson KW & Roberts DD (2012) Urea amidolyase (*DUR1,2*) contributes to virulence and kidney pathogenesis of *Candida albicans*. *PLoS One* **7**: e48475.

Nevitt T & Thiele DJ (2011) Host iron withholding demands siderophore utilization for *Candida glabrata* to survive macrophage killing. *PLoS Pathog* **7**: e1001322.

Noble JA, Tsai HF, Suffis SD, Su Q, Myers TG & Bennett JE (2013) STB5 is a negative regulator of azole resistance in *Candida glabrata*. *Antimicrob Agents Chemother* **57**: 959-967.

Pfaffl MW (2001) A new mathematical model for relative quantification in real-time RT-PCR. *Nucleic Acids Res* **29**: e45.

Pla J, Gil C, Monteoliva L, Navarro-Garcia F, Sanchez M & Nombela C (1996) Understanding *Candida albicans* at the molecular level. *Yeast* **12**: 1677-1702.

Rando OJ & Winston F (2012) Chromatin and transcription in yeast. *Genetics* **190**: 351-387.

Samols D, Thornton CG, Murtif VL, Kumar GK, Haase FC & Wood HG (1988) Evolutionary conservation among biotin enzymes. *J Biol Chem* **263**: 6461-6464.

Sanglard D, Ischer F, Monod M & Bille J (1996) Susceptibilities of *Candida albicans* multidrug transporter mutants to various antifungal agents and other metabolic inhibitors. *Antimicrob Agents Chemother* **40**: 2300-2305.

Schwarzmüller T, Ma B, Hiller E*, et al.* (2014) Systematic phenotyping of a large-scale *Candida glabrata* deletion collection reveals novel antifungal tolerance genes. *PLoS Pathog* **10**: e1004211.

Seider K, Gerwien F, Kasper L*, et al.* (2014) Immune evasion, stress resistance, and efficient nutrient acquisition are crucial for intracellular survival of *Candida glabrata* within macrophages. *Eukaryot Cell* **13**: 170-183.

Skrzypek MS, Binkley J, Binkley G, Miyasato SR, Simison M & Sherlock G (2017) The *Candida* Genome Database (CGD): incorporation of Assembly 22, systematic identifiers and visualization of high throughput sequencing data. *Nucleic Acids Res* **45**: D592-D596.

Sprenger M, Hartung TS, Allert S, Wisgott S, Niemiec MJ, Graf K, Jacobsen ID, Kasper L & Hube B (2020) Fungal biotin homeostasis is essential for immune evasion after macrophage phagocytosis and virulence. *Cell Microbiol*.

Staab JF, Bahn YS & Sundstrom P (2003) Integrative, multifunctional plasmids for hypha-specific or constitutive expression of green fluorescent protein in *Candida albicans*. *Microbiology* **149**: 2977-2986.

Sternicki LM, Wegener KL, Bruning JB, Booker GW & Polyak SW (2017) Mechanisms Governing Precise Protein Biotinylation. *Trends Biochem Sci* **42**: 383-394.

Ueno K, Matsumoto Y, Uno J, Sasamoto K, Sekimizu K, Kinjo Y & Chibana H (2011) Intestinal resident yeast *Candida glabrata* requires Cyb2p-mediated lactate assimilation to adapt in mouse intestine. *PLoS One* **6**: e24759.

Walther A & Wendland J (2003) An improved transformation protocol for the human fungal pathogen *Candida albicans*. *Curr Genet* **42**: 339-343.

Wilson RB, Davis D & Mitchell AP (1999) Rapid hypothesis testing with *Candida albicans* through gene disruption with short homology regions. *J Bacteriol* **181**: 1868-1874.

Xu QR, Yan L, Lv QZ, Zhou M, Sui X, Cao YB & Jiang YY (2014) Molecular genetic techniques for gene manipulation in *Candida albicans*. *Virulence* **5**: 507-520.

Yánez-Carrillo P, Orta-Zavalza E, Gutierrez-Escobedo G, Patron-Soberano A, De Las Penas A & Castano I (2015) Expression vectors for C-terminal fusions with fluorescent proteins and epitope tags in *Candida glabrata*. *Fungal Genet Biol* **80**: 43-52.

Zempleni J, Hassan YI & Wijeratne SS (2008) Biotin and biotinidase deficiency. *Expert Rev Endocrinol Metab* **3**: 715-724.

Zordan RE, Ren Y, Pan SJ, Rotondo G, De Las Penas A, Iluore J & Cormack BP (2013) Expression plasmids for use in *Candida glabrata*. *G3 (Bethesda)* **3**: 1675-1686.

Figures and legends
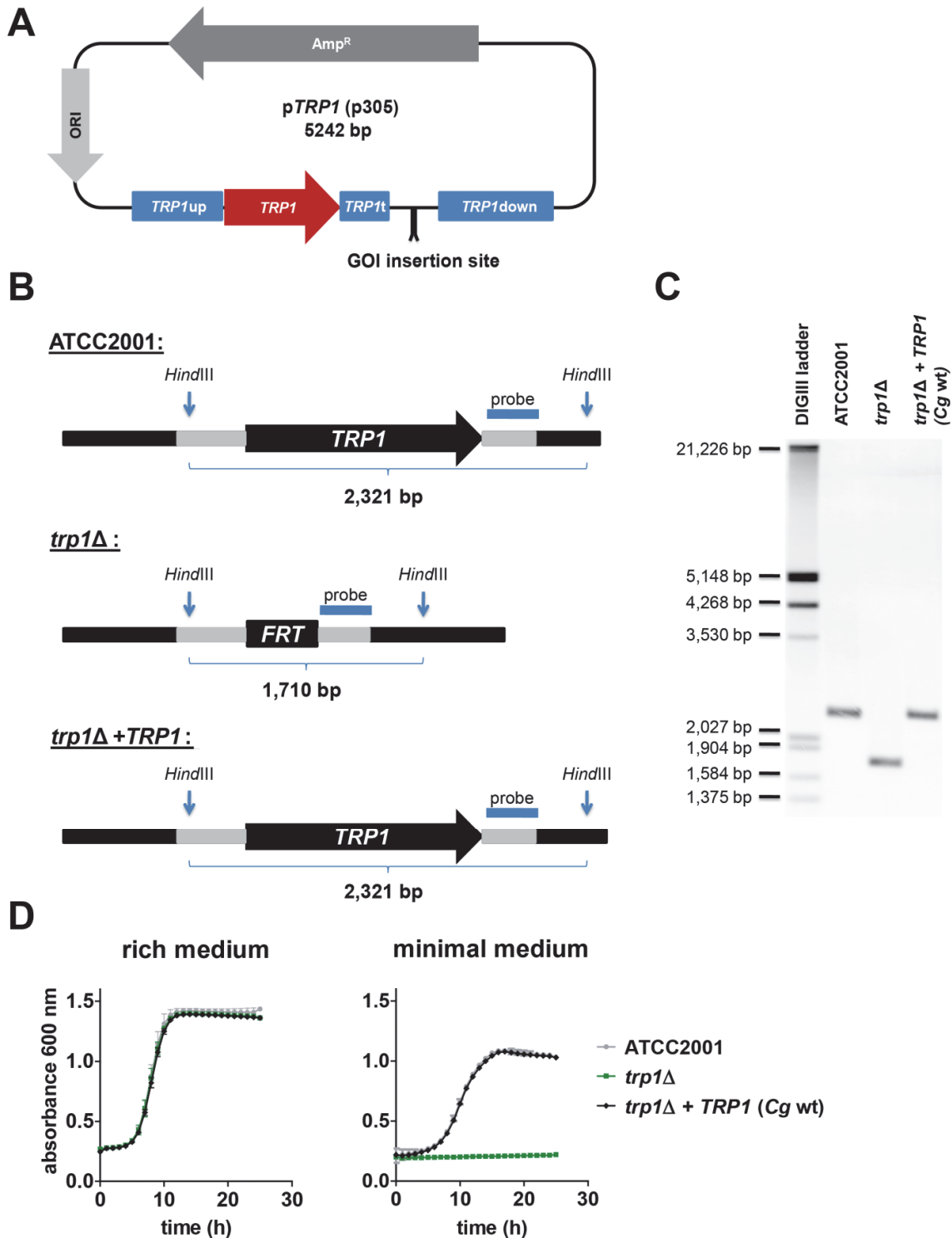
FIGURE 1: Construction and verification of *TRP1* complemented strains.

(A) Overview of the plasmid used for gene complementation in *C. glabrata*. The insertion site allows cloning of GOI sequences with their promotor and terminator

(B) Depiction of the *TRP1* gene locus in the *C. glabrata* ATCC2001 reference genome, the *trp1* deletion mutant (*trp1Δ*) and our complementation strain (*trp1Δ + TRP1*). A

DNA probe was designed for the terminator region to detect gene-specific fragments by Southern blotting. (C) Southern blot of *Hind*III-digested genomic DNA of ATCC2001, *trp1*Δ, and *trp1*Δ + *TRP1* (*Cg* wt). The expected sizes from (B) correspond to the visible bands. (D) Growth analysis of *C. glabrata* ATCC2001, *trp1*Δ, and *trp1*Δ + *TRP1* in nutrient-rich medium (YPD) and minimal medium (SD) at 37°C for 24 h. Values are absorption at 600 nm and shown as mean ± SD of at least three replicates.
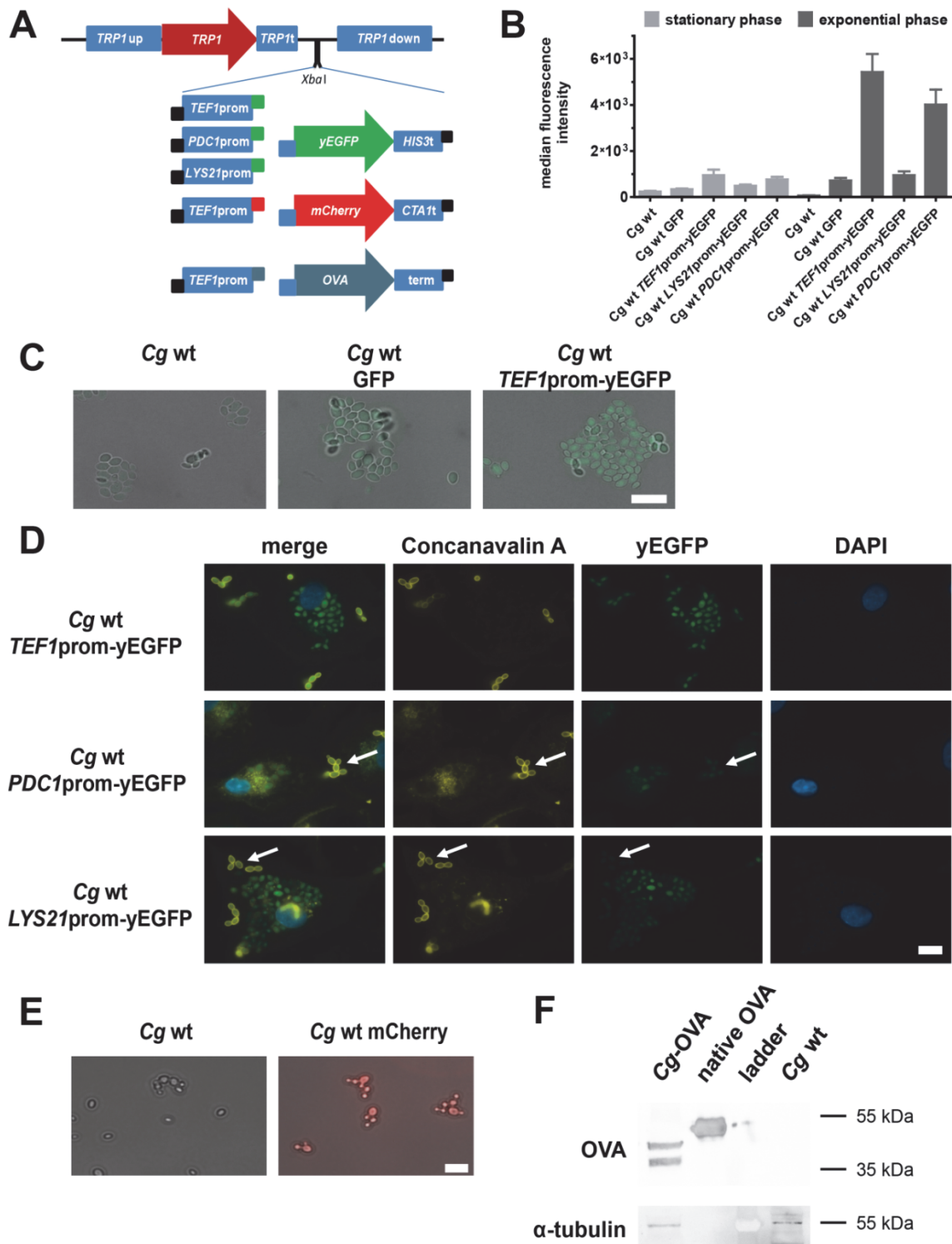
FIGURE 2: Heterologous expression of yEGFP, mCherry, and ovalbumin in *C. glabrata*. (A) Overview of constructed plasmids for yEGFP, mCherry, and ovalbumin (OVA) expression in *C. glabrata*. Three different promotors were fused with yEGFP, and the constitutive *CgTEF1* promotor was fused either with mCherry or OVA. The constructs were subsequently cloned into the XbaI-linearized pTRP1 plasmid. (B-

E) The fluorescence of the different strains was evaluated by (B) flow cytometry of cells grown in culture medium and (C-E) by fluorescence microscopy, during (D) infection of macrophages and (C and E) *in vitro* growth in minimal medium of stationary phase yeast cells (scale bar: 10 μm). (B) All strains, grown in YPD at 37°C and 180 rpm (stationary phase), were diluted 1:20 in fresh YPD and incubated 2 h under the same growth conditions (exponential phase). Yeast cells of both growth phases were analyzed for green fluorescence (FITC channel) using BD FACS Verse. (D) Primary human macrophages (hMDMs) were infected with yeast cells at an MOI of 5 and incubated for 3 h at 37°C and 5% CO_2. Non-phagocytosed yeast cells were counterstained with Alexa Fluor 647-coupled concanavalin A (representative examples shown by arrows). (F) Equal amounts of protein extracts were of the OVA-expressing *C. glabrata* (*Cg*-OVA), the parental strain (*Cg* wt) and isolated egg white ovalbumin (OVA) were blotted and probed for OVA. A separate gel with the same amounts was probed for α-tubulin (loading control). The protein sizes were estimates by using PageRuler Plus prestained (Fisher Scientific).
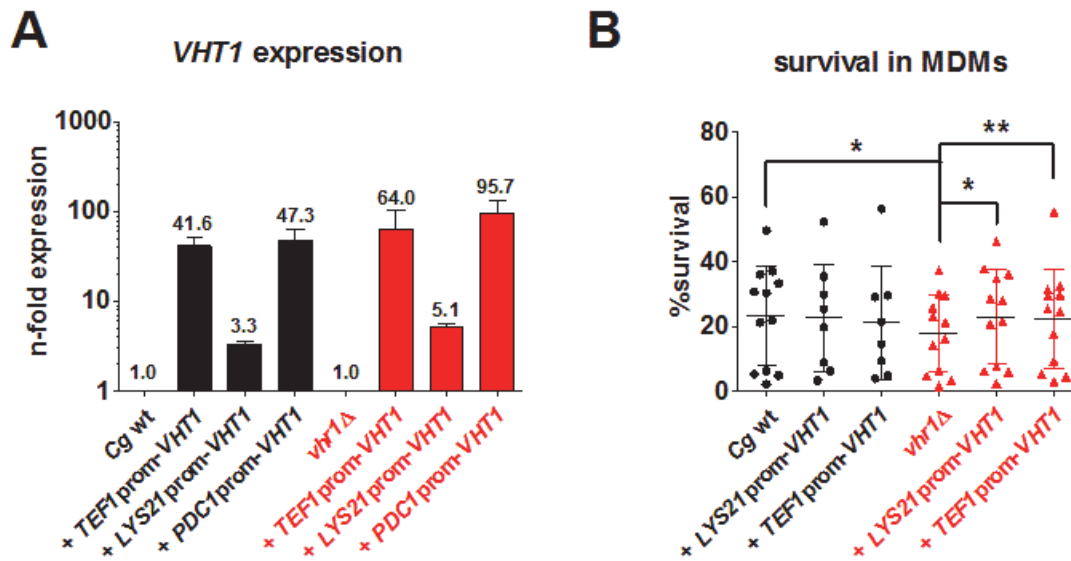
FIGURE 3: The overexpression of _VHT1_ increases intracellular fitness of _vhr1Δ_.

(A) _C. glabrata_ wt (black letters), mutant (_vhr1Δ_, red letters), and corresponding overexpression strains (+_LYS21_prom-_VHT1_, +_TEF1_prom-_VHT1_, +_PDC1_prom-_VHT1_) were cultivated in YPD for 90 min at 37 °C and 180 rpm. Target gene expression was analyzed by qRT-PCR and normalized to _ACT1_ and _EFB1_. Expression is shown relative to the parental strain. Data are shown as mean ± SD of two independent experiments. (B) _C. glabrata_ wt (black letters), mutant (_vhr1Δ_, red letters), and corresponding overexpression strains (+p_LYS21_-_VHT1_, +p_TEF1_-_VHT1_) were pre-cultured in YPD + 2 mg/L biotin before confrontation with hMDMs. Survival of _C. glabrata_ strains after 3 h co-incubation with hMDMs at an MOI of 1, shown as % of survival (mean ± SD). Each single dot represents one technical replicate/blood donor (at least eight donors in two independent experiments). For statistical analysis, a repeated measures ANOVA with Bonferroni's multiple comparison test was performed comparing all strains (* $p \leq 0.05$, ** $p \leq 0.01$).
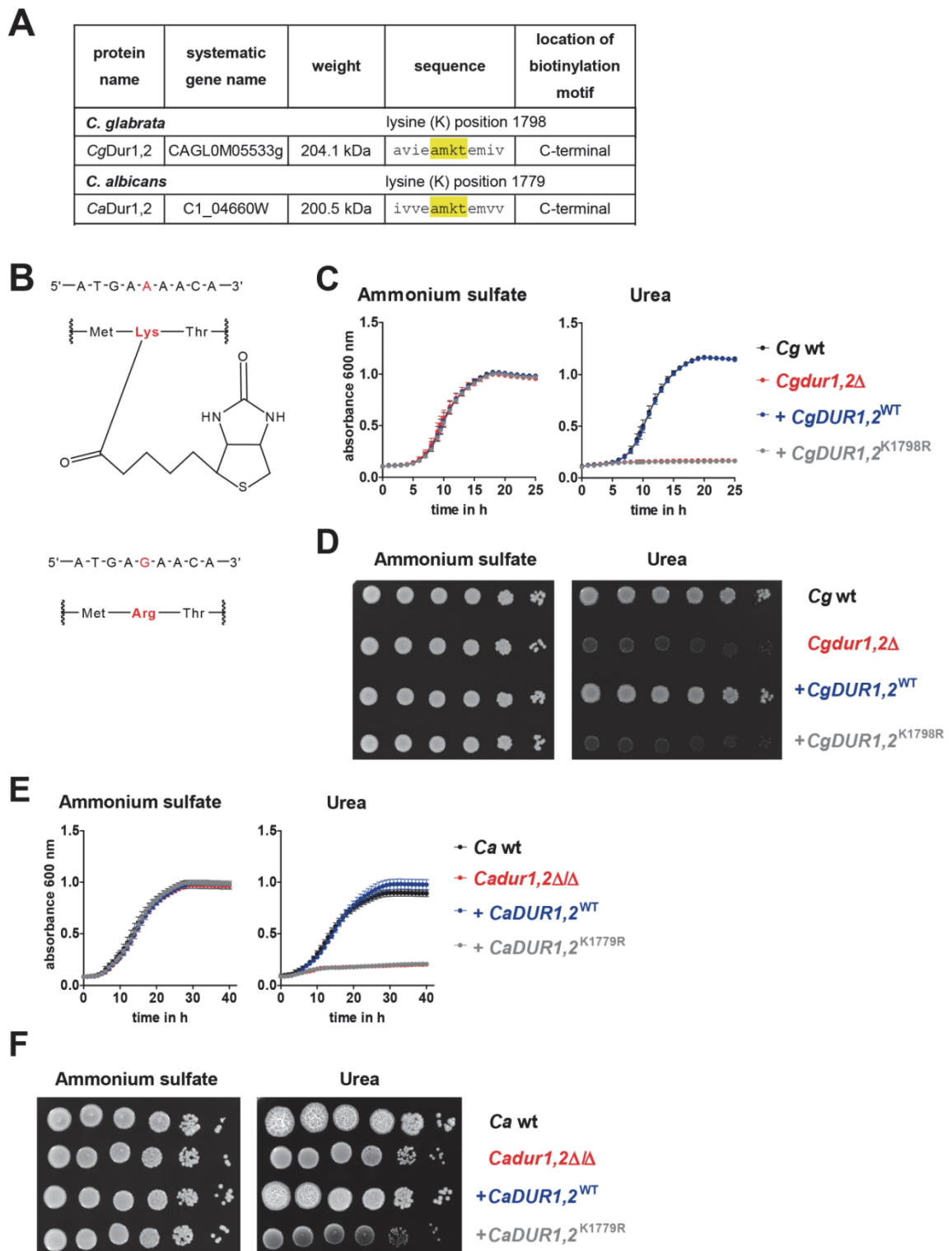
FIGURE 4: **Biotinylation of Dur1,2 is essential for urea utilization.** (A) Dur1,2 possess a highly conserved biotinylation motif (AMKT) in *C. glabrata* and *C. albicans*. (B) Upper part: DNA sequence which is transcribed into the lysine (K) residue essential for biotinylation and biotin structure coupled to lysine. Lower part: The adenine of the triplet codon was mutated to guanine to induce an amino acid exchange to arginine.

(C-F) Growth analysis of (C-D) *C. glabrata* wt, *Cgdur1,2Δ, + CgDUR1,2*^{WT}*, and CgDUR1,2*^{K1798R} and (E-F) *C. albicans* wt, *Cadur1,2Δ/Δ, + CaDUR1,2*^{WT}*, and CaDUR1,2*^{K1779R} in (C, E) liquid and on (D, F) solid minimal medium at 30°C (E) or 37°C (C, D, and F) containing either 0.5% ammonium sulfate or 0.5% urea as sole nitrogen source. Values are represented as mean ± SD of at least three replicates and representative picture are shown.

3 Additional results on manuscript II

The following results are related to **manuscript II**.

3.1 The conservation of the biotin biosynthesis gene cluster and the regulated biotin transport among pathogenic *Candida* species

A common ancestor of *Candida* and *Saccharomyces* species has lost the biotin biosynthetic pathway, and parts of the biosynthetic pathway were rebuilt through horizontal gene transfer from different proteobacteria and neofunctionalization [317]. Some *S. cerevisiae* strains possess the biosynthesis genes *BIO1* and *BIO6* enabling the *de novo* synthesis of biotin ([318], **Figure 3A**). Most strikingly is the comparison to, mainly in the environment found, fungal pathogens, like *Aspergillus* and *Histoplasma*, which possesses a complete biosynthetic pathway to produce biotin *de novo* [299].
Interestingly, different *Candida* species contain a different set of genes in the pathway of biotin synthesis as indicated in **manuscript II, Figure S1**. The biosynthesis starting from KAPA is present in *C. albicans* and *C. tropicalis*, whereas *C. dubliniensis* and *C. auris* progressively minimized the pathway and only the *BIO2* remains in the genome. Interestingly, the closest relative of *C. albicans*, *C. dubliniensis* possesses no orthologues of *BIO3-5* and was only able to use DTB (**manuscript II, Figure S1**). *C. glabrata* and *C. parapsilosis* have lost the whole biosynthetic pathway and probably rely only on biotin uptake from the environment (**Figure 3B**). **Manuscript II** showed that orthologs of the biotin transporter *Ca*Vht1 and the biotin regulator *Ca*Vhr1 are present in *C. glabrata* and *C. albicans*. *In silico* analyses revealed that orthologs of these genes can be found in as well in other medically important *Candida species* (**Table 3**).
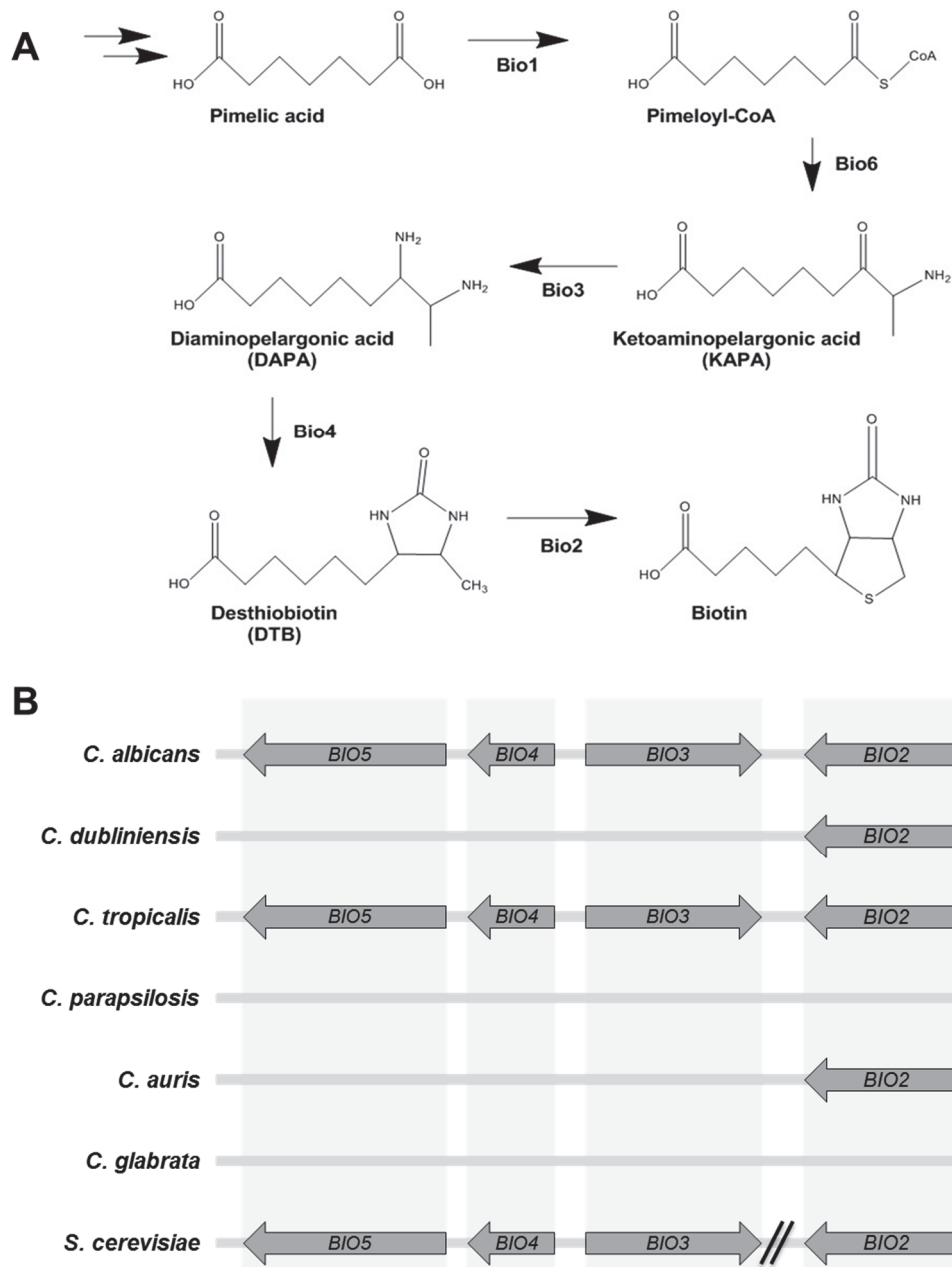
Figure 3. The biotin biosynthetic gene cluster in medically important *Candida* species and *S. cerevisiae*. (A) Biotin biosynthetic pathway. (B) [317] showed and *in vitro* growth analyses suggested that *C. albicans*, *C. tropicalis*, and *S. cerevisiae* are equipped with *BIO2-5*, whereas *C. dubliniensis* and *C. auris* can exclusively use DTB and *C. glabrata* and *C. parapsilosis* are not able to use biotin precursors. *II BIO2* in *S. cerevisiae* is not located in the cluster with *BIO3-5*.

Table 3: Putative orthologs of *Ca*Vht1 and *Ca*Vhr1 in other medically important *Candida* species. The percentage of identical amino acids between *Candida* species and *S. cerevisiae* was analyzed with CDG [31] or CloneManager 9 (with asterisks).

| *C. albicans*	*Ca*Vht1 orf19.2397	Identities	*Ca*Vhr1 orf19.7468	Identities
C. dubliniensis	Cd36_28410	91.2%	Cd36_25730	89.6%
C. parapsilosis	CPAR2_802240	78.4%	CPAR2_804070	49.7%
C. tropicalis	CTRG_00773	76.4%	CTRG_01006	64.2%
C. auris	B9J08_002974	70.3%	B9J08_000684	38.4%
C. glabrata	CAGL0K04609g	25.9%*	CAGL0M12496g	26%*
S. cerevisiae	YGR065C	19%*	YIL056W	21.7%

3.2 The transcriptional regulation of *CgVHT1* and *CgBPL1* depends on nutrient sources, but not *CgVHR2*

The availability of different nutrients affects the transcription of *C. albicans* metabolic genes to improve metabolization of these nutrients, or to shut down other, unneeded metabolic pathways [281, 319]. To analyze how the expression of biotin-related genes is affected by different nutrient conditions, the transcription of the biotin transporter gene *CgVHT1* and the biotin protein ligase *CgBPL1* in response to different carbon- and nitrogen sources in combination with variations in biotin levels was analyzed.

The expression of *CgVHT1* and *CgBPL1* was strongly induced during logarithmic growth under biotin limitation in the presence of glucose (**manuscript II** and [320]). When comparing the expression of both genes between logarithmic and stationary *C. glabrata* cultures in nutrient-rich YPD medium, transcript levels were reduced during logarithmic compared to stationary growth. This suggests that progressive biotin depletion or accumulated metabolites caused increasing expression of biotin-responsive genes upon prolonged (stationary) growth (**Figure 4A**). Overall, the level of regulation was similar between *CgVHT1* and *CgBPL1*, suggesting similar regulation mechanisms of these genes (**Figure 4B**). While the expression of *CgVHT1* and *CgBPL1* was strongly induced in media lacking biotin and containing glucose as carbon source and ammonium sulfate as nitrogen source, media with non-fermentable carbon sources like glycerol and amino acids only marginally induced *CgVHT1* and *CgBPL1* expression (**Figure 4B**). Furthermore, the addition of amino acids to glucose-containing media reduced the transcript abundance of *CgVHT1* and *CgBPL1* by app. 50% (**Figure 4B**). This indicates that amino acid-dependent processes can overcome the need for *VHT1* under biotin limitation (see also **manuscript II**) and that potentially other regulators in addition to *Cg*Vhr1 are involved in the regulation of these genes.

Upregulation of *CgVHT1* and *CgBPL1* under biotin limitation was strongly dependent on *Cg*Vhr1 at early time points (90 min) (**manuscript II**). *CgVHT1* expression, however, gets induced to wild type (wt)-like levels at later time points (180 min) in the absence of *VHR1* (**Figure 4C),** suggesting a role of *Cg*Vhr1 for an initial upregulation of *CgVHT1*. However, this also suggests that additional regulators exits, which are involved in *CgVHT1* regulation at later time points.
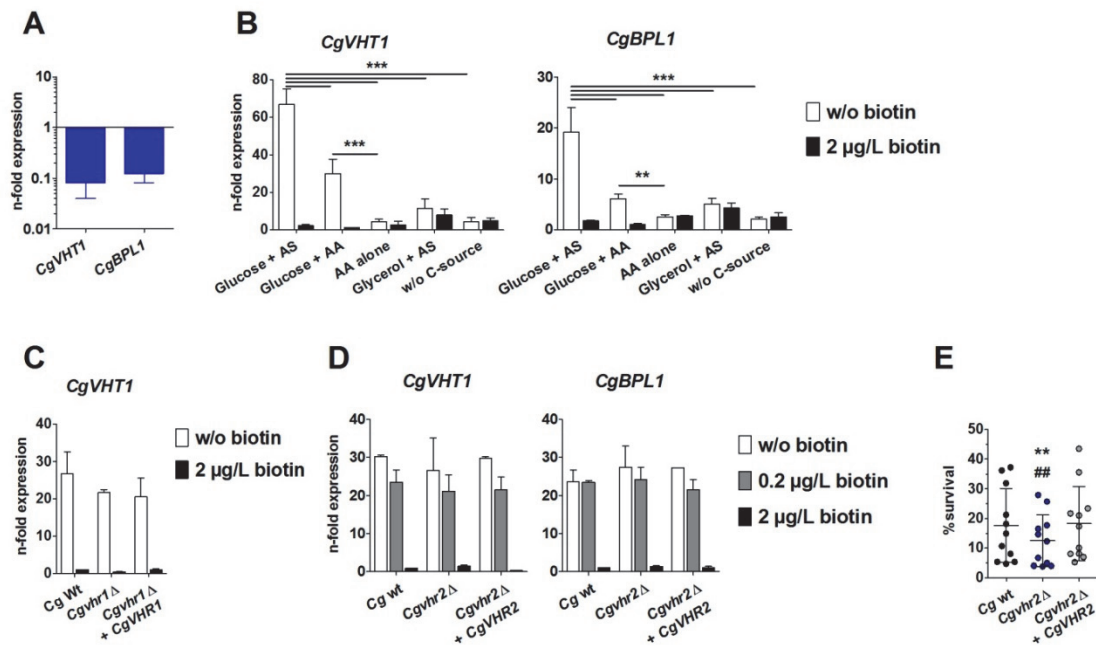
Figure 4: Growth phase and nutrient sources dependent expression of *CgVHT1* and *CgBPL1*. Stationary *C. glabrata* cells were incubated in (A) fresh YPD, (B) minimal medium containing 2% glucose and 0.5% ammonium sulfate (AS), 1% casamino acids (AA) or 3% glycerol, or (C) minimal medium containing 2% glucose and 0.5% ammonium sulfate (AS) for (A-B) 90 min or (C) 180 min at 37°C and 180 rpm with or without biotin. Target gene expression was analyzed by qRT-PCR and normalized to *CgACT1*, *CgEFB1* and *CgEFT2*. Values are represented as mean + SD of three independent experiments, whereby n-fold expression for each gene is shown relative to (A) stationary phase culture or (B-C) culture with glucose and ammonium sulfate and 2 µg/L biotin. For statistical analysis, a Two-way ANOVA with Bonferroni post-tests was used (**$p \le 0.01$, *** $p \le 0.001$; comparing different nutrient sources). (D) Stationary *C. glabrata* cells were incubated in minimal medium containing 2% glucose and 0.5% ammonium sulfate for 90 min at 37°C and 180 rpm with indicated biotin concentrations. Target gene expression was analyzed by qRT-PCR and normalized to *CgACT1*, *CgEFB1* and *CgEFT2*. Values are represented as mean + SD of three independent experiments, whereby n-fold expression for each gene is shown relative to glucose and ammonium sulfate with 2 µg/L biotin. (E) *C. glabrata* wild type (wt), mutant (*Cgvhr2Δ*), or complemented strain (*Cgvhr2Δ + CgVHR2*) were confronted with human blood monocyte-derived macrophages (hMDMs). Survival of *C. glabrata* strains after 3 h, (% survival of inoculum) is shown. Values are represented as scatterplots with mean ± SD and each single dot corresponds to one blood donor (total of eleven different donors in at least three independent experiments). For statistical analysis, a Repeated Measures ANOVA with Bonferroni's multiple comparison test was performed (** $p \le 0.01$ comparing wt and deletion mutant; ## $p \le 0.01$ comparing deletion mutant to the complemented strain).

S. cerevisiae possesses the putative transcription factor Vhr2 (YER064C) with high similarities to Vhr1 in terms of the protein sequence as well as DNA binding specificity [321]. The *VHR2* gene arose from whole genome duplication in the ancestor of *S. cerevisiae*, belongs to the basic leucine zipper domain (bZIP) transcription factor family and is also present in *C. glabrata* (CAGL0J03014g), but not in *C. albicans* [31, 322]. To analyze whether *Cg*Vhr2 is an additional *CgVHT1* regulator, a deletion strain of CAGL0J03014g (*Cgvhr2Δ*) and a complemented strain (*Cgvhr2Δ + CgVHR2*) with its native promotor were constructed. These strains were analyzed for transcriptional inducibility of *CgVHT1* and *CgBPL1* under biotin limitation and for survival within primary human monocyte-derived macrophages (hMDMs). *CgVHR2* was not involved in the transcriptional control of *CgVHT1* and *CgBPL1* (**Figure 4D**), but was necessary for survival of *C. glabrata* inside macrophages (**Figure 4E**). These data suggest that *CgVHR2* has yet unknown regulatory functions in *C. glabrata* that are independent of biotin transport (**Figure 4E**).
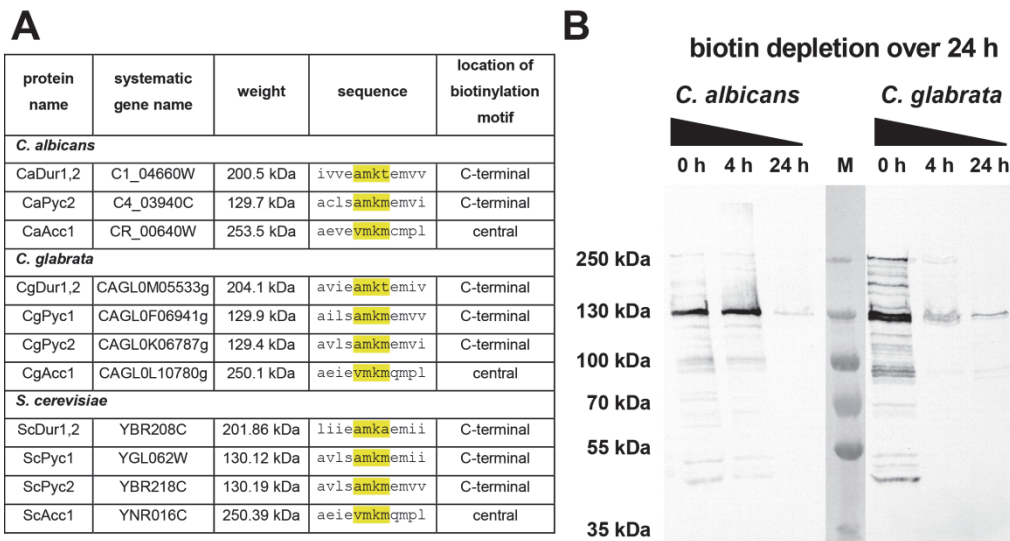
In summary, these data show that the regulation of biotin-related genes in *C. glabrata* is influenced by nutritional conditions. It also suggests that additional transcriptional regulators, in addition to Vhr1, affect *VHT1* and *BPL1* expression in order to fine-tune the biotin levels of *C. glabrata* in response to environmental stimuli.

3.3 Major biotin-dependent carboxylases possess a biotinylation motif, and pyruvate-carboxylase genes are regulated by biotin

The depletion of biotin increases the expression of the biotin transporter gene *VHT1* and biotin protein ligase gene *BPL1* to sustain sufficient biotin import and attach biotin to biotin dependent proteins to ensure functioning of biotin-dependent processes (**manuscript II**). These are essential for key metabolic pathways, like fatty acid metabolism, gluconeogenesis and amino acid metabolism, requiring most highly biotinylated pyruvate carboxylase Pyc1/2 and acetyl carboxylase Acc1 (**Figure 5B**)[323, 324]. Corrspondingly, several studies in *S. cerevisiae* show that Pyc1/2- and Acc1-deficient strains are severely attenuated in general growth [325-328]. Biotinylation is a covalent posttranslational modification of lysine residues in proteins being essential for carboxylation reactions [329]. The specific biotinylated lysine residue in pyruvate carboxylases Pyc1/2, acetyl-CoA carboxylase Acc1 and urea amidolyase Dur1,2 of *S. cerevisiae* is located in a highly conserved AMKM motif [330, 331]. Previous studies showed that site-directed mutagenesis of this lysine residue affects biotinylation [330] and the first methionine residue is critical for carboxylase activity [332].

By using *in silico* analyses biotin-dependent carboxylases were found in *C. albicans* and *C. glabrata* possessing this motif with slight sequence modifications (**Figure 5A**). Alanine in the biotinylation motif of Acc1 was substituted by valine (AMKM → VMKM), and the last methionine in the biotinylation motif of Dur1,2 was replaced by threonine (AMKM → AMKT) in both *Candida* spp. and by alanine in *S. cerevisiae*. The impact of these amino acid substitutions on biotinylation efficiency and enzymatic activity of the respective carboxylase is unknown. Still, the first methionine, required for enzymatic activity, is present in all of these biotinylation motifs. The necessity of the lysine residue in the biotinylation motif of Dur1,2 is demonstrated in **manuscript V**.

protein name	systematic gene name	weight	sequence	location of biotinylation motif
C. albicans				
CaDur1,2	C1_04660W	200.5 kDa	ivve<mark>amkt</mark>emvv	C-terminal
CaPyc2	C4_03940C	129.7 kDa	acls<mark>amkm</mark>emvi	C-terminal
CaAcc1	CR_00640W	253.5 kDa	aeve<mark>vmkm</mark>cmpl	central
C. glabrata				
CgDur1,2	CAGL0M05533g	204.1 kDa	avie<mark>amkt</mark>emiv	C-terminal
CgPyc1	CAGL0F06941g	129.9 kDa	ails<mark>amkm</mark>emvv	C-terminal
CgPyc2	CAGL0K06787g	129.4 kDa	avls<mark>amkm</mark>emvi	C-terminal
CgAcc1	CAGL0L10780g	250.1 kDa	aeie<mark>vmkm</mark>qmpl	central
S. cerevisiae				
ScDur1,2	YBR208C	201.86 kDa	liie<mark>amka</mark>emii	C-terminal
ScPyc1	YGL062W	130.12 kDa	avls<mark>amkm</mark>emii	C-terminal
ScPyc2	YBR218C	130.19 kDa	avls<mark>amkm</mark>emvv	C-terminal
ScAcc1	YNR016C	250.39 kDa	aeie<mark>vmkm</mark>qmpl	central

Figure 5: Protein biotinylation in *C. albicans* and *C. glabrata*. (A) Biotin-dependent carboxylases possess a highly conserved biotinylation motif (AMKM, with single amino acid divergence) in *C. glabrata*, *C. albicans* and *S. cerevisiae*. (B) Western blot of biotinylated proteins of *C. albicans* (SC5314; left) and *C. glabrata* (ATCC2001; right). Both strains were cultivated in biotin-free SD medium at 180 rpm and 30°C or 37°C, respectively. The yeast cell suspension was harvested after 4 and 24 h by centrifugation. The 0 h time point (stationary phase culture, YPD) was used as control.

Biotinylated proteins are recognized by high affinity biotin-binding proteins like avidin and streptavidin [333], and are detectable in Western blots with avidin/streptavidin conjugated to horseradish peroxidase (HRP). To analyze the biotinylated protein pattern during biotin depletion, Western blots of whole cell extracts of *C. glabrata* and *C. albicans* after 4 and 24 h were performed. The most prominent and stable biotinylated protein had a size of approximately 130 kDa, which, according to size prediction ((**Figure 5A**) and [31]), correlates to a pyruvate carboxylase (**Figure 5B**). As predicted by the *in silico* analyses (**Figure 5A**), *C. glabrata* extracts showed two protein bands, corresponding to two pyruvate carboxylase isoforms (Pyc1 and Pyc2), similar to *S. cerevisiae* [325]. The larger band, likely corresponding to CgPyc1 (129.9 kDa),

remained more biotinylated after 24 h of biotin depletion. Comparing both *Candida* species, *in silico* analyses suggest that *C. albicans* reduced the number of carboxylases and relies on one pyruvate carboxylase, encoded by *CaPYC2* (**Figure 5A**). A biotinylated protein with a molecular size of approximately 250 kDa, correlating to the predicted size of the acetyl-CoA carboxylase Acc1, was present in the stationary phase culture of both species, but it diminished during cultivation under biotin limitation (**Figure 5B**).
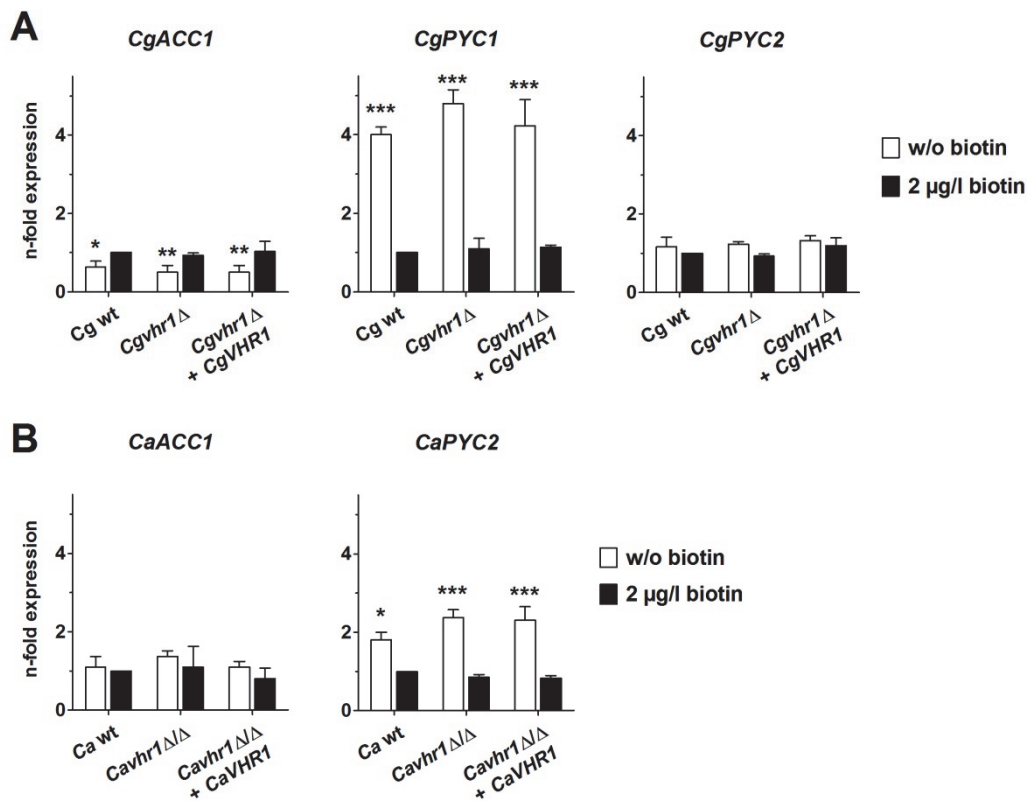
Figure 6: Expression of biotin-dependent carboxylase genes *ACC1* and *PYC1/2* in *C. albicans* and *C. glabrata*. (A) *C. glabrata* wt, mutant (*Cgvhr1Δ*), and complemented strain (*Cgvhr1Δ+CgVHR1*) and (B) *C. albicans* wt, mutant (*Cavhr1Δ/Δ*), and complemented strain (*Cavhr1Δ/Δ+CaVHR1*) were pre-cultivated in YPD and then incubated in minimal medium for 180 min at 37°C and 180 rpm. Target gene expression was analyzed by qRT-PCR and normalized to *CgACT1, CgEFT2, CgEFB1,* or *CaTDH3* and *CaEFB1*. Values are represented as mean + SD of three independent experiments, whereby n-fold expression for each gene is shown relative to the wt in 2 µg/L biotin. For statistical analysis, a Two-way ANOVA with Bonferroni post-tests was used (*$p \leq 0.05$, **$p \leq 0.01$, *** $p \leq 0.001$; comparing 2 µg/L biotin and w/o biotin).

Studies in *S. cerevisiae* hinted at the pyruvate carboxylases of importance in, both, biotin sensing and inducing a biotin-starvation response (upregulation of Vhr1-dependent genes) [334], but it remained unknown how biotin availability affects the

expression of biotin acceptor genes in *Candida* species. Therefore, the transcript levels of the corresponding *PYC* and *ACC* genes in *C. glabrata* and *C. albicans* were analyzed. The expression of the both *ACC1* genes, in *C. glabrata* and *C. albicans*, was only marginally regulated by biotin, whereas the transcript abundance of *CgPYC1* and *CaPYC2* increased upon biotin limitation (**Figure 6A-B**). Taken together, the upregulation of *CgPYC1* and *CaPYC2* together with the mostly stable biotinylation upon biotin limitation indicate the importance of these enzymes for cellular metabolism.

3.4   The usage of alternative biotin-sources is Vht1-dependent

In association with the mammalian host, free biotin could be restricted to invading microbes as mammalian cells are also auxotrophic for biotin and need to recycle biotin by proteolytic digestion of biotinylated proteins, releasing biocytin [335]. This intermediate is degraded to lysine and biotin by biotinidase activity (**Figure 7A**)[335]. During host invasion and damage of various cell types, alternative host-derived biotin sources like biotinylated proteins or biocytin could be available. Therefore, growth analyses with these potential host-derived biotin sources were performed. Analogous to the experiments in **manuscript II**, biotin-starved *Candida* cells were used.

C. albicans and *C. glabrata* wild type cells were able to use these alternative biotin sources for robust growth suggesting that both fungi are enzymatically equipped to further process these sources as shown in **manuscript II** (**Figure S1**). *VHT1* but not *VHR1* deletion mutants of both species, however, were defective in growth with biotinylated BSA and biocytin (**Figure 7B-C**), suggesting that Vht1 may import these host biotin sources. Previous studies, however, showed that uptake of labeled biotin cannot be inhibited by biocytin, indicating that Vht1 is high selective for biotin [336]. These data suggest that extracellular enzymatic processing of biotinylated substrates and biocytin to biotin might be required, followed by biotin uptake depending on the biotin transporter Vht1 (**manuscript II, Figure 3**).
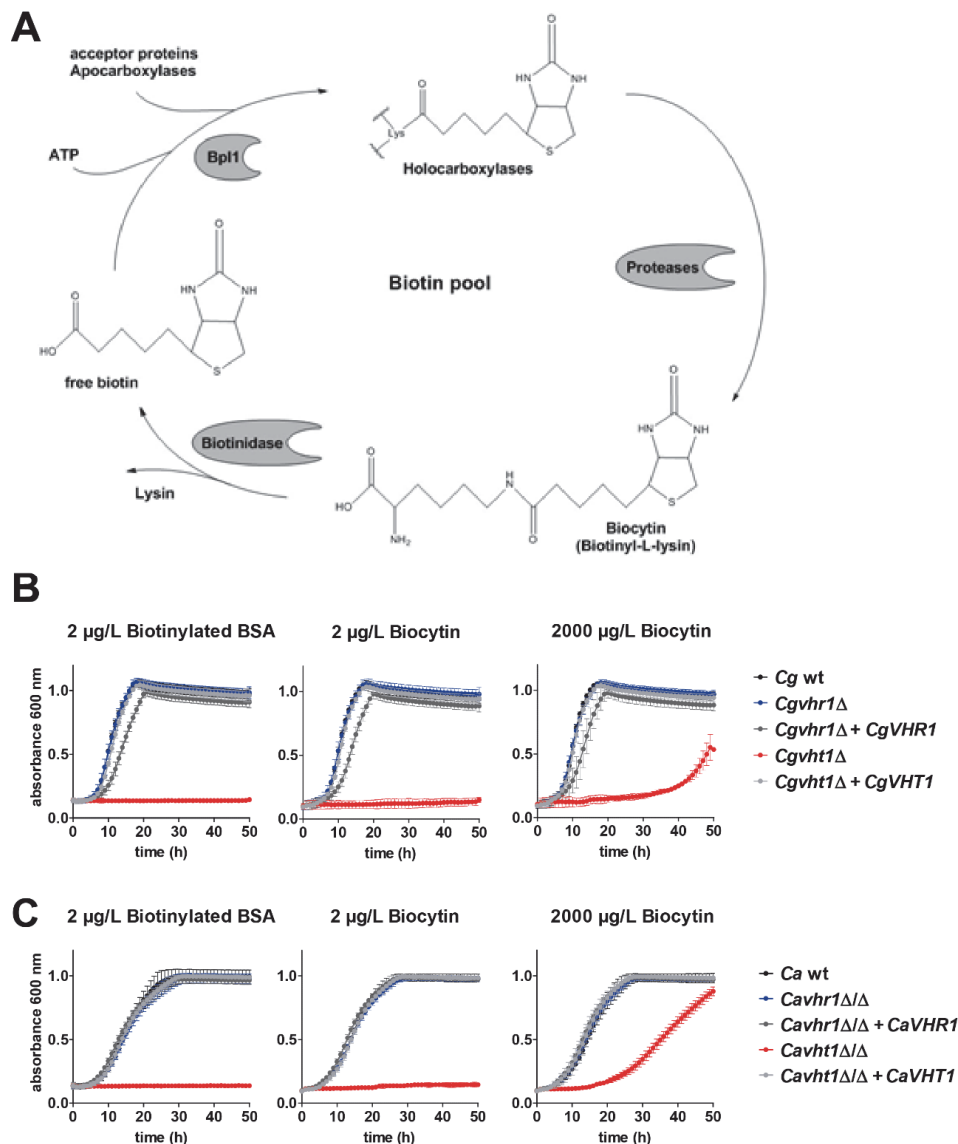
Figure 7. The usage of alternative biotin sources is Vht1-dependent.
(A) Biotin is cycled within the cell during an uncoupled (free) and coupled state mediated by enzymatic reactions. The biotin-protein ligase 1 (Bpl1) covalently links biotin to acceptor proteins like apocarboxylases, generating functional active holocarboxylases. Protein turnover by proteases releases biocytin (biotinyl-L-lysine), which is further metabolized to lysine and biotin by biotinidase activity. (B-C) Yeast growth of biotin pre-starved wt, mutants (*vhr1Δ*, *vht1Δ*), or complemented strains (*vhr1Δ + VHR1*, *vht1Δ + VHT1*) of (B) *C. glabrata* (37°C) or (C) *C. albicans* (30°C) in minimal medium containing 2 µg/L biotinylated BSA, 2 µg/L or 2 mg/L biocytin. Values are represented as mean ± SD of at least three replicates.

3.5 Biotin promotes amino acid-induced growth by increasing environmental pH and ammonia release

Certain conditions can bypass the need for biotin. *C. glabrata* is able to grow in media with casamino acids (CAA) as a sole carbon- and nitrogen source in the absence of biotin dependent on *CgVHR1* (**manuscript II, Figure S3**). Still, growth is significantly enhanced under such conditions, when biotin is present (**Figure 8A**), suggesting that amino acids can only partially bypass the requirement for biotin. In medium with CAA

as a sole carbon- and nitrogen source, *C. albicans* is known to induce filamentation associated with an increase in environmental pH [283]. This *C. albicans*-driven alkalinization is caused by ammonia release due to the catabolism of amino acids [283]. As biotin promotes filamentation in *C. albicans* [337, 338], we analyzed the impact of biotin on filamentation under alkalinization-inducing conditions.

In medium with an initial pH of 4.5, colony wrinkling, indicating filamentation of the *C. albicans* wild type, was only visible when sufficient amounts of biotin (2 µg/L) were added (**Figure 8B**). Noteworthy, the initial increase to a neutral pH (pH 6.5) abolished this phenotype and the *C. albicans* wild type showed a fuzzy-wrinkled colony morphology independent of biotin addition, suggesting that a neutral pH bypasses the requirement of biotin-promoted alkalinization for filamentation (**Figure 8B**).

C. glabrata requires *CgVHR1* for growth under conditions that combine low biotin with limitations of optimal C- and N-sources, like the growth with amino acids [338]. To find out whether *CaVHR1* and other *C. albicans* biotin-metabolic genes have an impact on the above-described colony wrinkling, we investigated the colony morphology of biotin-metabolic mutants when growing on agar containing CAA adjusted to an initial pH of 4.5. The degree of colony wrinkling was reduced in the *CaVHR1* deletion mutant and remained unaffected by addition of either higher amounts of biotin or biotin precursors (**Figure 8C**). The deletion of the partial biotin biosynthesis pathway genes *BIO2-5* demolished the ability of *C. albicans* to grow with the biotin precursors KAPA and DTB [338]. This result was further supported by the fact that the *Cabio2-5Δ/Δ* mutant did not show colony wrinkling on agar with KAPA or DTB as biotin precursors. The *Cavht1Δ/Δ* mutant showed only growth and colony wrinkling with KAPA and high amounts of biotin (**Figure 8C**). This is in line with the fact that high external biotin was needed to support growth in liquid medium in the absence of *VHT1* (**manuscript II**). Similar to this observation, the growth defect of *Cavht1Δ/Δ* was also rescued by addition of KAPA, but not DTB (**Figure 8D**). This indicates that *CaVHT1*, similar to its *S. cerevisiae* ortholog, is also required for DTB uptake [339], whereas KAPA usage does not require *VHT1*.

Environmental alkalinization by *C. albicans* is associated with ammonia release and a rise in environmental pH [283]. Therefore, the impact on ammonia release and environmental pH changes during *C. albicans* and *C. glabrata* growth was visualized with phenol red and measured spectrometrically, respectively. In all experiments, the initial pH was adjusted to 4.5 (yellow color). In the presence of biotin, *C. albicans* and *C. glabrata* wild type growth caused increased pH values, as indicated by an orange to red color (**Figure 9A**) and ammonia release (**Figure 9B**). Of note, *C. glabrata* increased the environmental pH much slower and released ammonia to a lower extent than *C. albicans* (**Figure 9A-B**).
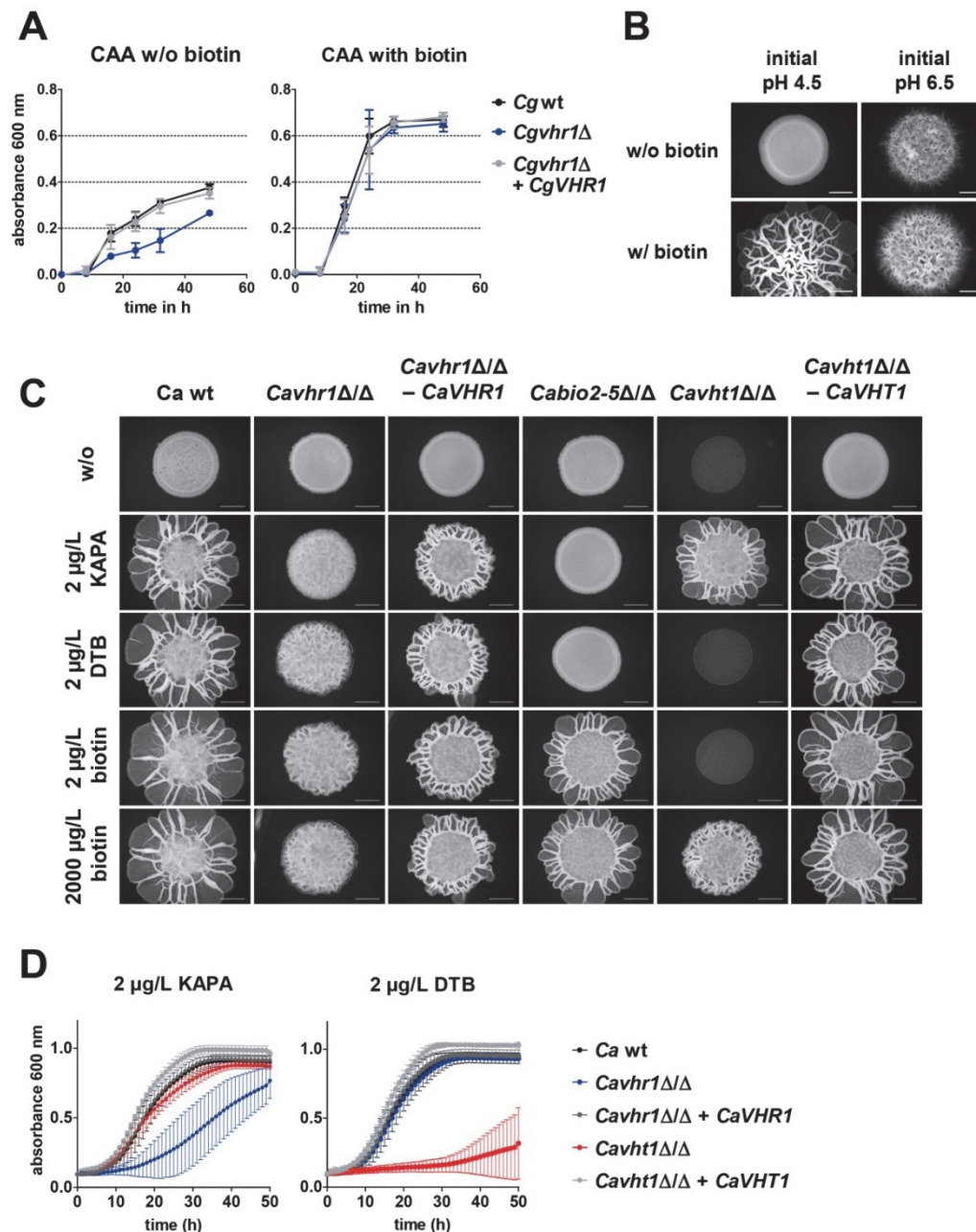
Figure 8: Growth and colony morphology is dependent on biotin availability. (A) Growth of *C. glabrata* wt, *Cgvhr1Δ* and *Cgvhr1Δ + CgVHR1* in liquid YNB-CAA medium without or with 2 µg/L biotin at 37°C and 180 rpm measured every 8 h. (B) The initial pH and the presence of 2 µg/L biotin impaired the colony morphology of 1x10^5 *C. albicans* wt cells grown on YNB-CAA at 37°C for 48 h. (C) *C. albicans* wt, mutants (*Cavhr1Δ/Δ, Cavht1Δ/Δ, Cabio2-5Δ/Δ*), and complemented strains (*Cavhr1Δ/Δ + CaVHR1* or *Cavht1Δ/Δ + CaVHT1*) were spotted on YNB-CAA (initial pH 4.5) in separate wells of a 12-well plate and incubated at 37 °C for 48 h. The colony morphology was documented with binocular microscope (Zeiss), scale bar: 1 mm. (D) Yeast growth of biotin pre-starved *C. albicans* wt, *Cavhr1Δ/Δ, Cavhr1Δ/Δ + CaVHR1, Cavht1Δ/Δ* or *Cavht1Δ/Δ + CaVHT1* at 30°C in minimal medium containing 2 µg/L KAPA or DTB. Values (in A and D) are represented as mean ± SD of at least three replicates.

As expected from our growth and filamentation analyses (**Figure 8A-C**), alkalinization, as seen by the rise in medium pH, and the release of ammonia was enhanced in the presence of biotin. The deletion of *CaVHR1*, but not *CgVHR1*, caused a reduced

medium pH change and ammonia release (**Figure 9B-C**). As expected from previous data (**manuscript II**), the biotin transporter mutants (*vht1Δ*) of both species were unable to grow with intermediate biotin concentrations. This deficiency correlated with the reduced ammonia secretion (**Figure 9C-D**). Collectively, these data suggest that *VHR1* plays a role in the utilization of amino acids in both *Candida* species, and influences the induction of proper *C. albicans* filaments under this specific condition.
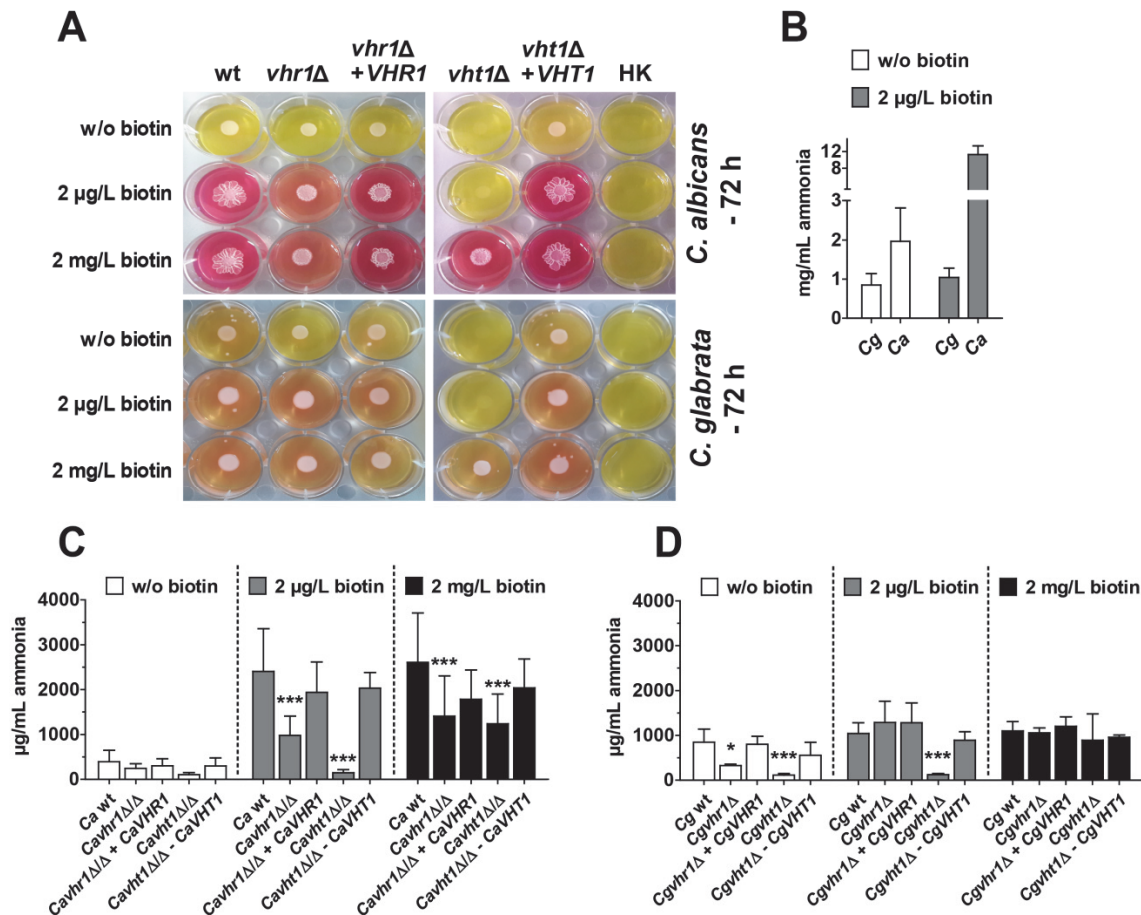
Figure 9: *Candida*-**driven alkalinization and ammonia release is enhanced by biotin and VHR1.** (A) Alkalinization of YNB-CAA-Allantoin agar by wt, mutants (*vhr1Δ*, *vht1Δ*), or complemented strains (*vhr1Δ + VHR1*, *vht1Δ + VHT1*) of *C. albicans* (above) and *C. glabrata* (below) after 72 h incubation at 37°C. HK indicated heat-killed *Candida* cells (70°C, 30 min). The pH was visualized by 20 mg/L phenolred. A pH-increase causes a color change from yellow (initial pH 4.5) over orange to red. Volatile ammonia released by (B) wt cells of *C. albicans* and *C. glabrata* grown 72 h on YNB-CAA-allantoin agar and (C-D) wt, mutants (*vhr1Δ*, *vht1Δ*), or complemented strains (*vhr1Δ + VHR1*, *vht1Δ + VHT1*) of (C) *C. albicans* and (D) *C. glabrata* grown 48 h on YNB-CAA-allantoin agar. Values (in B-D) are represented as mean ± SD of at least three replicates. For statistical analysis, a Two-way ANOVA with Bonferroni post-tests was used (*$p \leq 0.05$, **$p \leq 0.01$, *** $p \leq 0.001$; comparing wt and mutant strains).

3.6 Biotin availability during infection has no influence on the interaction between *C. glabrata* and *C. albicans* and macrophages

Biotin uptake is essential to maintain cellular homeostasis of *Candida* spp. but also of the mammalian host. The host can experience biotin limitation due to specific diets and also during infection by biotin-consuming pathogens. This can have an influence of activities of immune cells. For example, it was shown that human dendritic cells and CD4^{+} T lymphocytes react to biotin limitation with an enhanced pro-inflammatory response [340, 341], whereas monocytic myeloid cells react *vice versa* [342].

The impact of biotin on the ability of macrophages to phagocytose and kill ingested *Candida* cells as well as the *Candida*-induced cytolysis and pro-inflammatory response was so far unknown. To test different macrophage polarization states, primary M-CSF-treated macrophages (hMDMs) were stimulated for 24 h with the Th1 cytokine IFN-γ or the Th2 cytokine IL-4 to favor a pro- or anti-inflammatory macrophage polarization phenotype [343]. Macrophages were then infected with *C. albicans* or *C. glabrata* wild type cells and co-incubated for 1 and 3 h in biotin-depleted or biotin-rich medium to determine phagocytosis and survival rates, respectively. Phagocytosis was nearly unaffected by biotin (**Figure 10A**). Exclusively, the phagocytosis of *C. albicans* by anti-inflammatory macrophages was marginally reduced (**Figure 10A**). While fungal biotin conditions before macrophage confrontation had an impact on *C. glabrata* and *C. albicans* survival (**manuscript II**), the survival of both *Candida* spp. was not affected by the availability of biotin during the infection. Interestingly, the stimulation with IFN-γ increased phagocytosis-mediated killing of *C. glabrata*, whereas *C. albicans* killing efficiency was unaffected by macrophage stimulation (**Figure 10B**).

In order to determine the impact of biotin on fungus-driven cytolysis and release of pro-inflammatory mediators (IL-1β, TNFα, IL-6 and IL-8), unstimulated macrophages (M-CSF-treated) were infected with *C. albicans* and *C. glabrata* wild type cells and co-incubated for 24 h in presence or absence of biotin. In accordance with previous studies [178, 211, 344], *C. albicans* induced a strong cytokine release by and damage of macrophages (app. 70% cytotoxicity), whereas *C. glabrata* induced no visible macrophage damage and low IL-1β secretion (**Figure 10C-D**). However, the release of IL-6 and TNF-α was comparable between both fungal species, and only the secretion of IL-1β and the chemokine IL-8 were attenuated in *C. glabrata* infected macrophages (**Figure 10D**). Biotin had no effect on the secretion of the tested pro-inflammatory cytokines and there were only marginal survival differences for *C. glabrata* between the two macrophage polarization states.
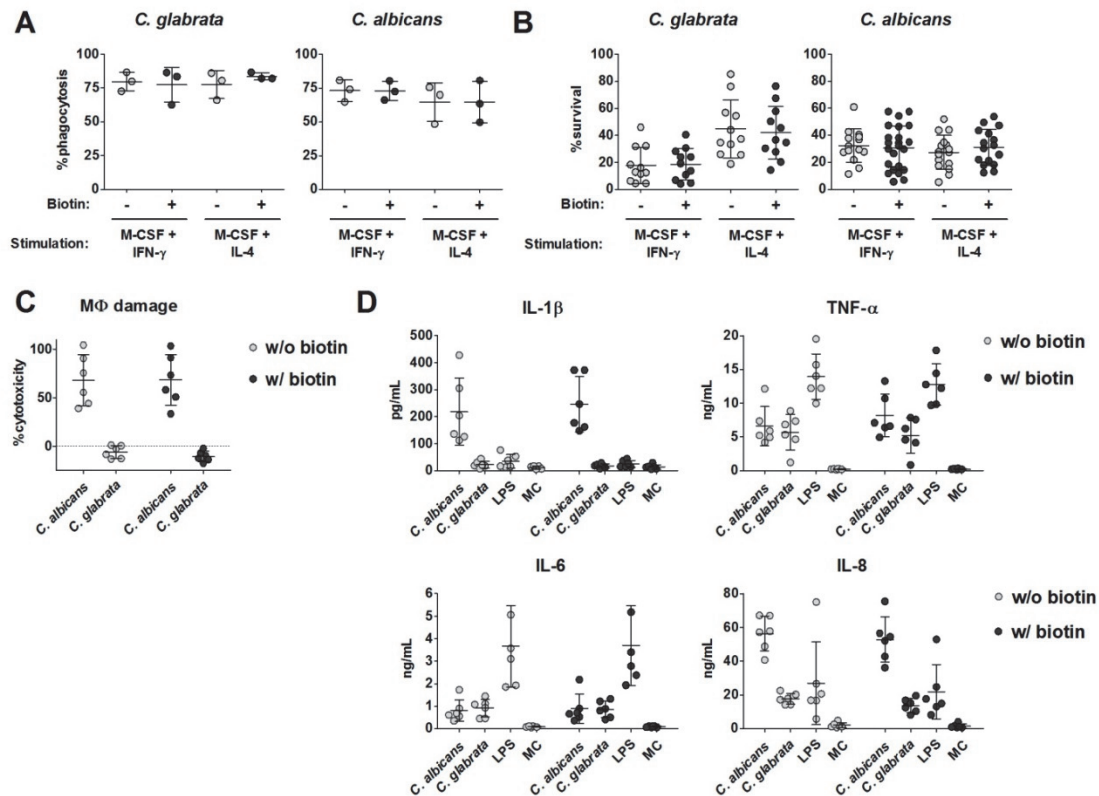
Figure 10: Interaction of *C. albicans* and *C. glabrata* with macrophages depending on biotin availability. *C. glabrata* or *C. albicans* wt cells were confronted with human blood monocyte-derived macrophages (hMDMs) pre-cultivated either IFN-γ and M-CSF or IL-4 and M-CSF without (-) or with (++) 200 µg/L biotin. (A) Uptake of yeast cells (% phagocytosis) was quantified by differential staining after 1 h of co-incubation (MOI 2). (B) Fungal survival after 3 h, (% survival of inoculum). (C) Cytolysis (% cytotoxicity; 100% refers to full lysis) of and (D) release of pro-inflammatory cytokines and chemokines by unstimulated macrophages after infection with *C. albicans* and *C. glabrata* after 24 h of co-incubation (MOI 5). Positive (LPS; 1 µg/mL) and negative control (MC, medium control) were included. Values are represented as scatterplots (mean ± SD). Each single dot represents one technical replicate/blood donor (at least three donors in two independent experiments).

These data suggest that external biotin levels during interaction of *Candida* cells with macrophages have no influence on host activities like phagocytosis, fungal killing, susceptibility to fungus-driven cell lysis and release of pro-inflammatory mediators. This is in contrast to the fungal internal biotin pool, which is essential for survival and proliferation within macrophages (**manuscript II**).

3.7 Biotin impacts on Ca*VHT1*-dependent macrophage lysis and pro-inflammatory cytokine secretion

The uptake of biotin by the putative biotin transporter Vht1 is essential for *C. albicans* and *C. glabrata* to proliferate in environments with limited biotin, likely encountered in host niches like the macrophage phagosome. Deletion of *VHT1* attenuated fungal

proliferation within macrophages (both species), survival and macrophage lysis (*C. albicans*) (**manuscript II**).

To see whether biotin availability during *C. albicans*-macrophage interaction influences the infection outcome of a strain that strongly depends on biotin, we monitored inflammasome activation, macrophage cytotoxicity and cytokine release after infection with the *CaVHT1* deletion strain. To exclude variations in the fungal biotin pool, all strains were biotin pre-starved. This pre-starvation significantly lowered the intracellular survival of *Cavht1Δ/Δ* (**manuscript II**).

C. albicans is, unlike *C. glabrata*, a potent activator of the NLRP3 inflammasome in macrophages [345]. To study the influence of *CaVHT1* on inflammasome activation, IL-1β secretion by LPS-primed primary hMDMs after infection with biotin-starved *C. albicans* wt, deletion and complemented strains was measured 5 h p.i. The *Caece1Δ/Δ* mutant, known to trigger less IL-1β secretion in hMDMs, was included as control [218, 346]. The *Cavht1Δ/Δ* mutant was completely unable to induce secretion of IL-1β when interacting with macrophages in biotin-free culture medium (**Figure 11A**), while the addition of 2 mg/L biotin restored a wt-like IL-1β secretion. This biotin concentration was sufficient to promote wt-like growth of *Cavht1Δ/Δ* (**manuscript II**).

In order to determine whether the reduced intracellular survival and inflammasome activation of the biotin transporter mutant *Cavht1Δ/Δ* is associated with an altered late cytolysis and progressive pro-inflammatory host response, the release of LDH and the secretion of IL-1β, IL-6, IL-8 and TNF-α was quantified after 24 h of co-incubation. As described in **manuscript II**, the *VHT1* deletion mutant was severely attenuated in damage. The addition of biotin (2 mg/L) partly rescued the damage potential of this mutant (**Figure 11B**). In accordance to that, the secretion of the cytokines IL-1β, IL-6 and TNF-α and chemokine IL-8 was strongly reduced in *Cavht1Δ/Δ*-infected macrophages in a biotin-limited environment and reached wt level in biotin-enriched medium (**Figure 11D-F**).
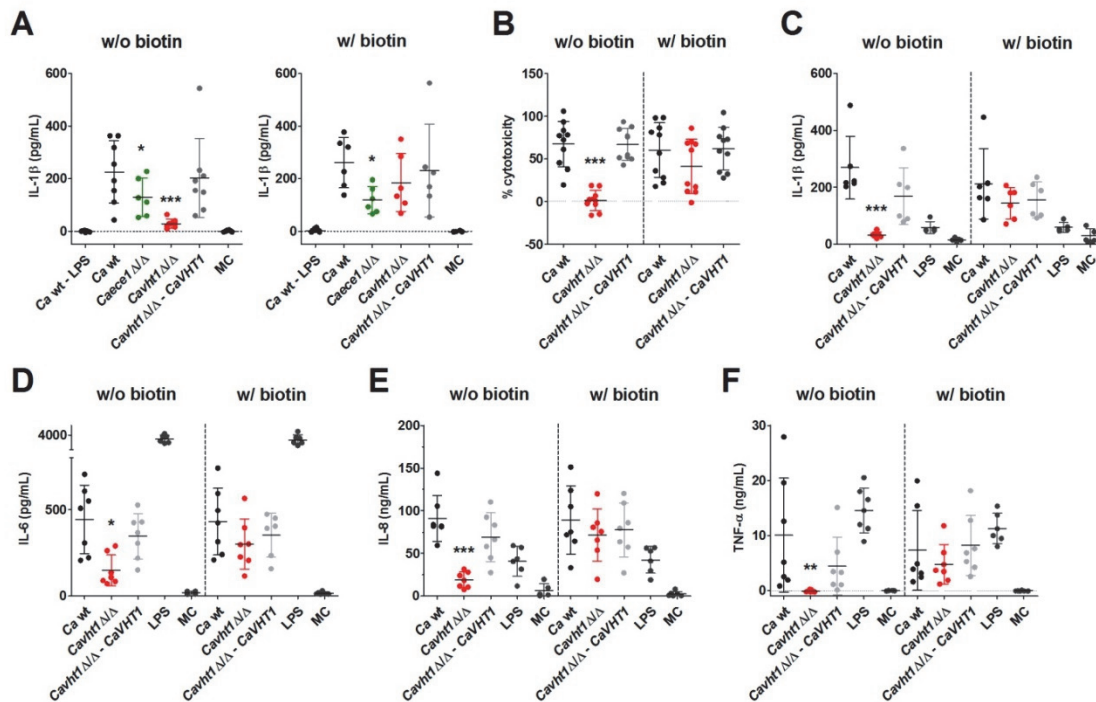
Figure 11: Impact of *VHT1* on interaction of *C. albicans* with macrophages dependent on biotin availability. Biotin-prestarved *C. albicans* wt, mutants (*Cavht1Δ/Δ*, *Caece1Δ/Δ*), or complemented strains (*Cavht1Δ/Δ + CaVHT1*) were confronted with human blood monocyte-derived macrophages (hMDMs) in the absence (w/o) or presence of 2 mg/L biotin (w/). (A) The early IL-1β release was quantified 5 h p.i. with *C. albicans* (MOI 5) of LPS-primed hMDMs (2 h pre-incubation with 50 ng/mL LPS. (B) Cytolysis (% cytotoxicity; 100% refers to full lysis) of and (D-F) release of pro-inflammatory cytokines and chemokines by hMDMs after infection with *C. albicans* 24 h p.i. (MOI 5). Positive (LPS; 1 μg/mL and negative control (MC, medium control) were included. Values are represented as scatterplots (mean ± SD). Each single dot represents one technical replicate/blood donor (at least five donors in two independent experiments). For statistical analysis, a repeated measures ANOVA with Bonferroni's multiple comparison test was performed (* p ≤ 0.05, ** p ≤ 0.01, *** p ≤ 0.001 comparing wt and deletion mutant).

These data imply that Vht1-dependent proliferation of *C. albicans* in biotin-scarce environments mediates cytolysis of macrophages and activation of a pro-inflammatory response. This requirement for *VHT1* can only be overcome when high amounts of biotin are available continuously.

4 Discussion

Pathogenic *Candida* species have evolved sophisticated immune evasion strategies to thrive within macrophages, by surviving antimicrobial activities, adapting to nutrient scarceness, and persisting within or escaping from these cells. The adaptation to the nutritional environment within the phagosome of macrophages needs rapid transcriptional responses. Such responses are common among facultative intracellular pathogens, but need to be fine-tuned dependent on cellular localization of the pathogen, extrinsic nutrient availability, and intrinsic nutrient requirements. In **manuscript I**, these adaptation mechanisms were summarized and discussed, comparing *Candida* species with bacterial and other fungal pathogens. Fungal pathogens often show common responses leading to repression of energy-consuming processes and activation of alternative carbon- and nitrogen assimilation pathways, whereas pathogenic bacteria rely on species-specific responses dependent on intrinsic nutritional requirements and their intracellular localization.

The ability of pathogenic *Candida* species to acquire and metabolize macro- and micronutrients is essential for survival in the hostile phagosomal environment [251, 253-255, 258, 314]. In general, *Candida* species have a remarkable metabolic flexibility that allows them to switch between metabolization of different nutrients, depending on their availability in different host niches [319]. However, this metabolic flexibility mainly accounts for macronutrients. The requirement of essential micronutrients such as vitamins or trace metals, that are often co-factors of important metabolic enzymes, cannot be bypassed. The strong impact of the essential vitamin biotin (vitamin H) on survival inside macrophages and virulence of *C. glabrata* and *C. albicans* was demonstrated in **manuscript II**. Furthermore, the importance of copper and redox homeostasis for *C. parapsilosis* during contact with macrophages and predatory amoebae was stressed in **manuscript IV**. To extend the genetic toolbox for research on *C. glabrata* and *C. parapsilosis*, to get further insights into gene functions and to identify new virulence genes as well as targets of antifungal substances, RNA-interference for *C. glabrata* (**manuscript III**), and gene complementation strategies for *C. glabrata* (**manuscript V**) and *C. parapsilosis* (**manuscript IV**) were developed.

4.1 Establishment of new genetic manipulation tools to study biology and virulence of *C. glabrata* and *C. parapsilosis*

Gene deletion is a broadly employed and long used approach to study the function of potential virulence-associated genes in the major *Candida* species *C. albicans* [99]. However, due to the increasing prevalence of other *Candida* spp., the understanding of pathogenicity mechanisms of these NAC species like *C. glabrata* or *C. parapsilosis* has recently come into focus.

The approaches used so far for the creation of deletion mutants in these two NAC species resemble the strategies used in *C. albicans*, relying on selective markers like *NAT1*, *HIS3* or *URA3* [347, 348]. To describe molecular mechanisms of pathogenesis and gene functions, the molecular Koch´s postulates [108] should be fulfilled, which comprise the reintroduction of the deleted gene to regain wild type phenotypes and thus exclude pleiotropic effects associated with the gene deletion process. In *C. albicans*, genomic integration is a commonly used tool for reintroducing a certain gene into a knock-out strain. However, in *C. glabrata* and *C. parapsilosis* this approaches are less commonly used. We established a genomic reintegration strategy in *C. glabrata* that can be used to complement deletion mutants with their original gene, either expressed by the native or any conditional promotor (**manuscript V**). In addition, this strategy can be used to reintroduce modified versions of a gene, to investigate not only the gene function itself, but also specific nucleotide exchanges (respectively amino acid exchanges in the corresponding protein) and changes in gene expression pattern. Moreover, the new complementation strategy was applied for labeling of *C. glabrata* with two well-known fluorophores yEGFP and mCherry as well as the antigen ovalbumin (**manuscript V, Figure 2**). Fluorescent markers can be useful to tag different mutant strains and perform fluorescence-based experiments and intraspecies or interspecies competition assays, a strategy broadly used for *C. albicans* [349, 350]. By using additional selection markers, like *HIS3*, *LEU2* or *HygB* [351], our new protocol could also be extended to generate double fluorescently labeled strains for monitoring protein-protein interactions *in vivo*.

The newly developed *C. glabrata* complementation strategy relies on integration into the *TRP1* locus, a gene coding for an enzyme involved in the tryptophan biosynthesis [352]. Complementation with *TRP1* in a non-native locus could raises the problem of inefficient transcription and growth defects in tryptophan-poor niches. This possibility was excluded by choosing the native gene locus of the selection marker (**manuscript V**). In addition, deletion of *TRP1* had no influence on the systemic *C. glabrata* infection [68] and this locus was shown to be suitable for a sufficiently high expression level of other genes (**manuscript V**). Nevertheless, a minor risk remains that a certain gene in

the *TRP1* locus is transcribed differently due to the local chromatin structure. Alternatively, gene complementation may be also done in neutral loci, like *NEUT5L* in *C. albicans* [353]. The *NEUT5L* was also suitable to generate complemented strains in *C. parapsilosis* (**manuscript IV** and [354]). Such a neutral locus has also been used in *C. glabrata* on chromosome F [276].

The creation of gene deletions can fail in case of essential genes. Studying such genes is of high importance as these might encode virulence factors and/or potential targets for novel antifungals [103, 355]. For that reason alternative techniques are required, which use knock-down approaches such as targeted transcriptional repression (or induction) of tetracycline promotor-regulated genes (GRACE; gene replacement and conditional expression) or RNA-mediated downregulation [103]. Both methods are also suitable to perform large-scale identification of essential and virulence-associated genes [103] and (**manuscript III**). The established RNA interference (RNAi) strategy for *C. glabrata* has the advantage that no external substances like tetracyclin have to be added to achieve transcriptional gene repression. As members of the *Saccharomyces* complex, including *C. glabrata*, do not possess the mechanism of RNA-based gene silencing, Dicer (*DCR1*) and Argonaute (*AGO1*) were heterologously expressed in *C. glabrata*. In contrast, some pathogenic *Candida* species including *C. albicans* intrinsically possess the RNAi pathway [356]. A disadvantage (or desired advantage in the case of essential genes) of the RNAi technology in the investigation of gene function is that complete gene repression is often not possible and compensation of translation efficiency could overlay differences in transcription [357]. Certainly, the quantitative downregulation efficiency could be affected by the type of RNAi (**manuscript III, Figure 1**) or by using either antisense or hairpin constructs. Thus, different strategies may have to be compared for each gene.

Together, the techniques established in this work add important new genetic tools to investigate the function of novel genes and their role in pathobiology of the second and third-to-fourth most prevalent *Candida* species *C. glabrata* and *C. parapsilosis*.

4.2 Metal and redox homeostasis are essential for intraphagosomal survival

Besides macronutrients, micronutrients like trace metals and vitamins are essential in fine-tuning and maintaining metabolic fluxes – as cofactors of important metabolic enzymes. Concerning the acquisition of trace metals, one important group of micronutrients, two sides of a coin have to be considered. When low amounts of essential trace metals are present, microbes need high-affinity transport systems for the uptake of these metals from the environment. On the other hand, high metal

concentrations are toxic mainly due to the Fenton reaction and ROS production [358]. Metal intoxication by zinc and copper is also one mechanism used by phagocytic cells to kill ingested microbes [233, 359]. It has already been demonstrated that not only the uptake of metals, but also the homeostasis, either the acquisition or detoxification, of trace metals, and their complex regulatory processes, are indispensable for bacterial and fungal pathogens [270, 360].

In **manuscript IV**, it was demonstrated that predation by fungivorous amoebae increases the expression of genes necessary to cope with high copper concentrations in *C. parapsilosis*. The deletion of the copper exporter Crp1, involved in fungal copper resistance, made phagocytosed *C. parapsilosis* cells more susceptible to the antimicrobial activity of predatory amoebae and, to a lower extend, of macrophages **(manuscript IV, Figure 8)**. This indicated that *C. parapsilosis* is exposed to copper poisoning in amoebae, whereas the phenotype in macrophages is more ambiguous. In fact, the stable expression of *CpCRP1* within macrophages, compared to the increased expression of the copper transporter *CpCTR1* may indicate that *C. parapsilosis* is rather exposed to copper limitation in macrophages **(manuscript IV, Figure 4)**. This reveals differences in the two different phagocyte infection models used in that study. Further survival assays with a *CpCTR1* deletion mutant may address the question of copper restriction or intoxication by amoebae or macrophages.

Copper poisoning in macrophages has been described for other fungal species. In *C. albicans*, *Ca*Sur7 mediates high copper resistance and promotes intraphagosomal growth *in vitro* [236, 237], indicating toxic copper concentrations during *C. albicans´* intraphagosomal stay. Further studies focused on *C. albicans* or *A. fumigatus* infections showed that copper poisoning plays a role during systemic infections [361, 362].

While the pathogen can directly react towards an antimicrobial response, the immune system can also modulate this response. Cytokines like IFN-γ can not only influence the macrophage activation status [363] but also the content and pH of the phagosome [137], and even the degree of copper restriction and possibly also intoxication [364]. The copper transporter gene *HcCTR3*, for example, is necessary for replication of *H. capsulatum* in IFN-γ-activated but not non-activated macrophages [364]. Recently, similar results were observed for *C. glabrata*, as *CgCTR2* is needed for survival in IFN-γ stimulated macrophages [365]. These data open up the interesting perspective that the phagosome content is a consequence of macrophage stimulation. The modulation of macrophage polarization by fungal pathogens [198, 366] may thus be a strategy of these pathogens to alter intraphagosomal nutrition and the toxicity status in favor of the fungus. Alternatively, fungal pathogens may actively modulate the phagosome content,

similar to many bacterial intracellular pathogens, which create a distinct and degradation-permissive pathogen-containing vacuole [367].

Phagocytes can bombard microbes with high phagosomal metal concentrations, but also ROS are produced in high amounts [368]. Therefore, successful intracellular pathogens require efficient oxidative stress detoxification mechanisms [369]. Peroxiredoxins (Prxs) are thiol-specific antioxidant proteins [370]. Deletion of *PRX1*, encoding a Prx, caused attenuated survival of *C. parapsilosis* in amoebae and macrophages (**manuscript IV, Figure 8**), and the increased expression of a homologous gene in *C. albicans* during confrontation with macrophages [175] suggests a similar response pattern. However, the impact on the highly conserved *PRX1* gene in *C. albicans* and *C. glabrata* macrophage interaction remains to be elucidated.

4.3 Fungal factors involved in biotin homeostasis

The intrinsic biotin auxotrophy of *Candida* species has long been known [310, 311], but recent studies highlighted infection-relevant roles of biotin by showing that *C. albicans* requires biotin in parenteral nutrition solutions or filament-inducing media to promote proliferation [337, 371, 372].

4.3.1 Biotin uptake and biosynthesis

The necessity of biotin for growth of *C. albicans* and *C. glabrata* was confirmed, and the biotin transporter *VHT1* and the regulator of biotin-metabolic genes *VHR1* were identified as important players of biotin acquisition (**manuscript II**). This acquisition system likely extends to other medically relevant *Candida* species (*C. tropicalis*, *C. parapsilosis*, *C. auris* and *C. dubliniensis*) as these species contain orthologs of *VHR1* and *VHT1* (**Table 3**). A difference between *Candida* species is the presence or absence of the genes *BIO2-5*, which enable the partial synthesis of biotin from precursors (**manuscript II, Figure S1; Figure 3;** [317]). To date, it is unknown whether and how the presence of *BIO2-5* impacts on *C. albicans* colonization or virulence. The partial biosynthetic pathway does not largely affect pathogenicity of *Candida* species, as *C. glabrata* and *C. parapsilosis* (which both lack *BIO2-5)* are still the second and third frequent *Candida* species isolated from patients, while infections with *C. tropicalis* (possessing *BIO2-5*) are less frequent [64]. Also, a loss of *BIO2-5* was dispensable for *C. albicans´* survival and proliferation within macrophages (**manuscript II, Figure S4**). While most *S. cerevisiae* strains contain parts of the biotin biosynthesis cluster (*BIO2-5* genes), prototrophic *S. cerevisiae* strains exist, which additionally possess the genes *BIO1* and *BIO6* and are fully able to synthesize biotin [318]. It is tempting to speculate that there are also clinical *Candida* isolates that are capable of biotin synthesis.

The existence of the incomplete biotin biosynthesis gene cluster (*BIO2-5*) may be a benefit for *C. albicans* or *C. tropicalis* during commensalism on mucosal surfaces, promoting acquisition of biotin precursors from microbes living in close proximity. Also 20% of biotin-auxotrophic bacteria of the human microbiome possess similar incomplete biotin biosynthetic gene clusters [373], indicating that this phenomenon is also found in other kingdoms. As mammalian hosts are biotin auxotroph [335] other microbes are likely the only potential source of such precursors for *Candida* species in the host. Conceivably, the *BIO2-5* cluster could also benefit the competition of *Candida* species with other microbes, which have completely lost the ability to synthesize biotin, like bacteria of the Actinobacteria and Firmicutes phylum or other *Candida* species [374]. Ohsugi *et al.* described that members of the Enterobacteriaceae excrete biotin and biotin precursors, which further stresses a role of biotin and biotin intermediates in cross-feeding within microbial communities [373, 375].

To date, the influence of biotin or biotin precursor acquisition on *C. albicans* colonization of the gut, the main reservoir of *C. albicans* [50, 51] has not been elucidated. While many studies about *C. albicans* gut colonization are published, most of these studies used antibiotic-treated mice to accomplish stable gut colonization with *C. albicans* [376]. This could be problematic to interpret the impact of biotin on colonization in a healthy situation as the intact microbiota is essential to producing B-vitamins, especially biotin or biotin precursors, for the host and very likely for *Candida* [374]. Probably, the stable gut colonization with *C. albicans* in antibiotic-treated mice may be depending on biotin of the daily diet. The amount of biotin in the gastrointestinal tract, exemplary documented for chicken in the cecal content, is in the range of nanograms [377], while amounts of its precursors are not investigated. Of note, *Candida* species require only 0.2-2 ng biotin per mL for robust growth *in vitro* (**manuscript II, Figure S3**), suggesting enough biotin for *Candida* cells in the gastrointestinal tract containing a functional microbiota. Moreover, dietary fluctuation, the mode of nutrition (dietary source) and the microbiota composition of the large intestine (bacterial source) potentially impair the biotin content [378].

CgVHT1 (CAGL0K04609g) and *CaVHT1* (CR_03270W) were identified as the main factors responsible for biotin uptake in *C. glabrata* and *C. albicans* (**manuscript II, Figure 3**). Both genes show high similarity to the *S. cerevisiae* high affinity biotin transporter gene *VHT1* [379], coding for Vht1, which functions as a biotin-proton symporter with twelve putative transmembrane helices [379]. According to *in silico* analyses, Vht1 in *C. albicans* belongs to the anion: cation symporter (ACS) family as part of the major facilitator superfamily (MFS) [380]. BLASTp analyses revealed that

orthologs of *VHT1* were also found in other *Candida* spp., *Aspergillus* spp. and other fungal species suggesting that biotin uptake is facilitated in a similar way in distantly related fungi [381]. Even mammals use a similar transport system consisting of a sodium-driven symporter (SMVT) or proton-driven symporter (MCT1) with twelve membrane-spanning domains [336]. In contrast, bacteria use an ATP-mediated transport system BioY [336], and some species additionally employ a secondary transporter, YigM [336].

Although our data strongly indicate that Vht1 is the main biotin transporter in *C. glabrata* and *C. albicans*, growth of *vht1Δ* mutants was still possible in presence of high external biotin. This may be due to passive diffusion of highly concentrated biotin into the cells. However, it cannot be excluded that a low affinity biotin transporter or other transporters of the MFS family, which are structurally similar to Vht1, contribute to biotin import [380]. Besides, *C. glabrata* and *C. albicans* genomes contain other genes with sequence similarities to *ScVHT1* (**manuscript II, Figure 2**). These genes did not show any biotin- or *VHR1*-dependent transcriptional regulation, but could still mediate low affinity biotin uptake (**manuscript II, Figure S2**). Creating additional, possibly conditional, knock-outs in a *vht1Δ* mutant background strain might help to understand how this mutant can acquire biotin when present in high amounts.

C. albicans and *C. glabrata* can use biotinylated proteins and biocytin as biotin source dependent on *VHT1* (**Figure 7**). Consequently, these *Candida* species must possess a biotin salvage pathway that releases biotin from proteins or amino acids [382]. It remains to be elucidated which protease is required for the cleavage of biotinylated proteins and where this process takes place. Interestingly, the abundance of the GPI-anchored protease Mkc7 is increased in *S. cerevisiae* upon biotin limitation [383]. The involvement of this protease in the usage of biotinylated proteins could be further tested, as orthologous genes are also present in *C. albicans* (*CaSAP99*) and *C. glabrata* (*CgYPS2*). It is also conceivable to assume that small biotinylated peptides, which are released by extracellular fungal proteases like yapsins [72] or Saps [44], are transported into fungal cells, followed by further intracellular processing. Independent on where biotinylated proteins are processed, a result will be the release of biocytin (biotinyl-L-lysine). In mammalian cells, a hydrolytic enzyme, called biotinidase [335], can hydrolyze biotin from biocytin to make this freely available, *e.g.* for later coupling to other acceptor proteins, or for transfer of biotin to histones [384]. The eukaryotic biotinidase belongs to the nitrilase superfamily, with an amidase activity on non-peptide bonds [384, 385]. Whether *Candida* species or related yeasts possess a biotinidase gene is unknown, but the ability to use biocytin and biotinylated proteins suggests the presence of such enzymatic activity.

4.3.2 Regulation of biotin uptake and biosynthesis

The transcriptional regulation of biotin-related genes by Vhr1 revealed species-specific differences (**manuscript II, Figure 4**). *C. glabrata* showed a Vhr1-dependent transcriptional activation of *CgVHT1*, similar to *S. cerevisiae* [386]. In contrast, *Ca*Vhr1 activated the expression of the incomplete biosynthetic pathway (*CaBIO3-5*), but not *CaVHT1*. The impact of *Sc*Vhr1 on *BIO* gene expression is described in baker´s yeast [386, 387]. In line with this, the deletion of *CaVHR1* led to impaired growth with the biotin precursors KAPA and DTB (**Figure 8D**). This Vhr1-mediated activation of partial biotin biosynthesis could become important for acquisition of bacteria-produced biotin precursors (see above) during colonization of *C. albicans* of the mammalian gastrointestinal tract, where *CaVHR1* was shown to be upregulated [388]. BLASTp analyses of the Vhr1 protein sequence exhibited that this putative transcription factor was exclusively found in members of the order Saccharomycetales ([381]; unpublished own observations), which have an enriched repertoire of genes associated with transcription compared to other phyla [389]. This indicates that Saccharomycetales may use a different regulation mechanism probably due to the biotin auxotrophy, which is not present in other environmental fungi.

The *CaVHR1*-independent transcriptional activation *CaVHT1* (**manuscript II, Figure 4**) and the delayed *CgVHR1*-independent upregulation of *CgVHT1* (**Figure 4C**) upon biotin limitation suggested the presence of other, yet unknown, *VHT1* regulators in both species. This was underlined by transcriptional analyses of *CgVHT1* in response to nutrient availability and growth phase (**manuscript II, Figure 3**).

The genome of *S. cerevisiae* possesses a *VHR1* paralog, *VHR2*, which is present in the genome of *C. glabrata*, but not *C. albicans*. Both genes encode factors which share similarities in their DNA-binding motif and are predicted to be involved in amino acid metabolism [321]. Vhr2 was not involved in the transcriptional control of *CgVHT1* and *CgBPL1* (**Figure 4**). However, *CgVHR2* was, similar to *CgVHR1*, necessary for survival after phagocytosis by macrophages. It might be possible that a Vhr1-Vhr2 core response improves fungal survival within macrophages. Future transcriptional profiling of *vhr1Δ* and *vhr2Δ* mutants may verify how and which genes are regulated by both or only one factor. Using a *vhr1Δvhr2Δ* deletion strain may improve the interpretation of transcriptional profiles and survival experiments.

The chromatin-remodeling protein *SNF2* or the iron regulators *AFT1/2* modulate the expression of *VHT1* in baker´s yeast [390, 391]. Orthologs of *SNF2* or *AFT1/2* are therefore candidates for additional regulators in *C. glabrata* or *C. albicans*. In *S. cerevisiae*, *VHT1* and most *BIO* genes showed Gcn4-dependent induction in response to amino acid limitation [392]. DNA-binding motifs of Vhr1 and Gcn4 binding

are similar. BLAST analyses exhibited potential binding sites for both regulators in the promotor region of *CgVHT1* (done in this study, not shown). In addition to that, the expression of *CgVHT1* was not upregulated in biotin-poor medium with amino acids as a sole carbon- and nitrogen source - conditions at which Gcn4 is degraded [393]. Together, these data suggest that Gcn4 may be an additional regulator of *CgVHT1*. Therefore, it was intended to delete *CgGCN4* in order to analyze the effect on *CgVHT1* expression. Unfortunately, this approach failed several times, possibly due to essential gene functions of *CgGCN4*.

In order to identify more regulators involved in the response to biotin limitation, screening of transcription factor knock-out libraries in *C. glabrata* [347] and *C. albicans* [245] for failed *VHT1* induction upon biotin limitation could be realized in future.

4.3.3 Influence of biotin and *VHR1* on cellular processes

C. glabrata and *C. albicans* are able to grow with amino acids despite biotin limitation, while growth in media with glucose and ammonium was not possible without biotin. Interestingly, deletion of *CgVHR1* showed a growth defect in biotin-limited media with amino acids, which did not occur when only biotin limitation or only amino acids as sole carbon- and nitrogen-source were present. These data may indicate a putative function of *CgVHR1* in amino acid usage, while biotin is limited, suggesting Vhr1 as regulating screw between macronutrient availability and biotin acquisition. Data from *S. cerevisiae* suggest that, Vhr1 might indeed regulate Gcn4-related processes like the utilization of amino acids as sole carbon- and nitrogen source [321].

This and a previous study found that biotin promotes filamentous growth of *C. albicans* ([337]; **manuscript II, Figure 1**). This effect is more pronounced when amino acids are the sole carbon- and nitrogen source (**Figure 8B**). Our data suggest that this is due to an enhanced alkalinization and ammonia release in presence of biotin – a process that promotes hypha formation [283]. This process seems to depend on *CaVHR1*, since mutants lacking *CaVHR1* showed less ammonia release and alkalinization (**Figure 8C, 9A,C**), which may be due to a disturbed usage of amino acids, similar to effects seen when *CgVHR1* was deleted. Future studies with amino acids drop out media or transcriptional profiling would be helpful to get insights, which amino acid pathway is affected.

The availability of biotin increases the nutritional flexibility for *C. albicans* and *C. glabrata*, as biotin-dependent enzymes like pyruvate carboxylase (Pyc), acetyl-CoA carboxylase (Acc) and urea amidolyase (Dur1,2) can promote gluconeogenesis, fatty acid synthesis and metabolization of urea. On the other hand, the present work shows that biotin limitation makes the cell more dependent on the presence of certain

metabolites that overcome the missing function of biotin-dependent enzymes. The deficiency in acetyl-CoA carboxylase or pyruvate carboxylase activities under biotin deprivation may be bypassed by feeding with the fatty acids or aspartate, respectively [394, 395]. In line with this, casamino acids (mixture of all amino acids except tryptophan; see also above) and aspartate bypassed the need for biotin in *C. glabrata* and *C. albicans* (**manuscript II, Figure S1C, S3B,G**). These data suggest that biotin-auxotrophic *C. albicans* and *C. glabrata* can grow albeit solely in certain biotin-poor niches containing amino acids.

The focus of this thesis was the elucidation of biotin uptake by pathogenic *Candida* species. Further studies may investigate which function of biotin within the fungal cell is essential to withstand macrophage killing and initiate proliferation. An important player may be the biotin-protein ligase 1 (Bpl1), coupling biotin to biotin-dependent enzymes. This factor is essential in *S. cerevisiae* [395] and shows Vhr1- and biotin-dependent regulation in *C. glabrata* and *C. albicans* (**manuscript II, Figure 4**). A conditional knock-down, probably by the established RNAi in *C. glabrata*, could be used to investigate its role during interaction with macrophages. The last parts of the biotin cycle in the cell are biotinylated enzymes as mentioned above. Protein biotinylation in *C. glabrata* and *C. albicans* decreased upon biotin limitation, but less in the pyruvate carboxylase, confirming the importance of pyruvate carboxylation for the cell (**Figure 5B**).

Besides the role of biotin in carboxylase reactions, recent studies found that non-carboxylase proteins and histones are targets of biotinylation. This posttranslational modification was already observed in *C. albicans* [396] and studies in mammalian cells revealed the impact of biotinylated histones in cell proliferation, gene silencing and cellular response to DNA damage [397]. The impact of biotinylated non-carboxylase proteins and histones on fungal biology and virulence needs to be determined. Likely the biotinylation of histones could be detrimental after engulfment by phagocytes.

4.4   Biotin homeostasis in fungal virulence

The shift from commensalism to pathogenicity requires the adaptation to new host environments with altering nutrient compositions [319, 398]. The necessity of biotin differs quite a lot for different pathogens; many pathogenic bacteria possess the advantageous ability to synthesize this vitamin *de novo*, being independent of the external supply during infection [293, 299, 399], whereas *Candida* species have to struggle for sufficient biotin uptake to grow properly. Phagocytic cells use direct (active sequestration of nutrients) or indirect (no influx of nutrients) nutrient limitation mechanisms to starve ingested microbes and potentially kill them [400]. Hence,

enduring nutrient limitations within phagocytic cells is essential for pathogenic microbes to survive and proliferate. At the beginning of this thesis it was unknown, whether biotin limitation is one stressor *C. albicans* and *C. glabrata* encounter within the phagosome or other host niches.

4.4.1 Fungal biotin homeostasis is required for adaptation to macrophages

The two unlike *Candida* species, *C. albicans* and *C. glabrata*, evolved different strategies to evade immune cell-mediated killing [401]. *C. albicans* favors an aggressive route by rapidly forming hyphae, inducing an inflammatory response and escape, while *C. glabrata* keeps the inflammatory response low, replicates as yeast and persists inside macrophages for days [178]. However, the phagocytosis of *C. albicans* and *C. glabrata* yeast cells induces a similar initial transcriptional response, enabling fungal survival and proliferation within the harmful phagosome [72, 175]. This indicates that both species have similar metabolic adaptation strategies.

While biotin limitation prior to infection reduced survival and proliferation of *C. glabrata* and *C. albicans* wild type cells in macrophages (**manuscript II, Figure 5**), external biotin levels during the interaction had no impact on the interaction of the two *Candida* species with macrophages or the secretion of pro-inflammatory cytokines by these immune cells (**Figure 9**). This indicates that external biotin levels had no detectable or visible impact on macrophage activities in the experimental setting used. This is in contrast to other immune cells which showed an altered pro-inflammatory response depending on biotin availability [340-342].

While *VHT1* was necessary for biotin-dependent growth *in vitro* and proliferation within macrophages, Vhr1, as transcriptional regulator of biotin-related genes, was essential for survival and the initial proliferation of both *Candida* species (**manuscript II**). The importance of *VHR1* for the interaction with macrophages is supported by the strong upregulation of this gene upon phagocytosis (**manuscript II, Figure 5G-H**). When the intracellular biotin pool of *C. albicans* and *C. glabrata* was lowered by cultivation in biotin-free medium prior to infection, the intracellular survival of wild type cells and *VHR1* deletion mutant cells was similar (**manuscript II, Figure S5**). This implies that Vhr1 functions for survival are only important when the fungus has access to a sufficiently high internal biotin pool. Possibly, Vhr1 functions in the reorganization of stored biotin. Alternatively, potential Vhr1-dependent amino acid-related processes may affect initial survival and proliferation (**manuscript II, Figure S3B; Figure 8A,C**; see above 4.3.3). The upregulation of amino acid permease genes upon phagocytosis

implies that amino acids are indeed available to internalized *Candida* cells [72, 175] and the impact of efficient amino acid metabolism on survival and proliferation of described for *C. albicans* has been extensively studied [253, 256, 285]. Nevertheless, the reduced survival and initially delayed proliferation of *VHR1* deletion mutant cells in *C. albicans* did not cause a reduced cytolysis or cytokine response (**manuscript II, Figure 6F and data not shown**). This could be due to the delayed transcriptional regulation of Vhr1 targets by other factors (see *CgVHT1* expression) or compensation by other factors. To get further insights into the potential targets of Vhr1, comparative transcriptional profiling during growth with amino acids as sole carbon- and nitrogen sources and during phagocytosis could be performed in future.

One critical question for all studies on facultative intracellular pathogens is related to the access of nutrients after phagocytosis: Which nutrients are available within the phagosome, and which of these are used by the pathogen? Inherent or acquired auxotrophies in pathogens might be a useful tool to define metabolite availabilities in different host niches [263], and to study how pathogens acquire and exploit essential micronutrients during infection. This has been described nicely for *Pseudomonas aeruginosa* [402]. Previous work with biotin-auxotrophic *M. tuberculosis* and *F. tulariensis* mutants [403-406], and this thesis suggest that the intracellular compartment of those pathogens is biotin-depleted. This was mainly concluded from the transcriptional increase in biotin-related genes in both *Candida* species upon phagocytosis, which is underlined by previous large-scale transcriptional profiling of *C. albicans* (*e.g.* upregulation of *BIO2*, *VHR1*, *BIO5*, and *BPL1*) [175] and *C. glabrata* (*e.g.* upregulation of *BPL1* and *VHT1*) [72]. Taken together, a rich biotin storage and a functional biotin acquisition pathway (Vhr1-Vht1) increased fungal fitness inside macrophages (**manuscript II, Figure 5-6**), suggesting that a functional biotin homeostasis is even more beneficial for the fungus within a biotin-depleted phagosome. Similarly, other vitamins may be limited in the phagosome. The fungus *H. capsulatum*, for example, needs riboflavin biosynthesis for proliferation within macrophages and virulence *in vivo* [305]. All in all, the depletion of essential vitamins can be assumed as new form of nutritional immunity [265]. It is so far unknown, however, whether this process is active or passive.

As discussed above, the scarcity of biotin in host niches like the phagosome may be bypassed by amino acids (**manuscript II, Figure S3; Figure 8**). In addition, proliferation of *C. albicans* (as hypha) and *C. glabrata* (as yeast) followed by bursting of, possibly, first the phagosomal and second the cytosolic membrane could allow fungal access to host-derived biotin or other alternative biotin sources (biotinylated proteins or biocytin), which can be used in a Vht1-dependent manner (**manuscript II,**

Figure S1; Figure 7). Such host-derived biotin sources may explain why a *CaVHR1* deletion mutant had initial survival and proliferation defects, but caused wild type-like-like late macrophage damage, while a *CaVHT1* deletion mutant was attenuated in both, proliferation and host cell damage. To further elucidate whether *Candida* can indeed use host-derived biotin sources during infection, feeding macrophages with radiolabeled biotin could be performed. This method is commonly used for other nutrient sources like amino acids (stable isotope labeling with amino acids; SILAC [407]). In case *Candida* cells can use host-derived biotin, radiolabeled biotin should appear inside of *Candida* cells.

Besides the effects of Vht1 on fungal proliferation and macrophage damage, the *C. albicans*-induced inflammatory response was also diminished. The inflammasome, an important inflammatory pathway, lead to secretion by IL-1β secretion [408] and is activated by *C. albicans* and not by *C. glabrata* [345]. Early secretion of IL-1β by macrophages was highly attenuated after challenge with a biotin-starved *Cavht1Δ/Δ* mutant (**Figure 11A**). Of note, this phenomenon was only observed in biotin-free infection medium, whereas the presence of 2 mg/L biotin during infection, which is sufficient to support growth of this mutant in culture medium (**manuscript II, Figure 3**), led to wild type-like IL-1β release (**Figure 11A**). Similarly, the biotin-starved *Cavht1Δ/Δ* mutant caused reduced macrophage damage and release of pro-inflammatory cytokines at later time points (**Figure 11B-F**). This indicates that *CaVHT1*-dependent proliferation within macrophages is essential for the early and late inflammatory response, linked to macrophage lysis. The activation of the inflammasome in macrophages finally leads to a programmed cell death, caused by pyroptosis [408], which increases fungal survival [409]. Thus, the reduced survival of the biotin-starved *Cavht1Δ/Δ* mutant (**manuscript II, Figure S5B**) may be linked to reduced inflammasome activation (**Figure 11A**). Either the pre-feeding or the presence of high amounts biotin during infection can increase survival and inflammasome activation (**manuscript II, Figure 6C; Figure 11A**). Probably biotin can be taken up with one yeast cell during phagocytosis and promoting intraphagosomal growth of the *Cavht1Δ/Δ* mutant and progressive cytolysis. A large scale screening of macrophage inflammasome activation upon challenge with different *C. albicans* strains suggests that *CaVHT1* is involved inflammasome activation by *C. albicans* [409]. Several studies showed that *C. albicans* filamentation and cell wall remodeling activated the inflammasome in macrophages [345, 410, 411], which, both, might be lacking in the biotin-starved *Cavht1Δ/Δ* mutant. The lack of filamentation of the *Cavht1Δ/Δ* mutant in biotin-limited environments supports this view and may explain the attenuated induction of IL-1β caused by this mutant.

4.4.2 *VHT1*-mediated biotin acquisition promotes fungal fitness in the murine host and virulence

C. glabrata and C. albicans are able to disseminate to almost all organs during systemic infection but cause different infection outcomes in commonly used mouse models. *C. albicans* induces a fast and progressive immune reaction and mice die from dysregulated inflammatory response, immunopathology and sepsis [412]. In contrast, *C. glabrata* persists over weeks in various mouse tissues [68, 413-415], induces only a transient pro-inflammatory cytokine response within colonized host tissues and causes a minor influx of immune cells [66, 68, 413, 415, 416].

In stark contrast to these differences *in vivo*, *C. albicans*, like *C. glabrata*, requires an external biotin supply for robust growth facilitated by the putative high affinity biotin transporter Vht1 (**manuscript II**). The attenuated virulence of a *C. albicans vht1Δ/Δ* mutant during systemic challenge therefore strongly suggests that biotin acquisition is necessary for *C. albicans* virulence. Importantly, the reduced burdens in *C. glabrata vht1Δ* mutant-infected brains and *C. albicans vht1Δ/Δ* mutant-infected kidneys and brains implied a biotin-dependent proliferation in those organs (**manuscript II, Figure 7**). Importantly, kidney and temporarily the brain are target organs in which *C. albicans* filaments, but not in liver and spleen [66, 143, 147, 417-420]. The morphological plasticity of *C. albicans* is necessary for virulence and mutants that cannot change between yeast and hyphal morphology are often attenuated [33]. As known from the *in vitro* and macrophage studies, *VHT1* deletion leads to a reduction in hyphal growth when biotin is limiting (**manuscript II, Figure 3, 6**). The lack of hyphae, thus, may be one reason for reduced virulence of the *Cavht1Δ/Δ* mutant. Histological analyses would be required to elucidate the fungal morphology of the *Cavht1Δ/Δ* mutant in these organs. Moreover, previous observations showed also that *C. glabrata* is able to temporarily proliferate in the brain (**manuscript II, Figure 7;** [66, 68, 421]), the organ with a *VHT1*-dependent colonization effect.

The bioavailability and the accessibility of biotin during infection of mouse organs with *C. albicans* and *C. glabrata* remain unclear. However, several studies showed that the blood is richest in biotin, followed by the liver and kidney tissues, and lowest biotin amounts are found in brain and spleen (**Table 4**).

Another explanation for the reduced cfus of a *VHT1* deletion mutant in the brain may, however, also be a differential organ tropism of this mutant. So far, the exact location of brain-colonizing *C. glabrata* and how it crosses the blood brain barrier (BBB) is unknown. *C. albicans* and *Cryptococcus neoformans* are able to cross the BBB *in vivo* and *in vitro* [422-424]. *C. glabrata* may use pathways for BBB passage similar to those

described for *Cr. neoformans* - transcytosis across endothelial cells [425], or paracellular passage [423, 426]. Alternatively, the use of migrating macrophages as "Trojan horse" has been reported for *Cr. neoformans* [427]. Interestingly, fungal inositol transporters are required for the transmigration of *Cr. neoformans* across the BBB, suggesting alterations of the fungal metabolism during passages [428]. However, in contrast to biotin (**Table 4**), inositol is highly abundant in brain tissue [429, 430], which could be an attractant for disseminating cryptococcal cells. To distinguish between Vht1-dependent organ trafficking and subsequent proliferation, quantification of initial brain and kidney colonization by the *vht1Δ* mutants at early section time points (6 and 12 h) may be necessary. Sensing the vitamin status in certain niches may influence not only organ tropism but also virulence traits, as *e.g.* nicotinic acid can modulate adhesion of *C. glabrata* [309], differentiation of *Legionella pneumophila* [431], and virulence gene expression in *Bordetella pertussis* [432]. It would be highly interesting to elucidate whether biotin availability can directly modulate the expression of virulence-associated genes. In the case of *C. albicans* it seems clear that the presence of biotin promotes filamentation in *C. albicans*, an important virulence trait and associated with the expression of several further virulence factors [32].

Table 4: Documented amounts of biotin in various host tissues.

organ	host	Concentration		reference
brain	rat	0.046	µg/g	[434]
		0.073	µg/g	[435]
blood	rat	13.34	µg/L	[434]
cerebrospinal fluid (CSF)	rabbit	1.95	µg/L	[435]
liver	Rat	0.44	µg/g	[434]
	Pig	0.51* – 0.83#	µg/g	[436]
	chicken	2.02* – 5.59#	µg/g	[436]
kidney	Rat	0.3	µg/g	[434]
spleen	Rat	0.012	µg/g	[434]

* biotin-depleted, # biotin-supplemented, 4.09316 nmol/g ≙ 1 µg/g. *Candida* species require only 0.2-2 µg/L (app. 0.0002-0.002 µg/g) biotin for robust growth *in vitro*.

The importance of biotin for *C. albicans* and *C. glabrata* shown in this thesis resembles the results of studies with the bacterial pathogens *M. tuberculosis* and *F. tulariensis*, which provided evidence that biotin is required for intraphagosomal fitness and virulence [403, 404, 406]. Nevertheless, inhibition of biotin synthesis in other fungal and bacterial pathogens was not accompanied with attenuated virulence [305, 433], due to

the presence of biotin transporter genes and high plasma biotin level in mice [433]. This could also explain why the *CaVHT1* deletion mutant was not completely avirulent during systemic candidiasis, depicted by a delayed infection progression in at least some mice (**manuscript II, Figure 7B**).

It was surprising that, despite a strict requirement for high external biotin, *vht1Δ* mutants of both *Candida* species colonized liver and spleen similarly to the wild type (**manuscript II, Figure S6**). Possibly, both species have access to excessive biotin in these organs, or fungal proliferation *per se* is restricted in these tissues, making Vht1-dependent biotin acquisition dispensable. Of note, *C. albicans´* filamentation, as indicator of proliferation, is actively inhibited by specialized phagocytes in the liver [174], which likely support the growth inhibition in this organ. Histological sections from different *C. glabrata*-infected mouse organs showed accumulated yeast cells (each > 5 yeast cells) [68], which can be explained by either proliferation of few yeast cells in the tissue or by bursting of a group of initially administrated yeast cells from the blood stream into the tissue. Further approaches are required to distinguish between injected mother cells and daughter cells, and to learn about the level of organ-specific proliferation in the host. For such experiments, fluorescently labeled yeast cells, similarly to those used in **manuscript II**, or fluorometric cell cycle assays would be useful to track cell division [437, 438].

Similar to the organ cfu kinetics during persistence of *in vivo*, the viability and resulting cfu count of *C. glabrata* under nutrient-limited conditions (staying in PBS) lowered continuously. Also, a macrophage persistence model showed only weak intracellular proliferation of *C. glabrata* over the duration of one week, and a continuous decline in fungal burden due to fungal killing [Fischer *et al*., unpublished data]. Consequently, weak or no fungal proliferation together with fungal clearance by decreased viability or host-mediated mechanisms lead to the diminished fungal burden over time. Indeed, growth is not always required in the lifestyle of pathogens. Cellular quiescence represents a strategy to slow down or arrest microbial growth favoring persistence for days or months up to years [439], leading to chronic infections [440]. Those microbial populations are better tolerated by the immune system and resist antimicrobial therapies [440], which could be a characteristic for the chronic phase of *C. glabrata* infections [68].

In conclusion, *C. glabrata* and *C. albicans*, different in their infection strategies, employ a similar biotin uptake system, which is essential for the interaction with macrophages and during systemic infections. The usage of the biotin transporter mutant allows investigating in which niches biotin may be limited and where biotin is important for

fungal proliferation. Thus, the uptake of biotin by pathogenic *Candida* species represents a metabolic adaptation strategy during infection.

4.5   Outlook

It needs to be clarified whether the role of biotin on the interaction of *Candida* cells with macrophages is indeed linked to the phenotypes observed *in vivo*. During systemic infection with *C. albicans*, inflammatory monocytes and macrophages expand, especially in spleen and liver and promote fungal clearance [147]. Apart from the histological association of *C. glabrata* with and the attraction of monocytic cells *ex vivo* [68, 194], the role of monocytic cells for the dissemination and the persistence or clearance of *C. glabrata* during systemic infection is unknown. However, the importance of macrophages for protection from fungal infection seems to hold true for different pathogens besides *C. albicans*. Macrophage depletion curtailed *Blastomyces dermatitidis* infection [441], and monocytes are used as "Trojan horse" for dissemination and BBB translocation by *Cr. neoformans* [427, 442]. Macrophage depletion experiments [443] together with immunohistochemical analyses could be used to further characterize the interaction of *C. glabrata* with monocytic cells *in vivo*. Furthermore, the mechanism of brain colonization by *C. glabrata*, probably by crossing the BBB, could be further investigated using a microfluidic chip model to mimic the blood circulation, the endothelial barrier and the barrier supporting brain parenchyma, mainly astrocytes and microglial cells.

The *C. glabrata* mouse model used does not lead to killing of the host, while human patients can die from systemic *C. glabrata* infections. Consequently, we do not know whether *VHT1* and biotin acquisition are required for *C. glabrata´* virulence, similar to *C. albicans*. The prevalence of *C. glabrata* infections is increased in elderly people, which is often associated with a senescent immune system and metabolic disorders [64, 65]. Therefore, a novel systemic candidiasis infection model with aged mice could be developed, which mimics more the human situation.

This thesis revealed many aspects of the biotin metabolism in two highly prevalent *Candida* species, but the exact role of the biotin biosynthesis cluster in the viability and pathogenicity or commensalism of *C. albicans* (and also *C. tropicalis*) remains unclear. The reintegrating of the biotin prototrophy in *C. albicans*, by using *BIO1* and *BIO6* from prototrophic *S. cerevisiae* strains [318], could be a useful tool to study the effect on colonization and virulence to answer another key question: whether a biotin auxotrophy is a fitness cost, which makes *Candida* cells dependent on the microbiota and the host?

5   References

1. Brown GD, Denning DW, Gow NA, Levitz SM, Netea MG, White TC. Hidden killers: human fungal infections. Sci Transl Med. 2012;4(165):165rv13. Epub 2012/12/21. doi: 10.1126/scitranslmed.3004404. PubMed PMID: 23253612.

2. Gow NAR, Yadav B. Microbe Profile: *Candida albicans*: a shape-changing, opportunistic pathogenic fungus of humans. Microbiology. 2017;163(8):1145-7. Epub 2017/08/16. doi: 10.1099/mic.0.000499. PubMed PMID: 28809155.

3. Bensasson D, Dicks J, Ludwig JM, Bond CJ, Elliston A, Roberts IN, et al. Diverse Lineages of *Candida albicans* Live on Old Oaks. Genetics. 2019;211(1):277-88. Epub 2018/11/23. doi: 10.1534/genetics.118.301482. PubMed PMID: 30463870; PubMed Central PMCID: PMCPMC6325710.

4. Pfaller MA, Diekema DJ. Epidemiology of invasive candidiasis: a persistent public health problem. Clin Microbiol Rev. 2007;20(1):133-63. Epub 2007/01/16. doi: 10.1128/CMR.00029-06. PubMed PMID: 17223626; PubMed Central PMCID: PMCPMC1797637.

5. Kullberg BJ, Verweij PE, Akova M, Arendrup MC, Bille J, Calandra T, et al. European expert opinion on the management of invasive candidiasis in adults. Clin Microbiol Infect. 2011;17 Suppl 5:1-12. Epub 2011/10/12. doi: 10.1111/j.1469-0691.2011.03615.x. PubMed PMID: 21884296.

6. Tortorano AM, Peman J, Bernhardt H, Klingspor L, Kibbler CC, Faure O, et al. Epidemiology of candidaemia in Europe: results of 28-month European Confederation of Medical Mycology (ECMM) hospital-based surveillance study. Eur J Clin Microbiol Infect Dis. 2004;23(4):317-22. Epub 2004/03/19. doi: 10.1007/s10096-004-1103-y. PubMed PMID: 15029512.

7. Morgan J, Meltzer MI, Plikaytis BD, Sofair AN, Huie-White S, Wilcox S, et al. Excess mortality, hospital stay, and cost due to candidemia: a case-control study using data from population-based candidemia surveillance. Infect Control Hosp Epidemiol. 2005;26(6):540-7. Epub 2005/07/16. doi: 10.1086/502581. PubMed PMID: 16018429.

8. Fridkin SK. Candidemia is costly--plain and simple. Clin Infect Dis. 2005;41(9):1240-1. Epub 2005/10/06. doi: 10.1086/496935. PubMed PMID: 16206096.

9. Krcmery V, Barnes AJ. Non-albicans *Candida* spp. causing fungaemia: pathogenicity and antifungal resistance. J Hosp Infect. 2002;50(4):243-60. Epub 2002/05/17. doi: 10.1053/jhin.2001.1151. PubMed PMID: 12014897.

10. Chi HW, Yang YS, Shang ST, Chen KH, Yeh KM, Chang FY, et al. *Candida albicans* versus non-albicans bloodstream infections: the comparison of risk factors and outcome. J Microbiol Immunol Infect. 2011;44(5):369-75. Epub 2011/04/29. doi: 10.1016/j.jmii.2010.08.010. PubMed PMID: 21524971.

11. Arendrup MC. *Candida* and candidaemia. Susceptibility and epidemiology. Dan Med J. 2013;60(11):B4698. Epub 2013/11/07. PubMed PMID: 24192246.

12. Pappas PG, Kauffman CA, Andes D, Benjamin DK, Jr., Calandra TF, Edwards JE, Jr., et al. Clinical practice guidelines for the management of candidiasis: 2009 update by the Infectious Diseases Society of America. Clin Infect Dis. 2009;48(5):503-35. Epub 2009/02/05. doi: 10.1086/596757. PubMed PMID: 19191635.

13. Perlroth J, Choi B, Spellberg B. Nosocomial fungal infections: epidemiology, diagnosis, and treatment. Med Mycol. 2007;45(4):321-46. Epub 2007/05/19. doi: 10.1080/13693780701218689. PubMed PMID: 17510856.

14. Kullberg BJ, Arendrup MC. Invasive Candidiasis. N Engl J Med. 2015;373(15):1445-56. Epub 2015/10/09. doi: 10.1056/NEJMra1315399. PubMed PMID: 26444731.

15. Akpan A, Morgan R. Oral candidiasis. Postgrad Med J. 2002;78(922):455-9. Epub 2002/08/20. doi: 10.1136/pmj.78.922.455. PubMed PMID: 12185216; PubMed Central PMCID: PMCPMC1742467.

16. Sobel JD. Vulvovaginal candidosis. Lancet. 2007;369(9577):1961-71. Epub 2007/06/15. doi: 10.1016/S0140-6736(07)60917-9. PubMed PMID: 17560449.

17. Rantala A, Niinikoski J, Lehtonen OP. Yeasts in blood cultures: impact of early therapy. Scand J Infect Dis. 1989;21(5):557-61. Epub 1989/01/01. doi: 10.3109/00365548909037885. PubMed PMID: 2587957.

18. Yeo SF, Wong B. Current status of nonculture methods for diagnosis of invasive fungal infections. Clin Microbiol Rev. 2002;15(3):465-84. Epub 2002/07/05. doi: 10.1128/cmr.15.3.465-484.2002. PubMed PMID: 12097252; PubMed Central PMCID: PMCPMC118074.

19. Mayer FL, Wilson D, Hube B. *Candida albicans* pathogenicity mechanisms. Virulence. 2013;4(2):119-28. Epub 2013/01/11. doi: 10.4161/viru.22913. PubMed PMID: 23302789; PubMed Central PMCID: PMCPMC3654610.

20. Fitzpatrick DA, Logue ME, Stajich JE, Butler G. A fungal phylogeny based on 42 complete genomes derived from supertree and combined gene analysis. BMC Evol Biol. 2006;6:99. Epub 2006/11/24. doi: 10.1186/1471-2148-6-99. PubMed PMID: 17121679; PubMed Central PMCID: PMCPMC1679813.

21. Moran GPC, D.; Sullivan, D. An Introduction to the Medically Important *Candida* Species. In: Calderone RAC, C.J. , editor. Candida and Candidasis 2nd Edition. Washington, DC: ASM Press; 2012.

22. Yapar N. Epidemiology and risk factors for invasive candidiasis. Ther Clin Risk Manag. 2014;10:95-105. Epub 2014/03/13. doi: 10.2147/TCRM.S40160. PubMed PMID: 24611015; PubMed Central PMCID: PMCPMC3928396.

23. Diekema D, Arbefeville S, Boyken L, Kroeger J, Pfaller M. The changing epidemiology of healthcare-associated candidemia over three decades. Diagn Microbiol Infect Dis. 2012;73(1):45-8. doi: 10.1016/j.diagmicrobio.2012.02.001. PubMed PMID: 22578938.

24. Papon N, Courdavault V, Clastre M, Bennett RJ. Emerging and emerged pathogenic *Candida* species: beyond the *Candida albicans* paradigm. PLoS Pathog. 2013;9(9):e1003550. Epub 2013/10/03. doi: 10.1371/journal.ppat.1003550. PubMed PMID: 24086128; PubMed Central PMCID: PMCPMC3784480.

25. Lone SA, Ahmad A. *Candida auris*-the growing menace to global health. Mycoses. 2019;62(8):620-37. Epub 2019/02/19. doi: 10.1111/myc.12904. PubMed PMID: 30773703.

26. Csank C, Haynes K. *Candida glabrata* displays pseudohyphal growth. FEMS Microbiol Lett. 2000;189(1):115-20. Epub 2000/07/29. doi: 10.1111/j.1574-6968.2000.tb09216.x. PubMed PMID: 10913876.

27. Borman AM, Szekely A, Johnson EM. Comparative Pathogenicity of United Kingdom Isolates of the Emerging Pathogen *Candida auris* and Other Key Pathogenic *Candida* Species. mSphere. 2016;1(4). Epub 2016/08/23. doi: 10.1128/mSphere.00189-16. PubMed PMID: 27547827; PubMed Central PMCID: PMCPMC4990711.

28. Santos MA, Tuite MF. The CUG codon is decoded in vivo as serine and not leucine in *Candida albicans*. Nucleic Acids Res. 1995;23(9):1481-6. Epub 1995/05/11. doi: 10.1093/nar/23.9.1481. PubMed PMID: 7784200; PubMed Central PMCID: PMCPMC306886.

29. Gabaldón T, Martin T, Marcet-Houben M, Durrens P, Bolotin-Fukuhara M, Lespinet O, et al. Comparative genomics of emerging pathogens in the *Candida glabrata* clade. BMC Genomics. 2013;14:623. Epub 2013/09/17. doi: 10.1186/1471-2164-14-623. PubMed PMID: 24034898; PubMed Central PMCID: PMCPMC3847288.

30. Suzuki T, Nishibayashi S, Kuroiwa T, Kanbe T, Tanaka K. Variance of ploidy in *Candida albicans*. J Bacteriol. 1982;152(2):893-6. Epub 1982/11/01. PubMed PMID: 6752122; PubMed Central PMCID: PMCPMC221545.

31. Skrzypek MS, Binkley J, Binkley G, Miyasato SR, Simison M, Sherlock G. The *Candida* Genome Database (CGD): incorporation of Assembly 22, systematic identifiers and visualization of high throughput sequencing data. Nucleic Acids Res. 2017;45(D1):D592-

References

D6. Epub 2016/10/16. doi: 10.1093/nar/gkw924. PubMed PMID: 27738138; PubMed Central PMCID: PMCPMC5210628.

32. Jacobsen ID, Wilson D, Wächtler B, Brunke S, Naglik JR, Hube B. *Candida albicans* dimorphism as a therapeutic target. Expert Rev Anti Infect Ther. 2012;10(1):85-93. Epub 2011/12/14. doi: 10.1586/eri.11.152. PubMed PMID: 22149617.

33. Lo HJ, Kohler JR, DiDomenico B, Loebenberg D, Cacciapuoti A, Fink GR. Nonfilamentous *C. albicans* mutants are avirulent. Cell. 1997;90(5):939-49. Epub 1997/09/23. doi: 10.1016/s0092-8674(00)80358-x. PubMed PMID: 9298905.

34. Veses V, Gow NA. Pseudohypha budding patterns of *Candida albicans*. Med Mycol. 2009;47(3):268-75. Epub 2009/04/07. doi: 10.1080/13693780802245474. PubMed PMID: 19347739.

35. Odds FC. *Candida* and candidosis: a review and bibliography. 2nd edition.: Baillière Tindall; 1988.

36. Soll DR. The role of phenotypic switching in the basic biology and pathogenesis of *Candida albicans*. J Oral Microbiol. 2014;6. Epub 2014/01/24. doi: 10.3402/jom.v6.22993. PubMed PMID: 24455104; PubMed Central PMCID: PMCPMC3895265.

37. Miller MG, Johnson AD. White-opaque switching in *Candida albicans* is controlled by mating-type locus homeodomain proteins and allows efficient mating. Cell. 2002;110(3):293-302. Epub 2002/08/15. doi: 10.1016/s0092-8674(02)00837-1. PubMed PMID: 12176317.

38. Staib P, Morschhäuser J. Chlamydospore formation in *Candida albicans* and *Candida dubliniensis*--an enigmatic developmental programme. Mycoses. 2007;50(1):1-12. Epub 2007/02/17. doi: 10.1111/j.1439-0507.2006.01308.x. PubMed PMID: 17302741.

39. Staab JF, Bradway SD, Fidel PL, Sundstrom P. Adhesive and mammalian transglutaminase substrate properties of *Candida albicans* Hwp1. Science. 1999;283(5407):1535-8. Epub 1999/03/05. doi: 10.1126/science.283.5407.1535. PubMed PMID: 10066176.

40. Liu Y, Filler SG. *Candida albicans* Als3, a multifunctional adhesin and invasin. Eukaryot Cell. 2011;10(2):168-73. Epub 2010/12/01. doi: 10.1128/EC.00279-10. PubMed PMID: 21115738; PubMed Central PMCID: PMCPMC3067396.

41. Phan QT, Myers CL, Fu Y, Sheppard DC, Yeaman MR, Welch WH, et al. Als3 is a *Candida albicans* invasin that binds to cadherins and induces endocytosis by host cells. PLoS Biol. 2007;5(3):e64. Epub 2007/02/22. doi: 10.1371/journal.pbio.0050064. PubMed PMID: 17311474; PubMed Central PMCID: PMCPMC1802757.

42. Sun JN, Solis NV, Phan QT, Bajwa JS, Kashleva H, Thompson A, et al. Host cell invasion and virulence mediated by *Candida albicans* Ssa1. PLoS Pathog. 2010;6(11):e1001181. Epub 2010/11/19. doi: 10.1371/journal.ppat.1001181. PubMed PMID: 21085601; PubMed Central PMCID: PMCPMC2978716.

43. Moyes DL, Wilson D, Richardson JP, Mogavero S, Tang SX, Wernecke J, et al. Candidalysin is a fungal peptide toxin critical for mucosal infection. Nature. 2016;532(7597):64-8. Epub 2016/03/31. doi: 10.1038/nature17625. PubMed PMID: 27027296; PubMed Central PMCID: PMCPMC4851236.

44. Naglik JR, Challacombe SJ, Hube B. *Candida albicans* secreted aspartyl proteinases in virulence and pathogenesis. Microbiol Mol Biol Rev. 2003;67(3):400-28, table of contents. Epub 2003/09/11. doi: 10.1128/mmbr.67.3.400-428.2003. PubMed PMID: 12966142; PubMed Central PMCID: PMCPMC193873.

45. Saville SP, Lazzell AL, Monteagudo C, Lopez-Ribot JL. Engineered control of cell morphology in vivo reveals distinct roles for yeast and filamentous forms of *Candida albicans* during infection. Eukaryot Cell. 2003;2(5):1053-60. Epub 2003/10/14. doi: 10.1128/ec.2.5.1053-1060.2003. PubMed PMID: 14555488; PubMed Central PMCID: PMCPMC219382.

46. Böhm L, Torsin S, Tint SH, Eckstein MT, Ludwig T, Perez JC. The yeast form of the fungus *Candida albicans* promotes persistence in the gut of gnotobiotic mice. PLoS Pathog.

2017;13(10):e1006699. Epub 2017/10/27. doi: 10.1371/journal.ppat.1006699. PubMed PMID: 29069103; PubMed Central PMCID: PMCPMC5673237.

47. Witchley JN, Penumetcha P, Abon NV, Woolford CA, Mitchell AP, Noble SM. *Candida albicans* Morphogenesis Programs Control the Balance between Gut Commensalism and Invasive Infection. Cell Host Microbe. 2019;25(3):432-43 e6. Epub 2019/03/15. doi: 10.1016/j.chom.2019.02.008. PubMed PMID: 30870623; PubMed Central PMCID: PMCPMC6581065.

48. Lockhart SR, Reed BD, Pierson CL, Soll DR. Most frequent scenario for recurrent *Candida* vaginitis is strain maintenance with "substrain shuffling": demonstration by sequential DNA fingerprinting with probes Ca3, C1, and CARE2. J Clin Microbiol. 1996;34(4):767-77. Epub 1996/04/01. PubMed PMID: 8815082; PubMed Central PMCID: PMCPMC228891.

49. Odds FC, Davidson AD, Jacobsen MD, Tavanti A, Whyte JA, Kibbler CC, et al. *Candida albicans* strain maintenance, replacement, and microvariation demonstrated by multilocus sequence typing. J Clin Microbiol. 2006;44(10):3647-58. Epub 2006/10/06. doi: 10.1128/JCM.00934-06. PubMed PMID: 17021093; PubMed Central PMCID: PMCPMC1594753.

50. Nucci M, Anaissie E. Revisiting the source of candidemia: skin or gut? Clin Infect Dis. 2001;33(12):1959-67. Epub 2001/11/10. doi: 10.1086/323759. PubMed PMID: 11702290.

51. Miranda LN, van der Heijden IM, Costa SF, Sousa AP, Sienra RA, Gobara S, et al. *Candida* colonisation as a source for candidaemia. J Hosp Infect. 2009;72(1):9-16. Epub 2009/03/24. doi: 10.1016/j.jhin.2009.02.009. PubMed PMID: 19303662.

52. Pfaller MA, Diekema DJ, Gibbs DL, Newell VA, Ellis D, Tullio V, et al. Results from the ARTEMIS DISK Global Antifungal Surveillance Study, 1997 to 2007: a 10.5-year analysis of susceptibilities of *Candida* Species to fluconazole and voriconazole as determined by CLSI standardized disk diffusion. J Clin Microbiol. 2010;48(4):1366-77. Epub 2010/02/19. doi: 10.1128/JCM.02117-09. PubMed PMID: 20164282; PubMed Central PMCID: PMCPMC2849609.

53. Ghanem-Zoubi N, Khoury J, Arnon M, Zorbavel D, Geffen Y, Paul M. Risk Factors for Non-Albicans Candidemia Focusing on Prior Antifungal and Immunosuppressive Therapy. Isr Med Assoc J. 2019;5(21):303-7. Epub 2019/05/30. PubMed PMID: 31140219.

54. Meis JF, Chowdhary A. *Candida auris*: a global fungal public health threat. Lancet Infect Dis. 2018;18(12):1298-9. Epub 2018/10/09. doi: 10.1016/S1473-3099(18)30609-1. PubMed PMID: 30293876.

55. Spivak ES, Hanson KE. *Candida auris*: an Emerging Fungal Pathogen. J Clin Microbiol. 2018;56(2). Epub 2017/11/24. doi: 10.1128/JCM.01588-17. PubMed PMID: 29167291; PubMed Central PMCID: PMCPMC5786713.

56. Kordalewska M, Perlin DS. Identification of Drug Resistant *Candida auris*. Front Microbiol. 2019;10:1918. Epub 2019/09/05. doi: 10.3389/fmicb.2019.01918. PubMed PMID: 31481947; PubMed Central PMCID: PMCPMC6710336.

57. Kurtzman CP, Robnett CJ. Identification of clinically important ascomycetous yeasts based on nucleotide divergence in the 5' end of the large-subunit (26S) ribosomal DNA gene. J Clin Microbiol. 1997;35(5):1216-23. Epub 1997/05/01. PubMed PMID: 9114410; PubMed Central PMCID: PMCPMC232732.

58. Srikantha T, Lachke SA, Soll DR. Three mating type-like loci in *Candida glabrata*. Eukaryot Cell. 2003;2(2):328-40. Epub 2003/04/10. doi: 10.1128/ec.2.2.328-340.2003. PubMed PMID: 12684382; PubMed Central PMCID: PMCPMC154844.

59. Dodgson AR, Pujol C, Pfaller MA, Denning DW, Soll DR. Evidence for recombination in *Candida glabrata*. Fungal Genet Biol. 2005;42(3):233-43. Epub 2005/02/15. doi: 10.1016/j.fgb.2004.11.010. PubMed PMID: 15707844.

60. Gabaldón T, Fairhead C. Genomes shed light on the secret life of *Candida glabrata*: not so asexual, not so commensal. Curr Genet. 2019;65(1):93-8. Epub 2018/07/22. doi: 10.1007/s00294-018-0867-z. PubMed PMID: 30027485; PubMed Central PMCID: PMCPMC6342864.

References

61. Brockert PJ, Lachke SA, Srikantha T, Pujol C, Galask R, Soll DR. Phenotypic switching and mating type switching of *Candida glabrata* at sites of colonization. Infect Immun. 2003;71(12):7109-18. Epub 2003/11/26. doi: 10.1128/iai.71.12.7109-7118.2003. PubMed PMID: 14638801; PubMed Central PMCID: PMCPMC308932.

62. Kadir T, Pisiriciler R, Akyuz S, Yarat A, Emekli N, Ipbuker A. Mycological and cytological examination of oral candidal carriage in diabetic patients and non-diabetic control subjects: thorough analysis of local aetiologic and systemic factors. J Oral Rehabil. 2002;29(5):452-7. Epub 2002/05/25. PubMed PMID: 12028493.

63. Lockhart SR, Joly S, Vargas K, Swails-Wenger J, Enger L, Soll DR. Natural defenses against *Candida* colonization breakdown in the oral cavities of the elderly. J Dent Res. 1999;78(4):857-68. Epub 1999/05/18. doi: 10.1177/00220345990780040601. PubMed PMID: 10326730.

64. Pfaller MA, Andes DR, Diekema DJ, Horn DL, Reboli AC, Rotstein C, et al. Epidemiology and outcomes of invasive candidiasis due to non-albicans species of *Candida* in 2,496 patients: data from the Prospective Antifungal Therapy (PATH) registry 2004-2008. PLoS One. 2014;9(7):e101510. Epub 2014/07/06. doi: 10.1371/journal.pone.0101510. PubMed PMID: 24991967; PubMed Central PMCID: PMCPMC4081561.

65. Khatib R, Johnson LB, Fakih MG, Riederer K, Briski L. Current trends in candidemia and species distribution among adults: *Candida glabrata* surpasses *C. albicans* in diabetic patients and abdominal sources. Mycoses. 2016;59(12):781-6. Epub 2016/07/13. doi: 10.1111/myc.12531. PubMed PMID: 27402377.

66. Brieland J, Essig D, Jackson C, Frank D, Loebenberg D, Menzel F, et al. Comparison of pathogenesis and host immune responses to *Candida glabrata* and *Candida albicans* in systemically infected immunocompetent mice. Infect Immun. 2001;69(8):5046-55. Epub 2001/07/12. doi: 10.1128/IAI.69.8.5046-5055.2001. PubMed PMID: 11447185; PubMed Central PMCID: PMCPMC98599.

67. Arendrup M, Horn T, Frimodt-Moller N. *In vivo* pathogenicity of eight medically relevant *Candida* species in an animal model. Infection. 2002;30(5):286-91. Epub 2002/10/17. doi: 10.1007/s15010-002-2131-0. PubMed PMID: 12382088.

68. Jacobsen ID, Brunke S, Seider K, Schwarzmüller T, Firon A, d'Enfert C, et al. *Candida glabrata* persistence in mice does not depend on host immunosuppression and is unaffected by fungal amino acid auxotrophy. Infect Immun. 2010;78(3):1066-77. doi: 10.1128/IAI.01244-09. PubMed PMID: 20008535; PubMed Central PMCID: PMC2825948.

69. Cormack BP, Ghori N, Falkow S. An adhesin of the yeast pathogen *Candida glabrata* mediating adherence to human epithelial cells. Science. 1999;285(5427):578-82. Epub 1999/07/27. doi: 10.1126/science.285.5427.578. PubMed PMID: 10417386.

70. Mundy RD, Cormack B. Expression of *Candida glabrata* adhesins after exposure to chemical preservatives. J Infect Dis. 2009;199(12):1891-8. Epub 2009/05/12. doi: 10.1086/599120. PubMed PMID: 19426114; PubMed Central PMCID: PMCPMC4019233.

71. Kantarcioglu AS, Yucel A. Phospholipase and protease activities in clinical *Candida* isolates with reference to the sources of strains. Mycoses. 2002;45(5-6):160-5. Epub 2002/07/09. doi: 10.1046/j.1439-0507.2002.00727.x. PubMed PMID: 12100532.

72. Kaur R, Ma B, Cormack BP. A family of glycosylphosphatidylinositol-linked aspartyl proteases is required for virulence of *Candida glabrata*. Proc Natl Acad Sci U S A. 2007;104(18):7628-33. doi: 10.1073/pnas.0611195104. PubMed PMID: 17456602; PubMed Central PMCID: PMC1863504.

73. Bairwa G, Kaur R. A novel role for a glycosylphosphatidylinositol-anchored aspartyl protease, CgYps1, in the regulation of pH homeostasis in *Candida glabrata*. Mol Microbiol. 2011;79(4):900-13. Epub 2011/02/09. doi: 10.1111/j.1365-2958.2010.07496.x. PubMed PMID: 21299646.

74. Bairwa G, Rasheed M, Taigwal R, Sahoo R, Kaur R. GPI (glycosylphosphatidylinositol)-linked aspartyl proteases regulate vacuole homoeostasis in *Candida glabrata*. Biochem J. 2014;458(2):323-34. Epub 2013/12/18. doi: 10.1042/BJ20130757. PubMed PMID: 24341558.

75. Rasheed M, Battu A, Kaur R. Aspartyl proteases in *Candida glabrata* are required for suppression of the host innate immune response. J Biol Chem. 2018;293(17):6410-33. Epub 2018/03/02. doi: 10.1074/jbc.M117.813741. PubMed PMID: 29491142; PubMed Central PMCID: PMCPMC5925793.

76. Whaley SG, Rogers PD. Azole Resistance in *Candida glabrata*. Curr Infect Dis Rep. 2016;18(12):41. Epub 2016/10/21. doi: 10.1007/s11908-016-0554-5. PubMed PMID: 27761779.

77. Garnacho-Montero J, Diaz-Martin A, Garcia-Cabrera E, Ruiz Perez de Pipaon M, Hernandez-Caballero C, Aznar-Martin J, et al. Risk factors for fluconazole-resistant candidemia. Antimicrob Agents Chemother. 2010;54(8):3149-54. Epub 2010/05/26. doi: 10.1128/AAC.00479-10. PubMed PMID: 20498325; PubMed Central PMCID: PMCPMC2916332.

78. Lee I, Fishman NO, Zaoutis TE, Morales KH, Weiner MG, Synnestvedt M, et al. Risk factors for fluconazole-resistant *Candida glabrata* bloodstream infections. Arch Intern Med. 2009;169(4):379-83. Epub 2009/02/25. doi: 10.1001/archinte.169.4.379. PubMed PMID: 19237722; PubMed Central PMCID: PMCPMC2890272.

79. Dujon B, Sherman D, Fischer G, Durrens P, Casaregola S, Lafontaine I, et al. Genome evolution in yeasts. Nature. 2004;430(6995):35-44. Epub 2004/07/02. doi: 10.1038/nature02579. PubMed PMID: 15229592.

80. Wong S, Wolfe KH. Birth of a metabolic gene cluster in yeast by adaptive gene relocation. Nat Genet. 2005;37(7):777-82. Epub 2005/06/14. doi: 10.1038/ng1584. PubMed PMID: 15951822.

81. Butler G, Rasmussen MD, Lin MF, Santos MA, Sakthikumar S, Munro CA, et al. Evolution of pathogenicity and sexual reproduction in eight *Candida* genomes. Nature. 2009;459(7247):657-62. Epub 2009/05/26. doi: 10.1038/nature08064. PubMed PMID: 19465905; PubMed Central PMCID: PMCPMC2834264.

82. Nosek J, Holesova Z, Kosa P, Gacser A, Tomaska L. Biology and genetics of the pathogenic yeast *Candida parapsilosis*. Curr Genet. 2009;55(5):497-509. Epub 2009/08/08. doi: 10.1007/s00294-009-0268-4. PubMed PMID: 19662416.

83. Bonassoli LA, Bertoli M, Svidzinski TI. High frequency of *Candida parapsilosis* on the hands of healthy hosts. J Hosp Infect. 2005;59(2):159-62. Epub 2004/12/29. doi: 10.1016/j.jhin.2004.06.033. PubMed PMID: 15620452.

84. Suh SO, Nguyen NH, Blackwell M. Yeasts isolated from plant-associated beetles and other insects: seven novel *Candida* species near *Candida albicans*. FEMS Yeast Res. 2008;8(1):88-102. Epub 2007/11/08. doi: 10.1111/j.1567-1364.2007.00320.x. PubMed PMID: 17986254.

85. Gadanho M, Sampaio JP. Occurrence and diversity of yeasts in the mid-atlantic ridge hydrothermal fields near the Azores Archipelago. Microb Ecol. 2005;50(3):408-17. Epub 2005/12/06. doi: 10.1007/s00248-005-0195-y. PubMed PMID: 16328655.

86. Medeiros AO, Kohler LM, Hamdan JS, Missagia BS, Barbosa FA, Rosa CA. Diversity and antifungal susceptibility of yeasts from tropical freshwater environments in Southeastern Brazil. Water Res. 2008;42(14):3921-9. Epub 2008/08/06. doi: 10.1016/j.watres.2008.05.026. PubMed PMID: 18678387.

87. van Asbeck EC, Huang YC, Markham AN, Clemons KV, Stevens DA. *Candida parapsilosis* fungemia in neonates: genotyping results suggest healthcare workers hands as source, and review of published studies. Mycopathologia. 2007;164(6):287-93. Epub 2007/09/18. doi: 10.1007/s11046-007-9054-3. PubMed PMID: 17874281.

88. Welbel SF, McNeil MM, Kuykendall RJ, Lott TJ, Pramanik A, Silberman R, et al. *Candida parapsilosis* bloodstream infections in neonatal intensive care unit patients: epidemiologic and laboratory confirmation of a common source outbreak. Pediatr Infect Dis J. 1996;15(11):998-1002. Epub 1996/11/01. PubMed PMID: 8933548.

89. Campbell JR, Zaccaria E, Baker CJ. Systemic candidiasis in extremely low birth weight infants receiving topical petrolatum ointment for skin care: a case-control study. Pediatrics.

References

2000;105(5):1041-5. Epub 2000/05/03. doi: 10.1542/peds.105.5.1041. PubMed PMID: 10790460.

90. Meunier-Carpentier F, Kiehn TE, Armstrong D. Fungemia in the immunocompromised host. Changing patterns, antigenemia, high mortality. Am J Med. 1981;71(3):363-70. Epub 1981/09/01. doi: 10.1016/0002-9343(81)90162-5. PubMed PMID: 6792913.

91. van Asbeck EC, Clemons KV, Stevens DA. *Candida parapsilosis*: a review of its epidemiology, pathogenesis, clinical aspects, typing and antimicrobial susceptibility. Crit Rev Microbiol. 2009;35(4):283-309. Epub 2009/10/14. doi: 10.3109/10408410903213393. PubMed PMID: 19821642.

92. Bistoni F, Vecchiarelli A, Cenci E, Sbaraglia G, Perito S, Cassone A. A comparison of experimental pathogenicity of *Candida* species in cyclophosphamide-immunodepressed mice. Sabouraudia. 1984;22(5):409-18. Epub 1984/01/01. PubMed PMID: 6505914.

93. Silva S, Negri M, Henriques M, Oliveira R, Williams DW, Azeredo J. Adherence and biofilm formation of non-*Candida albicans Candida* species. Trends Microbiol. 2011;19(5):241-7. Epub 2011/03/18. doi: 10.1016/j.tim.2011.02.003. PubMed PMID: 21411325.

94. Silva S, Henriques M, Martins A, Oliveira R, Williams D, Azeredo J. Biofilms of non-*Candida albicans Candida* species: quantification, structure and matrix composition. Med Mycol. 2009;47(7):681-9. Epub 2009/11/06. doi: 10.3109/13693780802549594. PubMed PMID: 19888800.

95. Horvath P, Nosanchuk JD, Hamari Z, Vagvolgyi C, Gacser A. The identification of gene duplication and the role of secreted aspartyl proteinase 1 in *Candida parapsilosis* virulence. J Infect Dis. 2012;205(6):923-33. Epub 2012/02/04. doi: 10.1093/infdis/jir873. PubMed PMID: 22301631.

96. Gácser A, Trofa D, Schafer W, Nosanchuk JD. Targeted gene deletion in *Candida parapsilosis* demonstrates the role of secreted lipase in virulence. J Clin Invest. 2007;117(10):3049-58. Epub 2007/09/15. doi: 10.1172/JCI32294. PubMed PMID: 17853941; PubMed Central PMCID: PMCPMC1974868.

97. Tóth R, Alonso MF, Bain JM, Vágvölgyi C, Erwig LP, Gácser A. Different *Candida parapsilosis* clinical isolates and lipase deficient strain trigger an altered cellular immune response. Front Microbiol. 2015;6:1102. Epub 2015/11/04. doi: 10.3389/fmicb.2015.01102. PubMed PMID: 26528256; PubMed Central PMCID: PMCPMC4602145.

98. Tóth R, Tóth A, Vágvölgyi C, Gácser A. *Candida parapsilosis* Secreted Lipase as an Important Virulence Factor. Curr Protein Pept Sci. 2017;18(10):1043-9. Epub 2016/08/17. doi: 10.2174/1389203717666160813163054. PubMed PMID: 27526931.

99. Xu QR, Yan L, Lv QZ, Zhou M, Sui X, Cao YB, et al. Molecular genetic techniques for gene manipulation in *Candida albicans*. Virulence. 2014;5(4):507-20. Epub 2014/04/25. doi: 10.4161/viru.28893. PubMed PMID: 24759671; PubMed Central PMCID: PMCPMC4063812.

100. Wilson RB, Davis D, Enloe BM, Mitchell AP. A recyclable *Candida albicans URA3* cassette for PCR product-directed gene disruptions. Yeast. 2000;16(1):65-70. Epub 2000/01/06. doi: 10.1002/(SICI)1097-0061(20000115)16:1<65::AID-YEA508>3.0.CO;2-M. PubMed PMID: 10620776.

101. Schaub Y, Dunkler A, Walther A, Wendland J. New pFA-cassettes for PCR-based gene manipulation in *Candida albicans*. J Basic Microbiol. 2006;46(5):416-29. Epub 2006/09/30. doi: 10.1002/jobm.200510133. PubMed PMID: 17009297.

102. Milne SW, Cheetham J, Lloyd D, Aves S, Bates S. Cassettes for PCR-mediated gene tagging in *Candida albicans* utilizing nourseothricin resistance. Yeast. 2011;28(12):833-41. Epub 2011/11/11. doi: 10.1002/yea.1910. PubMed PMID: 22072586.

103. Roemer T, Jiang B, Davison J, Ketela T, Veillette K, Breton A, et al. Large-scale essential gene identification in *Candida albicans* and applications to antifungal drug discovery. Mol Microbiol. 2003;50(1):167-81. Epub 2003/09/26. doi: 10.1046/j.1365-2958.2003.03697.x. PubMed PMID: 14507372.

104. Lavoie H, Sellam A, Askew C, Nantel A, Whiteway M. A toolbox for epitope-tagging and genome-wide location analysis in *Candida albicans*. BMC Genomics. 2008;9:578. Epub

2008/12/06. doi: 10.1186/1471-2164-9-578. PubMed PMID: 19055720; PubMed Central PMCID: PMCPMC2607300.

105. Bain JM, Stubberfield C, Gow NA. Ura-status-dependent adhesion of *Candida albicans* mutants. FEMS Microbiol Lett. 2001;204(2):323-8. Epub 2001/12/04. doi: 10.1111/j.1574-6968.2001.tb10905.x. PubMed PMID: 11731143.

106. Staab JF, Sundstrom P. *URA3* as a selectable marker for disruption and virulence assessment of *Candida albicans* genes. Trends Microbiol. 2003;11(2):69-73. Epub 2003/02/25. doi: 10.1016/s0966-842x(02)00029-x. PubMed PMID: 12598128.

107. Brand A, MacCallum DM, Brown AJ, Gow NA, Odds FC. Ectopic expression of *URA3* can influence the virulence phenotypes and proteome of *Candida albicans* but can be overcome by targeted reintegration of *URA3* at the *RPS10* locus. Eukaryot Cell. 2004;3(4):900-9. Epub 2004/08/11. doi: 10.1128/EC.3.4.900-909.2004. PubMed PMID: 15302823; PubMed Central PMCID: PMCPMC500875.

108. Falkow S. Molecular Koch's postulates applied to microbial pathogenicity. Rev Infect Dis. 1988;10 Suppl 2:S274-6. PubMed PMID: 3055197.

109. Reuss O, Vik A, Kolter R, Morschhauser J. The SAT1 flipper, an optimized tool for gene disruption in *Candida albicans*. Gene. 2004;341:119-27. Epub 2004/10/12. doi: 10.1016/j.gene.2004.06.021. PubMed PMID: 15474295.

110. Murad AM, Lee PR, Broadbent ID, Barelle CJ, Brown AJ. CIp10, an efficient and convenient integrating vector for *Candida albicans*. Yeast. 2000;16(4):325-7. doi: 10.1002/1097-0061(20000315)16:4<325::AID-YEA538>3.0.CO;2-#. PubMed PMID: 10669870.

111. Ohama T, Suzuki T, Mori M, Osawa S, Ueda T, Watanabe K, et al. Non-universal decoding of the leucine codon CUG in several *Candida* species. Nucleic Acids Res. 1993;21(17):4039-45. Epub 1993/08/25. doi: 10.1093/nar/21.17.4039. PubMed PMID: 8371978; PubMed Central PMCID: PMCPMC309997.

112. Ueno K, Uno J, Nakayama H, Sasamoto K, Mikami Y, Chibana H. Development of a highly efficient gene targeting system induced by transient repression of YKU80 expression in *Candida glabrata*. Eukaryot Cell. 2007;6(7):1239-47. Epub 2007/05/22. doi: 10.1128/EC.00414-06. PubMed PMID: 17513567; PubMed Central PMCID: PMCPMC1951112.

113. Corrigan MW, Kerwin-Iosue CL, Kuczmarski AS, Amin KB, Wykoff DD. The fate of linear DNA in *Saccharomyces cerevisiae* and *Candida glabrata*: the role of homologous and non-homologous end joining. PLoS One. 2013;8(7):e69628. Epub 2013/07/31. doi: 10.1371/journal.pone.0069628. PubMed PMID: 23894512; PubMed Central PMCID: PMCPMC3722132.

114. Cen Y, Fiori A, Van Dijck P. Deletion of the DNA Ligase IV Gene in Candida glabrata Significantly Increases Gene-Targeting Efficiency. Eukaryot Cell. 2015;14(8):783-91. Epub 2015/06/07. doi: 10.1128/EC.00281-14. PubMed PMID: 26048009; PubMed Central PMCID: PMCPMC4519754.

115. Janeway Jr CA, Travers P, Walport M, Shlomchik MJ. Principles of innate and adaptive immunity. Immunobiology, 5th edition The Immune System in Health and Disease. New York.: Garland Science; 2001.; 2001.

116. Janeway CA, Jr., Medzhitov R. Innate immune recognition. Annu Rev Immunol. 2002;20:197-216. Epub 2002/02/28. doi: 10.1146/annurev.immunol.20.083001.084359. PubMed PMID: 11861602.

117. Zipfel PF. Complement and immune defense: from innate immunity to human diseases. Immunol Lett. 2009;126(1-2):1-7. Epub 2009/07/21. doi: 10.1016/j.imlet.2009.07.005. PubMed PMID: 19616581.

118. Kozel TR. Activation of the complement system by pathogenic fungi. Clin Microbiol Rev. 1996;9(1):34-46. Epub 1996/01/01. PubMed PMID: 8665475; PubMed Central PMCID: PMCPMC172880.

References

119. Mullick A, Elias M, Picard S, Bourget L, Jovcevski O, Gauthier S, et al. Dysregulated inflammatory response to *Candida albicans* in a C5-deficient mouse strain. Infect Immun. 2004;72(10):5868-76. Epub 2004/09/24. doi: 10.1128/IAI.72.10.5868-5876.2004. PubMed PMID: 15385488; PubMed Central PMCID: PMCPMC517586.

120. Cheng SC, Sprong T, Joosten LA, van der Meer JW, Kullberg BJ, Hube B, et al. Complement plays a central role in *Candida albicans*-induced cytokine production by human PBMCs. Eur J Immunol. 2012;42(4):993-1004. Epub 2012/04/26. doi: 10.1002/eji.201142057. PubMed PMID: 22531923.

121. Gelfand JA, Hurley DL, Fauci AS, Frank MM. Role of complement in host defense against experimental disseminated candidiasis. J Infect Dis. 1978;138(1):9-16. Epub 1978/07/01. doi: 10.1093/infdis/138.1.9. PubMed PMID: 355578.

122. Tsoni SV, Kerrigan AM, Marakalala MJ, Srinivasan N, Duffield M, Taylor PR, et al. Complement C3 plays an essential role in the control of opportunistic fungal infections. Infect Immun. 2009;77(9):3679-85. Epub 2009/07/08. doi: 10.1128/IAI.00233-09. PubMed PMID: 19581397; PubMed Central PMCID: PMCPMC2738051.

123. Zipfel PF, Skerka C. Complement, *Candida*, and cytokines: the role of C5a in host response to fungi. Eur J Immunol. 2012;42(4):822-5. Epub 2012/04/26. doi: 10.1002/eji.201242466. PubMed PMID: 22531909.

124. Speth C, Lass-Flörl C, Würzner R. Complement in fungal infections and complement evasion strategies. In: Brown GD, Netea MG, editors. Immunology of fungal infections. Dordrecht, The Netherlands: Springer; 2007. p. p. 177-99.

125. Heinsbroek SE, Taylor PR, Martinez FO, Martinez-Pomares L, Brown GD, Gordon S. Stage-specific sampling by pattern recognition receptors during *Candida albicans* phagocytosis. PLoS Pathog. 2008;4(11):e1000218. Epub 2008/12/02. doi: 10.1371/journal.ppat.1000218. PubMed PMID: 19043561; PubMed Central PMCID: PMCPMC2583056.

126. Netea MG, Brown GD, Kullberg BJ, Gow NA. An integrated model of the recognition of *Candida albicans* by the innate immune system. Nat Rev Microbiol. 2008;6(1):67-78. Epub 2007/12/15. doi: 10.1038/nrmicro1815. PubMed PMID: 18079743.

127. Richardson JP, Moyes DL. Adaptive immune responses to *Candida albicans* infection. Virulence. 2015;6(4):327-37. Epub 2015/01/22. doi: 10.1080/21505594.2015.1004977. PubMed PMID: 25607781; PubMed Central PMCID: PMCPMC4601188.

128. d'Ostiani CF, Del Sero G, Bacci A, Montagnoli C, Spreca A, Mencacci A, et al. Dendritic cells discriminate between yeasts and hyphae of the fungus *Candida albicans*. Implications for initiation of T helper cell immunity *in vitro* and *in vivo*. J Exp Med. 2000;191(10):1661-74. Epub 2000/05/17. doi: 10.1084/jem.191.10.1661. PubMed PMID: 10811860; PubMed Central PMCID: PMCPMC2193147.

129. van de Veerdonk FL, Joosten LA, Shaw PJ, Smeekens SP, Malireddi RK, van der Meer JW, et al. The inflammasome drives protective Th1 and Th17 cellular responses in disseminated candidiasis. Eur J Immunol. 2011;41(8):2260-8. Epub 2011/06/18. doi: 10.1002/eji.201041226. PubMed PMID: 21681738; PubMed Central PMCID: PMCPMC3939807.

130. Latgé JP. Tasting the fungal cell wall. Cell Microbiol. 2010;12(7):863-72. Epub 2010/05/21. doi: 10.1111/j.1462-5822.2010.01474.x. PubMed PMID: 20482553.

131. Gow NAR, Latge JP, Munro CA. The Fungal Cell Wall: Structure, Biosynthesis, and Function. Microbiol Spectr. 2017;5(3). Epub 2017/05/18. doi: 10.1128/microbiolspec.FUNK-0035-2016. PubMed PMID: 28513415.

132. Gow NA, Hube B. Importance of the *Candida albicans* cell wall during commensalism and infection. Curr Opin Microbiol. 2012;15(4):406-12. Epub 2012/05/23. doi: 10.1016/j.mib.2012.04.005. PubMed PMID: 22609181.

133. Plato A, Hardison SE, Brown GD. Pattern recognition receptors in antifungal immunity. Semin Immunopathol. 2015;37(2):97-106. Epub 2014/11/26. doi: 10.1007/s00281-014-0462-4. PubMed PMID: 25420452; PubMed Central PMCID: PMCPMC4326652.

134. Netea MG, Joosten LA, van der Meer JW, Kullberg BJ, van de Veerdonk FL. Immune defence against *Candida* fungal infections. Nat Rev Immunol. 2015;15(10):630-42. Epub 2015/09/22. doi: 10.1038/nri3897. PubMed PMID: 26388329.

135. Nathan C. Metchnikoff's Legacy in 2008. Nat Immunol. 2008;9(7):695-8. Epub 2008/06/20. doi: 10.1038/ni0708-695. PubMed PMID: 18563074.

136. Media N. Ilya Mechnikov – Biographical. 2019 [11. Nov 2019]. Available from: https://www.nobelprize.org/prizes/medicine/1908/mechnikov/biographical/.

137. Levin R, Grinstein S, Canton J. The life cycle of phagosomes: formation, maturation, and resolution. Immunol Rev. 2016;273(1):156-79. Epub 2016/08/26. doi: 10.1111/imr.12439. PubMed PMID: 27558334.

138. Haider M, Dambuza IM, Asamaphan P, Stappers M, Reid D, Yamasaki S, et al. The pattern recognition receptors dectin-2, mincle, and FcRgamma impact the dynamics of phagocytosis of *Candida*, *Saccharomyces*, *Malassezia*, and *Mucor* species. PLoS One. 2019;14(8):e0220867. Epub 2019/08/09. doi: 10.1371/journal.pone.0220867. PubMed PMID: 31393930; PubMed Central PMCID: PMCPMC6687134.

139. Flannagan RS, Jaumouille V, Grinstein S. The cell biology of phagocytosis. Annu Rev Pathol. 2012;7:61-98. Epub 2011/09/14. doi: 10.1146/annurev-pathol-011811-132445. PubMed PMID: 21910624.

140. Flannagan RS, Heit B, Heinrichs DE. Antimicrobial Mechanisms of Macrophages and the Immune Evasion Strategies of *Staphylococcus aureus*. Pathogens. 2015;4(4):826-68. Epub 2015/12/04. doi: 10.3390/pathogens4040826. PubMed PMID: 26633519; PubMed Central PMCID: PMCPMC4693167.

141. Mayadas TN, Cullere X, Lowell CA. The multifaceted functions of neutrophils. Annu Rev Pathol. 2014;9:181-218. Epub 2013/09/21. doi: 10.1146/annurev-pathol-020712-164023. PubMed PMID: 24050624; PubMed Central PMCID: PMCPMC4277181.

142. Hong CW. Current Understanding in Neutrophil Differentiation and Heterogeneity. Immune Netw. 2017;17(5):298-306. Epub 2017/11/03. doi: 10.4110/in.2017.17.5.298. PubMed PMID: 29093651; PubMed Central PMCID: PMCPMC5662779.

143. Fulurija A, Ashman RB, Papadimitriou JM. Neutrophil depletion increases susceptibility to systemic and vaginal candidiasis in mice, and reveals differences between brain and kidney in mechanisms of host resistance. Microbiology. 1996;142 (Pt 12):3487-96. Epub 1996/12/01. doi: 10.1099/13500872-142-12-3487. PubMed PMID: 9004511.

144. Hamood M, Bluche PF, De Vroey C, Corazza F, Bujan W, Fondu P. Effects of recombinant human granulocyte-colony stimulating factor on neutropenic mice infected with *Candida albicans*: acceleration of recovery from neutropenia and potentiation of anti-*C. albicans* resistance. Mycoses. 1994;37(3-4):93-9. Epub 1994/03/01. doi: 10.1111/j.1439-0507.1994.tb00783.x. PubMed PMID: 7531290.

145. Koh AY, Kohler JR, Coggshall KT, Van Rooijen N, Pier GB. Mucosal damage and neutropenia are required for *Candida albicans* dissemination. PLoS Pathog. 2008;4(2):e35. Epub 2008/02/20. doi: 10.1371/journal.ppat.0040035. PubMed PMID: 18282097; PubMed Central PMCID: PMCPMC2242836.

146. Romani L, Mencacci A, Cenci E, Del Sero G, Bistoni F, Puccetti P. An immunoregulatory role for neutrophils in CD4+ T helper subset selection in mice with candidiasis. J Immunol. 1997;158(5):2356-62. Epub 1997/03/01. PubMed PMID: 9036985.

147. Lionakis MS, Lim JK, Lee CC, Murphy PM. Organ-specific innate immune responses in a mouse model of invasive candidiasis. J Innate Immun. 2011;3(2):180-99. Epub 2010/11/11. doi: 10.1159/000321157. PubMed PMID: 21063074; PubMed Central PMCID: PMCPMC3072204.

148. Altmeier S, Toska A, Sparber F, Teijeira A, Halin C, LeibundGut-Landmann S. IL-1 Coordinates the Neutrophil Response to *C. albicans* in the Oral Mucosa. PLoS Pathog. 2016;12(9):e1005882. Epub 2016/09/16. doi: 10.1371/journal.ppat.1005882. PubMed PMID: 27632536; PubMed Central PMCID: PMCPMC5025078.

References

149. Huppler AR, Conti HR, Hernandez-Santos N, Darville T, Biswas PS, Gaffen SL. Role of neutrophils in IL-17-dependent immunity to mucosal candidiasis. J Immunol. 2014;192(4):1745-52. Epub 2014/01/21. doi: 10.4049/jimmunol.1302265. PubMed PMID: 24442441; PubMed Central PMCID: PMCPMC3946223.

150. Brown GD. Innate antifungal immunity: the key role of phagocytes. Annu Rev Immunol. 2011;29:1-21. Epub 2010/10/13. doi: 10.1146/annurev-immunol-030409-101229. PubMed PMID: 20936972; PubMed Central PMCID: PMCPMC3434799.

151. Amulic B, Cazalet C, Hayes GL, Metzler KD, Zychlinsky A. Neutrophil function: from mechanisms to disease. Annu Rev Immunol. 2012;30:459-89. Epub 2012/01/10. doi: 10.1146/annurev-immunol-020711-074942. PubMed PMID: 22224774.

152. Rosales C. Neutrophil: A Cell with Many Roles in Inflammation or Several Cell Types? Front Physiol. 2018;9:113. Epub 2018/03/09. doi: 10.3389/fphys.2018.00113. PubMed PMID: 29515456; PubMed Central PMCID: PMCPMC5826082.

153. Aratani Y, Koyama H, Nyui S, Suzuki K, Kura F, Maeda N. Severe impairment in early host defense against *Candida albicans* in mice deficient in myeloperoxidase. Infect Immun. 1999;67(4):1828-36. Epub 1999/03/20. PubMed PMID: 10085024; PubMed Central PMCID: PMCPMC96534.

154. Lehrer RI, Cline MJ. Leukocyte myeloperoxidase deficiency and disseminated candidiasis: the role of myeloperoxidase in resistance to *Candida* infection. J Clin Invest. 1969;48(8):1478-88. Epub 1969/08/01. doi: 10.1172/JCI106114. PubMed PMID: 5796360; PubMed Central PMCID: PMCPMC322375.

155. Lehrer RI. Measurement of candidacidal activity of specific leukocyte types in mixed cell populations I. Normal, myeloperoxidase-deficient, and chronic granulomatous disease neutrophils. Infect Immun. 1970;2(1):42-7. Epub 1970/07/01. PubMed PMID: 16557797; PubMed Central PMCID: PMCPMC415961.

156. Brothers KM, Gratacap RL, Barker SE, Newman ZR, Norum A, Wheeler RT. NADPH oxidase-driven phagocyte recruitment controls *Candida albicans* filamentous growth and prevents mortality. PLoS Pathog. 2013;9(10):e1003634. Epub 2013/10/08. doi: 10.1371/journal.ppat.1003634. PubMed PMID: 24098114; PubMed Central PMCID: PMCPMC3789746.

157. Stevenhagen A, van Furth R. Interferon-gamma activates the oxidative killing of *Candida albicans* by human granulocytes. Clin Exp Immunol. 1993;91(1):170-5. Epub 1993/01/01. doi: 10.1111/j.1365-2249.1993.tb03374.x. PubMed PMID: 8419079; PubMed Central PMCID: PMCPMC1554646.

158. Donini M, Zenaro E, Tamassia N, Dusi S. NADPH oxidase of human dendritic cells: role in *Candida albicans* killing and regulation by interferons, dectin-1 and CD206. Eur J Immunol. 2007;37(5):1194-203. Epub 2007/04/05. doi: 10.1002/eji.200636532. PubMed PMID: 17407098.

159. Rubin-Bejerano I, Fraser I, Grisafi P, Fink GR. Phagocytosis by neutrophils induces an amino acid deprivation response in *Saccharomyces cerevisiae* and *Candida albicans*. Proc Natl Acad Sci U S A. 2003;100(19):11007-12. Epub 2003/09/06. doi: 10.1073/pnas.1834481100. PubMed PMID: 12958213; PubMed Central PMCID: PMCPMC196917.

160. Fradin C, De Groot P, MacCallum D, Schaller M, Klis F, Odds FC, et al. Granulocytes govern the transcriptional response, morphology and proliferation of *Candida albicans* in human blood. Mol Microbiol. 2005;56(2):397-415. Epub 2005/04/09. doi: 10.1111/j.1365-2958.2005.04557.x. PubMed PMID: 15813733.

161. Enjalbert B, MacCallum DM, Odds FC, Brown AJ. Niche-specific activation of the oxidative stress response by the pathogenic fungus *Candida albicans*. Infect Immun. 2007;75(5):2143-51. Epub 2007/03/07. doi: 10.1128/IAI.01680-06. PubMed PMID: 17339352; PubMed Central PMCID: PMCPMC1865731.

162. Geissmann F, Manz MG, Jung S, Sieweke MH, Merad M, Ley K. Development of monocytes, macrophages, and dendritic cells. Science. 2010;327(5966):656-61. Epub

2010/02/06. doi: 10.1126/science.1178331. PubMed PMID: 20133564; PubMed Central PMCID: PMCPMC2887389.

163. Tussiwand R, Gautier EL. Transcriptional Regulation of Mononuclear Phagocyte Development. Front Immunol. 2015;6:533. Epub 2015/11/06. doi: 10.3389/fimmu.2015.00533. PubMed PMID: 26539196; PubMed Central PMCID: PMCPMC4609886.

164. Yong SB, Song Y, Kim HJ, Ain QU, Kim YH. Mononuclear phagocytes as a target, not a barrier, for drug delivery. J Control Release. 2017;259:53-61. Epub 2017/01/22. doi: 10.1016/j.jconrel.2017.01.024. PubMed PMID: 28108325.

165. O'Connell KE, Mikkola AM, Stepanek AM, Vernet A, Hall CD, Sun CC, et al. Practical murine hematopathology: a comparative review and implications for research. Comp Med. 2015;65(2):96-113. Epub 2015/05/01. PubMed PMID: 25926395; PubMed Central PMCID: PMCPMC4408895.

166. Serbina NV, Jia T, Hohl TM, Pamer EG. Monocyte-mediated defense against microbial pathogens. Annu Rev Immunol. 2008;26:421-52. Epub 2008/02/29. doi: 10.1146/annurev.immunol.26.021607.090326. PubMed PMID: 18303997; PubMed Central PMCID: PMCPMC2921669.

167. Ginhoux F, Guilliams M. Tissue-Resident Macrophage Ontogeny and Homeostasis. Immunity. 2016;44(3):439-49. Epub 2016/03/18. doi: 10.1016/j.immuni.2016.02.024. PubMed PMID: 26982352.

168. Davies LC, Jenkins SJ, Allen JE, Taylor PR. Tissue-resident macrophages. Nat Immunol. 2013;14(10):986-95. Epub 2013/09/21. doi: 10.1038/ni.2705. PubMed PMID: 24048120; PubMed Central PMCID: PMCPMC4045180.

169. Qian Q, Jutila MA, Van Rooijen N, Cutler JE. Elimination of mouse splenic macrophages correlates with increased susceptibility to experimental disseminated candidiasis. J Immunol. 1994;152(10):5000-8. Epub 1994/05/15. PubMed PMID: 8176217.

170. van 't Wout JW, Linde I, Leijh PC, van Furth R. Contribution of granulocytes and monocytes to resistance against experimental disseminated *Candida albicans* infection. Eur J Clin Microbiol Infect Dis. 1988;7(6):736-41. Epub 1988/12/01. PubMed PMID: 3145854.

171. Ngo LY, Kasahara S, Kumasaka DK, Knoblaugh SE, Jhingran A, Hohl TM. Inflammatory monocytes mediate early and organ-specific innate defense during systemic candidiasis. J Infect Dis. 2014;209(1):109-19. Epub 2013/08/08. doi: 10.1093/infdis/jit413. PubMed PMID: 23922372; PubMed Central PMCID: PMCPMC3864383.

172. Thompson A, Davies LC, Liao CT, da Fonseca DM, Griffiths JS, Andrews R, et al. The protective effect of inflammatory monocytes during systemic *C. albicans* infection is dependent on collaboration between C-type lectin-like receptors. PLoS Pathog. 2019;15(6):e1007850. Epub 2019/06/27. doi: 10.1371/journal.ppat.1007850. PubMed PMID: 31242262; PubMed Central PMCID: PMCPMC6594653.

173. Dominguez-Andres J, Feo-Lucas L, Minguito de la Escalera M, Gonzalez L, Lopez-Bravo M, Ardavin C. Inflammatory Ly6C(high) Monocytes Protect against Candidiasis through IL-15-Driven NK Cell/Neutrophil Activation. Immunity. 2017;46(6):1059-72 e4. Epub 2017/06/22. doi: 10.1016/j.immuni.2017.05.009. PubMed PMID: 28636955.

174. Sun D, Sun P, Li H, Zhang M, Liu G, Strickland AB, et al. Fungal dissemination is limited by liver macrophage filtration of the blood. Nat Commun. 2019;10(1):4566. Epub 2019/10/09. doi: 10.1038/s41467-019-12381-5. PubMed PMID: 31594939; PubMed Central PMCID: PMCPMC6783440.

175. Lorenz MC, Bender JA, Fink GR. Transcriptional response of *Candida albicans* upon internalization by macrophages. Eukaryot Cell. 2004;3(5):1076-87. Epub 2004/10/08. doi: 10.1128/EC.3.5.1076-1087.2004. PubMed PMID: 15470236; PubMed Central PMCID: PMCPMC522606.

176. Marcil A, Harcus D, Thomas DY, Whiteway M. *Candida albicans* killing by RAW 264.7 mouse macrophage cells: effects of *Candida* genotype, infection ratios, and gamma

217

interferon treatment. Infect Immun. 2002;70(11):6319-29. Epub 2002/10/16. doi: 10.1128/iai.70.11.6319-6329.2002. PubMed PMID: 12379711; PubMed Central PMCID: PMCPMC130362.

177. Wellington M, Dolan K, Haidaris CG. Monocyte responses to *Candida albicans* are enhanced by antibody in cooperation with antibody-independent pathogen recognition. FEMS Immunol Med Microbiol. 2007;51(1):70-83. Epub 2007/07/06. doi: 10.1111/j.1574-695X.2007.00278.x. PubMed PMID: 17610517.

178. Seider K, Brunke S, Schild L, Jablonowski N, Wilson D, Majer O, et al. The facultative intracellular pathogen *Candida glabrata* subverts macrophage cytokine production and phagolysosome maturation. J Immunol. 2011;187(6):3072-86. Epub 2011/08/19. doi: 10.4049/jimmunol.1003730. PubMed PMID: 21849684.

179. Koller B, Schramm C, Siebert S, Triebel J, Deland E, Pfefferkorn AM, et al. *Dictyostelium discoideum* as a Novel Host System to Study the Interaction between Phagocytes and Yeasts. Front Microbiol. 2016;7:1665. Epub 2016/11/08. doi: 10.3389/fmicb.2016.01665. PubMed PMID: 27818653; PubMed Central PMCID: PMCPMC5073093.

180. Radosa S, Ferling I, Sprague JL, Westermann M, Hillmann F. The different morphologies of yeast and filamentous fungi trigger distinct killing and feeding mechanisms in a fungivorous amoeba. Environ Microbiol. 2019;21(5):1809-20. Epub 2019/03/15. doi: 10.1111/1462-2920.14588. PubMed PMID: 30868709.

181. Priest SJ, Lorenz MC. Characterization of Virulence-Related Phenotypes in *Candida* Species of the CUG Clade. Eukaryot Cell. 2015;14(9):931-40. Epub 2015/07/08. doi: 10.1128/EC.00062-15. PubMed PMID: 26150417; PubMed Central PMCID: PMCPMC4551586.

182. Hernández-Chávez MJ, Pérez-García LA, Nino-Vega GA, Mora-Montes HM. Fungal Strategies to Evade the Host Immune Recognition. J Fungi (Basel). 2017;3(4). Epub 2018/01/27. doi: 10.3390/jof3040051. PubMed PMID: 29371567; PubMed Central PMCID: PMCPMC5753153.

183. Gantner BN, Simmons RM, Underhill DM. Dectin-1 mediates macrophage recognition of *Candida albicans* yeast but not filaments. EMBO J. 2005;24(6):1277-86. Epub 2005/02/25. doi: 10.1038/sj.emboj.7600594. PubMed PMID: 15729357; PubMed Central PMCID: PMCPMC556398.

184. Erwig LP, Gow NA. Interactions of fungal pathogens with phagocytes. Nat Rev Microbiol. 2016;14(3):163-76. Epub 2016/02/09. doi: 10.1038/nrmicro.2015.21. PubMed PMID: 26853116.

185. Wheeler RT, Kombe D, Agarwala SD, Fink GR. Dynamic, morphotype-specific *Candida albicans* beta-glucan exposure during infection and drug treatment. PLoS Pathog. 2008;4(12):e1000227. Epub 2008/12/06. doi: 10.1371/journal.ppat.1000227. PubMed PMID: 19057660; PubMed Central PMCID: PMCPMC2587227.

186. Hopke A, Nicke N, Hidu EE, Degani G, Popolo L, Wheeler RT. Neutrophil Attack Triggers Extracellular Trap-Dependent *Candida* Cell Wall Remodeling and Altered Immune Recognition. PLoS Pathog. 2016;12(5):e1005644. Epub 2016/05/26. doi: 10.1371/journal.ppat.1005644. PubMed PMID: 27223610; PubMed Central PMCID: PMCPMC4880299.

187. Sherrington SL, Sorsby E, Mahtey N, Kumwenda P, Lenardon MD, Brown I, et al. Adaptation of *Candida albicans* to environmental pH induces cell wall remodelling and enhances innate immune recognition. PLoS Pathog. 2017;13(5):e1006403. Epub 2017/05/26. doi: 10.1371/journal.ppat.1006403. PubMed PMID: 28542528; PubMed Central PMCID: PMCPMC5456412.

188. Ballou ER, Avelar GM, Childers DS, Mackie J, Bain JM, Wagener J, et al. Lactate signalling regulates fungal beta-glucan masking and immune evasion. Nat Microbiol. 2016;2:16238. Epub 2016/12/13. doi: 10.1038/nmicrobiol.2016.238. PubMed PMID: 27941860; PubMed Central PMCID: PMCPMC5704895.

189. Pradhan A, Avelar GM, Bain JM, Childers DS, Larcombe DE, Netea MG, et al. Hypoxia Promotes Immune Evasion by Triggering beta-Glucan Masking on the *Candida albicans*

Cell Surface via Mitochondrial and cAMP-Protein Kinase A Signaling. mBio. 2018;9(6). Epub 2018/11/08. doi: 10.1128/mBio.01318-18. PubMed PMID: 30401773; PubMed Central PMCID: PMCPMC6222127.

190. Lopes JP, Stylianou M, Backman E, Holmberg S, Jass J, Claesson R, et al. Evasion of Immune Surveillance in Low Oxygen Environments Enhances *Candida albicans* Virulence. mBio. 2018;9(6). Epub 2018/11/08. doi: 10.1128/mBio.02120-18. PubMed PMID: 30401781; PubMed Central PMCID: PMCPMC6222133.

191. Glass KA, Longley SJ, Bliss JM, Shaw SK. Protection of *Candida parapsilosis* from neutrophil killing through internalization by human endothelial cells. Virulence. 2015;6(5):504-14. Epub 2015/06/04. doi: 10.1080/21505594.2015.1042643. PubMed PMID: 26039751; PubMed Central PMCID: PMCPMC4601288.

192. Snarr BD, Qureshi ST, Sheppard DC. Immune Recognition of Fungal Polysaccharides. J Fungi (Basel). 2017;3(3). Epub 2018/01/27. doi: 10.3390/jof3030047. PubMed PMID: 29371564; PubMed Central PMCID: PMCPMC5715945.

193. Kasper L, Seider K, Gerwien F, Allert S, Brunke S, Schwarzmuller T, et al. Identification of Candida glabrata genes involved in pH modulation and modification of the phagosomal environment in macrophages. PLoS One. 2014;9(5):e96015. Epub 2014/05/03. doi: 10.1371/journal.pone.0096015. PubMed PMID: 24789333; PubMed Central PMCID: PMCPMC4006850.

194. Duggan S, Essig F, Hunniger K, Mokhtari Z, Bauer L, Lehnert T, et al. Neutrophil activation by *Candida glabrata* but not *Candida albicans* promotes fungal uptake by monocytes. Cell Microbiol. 2015;17(9):1259-76. Epub 2015/04/09. doi: 10.1111/cmi.12443. PubMed PMID: 25850517.

195. MacCallum DM, Castillo L, Brown AJ, Gow NA, Odds FC. Early-expressed chemokines predict kidney immunopathology in experimental disseminated *Candida albicans* infections. PLoS One. 2009;4(7):e6420. Epub 2009/07/31. doi: 10.1371/journal.pone.0006420. PubMed PMID: 19641609; PubMed Central PMCID: PMCPMC2712765.

196. Hünniger K, Lehnert T, Bieber K, Martin R, Figge MT, Kurzai O. A virtual infection model quantifies innate effector mechanisms and *Candida albicans* immune escape in human blood. PLoS Comput Biol. 2014;10(2):e1003479. doi: 10.1371/journal.pcbi.1003479. PubMed PMID: 24586131; PubMed Central PMCID: PMC3930496.

197. Swidergall M, Khalaji M, Solis NV, Moyes DL, Drummond RA, Hube B, et al. Candidalysin Is Required for Neutrophil Recruitment and Virulence During Systemic *Candida albicans* Infection. J Infect Dis. 2019;220(9):1477-88. Epub 2019/08/12. doi: 10.1093/infdis/jiz322. PubMed PMID: 31401652; PubMed Central PMCID: PMCPMC6761979.

198. Wagener J, MacCallum DM, Brown GD, Gow NA. *Candida albicans* Chitin Increases Arginase-1 Activity in Human Macrophages, with an Impact on Macrophage Antimicrobial Functions. MBio. 2017;8(1). Epub 2017/01/26. doi: 10.1128/mBio.01820-16. PubMed PMID: 28119468; PubMed Central PMCID: PMCPMC5263244.

199. Chakraborty T, Thuer E, Heijink M, Tóth R, Bodai L, Vágvölgyi C, et al. Eicosanoid biosynthesis influences the virulence of *Candida parapsilosis*. Virulence. 2018;9(1):1019-35. Epub 2018/07/28. doi: 10.1080/21505594.2018.1475797. PubMed PMID: 30052120; PubMed Central PMCID: PMCPMC6086292.

200. Chakraborty T, Tóth R, Gácser A. Eicosanoid production by *Candida parapsilosis* and other pathogenic yeasts. Virulence. 2018. Epub 2018/12/19. doi: 10.1080/21505594.2018.1559674. PubMed PMID: 30558484.

201. Noverr MC, Phare SM, Toews GB, Coffey MJ, Huffnagle GB. Pathogenic yeasts *Cryptococcus neoformans* and *Candida albicans* produce immunomodulatory prostaglandins. Infect Immun. 2001;69(5):2957-63. Epub 2001/04/09. doi: 10.1128/IAI.69.5.2957-2963.2001. PubMed PMID: 11292712; PubMed Central PMCID: PMCPMC98248.

References

202. Smith LM, May RC. Mechanisms of microbial escape from phagocyte killing. Biochem Soc Trans. 2013;41(2):475-90. Epub 2013/03/22. doi: 10.1042/BST20130014. PubMed PMID: 23514140.

203. Hybiske K, Stephens R. Cellular Exit Strategies of Intracellular Bacteria. Microbiol Spectr. 2015;3(6). Epub 2016/06/24. doi: 10.1128/microbiolspec.VMBF-0002-2014. PubMed PMID: 27337274.

204. Flieger A, Frischknecht F, Häcker G, Hornef MW, Pradel G. Pathways of host cell exit by intracellular pathogens. Microb Cell. 2018;5(12):525-44. Epub 2018/12/12. doi: 10.15698/mic2018.12.659. PubMed PMID: 30533418; PubMed Central PMCID: PMCPMC6282021.

205. Alvarez M, Casadevall A. Phagosome extrusion and host-cell survival after *Cryptococcus neoformans* phagocytosis by macrophages. Curr Biol. 2006;16(21):2161-5. Epub 2006/11/07. doi: 10.1016/j.cub.2006.09.061. PubMed PMID: 17084702.

206. Ma H, Croudace JE, Lammas DA, May RC. Expulsion of live pathogenic yeast by macrophages. Curr Biol. 2006;16(21):2156-60. Epub 2006/11/07. doi: 10.1016/j.cub.2006.09.032. PubMed PMID: 17084701.

207. Bain JM, Lewis LE, Okai B, Quinn J, Gow NA, Erwig LP. Non-lytic expulsion/exocytosis of *Candida albicans* from macrophages. Fungal Genet Biol. 2012;49(9):677-8. Epub 2012/02/14. doi: 10.1016/j.fgb.2012.01.008. PubMed PMID: 22326419; PubMed Central PMCID: PMCPMC3430864.

208. Tóth R, Tóth A, Papp C, Jankovics F, Vagvolgyi C, Alonso MF, et al. Kinetic studies of *Candida parapsilosis* phagocytosis by macrophages and detection of intracellular survival mechanisms. Front Microbiol. 2014;5:633. Epub 2014/12/06. doi: 10.3389/fmicb.2014.00633. PubMed PMID: 25477874; PubMed Central PMCID: PMCPMC4238376.

209. Kasper L, Seider K, Hube B. Intracellular survival of *Candida glabrata* in macrophages: immune evasion and persistence. FEMS Yeast Res. 2015;15(5):fov042. Epub 2015/06/13. doi: 10.1093/femsyr/fov042. PubMed PMID: 26066553.

210. Kaposzta R, Marodi L, Hollinshead M, Gordon S, da Silva RP. Rapid recruitment of late endosomes and lysosomes in mouse macrophages ingesting *Candida albicans*. J Cell Sci. 1999;112 (Pt 19):3237-48. Epub 1999/10/03. PubMed PMID: 10504329.

211. McKenzie CG, Koser U, Lewis LE, Bain JM, Mora-Montes HM, Barker RN, et al. Contribution of *Candida albicans* cell wall components to recognition by and escape from murine macrophages. Infect Immun. 2010;78(4):1650-8. Epub 2010/02/04. doi: 10.1128/IAI.00001-10. PubMed PMID: 20123707; PubMed Central PMCID: PMCPMC2849426.

212. Ghosh S, Navarathna DH, Roberts DD, Cooper JT, Atkin AL, Petro TM, et al. Arginine-induced germ tube formation in *Candida albicans* is essential for escape from murine macrophage line RAW 264.7. Infect Immun. 2009;77(4):1596-605. Epub 2009/02/04. doi: 10.1128/IAI.01452-08. PubMed PMID: 19188358; PubMed Central PMCID: PMCPMC2663133.

213. Wellington M, Koselny K, Sutterwala FS, Krysan DJ. *Candida albicans* triggers NLRP3-mediated pyroptosis in macrophages. Eukaryot Cell. 2014;13(2):329-40. Epub 2014/01/01. doi: 10.1128/EC.00336-13. PubMed PMID: 24376002; PubMed Central PMCID: PMCPMC3910967.

214. Uwamahoro N, Verma-Gaur J, Shen HH, Qu Y, Lewis R, Lu J, et al. The pathogen *Candida albicans* hijacks pyroptosis for escape from macrophages. MBio. 2014;5(2):e00003-14. Epub 2014/03/29. doi: 10.1128/mBio.00003-14. PubMed PMID: 24667705; PubMed Central PMCID: PMCPMC3977349.

215. O'Meara TR, Veri AO, Ketela T, Jiang B, Roemer T, Cowen LE. Global analysis of fungal morphology exposes mechanisms of host cell escape. Nat Commun. 2015;6:6741. Epub 2015/04/01. doi: 10.1038/ncomms7741. PubMed PMID: 25824284; PubMed Central PMCID: PMCPMC4382923.

216. O'Meara TR, Duah K, Guo CX, Maxson ME, Gaudet RG, Koselny K, et al. High-Throughput Screening Identifies Genes Required for *Candida albicans* Induction of Macrophage Pyroptosis. MBio. 2018;9(4). Epub 2018/08/23. doi: 10.1128/mBio.01581-18. PubMed PMID: 30131363; PubMed Central PMCID: PMCPMC6106084.

217. Vylkova S, Lorenz MC. Phagosomal Neutralization by the Fungal Pathogen *Candida albicans* Induces Macrophage Pyroptosis. Infect Immun. 2017;85(2). Epub 2016/11/23. doi: 10.1128/IAI.00832-16. PubMed PMID: 27872238; PubMed Central PMCID: PMCPMC5278172.

218. Kasper L, Konig A, Koenig PA, Gresnigt MS, Westman J, Drummond RA, et al. The fungal peptide toxin Candidalysin activates the NLRP3 inflammasome and causes cytolysis in mononuclear phagocytes. Nat Commun. 2018;9(1):4260. Epub 2018/10/17. doi: 10.1038/s41467-018-06607-1. PubMed PMID: 30323213; PubMed Central PMCID: PMCPMC6189146.

219. Westman J, Moran G, Mogavero S, Hube B, Grinstein S. *Candida albicans* Hyphal Expansion Causes Phagosomal Membrane Damage and Luminal Alkalinization. MBio. 2018;9(5). Epub 2018/09/13. doi: 10.1128/mBio.01226-18. PubMed PMID: 30206168; PubMed Central PMCID: PMCPMC6134096.

220. Rai MN, Balusu S, Gorityala N, Dandu L, Kaur R. Functional genomic analysis of *Candida glabrata*-macrophage interaction: role of chromatin remodeling in virulence. PLoS Pathog. 2012;8(8):e1002863. Epub 2012/08/24. doi: 10.1371/journal.ppat.1002863. PubMed PMID: 22916016; PubMed Central PMCID: PMCPMC3420920.

221. Lewis LE, Bain JM, Lowes C, Gillespie C, Rudkin FM, Gow NA, et al. Stage specific assessment of *Candida albicans* phagocytosis by macrophages identifies cell wall composition and morphogenesis as key determinants. PLoS Pathog. 2012;8(3):e1002578. Epub 2012/03/23. doi: 10.1371/journal.ppat.1002578. PubMed PMID: 22438806; PubMed Central PMCID: PMCPMC3305454.

222. Bain JM, Louw J, Lewis LE, Okai B, Walls CA, Ballou ER, et al. *Candida albicans* hypha formation and mannan masking of beta-glucan inhibit macrophage phagosome maturation. MBio. 2014;5(6):e01874. Epub 2014/12/04. doi: 10.1128/mBio.01874-14. PubMed PMID: 25467440; PubMed Central PMCID: PMCPMC4324242.

223. Hwang CS, Rhie GE, Oh JH, Huh WK, Yim HS, Kang SO. Copper- and zinc-containing superoxide dismutase (Cu/ZnSOD) is required for the protection of *Candida albicans* against oxidative stresses and the expression of its full virulence. Microbiology. 2002;148(Pt 11):3705-13. Epub 2002/11/13. doi: 10.1099/00221287-148-11-3705. PubMed PMID: 12427960.

224. Miramón P, Dunker C, Windecker H, Bohovych IM, Brown AJ, Kurzai O, et al. Cellular responses of *Candida albicans* to phagocytosis and the extracellular activities of neutrophils are critical to counteract carbohydrate starvation, oxidative and nitrosative stress. PLoS One. 2012;7(12):e52850. Epub 2013/01/04. doi: 10.1371/journal.pone.0052850. PubMed PMID: 23285201; PubMed Central PMCID: PMCPMC3528649.

225. Patterson MJ, McKenzie CG, Smith DA, da Silva Dantas A, Sherston S, Veal EA, et al. Ybp1 and Gpx3 signaling in *Candida albicans* govern hydrogen peroxide-induced oxidation of the Cap1 transcription factor and macrophage escape. Antioxid Redox Signal. 2013;19(18):2244-60. Epub 2013/05/28. doi: 10.1089/ars.2013.5199. PubMed PMID: 23706023; PubMed Central PMCID: PMCPMC3869436.

226. Miramón P, Dunker C, Kasper L, Jacobsen ID, Barz D, Kurzai O, et al. A family of glutathione peroxidases contributes to oxidative stress resistance in *Candida albicans*. Med Mycol. 2014;52(3):223-39. Epub 2014/03/15. doi: 10.1093/mmy/myt021. PubMed PMID: 24625675.

227. Tillmann AT, Strijbis K, Cameron G, Radmaneshfar E, Thiel M, Munro CA, et al. Contribution of Fdh3 and Glr1 to Glutathione Redox State, Stress Adaptation and Virulence in *Candida albicans*. PLoS One. 2015;10(6):e0126940. Epub 2015/06/04. doi:

10.1371/journal.pone.0126940. PubMed PMID: 26039593; PubMed Central PMCID: PMCPMC4454436.

228. Cuéllar-Cruz M, López-Romero E, Ruiz-Baca E, Zazueta-Sandoval R. Differential response of *Candida albicans* and *Candida glabrata* to oxidative and nitrosative stresses. Curr Microbiol. 2014;69(5):733-9. Epub 2014/07/09. doi: 10.1007/s00284-014-0651-3. PubMed PMID: 25002360.

229. Chinen T, Qureshi MH, Koguchi Y, Kawakami K. *Candida albicans* suppresses nitric oxide (NO) production by interferon-gamma (IFN-gamma) and lipopolysaccharide (LPS)-stimulated murine peritoneal macrophages. Clin Exp Immunol. 1999;115(3):491-7. Epub 1999/04/08. doi: 10.1046/j.1365-2249.1999.00822.x. PubMed PMID: 10193423; PubMed Central PMCID: PMCPMC1905260.

230. Cuellar-Cruz M, Briones-Martin-del-Campo M, Canas-Villamar I, Montalvo-Arredondo J, Riego-Ruiz L, Castano I, et al. High resistance to oxidative stress in the fungal pathogen *Candida glabrata* is mediated by a single catalase, Cta1p, and is controlled by the transcription factors Yap1p, Skn7p, Msn2p, and Msn4p. Eukaryot Cell. 2008;7(5):814-25. Epub 2008/04/01. doi: 10.1128/EC.00011-08. PubMed PMID: 18375620; PubMed Central PMCID: PMCPMC2394966.

231. Roetzer A, Gratz N, Kovarik P, Schuller C. Autophagy supports *Candida glabrata* survival during phagocytosis. Cell Microbiol. 2010;12(2):199-216. Epub 2009/10/09. doi: 10.1111/j.1462-5822.2009.01391.x. PubMed PMID: 19811500; PubMed Central PMCID: PMCPMC2816358.

232. Whittaker JW. The irony of manganese superoxide dismutase. Biochem Soc Trans. 2003;31(Pt 6):1318-21. Epub 2003/12/04. doi: 10.1042/bst0311318. PubMed PMID: 14641053.

233. Djoko KY, Ong CL, Walker MJ, McEwan AG. The Role of Copper and Zinc Toxicity in Innate Immune Defense against Bacterial Pathogens. J Biol Chem. 2015;290(31):18954-61. Epub 2015/06/10. doi: 10.1074/jbc.R115.647099. PubMed PMID: 26055706; PubMed Central PMCID: PMCPMC4521016.

234. Valko M, Morris H, Cronin MT. Metals, toxicity and oxidative stress. Curr Med Chem. 2005;12(10):1161-208. Epub 2005/05/17. doi: 10.2174/0929867053764635. PubMed PMID: 15892631.

235. Weissman Z, Berdicevsky I, Cavari BZ, Kornitzer D. The high copper tolerance of Candida albicans is mediated by a P-type ATPase. Proc Natl Acad Sci U S A. 2000;97(7):3520-5. Epub 2000/03/29. doi: 10.1073/pnas.97.7.3520. PubMed PMID: 10737803; PubMed Central PMCID: PMCPMC16272.

236. Douglas LM, Wang HX, Keppler-Ross S, Dean N, Konopka JB. Sur7 promotes plasma membrane organization and is needed for resistance to stressful conditions and to the invasive growth and virulence of *Candida albicans*. MBio. 2012;3(1). Epub 2011/12/29. doi: 10.1128/mBio.00254-11. PubMed PMID: 22202230; PubMed Central PMCID: PMCPMC3244266.

237. Douglas LM, Konopka JB. Plasma membrane architecture protects *Candida albicans* from killing by copper. PLoS Genet. 2019;15(1):e1007911. Epub 2019/01/12. doi: 10.1371/journal.pgen.1007911. PubMed PMID: 30633741; PubMed Central PMCID: PMCPMC6345494.

238. Riedelberger M, Penninger P, Tscherner M, Hadriga B, Brunnhofer C, Jenull S, et al. Type I Interferons Ameliorate Zinc Intoxication of *Candida glabrata* by Macrophages and Promote Fungal Immune Evasion. iScience. 2020;23(5):101121. Epub 2020/05/20. doi: 10.1016/j.isci.2020.101121. PubMed PMID: 32428860; PubMed Central PMCID: PMCPMC7232100.

239. Ene IV, Brunke S, Brown AJ, Hube B. Metabolism in fungal pathogenesis. Cold Spring Harb Perspect Med. 2014;4(12):a019695. Epub 2014/09/06. doi: 10.1101/cshperspect.a019695. PubMed PMID: 25190251; PubMed Central PMCID: PMCPMC4292087.

240. Van Dijck P, Brown NA, Goldman GH, Rutherford J, Xue C, Van Zeebroeck G. Nutrient Sensing at the Plasma Membrane of Fungal Cells. Microbiol Spectr. 2017;5(2). Epub 2017/03/04. doi: 10.1128/microbiolspec.FUNK-0031-2016. PubMed PMID: 28256189.

241. Conrad M, Schothorst J, Kankipati HN, Van Zeebroeck G, Rubio-Texeira M, Thevelein JM. Nutrient sensing and signaling in the yeast *Saccharomyces cerevisiae*. FEMS Microbiol Rev. 2014;38(2):254-99. Epub 2014/02/04. doi: 10.1111/1574-6976.12065. PubMed PMID: 24483210; PubMed Central PMCID: PMCPMC4238866.

242. Ramírez-Zavala B, Mottola A, Haubenreisser J, Schneider S, Allert S, Brunke S, et al. The Snf1-activating kinase Sak1 is a key regulator of metabolic adaptation and *in vivo* fitness of *Candida albicans*. Mol Microbiol. 2017;104(6):989-1007. Epub 2017/03/25. doi: 10.1111/mmi.13674. PubMed PMID: 28337802.

243. Tripathi G, Wiltshire C, Macaskill S, Tournu H, Budge S, Brown AJ. Gcn4 co-ordinates morphogenetic and metabolic responses to amino acid starvation in *Candida albicans*. EMBO J. 2002;21(20):5448-56. Epub 2002/10/11. doi: 10.1093/emboj/cdf507. PubMed PMID: 12374745; PubMed Central PMCID: PMCPMC129063.

244. Inglis DO, Sherlock G. Ras signaling gets fine-tuned: regulation of multiple pathogenic traits of *Candida albicans*. Eukaryot Cell. 2013;12(10):1316-25. Epub 2013/08/06. doi: 10.1128/EC.00094-13. PubMed PMID: 23913542; PubMed Central PMCID: PMCPMC3811338.

245. Homann OR, Dea J, Noble SM, Johnson AD. A phenotypic profile of the *Candida albicans* regulatory network. PLoS Genet. 2009;5(12):e1000783. Epub 2009/12/31. doi: 10.1371/journal.pgen.1000783. PubMed PMID: 20041210; PubMed Central PMCID: PMCPMC2790342.

246. Shimamura S, Miyazaki T, Tashiro M, Takazono T, Saijo T, Yamamoto K, et al. Autophagy-Inducing Factor Atg1 Is Required for Virulence in the Pathogenic Fungus *Candida glabrata*. Front Microbiol. 2019;10:27. Epub 2019/02/15. doi: 10.3389/fmicb.2019.00027. PubMed PMID: 30761093; PubMed Central PMCID: PMCPMC6362428.

247. Lorenz MC, Fink GR. The glyoxylate cycle is required for fungal virulence. Nature. 2001;412(6842):83-6. Epub 2001/07/14. doi: 10.1038/35083594. PubMed PMID: 11452311.

248. Brega E, Zufferey R, Mamoun CB. *Candida albicans* Csy1p is a nutrient sensor important for activation of amino acid uptake and hyphal morphogenesis. Eukaryot Cell. 2004;3(1):135-43. Epub 2004/02/12. doi: 10.1128/ec.3.1.135-143.2004. PubMed PMID: 14871944; PubMed Central PMCID: PMCPMC329513.

249. Martínez P, Ljungdahl PO. Divergence of Stp1 and Stp2 transcription factors in *Candida albicans* places virulence factors required for proper nutrient acquisition under amino acid control. Mol Cell Biol. 2005;25(21):9435-46. Epub 2005/10/18. doi: 10.1128/MCB.25.21.9435-9446.2005. PubMed PMID: 16227594; PubMed Central PMCID: PMCPMC1265835.

250. Martínez P, Ljungdahl PO. An ER packaging chaperone determines the amino acid uptake capacity and virulence of *Candida albicans*. Mol Microbiol. 2004;51(2):371-84. Epub 2004/02/06. doi: 10.1046/j.1365-2958.2003.03845.x. PubMed PMID: 14756779.

251. Ramírez MA, Lorenz MC. Mutations in alternative carbon utilization pathways in *Candida albicans* attenuate virulence and confer pleiotropic phenotypes. Eukaryot Cell. 2007;6(2):280-90. Epub 2006/12/13. doi: 10.1128/EC.00372-06. PubMed PMID: 17158734; PubMed Central PMCID: PMCPMC1797957.

252. Chew SY, Ho KL, Cheah YK, Ng TS, Sandai D, Brown AJP, et al. Glyoxylate cycle gene *ICL1* is essential for the metabolic flexibility and virulence of *Candida glabrata*. Sci Rep. 2019;9(1):2843. Epub 2019/02/28. doi: 10.1038/s41598-019-39117-1. PubMed PMID: 30808979; PubMed Central PMCID: PMCPMC6391369.

253. Vylkova S, Lorenz MC. Modulation of phagosomal pH by *Candida albicans* promotes hyphal morphogenesis and requires Stp2p, a regulator of amino acid transport. PLoS

Pathog. 2014;10(3):e1003995. Epub 2014/03/15. doi: 10.1371/journal.ppat.1003995. PubMed PMID: 24626429; PubMed Central PMCID: PMCPMC3953444.

254. Danhof HA, Lorenz MC. The *Candida albicans* ATO Gene Family Promotes Neutralization of the Macrophage Phagolysosome. Infect Immun. 2015;83(11):4416-26. Epub 2015/09/10. doi: 10.1128/IAI.00984-15. PubMed PMID: 26351284; PubMed Central PMCID: PMCPMC4598414.

255. Danhof HA, Vylkova S, Vesely EM, Ford AE, Gonzalez-Garay M, Lorenz MC. Robust Extracellular pH Modulation by *Candida albicans* during Growth in Carboxylic Acids. mBio. 2016;7(6). Epub 2016/12/10. doi: 10.1128/mBio.01646-16. PubMed PMID: 27935835; PubMed Central PMCID: PMCPMC5111404.

256. Miramón P, Lorenz MC. The SPS amino acid sensor mediates nutrient acquisition and immune evasion in *Candida albicans*. Cell Microbiol. 2016;18(11):1611-24. Epub 2016/10/26. doi: 10.1111/cmi.12600. PubMed PMID: 27060451; PubMed Central PMCID: PMCPMC5501722.

257. Williams RB, Lorenz MC. Multiple Alternative Carbon Pathways Combine To Promote *Candida albicans* Stress Resistance, Immune Interactions, and Virulence. mBio. 2020;11(1). Epub 2020/01/16. doi: 10.1128/mBio.03070-19. PubMed PMID: 31937647; PubMed Central PMCID: PMCPMC6960290.

258. Vesely EM, Williams RB, Konopka JB, Lorenz MC. *N*-Acetylglucosamine Metabolism Promotes Survival of *Candida albicans* in the Phagosome. mSphere. 2017;2(5). Epub 2017/09/15. doi: 10.1128/mSphere.00357-17. PubMed PMID: 28904994; PubMed Central PMCID: PMCPMC5588037.

259. Brown AJ, Brown GD, Netea MG, Gow NA. Metabolism impacts upon *Candida* immunogenicity and pathogenicity at multiple levels. Trends Microbiol. 2014;22(11):614-22. Epub 2014/08/05. doi: 10.1016/j.tim.2014.07.001. PubMed PMID: 25088819; PubMed Central PMCID: PMCPMC4222764.

260. Ries LNA, Beattie S, Cramer RA, Goldman GH. Overview of carbon and nitrogen catabolite metabolism in the virulence of human pathogenic fungi. Mol Microbiol. 2018;107(3):277-97. Epub 2017/12/03. doi: 10.1111/mmi.13887. PubMed PMID: 29197127; PubMed Central PMCID: PMCPMC5777862.

261. Zaman S, Lippman SI, Zhao X, Broach JR. How *Saccharomyces* responds to nutrients. Annu Rev Genet. 2008;42:27-81. Epub 2008/02/29. doi: 10.1146/annurev.genet.41.110306.130206. PubMed PMID: 18303986.

262. Basson NJ. Competition for glucose between *Candida albicans* and oral bacteria grown in mixed culture in a chemostat. J Med Microbiol. 2000;49(11):969-75. Epub 2000/11/10. doi: 10.1099/0022-1317-49-11-969. PubMed PMID: 11073150.

263. Fleck CB, Schobel F, Brock M. Nutrient acquisition by pathogenic fungi: nutrient availability, pathway regulation, and differences in substrate utilization. Int J Med Microbiol. 2011;301(5):400-7. Epub 2011/05/10. doi: 10.1016/j.ijmm.2011.04.007. PubMed PMID: 21550848.

264. Weinberg ED. Nutritional immunity. Host's attempt to withold iron from microbial invaders. JAMA. 1975;231(1):39-41. Epub 1975/01/06. doi: 10.1001/jama.231.1.39. PubMed PMID: 1243565.

265. Kehl-Fie TE, Skaar EP. Nutritional immunity beyond iron: a role for manganese and zinc. Curr Opin Chem Biol. 2010;14(2):218-24. Epub 2009/12/18. doi: 10.1016/j.cbpa.2009.11.008. PubMed PMID: 20015678; PubMed Central PMCID: PMCPMC2847644.

266. Hood MI, Skaar EP. Nutritional immunity: transition metals at the pathogen-host interface. Nat Rev Microbiol. 2012;10(8):525-37. Epub 2012/07/17. doi: 10.1038/nrmicro2836. PubMed PMID: 22796883; PubMed Central PMCID: PMCPMC3875331.

267. Cellier MF. Nramp: from sequence to structure and mechanism of divalent metal import. Curr Top Membr. 2012;69:249-93. Epub 2012/10/11. doi: 10.1016/B978-0-12-394390-3.00010-0. PubMed PMID: 23046654.

268. Van Zandt KE, Sow FB, Florence WC, Zwilling BS, Satoskar AR, Schlesinger LS, et al. The iron export protein ferroportin 1 is differentially expressed in mouse macrophage populations and is present in the mycobacterial-containing phagosome. J Leukoc Biol. 2008;84(3):689-700. Epub 2008/07/01. doi: 10.1189/jlb.1107781. PubMed PMID: 18586980; PubMed Central PMCID: PMCPMC2516892.

269. Riedelberger M, Penninger P, Tscherner M, Seifert M, Jenull S, Brunnhofer C, et al. Type I Interferon Response Dysregulates Host Iron Homeostasis and Enhances *Candida glabrata* Infection. Cell Host Microbe. 2020. Epub 2020/02/23. doi: 10.1016/j.chom.2020.01.023. PubMed PMID: 32075740.

270. Gerwien F, Skrahina V, Kasper L, Hube B, Brunke S. Metals in fungal virulence. FEMS Microbiol Rev. 2018;42(1). Epub 2017/10/27. doi: 10.1093/femsre/fux050. PubMed PMID: 29069482; PubMed Central PMCID: PMCPMC5812535.

271. Nevitt T, Thiele DJ. Host iron withholding demands siderophore utilization for *Candida glabrata* to survive macrophage killing. PLoS Pathog. 2011;7(3):e1001322. doi: 10.1371/journal.ppat.1001322. PubMed PMID: 21445236; PubMed Central PMCID: PMC3060170.

272. Srivastava VK, Suneetha KJ, Kaur R. A systematic analysis reveals an essential role for high-affinity iron uptake system, haemolysin and CFEM domain-containing protein in iron homoeostasis and virulence in *Candida glabrata*. Biochem J. 2014;463(1):103-14. doi: 10.1042/BJ20140598. PubMed PMID: 24987864.

273. Towle HC. Glucose as a regulator of eukaryotic gene transcription. Trends Endocrinol Metab. 2005;16(10):489-94. Epub 2005/11/05. doi: 10.1016/j.tem.2005.10.003. PubMed PMID: 16269245.

274. Lorenz MC. Carbon catabolite control in *Candida albicans*: new wrinkles in metabolism. mBio. 2013;4(1):e00034-13. Epub 2013/02/07. doi: 10.1128/mBio.00034-13. PubMed PMID: 23386434; PubMed Central PMCID: PMCPMC3624514.

275. Sabina J, Brown V. Glucose sensing network in *Candida albicans*: a sweet spot for fungal morphogenesis. Eukaryot Cell. 2009;8(9):1314-20. Epub 2009/07/21. doi: 10.1128/EC.00138-09. PubMed PMID: 19617394; PubMed Central PMCID: PMCPMC2747818.

276. Ueno K, Matsumoto Y, Uno J, Sasamoto K, Sekimizu K, Kinjo Y, et al. Intestinal resident yeast *Candida glabrata* requires Cyb2p-mediated lactate assimilation to adapt in mouse intestine. PLoS One. 2011;6(9):e24759. Epub 2011/09/21. doi: 10.1371/journal.pone.0024759. PubMed PMID: 21931845; PubMed Central PMCID: PMCPMC3170380.

277. Barelle CJ, Priest CL, MacCallum DM, Gow NA, Odds FC, Brown AJ. Niche-specific regulation of central metabolic pathways in a fungal pathogen. Cell Microbiol. 2006;8(6):961-71. Epub 2006/05/10. doi: 10.1111/j.1462-5822.2005.00676.x. PubMed PMID: 16681837; PubMed Central PMCID: PMCPMC1472618.

278. Rodaki A, Bohovych IM, Enjalbert B, Young T, Odds FC, Gow NA, et al. Glucose promotes stress resistance in the fungal pathogen *Candida albicans*. Mol Biol Cell. 2009;20(22):4845-55. Epub 2009/09/18. doi: 10.1091/mbc.E09-01-0002. PubMed PMID: 19759180; PubMed Central PMCID: PMCPMC2777113.

279. Ene IV, Adya AK, Wehmeier S, Brand AC, MacCallum DM, Gow NA, et al. Host carbon sources modulate cell wall architecture, drug resistance and virulence in a fungal pathogen. Cell Microbiol. 2012;14(9):1319-35. Epub 2012/05/17. doi: 10.1111/j.1462-5822.2012.01813.x. PubMed PMID: 22587014; PubMed Central PMCID: PMCPMC3465787.

280. Ng TS, Desa MNM, Sandai D, Chong PP, Than LTL. Growth, biofilm formation, antifungal susceptibility and oxidative stress resistance of *Candida glabrata* are affected by different glucose concentrations. Infect Genet Evol. 2016;40:331-8. Epub 2015/09/12. doi: 10.1016/j.meegid.2015.09.004. PubMed PMID: 26358577.

281. Van Ende M, Wijnants S, Van Dijck P. Sugar Sensing and Signaling in *Candida albicans* and *Candida glabrata*. Front Microbiol. 2019;10:99. doi: 10.3389/fmicb.2019.00099. PubMed PMID: 30761119; PubMed Central PMCID: PMC6363656.

282. Chew SY, Ho KL, Cheah YK, Sandai D, Brown AJP, Than LTL. Physiologically Relevant Alternative Carbon Sources Modulate Biofilm Formation, Cell Wall Architecture, and the Stress and Antifungal Resistance of *Candida glabrata*. Int J Mol Sci. 2019;20(13). Epub 2019/07/03. doi: 10.3390/ijms20133172. PubMed PMID: 31261727; PubMed Central PMCID: PMCPMC6651560.

283. Vylkova S, Carman AJ, Danhof HA, Collette JR, Zhou H, Lorenz MC. The fungal pathogen *Candida albicans* autoinduces hyphal morphogenesis by raising extracellular pH. MBio. 2011;2(3):e00055-11. doi: 10.1128/mBio.00055-11. PubMed PMID: 21586647; PubMed Central PMCID: PMC3101780.

284. Schrevens S, Van Zeebroeck G, Riedelberger M, Tournu H, Kuchler K, Van Dijck P. Methionine is required for cAMP-PKA mediated morphogenesis and virulence of *Candida albicans*. Mol Microbiol. 2018;109(3):415-6. Epub 2018/09/07. doi: 10.1111/mmi.14065. PubMed PMID: 30187986.

285. Silao FGS, Ward M, Ryman K, Wallstrom A, Brindefalk B, Udekwu K, et al. Mitochondrial proline catabolism activates Ras1/cAMP/PKA-induced filamentation in *Candida albicans*. PLoS Genet. 2019;15(2):e1007976. doi: 10.1371/journal.pgen.1007976. PubMed PMID: 30742618; PubMed Central PMCID: PMC6386415.

286. Rajendran R, May A, Sherry L, Kean R, Williams C, Jones BL, et al. Integrating *Candida albicans* metabolism with biofilm heterogeneity by transcriptome mapping. Sci Rep. 2016;6:35436. Epub 2016/10/22. doi: 10.1038/srep35436. PubMed PMID: 27765942; PubMed Central PMCID: PMCPMC5073228.

287. Combs JGFM, J.P. The Vitamins: Fundamental Aspects in Nutrition and Health: Academic Press; 2017.

288. Suzuki H, Kunisawa J. Vitamin-mediated immune regulation in the development of inflammatory diseases. Endocr Metab Immune Disord Drug Targets. 2015;15(3):212-5. Epub 2015/03/17. PubMed PMID: 25772180.

289. Dakshinamurti K. Biotin--a regulator of gene expression. J Nutr Biochem. 2005;16(7):419-23. doi: 10.1016/j.jnutbio.2005.03.015. PubMed PMID: 15992682.

290. Sprenger M, Kasper L, Hensel M, Hube B. Metabolic adaptation of intracellular bacteria and fungi to macrophages. Int J Med Microbiol. 2018;308(1):215-27. Epub 2017/11/19. doi: 10.1016/j.ijmm.2017.11.001. PubMed PMID: 29150190.

291. Zengler K, Zaramela LS. The social network of microorganisms - how auxotrophies shape complex communities. Nat Rev Microbiol. 2018;16(6):383-90. Epub 2018/03/31. doi: 10.1038/s41579-018-0004-5. PubMed PMID: 29599459; PubMed Central PMCID: PMCPMC6059367.

292. Long Q, Ji L, Wang H, Xie J. Riboflavin biosynthetic and regulatory factors as potential novel anti-infective drug targets. Chem Biol Drug Des. 2010;75(4):339-47. Epub 2010/02/13. doi: 10.1111/j.1747-0285.2010.00946.x. PubMed PMID: 20148904.

293. Salaemae W, Booker GW, Polyak SW. The Role of Biotin in Bacterial Physiology and Virulence: a Novel Antibiotic Target for *Mycobacterium tuberculosis*. Microbiol Spectr. 2016;4(2). Epub 2016/05/27. doi: 10.1128/microbiolspec.VMBF-0008-2015. PubMed PMID: 27227307.

294. Dick T, Manjunatha U, Kappes B, Gengenbacher M. Vitamin B6 biosynthesis is essential for survival and virulence of *Mycobacterium tuberculosis*. Mol Microbiol. 2010;78(4):980-8. Epub 2010/09/08. doi: 10.1111/j.1365-2958.2010.07381.x. PubMed PMID: 20815826.

295. Sambandamurthy VK, Wang X, Chen B, Russell RG, Derrick S, Collins FM, et al. A pantothenate auxotroph of *Mycobacterium tuberculosis* is highly attenuated and protects mice against tuberculosis. Nat Med. 2002;8(10):1171-4. Epub 2002/09/10. doi: 10.1038/nm765. PubMed PMID: 12219086.

296. Vitreschak AG, Rodionov DA, Mironov AA, Gelfand MS. Regulation of riboflavin biosynthesis and transport genes in bacteria by transcriptional and translational

attenuation. Nucleic Acids Res. 2002;30(14):3141-51. Epub 2002/07/24. doi: 10.1093/nar/gkf433. PubMed PMID: 12136096; PubMed Central PMCID: PMCPMC135753.

297. Deka RK, Brautigam CA, Biddy BA, Liu WZ, Norgard MV. Evidence for an ABC-type riboflavin transporter system in pathogenic spirochetes. MBio. 2013;4(1):e00615-12. Epub 2013/02/14. doi: 10.1128/mBio.00615-12. PubMed PMID: 23404400; PubMed Central PMCID: PMCPMC3573665.

298. Mansjö M, Johansson J. The riboflavin analog roseoflavin targets an FMN-riboswitch and blocks *Listeria monocytogenes* growth, but also stimulates virulence gene-expression and infection. RNA Biol. 2011;8(4):674-80. Epub 2011/05/20. doi: 10.4161/rna.8.4.15586. PubMed PMID: 21593602; PubMed Central PMCID: PMCPMC3225981.

299. Meir Z, Osherov N. Vitamin Biosynthesis as an Antifungal Target. J Fungi (Basel). 2018;4(2). Epub 2018/06/20. doi: 10.3390/jof4020072. PubMed PMID: 29914189; PubMed Central PMCID: PMCPMC6023522.

300. Spry C, Kirk K, Saliba KJ. Coenzyme A biosynthesis: an antimicrobial drug target. FEMS Microbiol Rev. 2008;32(1):56-106. Epub 2008/01/05. doi: 10.1111/j.1574-6976.2007.00093.x. PubMed PMID: 18173393.

301. Kronenberger T, Lindner J, Meissner KA, Zimbres FM, Coronado MA, Sauer FM, et al. Vitamin B6-dependent enzymes in the human malaria parasite *Plasmodium falciparum*: a druggable target? Biomed Res Int. 2014;2014:108516. Epub 2014/02/14. doi: 10.1155/2014/108516. PubMed PMID: 24524072; PubMed Central PMCID: PMCPMC3912857.

302. Kundu B, Sarkar D, Ray N, Talukdar A. Understanding the riboflavin biosynthesis pathway for the development of antimicrobial agents. Med Res Rev. 2019;39(4):1338-71. Epub 2019/03/31. doi: 10.1002/med.21576. PubMed PMID: 30927319.

303. Dietl AM, Meir Z, Shadkchan Y, Osherov N, Haas H. Riboflavin and pantothenic acid biosynthesis are crucial for iron homeostasis and virulence in the pathogenic mold *Aspergillus fumigatus*. Virulence. 2018;9(1):1036-49. Epub 2018/07/28. doi: 10.1080/21505594.2018.1482181. PubMed PMID: 30052132; PubMed Central PMCID: PMCPMC6068542.

304. Purnell DM. The effects of specific auxotrophic mutations on the virulence of *Aspergillus nidulans* for mice. Mycopathol Mycol Appl. 1973;50(3):195-203. Epub 1973/07/31. doi: 10.1007/bf02053368. PubMed PMID: 4580921.

305. Garfoot AL, Zemska O, Rappleye CA. *Histoplasma capsulatum* depends on *de novo* vitamin biosynthesis for intraphagosomal proliferation. Infect Immun. 2014;82(1):393-404. Epub 2013/11/06. doi: 10.1128/IAI.00824-13. PubMed PMID: 24191299; PubMed Central PMCID: PMCPMC3911860.

306. Becker JM, Kauffman SJ, Hauser M, Huang L, Lin M, Sillaots S, et al. Pathway analysis of *Candida albicans* survival and virulence determinants in a murine infection model. Proc Natl Acad Sci U S A. 2010;107(51):22044-9. Epub 2010/12/08. doi: 10.1073/pnas.1009845107. PubMed PMID: 21135205; PubMed Central PMCID: PMCPMC3009777.

307. Brown JS, Aufauvre-Brown A, Brown J, Jennings JM, Arst H, Jr., Holden DW. Signature-tagged and directed mutagenesis identify PABA synthetase as essential for Aspergillus fumigatus pathogenicity. Mol Microbiol. 2000;36(6):1371-80. Epub 2000/08/10. doi: 10.1046/j.1365-2958.2000.01953.x. PubMed PMID: 10931287.

308. Tang CM, Smith JM, Arst HN, Jr., Holden DW. Virulence studies of *Aspergillus nidulans* mutants requiring lysine or p-aminobenzoic acid in invasive pulmonary aspergillosis. Infect Immun. 1994;62(12):5255-60. Epub 1994/12/01. PubMed PMID: 7960102; PubMed Central PMCID: PMCPMC303262.

309. Domergue R, Castano I, De Las Penas A, Zupancic M, Lockatell V, Hebel JR, et al. Nicotinic acid limitation regulates silencing of *Candida* adhesins during UTI. Science.

2005;308(5723):866-70. Epub 2005/03/19. doi: 10.1126/science.1108640. PubMed PMID: 15774723.

310. McVeigh IB, E. The amino acid and vitamin requirements of *Candida albicans* Y-475 and *Mycoderma vini* Y-939. Bull Torrey Botan Club. 1951;Vol. 78(No. 2 (Mar. - Apr., 1951):134–44. doi: doi: 10.2307/2482046.

311. Littman ML, Miwatani T. Effect of Water Soluble Vitamins and Their Analogues on the Growth of *Candida Albicans*. I. Biotin, Pyridoxamine, Pyridoxine and Fluorinated Pyrimidines. Mycopathol Mycol Appl. 1963;21:81-108. PubMed PMID: 14083424.

312. Seider K, Heyken A, Lüttich A, Miramón P, Hube B. Interaction of pathogenic yeasts with phagocytes: survival, persistence and escape. Curr Opin Microbiol. 2010;13(4):392-400. Epub 2010/07/16. doi: 10.1016/j.mib.2010.05.001. PubMed PMID: 20627672.

313. Lionakis MS, Swamydas M, Fischer BG, Plantinga TS, Johnson MD, Jaeger M, et al. CX$_3$CR1-dependent renal macrophage survival promotes *Candida* control and host survival. J Clin Invest. 2013;123(12):5035-51. Epub 2013/11/02. doi: 10.1172/JCI71307. PubMed PMID: 24177428; PubMed Central PMCID: PMCPMC3859390.

314. Seider K, Gerwien F, Kasper L, Allert S, Brunke S, Jablonowski N, et al. Immune evasion, stress resistance, and efficient nutrient acquisition are crucial for intracellular survival of *Candida glabrata* within macrophages. Eukaryot Cell. 2014;13(1):170-83. Epub 2013/12/24. doi: 10.1128/EC.00262-13. PubMed PMID: 24363366; PubMed Central PMCID: PMCPMC3910963.

315. Brunke S, Quintin J, Kasper L, Jacobsen ID, Richter ME, Hiller E, et al. Of mice, flies--and men? Comparing fungal infection models for large-scale screening efforts. Dis Model Mech. 2015;8(5):473-86. Epub 2015/03/20. doi: 10.1242/dmm.019901. PubMed PMID: 25786415; PubMed Central PMCID: PMCPMC4415897.

316. Casadevall A, Fu MS, Guimaraes AJ, Albuquerque P. The 'Amoeboid Predator-Fungal Animal Virulence' Hypothesis. J Fungi (Basel). 2019;5(1). Epub 2019/01/24. doi: 10.3390/jof5010010. PubMed PMID: 30669554; PubMed Central PMCID: PMCPMC6463022.

317. Fitzpatrick DA, O'Gaora P, Byrne KP, Butler G. Analysis of gene evolution and metabolic pathways using the *Candida* Gene Order Browser. BMC Genomics. 2010;11:290. doi: 10.1186/1471-2164-11-290. PubMed PMID: 20459735; PubMed Central PMCID: PMC2880306.

318. Hall C, Dietrich FS. The reacquisition of biotin prototrophy in *Saccharomyces cerevisiae* involved horizontal gene transfer, gene duplication and gene clustering. Genetics. 2007;177(4):2293-307. Epub 2007/12/13. doi: 10.1534/genetics.107.074963. PubMed PMID: 18073433; PubMed Central PMCID: PMCPMC2219469.

319. Miramón P, Lorenz MC. A feast for Candida: Metabolic plasticity confers an edge for virulence. PLoS Pathog. 2017;13(2):e1006144. doi: 10.1371/journal.ppat.1006144. PubMed PMID: 28182769; PubMed Central PMCID: PMC5300112.

320. Allert S. Der Einfluss spezifischer Gene der humanpathogenen Hefe *Candida glabrata* auf das Überleben in Makrophagen [Master Thesis]: Friedrich-Schiller University Jena; 2013.

321. Gordân R, Murphy KF, McCord RP, Zhu C, Vedenko A, Bulyk ML. Curated collection of yeast transcription factor DNA binding specificity data reveals novel structural and gene regulatory insights. Genome Biol. 2011;12(12):R125. Epub 2011/12/23. doi: 10.1186/gb-2011-12-12-r125. PubMed PMID: 22189060; PubMed Central PMCID: PMCPMC3334620.

322. Cherry JM, Hong EL, Amundsen C, Balakrishnan R, Binkley G, Chan ET, et al. *Saccharomyces* Genome Database: the genomics resource of budding yeast. Nucleic Acids Res. 2012;40(Database issue):D700-5. doi: 10.1093/nar/gkr1029. PubMed PMID: 22110037; PubMed Central PMCID: PMC3245034.

323. Jitrapakdee S, Wallace JC. Structure, function and regulation of pyruvate carboxylase. Biochem J. 1999;340 (Pt 1):1-16. Epub 1999/05/07. PubMed PMID: 10229653; PubMed Central PMCID: PMCPMC1220216.

324. Tehlivets O, Scheuringer K, Kohlwein SD. Fatty acid synthesis and elongation in yeast. Biochim Biophys Acta. 2007;1771(3):255-70. Epub 2006/09/05. doi: 10.1016/j.bbalip.2006.07.004. PubMed PMID: 16950653.

325. Stucka R, Dequin S, Salmon JM, Gancedo C. DNA sequences in chromosomes II and VII code for pyruvate carboxylase isoenzymes in *Saccharomyces cerevisiae*: analysis of pyruvate carboxylase-deficient strains. Mol Gen Genet. 1991;229(2):307-15. PubMed PMID: 1921979.

326. Hasslacher M, Ivessa AS, Paltauf F, Kohlwein SD. Acetyl-CoA carboxylase from yeast is an essential enzyme and is regulated by factors that control phospholipid metabolism. J Biol Chem. 1993;268(15):10946-52. Epub 1993/05/25. PubMed PMID: 8098706.

327. Brewster NK, Val DL, Walker ME, Wallace JC. Regulation of pyruvate carboxylase isozyme (*PYC1*, *PYC2*) gene expression in *Saccharomyces cerevisiae* during fermentative and nonfermentative growth. Arch Biochem Biophys. 1994;311(1):62-71. doi: 10.1006/abbi.1994.1209. PubMed PMID: 8185321.

328. Hoja U, Marthol S, Hofmann J, Stegner S, Schulz R, Meier S, et al. *HFA1* encoding an organelle-specific acetyl-CoA carboxylase controls mitochondrial fatty acid synthesis in *Saccharomyces cerevisiae*. J Biol Chem. 2004;279(21):21779-86. Epub 2004/02/06. doi: 10.1074/jbc.M401071200. PubMed PMID: 14761959.

329. Lane MD, Rominger KL, Young DL, Lynen F. The Enzymatic Synthesis of Holotranscarboxylase from Apotranscarboxylase and (+)-Biotin. Ii. Investigation of the Reaction Mechanism. J Biol Chem. 1964;239:2865-71. Epub 1964/09/01. PubMed PMID: 14216437.

330. Samols D, Thornton CG, Murtif VL, Kumar GK, Haase FC, Wood HG. Evolutionary conservation among biotin enzymes. J Biol Chem. 1988;263(14):6461-4. PubMed PMID: 2896195.

331. Chapman-Smith A, Cronan JE, Jr. Molecular biology of biotin attachment to proteins. J Nutr. 1999;129(2S Suppl):477S-84S. doi: 10.1093/jn/129.2.477S. PubMed PMID: 10064313.

332. Shenoy BC, Xie Y, Park VL, Kumar GK, Beegen H, Wood HG, et al. The importance of methionine residues for the catalysis of the biotin enzyme, transcarboxylase. Analysis by site-directed mutagenesis. J Biol Chem. 1992;267(26):18407-12. PubMed PMID: 1526981.

333. Diamandis EP, Christopoulos TK. The biotin-(strept)avidin system: principles and applications in biotechnology. Clin Chem. 1991;37(5):625-36. Epub 1991/05/01. PubMed PMID: 2032315.

334. Ringlstetter SL. Identification of the biotin transporter in *Escherichia coli*, biotinylation of histones in *Saccharomyces cerevisiae* and analysis of biotin sensing in *Saccharomyces cerevisiae*: Universität Regensburg; 2010.

335. Zempleni J, Hassan YI, Wijeratne SS. Biotin and biotinidase deficiency. Expert Rev Endocrinol Metab. 2008;3(6):715-24. doi: 10.1586/17446651.3.6.715. PubMed PMID: 19727438; PubMed Central PMCID: PMC2726758.

336. Azhar A, Booker GW, Polyak SW. Mechanisms of Biotin Transport. Biochem Anal Biochem. 2015;4. doi: 10.4172/2161-1009.1000210.

337. Ahmad Hussin N, Pathirana RU, Hasim S, Tati S, Scheib-Owens JA, Nickerson KW. Biotin Auxotrophy and Biotin Enhanced Germ Tube Formation in *Candida albicans*. Microorganisms. 2016;4(3). Epub 2016/09/30. doi: 10.3390/microorganisms4030037. PubMed PMID: 27681931; PubMed Central PMCID: PMCPMC5039597.

338. Sprenger M, Hartung TS, Allert S, Wisgott S, Niemiec MJ, Graf K, et al. Fungal biotin homeostasis is essential for immune evasion after macrophage phagocytosis and virulence. Cell Microbiol. 2020. Epub 2020/02/23. doi: 10.1111/cmi.13197. PubMed PMID: 32083801.

339. Stolz J. Isolation and characterization of the plasma membrane biotin transporter from *Schizosaccharomyces pombe*. Yeast. 2003;20(3):221-31. Epub 2003/01/31. doi: 10.1002/yea.959. PubMed PMID: 12557275.

References

340. Agrawal S, Agrawal A, Said HM. Biotin deficiency enhances the inflammatory response of human dendritic cells. Am J Physiol Cell Physiol. 2016;311(3):C386-91. doi: 10.1152/ajpcell.00141.2016. PubMed PMID: 27413170; PubMed Central PMCID: PMC5129763.

341. Elahi A, Sabui S, Narasappa NN, Agrawal S, Lambrecht NW, Agrawal A, et al. Biotin Deficiency Induces Th1- and Th17-Mediated Proinflammatory Responses in Human CD4(+) T Lymphocytes via Activation of the mTOR Signaling Pathway. J Immunol. 2018;200(8):2563-70. doi: 10.4049/jimmunol.1701200. PubMed PMID: 29531163; PubMed Central PMCID: PMC5893381.

342. Xue J, Zempleni J. Epigenetic synergies between biotin and folate in the regulation of pro-inflammatory cytokines and repeats. Scand J Immunol. 2013;78(5):419-25. Epub 2013/09/07. doi: 10.1111/sji.12108. PubMed PMID: 24007195; PubMed Central PMCID: PMCPMC3817955.

343. Muraille E, Leo O, Moser M. TH1/TH2 paradigm extended: macrophage polarization as an unappreciated pathogen-driven escape mechanism? Front Immunol. 2014;5:603. Epub 2014/12/17. doi: 10.3389/fimmu.2014.00603. PubMed PMID: 25505468; PubMed Central PMCID: PMCPMC4244692.

344. Qin Y, Zhang L, Xu Z, Zhang J, Jiang YY, Cao Y, et al. Innate immune cell response upon *Candida albicans* infection. Virulence. 2016;7(5):512-26. Epub 2016/04/15. doi: 10.1080/21505594.2016.1138201. PubMed PMID: 27078171; PubMed Central PMCID: PMCPMC5026795.

345. Joly S, Ma N, Sadler JJ, Soll DR, Cassel SL, Sutterwala FS. Cutting edge: *Candida albicans* hyphae formation triggers activation of the Nlrp3 inflammasome. J Immunol. 2009;183(6):3578-81. Epub 2009/08/18. doi: 10.4049/jimmunol.0901323. PubMed PMID: 19684085; PubMed Central PMCID: PMCPMC2739101.

346. Rogiers O, Frising UC, Kucharikova S, Jabra-Rizk MA, van Loo G, Van Dijck P, et al. Candidalysin Crucially Contributes to Nlrp3 Inflammasome Activation by *Candida albicans* Hyphae. MBio. 2019;10(1). Epub 2019/01/10. doi: 10.1128/mBio.02221-18. PubMed PMID: 30622184; PubMed Central PMCID: PMCPMC6325245.

347. Schwarzmüller T, Ma B, Hiller E, Istel F, Tscherner M, Brunke S, et al. Systematic phenotyping of a large-scale *Candida glabrata* deletion collection reveals novel antifungal tolerance genes. PLoS Pathog. 2014;10(6):e1004211. Epub 2014/06/20. doi: 10.1371/journal.ppat.1004211. PubMed PMID: 24945925; PubMed Central PMCID: PMCPMC4063973.

348. Zhou P, Szczypka MS, Young R, Thiele DJ. A system for gene cloning and manipulation in the yeast *Candida glabrata*. Gene. 1994;142(1):135-40. Epub 1994/05/03. doi: 10.1016/0378-1119(94)90368-9. PubMed PMID: 8181748.

349. Keppler-Ross S, Douglas L, Konopka JB, Dean N. Recognition of yeast by murine macrophages requires mannan but not glucan. Eukaryot Cell. 2010;9(11):1776-87. Epub 2010/09/14. doi: 10.1128/EC.00156-10. PubMed PMID: 20833894; PubMed Central PMCID: PMCPMC2976302.

350. Prieto D, Roman E, Correia I, Pla J. The HOG pathway is critical for the colonization of the mouse gastrointestinal tract by *Candida albicans*. PLoS One. 2014;9(1):e87128. Epub 2014/01/30. doi: 10.1371/journal.pone.0087128. PubMed PMID: 24475243; PubMed Central PMCID: PMCPMC3903619.

351. Basso LR, Jr., Bartiss A, Mao Y, Gast CE, Coelho PS, Snyder M, et al. Transformation of *Candida albicans* with a synthetic hygromycin B resistance gene. Yeast. 2010;27(12):1039-48. Epub 2010/08/26. doi: 10.1002/yea.1813. PubMed PMID: 20737428; PubMed Central PMCID: PMCPMC4243612.

352. Kitada K, Yamaguchi E, Arisawa M. Cloning of the *Candida glabrata TRP1* and *HIS3* genes, and construction of their disruptant strains by sequential integrative transformation. Gene. 1995;165(2):203-6. Epub 1995/11/20. doi: 10.1016/0378-1119(95)00552-h. PubMed PMID: 8522176.

353. Gerami-Nejad M, Zacchi LF, McClellan M, Matter K, Berman J. Shuttle vectors for facile gap repair cloning and integration into a neutral locus in *Candida albicans*. Microbiology. 2013;159(Pt 3):565-79. Epub 2013/01/12. doi: 10.1099/mic.0.064097-0. PubMed PMID: 23306673; PubMed Central PMCID: PMCPMC3709822.

354. Singh DK, Nemeth T, Papp A, Toth R, Lukacsi S, Heidingsfeld O, et al. Functional Characterization of Secreted Aspartyl Proteases in *Candida parapsilosis*. mSphere. 2019;4(4). Epub 2019/08/23. doi: 10.1128/mSphere.00484-19. PubMed PMID: 31434748; PubMed Central PMCID: PMCPMC6706470.

355. Hu W, Sillaots S, Lemieux S, Davison J, Kauffman S, Breton A, et al. Essential gene identification and drug target prioritization in *Aspergillus fumigatus*. PLoS Pathog. 2007;3(3):e24. Epub 2007/03/14. doi: 10.1371/journal.ppat.0030024. PubMed PMID: 17352532; PubMed Central PMCID: PMCPMC1817658.

356. Bernstein DA, Vyas VK, Weinberg DE, Drinnenberg IA, Bartel DP, Fink GR. *Candida albicans* Dicer (CaDcr1) is required for efficient ribosomal and spliceosomal RNA maturation. Proc Natl Acad Sci U S A. 2012;109(2):523-8. Epub 2011/12/17. doi: 10.1073/pnas.1118859109. PubMed PMID: 22173636; PubMed Central PMCID: PMCPMC3258626.

357. Beaupere C, Chen RB, Pelosi W, Labunskyy VM. Genome-wide Quantification of Translation in Budding Yeast by Ribosome Profiling. J Vis Exp. 2017;(130). Epub 2017/12/30. doi: 10.3791/56820. PubMed PMID: 29286414; PubMed Central PMCID: PMCPMC5755679.

358. Fenton HJH. Oxidation of tartaric acid in presence of iron. J Chem Soc Trans. 1894;(65):899–910.

359. Neyrolles O, Wolschendorf F, Mitra A, Niederweis M. Mycobacteria, metals, and the macrophage. Immunol Rev. 2015;264(1):249-63. Epub 2015/02/24. doi: 10.1111/imr.12265. PubMed PMID: 25703564; PubMed Central PMCID: PMCPMC4521620.

360. Palmer LD, Skaar EP. Transition Metals and Virulence in Bacteria. Annu Rev Genet. 2016;50:67-91. Epub 2016/09/13. doi: 10.1146/annurev-genet-120215-035146. PubMed PMID: 27617971; PubMed Central PMCID: PMCPMC5125913.

361. Mackie J, Szabo EK, Urgast DS, Ballou ER, Childers DS, MacCallum DM, et al. Host-Imposed Copper Poisoning Impacts Fungal Micronutrient Acquisition during Systemic *Candida albicans* Infections. PLoS One. 2016;11(6):e0158683. Epub 2016/07/01. doi: 10.1371/journal.pone.0158683. PubMed PMID: 27362522; PubMed Central PMCID: PMCPMC4928837.

362. Wiemann P, Perevitsky A, Lim FY, Shadkchan Y, Knox BP, Landero Figueora JA, et al. Aspergillus fumigatus Copper Export Machinery and Reactive Oxygen Intermediate Defense Counter Host Copper-Mediated Oxidative Antimicrobial Offense. Cell Rep. 2017;19(10):2174-6. Epub 2017/06/08. doi: 10.1016/j.celrep.2017.05.075. PubMed PMID: 28591586.

363. Atri C, Guerfali FZ, Laouini D. Role of Human Macrophage Polarization in Inflammation during Infectious Diseases. Int J Mol Sci. 2018;19(6). Epub 2018/06/21. doi: 10.3390/ijms19061801. PubMed PMID: 29921749; PubMed Central PMCID: PMCPMC6032107.

364. Shen Q, Beucler MJ, Ray SC, Rappleye CA. Macrophage activation by IFN-gamma triggers restriction of phagosomal copper from intracellular pathogens. PLoS Pathog. 2018;14(11):e1007444. Epub 2018/11/20. doi: 10.1371/journal.ppat.1007444. PubMed PMID: 30452484; PubMed Central PMCID: PMCPMC6277122.

365. Pieper F. The role of the putative vacuole transporter Ctr2 of *Candida glabrata* under copper stress and during macrophage interaction [Master Thesis]: Friedrich-Schiller University Jena; 2020.

366. Davis MJ, Tsang TM, Qiu Y, Dayrit JK, Freij JB, Huffnagle GB, et al. Macrophage M1/M2 polarization dynamically adapts to changes in cytokine microenvironments in Cryptococcus

neoformans infection. mBio. 2013;4(3):e00264-13. Epub 2013/06/20. doi: 10.1128/mBio.00264-13. PubMed PMID: 23781069; PubMed Central PMCID: PMCPMC3684832.

367. Herweg JA, Hansmeier N, Otto A, Geffken AC, Subbarayal P, Prusty BK, et al. Purification and proteomics of pathogen-modified vacuoles and membranes. Front Cell Infect Microbiol. 2015;5:48. Epub 2015/06/18. doi: 10.3389/fcimb.2015.00048. PubMed PMID: 26082896; PubMed Central PMCID: PMCPMC4451638.

368. Slauch JM. How does the oxidative burst of macrophages kill bacteria? Still an open question. Mol Microbiol. 2011;80(3):580-3. Epub 2011/03/08. doi: 10.1111/j.1365-2958.2011.07612.x. PubMed PMID: 21375590; PubMed Central PMCID: PMCPMC3109634.

369. Reniere ML. Reduce, Induce, Thrive: Bacterial Redox Sensing during Pathogenesis. J Bacteriol. 2018;200(17). Epub 2018/06/13. doi: 10.1128/JB.00128-18. PubMed PMID: 29891640; PubMed Central PMCID: PMCPMC6088161.

370. Wood ZA, Schroder E, Robin Harris J, Poole LB. Structure, mechanism and regulation of peroxiredoxins. Trends Biochem Sci. 2003;28(1):32-40. Epub 2003/01/09. doi: 10.1016/s0968-0004(02)00003-8. PubMed PMID: 12517450.

371. Omotani S, Tani K, Nagai K, Hatsuda Y, Mukai J, Myotoku M. Water Soluble Vitamins Enhance the Growth of Microorganisms in Peripheral Parenteral Nutrition Solutions. Int J Med Sci. 2017;14(12):1213-9. Epub 2017/11/07. doi: 10.7150/ijms.21424. PubMed PMID: 29104477; PubMed Central PMCID: PMCPMC5666554.

372. Kuwahara T, Kaneda S, Shimono K. Adding Biotin to Parenteral Nutrition Solutions Without Lipid Accelerates the Growth of *Candida albicans*. Int J Med Sci. 2016;13(9):724-9. Epub 2016/09/21. doi: 10.7150/ijms.15951. PubMed PMID: 27648003; PubMed Central PMCID: PMCPMC5027192.

373. Rodionov DA, Arzamasov AA, Khoroshkin MS, Iablokov SN, Leyn SA, Peterson SN, et al. Micronutrient Requirements and Sharing Capabilities of the Human Gut Microbiome. Front Microbiol. 2019;10:1316. Epub 2019/07/06. doi: 10.3389/fmicb.2019.01316. PubMed PMID: 31275260; PubMed Central PMCID: PMCPMC6593275.

374. Magnusdottir S, Ravcheev D, de Crecy-Lagard V, Thiele I. Systematic genome assessment of B-vitamin biosynthesis suggests co-operation among gut microbes. Front Genet. 2015;6:148. doi: 10.3389/fgene.2015.00148. PubMed PMID: 25941533; PubMed Central PMCID: PMC4403557.

375. Ohsugi M, Imanishi Y, Teraoka T, Nishimura K, Nakao S. Biosynthesis of biotin-vitamers by family Enterobacteriaceae. J Nutr Sci Vitaminol (Tokyo). 1990;36(5):447-56. Epub 1990/10/01. doi: 10.3177/jnsv.36.447. PubMed PMID: 2097319.

376. Mishra AA, Koh AY. Adaptation of *Candida albicans* during gastrointestinal tract colonization. Curr Clin Microbiol Rep. 2018;5(3):165-72. Epub 2018/12/19. doi: 10.1007/s40588-018-0096-8. PubMed PMID: 30560045; PubMed Central PMCID: PMCPMC6294318.

377. Bryden WL. Intestinal distribution and absorption of biotin in the chicken. Br J Nutr. 1989;62(2):389-98. Epub 1989/09/01. doi: 10.1079/bjn19890039. PubMed PMID: 2819022.

378. Said HM. Cell and molecular aspects of human intestinal biotin absorption. J Nutr. 2009;139(1):158-62. Epub 2008/12/06. doi: 10.3945/jn.108.092023. PubMed PMID: 19056639; PubMed Central PMCID: PMCPMC2646215.

379. Stolz J, Hoja U, Meier S, Sauer N, Schweizer E. Identification of the plasma membrane H+-biotin symporter of *Saccharomyces cerevisiae* by rescue of a fatty acid-auxotrophic mutant. J Biol Chem. 1999;274(26):18741-6. Epub 1999/06/22. doi: 10.1074/jbc.274.26.18741. PubMed PMID: 10373489.

380. Gaur M, Puri N, Manoharlal R, Rai V, Mukhopadhayay G, Choudhury D, et al. MFS transportome of the human pathogenic yeast *Candida albicans*. BMC Genomics. 2008;9:579. Epub 2008/12/06. doi: 10.1186/1471-2164-9-579. PubMed PMID: 19055746; PubMed Central PMCID: PMCPMC2636803.

381. Altschul SF, Madden TL, Schaffer AA, Zhang J, Zhang Z, Miller W, et al. Gapped BLAST and PSI-BLAST: a new generation of protein database search programs. Nucleic Acids Res. 1997;25(17):3389-402. Epub 1997/09/01. doi: 10.1093/nar/25.17.3389. PubMed PMID: 9254694; PubMed Central PMCID: PMCPMC146917.

382. Zempleni J, Wijeratne SS, Hassan YI. Biotin. Biofactors. 2009;35(1):36-46. Epub 2009/03/26. doi: 10.1002/biof.8. PubMed PMID: 19319844; PubMed Central PMCID: PMCPMC4757853.

383. Madsen CT, Sylvestersen KB, Young C, Larsen SC, Poulsen JW, Andersen MA, et al. Biotin starvation causes mitochondrial protein hyperacetylation and partial rescue by the SIRT3-like deacetylase Hst4p. Nat Commun. 2015;6:7726. doi: 10.1038/ncomms8726. PubMed PMID: 26158509; PubMed Central PMCID: PMC4510963.

384. Wolf B. Biotinidase: its role in biotinidase deficiency and biotin metabolism. J Nutr Biochem. 2005;16(7):441-5. Epub 2005/07/05. doi: 10.1016/j.jnutbio.2005.03.024. PubMed PMID: 15992688.

385. Pace HC, Brenner C. The nitrilase superfamily: classification, structure and function. Genome Biol. 2001;2(1):REVIEWS0001. Epub 2001/09/06. doi: 10.1186/gb-2001-2-1-reviews0001. PubMed PMID: 11380987; PubMed Central PMCID: PMCPMC150437.

386. Weider M, Machnik A, Klebl F, Sauer N. Vhr1p, a new transcription factor from budding yeast, regulates biotin-dependent expression of *VHT1* and *BIO5*. J Biol Chem. 2006;281(19):13513-24. Epub 2006/03/15. doi: 10.1074/jbc.M512158200. PubMed PMID: 16533810.

387. Stüer H. Wahrnehmung von Biotinmangel durch *Saccharomyces cerevisiae*: Universität Regensburg; 2009.

388. Rosenbach A, Dignard D, Pierce JV, Whiteway M, Kumamoto CA. Adaptations of *Candida albicans* for growth in the mammalian intestinal tract. Eukaryot Cell. 2010;9(7):1075-86. Epub 2010/05/04. doi: 10.1128/EC.00034-10. PubMed PMID: 20435697; PubMed Central PMCID: PMCPMC2901676.

389. Arvas M, Kivioja T, Mitchell A, Saloheimo M, Ussery D, Penttila M, et al. Comparison of protein coding gene contents of the fungal phyla Pezizomycotina and Saccharomycotina. BMC Genomics. 2007;8:325. Epub 2007/09/18. doi: 10.1186/1471-2164-8-325. PubMed PMID: 17868481; PubMed Central PMCID: PMCPMC2045113.

390. Weider M, Schroder A, Klebl F, Sauer N. A novel mechanism for target gene-specific SWI/SNF recruitment via the Snf2p N-terminus. Nucleic Acids Res. 2011;39(10):4088-98. Epub 2011/02/01. doi: 10.1093/nar/gkr004. PubMed PMID: 21278159; PubMed Central PMCID: PMCPMC3105400.

391. Shakoury-Elizeh M, Tiedeman J, Rashford J, Ferea T, Demeter J, Garcia E, et al. Transcriptional remodeling in response to iron deprivation in *Saccharomyces cerevisiae*. Mol Biol Cell. 2004;15(3):1233-43. Epub 2003/12/12. doi: 10.1091/mbc.e03-09-0642. PubMed PMID: 14668481; PubMed Central PMCID: PMCPMC363115.

392. Natarajan K, Meyer MR, Jackson BM, Slade D, Roberts C, Hinnebusch AG, et al. Transcriptional profiling shows that Gcn4p is a master regulator of gene expression during amino acid starvation in yeast. Mol Cell Biol. 2001;21(13):4347-68. Epub 2001/06/08. doi: 10.1128/MCB.21.13.4347-4368.2001. PubMed PMID: 11390663; PubMed Central PMCID: PMCPMC87095.

393. Kornitzer D, Raboy B, Kulka RG, Fink GR. Regulated degradation of the transcription factor Gcn4. EMBO J. 1994;13(24):6021-30. Epub 1994/12/15. PubMed PMID: 7813440; PubMed Central PMCID: PMCPMC395579.

394. Ruiz-Amil M, De Torrontegui G, Palacián E, Catalina L, Losada M. Properties and function of yeast pyruvate carboxylase. J Biol Chem. 1965;240(9):3485-92. Epub 1965/09/01. PubMed PMID: 5891073.

395. Hoja U, Wellein C, Greiner E, Schweizer E. Pleiotropic phenotype of acetyl-CoA-carboxylase-defective yeast cells--viability of a BPL1-amber mutation depending on its

233

readthrough by normal tRNA(Gln)(CAG). Eur J Biochem. 1998;254(3):520-6. PubMed PMID: 9688262.

396. Hasim S, Tati S, Madayiputhiya N, Nandakumar R, Nickerson KW. Histone biotinylation in *Candida albicans*. FEMS Yeast Res. 2013;13(6):529-39. Epub 2013/05/31. doi: 10.1111/1567-1364.12056. PubMed PMID: 23718707.

397. Kothapalli N, Camporeale G, Kueh A, Chew YC, Oommen AM, Griffin JB, et al. Biological functions of biotinylated histones. J Nutr Biochem. 2005;16(7):446-8. Epub 2005/07/05. doi: 10.1016/j.jnutbio.2005.03.025. PubMed PMID: 15992689; PubMed Central PMCID: PMCPMC1226983.

398. Brock M. Fungal metabolism in host niches. Curr Opin Microbiol. 2009;12(4):371-6. Epub 2009/06/19. doi: 10.1016/j.mib.2009.05.004. PubMed PMID: 19535285.

399. Napier BA, Meyer L, Bina JE, Miller MA, Sjostedt A, Weiss DS. Link between intraphagosomal biotin and rapid phagosomal escape in *Francisella*. Proc Natl Acad Sci U S A. 2012;109(44):18084-9. Epub 2012/10/17. doi: 10.1073/pnas.1206411109. PubMed PMID: 23071317; PubMed Central PMCID: PMCPMC3497780.

400. Appelberg R. Macrophage nutriprive antimicrobial mechanisms. J Leukoc Biol. 2006;79(6):1117-28. Epub 2006/04/11. doi: 10.1189/jlb.0206079. PubMed PMID: 16603587.

401. Brunke S, Hube B. Two unlike cousins: *Candida albicans* and *C. glabrata* infection strategies. Cell Microbiol. 2013;15(5):701-8. Epub 2012/12/21. doi: 10.1111/cmi.12091. PubMed PMID: 23253282; PubMed Central PMCID: PMCPMC3654559.

402. Turner KH, Everett J, Trivedi U, Rumbaugh KP, Whiteley M. Requirements for *Pseudomonas aeruginosa* acute burn and chronic surgical wound infection. PLoS Genet. 2014;10(7):e1004518. Epub 2014/07/25. doi: 10.1371/journal.pgen.1004518. PubMed PMID: 25057820; PubMed Central PMCID: PMCPMC4109851.

403. Sassetti CM, Rubin EJ. Genetic requirements for mycobacterial survival during infection. Proc Natl Acad Sci U S A. 2003;100(22):12989-94. Epub 2003/10/22. doi: 10.1073/pnas.2134250100. PubMed PMID: 14569030; PubMed Central PMCID: PMCPMC240732.

404. Rengarajan J, Bloom BR, Rubin EJ. Genome-wide requirements for *Mycobacterium tuberculosis* adaptation and survival in macrophages. Proc Natl Acad Sci U S A. 2005;102(23):8327-32. Epub 2005/06/02. doi: 10.1073/pnas.0503272102. PubMed PMID: 15928073; PubMed Central PMCID: PMCPMC1142121.

405. Feng Y, Napier BA, Manandhar M, Henke SK, Weiss DS, Cronan JE. A Francisella virulence factor catalyses an essential reaction of biotin synthesis. Mol Microbiol. 2014;91(2):300-14. Epub 2013/12/10. doi: 10.1111/mmi.12460. PubMed PMID: 24313380; PubMed Central PMCID: PMCPMC3933004.

406. Feng Y, Chin CY, Chakravartty V, Gao R, Crispell EK, Weiss DS, et al. The Atypical Occurrence of Two Biotin Protein Ligases in *Francisella novicida* Is Due to Distinct Roles in Virulence and Biotin Metabolism. MBio. 2015;6(3):e00591. Epub 2015/06/11. doi: 10.1128/mBio.00591-15. PubMed PMID: 26060274; PubMed Central PMCID: PMCPMC4462617.

407. Ong SE, Blagoev B, Kratchmarova I, Kristensen DB, Steen H, Pandey A, et al. Stable isotope labeling by amino acids in cell culture, SILAC, as a simple and accurate approach to expression proteomics. Mol Cell Proteomics. 2002;1(5):376-86. Epub 2002/07/16. doi: 10.1074/mcp.m200025-mcp200. PubMed PMID: 12118079.

408. Bergsbaken T, Fink SL, Cookson BT. Pyroptosis: host cell death and inflammation. Nat Rev Microbiol. 2009;7(2):99-109. Epub 2009/01/17. doi: 10.1038/nrmicro2070. PubMed PMID: 19148178; PubMed Central PMCID: PMCPMC2910423.

409. O'Meara TR, Cowen LE. Insights into the host-pathogen interaction: *C. albicans* manipulation of macrophage pyroptosis. Microb Cell. 2018;5(12):566-8. Epub 2018/12/12. doi: 10.15698/mic2018.12.662. PubMed PMID: 30533421; PubMed Central PMCID: PMCPMC6282020.

410. Gross O, Poeck H, Bscheider M, Dostert C, Hannesschlager N, Endres S, et al. Syk kinase signalling couples to the Nlrp3 inflammasome for anti-fungal host defence. Nature. 2009;459(7245):433-6. Epub 2009/04/03. doi: 10.1038/nature07965. PubMed PMID: 19339971.

411. Hise AG, Tomalka J, Ganesan S, Patel K, Hall BA, Brown GD, et al. An essential role for the NLRP3 inflammasome in host defense against the human fungal pathogen *Candida albicans*. Cell Host Microbe. 2009;5(5):487-97. Epub 2009/05/21. doi: 10.1016/j.chom.2009.05.002. PubMed PMID: 19454352; PubMed Central PMCID: PMCPMC2824856.

412. Spellberg B, Ibrahim AS, Edwards JE, Jr., Filler SG. Mice with disseminated candidiasis die of progressive sepsis. J Infect Dis. 2005;192(2):336-43. Epub 2005/06/18. doi: 10.1086/430952. PubMed PMID: 15962230.

413. Jacobsen ID, Grosse K, Berndt A, Hube B. Pathogenesis of *Candida albicans* infections in the alternative chorio-allantoic membrane chicken embryo model resembles systemic murine infections. PLoS One. 2011;6(5):e19741. Epub 2011/05/24. doi: 10.1371/journal.pone.0019741. PubMed PMID: 21603634; PubMed Central PMCID: PMCPMC3094387.

414. Quintin J, Asmar J, Matskevich AA, Lafarge MC, Ferrandon D. The Drosophila Toll pathway controls but does not clear *Candida glabrata* infections. J Immunol. 2013;190(6):2818-27. Epub 2013/02/13. doi: 10.4049/jimmunol.1201861. PubMed PMID: 23401590.

415. Cheng S, Clancy CJ, Hartman DJ, Hao B, Nguyen MH. *Candida glabrata* intra-abdominal candidiasis is characterized by persistence within the peritoneal cavity and abscesses. Infect Immun. 2014;82(7):3015-22. Epub 2014/05/07. doi: 10.1128/IAI.00062-14. PubMed PMID: 24799629; PubMed Central PMCID: PMCPMC4097615.

416. Nash EE, Peters BM, Lilly EA, Noverr MC, Fidel PL, Jr. A Murine Model of *Candida glabrata* Vaginitis Shows No Evidence of an Inflammatory Immunopathogenic Response. PLoS One. 2016;11(1):e0147969. Epub 2016/01/26. doi: 10.1371/journal.pone.0147969. PubMed PMID: 26807975; PubMed Central PMCID: PMCPMC4726552.

417. Odds FC, Van Nuffel L, Gow NA. Survival in experimental *Candida albicans i*nfections depends on inoculum growth conditions as well as animal host. Microbiology. 2000;146 (Pt 8):1881-9. Epub 2000/08/10. doi: 10.1099/00221287-146-8-1881. PubMed PMID: 10931892.

418. MacCallum DM, Odds FC. Temporal events in the intravenous challenge model for experimental *Candida albicans* infections in female mice. Mycoses. 2005;48(3):151-61. Epub 2005/04/22. doi: 10.1111/j.1439-0507.2005.01121.x. PubMed PMID: 15842329.

419. Drummond RA, Collar AL, Swamydas M, Rodriguez CA, Lim JK, Mendez LM, et al. CARD9-Dependent Neutrophil Recruitment Protects against Fungal Invasion of the Central Nervous System. PLoS Pathog. 2015;11(12):e1005293. Epub 2015/12/19. doi: 10.1371/journal.ppat.1005293. PubMed PMID: 26679537; PubMed Central PMCID: PMCPMC4683065.

420. Drummond RA, Swamydas M, Oikonomou V, Zhai B, Dambuza IM, Schaefer BC, et al. CARD9(+) microglia promote antifungal immunity via IL-1beta- and CXCL1-mediated neutrophil recruitment. Nat Immunol. 2019;20(5):559-70. Epub 2019/04/19. doi: 10.1038/s41590-019-0377-2. PubMed PMID: 30996332; PubMed Central PMCID: PMCPMC6494474.

421. Beyer R, Jandric Z, Zutz C, Gregori C, Willinger B, Jacobsen ID, et al. Competition of *Candida glabrata* against Lactobacillus is Hog1 dependent. Cell Microbiol. 2018;20(12):e12943. Epub 2018/08/17. doi: 10.1111/cmi.12943. PubMed PMID: 30112857; PubMed Central PMCID: PMCPMC6283251.

422. Jong AY, Stins MF, Huang SH, Chen SH, Kim KS. Traversal of *Candida albicans* across human blood-brain barrier in vitro. Infect Immun. 2001;69(7):4536-44. Epub 2001/06/13.

doi: 10.1128/IAI.69.7.4536-4544.2001. PubMed PMID: 11401997; PubMed Central PMCID: PMCPMC98530.

423. Chen SH, Stins MF, Huang SH, Chen YH, Kwon-Chung KJ, Chang Y, et al. *Cryptococcus neoformans* induces alterations in the cytoskeleton of human brain microvascular endothelial cells. J Med Microbiol. 2003;52(Pt 11):961-70. doi: 10.1099/jmm.0.05230-0. PubMed PMID: 14532340.

424. Navarathna DH, Munasinghe J, Lizak MJ, Nayak D, McGavern DB, Roberts DD. MRI confirms loss of blood-brain barrier integrity in a mouse model of disseminated candidiasis. NMR Biomed. 2013;26(9):1125-34. Epub 2013/04/23. doi: 10.1002/nbm.2926. PubMed PMID: 23606437; PubMed Central PMCID: PMCPMC3744627.

425. Chang YC, Stins MF, McCaffery MJ, Miller GF, Pare DR, Dam T, et al. Cryptococcal yeast cells invade the central nervous system via transcellular penetration of the blood-brain barrier. Infect Immun. 2004;72(9):4985-95. doi: 10.1128/IAI.72.9.4985-4995.2004. PubMed PMID: 15321990; PubMed Central PMCID: PMC517459.

426. Shi M, Li SS, Zheng C, Jones GJ, Kim KS, Zhou H, et al. Real-time imaging of trapping and urease-dependent transmigration of *Cryptococcus neoformans* in mouse brain. J Clin Invest. 2010;120(5):1683-93. doi: 10.1172/JCI41963. PubMed PMID: 20424328; PubMed Central PMCID: PMC2860939.

427. Santiago-Tirado FH, Onken MD, Cooper JA, Klein RS, Doering TL. Trojan Horse Transit Contributes to Blood-Brain Barrier Crossing of a Eukaryotic Pathogen. MBio. 2017;8(1). doi: 10.1128/mBio.02183-16. PubMed PMID: 28143979; PubMed Central PMCID: PMC5285505.

428. Liu TB, Kim JC, Wang Y, Toffaletti DL, Eugenin E, Perfect JR, et al. Brain inositol is a novel stimulator for promoting *Cryptococcus* penetration of the blood-brain barrier. PLoS Pathog. 2013;9(4):e1003247. doi: 10.1371/journal.ppat.1003247. PubMed PMID: 23592982; PubMed Central PMCID: PMC3617100.

429. Fisher SK, Novak JE, Agranoff BW. Inositol and higher inositol phosphates in neural tissues: homeostasis, metabolism and functional significance. J Neurochem. 2002;82(4):736-54. Epub 2002/10/03. doi: 10.1046/j.1471-4159.2002.01041.x. PubMed PMID: 12358779.

430. Wang Y, Liu TB, Delmas G, Park S, Perlin D, Xue C. Two major inositol transporters and their role in cryptococcal virulence. Eukaryot Cell. 2011;10(5):618-28. doi: 10.1128/EC.00327-10. PubMed PMID: 21398509; PubMed Central PMCID: PMC3127654.

431. Edwards RL, Bryan A, Jules M, Harada K, Buchrieser C, Swanson MS. Nicotinic acid modulates Legionella pneumophila gene expression and induces virulence traits. Infect Immun. 2013;81(3):945-55. Epub 2013/01/16. doi: 10.1128/IAI.00999-12. PubMed PMID: 23319553; PubMed Central PMCID: PMCPMC3584888.

432. McPheat WL, Wardlaw AC, Novotny P. Modulation of *Bordetella pertussis* by nicotinic acid. Infect Immun. 1983;41(2):516-22. Epub 1983/08/01. PubMed PMID: 6307872; PubMed Central PMCID: PMCPMC264671.

433. Carfrae LA, MacNair CR, Brown CM, Tsai CN, Weber BS, Zlitni S, et al. Mimicking the human environment in mice reveals that inhibiting biotin biosynthesis is effective against antibiotic-resistant pathogens. Nat Microbiol. 2020;5(1):93-101. Epub 2019/10/30. doi: 10.1038/s41564-019-0595-2. PubMed PMID: 31659298.

434. Moriya A, Fukuwatari T, Sano M, Shibata K. Different variations of tissue B-group vitamin concentrations in short- and long-term starved rats. Br J Nutr. 2012;107(1):52-60. Epub 2011/07/08. doi: 10.1017/S0007114511002339. PubMed PMID: 21733331.

435. Spector R, Johanson CE. Vitamin transport and homeostasis in mammalian brain: focus on Vitamins B and E. J Neurochem. 2007;103(2):425-38. Epub 2007/07/25. doi: 10.1111/j.1471-4159.2007.04773.x. PubMed PMID: 17645457.

436. Cooper KM, Kennedy S, McConnell S, Kennedy DG, Frigg M. An immunohistochemical study of the distribution of biotin in tissues of pigs and chickens. Res Vet Sci. 1997;63(3):219-25. PubMed PMID: 9491447.

437. Dagher Z, Xu S, Negoro PE, Khan NS, Feldman MB, Reedy JL, et al. Fluorescent Tracking of Yeast Division Clarifies the Essential Role of Spleen Tyrosine Kinase in the Intracellular Control of *Candida glabrata* in Macrophages. Front Immunol. 2018;9:1058. Epub 2018/06/06. doi: 10.3389/fimmu.2018.01058. PubMed PMID: 29868018; PubMed Central PMCID: PMCPMC5964189.

438. Cote P, Hogues H, Whiteway M. Transcriptional analysis of the *Candida albicans* cell cycle. Mol Biol Cell. 2009;20(14):3363-73. Epub 2009/05/30. doi: 10.1091/mbc.E09-03-0210. PubMed PMID: 19477921; PubMed Central PMCID: PMCPMC2710843.

439. Corper HJ, Cohn ML. The viability and virulence of old cultures of tubercle bacilli; studies on 30-year-old broth cultures maintained at 37 degrees C. Tubercle. 1951;32(11):232-7. Epub 1951/11/01. PubMed PMID: 14893467.

440. Rittershaus ES, Baek SH, Sassetti CM. The normalcy of dormancy: common themes in microbial quiescence. Cell Host Microbe. 2013;13(6):643-51. Epub 2013/06/19. doi: 10.1016/j.chom.2013.05.012. PubMed PMID: 23768489; PubMed Central PMCID: PMCPMC3743100.

441. Sterkel AK, Mettelman R, Wuthrich M, Klein BS. The unappreciated intracellular lifestyle of *Blastomyces dermatitidis*. J Immunol. 2015;194(4):1796-805. Epub 2015/01/16. doi: 10.4049/jimmunol.1303089. PubMed PMID: 25589071; PubMed Central PMCID: PMCPMC4373353.

442. Charlier C, Nielsen K, Daou S, Brigitte M, Chretien F, Dromer F. Evidence of a role for monocytes in dissemination and brain invasion by *Cryptococcus neoformans*. Infect Immun. 2009;77(1):120-7. Epub 2008/10/22. doi: 10.1128/IAI.01065-08. PubMed PMID: 18936186; PubMed Central PMCID: PMCPMC2612285.

443. Kozicky LK, Sly LM. Depletion and Reconstitution of Macrophages in Mice. Methods Mol Biol. 2019;1960:101-12. Epub 2019/02/25. doi: 10.1007/978-1-4939-9167-9_9. PubMed PMID: 30798525.

444. Gola S, Martin R, Walther A, Dunkler A, Wendland J. New modules for PCR-based gene targeting in *Candida albicans*: rapid and efficient gene targeting using 100 bp of flanking homology region. Yeast. 2003;20(16):1339-47. Epub 2003/12/10. doi: 10.1002/yea.1044. PubMed PMID: 14663826.

445. Hartung TS. The role of biotin metabolism for the interaction of *Candida albicans* with macrophages [Master Thesis]: Friedrich Schiller University Jena; 2018.

446. Walther A, Wendland J. An improved transformation protocol for the human fungal pathogen *Candida albicans*. Curr Genet. 2003;42(6):339-43. Epub 2003/03/04. doi: 10.1007/s00294-002-0349-0. PubMed PMID: 12612807.

447. Gori K, Mortensen HD, Arneborg N, Jespersen L. Ammonia production and its possible role as a mediator of communication for *Debaryomyces hansenii* and other cheese-relevant yeast species. J Dairy Sci. 2007;90(11):5032-41. doi: 10.3168/jds.2006-750. PubMed PMID: 17954742.

6 Appendix

6.1 Additional experimental procedures

The following sections contain a more detailed description of the mutagenesis in *C. albicans* and *C. glabrata* and methods referring to the additional data.

6.1.1 Additional *in silico* tools

To design primer sequences and develop cloning strategies the software CloneManager 9 was used. Chemical structures and formulas were constructed with ChemBioDraw Ultra13.0. All figures were created with Adobe Illustrator CS5.1, Microsoft PowerPoint or GraphPad 5. The expression data were analyzed with Bio-Rad CFX Manager.

6.1.2 Additional strains, plasmids and oligonucleotides

Additional strains (**Table 5**), oligonucleotides (**Table 6**), and plasmids (**Table 7**) are not mentioned in **manuscript II** and **V** and referred to the additional data.

Table 5. Strains.

name	internal ID	designation/ genotype	reference
C. glabrata strains			
Cgtrp1Δ Cgvhr2Δ	G318	*trp1*::*FRT;* CAGL0J03014g::*NAT1*	this work
Cgvhr2Δ	G320	*trp1*::*TRP1;* CAGL0J03014g::*NAT1*	this work
Cgvhr2Δ + CgVHR2	G319	CAGL0J03014g::*NAT1;* *trp1*::(*TRP1*- CAGL0J03014g)	this work

Table 6. Oligonucleotides.

oligonucleotide name	sequence (5´→ 3´)	used for	reference
CgVHR2 cloning			
pUC19-*VHR2*-up-fwd	CCGGGGATCCTCTAGAATTTCGAGCTCTCGTTTATC	cloning of *VHR2* deletion construct	this study
VHR2-up-U1-rev	CGCGCCTAGCAGCGGTGTGTATCTCTGCTGTTGTGGC		this study
VHR2-down-D1-fwd	CGGCCGCATCCCTGCTTCTCCTAGGGACAATTTGGATC		this study
pUC19-*VHR2*-down-rev	CAGGTCGACTCTAGAACCTAACGAACTTTTGTGTTTAATAC		this study
VHR2del-amp-fwd	TCTCGTTTATCTTATATATTC	amplification of *VHR2* deletion construct from plasmid	this study
VHR2del-amp-rev	ACGAACTTTTGTGTTTAATAC		this study
VHR2-up-fwd	TGGGCCAACTGGGCTACATC	verification	this study
VHR2-down-rev	AGCCAGCGGAAGCTAGTGAG		this study

pTRP1-*VHR2* fwd	GCAGGTCGACTCTAGATTTCGAG CTCTCGTTTATC	cloning of *VHR2* complementation construct	this study
pTRP1-*VHR2* rev	CCGGGGATCCTCTAGAACGATGA CAAGGCCAAGGAG		this study
CgVHR2 RT fwd	CAGCATAACAGCCAGATGAC	verification	this study
CgVHR2 RT rev	AAAGCGCTGACGGACCTTGG		this study
VHR2 ctrl rev	AATTGCTCGCGGATCTTGTG		this study
VHR2 seq-fwd	GATACGGTACCACCCACAAG	verification	this study
probe synthesis			
VHR2 prom Sonde fwd	TTTCGAGTGATGGCCCAATG		this study
VHR2 prom Sonde rev	GCGCATGATCCATTGTGCAG		this study
*CgDUR1,2*prom Probe fwd	TCAGCCGATAAGAGTTACCC		this study
*CgDUR1,2*prom Probe rev	GCAATTTCCAGCCAAAATAC		this study
*CaDUR1,2*prom Probe fwd	CCACATCTCATCCTCATTATC		this study
*CaDUR1,2*prom Probe rev	GGGACCATCAAATGCCATAG		this study
quantitative RT-PCR oligonucleotides			
***C. glabrata* genes**			
CgACC1 RT fwd	GAGTGAGAAGGGTCTATCTG		this study
CgACC1 RT rev	CCTCGTTCAAACGGCGTCTC		this study
CgPYC1-RT fwd	GAGAAAGATTCGCGTACCTG		this study
CgPYC1-RT rev	TTTACCTGGCCATCTGCTTG		this study
CgPYC2-RT fwd	TTGGCACCATTCGACTTAGC		this study
CgPYC2-RT rev	CTCTGATACCGGTTTCTTCG		this study
***C. albicans* genes**			
CaPYC2 RT fwd	TGGCTGTTGGTGATGTTTCG		this study
CaPYC2 RT rev	CGGCAATTGGATCACCTTTAGC		this study
CaACC1 RT fwd	GCAGGTCAAGTGTGGTATCC		this study
CaACC1 RT rev	GAGCCACCTCTCAATTCTCC		this study

green: homolog to *Xba*I-linearized vector pUC19
blue: homolog to *Xba*I- linearized vector pTRP1

Table 7. Plasmids.

plasmid	features/Use	reference
p*CgNAT1*-VHR2	Amplification of *CgNAT1* cassette with up- and downstream flanking sequences of CAGL0J03014g	this study
p*CgTRP1*-VHR2	Amplification of *CgTRP1* and CAGL0J03014g, complementation of tryptophan auxotrophy and *CgVHR1* deletion	this study

6.1.3 Isolation of genomic DNA

Dependent on the follow-up experiments, genomic DNA was either isolated with a quick isolation protocol for standard PCR or the lyticase protocol for high-molecular DNA preparation used for Southern blotting. For both protocols, a liquid culture of *Candida* cells was grown overnight at 30°C (*C. albicans*) or 37°C (*C. glabrata*) in YPD or SD medium. Cells were harvested by centrifugation (4,000g; 2 min, RT).

Quick DNA isolation
The cells were disrupted by two freeze and thaw steps (2 min at -80°C and 1 min at 95°C) in 250 µL Harju buffer (2% Triton™ X-100, 1% SDS, 100 mM NaCl, 10 mM Tris-HCl pH 8.0, 1 mM EDTA) followed by vortexing. The cell debris was precipitated by adding 250 µL chloroform and centrifugation (20,000g; 5 min, RT). Following, the hydrophilic phase was transferred into a new microcentrifuge tube containing 500 µL ice-cold 100% ethanol. The DNA was precipitated by centrifugation (20,000g; 5 min, RT), washed once with 70% ethanol and air-dried. The transparent DNA pellet was reconstituted in 100-200 µL ddH$_2$O.

Isolation of high-molecular DNA
The cells were washed with 1 mL ddH$_2$O, transferred in 2 mL screw tubes and centrifuged (20,000g; 1 min, RT). The cells were resuspended in 1 mL lysis buffer (1 M sorbitol; 100 mM sodium citrate, pH 5.8; 50 mM EDTA, pH 8.0; 0.6 mg/mL lyticase and 2.5% β-mercaptoethanol) and incubated at 37°C for 45 min. Afterwards the cells were centrifuged, resuspended in 800 µL proteinase buffer (10 mM Tris-HCl, pH 7.5; 50 mM EDTA, pH 7.5; 0.5% SDS; 1 mg/mL proteinase K) and incubated at 60°C for 30 min. The cell debris was precipitated by adding 800 µL phenol/chloroform/isoamylalcohol (25:24:1), mixed with vortex device for 4 min and centrifuged (20,000g; 5 min, RT). The hydrophilic phase was transferred into a new microcentrifuge tube containing 750 µL isopropanol. The precipitated DNA was centrifuged (20,000g; 5 min, RT), washed with 600 µL 70% ethanol and air-dried. The transparent DNA pellet was reconstituted in 200 µL ddH$_2$O containing 10 mg/mL RNase A.
The DNA quantity was evaluated using a NanoDrop Spectrophotometer (ND-100, Peqlab). The DNA was stored at 4°C (short term) or -20°C (long term). Dilutions of DNA were made freshly.

6.1.4 Polymerase Chain Reaction (PCR) and gel electrophoresis

***Taq*-PCR**
This PCR was used for all standard reactions (genotyping of mutants), which do not require proof-reading activity (**Table 8**).

Table 8: Components and conditions of Taq-PCR.

Component	per reaction	PCR program:			
nuclease-free water	14.3 µL				
10× ThermoPol® Puffer	2 µL	Initial denaturation	95°C	30 sec	
10 mM dNTPs	0.5 µL	Denaturation	95°C	30 sec	
10 µM forward Primer	0.5 µL	Annealing	xx°C[1]	30 sec	30×
10 µM reverse Primer	0.5 µL	Extension	68°C	xx sec[2]	
Taq DNA Polymerase	0.2 µL	Final extension	68°C	10 min	
template DNA	100 ng (1 µL)	hold	4°C	∞	

[1] The annealing temperature was calculated with T_m calculator v 1.12.0 from NEB.
[2] The extension time was dependent on fragment length; 1,000 bp = 60 sec.

Colony PCR

The colony PCR was performed to directly check *E. coli* transformants for correct plasmid constructs. Instead of 1 µL of DNA, a small amount of colony material was inoculated into one 20 µL reaction. The initial denaturation step was extended to 5 min.

High fidelity PCR

This PCR was used for the synthesis of all cloning and transformation constructs (**Table 9**).

Table 9: Components and conditions of High fidelity PCR.

Component	per reaction	PCR program:			
nuclease-free water	32.5 µL				
5× Phusion HF	10 µL	Initial denaturation	98°C	30 sec	
10 mM dNTPs	1 µL	Denaturation	98°C	10 sec	
10 µM forward Primer	2.5 µL	Annealing	xx°C[1]	20 sec	35×
10 µM reverse Primer	2.5 µL	Extension	72°C	xx sec[2]	
Phusion® DNA Polymerase	0.5 µL	Final extension	72°C	10 min	
template DNA	100 ng (1 µL)	hold	4°C	∞	

[1] The annealing temperature was calculated with T_m calculator v 1.12.0 from NEB.
[2] The extension time was dependent on fragment length; 1,000 bp = 30 sec.

Probe PCR

The synthesis of Southern blot probes required the incorporation of digoxigenin (DIG)-labeled dNTPs into the PCR product to detect gene-specific fragments in the Southern blot. All components are part of the PCR DIG Probe Synthesis Kit (Roche, **Table 10**). The high fidelity PCR program (**Table 9**) was used.

Table 10: Components of the PCR synthesizing Southern blot probes.

Component	labeling reaction	control reaction
nuclease-free water	34.25 µL	34.25 µL
PCR Buffer with MgCl$_2$ (3)	5 µL	5 µL
PCR DIG mix labeled (2)	2.5 µL	-
PCR DIG mix unlabeled (4)	2.5 µL	5 µL
10 µM forward Primer	2.5 µL	2.5 µL
10 µM reverse Primer	2.5 µL	2.5 µL
Expand High Fidelity DNA Polymerase (1)	0.75 µL	0.75 µL
template DNA	100 ng (1 µL)	100 ng (1 µL)

The synthesized fragments were mixed with 1× loading dye, separated by size in 1% agarose gels in 1× TAE buffer (40 mM Tris, 20 mM acetic acid, 1 mM EDTA) for 40-60 min at 90-130 V and for size comparison 0.6 µg GeneRuler™ 1 kb DNA Ladder, ready-to-use (Thermo Fisher) was carried along. DNA fragments were stained in an ethidium bromide bath (0.15% staining solution, Fisher BioReagents) and visualized under UV light using an INFINITY3026 Imager with a camera and InfinityCapt V14.2 software.

6.1.5 Transformation of *E. coli* and isolation of plasmid DNA

One aliquot (app. 50 µL) of chemically competent *E. coli* cells (Stellar™ cells or DH5α) was thawed on ice. One hundred ng pure plasmid DNA or 5 to 10 µL ligation mixture was added to the cells and chilled on ice for additional 15 min. The uptake of DNA was facilitated by the heat shock method (42°C, 90 sec) and incubation in ice-cold water for 1 min. To express the antibiotic resistance gene, 450 µL LB or SOC medium was added and the cell suspension was incubated for 1 h at 37°C and 180 rpm. Different dilutions (1:10 and 1:100) were platted on LB agar (with 50 µg/mL ampicillin; LB-Amp) and incubated over night at 37°C. Grown colonies were checked for positive constructed plasmids *via* colony-PCR, streaked on fresh LB-Amp agar and grown o/n 37°C. For plasmid isolation, positive clones were incubated in LB-Amp medium at 37°C and 180 rpm, dependent on the required amount of plasmid DNA, 5 or 25 mL cultures were used. The cultures were harvested by centrifugation, washed with water and the cell pellet was resuspended in 350 µL P1 buffer (50 mM Tris-HCl pH 8.0, 10 mM EDTA and freshly added 100 µg/mL RNase A). The bacterial lysis was executed by adding 350 µL P2 buffer (200 mM NaOH, 1% SDS) and inverting the cell suspension. After 5 minutes, the lysis was neutralized by adding 350 µL P3 buffer (3 M potassium acetate pH 5.5). The precipitated cell debris and chromosomal DNA was removed by centrifugation (20,000*g*; 5 min, RT). One milliliter supernatant was transferred in a new tube containing 500 µL isopropanol and mixed by vortexing followed by centrifugation (full spin, 10 min, RT). The precipitated plasmid DNA was washed once with 500 µL 70% ethanol, air-dried and reconstituted in 30-100 µL ddH$_2$O.

6.1.6 Southern blot

High-molecular genomic DNA was digested with the appropriate restriction enzyme for 2 h to 16 h in the thermo-cycler. The reaction buffer and time, as well as inactivation procedure were selected according to the manufacturer's recommendations. The digested DNA was separated in a 1% agarose gel for 16 h with a current potential of 27 V. For size comparison, the DNA Molecular Weight Marker III, DIG-labeled (50 pg per lane, Roche) was carried along. A small gel was loaded and stained with ethidium bromide (0.15% staining solution, Fisher BioReagents) to check for successful digestion. The DNA was pretreated in acid to ensure efficient transfer. The agarose gel was rinsed 10 min in Depurination solution (0.25 M HCl) and shortly in water. The gel was denatured two times for 15 min in Denaturing solution (0.5 M NaOH, 1.5 M NaCl) and washed briefly in water. Finally, the gel was rinsed in Neutralization buffer (1 M Tris-HCl pH 7.5; 1.5 M NaCl) two times for 15 min and equilibrated for at least 10 min in 20× SSC (3.0 M NaCl, 0.3 M Sodium Citrate, adjust pH to 7.0).
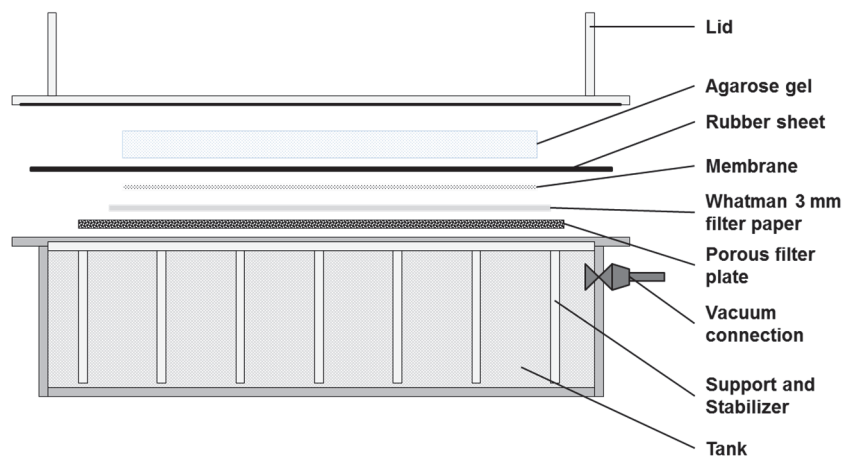
Figure 12: Setup of vacuum blotting to transfer DNA from agarose gel to positively-charged nylon membrane.

The nylon membrane (positively charged, Roche) was rinsed 2 min in water and 15 min in 20× SSC to activate the membrane, before the DNA was blotted 1.5 h at 50-100 mbar (**Figure 12**). In between fresh 20× SSC was added to the agarose gel preventing dehydration. Before DNA crosslinking, the membrane was rinsed 30 sec in 0.4 M NaOH, 30 sec in 0.2 M Tris-HCl pH 7.5 and dried 10-15 min on a piece of Whatman™ filter paper. The DNA was crosslinked to the membrane by UV light (120 mJ/cm^2) for at least 60 sec and the membrane was rinsed with 2× SSC. The membrane was incubated for at least 45 min at 40-44°C in 20 mL pre-warmed DIG Easy Hyb™ under rotation in hybridization flasks (Biometra). The optimal hybridization temperature is dependent on GC content and length of the probe. The probe was denaturized at 99°C for 5 min, cooled on ice and 5-20 µL, depending on strength of PCR product, were added to the pre-hybridization solution. The probe was hybridized overnight at 40-44°C under rotation.

The membrane was washed two times in low stringency buffer (2× SSC, 0.1% SDS) for 5 min and two times in pre-warmed high stringency buffer (0.1× SSC, 0.1% SDS, 68°C or 0.5× SSC, 0.1% SDS, 65°C) for 15 min. Afterwards, the membrane was rinsed twice with maleic acid buffer (0.1 M maleic acid, 0.15 M NaCl, pH 7.5 with 0.3% Tween®20) and once with maleic acid buffer without Tween®20 for 5 min each. Unspecific binding sites on the membrane were blocked with 1% blocking solution (Roche) in 1× maleic

acid buffer for 30 min at RT. Then, anti-Digoxiginin-AP, Fab fragments (Roche, 1:10,000 diluted) were added and incubated for 1 h at RT under rotation. Afterwards, the membrane was rinsed twice with maleic acid buffer (0.1 M maleic acid, 0.15 M NaCl, pH 7.5 with 0.3% Tween®20) and twice with maleic acid buffer without Tween®20 for 15 min each. The membrane was equilibrated for 5 min in alkaline phosphatase buffer (0.1 M Tris-HCl, 0.1 M NaCl, pH 9.5) under shaking in a plastic shell. The chemiluminescence reaction was started by adding CDP-*Star*® (Roche, 1:100 diluted in alkaline phosphatase buffer) onto the membrane in the plastic foil and incubated 5 min at RT in the dark. The membrane was shortly dried on Whatman™ filter paper and the chemiluminescence was detected in the Chemoimager with an exposure time of 1 h.

6.1.7 Protein isolation and Western blot of biotinylated proteins

For preparation of whole protein extracts, stationary phase cells were washed three times in PBS, diluted to OD600 0.2 into minimal medium without biotin and incubated at 30°C (*C. albicans*) or 37°C (*C. glabrata*) at 180 rpm for 4 and 24 h. The cells were harvested and mechanically lysed in PBS-KMT (PBS + 3 mM KCl, 2.5 mM $MgCl_2$, 0.1% Triton-X-100) + protease inhibitor cocktail (Roche) with acid-washed glass beads by bead beating in a Precellys 24 homogenizer (Peqlab; 6.500 rpm, 2 cycles, each 30 sec, 30 sec pause). The lysate was centrifuged (14,000 rpm, 4°C for 5 min) and the protein concentration of the supernatant was determined by Pierce™ BCA Protein Assay Kit (Thermo Fisher Scientific). Fifteen µg protein per condition and strain were denatured in one-fourth volume of 4× Lämmli buffer (125 mM Tris-HCl pH 6.8, 50% glycerol, 4% SDS, 0.02% bromophenol blue, 1:10 β-mercaptoethanol) at 95°C for 5 min and separated by denaturing SDS-PAGE with Rotiphorese® Gel 30 (final 8% acrylamide mix (Roth)). Proteins were electro-transferred to nitrocellulose membranes (Whatman) in blotting buffer (25 mM Tris, 192 mM glycine, 10% methanol and 0.1% SDS) and free binding sites were blocked with 5% milk powder in TBS (0.5 M Tris, 1.5 M NaCl, pH 7.6) + 0.05% Tween®20 (TBS-T) overnight. The membrane was incubated with Streptavidin-HRP (CST), which was diluted 1:4000 in TBS-T containing 2% BSA (Serva), and incubated for 2 h at room temperature and gentle shaking. The membrane was rinsed three times in TBS-T and two times in TBS, followed by chemiluminescence detection using Pierce™ ECL Plus Western Blotting Substrate (Thermo Fisher Scientific) according to the manufacturer´s instructions.

6.1.8 Construction of *Candida* mutant strains

6.1.8.1 Mutagenesis strategy in *C. albicans*

All *C. albicans* mutants were generated in the Arg⁻, His⁻, and Ura⁻-auxotrophic parental strain background BWP17 using a PCR-based gene disruption strategy [444]. The detailed description of the construction of the *CaVHR1* and *CaBIO2-5* deletion mutants in *C. albicans* is enclosed in the Master thesis of Teresa Sofie Hartung [445]. The construction of the *CaVHT1* (CR_03270WΔ/Δ) and *CaDUR1,2* (C1_04660WΔ/Δ) deletion mutants is exemplarily depicted for *CaVHT1* (**Figure 13**) and described in **manuscript II** and **manuscript V**, respectively.
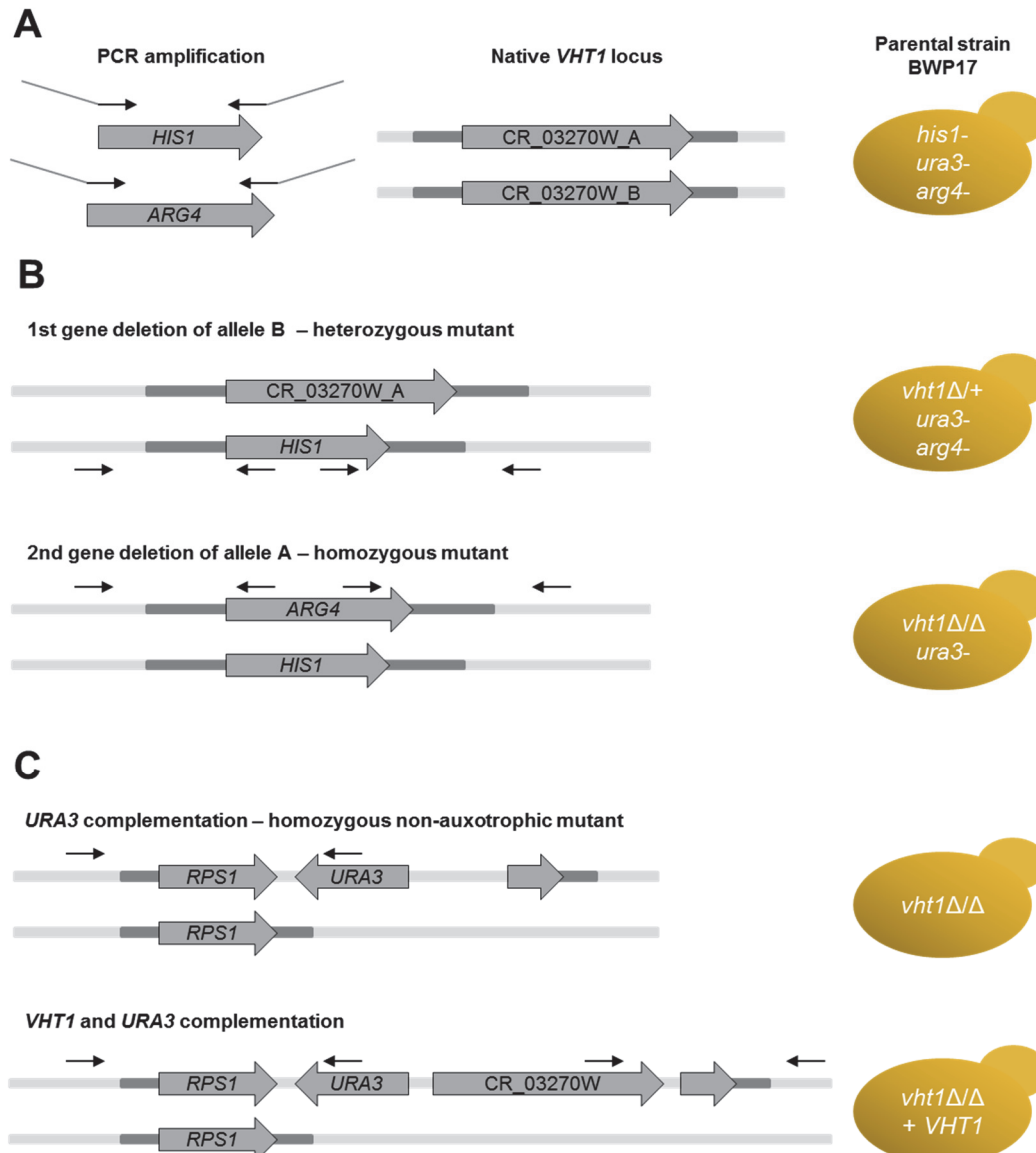
Figure 13: Gene mutagenesis and complementation in *C. albicans*, exemplary shown for *CaVHT1*. (A) Left: Separate amplification of *HIS1* and *ARG4* deletion cassettes with long oligonucleotides from pFA-HIS1 and pFA-ARG4 [444], respectively. The gray overlapping sequences of the primers are homologous to the up- and downstream regions of the GOI. Middle: Structure of the GOI (*VHT1*) locus in the diploid parental strain BWP17. (B) Sequential deletion of both gene alleles by two subsequent transformations with *HIS1* and *ARG4* constructs and homologous recombination. (C) After correct gene deletion, the strain was either complemented with *URA3* by using the CIp10 plasmid [110] (non-auxotrophic mutant) or reconstituted with *URA3* and the GOI by cloning the GOI into CIp10. The black arrows indicate the location of primers used to verify the correct insertion in the transformed yeast cell.

The transformation protocol was adapted from [446]. Briefly, *C. albicans* cells from a stationary culture were adjusted to OD_{600} 0.2 in 24 mL YPD medium and grown to exponential phase (until OD_{600} 0.8 was reached) for 3-4 h at 180 rpm and 30°C The cell suspension was harvested by centrifugation (5 min; 3,000g) and washed with 10 mL water resuspended in 500 µL TELiAc. In a new microcentrifuge tube, 10 µL of carrier DNA (UltraPure™ Salomon Sperm DNA Solution, Life Technology GmbH, boiled 10 min at 98°C prior to use and stored on ice), 1-10 µg of linearized DNA (plasmid DNA or PCR product) and 100 µL of *Candida* cells in TELiAc (1× TE, pH 7.4;

0.1 M lithium acetate) were mixed. Next, 600 µL PEG/LiAc solution (40% PEG3350, 0.1 M lithium acetate, 1x TE) was added and mixed by pipetting gently up and down. The transformation mixture was incubated o/n at 30°C. On the next day, the DNA uptake was facilitated by the heat shock at 44°C for 15 min in the water bath followed by cooling on ice for 1 min. The cells were centrifuged (5 min; 6,000 rpm) and washed once with YPD medium. Finally, the cells were washed and resuspended in 450 µL PBS and spread on three SD plates in equal proportions. The agar plates were incubated at 30°C for 2-4 days. Grown colonies were streaked on fresh plates and used for genomic DNA isolation. The correct integration of deletion and complementation cassettes was confirmed by PCR and Southern blot (**Figure 14-15**).
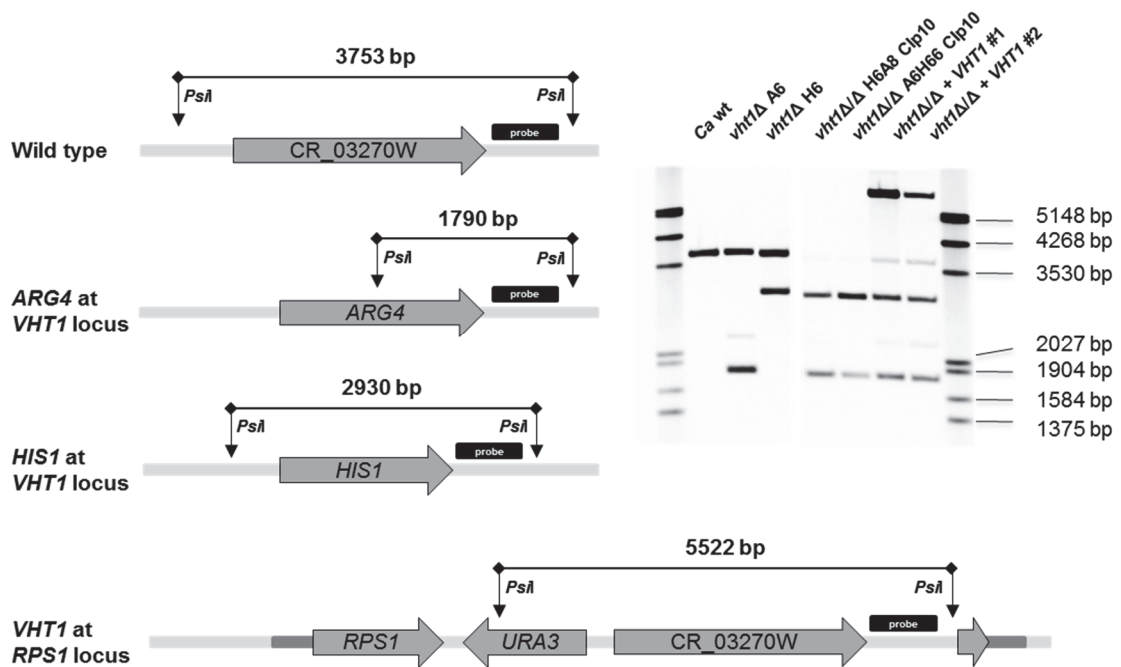
Figure 14: Verification of *CaVHT1* deletion and complementation by Southern blot. A *CaVHT1*-specific probe, generated by PCR using primers *Ca*19.2397term Sonde fwd (4/74) and *Ca*19.2397term Sonde rev (4/75) (product size: 199 bp). The high molecular genomic DNA was digested with *Psi*I, giving different bands in strains with the native gene (*Ca* wt [BWP17]), heterozygous deletion mutant (*vht1Δ*), homozygous deletion mutant (*vht1Δ/Δ* CIp10) and complemented strains (*vht1Δ/Δ+VHT1*).
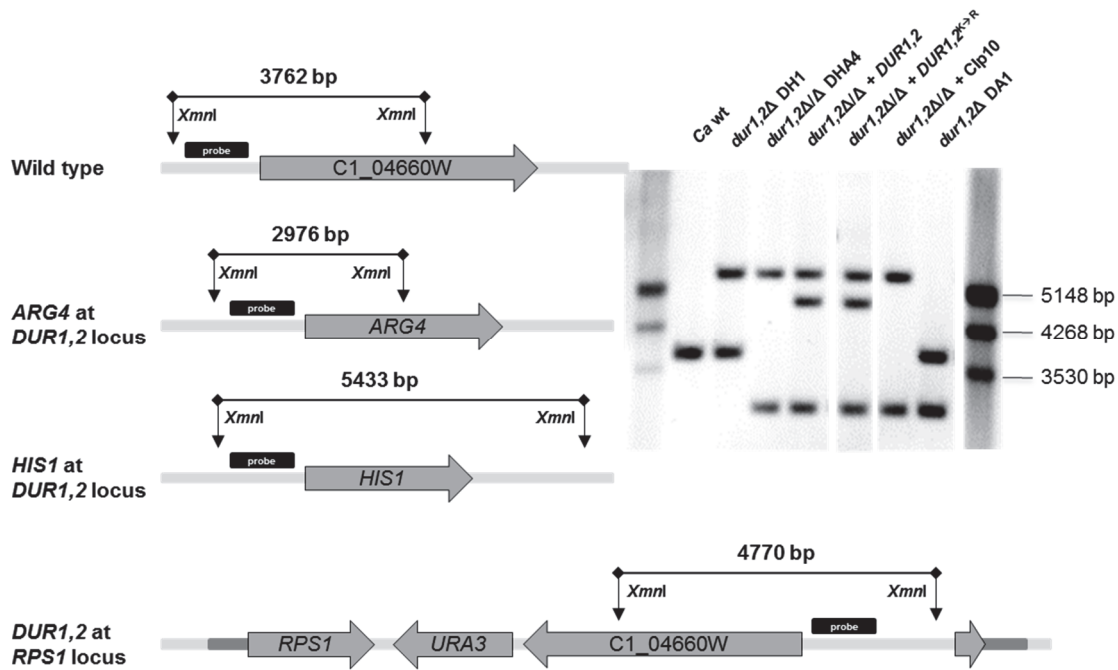
Figure 15: Verification of *CaDUR1,2* deletion and complementation by Southern blot. A *CaDUR1,2*-specific probe, generated by PCR using primers *CaDUR1,2*prom Probe fwd (5/28) and *CaDUR1,2*prom Probe rev (5/29) (product size: 236 bp). The high molecular genomic DNA was digested with *Psi*I, giving different bands in strains with the native gene (*Ca* wt [BWP17]), heterozygous deletion mutant (*dur1,2Δ*), homozygous deletion mutant (*dur1,2Δ/Δ* CIp10) and complemented strains (*dur1,2Δ/Δ+DUR1,2*; *dur1,2Δ/Δ+DUR1,2*$^{K\rightarrow R}$).

6.1.8.2 Mutagenesis strategy in *C. glabrata*

All *C. glabrata* mutants were generated in the parental strain background ATCC2001. Flanking homologous regions were cloned into pTS50 to construct a gene-specific *CgNAT1* deletion cassette [347]. The detailed description of the construction of the *CgVHR1* and *CgVHT1* deletion mutants is enclosed in the Master thesis of Stefanie Allert [320]. For gene complementation studies, the additional auxotrophic marker *CgTRP1* was chosen and requires a *CgTRP1* deletion background (**manuscript II and V**). Therefore, the deletion cassettes were amplified from existing *CgVHR1* and *CgVHT1* deletion mutants and transformed into *Cgtrp1Δ*, complemented either with *CgTRP1* or with *CgTRP1* together with the gene of interest at the native *CgTRP1* locus. The construction of the complementation plasmids is described in **manuscript II**. The *Cgdur1,2Δ* mutant (CAGL0M05533gΔ) was generated in the same way (described in **manuscript V**), as the *Cgdur1,2Δ* exists an triple-auxotrophic strain background [347].

The transformation protocol was adapted from [446]. Briefly, *C. glabrata* cells from a stationary culture were adjusted to OD_{600} 0.2 in 50 mL YPD medium and grown to exponential phase (until OD_{600} 0.8 was reached) for 3-4 h at 180 rpm and 37°C. The cell suspension was harvested by centrifugation (5 min; 3,000g). The cell pellet was first washed with 5 mL 1× TE and then with 5 mL TELiAc and finally resuspended in 500 µL TELiAc. Fifty microliter aliquots were either used directly or frozen at -80°C if needed and 5 µL of carrier DNA (UltraPure™ Salomon Sperm DNA Solution, Life Technology GmbH, boiled 10 min at 98°C prior to use and stored on ice) and 4 µg of PCR product were added. The transformation mixture was completed with 300 µL

Plate-Puffer (40% PEG3350 in TELiAc), mixed and incubated at 30°C for 30 min. The DNA uptake was facilitated by heat shock at 45°C for 15 min in the water bath followed by cooling on ice for 1 min. The cells were centrifuged (5 min; 6,000 rpm) and washed once with YPD medium. Dependent on the selection marker, the cells were additionally incubated for 3-4 h at 30°C and 180 rpm in 1 mL YPD to express the *NAT1* resistance gene. Finally, the cells were washed and resuspended in 450 µL PBS and spread on three YPD-NTC (250 µg/mL nourseothricin) or three SD plates dependent on the selection marker. The agar plates were incubated at 37°C for 1-3 days. The growth time is dependent on nutrient-rich (YPD) and nutrient-defined media (SD). Grown colonies were streaked on fresh plates and used for genomic DNA isolation.
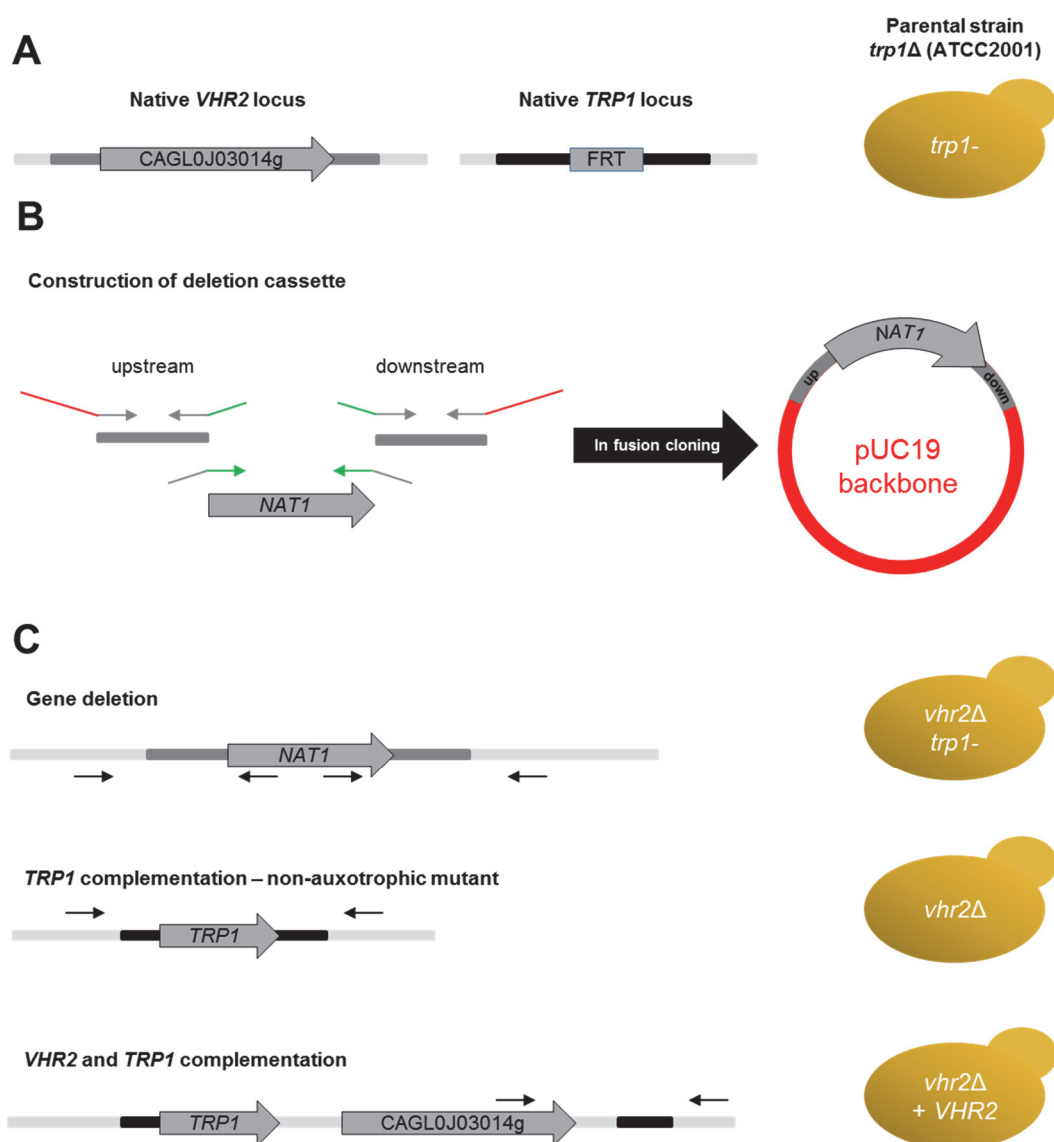

Figure 16: Gene mutagenesis and complementation in *C. glabrata*, exemplary shown for *CgVHR2*. (A) Structure of the GOI (*VHR2*) and *TRP1* loci in the parental strain *trp1Δ*. (B) Deletion cassette construction by infusion cloning of up- and downstream homologous regions referring to the GOI into the 5' and 3' region of the *NAT1* cassette of pTS50 [347]. Red regions of the primer overlap with the pUC19 backbone and gene regions (green) overlap with the *NAT1* cassette. (C) Mutagenesis in *C. glabrata* is done by homologous recombination. After gene deletion, the strain was either complemented with *TRP1* alone (non-auxotrophic mutant) or reconstituted with *TRP1* and the GOI. The black arrows indicate the location of primers used to verify the correct insertion in the transformed yeast cell.

The *CgVHR2* (CAGL0J03014g) deletion mutant was generated by flanking the barcoded *NAT1* cassette of *Cgfre8Δ* [314, 347] with *CgVHR2*-specific 5′- and 3′-flanks (701 bp upstream and 807 bp downstream) and integrating into an *XbaI*-linearized pUC19 vector using the Infusion HD Cloning Kit (Clontech). The plasmid was verified by control digest and sequencing. The deletion construct was amplified by PCR, purified with QIAquick PCR Purification Kit (Qiagen) and used for transformation of the *Cgtrp1Δ* parental strain. The *Cgvhr2Δ Cgtrp1Δ* mutant was verified by PCR.

For gene complementation, the coding sequence of *CgVHR2* together with the up- and downstream intergenic regions was inserted into p*CgTRP1* using the In-Fusion® HD Cloning Kit (Clontech) to generate p*CgTRP1-CgVHR2* and the correct plasmid was confirmed by sequencing. The tryptophan auxotrophy in the *Cgvhr2Δ Cgtrp1Δ* mutant was restored by transformation of PCR-amplified *CgTRP1* or *CgTRP1 + CgVHR2* cassettes to generate a non-auxotrophic mutant or gene complemented strain, respectively. All strains were verified by PCR and further analyzed by Southern blot (**Figure 17-20**).
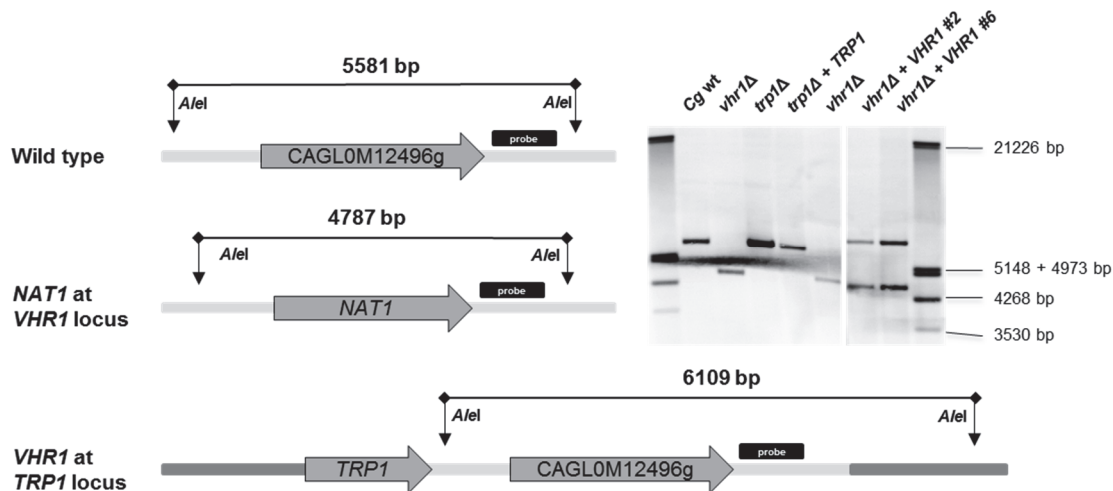
Figure 17: Verification of *CgVHR1* deletion and complementation by Southern blot. A *CgVHR1*-specific probe, generated by PCR using primers *CgVHR1*-term Sonde new fwd (3/51) and *CgVHR1*-term Sonde new rev (3/52) (product size: 428 bp). The high molecular genomic DNA was digested with *AleI*, giving different bands in strains with the native gene (*Cg* wt [ATCC2001]; *trp1Δ*; *trp1Δ+TRP1*), deletion mutant (*vhr1Δ*) and complemented strains (*vhr1Δ+VHR1*).
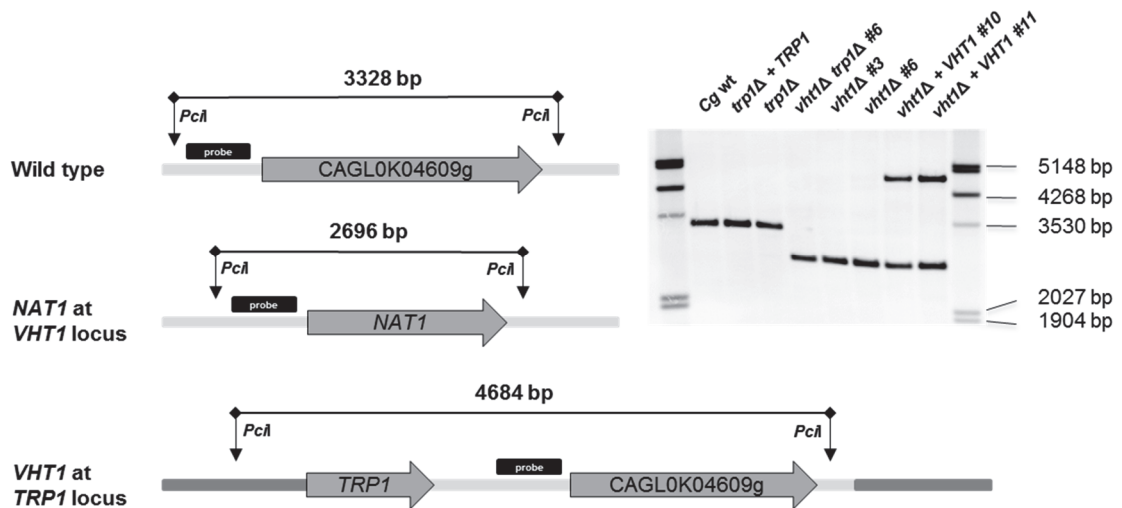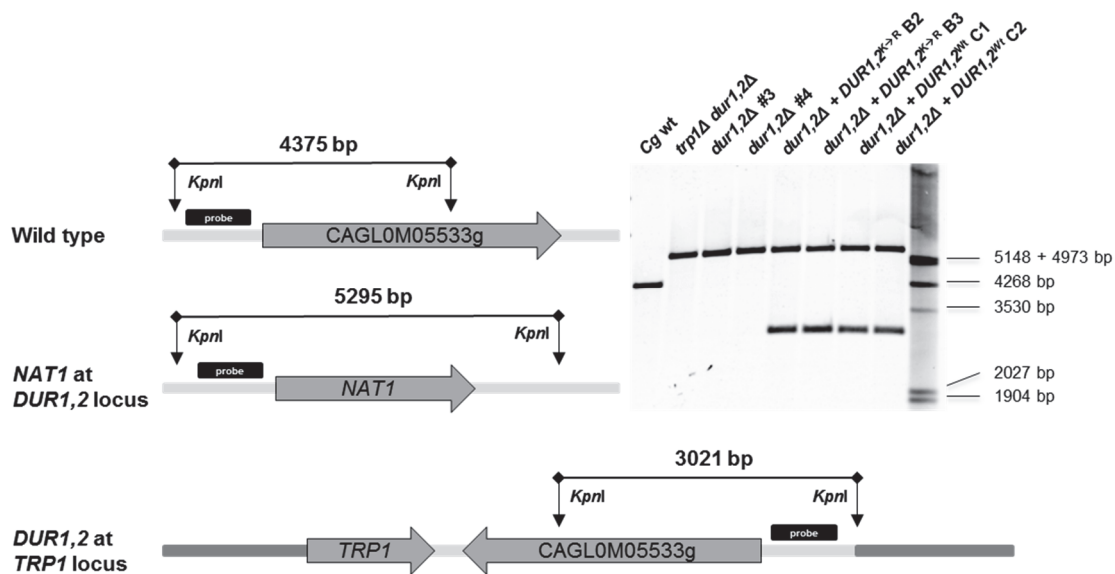
Figure 18: Verification of *CgVHT1* deletion and complementation by Southern blot. A *CgVHT1*-specific probe, generated by PCR using primers *CgVHT1*-prom Sonde fwd (2/15) and *CgVHT1*-prom Sonde rev (2/16) (product size: 398 bp). The high molecular genomic DNA was digested with *Pci*I, giving different bands in strains with the native gene (*Cg* wt [ATCC2001]; *trp1*Δ; *trp1*Δ+*TRP1*), deletion mutant (*vht1*Δ; *trp1*Δ *vht1*Δ) and complemented strains (*vht1*Δ+*VHT1*).
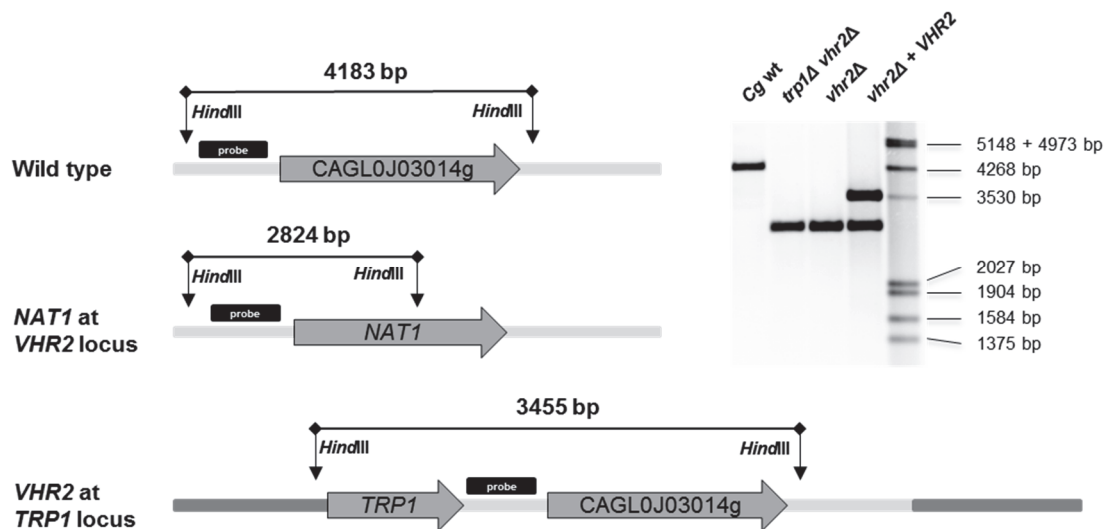
Figure 19: Verification of *CgVHR2* deletion and complementation by Southern blot. A *CgVHR2*-specific probe, generated by PCR using primers *CgVHR2* prom Sonde fwd (4/31) and *CgVHR2* prom Sonde rev (4/32) (product size: 413 bp). The high molecular genomic DNA was digested with *Hind*III, giving different bands in strains with the native gene (*Cg* wt [*trp1*Δ+*TRP1*]), deletion mutant (*vhr2*Δ; *trp1*Δ *vhr2*Δ) and complemented strains (*vhr2*Δ+*VHR2*).

Figure 20: Verification of *CgDUR1,2* deletion and complementation by Southern blot. A *CgDUR1,2*-specific probe, generated by PCR using primers *CgDUR1,2*prom Probe fwd (5/48) and *CgDUR1,2*prom Probe rev (5/49) (product size: 276 bp). The high molecular genomic DNA was digested with *Kpn*I, giving different bands in strains with the native gene (*Cg* wt [*trp1*Δ+*TRP1*]), deletion mutant (*dur1,2*Δ; *trp1*Δ *dur1,2*Δ) and complemented strains (*dur1,2*Δ+*DUR1,2*; *dur1,2*Δ+*DUR1,2*^K→R).

6.1.9 Alkalinization assay and ammonia quantification

The alkalinization assay on solid agar was adapted from [283]. Briefly, $1×10^5$ *Candida* cells were spotted onto agar (0.69% YNB without amino acids, ammonium sulfate and biotin (Formedium); 20 mg/L phenol red; 1% casamino acids; 0.5% allantoin; 2% oxoid agar; initially adjusted to pH 4.5 with HCl) in a 12-well plate and incubated at 37°C for 48-72 h. The quantification of volatile ammonia released from *Candida* cells was adapted from [283, 447]. Briefly, an acidic trap consisting of 100 µL of 10% citric acid was placed underneath the colonies in the lid of an inverted 12-well plate. After 24 to 72 h incubation, the acidic trap was removed and the ammonia was quantified by adding 160 µL of Nessler´s reagent to 40 µL diluted sample. Ammonia was calculated with the help of a standard curve of eight dilutions of an ammonium chloride solution (500 µg/mL). Heat killed *Candida* cells (70°C, 30 min) were included as negative control.

6.1.10 Macrophage experiments

For all macrophages, primary human monocyte-derived macrophages were used and isolated and differentiated like previously described.

6.1.10.1　　Phagocytosis assay

Macrophages (1.5×10^5 MΦ) were allowed to adhere onto coverslips in a 24-well plate overnight at 37°C and 5% CO_2 in RPMI + 10% FBS and 50 ng/mL rh M-CSF. On the next day, macrophages were washed twice with RPMI and finally 250 µL RPMI were added. Stationary phase yeast cells were washed, stained with 0.2 mg/mL FITC for 30 min in carbonate buffer (0.15 M NaCl, 0.1 M Na_2CO_3, pH 9.0) and adjusted to 1.2×10^6 *Candida*/mL in cold RPMI and the macrophages were infected with 250 µL yeast suspension to get an MOI of 2. Phagocytosis was synchronized for 30 min on ice. Afterwards, unbound *Candida* cells were removed by two washing steps with pre-warmed RPMI and finally 500 µL RPMI were added and the infected macrophages were incubated at 37°C and 5% CO_2 for 1 h. Phagocytosis was stopped by two washing steps with PBS, adding 300 µL Roti®-Histofix 4%, and infected macrophages were stained with 50 µg/mL Concanavalin A conjugated with Alexa Fluor™ 647 (ConA-AF647; Thermo Fisher Scientific) at 37°C for 30 min to visualize external *Candida* cells. Coverslips were mounted with Mowiol mounting medium and fluorescence images were recorded using the Zeiss AXIO Observer.Z1 (Carl Zeiss Microscopy).

6.1.10.2　　Cytokine and chemokine measurements

Macrophages (2×10^5 MΦ) were allowed to adhere in a 24-well plate overnight at 37°C and 5% CO_2 in RPMI + 10% FBS and 50 ng/mL rh M-CSF. On the next day, macrophages were washed twice with RPMI and finally 400 µL RPMI were added. Stationary phase yeast cells were washed and adjusted to 4×10^6 and 1×10^7 *Candida*/mL in cold RPMI and the macrophages were infected with 100 µL yeast suspension to get an MOI of 2 or 5, respectively. For comparison, macrophages were stimulated with 1 µg/mL LPS (positive control; from *E. coli* O55:B5, Sigma) or only RPMI (medium control). After 24 h incubation at 37°C and 5% CO_2, infected macrophages were centrifuged ($300g$, 10 min), the supernatant was collected in micro-centrifuge tubes and stored at -80°C until measurement. The release of IL-1β, IL-6, IL-8, and TNF-α was quantified using commercial eBioscience™ ELISA Ready-SET-Go!™ kits according to the manufacturer's instructions. The supernatants defrosted on ice, were diluted appropriate in 1× assay diluent.

6.2   Abbreviations

AA	amino acids – not specified
Amp	ampicillin
AS	ammonium sulfate
ATP	adenosine triphosphate
BBB	blood brain barrier
BLAST	basic local alignment search tool
bp	base pair
BSA	bovine serum albumin
bZIP	basic leucine zipper
C-	carbon-
CAA	casamino acids
cfu	colony forming units
CGD	*Candida* genome database
CIp10	*Candida* Integration plasmid 10
CLRs	C-type lectin receptors
ConA	Concanavalin A
CUG	stands for the nucleobases: cytosine, uracil, guanine
DAPA	7,8-diaminopelargonic acid
DCs	dendritic cells
DNA	deoxyribonucleic acid
ddH$_2$O	double distilled water
DIG	digoxigenin
dNTPs	desoxynucleotide triphosphate
DTB	desthiobiotin
EDTA	ethylenediaminetetraacetic acid
e.g.	latin: *exempli gratia,* for example
ELISA	enzyme-linked immunosorbent assay
FBS	fetal bovine serum
FITC	fluorescein isothiocyanate
GPI	glycosylphosphatidylinositol
GOI	gene of interest
HK	heat-killed
HIV	human immunodeficiency virus
HRP	horse radish peroxidase
IFN-γ	interferon gamma
IL-1β	interleukin 1 beta
IL-4	interleukin 4
IL-6	interleukin 6
IL-8	interleukin 8
KAPA	8-Amino-7-oxononanoic acid
LB	lysogeny broth
LDH	lactate dehydrogenase
LPS	lipopolysaccharide
MΦ	macrophages
MCT1	monocarboxylate transporter 1
M-CSF	macrophage colony-stimulating factor
MDMs	monocyte-derived macrophages
MPO	myeloperoxidase
MOI	multiplicity of infection
N-	nitrogen-
NAC	non-*albicans Candida*

Abbreviations

NADPH	Nicotinamide adenine dinucleotide phosphate hydrogen
NTC	nourseothricin
NOD	Nucleotide-binding oligomerization domain
OD	optical density
ORF	open reading frame
o/n	overnight
PAMPs	pathogen associated molecular patterns
PBS	phosphate buffered saline
PCR	polymerase chain reaction
PEG	polyethylene glycol
pH	latin: *potentia hydrogenii*
p.i.	post infection
PMNs	polymorphonuclear
PRRs	pattern recognition receptors
rh	recombinant human
RIGI	retinoic-acid-inducible gene I
RLRs	RIGI-like receptors
RNA	ribonucleic acid
RNS	reactive nitrogen species
ROS	reactive oxygen species
rpm	rotations per minute
RPMI	Roswell Park Memorial Institute
RT	room temperature
Saps	secretory aspartic proteases
SD	synthetic defined
SDS	sodium dodecyl sulfate
SILAC	stable isotope labeling with amino acids
SMVT	sodium dependent multivitamin transporter
spp.	species
SSC	sodium chloride sodium citrate
Taq	*Thermus aquaticus*
TBS(-T)	Tris-buffered saline (with 0.05% Tween®20)
TE	Tris-EDTA
TELiAc	Tris-EDTA lithium acetate
Th1	T helper cells, type 1
Th17	T helper cells, type 17
Th2	T helper cells, type 2
TLRs	toll-like receptors
T_m	melting temperature
TNF-α	tumor necrosis factor alpha
Tris	tris(hydroxymethyl)aminomethane
WBC	whole blood count
WGD	whole genome duplication
Wt	wild type
w/	with
w/o	without
YNB	yeast nitrogen base
YPD	yeast peptone dextrose

6.3 List of publications

2020   **Fungal biotin homeostasis is essential for immune evasion after macrophage phagocytosis and virulence.**
Sprenger M, Hartung TS, Allert S, Wisgott S, Niemiec JM, Graf K, Jacobsen ID, Kasper L, Hube B. *Cell Microbiol.* 2020 Feb 21:e13197. doi: 10.1111/cmi.13197. [Epub ahead of print]

     Phagocytic predation by the fungivorous amoeba *Protostelium aurantium* targets metal ion and redox homeostasis
Radosa S, Sprague JL, Tóth R, Wolf T, **Sprenger M**, Brunke S, Linde J, Panagiotou G, Gácser A, Hillmann F. *Cell Microbiol.* under revision, bioRxiv preprint doi: https://doi.org/10.1101/690503

2019   **RNAi as a Tool to Study Virulence in the Pathogenic Yeast *Candida glabrata*.**
Ishchuk OP, Ahmad KM, Koruza K, Bojanovič K, **Sprenger M**, Kasper L, Brunke S, Hube B, Säll T, Hellmark T, Gullstrand B, Brion C, Freel K, Schacherer J, Regenberg B, Knecht W, Piškur J. *Front Microbiol.* 2019 Jul 24;10:1679. doi: 10.3389/fmicb.2019.01679. eCollection 2019.

2018   **Metabolic adaptation of intracellular bacteria and fungi to macrophages.**
Sprenger M, Kasper L, Hensel M, Hube B. *Int J Med Microbiol.* 2018 Jan;308(1):215-227. doi: 10.1016/j.ijmm.2017.11.001. Epub 2017 Nov 7.

2017   **A functional link between hyphal maintenance and quorum sensing in *Candida albicans*.**
Polke M, **Sprenger M**, Scherlach K, Albán-Proaño MC, Martin R, Hertweck C, Hube B, Jacobsen ID. *Mol Microbiol.* 2017 Feb;103(4):595-617. doi: 10.1111/mmi.13526. Epub 2016 Oct 11.

2016   **Acid Sphingomyelinase Promotes Endothelial Stress Response in Systemic Inflammation and Sepsis.**
Chung HY, Hupe DC, Otto GP, **Sprenger M**, Bunck AC, Dorer MJ, Bockmeyer CL, Deigner HP, Gräler MH, Claus RA. *Mol Med.* 2016 Sep;22:412-423. doi: 10.2119/molmed.2016.00140. Epub 2016 Jun 15.

6.4 Posters and talks

Posters

2015   The role of biotin in *Candida glabrata* – macrophage interaction and virulence. SPP 1580 National Meeting, April 19 - 22, 2015 in Bonn, Germany

The role of biotin in *Candida glabrata* – macrophage interaction and virulence. 49. Wissenschaftliche Jahrestagung der Deutschsprachigen mykologischen Gesellschaft (DMykG), September 16 - 19, 2015 in Jena, Germany

2016 The role of biotin in *Candida glabrata* – macrophage interaction and virulence, Annual Conference 2016 of the Association for General and Applied Microbiology (VAAM). March 13 - 16, 2016 in Jena, Germany

The role of biotin in *Candida glabrata* – macrophage interaction and virulence, 5th Central European Summer Course and and the 2nd Rising Stars in Mycology Workshop. July 2 - 8, 2016 in Szeged, Hungary

2017 Fungal biotin homeostasis is crucial for intracellular fitness within macrophages. Gordon Research Seminar and Conference, Immunology of Fungal Infections. January 14 - 20, 2017 in Galveston, Texas, USA

Fungal biotin homeostasis is crucial for intracellular fitness within macrophages. 12th Symposium of the VAAM Special Group Biology and Biotechnology of Fungi. Molecular Biology of Fungi. September 28 - 30, 2017 in Jena, Germany

Scientific talks

2020 Biotin acquisition is crucial for immune evasion, *in vivo* persistence and virulence of *Candida glabrata* and *C. albicans*. Statusworkshop der DGHM-Fachgruppe „Eukaryontische Krankheitserreger". February 6 - 8, 2020 in Innsbruck, Austria

2018 Fungal biotin homeostasis is crucial for intracellular fitness within macrophages. 14th ASM Conference on *Candida* and *Candidiasis*. April 15 - 19, 2018 in Providence, Rhode Island, USA

Fungal biotin homeostasis is crucial for intracellular fitness within macrophages. 52. Wissenschaftliche Tagung der Deutschsprachigen Mykologischen Gesellschaft (DMykG). September 6 - 8, 2018 in Innsbruck, Austria

2015 The role of *Candida albicans EED1* in Quorum sensing. Statusworkshop der DGHM-Fachgruppe „Eukaryontische Krankheitserreger". February 26 - 27, 2015 in Erlangen, Germany

6.5   Supervision and public related activities

2016   Practical course "Molecular & Microbial Infection Biology" for Master Biochemistry July 11 - 22, 2016

2016 - 2018   Supervision Master Thesis Teresa Sofie Hartung

2018   Contribution to the "Forsche-Schüler Tag", HKI Jena, April 26, 2018

2019   Contribution to the Long Night of Science, HKI Jena, November 22, 2019

6.6   Travel grant and awards

- Picture award of DMykG (1st place), 48. Wissenschaftliche Tagung der Deutschsprachigen Mykologischen Gesellschaft (DMykG) e. V., September 4 - 6, 2014 in Salzburg, Austria.

- Travel grant at Microbiology and Infection - 4th Joint Conference of DGHM and VAAM, October 5 – 8, 2014 in Dresden, Germany

- Travels grant at 14th ASM Conference on Candida and Candidiasis 2018, April 15 - 19, 2018 in Providence, Rhode Island, USA.

- Picture award of DMykG (2nd place), 53. Wissenschaftliche Tagung der Deutschsprachigen Mykologischen Gesellschaft (DMykG) e. V., September 5 - 7, 2019 in Mannheim, Germany.

Selbstständigkeitserklärung

Hiermit erkläre ich, dass ich die vorliegende Arbeit selbst verfasst habe und keine anderen als die angegebenen Quellen und Hilfsmittel verwendet habe. Mir ist die geltende Promotionsordnung der Fakultät für Biowissenschaften der Friedrich-Schiller-Universität Jena bekannt. Personen, die mich bei den Experimenten, der Datenanalyse und der Verfassung der Manuskripte unterstützt haben, sind als Ko-Autoren auf den entsprechenden Manuskripten verzeichnet. Personen die mich bei der Verfassung der Dissertation unterstützt haben, sind in der Danksagung der Dissertation vermerkt. Die Hilfe eines Promotionsberaters wurde nicht in Anspruch genommen. Es haben Dritte weder unmittelbar noch mittelbar geldwerte Leistungen für Arbeiten erhalten, die im Zusammenhang mit dem Inhalt der vorgelegten Dissertation stehen. Die vorliegende Arbeit wurde in gleicher oder ähnlicher Form noch bei keiner anderen Hochschule als Dissertation eingereicht und auch nicht als Prüfungsarbeit für eine staatliche oder andere wissenschaftliche Prüfung verwendet.

Jena, den 29.05.2020

Marcel Sprenger